THE Leaching Properties of Co-combustion Residues

Anthe George

Department of Chemical Engineering & Chemical Technology
Imperial College
University of London

Thesis submitted in partial fulfilment of the requirements of the degree of
Doctor of Philosophy

ABSTRACT

The leaching susceptibility of toxic trace metals from co-combustion ashes has been studied experimentally. This study has been motivated by the urgent need to find uses for the fly ashes from fluidised bed boilers, firing biomass or waste fuels along with coal. Current legislation limits the use of fly ashes for road building or construction purposes to those derived from firing black coal alone. Use of ashes derived partially from biomass, or waste, for such purposes or even their disposal to landfill, depends on the stability of contained heavy metals, to avoid leaching of toxic ions into ground waters.

In this study ashes produced from two sets of fuels underwent leaching by the TCLP (Toxicity Characteristic Leaching Procedure) test. Trace element content in the fuels, the ashes and leachate from these ashes was evaluated. The first set of fuels was a mixture of pure coals, and coal/secondary fuel mixtures. These fuels underwent combustion in a fixed bed "hot-rod" reactor, and a muffle furnace at temperatures of 850 and 950 °C. The second set of fuels consisted of Chilean coals blended in different proportions. These fuels underwent combustion at 900 and 1500 °C.

The trace elements evaluated were ones considered to be of most concern when entering the environment, namely: Be, V, Cr, Zn, As, Se, Cd, Ba, Hg & Pb. The contents of these metals in the ashes were measured and the retention of these trace elements was calculated. Mercury and selenium were almost completely volatilised in all cases. For the other trace metals it was not possible to establish a hierarchy of relative trace element retention. Retention was primarily a function of combustion method and temperature used, depending on the fuel set being studied. No synergistic effects were observed from blending the fuels in different proportions. There was varying concurrence of results between equilibrium modelling of trace element behaviour in combustion and empirical data.

For trace element retention in the leachates, the elements which underwent a very low degree of leaching were V, As, Se, Ba. Those which underwent moderate leaching were Be, Cr, Cd and those which were leached to a great extent were Zn, Hg, Pb. This

hierarchy was followed for all fuels and conditions studied. Leaching was found to be a strong function of temperature and combustion method. The type of fuel used did not appear to influence the degree of leaching. No synergistic effects appeared to be relevant in the leaching of trace elements from fuel blends. There was excellent agreement between empirical leaching data and thermodynamic modelling of the leaching system when experimental values of system pH were used. When the model was allowed to compute equilibrium pH there was less agreement in results.

A dilution attenuation factor was applied to the absolute trace element concentration in the leachate and the toxicity and suitability of the ashes for landfill thereby assessed. All of the leachates studied contained trace element levels above those deemed acceptable. Arsenic was an element that was always present in higher than maximum allowable levels, whilst zinc and mercury never exceeded regulatory limits. The other elements exceeded these limits to varying degrees, not attributable to the variables studied. Therefore, none of the ashes in this study would be suitable for landfill, without steps taken to prevent leachate emission.

ACKNOWLEDGEMENTS

I feel enormously privileged to have had the opportunity to study at Imperial College; I valued every minute. Much more so however, I feel particular gratitude to have worked under the guidance of Prof. Denis Dugwell and Prof. Rafael Kandiyoti. To them I extend my heartfelt thanks.

A round of applause must also go to all the others in my group and department, too numerous to mention, who helped me on this journey with their knowledge, enthusiasm and friendship. As for my friends and family outside of college, who weren't quite sure what I was doing for the past few years,...here it is!

CONTENTS

ABSTRACT 01

ACKNOWLEDGEMENTS 02

TABLE OF CONTENTS 03

FIGURES 09

TABLES 16

ACRONYMS & NOMENCLATURE 18

1.0 INTRODUCTION 19

2.0 BACKGROUND 22

2.1 Biomass & Combustible Waste 22

2.1.1 Impetus for Biomass Use 27

2.1.1.1 Greenhouse Gas Reduction 27

2.1.1.2 Reduction of Regional & Atmospheric Pollutants 28

2.1.1.3 Sustainable Development 28

2.1.1.4 Fossil Fuel Preservation & Diversification 28

2.2 Co-firing of Coal Biomass and Wastes 30

2.2.1 Combustion of Coal 30

2.2.2 Combustion of Biomass 32

2.2.3 Co-firing of Biomass & Wastes With Coal 34

2.2.3.1 Objectives of Co-firing 34

2.2.3.2 Co-firing Technologies 35

2.2.3.3 Fluidised Bed Combustion 36

2.2.3.4 Pulverised Fuel Combustion 37

2.2.3.5 Fixed Grate Combustion 39

2.2.3.6 Cyclone Combustion 40

2.2.3.7 Fouling and Corrosion in Co-combustion 40

2.2.3.8 Waste Production in Co-combustion 43

2.2.3.9 Beneficial Uses of Combustion Wastes 43

2.2.3.10 Ash Disposal Methods 45

2.2.4 Physical & Chemical Characteristics of Ash 48

2.3 Trace Elements 51
2.3.1 Trace Element Speciation Migration & Toxicity 51
2.3.1.1 Arsenic 51
Speciation & Migration 51
Toxicity & Regulatory Limits 53
2.3.1.2 Barium 53
Speciation & Migration 53
Toxicity & Regulatory Limits 54
2.3.1.3 Beryllium 54
Speciation & Migration 54
Toxicity & Regulatory Limits 55
2.3.1.4 Cadmium 56
Speciation & Migration 56
Toxicity & Regulatory Limits 57
2.3.1.5 Chromium 57
Speciation & Migration 57
Toxicity & Regulatory Limits 58
2.3.1.6 Lead 59
Speciation & Migration 59
Toxicity & Regulatory Limits 59
2.3.1.7 Mercury 60
Speciation & Migration 60
Toxicity & Regulatory Limits 61
2.3.1.8 Zinc 61
Speciation & Migration 61
Toxicity & Regulatory Limits 62
2.3.1.9 Vanadium 62
Speciation & Migration 62
Toxicity & Regulatory Limits 62

2.3.3 Trace Element Occurrence in Coal 63
2.3.4 Trace Element Partitioning in Combustion 66
2.4 Leaching 69
2.4.3 Leaching of Combustion Residues 69
2.4.4 Factors and Mechanisms Controlling Release 70
2.4.5 Leaching Tests 72
2.4.6 Equilibrium Speciation Modelling-MINTEQA2 75
2.4.6.1 Adsoprtion Models 79
3.0 EXPERIMENTAL PROTOCOL 81
3.1 Sample Characterisation 81
3.1.1 Fuel Set 1 – Samples Used to Verify Validity of Modified TCLP Test and Analytical Procedures 82
3.1.2 Fuel Set 2 – Samples Provided by CERCHAR 83
3.1.3 Fuel Set 3 – Samples Provided by GENER Power Station 84
3.2 Combustion Apparatus 86
3.2.1 The Hot-rod Reactor 86
3.2.1.1 Reactor Specifications 87
3.2.1.2 Reactor Gas Circuit 90
3.2.1.3 Heating & Temperature Control System 91
3.2.1.4 Operating Parameters & Reactor Output 94
3.2.2 The Muffle Furnace 95
3.3 Leaching Experiments 96
3.3.1 Toxicity Characteristic Leaching Procedure (TCLP) 96
3.3.1.1 Apparatus & Materials 97
3.3.1.2 Reagents 100
3.3.1.3 Sample Collection, Preservation & Handling 100
3.3.1.4 Procedure 101
3.3.2 Modified Toxicity Characteristic Leaching Procedure 105
3.3.2.1 TCLP Method For Small Sample Sizes 105
3.3.2.2 Verifying the Validity of the Modified Test 107

3.4 Analytical Techniques 108
3.4.1 Wet Ashing Digestion 108
3.4.2 Microwave Digestion Method 109
3.4.3 Mercury Analysis 110
3.4.3.1 Procedure 110
3.4.4 Inductively Coupled Plasma Mass Spectrometry (ICP-MS) 112
3.4.4.1 Theory & Instrumentation 112
3.4.4.2 Procedure & Operating Conditions 115
4.0 RESULTS 119
4.1 Developing the Modified TCLP Test 119
4.1.1 Ascertaining Reproducibility of Modified TCLP With Small Sample Masses 119
4.1.1.1 Results For Sample RM-203 120
4.1.1.2 Results For Sample RM-205 125
4.1.1.3 Results For Polish Coal 130
4.1.1.4 Conclusions 134
4.2.2 Comparison of Certified Values with Modified TCLP 135
4.2.2.1 Conclusions 145
4.2 Trace Element Contents in Raw Fuels 146
4.2.1 Experimental Error & Error Calculations 146
4.2.2 CERCHAR Fuels 147
4.2.3 Chilean Fuels 159
4.3 Trace Element Retention In Ashes 172
4.3.1 Trace Element Retention in CERCHAR Ashes 172
4.3.2 The Effect of Temperature On Muffle Furnace Produced Ash 174
4.3.3 The Effect of Temperature on Hot-rod Produced Ash 185
4.3.4 Trace Element Retention in the Chilean Ashes 197
4.4 Trace Element Content in Leachates 210
4.4.1 Leaching Modelling 210
4.4.2 Trace Element Content In CERCHAR Leachates 212

4.4.2.1 Trace Element Content in Leachate From Muffle Ash 213
4.4.2.2 Trace Element Content in Leachate From Hot-rod Ash 229
4.4.2.3 Trace Element Content in Leachate in Relation to Regulatory Constraints 239
4.4.3 Trace Element Content in Chilean Leachates 251
4.4.3.1 Trace Element Content in Leachate in Relation to Regulatory Constraints 262
5.0 SUMMARY 269
5.1 Trace Element Concentration in the Raw Fuel 269
5.2 Trace Element Retention in the Ashes 272
5.2.1 Trace Element Retention as a Function of Temperature 272
5.2.2 Trace Element Retention as a Function of Combustion Method 275
5.3 Trace Element Leaching from Ashes 277
5.3.1 Trace Element Leaching as a Function of Temperature 278
5.3.2 Trace Element Leaching as a Function of Combustion Method 280
5.4 Toxicity of Leachates 281
6.0 CONCLUSIONS 283
6.1 Trace Element Concentration in the Raw Fuel 283
6.2 Trace Element Retention After Combustion 283
6.2.1 The Influence of Temperature on Trace Element Retention 283
6.2.2 The Influence of Combustion Method on Trace Element Retention 283
6.2.3 The Influence of Fuel Type on Trace Element Retention 282
6.2.4 Possible Synergistic Effects in the Chilean Fuels 284
6.3 Trace Element Leaching 284
6.3.1 The Influence of Temperature on Trace Element Leaching 284
6.3.2 The Influence of Combustion Method on Trace Element Leaching 284
6.3.3 The Influence of Fuel Type on Trace Element Leaching 284
6.3.4 Possible Synergistic Effects In the Chilean Fuels 284
6.4 Toxicity of Leachates 285

7.0 FURTHER STUDY 286

7.1 Continuation and Changes to Experimental Work 286

7.2 Further Modelling 287

REFERENCES 288

APPENDIX I: Trace Element Concentrations in CERCHAR Fuels 297

APPENDIX II: Trace Element Retentions in CERCHAR Fuels as a Function of Combustion Method 307

APPENDIX III : Trace Element Concentrations in Chilean Fuels 327

APPENDIX IV: Example of a MINTEQA2 Output File 336

APPENDIX V: Trace Element Leached in CERCHAR fuels as a Function of Combustion method 354

INDEX of FIGURES

Figure 2.1.1 Structural Unit and SEM image for Cellulose

Figure 2.1.2 Combustibles Content, Moisture and Ash in Selected Bio Fuels

Figure 2.2.1 Major Steps in Coal Combustion and NO_x Reaction Pathways

Figure 2.2.2 Typical Waste Production Variation With Varying Combustor Configurations

Figure 2.3.1 Modes of Occurrence of Trace Elements in Coal

Figure 2.3.2 Classification of Trace Elements by Their Partitioning Behaviour During Combustion (CERCHAR 1985, Clarke 1991, Conzemius 1984, Klein 1975)

Figure 2.4.1 Conceptual Model of Water Balance at Land-fill Site

Figure 2.4.2 Example of Field Lysimetre

Figure 2.4.3 Basic Column Leaching Test Apparatus

Figure 2.4.4 Flow Diagram of General MINTEQA2 Methodology

Figure 3.2.1 Schematic of the Hot-Rod Reactor, Kaowool Lining and Sample Placement

Figure 3.2.2 Gas Supply Circuit For Hot-Rod Reactor

Figure 3.2.3 Hot-Rod Reactor Thermocouples and Heating Elements

Figure 3.2.4 Overview of reactor control programme.

Figure 3.2.5 Temperature & Power Output From Typical Hot-Rod Combustion Run

Figure 3.3.1 Flow Diagram of US – EPA TCLP Test Procedure

Figure 3.3.2 Agitator Designed to Carry Out Leaching

Figure 4.1.1 Reproducibility of Modified TCLP Test for Sample RM203, 50mg & 16hrs

Figure 4.1.2 Reproducibility of Modified TCLP Test for Sample RM203, 50mg & 18hrs

Figure 4.1.3 Reproducibility of Modified TCLP Test for Sample RM203, 75mg & 16hrs

Figure 4.1.4 Reproducibility of Modified TCLP Test for Sample RM203, 75mg & 18hrs

Figure 4.1.5 Reproducibility of Modified TCLP Test for Sample RM203, 100mg & 16hrs

Figure 4.1.6 Reproducibility of Modified TCLP Test for Sample RM203, 100mg & 18hrs

Figure 4.1.7 Reproducibility of Modified TCLP Test for Sample RM203, 125mg & 16hrs

Figure 4.1.8 Reproducibility of Modified TCLP Test for Sample RM203, 125mg & 18hrs

Figure 4.1.9 Reproducibility of Modified TCLP Test for Sample RM205, 50mg & 16hrs

Figure 4.1.10 Reproducibility of Modified TCLP Test for Sample RM203, 50mg & 18hrs

Figure 4.1.11 Reproducibility of Modified TCLP Test for Sample RM205, 75mg & 16hrs
Figure 4.1.12 Reproducibility of Modified TCLP Test for Sample RM205, 75mg & 18hrs
Figure 4.1.13 Reproducibility of Modified TCLP Test for Sample RM205, 100mg & 16hrs
Figure 4.1.14 Reproducibility of Modified TCLP Test for Sample RM205, 100mg & 18hrs
Figure 4.1.15 Reproducibility of Modified TCLP Test for Sample RM205, 125mg & 16hrs
Figure 4.1.16 Reproducibility of Modified TCLP Test for Sample RM205, 125mg & 18hrs
Figure 4.1.17 Reproducibility of Modified TCLP Test for Polish Coal, 50mg & 16hrs
Figure 4.1.18 Reproducibility of Modified TCLP Test for Polish Coal, 50mg & 18hrs
Figure 4.1.19 Reproducibility of Modified TCLP Test for Polish Coal, 75mg & 16hrs
Figure 4.1.20 Reproducibility of Modified TCLP Test for Polish Coal, 75mg & 18hrs
Figure 4.1.21 Reproducibility of Modified TCLP Test for Polish Coal, 100mg & 16hrs
Figure 4.1.22 Reproducibility of Modified TCLP Test for Polish Coal, 100mg & 18hrs
Figure 4.1.23 Reproducibility of Modified TCLP Test for Polish Coal, 125mg & 16hrs
Figure 4.1.24 Reproducibility of Modified TCLP Test for Polish Coal, 125mg & 18hrs
Figure 4.1.25 Effect of Sample Mass on Certified Cadmium Concentration after 16hrs – Sample RM203
Figure 4.1.26 Effect of Sample Mass on Certified Cadmium Concentration after 18hrs – Sample RM203
Figure 4.1.27 Effect of Sample Mass on Certified Lead Concentration after 16 hrs – Sample RM203
Figure 4.1.28 Effect of Sample Mass on Certified Lead Concentration after 18 hrs – Sample RM203
Figure 4.1.29 Effect of Sample Mass on Certified Chromium Concentration after 16 hrs – Sample RM205
Figure 4.1.30 Effect of Sample Mass on Certified Chromium Concentration after 18 hrs – Sample RM205
Figure 4.1.31 Effect of Sample Mass on Certified Arsenic Concentration after 16 hrs – Sample RM205
Figure 4.1.32 Effect of Sample Mass on Certified Arsenic Concentration after 18 hrs – Sample 205

Figure 4.1.33 Effect of Sample Mass on Certified Cadmium Concentration after 16 hrs – Sample RM205
Figure 4.1.34 Effect of Sample Mass on Certified Cadmium Concentration after 18 hrs – Sample RM205

Figure 4.1.35 Effect of Sample Mass on Certified Barium Concentration after 16 hrs – Sample RM205
Figure 4.1.36 Effect of Sample Mass on Certified Barium Concentration after 18 hrs – Sample RM205
Figure 4.1.37 Effect of Sample Mass on Certified Lead Concentration after 16 hrs – Sample RM205
Figure 4.1.38 Effect of Sample Mass on Certified Lead Concentration after 16 hrs – Sample RM205
Figure 4.2.1 Beryllium Concentration in Eight CERCHAR fuels Studied
Figure 4.2.2 Vanadium Concentration in Eight CERCHAR fuels Studied
Figure 4.2.3 Chromium Concentration in Eight CERCHAR fuels Studied
Figure 4.2.4 Zinc Concentration in Eight CERCHAR fuels Studied
Figure 4.2.5 Arsenic Concentration in Eight CERCHAR fuels Studied
Figure 4.2.6 Selenium Concentration in Eight CERCHAR fuels Studied
Figure 4.2.7 Mercury Concentration in Eight CERCHAR fuels Studied
Figure 4.2.8 Cadmium Concentration in Eight CERCHAR fuels Studied
Figure 4.2.9 Barium Concentration in Eight CERCHAR fuels Studied
Figure 4.2.10 Lead Concentration in Eight CERCHAR fuels Studied
Figure 4.2.11 Trace Element Occurrence in CERCHAR Fuel 1
Figure 4.2.12 Trace Element Occurrence in CERCHAR Fuel 2
Figure 4.2.13 Trace Element Occurrence in CERCHAR Fuel 3
Figure 4.2.14 Trace Element Occurrence in CERCHAR Fuel 4
Figure 4.2.15 Trace Element Occurrence in CERCHAR Fuel 5
Figure 4.2.16 Trace Element Occurrence in CERCHAR Fuel 6
Figure 4.2.17 Trace Element Occurrence in CERCHAR Fuel 7
Figure 4.2.18 Trace Element Occurrence in CERCHAR Fuel 8

Figure 4.2.19 Beryllium Concentration in Chilean Fuels & Fuel Blends
Figure 4.2.20 Vanadium Concentration in Chilean Fuels & Fuel Blends
Figure 4.2.21 Chromium Concentration in Chilean Fuels & Fuel Blends
Figure 4.2.22 Zinc Concentration in Chilean Fuels & Fuel Blends
Figure 4.2.23 Arsenic Concentration in Chilean Fuels & Fuel Blends
Figure 4.2.24 Selenium Concentration in Chilean Fuels & Fuel Blends
Figure 4.2.25 Mercury Concentration in Chilean Fuels & Fuel Blends
Figure 4.2.26 Cadmium Concentration in Chilean Fuels & Fuel Blends
Figure 4.2.27 Barium Concentration in Chilean Fuels & Fuel Blends
Figure 4.2.28 Lead Concentration in Chilean Fuels & Fuel Blends
Figure 4.2.29 % Deviation from Theoretical Value of Concentration in Kideco-Lemington Coal Blend
Figure 4.2.30 % Deviation from Theoretical Value of Concentration in Lemington-Allied Coal Blend
Figure 4.2.31 Trace Element Concentrations in Kideco Coal
Figure 4.2.32 Trace Element Concentrations in Kideco-Lemington Coal Fuel Blend
Figure 4.2.33 Trace Element Concentrations in Lemington Coal
Figure 4.2.34 Trace Element Concentrations in Lemington-Allied Coal Fuel Blend
Figure 4.2.35 Trace Element Concentrations in Allied Coal
Figure 4.3.1 Beryllium Retention in Muffle Furnace Ashes of CERCHAR fuels
Figure 4.3.2 Vanadium Retention in Muffle Furnace Ashes of CERCHAR fuels
Figure 4.3.3 Chromium Retention in Muffle Furnace Ashes of CERCHAR fuels
Figure 4.3.4 Zinc Retention in Muffle Furnace Ashes of CERCHAR fuels
Figure 4.3.5 Arsenic Retention in Muffle Furnace Ashes of CERCHAR fuels
Figure 4.3.6 Selenium Retention in Muffle Furnace Ashes of CERCHAR fuels
Figure 4.3.7 Cadmium Retention in Muffle Furnace Ashes of CERCHAR fuels
Figure 4.3.8 Mercury Retention in Muffle Furnace Ashes of CERCHAR fuels
Figure 4.3.9 Barium Retention in Muffle Furnace Ashes of CERCHAR fuels
Figure 4.3.10 Lead Retention in Muffle Furnace Ashes of CERCHAR fuels
Figure 4.3.11 Beryllium Retention in Hot-Rod Ashes of CERCHAR fuels
Figure 4.3.12 Vanadium Retention in Hot-Rod Ashes of CERCHAR fuels

Figure 4.3.13 Chromium Retention in Hot-Rod Ashes of CERCHAR fuels
Figure 4.3.14 Zinc Retention in Hot-Rod Ashes of CERCHAR fuels
Figure 4.3.15 Arsenic Retention in Hot-Rod Ashes of CERCHAR fuels
Figure 4.3.16 Selenium Retention in Hot-Rod Ashes of CERCHAR fuels
Figure 4.3.17 Cadmium Retention in Hot-Rod Ashes of CERCHAR fuels
Figure 4.3.18 Mercury Retention in Hot-Rod Ashes of CERCHAR fuels
Figure 4.3.19 Barium Retention in Hot-Rod Ashes of CERCHAR fuels
Figure 4.3.20 Lead Retention in Hot-Rod Ashes of CERCHAR fuels
Figure 4.3.21 Beryllium Retention in Chilean Ashes Produced at 900 & 1500 °C
Figure 4.3.22 Vanadium Retention in Chilean Ashes Produced at 900 & 1500 °C
Figure 4.3.23 Chromium Retention in Chilean Ashes Produced at 900 & 1500 °C
Figure 4.3.24 Zinc Retention in Chilean Ashes Produced at 900 & 1500 °C
Figure 4.3.25 Arsenic Retention in Chilean Ashes Produced at 900 & 1500 °C
Figure 4.3.26 Selenium Retention in Chilean Ashes Produced at 900 & 1500 °C
Figure 4.3.27 Cadmium Retention in Chilean Ashes Produced at 900 & 1500 °C
Figure 4.3.28 Mercury Retention in Chilean Ashes Produced at 900 & 1500 °C
Figure 4.3.29 Barium Retention in Chilean Ashes Produced at 900 & 1500 °C
Figure 4.3.30 Lead Retention in Chilean Ashes Produced at 900 & 1500 °C
Figure 4.3.31 % Deviation from Theoretical Value of Trace Element Retention in Kideco Lemington Fuel
Figure 4.3.32 % Deviation from Theoretical Value of Trace Element Retention in Lemington-Allied Fuel
Figure 4.4.1 % Beryllium Leached from Ash Produced in Muffle Furnace at 850 & 950 °C
Figure 4.4.2 % Vanadium Leached from Ash Produced in Muffle Furnace at 850 & 950 °C
Figure 4.4.3 % Chromium Leached from Ash Produced in Muffle Furnace at 850 & 950 °C
Figure 4.4.4 % Zinc Leached from Ash Produced in Muffle Furnace at 850 & 950 °C
Figure 4.4.5 % Arsenic Leached from Ash Produced in Muffle Furnace at 850 & 950 °C
Figure 4.4.6 % Selenium Leached from Ash Produced in Muffle Furnace at 850 & 950 °C
Figure 4.4.7 % Cadmium Leached from Ash Produced in Muffle Furnace at 850 & 950 °C
Figure 4.4.8 % Barium Leached from Ash Produced in Muffle Furnace at 850 & 950 °C
Figure 4.4.9 % Lead Leached from Ash Produced in Muffle Furnace at 850 & 950 °C

Figure 4.4.10 Beryllium Leached as a Function of System pH
Figure 4.4.11 Vanadium Leached as a Function of System pH
Figure 4.4.12 Chromium Leached as a Function of System pH
Figure 4.4.13 Zinc Leached as a Function of System pH
Figure 4.4.14 Arsenic Leached as a Function of System pH
Figure 4.4.15 Selenium Leached as a Function of System pH
Figure 4.4.16 Cadmium Leached as a Function of System pH
Figure 4.4.17 Mercury Leached as a Function of System pH
Figure 4.4.18 Barium Leached as a Function of System pH
Figure 4.4.19 Lead Leached as a Function of System pH
Figure 4.4.20 % Beryllium Leached from Ash Produced in Hot-Rod at 850 & 950 °C
Figure 4.4.21 % Vanadium Leached from Ash Produced in Hot-Rod at 850 & 950 °C
Figure 4.4.22 % Chromium Leached from Ash Produced in Hot-Rod at 850 & 950 °C
Figure 4.4.23 % Zinc Leached from Ash Produced in Hot-Rod at 850 & 950 °C
Figure 4.4.24 % Arsenic Leached from Ash Produced in Hot-Rod at 850 & 950 °C
Figure 4.4.25 % Selenium Leached from Ash Produced in Hot-Rod at 850 & 950 °C
Figure 4.4.26 % Cadmium Leached from Ash Produced in Hot-Rod at 850 & 950 °C
Figure 4.4.27 % Barium Leached from Ash Produced in Hot-Rod at 850 & 950 °C
Figure 4.4.28 Beryllium Concentration in Muffle Furnace Ash Leachate
Figure 4.4.29 Vanadium Concentration in Muffle Furnace Ash Leachate
Figure 4.4.30 Chromium Concentration in Muffle Furnace Ash Leachate
Figure 4.4.31 Zinc Concentration in Muffle Furnace Ash Leachate
Figure 4.4.32 Arsenic Concentration in Muffle Furnace Ash Leachate
Figure 4.4.33 Selenium Concentration in Muffle Furnace Ash Leachate
Figure 4.4.34 Cadmium Concentration in Muffle Furnace Ash Leachate
Figure 4.4.35 Barium Concentration in Muffle Furnace Ash Leachate
Figure 4.4.36 Lead Concentration in Muffle Furnace Ash Leachate
Figure 4.4.37 Beryllium Concentration in Hot-Rod Furnace Ash Leachate
Figure 4.4.37 Vanadium Concentration in Hot-Rod Furnace Ash Leachate
Figure 4.4.37 Chromium Concentration in Hot-Rod Furnace Ash Leachate
Figure 4.4.37 Zinc Concentration in Hot-Rod Furnace Ash Leachate

Figure 4.4.37 Arsenic Concentration in Hot-Rod Furnace Ash Leachate
Figure 4.4.37 Selenium Concentration in Hot-Rod Furnace Ash Leachate
Figure 4.4.37 Cadmium Concentration in Hot-Rod Furnace Ash Leachate
Figure 4.4.37 Barium Concentration in Hot-Rod Furnace Ash Leachate
Figure 4.4.38 % Beryllium Leached from Chilean Ashes Produced at 900 & 1500 °C
Figure 4.4.39 % Vanadium Leached from Chilean Ashes Produced at 900 & 1500 °C
Figure 4.4.40 % Chromium Leached from Chilean Ashes Produced at 900 & 1500 °C
Figure 4.4.41 % Zinc Leached from Chilean Ashes Produced at 900 & 1500 °C
Figure 4.4.43 % Arsenic Leached from Chilean Ashes Produced at 900 & 1500 °C
Figure 4.4.43 % Selenium from Chilean Ashes Produced at 900 & 1500 °C
Figure 4.4.44 % Cadmium Leached from Chilean Ashes Produced at 900 & 1500 °C
Figure 4.4.45 % Barium Leached from Chilean Ashes Produced at 900 & 1500 °C
Figure 4.4.46 % Lead Leached from Chilean Ashes Produced at 900 & 1500 °C
Figure 4.4.47 % Deviation from Theoretical Value for Kideco-Lemington Fuel Blend
Figure 4.4.48 % Deviation from Theoretical Value for Lemington-Allied Fuel Blend
Figure 4.4.49 Beryllium Concentration in Chilean Ash Leachate
Figure 4.4.50 Vanadium Concentration in Chilean Ash Leachate
Figure 4.4.51 Chromium Concentration in Chilean Ash Leachate
Figure 4.4.52 Zinc Concentration in Chilean Ash Leachate
Figure 4.4.53 Arsenic Concentration in Chilean Ash Leachate
Figure 4.4.54 Selenium Concentration in Chilean Ash Leachate
Figure 4.4.55 Cadmium Concentration in Chilean Ash Leachate
Figure 4.4.56 Barium Concentration in Chilean Ash Leachate
Figure 4.4.57 Lead Concentration in Chilean Ash Leachate

INDEX of TABLES

Table 2.1.1 MSW Generation and Recovery in the USA in 1995

Table 2.1.2 Typical Chemical Analysis and Properties of Selected Biomass Fuels and Energy Crops

Table 2.1.3 Typical Chemical Analysis and Properties of Selected Wood Products and Wastes

Table 2.2.1 Stoker Technologies and their Corresponding Grates

Table 2.2.2 Quantities of Princple Combustion Waste Produced in the USA

Table 2.2.3 Possible Configuration of a Landfill Cover System

Table 2.2.4 Crystalline Compounds Identified in Selected Dry Ash Materials

Table 2.2.5 Analysis of the Main Components in A Selection of Fuels

Table 2.3.1 Trace Element Affinities to Sulphur, Silicon and Iron

Table 2.3.2 Typical Concentration Ranges for Trace Elements in Coal

Table 3.1.1 Fuel Set 1 – Samples Used To Verify Validity of Analytical Techniques

Table 3.1.2 Fuels Supplied by CERCHAR & Ratios of Mixtures Used

Table 3.1.3 Proximate and Ultimate Analysis of Fuels Provided by CERCHAR

Table 3.1.4 Proximate and Ultimate Analysis of Fuels Provided by CERCHAR

Table 3.1.5 Proximate and Ultimate Analysis of Fuels Provided by GENER, Chile

Table 3.2.1 Chemical Composition of Incoloy 800 HT alloy

Table 3.2.2 Hot-rod Reactor Operating Parameters

Table 3.4.1 Instrumental Operating Parameters

Table 3.4.2 Operating Parameters Governing ICP-MS Data Acquisition

Table 3.4.3 ICP-MS Operating Parameters Relating to Data Quality

Table 3.4.4 Isotope Values to Be Used in Instances of "Unequal Isotope" Behaviour

Table 4.1.1 Certified Values of Elements in TCLP Reference Materials

Table 4.1.2. Concentrations Obtained Using TCLP Test and Deviation from Certified Values

Table 4.4.1 Theoretical and Computed System pH for the CERCHAR fuels.

Table 4.4.2 Theoretical and Computed System pH for the Chilean fuels

Table 5.1.1 Trace Element Concentrations in the Raw CERCHAR Fuels With Emphasis on Order of Magnitude

Table 5.1.2 Trace Element Concentrations in the Raw Chilean Fuels With Emphasis on Order of Magnitude

Table 5.2.1 TE Retention Trends when Combustion Temperature Increased in CERCHAR fuels

Table 5.2.2 TE Retention Trends when Combustion Temperature Increased in Chilean fuels

Table 5.2.3 Trace Element Retention Trends when Combustion Method Changed

Table 5.3.1 Trends in TE Leaching with Increasing Temperature in CERCHAR fuels

Table 5.3.2 Trends in TE Leaching with Increasing Temperature in Chilean fuels

Table 5.3.3 Leaching Trends in CERCHAR Fuels as a Function of Combustion Method

Table 5.4.1 Trace Element Occurrence Above Toxicity Limits

ACRONYMS & NOMENCLATURE

ACAA	American Coal Ash Association
BFB	Bubbling Fluidised Bed
CERCHAR	Centre d'Etudes et de Recherches de la Combustion
CFB	Circulating Fluidised Bed
DAF	Dilution Attenuation Factor
daf	Dry Ash Free Basis
DCP	Direct Current Plasma
DF	Dilution Factor
EP-TOX	Extraction Procedure Toxicity Test
EU	European Union
FBC	Fluidised Bed Combustion
FGD	Flue Gas Desulphurisation
HHV	Higher Heating Value
IARC	International Agency for Research on Cancer
ICP-MS	Inductively Coupled Plasma Mass Spectrometry
LOD	Limits of Detection
LOQ	Limits of Quantification
MSW	Municipal Solid Waste
NCB	National Coal Board
PFC	Pulverised Fuel Combustion
RDF	Refuse Derived Fuel
RSD	Relative Standard Deviation
TCLP	Toxicity Characteristic Leaching Procedure
TDF	Tire Derived Fuel
TE	Trace Element
SEM	Scanning Electron Microscope
SI	Saturation Index
US-EPA	United States Environmental Protection Agency

1.0 INTRODUCTION

Large quantities of waste produced from industrial processes and the over-rapid consumption of fossil fuels, have lead to the development of co-combustion technologies. Co-combustion of wastes with fossil fuels not only furthers the renewable energy cause, but also reduces the need to dispose of potentially harmful materials in landfill sites.

Unfortunately once co-combustion occurs, further waste products are created which cannot be similarly used. Currently there are many innovative uses for the ash and other residues of combustion. The use of ash in cement is widely accepted; ash is also used in fields such as agriculture, waste stabilisation and road construction. There is however, more combustion waste than there are avenues for its use. Furthermore only certain qualities of ash may be used for these purposes legally. Currently ashes containing biomass or waste are precluded due to higher quantities of harmful trace elements. Thus the requirement for landfill remains.

Landfill sites are not ideal methods of combustion-waste disposal for several reasons. Landfills have been known to emit noxious gases. Rainwater infiltrating a landfill may cause leaching of harmful species out of the combustion-waste and into the broader environment, unrestrained. This can affect the quality of the groundwater, and the health of both plants and animals. Landfills are also considered unsightly and if inappropriately situated can damage the local ecosystems.

The legacy of landfill use in the past continues to leave its mark on the environment as remediation, after harmful substances have been emitted, is frequently impossible. In the present, sophisticated methods are being devised to mitigate many of the more pernicious problems associated with landfills, such as membrane liners, and groundwater monitoring systems. However the type of landfill to be used is often governed by how developed a region is economically and politically, such that inappropriate landfill construction, and indeed waste dumping, are still used on a global level.

There is therefore a need to understand and assess the leaching processes landfill sites undergo and how this leaching affects the surrounding environment. Groundwater analysis and modelling are often used in order to achieve this, but the first step is the identification and quantification of the harmful substances escaping from the waste. The harmful substances escaping into the leachate of combustion ash are trace elements.

The deleterious effects of excessive trace element levels in the environment vary, depending on the element in question. In the leachate of combustion ash from landfill, the elements which are of most relevance are arsenic, barium, beryllium, cadmium, chromium (particularly in a valency of six), lead, mercury, selenium, vanadium and zinc.

Many factors can affect the degree to which an element is leached from ash. These can be the chemical speciation of the trace element in the solid and the solution, the availability of the element (the fraction of the element ultimately available for leaching), the solubility or sorption tendency of the metal and finally any mass transfer limitations e.g. diffusion rates relevant to the system. These factors are primarily governed by the nature of the ash and the leachate matrix. If the nature of the leachate may be considered a constant (in this case rainwater) than the main variable is the nature of the ash. This is defined by the fuel type, and combustion conditions employed.

The aim of this study is therefore two fold. First, to investigate the retention of the aforementioned trace elements, in a variety of ashes, produced from combustion under certain conditions. Secondly, to investigate the leaching of these trace elements from the ashes produced under those conditions. The effect of three variables on the quantity of trace element in the ash and subsequent leachate were to be investigated, namely: different coals & coal/secondary fuel mixtures, different combustion temperatures and different combustion methods. Thermodynamic equilibrium predictions of both the combustion and leaching process were used to gain a further understanding of the processes involved.

2.0 BACKGROUND

2.1 Biomass & Combustible Waste

The use of biomass is often acknowledged as the oldest method of harnessing energy known to man. Biomass is the oldest form of stored solar energy.[22] Its lower heating value, in comparison to fossil fuels, (typically 10-20 MJ/kg dry as opposed to 35 MJ/kg for anthracitic coal) has seen it become superseded by these fuels. However, the increasing onus to produce sustainable, environmentally cleaner forms of energy, added to technological advances, has once more brought biomass to the fore as an economically feasible fuel in the industrial world. It is currently providing approximately 14% of the world's primary energy supply, whilst in developing countries it may be as high as 95%.[2]

Biomass is essentially composed of three main components, cellulose, hemicellulose and lignin. The proportions of these constituents vary with biomass type. Figure 2.1.1 depicts an SEM image for cellulose and its chemical structure, where n is the number of structural units.

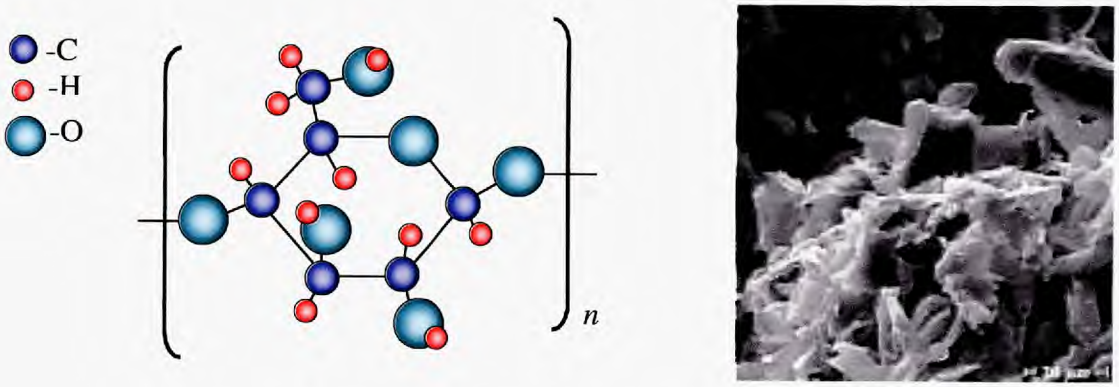


Figure 2.1.1 Structural Unit and SEM image for Cellulose

Biomass may be defined as carbonaceous material derived from plants or animals. For fuel categorisation purposes, the three primary groups maybe be defined energy crops, waste products, which would otherwise need to be disposed of, and organic derivatives such as paper.

Any plant matter may fall within the first category, however dedicated energy crops are often cultivated which exhibit superior properties as fuels, for example Sorghum or Miscanthus[3]. Subcategories of energy crops may be defined as herbaceous (e.g. grasses, stalks and straw), aquatic (e.g. kelp, reed or algae) or woody (e.g. hardwood or softwood).

Waste products may be subcategorised into various groups. Some biomass waste is included in municipal solid waste (MSW). MSW encompasses a broad range of wastes, some of which are non-organic. It is an important category from the perspective of a potential fuel and may be defined as wastes obtained from residential, commercial and industrial processes. This waste is either combusted, or land-filled and its energy content is typically 10.5 to 11.5 MJ/kg. Table 2.1.1 denotes the various products which may be referred to as MSW, the quantities generated in the United States and the amount recovered as energy.

Material	**Generated** (mt)	**Recovered** (mt)	**Landfilled** (mt)
Paper	70.5	24.0	46.6
Yard Trimmings	29.8	5.9	23.9
Plastics	17.5	0.6	16.9
Metals	15.5	4.7	10.8
Food	12.5	0	12.5
Glass	12.4	2.7	9.7
Wood	12.4	1.2	11.2
Rubber / Leather	5.6	0.4	5.4
Textiles	5.5	0.6	4.9
Misc. Organic	2.8	0	2.8
Other	3.0	0.6	2.4
Total	187.5	40.7	147.1

Table 2.1.1 MSW Generation and Recovery in the USA in 1995[4]

In the above group, plastics have the highest energy content at 30-44 MJ/kg[4], but are some of the most problematic wastes. Synthetic polymers do not readily degrade, and often generate environmentally hazardous materials such as chloride, phenyl and dioxins[5].

Pulp and paper manufacturing is one of the most pollution intensive and energy consuming industries[6]. The large quantity of sludge produced is a significant environmental problem. As with plastics, this sludge has traditionally been land-filled but its high content of process chemicals and other contaminants has promoted its use as a bio-fuel.

Another significant source is biomass waste is the agricultural industry. The most common agricultural residue is rice husk, which makes up 25% of rice by mass. Other residues include poultry and other animal litter, residue from the olive oil industry, molasses from beat sugar and bagasse, a sugar cane fibre.

Table 2.1.2 shows the chemical analysis for selected biomass fuels and energy crops. Table 2.1.3 denotes the analysis for various wood products and wastes. Comparisons are made with bituminous coal. All values are weight percentages unless otherwise specified. The higher heating value (HHV) of a sample may either be measured or estimated using the following relation[7]:

$$HHV(kJ/kg) = 35{,}150C + 116{,}225H - 11{,}090O + 6280N + 10{,}465S \qquad (1)$$

Where C, H, O, N and S are the elemental mass fractions in the coal. This heating value may be stated on a dry ash free basis or on an as received basis

Fuel Type	Coal [3]	Corn Stover[8]	Cotton Gin[9]	Rice Husk[10]	Olive Husk[11]	Corn Cobs[8]	Poplar [12]	Eucal-yptus[12]
Moisture	10.8	35.0	11.5	9.9	33.0	15.0	-	
Ash	5.7	3.3	14.5	20.6	1.6	1.4	1.3	0.5
Volatiles	30.7	54.6	-	54.7	-	76.6	-	-
Fixed C	52.8	7.2	-	15.0	-	7.0	16.4	16.9
C	54.9	42.5	42.0	34.9	47.8	48.4	48.5	48.3
H	4.3	5.0	5.4	5.5	5.1	5.6	5.9	5.9
O	23.3	42.6	35.0	38.9	45.4	44.3	43.7	45.1
N	0.8	0.8	1.4	0.11	0.1	0.3	0.5	0.2
S	0.3	0.2	0.5	-	-	-	0.01	0.01
HHV (MJ/kg)	25.5	10.7	15.50	13.5	18.0	15.5	19.4	19.4

Table 2.1.2 Typical Chemical Analysis and Properties of Selected Biomass Fuels and Energy Crops

Fuel Type	Coal[3]	Peat[13]	Sawdust[1] [4]	Switch grass[15]	Red wood[9]	MSW[16]	Tyres[17]	Manure[17]
Moisture	10.8	28.0	7.3	12.0	-	16-38	0.5	36.6
Ash	5.7	2.2	2.6	4.6	0.4	11-20	6.1	25.3
Volatiles	30.7	-	76.2	-	-	67-78	65.2	31.6
Fixed C	52.8	-	13.9	-	19.9	6-12	28.7	6.6
C	54.9	53.3	46.9	42.0	50.6	-	81.5	19.2
H	4.3	5.9	5.2	4.9	5.9	-	7.1	2.2
O	23.3	36.7	37.8	35.4	42.8	-	3.4	14.7
N	0.8	1.7	0.1	0.8	0.05	-	0.5	1.5
S	0.3	0.2	0.04	0.2	0.03	-	1.4	0.5
HHV (MJ/Kg)	25.5	15.30	18.1	15.9	20.7	15.9	36.8	7.9

Table 2.1.3 Typical Chemical Analysis and Properties of Selected Wood Products and Wastes

The data above illustrates the broad range of properties exhibited by various types of biomass. The figures illustrate well that it is not possible to categorise biomass, given the type of feedstock e.g. wood, waste etc., which would be necessary when determining combustion characteristics. Methods in which biomass may be categorised in order to predict combustion characteristics are given in Section 2.2.2.1. The data also illustrate the high moisture content of most biomass sources in comparison to coal.

The ash content of biomass may be classified as intrinsic or extrinsic. Intrinsic ash is contained in the matrix of the biomass, whereas extrinsic ash comes from the biomass collection process. The ash contents of woody biomasses are much lower than for coal. However, the ash content of non-woody biomass fuels can vary widely. Most of the ash in high ash biomass is extrinsic in nature, consisting of primarily SiO_2.

The heating value is generally proportional to the combustibles content in the fuel.[18] It is also a function of the ultimate analysis of the combustibles fraction. The heating value on an ash free basis increases with carbon and hydrogen content. Figure 2.1.2 is a graphical representation of the combustibles content in various bio-fuels, in decreasing order, and also depicts the moisture and ash content. The two ends of the combustibles spectrum are represented by sewage sludge, with the highest moisture content and tyre derived fuel (TDF) with the lowest. Consequently TDF has the highest heating value, even higher than that of bituminous coal.

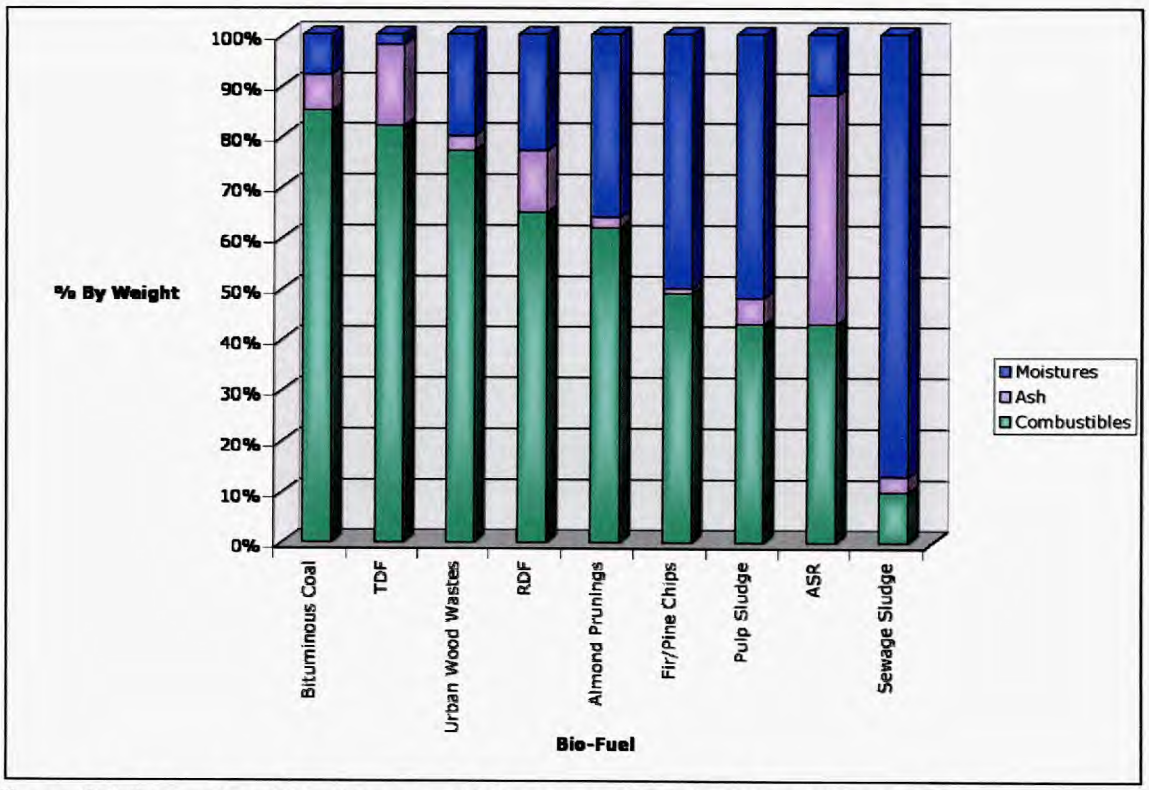


Figure 2.1.2 Combustibles Content, Moisture and Ash in Selected Bio Fuels

2.1.1 Impetus For Biomass Use

2.1.1.1 Greenhouse Gas Reduction

Both the 1992 Rio Earth Summit and the legally-binding Kyoto Protocol set targets to reduce CO_2 emissions. The EU agreed to an 8% reduction in anthropogenic CO_2 equivalent emissions by the period 2008-2012. When performing a life-cycle analysis of biomass combustion it may be considered CO_2 neutral, due to the intake of CO_2 in the biomass production phase[2]. Typically, fossil CO_2 equivalent emissions are reduced by 1 tonne for each tonne of biomass co-fired. This value increases to 3 tonnes of fossil CO_2 reduction if the biomass would have ordinarily been disposed of in an un-flared landfill site. [1] This is due to the fact that CH_4 produced in landfill is considered to be 21 times more potent then CO_2 in terms of global warming impact.[19] Therefore partially substituting fossil fuels with biomass which would ordinarily be landfilled greatly contributes to the overall reduction of greenhouse gases.

2.1.1.2 Reduction of Regional and Local Atmospheric Pollutants

The combustion of fossil fuels results in the production of significant quantities of nitrogen and sulphur oxides (NO_x and SO_x) which are linked to the formation of acid rain and ozone layer depletion. Many biomass fuels contain only a nominal quantity of bound nitrogen on a mass basis in comparison with coal (although nitrogen in straw for example can be higher than coal[20]). The nitrogen associated with biomass is released as NH radicals (primarily ammonia, NH_3) during the combustion process. The ammonia then reduces NO to molecular nitrogen, effectively acting as an in situ de-NO_x source. Therefore the combustion of biomass actively reduces NO_x emissions, although the extent to which this is effected is bio-fuel dependant.[21]

Sulphur oxide emissions are directly proportional to the sulphur content in the fuel. Most biomass fuels have a negligible quantity of sulphur and thus SO_x emissions are directly reduced. This attribute is particularly useful when co-firing with high sulphur coals. Desulphurisation may also be achieved in some cases due to SO_2 capture by the alkaline biomass ash. [21]

Other pollutants associated with the landfill of biomass, due to anaerobic digestion, are NH_3, amides, volatile organic acids, mercaptans, esters and other chemicals. Their production is also mitigated by the co-combustion of the biomass.

2.1.1.3 Sustainable Development

When biomass fuel is obtained as an energy crop (e.g. switchgrass, poplar or willow) there is a significant impact on agriculture and the local environment. Energy crops do not require the use of artificial fertilisers, pesticides or herbicides and are therefore "greener" than alternative crops such as cereal. When annual cereal crops are replaced with perennial energy crops, the level of cultivation is reduced. This results in a stable habitat and the ensuing encouragement of biodiversity. Land which is ordinarily inhospitable to the cultivation of cereal crops, such as derelict land, is often an ideal host for energy crops[22]. Indeed, studies show that no less than 29% of the world's land surface suffers moderate desertification and a further 6% is extremely desertified. In many simple bio-energy schemes, MSW-derived compost has been used to cultivate energy crops on land threatened by desertification.

2.1.1.4 Fossil Fuel Preservation and Fuel Diversification

The quantity of global fossil fuel reserves are a matter of debate although they are expected to last for several centuries yet.[23] Nevertheless, it is not debatable from an ecological perspective, that it would be advantageous to retard the depletion rate of fossil fuels.

For countries whose fossil fuel reserves are low, fuel diversification is an important strategic goal. Developing co-combustion technologies is also important for countries heavily dependant on fossil fuels, as heightened environmental concern and resource depletion drive fossil fuel costs upwards.[24]

The principle drivers for co-combustion of biomass with fossil fuels are described in the Section 2.2.3 describing co-firing.

2.2 Co-Firing Of Coal, Biomass & Wastes

2.2.1 Combustion of Coal

Before describing the basic combustion mechanisms of biomass, those of coal are first defined. Figure 2.2.1 is a schematic representation of the main combustion reactions which may be categorised as being heterogeneous or homogeneous.

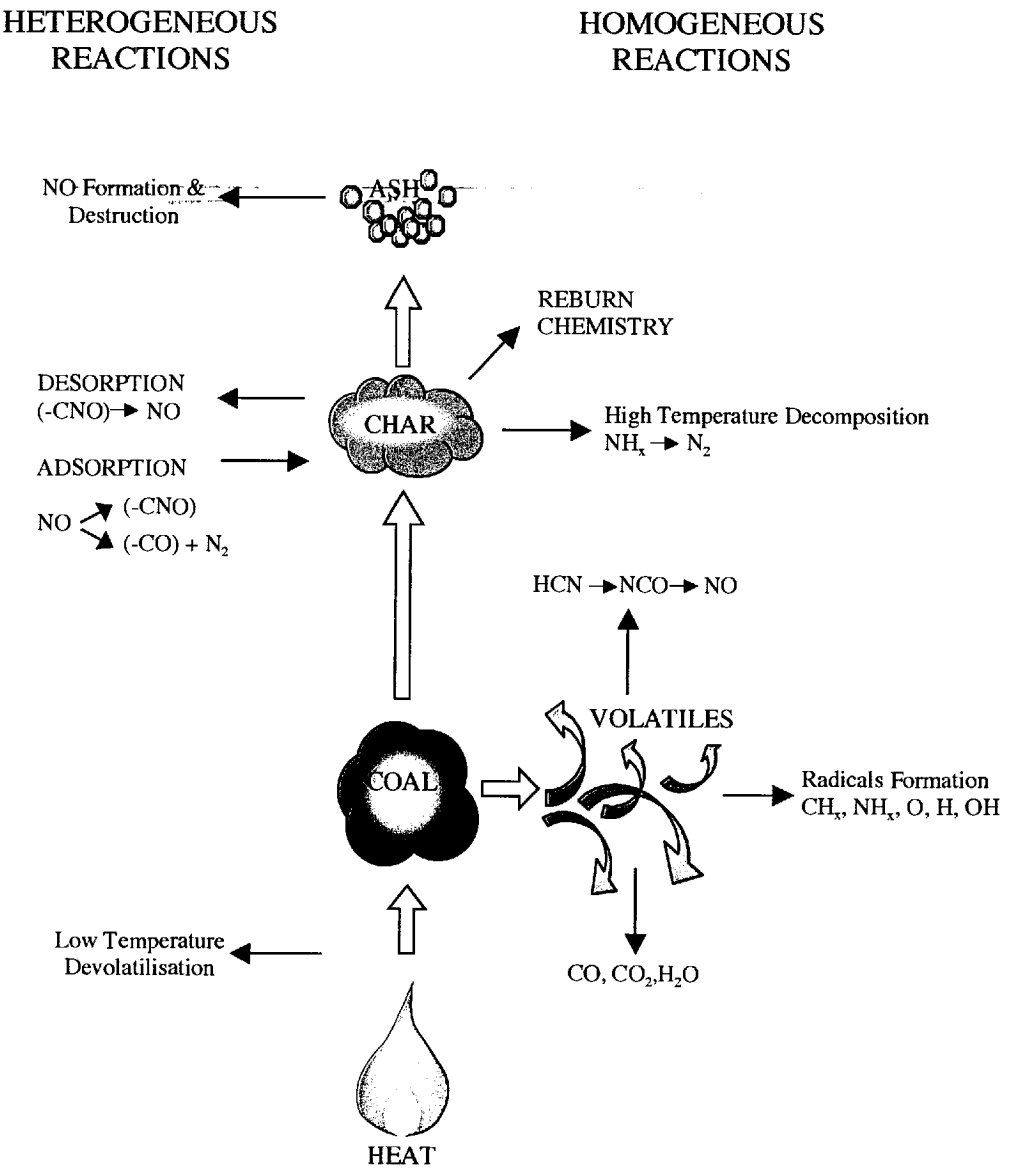


Figure 2.2.1 Major Steps in Coal Combustion and NO_x Reaction Pathways[27]

When a coal particle is heated devolatilisation occurs. Pyrolysis time scales in commercial combustion are of the order of 10-100 ms for particle diameters of 1mm. The temperature at which pyrolysis occurs is a function of fuel type and heating rate, typically for bituminous coal 450°C at heating rates <100°Cs^{-1} for bituminous coal[28]. At higher heating rates (>10,000°Cs^{-1}) pyrolysis is presumed to start at much higher temperatures. The heating rate is an important parameter as it determines the nature of the devolatilisation products and char. The products of this pyrolysis range from lighter volatiles (CH_4, C_2H_2, CO, CO_2, NH_3, H_2O etc) to heavy tars. Volatiles have been found to issue as jets from particles 80-100 μm in diameter.[29] Once the volatiles are released they undergo oxidation surrounding the particle. The temperature of the gas phase during this combustion step is much higher than that of the particle.[30] At this point a flame envelops the particle preventing heterogeneous oxidation of the char.

After pyrolysis char remains. The carbon undergoes heterogeneous reactions with the gaseous species which are principally governed by the following processes[31]:

- diffusion of gas phase oxidising reactant species to the particle surface
- adsorption of gas phase species (E=32,000 kJ/kmol)
- chemical reaction of the adsorbed species
- desorption of solid oxides (E=170,000 kJ/kmol)
- diffusion of gas phase products through the boundary layer to the bulk gas.

Oxygen transfer to the char can occur via O_2, CO_2, or H_2O and the heterogeneous combustion can occur via one of the following reactions:

$$C + {}^1/_2O_2 \rightarrow CO \qquad \text{(I)}$$

$$C + O_2 \rightarrow CO_2 \qquad \text{(II)}$$

$$C + CO_2 \rightarrow 2CO \qquad \text{(III)}$$

$$C + H_2O \rightarrow CO + H_2 \qquad \text{(IV)}$$

Once CO and H_2 are released via heterogeneous reactions (III) and (IV) they undergo oxidation in the gas phase.

Particle ignition occurs if the rate of heat release due to chemical reaction is higher than the rate of heat loss due to convection, radiation etc. Whether ignition of an isolated coal particle occurs heterogeneously or homogeneously depends on volatile matter, flammability of the volatiles and transport from the particle. If the volatiles burn early in the combustion sequence, they may remove oxygen from the internal pore surface area, thus preventing heterogeneous ignition. If coal is ignited homogeneously, the volatiles burn in the gas phase preventing oxygen from reaching the particle surface. If combustion is not complete or if volatile liberation occurs as jets, or intermittently from the pores, the oxygen can still reach the particle surface. In this instance, heterogeneous combustion of fixed carbon and combustion of in situ volatile matter can proceed in parallel with gas phase combustion.

2.2.2 Combustion of Biomass

The combustion of biomass may also be described in general terms as a two step process:

- devolatilisation to char and volatiles
- combustion of char and volatiles

However due to the high moisture content of biomass, a separate preliminary step is required to describe the drying phase. This step often dominates the combustion process. The devolatilisation of wood for example may be defined in five stages:[32]

1. Moisture and some volatile loss.
2. Breakdown of hemicellulose and emission of CO and CO_2.
3. Exothermic reaction causing the wood temperature to rise from 250 to 360 °C with emission of methane and ethane.
4. External energy input to continue the process.
5. Complete dissociation of the matter.

The ignition process of biomass is similar to that for coal although more volatile matter is available for reaction, therefore homogeneous ignition is more likely to occur in biomass fuels. Due to their more variable properties, bio-fuels exhibit a broader range of ignition temperatures for a given particle size than coal. Studies carried out on biomass char combustion[33] show that large amounts of oxygen and hydrogen are lost early on in the conversion, indicating volatile release. The lack of a visible flame suggests the these volatiles are primarily CO, CO_2 and H_2O as opposed to hydrocarbon gases. Unlike high-rank coals, oxygen levels remain almost an order of magnitude higher in biomass char. It has been shown that nitrogen is preferentially retained compared to carbon in pine and switchgrass chars.

When comparing pyrolysis, ignition and combustion of coal and biomass the following is generally true:

- pyrolysis starts earlier for biomass fuels compared to coal fuels
- volatile matter in biomass is higher than that of coal-often in excess of 90%.
- the heating value of volatiles (kJ/kg) in biomass fuels is lower than in coal
- the fractional heat contribution by volatile combustion in biomass is of the order of 70% compared to 36 % for coal
- biomass char contains more oxygen than coal (some coals can contain up to 20% oxygen, lignites more so)
- pyrolysis of biomass chars mostly releases CO, CO_2, and H_2O
- biomass fuels have ash that is more alkaline in nature, which aggravates fouling problems by forming low temperature melts
- the high SiO_2 content of biomass fuels e.g. straw can cause abrasion problems

2.2.2.1 Biomass Characterisation

Properties important for combustion purposes, such as tar yield, volatile composition and char yield and composition, vary greatly with biomass type. These need to be defined when designing co-combustion plants or adapting coal fired plants to co-combustion.

Instead of measuring relevant properties for each biomass feedstock, attempts have been made to find correlations in order to predict combustion behaviour. One such system is based on using a Van Krevelen Diagram[34]. Each biomass feedstock is plotted on a graph of H/C ratio versus O/C ratio. Biomass feedstocks which fall within the same clusters on this diagram will exhibit similar combustion properties irrespective of their biomass category (wood, waste etc.).

2.2.3 Co-firing of Biomass &Wastes with Coal

3.2.3.1 Objectives of Co-firing

Co-firing, the practice of substituting a portion of a base fuel with an alternative fuel, is being developed as a viable technology in order to achieve the following objectives[35], as elaborated upon in Section 2.1.2:

- Reducing greenhouse gas emissions
- Reducing atmospheric pollutants such as NO_x and SO_x
- Reducing fossil fuel depletion rates
- Reducing harmful impact of agriculture via the use of energy crops
- Sustainable waste management
- Fuel diversity – seasonally arising waste such as straw
- Stabilise combustion with fossil fuel foundation – co-combustion normally 70% coal and less than 30 % biomass.
- Improved economics – the capital costs of co-firing are less than those associated with single fuel biomass projects or indeed other renewable projects such as wind or hydro derived energy.[24]

3.2.3.2 Co-Firing Technologies

The relative profitability of the electricity generation industry, particularly that based on pulverised fuel technology has, historically, negated the need for co-combustion. Pulverised fuel furnaces are tailor made to suit the characteristics of a particular fuel and as such cannot readily handle the variety of fuel characteristics exhibited by the biofuels and wastes available. Thus the impetus to incorporate a degree of co-firing is recent, with the drivers being the reduction of CO_2 emissions and the declining profitability of running fossil fuels alone.

There are a number of co-firing options available. Co-firing may be achieved by. blending the biomass with coal prior to combustion. This is the simplest and least expensive approach to co-firing. However, the proportion of biomass which may be added to the fuel blend is limited, as are the types of biomass which may be used.

Another method is separate injection of the fuels into the boiler. In this instance more equipment is required than when blending the biomass directly with the coal but a higher percentage of biomass may be co-fired. In the case of separate injection, particle size is an important parameter. The kinetics of biomass combustion are faster than those of coal combustion[36] meaning particles up to 6mm may be combusted and, in the case of straws and switch grass, particle lengths, of up to 50 mm.

Remote biomass gasification may also be used as a co-firing technique. This is the most capital intensive approach but addresses many of the challenges associated with the above two techniques. For example gasification-based co-firing enables complete biomass consumption at a short residence time, the separation of biomass ash from coal ash. It is the most flexible with regard to the base fuel i.e. coal, oil or natural gas.

From a co-combustion perspective the technology options are as follows:

- fluidised bed combustion
- pulverised fuel combustion
- grate combustion
- cyclone combustion

A brief overview of each technology is given below.

2.2.3.3 Fluidised Bed Combustion

Fluidised bed combustion (FBC) is a versatile combustion technology, offering the capability to combust low grade fuels and fuels with a wide variety of chemical compositions and physical properties. The ability to cope with low grade fuels is attributable to the significant thermal inertia caused by the high combustor bed inventory of inert material, normally greater than 90% by weight. This enables combustion conditions to be optimised even for fuels with quite variable properties so that combustion conditions are stabilised and emissions minimised. Fluidised bed combustors are currently operated commercially using many wastes such as municipal sludge, waste paper and sludges from paper mills, as well as many agriculture based fuels such as wood bark, energy crops and straw. Fluidised bed combustion takes place at the comparatively low temperatures of approximately 850°C in a suspended bed of inert material. This temperature is chosen in order to avoid ash softening and fusion problems and to limit the generation of NO_x gases.

Sulphur capture is also optimised with a low bed combustion temperature. The SO_2 reduction is achieved due to the lower sulphur content of the substituted fuel and studies have shown that as such the reduction is proportional. However in many trials a higher than expected SO_2 reduction has been noted. This is due to the high alkali content in the bio-fuel and ash. FBC sulphur emissions are controlled by the addition of a sorbent, such as limestone or dolomite, to the bed. In some combustion operations, for example

those using sludge from paper and de-inking plants, the SO_2 reduction has been so significant that no added sorbent was required to meet emission regulations. Some FBC operations rely solely on the natural sorbent activity of the ash for SO_2 reduction.

There are two major types of fluidised bed combustor, namely the circulating fluidised bed (CFB) reactor and the bubbling fluidised bed (BFB) reactor. The primary differences are associated with the physics and fluid dynamics governing the two technologies. In the CFB the bed inventory and the fuel are continuously circulated via cyclones, such that combustion may take place in dilute phase throughout the combustor. In BFB, the bed inventory, is suspended immediately above a distributor plate, and eventually exits at the base of the combustor. The combustion in this instance takes place in or at the top of the bed, with volatile matter burning above in the freeboard. CFB operations have a higher fluidising velocity than BFB (5-8ms^{-1} as opposed to 1ms^{-1}). This leads to smaller combustor sizes as well as more efficient distribution of the fuel within the bed. There fore costs are minimised and combustion, and combustion control, improved. The ash produced from co-firing fuels in a BFB reactor are more likely to give rise to problems such as bed agglomeration fouling and slagging than when using a CFB reactor. All of these factors make the CFB configuration preferable to BFB.

2.2.3.4 Pulverised Fuel Combustion

Pulverised fuel combustion (PFC) is the established technology in the industrialised world, FBC technology being a relatively recent addition. PFC is an important technology for operations where fuel cost is significant, due to its higher efficiencies when compared to FBC or stoker firing techniques. To achieve these efficiencies, PFC systems require detailed definition of the combustion and thermodynamic processes taking place and therefore a detailed knowledge of the properties of the fuel to be burned. The main properties of interest when coal is the fuel are grindability, volatile matter, moisture content, ash content and ash softening temperatures. Fuel must be ground to 75-80% through BSS mesh sieve (74μ) for low volatiles matter or 65% bituminous coal.

Biomass produces a higher volatile fraction and more reactive char compared to coal. This higher volatile content promotes higher rates of ignition than when coal is burned alone. The volatile content of fuel in PFC systems is recommended to be above 15% (dry basis) and biomass and waste fuels easily meet these criteria. Conversely, the moisture content on an-as fired basis should not exceed 15%. Therefore, given the moisture content of many bio-fuels, in co-firing projects there is a maximum amount of biomass which may be added to the base fuel for this moisture content not to be exceeded (unless the fuel is pre-dried). Exceeding the 15% limit for the fuel mixture is likely to hamper flame stability and plant operation. The ash content in most bio-fuels in not significant enough to be of concern, but would need to be taken into consideration if it exceeded that of the base fuel. The ash softening temperature however is an important parameter as the constituents in biomass ash, such as potassium and other alkalis, contribute to the formation of eutectics. These in turn cause boiler fouling and slagging.

If supplementary fuels are to be used with coal, their particle size must be such that compatible combustion characteristics are obtained between the two fuels. The particle size of the bio-fuel must also complement that of the principle fuel in order to avoid blocking and settling in the pneumatic feeding systems. A small particle size favours high char reactivity as it facilitates the rapid removal of volatiles from the particle. The effect of particle size on combustion efficiency is fuel dependant as is the proportion of alternative fuel which may be co-fired with coal.

Co-combustion trials have shown that NO_x emissions in PFC installations are not only dependent on the initial nitrogen content in the fuel and the co-firing ratio, but also on the fuel injection mode (central or annular) as well as the primary and re-burn stoichiometry and flame injection. SO_2 emissions have been shown to be directly proportional to the sulphur in the original fuel.

Fuel supply logistics should also be considered in PFC. UK power stations based on 2000 MW, would require 2 million tonnes of coal per year. Supplying 1% of this coal inventory in biomass would require a significant catchment area.

2.2.3.5 Grate Combustion

Grate combustion of solid fuel predates PFC and is now limited to relatively small (a few tens at most) industrialised boilers. Grate combustor systems operate on the principle that the solid, non-volatile portion of the fuel is mixed with air and burnt on the grate itself. The stoker types may be overfeed or underfeed depending on whether the fuel is fed over or under the grate. Overfeed stokers may then be defined as spreader stokers or mass stokers. Table 2.2.1 shows the types of grate combustor configurations possible with the different stoker technologies. Grates are less flexible than fluidised beds with regard to fuel quality and are less suited to variable fuel mixtures.

Stoker Technology	Grate Type Used
Overfeed Spreader Stoker	Travelling
	Vibrating
	Stationary
Overfeed Mass Stoker	Travelling
	Vibrating
	Reciprocating
Underfeed Mass Stoker	Single retort
	Multiple retort

Table 2.2.1 Stoker Technologies and their Corresponding Grates

Various co-combustion trials have been undertaken in order to investigate whether alternative fuels may be co-fired economically. Tests have revealed that olive stones and wood chips may be mixed on coal conveyers and burned with a blend ratio of up to 20% bio-fuel (based on heat value), with little or no plant modifications and few problems.[30] Other tests using sawmill dust were found to be unviable due to the low volumetric heat value of the dust which required the handling of volumes in excess of the feeder capacity. Emissions of NO_x and SO_x were found to be fuel dependent.

2.2.3.6 Cyclone Combustion

Cyclone combustors were initially developed in order to overcome challenges with low grade coals and lignites containing ash of low softening and fusion temperatures. Cyclone furnace combustion provides the benefits of pf combustion plus reduction is fly ash quantities. Savings are also made due to the need for less costly particle size reduction equipment and a reduction of furnace size and cost for a given heat output.

A cyclone combustor is a water cooled cylinder lined internally with refractory material. A tangential inlet flow configuration for combustion air and fuel creates a stable vortex in the combustor which retains the crushed coal, about 95% passing a mesh screen, within the combustor until the combustion is complete. The high heat release rates and combustor gas temperatures in excess of 1600 °C are sufficient to melt the coal ash, which forms a liquid layer on the combustor walls, and which is removied from the combustor as a liquid by gravity. The reduced need for fuel preparation and the desirability of having low melting temperature ash make cyclone combustors particularly suitable for co-firing biomass/waste with coal.

2.2.3.7 Fouling and Corrosion in Co-Combustion

Fouling of combustor surfaces is a major issue in the design and operation of all of the above combustion technologies. Slagging and fouling reduces heat transfer and causes corrosion and erosion problems, reducing not only performance but life time of the apparatus. The main contributions to fouling come from the inorganic material in the fuel. The behaviour of these inorganics is less well understood than that of organic materials. Biomass fuels generally contain inorganic constituents radically different to that in coal. Thus issues of fouling, corrosion and pollutant emissions are important either when retrofitting an existing plant for bio-fuel use, or in new build operations. The bio-fuels of particular concern are certain agricultural residues and new woody materials which have a high alkaline metal content (especially sodium and potassium) which lower the melting point of the ash.[30] In studies relating to ash deposition and corrosion during

co-firing, Baxter[32] concluded that ash deposition from bio-fuels as opposed to coal would be higher, with smoother deposit surfaces and low deposit porosity. Thus deposits from biomass combustion are not only more prolific but are more difficult to remove. In fluidised bed combustion high reactivity alkali metals have the tendency to react with the inert bed material, forming sticky coatings on the surface of the bed particles. This enhances the tendency for the bed particles to form larger clusters, causing subsequent agglomeration and defluidisation of the bed.

2.2.3.8 Waste Production in Co-combustion

The characteristics of biomass and its co-firing have been thus far described. The next step, therefore, is a discussion of the issues relating to waste production and handling in co-combustion, and specifically of ash. Waste produced in coal combustion processes may be high volume or low volume. High volume wastes include:

- fly ash – the uncombusted material carried out of the boiler along with the flue gases.
- bottom ash – uncombusted material that does not melt and settles to the bottom of the boiler.
- boiler slag – uncombusted material that settles to the bottom of the boiler. Slag is formed when the operating temperatures exceed ash fusion temperatures and remains in a molten state until it is drained from the bottom of the boiler.
- flue gas desulphurisation waste – waste produced during the process of removing sulphur oxide gases from the flue gases.

Low volume wastes are produced as a result of ancillary processes. Amongst others these include:

- coal pile run-off – run off and drainage produced by precipitation falling on coal storage areas
- coal mill rejects/pyrites – waste produced by onsite processing of coal prior to use.
- boiler blow down – waste removed from boilers that recirculate water to maintain water quality
- cooling tower blowdown and sludge – wastes removed from recirculating cooling tower systems to maintain water quality
- water treatment sludge – wastes resulting from treatment for makeup water for the steam cycle or for non-contact cooling.
- air heater and precipitator wash water – wastes resulting from the periodic cleaning of the fireside of heat exchanging surfaces (i.e. the side exposed to hot combustion products).

Table 2.2.2 below indicates the quantity of each large volume waste generated in 1998 in the United States. The total quantity generated has increased steadily over the last decade. Globally, annual production of ash, from coal combustion alone, is thought to exceed 600 million tonnes[38]

Waste Type	Quantity Generated (mTonnes)	Quantity Generated (%)
Fly Ash	60.2	57
Bottom Ash	16.9	16
Boiler Slag	2.7	3
FGD Waste	25.2	24
Total	105.1	100

Table 2.2.2 Quantities of Princple Combustion Waste Produced in the USA (1998)[37]

The proportion of these wastes is dependant upon the combustion technology used. Figure 2.2.2 below show how ash production varies with combustion technologies PF, grate combustion and cyclone combustion.

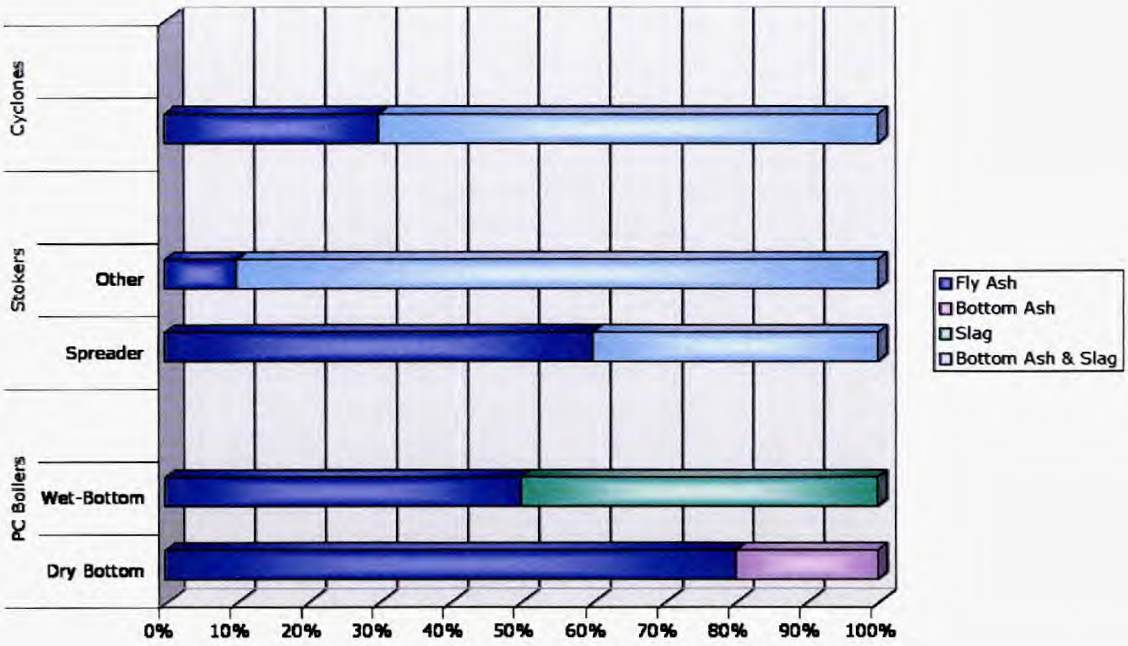


Figure 2.2.2 Typical Waste Production Variation With Varying Combustor Configurations

2.2.3.9 Beneficial Uses of Combustion Waste

In order to mitigate harmful environmental and economic effects of disposing the wastes described above, many innovative methods have been devised for their utilisation. These are described below.

Concrete and Cement Applications – This is the most common method for ash utilisation. When used alone, PFC fly ash imparts improved flow characteristics to fresh concrete due to its spherical shape and fineness. Additionally, the pozzolanic properties of fly ash increase the comprehensive strength and durability of the final concrete product. (A "pozzolan" is defined as "a siliceous or siliceous and aluminous material which in itself possesses little or no cementing property, but will in a finely divided form and in the presence of moisture chemically react with calcium hydroxide at ordinary temperatures to form compounds possessing cementitious properties")[39].

Construction Fills – Construction fills include structural fills, road base and sub-base applications. Most of the bottom ash and a considerable portion of PFC fly ash utilised are applied in construction fills. This is the second most common method of utilisation after the production of cement and concrete products. In structural fills fly ash and bottom ash replace natural materials and provide additional benefits not obtained from conventional fill materials, such as low compressibility, light unity weight, high shear strength and pozzolanic properties. In road bases and sub-bases the addition of ash allows for greater long term strength development.

Waste Stabilization/Solidification – Due to their high alkalinity solid combustion wastes may be used to chemically fix potentially hazardous wastes in a solid matrix. Through stabilisation, hazardous organic and inorganic constituents are immobilised and prevented from being released to the environment. Stabilisation may occur with or without solidification. Solidification consists of converting soils, liquids and sludges into a solid, structurally sound material prior to further utilisation. This method of ash utilisation is the third most common use for combustion waste.

Blasting Grit / Roofing Granules – More than 2 million tonnes of high volume combustion waste, primarily boiler slag was used as blasting grit and roofing granules in 1999.[100(2)]

Mining Applications – Mining application include controlling acid mining drainage, backfilling, blending mine soils and revegetation. Ash is used in remediation activities at coal mines because of its ability to neutralise the effects of acid drainage from mines and associated wastes.

Mineral Fillers – Mineral fillers include a variety of fine particles that are incorporated into a broad range of industrial products. Combustion waste has been used as substitutes for commercial fillers in asphalt products, plastics, metal alloys and fertilisers.

The uses receiving the most attention are fly ash and boiler slag in asphalt and plastics. Fly ash has also been proposed as a mineral filler in carpet backing, vinyl flooring, industrial coatings and paints and insecticides and pesticides.

Snow and Ice Control – Approximately one million tonnes of bottom ash and boiler slag were used in 1998 as a substitute for salt for road de-icing operations.

Agriculture – Fly ash, bottom ash and FGD sludge are used for agricultural soil amendment. In general, these wastes can benefit agricultural systems by changing physical and chemical characteristics of soils, thus improving crop yield. They affect the chemical properties of soils by supplying essential plant nutrients for crop production, modifying soil pH, and alleviating trace element deficiencies. Other benefits include modifying the soil physically in order to create a more favourable medium for plant growth for example reducing bulk density, increasing aeration, water filtration and drought tolerance. Biomass ashes rich in potassium are particularly beneficial for agricultural use.

2.2.3.10 Ash Disposal Methods

Waste management units common at coal combustion facilities include landfills and surface impoundments.

Surface Impoundments

Surface impoundments are natural depressions, excavated pounds, or diked basins that typically contain a mixture of liquids and solids. Ash managed in surface impoundments is typically sluiced with water from the point of generation to the impoundment. The ash gradually settles out of this slurry, accumulating at the bottom of the impoundment. This process leaves a standing layer of relatively clear water at the surface termed head. The distance between the surface of the head and the top edge of the impoundment is known as freeboard and indicates the remaining capacity of the impoundment.

The amount of freeboard in an impoundment may fluctuate as wastes are added, rainfall accumulates and liquids are removed for discharge to surface water or re-circulated to sluicing operations. Solids that accumulate at the bottom a surface impoundment may be left in place as a method of disposal. The impoundment may also be periodically dewatered and the solids removed for disposal in another unit such as landfill.

Landfill

Landfills are facilities in which wastes are placed for disposal on land. Landfills usually are constructed in cells. Wastes are places in the active cell and compacted until the predetermined cell area is filled. Completed cells are sometimes covered with soil or other material, and then the next cell is opened. Cells may be constructed on top of a layer of previously completed cells, called a lift. Landfills are usually natural depressions or excavations that are gradually filled with waste, although construction of lifts may continue to a level well about the natural grade. Ash managed in landfills may be transported dry from the point of generation, or may be placed after dredging from a surface impoundment. Some residual liquids may be placed along with the dredged solids.

Landfills were traditionally designed on the basis that the surrounding soil and groundwater have the ability to dilute, disperse or attenuate any leachate formed. Thus landfills were often deliberately sited in high permeability strata such as sandstone since the effect of mixing the leachate with a large volume of groundwater was thought to be sufficient to reduce the concentration of any pollutants to a safe level. The realisation that landfilling of wastes can pollute the surrounding groundwater has resulted in considerably greater emphasis being placed on controlling the outflow of polluting leachate from landfill sites. The USEPA has estimated that over 75% of landfills in the USA by 1995 have caused groundwater pollution.[40]

Environmental Control Technologies in Landfills and Surface Impoundments

Environmental controls are an essential part of landfill and impoundment design design and the common environmental control technologies used are briefly described below:

- Liners – Liners are barriers placed underneath a landfill or on the bottom or sides of surface impoundments. Depending on their construction, liners can slow or prevent the release of leachate from a landfill or liquids from a surface impoundment to underlying soils and ground water. Liners can consist of compacted soil, compacted clay, a synthetic material or membrane or a combination of barrier types. The current trend in the United Kingdom is to required that compacted soil liners be one meter in thickness, with a maximum hydraulic conductivity of 1×10^{-9} ms^{-1}.

- Covers – A cover or cap is a barrier placed over the top of a waste management unit. Covers can prevent precipitation runoff from becoming contaminated by contact with waste, prevent or slow percolation of precipitation in the unit, prevent windblown transport of waste, and control release of gas from the waste. Like liners, covers can consist of compacted clay, synthetic materials, membranes or a combination of materials. A combination of pulverised fuel and paper mill sludge for example has been shown to be an effective landfill cover due to its low permeability and plasticity. Covers may also be a layer of soil or sand. In order to achieve the aforementioned objectives covers are typically designed with several layers. Table 2.2.3 below depicts five possible components of an engineered cover system.

Layer	Layer Description	Typical Materials
1	Surface Layer	Top Soil; Geosynthetic Erosion Control Layer; Cobbles
2	Protection Layer	Soil; Recycled or Reused Waste; Cobbles
3	Drainage Layer	Sand or Gravel
4	Barrier Layer	Compacted Clay; Geomembrane; Geosynthetic Clay Liner; Waste Material
5	Gas Collection and/or Foundation layer	Sand or Gravel; Soil; Recycled or Reused Waste

Table 2.2.3 Possible Configuration of a Landfill Cover System

- Leachate Collection Systems – These are a series of drains placed beneath a unit, typically a landfill. These systems collect leachate for treatment or disposal, thus preventing it from reaching soils, groundwater or surface water.

- Ground Water Monitoring Systems – These consist of one or several wells drilled in the vicinity of a unit. Samples from these wells are periodically collected and analysed. Ground water monitoring is not strictly an environmental control but rather a warning system. Ground water samples that display contamination may trigger regulatory requirements to mitigate or eliminate the source of contamination.

2.2.4 Physical and Chemical Characteristics of Ash

The chemical characteristics of coal ash depend on the type and origin of the fuel as well as the combustion conditions. Mineral matter content in coal principally consists of well defined minerals such as kaolinite ($Al_2Si_2O_5 \bullet 2H_2O$), quartz ($SiO_2$), calcite ($CaCO_3$) and pyrite ($FeS_2$)[38]. These are formed within the coal strata or incorporated in the coal during the coalification process. A small part of the inorganic matter is present in the form of ions associated with the organic matrix. In biomass however the ash forming species are predominantly present in organic molecules and as ions dissolved in the cell fluid. Bio-fuels also contain sand and soil particles introduced by contamination of the fuel. Intermediate products such as peat contain both mineral grains and organically associated

ions. Combustion involves the liberation and transformation of the inorganic species to ash. Generally, clay minerals are dehydrated and decomposed, whilst carbonates are calcinated and sulphides oxidised.

Alkali and alkali earth metals, either from organic compounds or minerals, may also react with combustion gases to form chlorides and sulphates. In fluidised bed combustion ash melting is not common and the ash components are mainly crystalline. The higher temperatures of PF combustion cause the formation of glassy particles of solidified ash melt. Table 2.2.4 below indicates an example of the variety of minerals which may be found in fly ash. The fly ash produced in this study was via CFB combustion and the fuels used were co-combusted mixtures of wood, coal, peat and oil.

	Wood (70%) Coal (30 %	Wood (35%) Peat (65%)	Wood-Wet (80%) Oil (20%)	Wood-Dry (80%) Oil (20%)
SiO_2	√	√	√	√
CaO	√	√	√	√
$CaCO_2$	√		√	√
$Ca(OH)_2$			√	√
$CaSO_4$	√	√		√
$Ca_3Al_2O_6$		√		√
$Ca_2Al_2SiO_7$	√		√	√
$Ca_2Al_2Si_2O_8$		√	√	
MgO			√	√
$Ca_3Mg(SiO_4)_2$		√		
$Ca_2MgSi_2O_7$		√		
Ca_2SiO_4		√		
$Ca_5(PO_4)_3(OH)$	√			
$KAlSi_3O_8$		√		
$(NaCa)Al(SiAl)_3O_8$		√		
K_2SO_4		√		
$K_3Na(SO_4)_2$		√		
$K_2Ca(CO_3)_2$		√		
KCl				
NaCl		√		
Fe_2O_3	√			
TiO_2		√		
$MgFe_2O_4$		√		

Table 2.2.4 Crystalline Compounds Identified in Selected Dry Ash Materials

Table 2.2.5 below shows quantitatively the proportions of the various inorganic substances contained in a selection of bio-fuels compared to coals. It may be noted from the data that quantities of potassium and sodium are significantly higher in the biomass fuels than in coal. It has also been noted that it is not only the ash alkalinity itself which is of significance but also the reactivity of the alkaline material. Studies [40] documenting the chemical fractionation of the inorganic constituents in biomass demonstrate that the alkali matter is generally more available and reactive in the bio-fuels than in coals. It is this ash reactivity which can cause the difficulties in biomass combustion. Conversely alkali earth metals, particularly calcium, have lower mobility and vapour pressures and are thought to cause less deposition problems. Chlorine content is also important in that it facilitates the transfer of potassium in the gas phase, where it participates in further reactions or is deposited on cold reactor surfaces. Here it may be substituted by sulphur to form potassium sulphate deposits, or may react with the metal surface attacking the protective oxide layer thus initiating reactor corrosion.

	Black Thunder Coal[41]	Illinois No.6 Coal[41]	Sawdust[41]	Foot Cake 1<d<1.4mm[42]	Foot Cake < 1mm[42]	Wheat Straw[42]
SiO_2	35.3	44.3	23.7	32.2	31.4	28.0
Al_2O_3	17.2	19.3	4.1	5.2	3.9	3.4
TiO_2	1.2	0.9	0.4	-	-	-
Fe_2O_3	5.2	22.2	1.7	3.6	2.6	0.6
CaO	21.1	3.2	40.0	2.6	12.8	2.7
MgO	3.3	0.7	4.8	1.7	5.1	1.7
Na_2O	1.1	0.4	2.3	6.3	3.2	5.2
K_2O	0.56	2.1	9.8	12.6	21.7	24.0
P_2O_5	2.1	0.1	2.1	-	-	-
SO_3	13.1	2.5	1.9	3.0	3.1	3.8
Cl	-	-	-	0.5	1.4	12.8

Table 2.2.5 Analysis of the Main Components in A Selection of Fuels[41,42]

2.3 Trace Elements

In recent years , it has become recognised that the wide range of elements present in fuels in trace element quantities may be problematic from the standpoint of atmospheric pollution and pollution of ground waters by landfill ash leaching. Below follows a description of trace metals in fuels, their partitioning during combustion and their speciation, migration and toxicity in the environment.

2.3.1 Trace Element Speciation, Migration and Toxicity in the Environment

An investigation into the leaching characteristics of trace elements requires a knowledge of their speciation during combustion and subsequent migration in the environment. This knowledge is essential for modelling purposes and also in order to ascertain if trace element concentrations in leachates are likely to exist in valencies that are toxicologically important eg Cr^{6+}. Information is therefore given on the speciation, environmental fate and transport of each element studied in this project, as well as toxicity information and regulatory limits. Information is also given on naturally occurring concentrations of trace elements in aqueous environments

2.3.1.1 Arsenic

Speciation & Migration

Arsenic is a semi-metallic element which exists in several allotropic forms and oxidation states of (–III, 0, III & V). It is widely distributed throughout the Earth's crust and occurs most often as arsenic sulphide or as metal arsenates or arsenides. Other than the leaching of arsenic from combustion ash into ground waters, it is also introduced into water through the dissolution of minerals and ores, from industrial effluents and via atmospheric deposition.

Arsenic is present in most contaminated sites either as As_2O_3 or as arsenic compounds derived from As_2O_3. Arsenic also exists in organometallic forms such as methylarsenic acid, $H_2AsO_3CH_3$, and dimethlyarsenic acid, $(CH_3)_2AsO_2H$, active ingredients in many pesticides as well as arsine, AsH_3, and its methyl derivatives.

In soils arsenic exists again mainly as As_2O_3 or as species leached from As_2O_3, oxidised to As(V) and sorbed onto soil minerals. Due to the fact that many arsenic compounds are strongly sorbed on to soils and sediments, leaching from contaminated areas by rainfall or snowmelt usually results in the transport of these compounds over only short distances. Once in soils or sediments arsenic undergoes a complex series of transformations including redox reactions and ligand exchange and the factors influencing these processes include the red-ox conditions (Eh) pH, the presence of certain competing anions and complexing ions and salinity.

Transformations of arsenic in surface water and groundwater are similar to those occurring in soils and sediments. The predominant form of arsenic in well oxygenated surface waters is usually arsenate but under reducing conditions, such as those often found in deep lake sediments or ground waters, aquatic micro-organisms may reduce the arsenate to arsenite and a variety of methylated forms. Arsenate also occurs in groundwater but typically sorbs onto iron-bearing minerals so arsenite is often the major component in this case.

Once arsenic is bound to sediment it may be released back into the water by chemical or biological inter-conversions. Bioconcentration of arsenic can occur in aquatic organisms, primarily in algae and the lower invertebrates, however biomagnification in aquatic food chains does not appear to be significant.

Toxicity & Regulatory Limits

Although arsenic in trace quantities has proved to be an essential element for some animal species such as goats and chickens there is no evidence that it is required by humans. Arsenic is most toxic in its arsine form followed by arsenites, arsenates and finally organic arsenic compounds. Lethal doses of arsenic compounds range from 1.5mg/kg of body weight for As_2O_3 to 500 mg/kg of body weight for DMAA (dimethylarsenic acid). Arsenic in smaller quantities is carcinogenic, the most common form of exposure being ingestion via drinking water and fish.

The limits set by the WHO, US-EPA and the EC on the allowable quantities of As in drinking water vary. Whilst the WHO has set a value of 10 ppb, the EC and the UK have set the value to 50 ppb. In January 2001, EPA revised the standard from 50 ppb, ordering that it fall to 10 ppb by 2006. The level of arsenic in natural uncontaminated waters varies between 1 and 2 ppb.

2.3.1.2 Barium

Speciation & Migration

Barium is an alkaline earth metal whose ores comprise 0.5 % of the earths crust in the form of barium sulphate ($BaSO_4$) and barium carbonate ($BaCO_3$). The only oxidation state in which Barium may exist is +II and in aqueous environments barium occurs primarily as the dissolved divalent ion, Ba^{2+}, at pH < 9.3. The neutral ion species, $BaSO_4$ forms in the presence of high sulphate concentrations. Similarly, $BaCO_3$ becomes the dominant species in the presence of carbonate at pH > 9.3. Solid phases, $BaSO_4$ (barite) and $BaCO_3$ (witherite) exhibit fast precipitation kinetics and very low solubilities, and can limit barium concentration in aqueous solutions. Barium also forms salts of low solubility with arsenate (the least soluble arsenate), chromate, chloride and hydroxide

phosphate ions. In water barium can from complexes with natural organics such as fatty acids in acidic landfill leachates.

Barium is not very mobile in most soils. The rate of transport is dependent on the characteristics of soils, such as cation exchange capacity (CEC) and $CaCO_3$ content. In soils with high CEC values (such as clay minerals, or soils with high organic content), bariums mobility is limited by adsorption. High $CaCO_3$ content limits mobility by precipitation barium as $BaCO_3$. In the presence of sulphate ions, barium precipitates as $BaSO_4$. In the presence of Cl^- ions, barium is more mobile and is more likely to be leached to groundwater, from the solid medium, because of the increased solubility of $BaCl_2$, compared to other forms of barium compounds. Water-bourne barium may be taken up by fish and aquatic organisms. Barium in solids may be taken up by vegetation. However, relative to the amount found in soils, little barium is bio-concentrated by plants.

Toxicity and Regulatory Limits

Barium is not considered essential for human nutrition. Associations between barium content of drinking water and mortality from cardiovascular disease have been observed. At high concentrations it causes paralysis and depending on the solubility of the salt, death may occur in a few hours. There is no evidence that barium is carcinogenic. The WHO limit for barium in drinking water is 0.7mg/l. In natural waters the mean and maximum concentrations in a study of 500 sites in the Netherlands were 0.23 and 2.5 mg/l respectively.

2.3.1.3 Beryllium

Speciation and Migration

Beryllium is a hard, brittle metal and the lightest metal known. Elemental beryllium does not occur naturally, but it may be found as a component of coal, oil, soil and volcanic

dust. Beryllium is resistant to oxidation at ordinary temperatures. It has a high heat capacity and thermal conductivity.

Beryllium exhibits only the +II oxidation state under environmental conditions. Changes in redox potential do not affect its oxidation state and the reduction of Be^{2+} to elemental beryllium does not occur naturally. Beryllium forms strong complexes with OH^- ions. The solubility of $Be(OH)_2$ is very low at the pH of most natural systems. Beryllium also forms rather insoluble complexes with phosphate, silicate and aluminate. Beryllium does not form strong complexes with Cl^-, SO_4^{2-}, NO_3^-, or organic ligands.

In aqueous environments beryllium is often sorbed to suspended particulate matter or to the sediment. Therefore, beryllium concentrations in surface water usually are very low even in polluted conditions, where concentration of complexing agents are high. Beryllium in sediment is usually associated with the aluminium part of the sediment, ,indicating adsorption on to clay particles. Some beryllium also may be present in the sediment through formation and subsequent precipitation of insoluble complexes. Therefore beryllium is expected to have low mobility in soil, sediment and water. The formation of water soluble complexes with hydroxide ions at higher pH values, however, may increase the solubility and mobility of beryllium in surface water. Beryllium is extremely toxic to fresh water fish in soft water. However, bio-concentration in fish to high levels is not likely because of the low uptake of beryllium from water.

Toxicity and Regulatory Limits

No studies are available on the health effects of ingested beryllium, and its toxicity is considered to be low via this rout. However the International Agency for Research in Cancer (IARC) has classified beryllium and its compounds as being probably carcinogenic to humans. Concentrations in natural water are generally less than 1μg/l.

2.3.1.4 Cadmium

Speciation and Migration

Cadmium is a soft ductile metal which is rarely found in nature in its pure form. The main sources of cadmium are sulphide ores of lead, zinc and copper. Cadmium exists as Cd^{2+} ion, Cd-CN^- complexes, or $Cd(OH)_2$ sludge at most cadmium-contaminated sites, depending on pH. At pH <8.0 cadmium occurs primarily as the dissolved divalent ion, Cd^{2+}, or aqueous sulphate species. As pH increases, cadmium precipitates to form $Cd(OH)_2$, and $CdCO_3$. $CdCO_3$ is significantly less soluble than $Cd(OH)_2$ and its solubility increases as dissolved CO_2 concentration increases. Under reducing conditions and in the presence of sulphide, a stable cadmium compound, CdS, forms. Cadmium also forms precipitates with phosphate, selenide, selenate, arsenate and chromate; the solubilities of these precipitates vary under different pH and geochemical conditions.

Cadmium is more mobile in aquatic environments than most other heavy metals, such as lead. Cadmium exists in water as hydrate ions or complexes with humic substance or other organic ligands. Cadmium may be removed from water by precipitation or by sorption to mineral surfaces and organic materials. Studies reveal that cadmium concentrations in sediments are at least one order of magnitude 0higher than in the overlying water. Cadmium leaches into water particularly under acidic conditions to form more volatile compounds therefore, partitioning from water to air does not occur.

Precipitation and adsorption onto soils and sediments are the most common mechanisms governing the transformation and mobility of cadmium in the environment. Removal of cadmium from water increases with increasing pH through a critical range of pH 6-8. Below pH 6.0, little or no cadmium is removed. Above pH 8.0-9.0 cadmium may be completely removed. Cadmium adsorption often correlates with CEC of the clay minerals, carbonate minerals, oxides and organic matter in wastes and soils.

For example, sulphate and chloride ions often reduce cadmium adsorption by amorphous clay minerals, silica, and or alumina. Conversely ligands such as humic acids, glycine and phosphate increase cadmium adsorption. Aquatic and terrestrial organisms bio-accumulate cadmium. Cadmium concentrations in freshwater and marine animals can be hundreds to thousands of times higher than in the water itself. Cadmium is know to accumulate in grasses, food crops poultry, cattle and wildlife. However, bio-magnification of cadmium through the food chain has not been proven.

Toxicity and Regulatory Limits

The kidney is the most sensitive organ to ingestion of cadmium through contaminated food and drink. Cd ingestion causes itai – itai disease (osteoporosis accompanied by severe renal disease). Cadmium is not a known carcinogen although cigarette smoking increases cadmium concentrations inside homes and cadmium inhalation. Crops grown in polluted soil or irrigated with polluted water may contain increased concentrations as may meat from animals grazing on contaminated pastures. Kidneys and livers of animals have the propensity to bio-accumulate cadmium and very high levels have been found in shellfish. Cadmium concentrations in unpolluted waters are usually below 1μg/l. A level of 0.003 mg/l has been recommended as an acceptable limit in drinking water.

2.3.1.5 Chromium

Speciation and Migration

Chromium is one of the less common elements in the Earth's crust and occurs only in compounds. Chromium usually carries a valence of +VI or +III. Hexavalent chromium present as chromate or dichromate ions (CrO_2^{2-} and $Cr_2O_7^{2-}$) are the major chromium species encountered. Cr(VI) is both more mobile and more toxic than trivalent chromium. The stability of Cr(VI) and Cr(III) is Eh and pH dependent. Chromate

predominates between pH 6 and higher under oxidising conditions whilst Cr(III) predominates at lower pH.

Cr(VI) naturally precipitates with metal cations such as Ba^{2+}, and Pb^{2+} and also complexes with multiple sites on waste and soil surfaces having positively charged sites. These sites decrease with increasing soil pH. As a result, adsorption of Cr(VI) onto the surface of iron oxide, aluminium oxide or other solid components occurs only at an acidic on neutral pH. Cr(III) is less toxic and tends to adsorb on wastes and soils below pH 4.0 . Above pH 5.0, chromium's lack of mobility is attributed to the formation of $Cr(OH)_3$ solid and at pH range 4.0 and 5.0 to precipitation and adsorption. Cr (VI) is reduced to Cr(III) in the presence of ferrous iron, dissolved sulphides and organic compounds. The reduction reaction proceeds at a slow rate, under ambient temperature and alkaline conditions, increasing with increasing solid pH. Cr(III) can be oxidised to Cr(VI) by a large excess of MnO_2 and oxidation by oxygen occurs slowly under natural water conditions.

The leachability of Cr(VI) from waste or soil increases as the solid matrix pH increases. Most of chromium leached into water will ultimately be deposited in the sediment. The remaining soluble chromium is present as soluble Cr(VI) and Cr(III) complexes, with any Cr(VI) eventually becoming reduced to Cr(III) by organic matter in the water. It has been estimated that the residence time of total chromium in lake water ranges from 4.6 to 18 years.

Toxicity and Regulatory Limits

Chromium is known to bioacumulate in meat and fish and large quantities are also to be found in fruit and vegetables. Food is a higher contributor to human intake than water. There is a daily requirement for human intake of Cr(III) of 2-8μg. Cr(VI) however is known to be extremely carcinogenic. Different guideline values for the two valencies should be derived but current analytical methods favour a guideline value for total chromium. The WHO value is 0.05 mg/litre in drinking water. This value has been questioned but no toxicological data have supported a new value.

2.3.1.6 Lead

Speciation and Migration

Most of the lead released into the environment is in the form of lead metal, lead oxides and hydroxides. Its most common oxidations stares are 0 and +II. Pb(II) forms both mononuclear and polynuclear oxides and the corresponding hydrates and hydroxides. However, Pb^{2+}, and hydroxy complexes are the most stable species under most conditions.

The fate of lead in the solid matrix is affected by processes of adsorption, ion exchange, precipitation, and complexation to organic matter. After being released to a contaminated site, most lead is retained strongly in soil, with very little being transported to the surface water or groundwater. If the solid matrix has a high organic content and a pH of 6.0 – 8.0 lead may form insoluble organic lead complexes, if less organic matter exists hydrous lead oxide complexes or lead carbonates or phosphate precipitates may form. At a more acidic pH, the organic lead complexes become more soluble and are likely to leach out.

The amount of lead in water depends on the water pH and the total dissolved salt content. At pH> 5.4, the lead solubility is approximately 500μg/l in soft water and only 30 μg/l in hard water. Sulphate ions limit the lead concentration in solution by forming lead sulphate. Above pH 5.4 – 6.0 lead carbonates, $PbCO_3$ and $Pb_2(OH)_2CO_3$ form. As a result a significant fraction of lead is carried by river water in undissolved form, which consists of colloidal or larger particles.

Toxicity and Regulatory Limits

Lead is particularly toxic to children (children absorb 4 to 5 times as much as adults) and pregnant women and it is toxic to both the central and the peripheral nervous systems.

It severely impairs mental development and interferes with calcium and vitamin D metabolism. The IARC has classified inorganic lead as a possible human carcinogen although evidence is inconclusive due to the limited number of studies. Limits on drinking water have been set at 0.01 mg/l by the WHO (0.05 mg/l by the EC), and it exists in natural waters at the levels stated above.

2.3.1.7 Mercury

Speciation and Migration

The primary source of mercury is the sulphide ore, cinnabar. In a metals contaminated site, mercury exists in mercuric form (Hg^{2+}), mercurous form (Hg_2^{2+}), elemental form (Hg^0) or alkylated form (e.g. methyl and ethyl mercury). The alkylated compounds are both volatile in air and soluble in water. In general leaching is a relatively insignificant transport process in soils, but surface runoff does remove mercury from solids to water, particularly if a high humic content exists. In wastes soils and sediments, sorption is one of the most important controlling pathways for removal of mercury from solution and this increases with increasing pH. Inorganic mercury sorbed into soils is not readily desorbed, therefore freshwater and marine sediments are important repositories for inorganic mercury. Organic mercury however is is very soluble and mobile and quickly enters the aquatic food chain. Concentrations of methylmercury in fish, for example, can be up to 100,000 times the concentrations found in ambient waters.

The most important transformation process in the environmental fate of mercury in surface water and groundwater is biotransformation. Any form of mercury entering surface water and groundwater can be microbially converted to the methyl mercuric ion. Sulphur reducing bacteria are responsible for most of the mercury methylation, with anaerobic conditions favouring their activity.

Toxicity and Regulatory Limits

Methyl and ethyl mercury compounds have been the cause of the largest number of cases of mercury poisoning. The kidney is the main target organ for inorganic Hg, whereas methymercury affects mainly the central nervous system. Minamata disease, the most common form of Hg poisoning, is via ingestion of food rather than water. Almost all the mercury in uncontaminated drinking water is thought to be in the form of Hg^{2+} ions. The guideline for total mercury is 0.001mg/l in drinking water.

2.3.1.8 Zinc

Speciation and Migration

In surface water, zinc occurs in both suspended and dissolved forms. Dissolved zinc may occur as the free zinc ion or as dissolved complexes and compounds with varying degrees of stability and solubility. Suspended zinc may be dissolved following minor changes in water chemistry or sorbed to suspended particulate matter. Sorption is the dominant fate of zinc in aquatic environments. Zinc partitions to sediments or suspended solids in surface water through sorption onto hydrous iron and manganese oxides, clay minerals and organic matter. Sorption is affected by the nature and concentration of sorbents and the pH and salinity of solutions. Zinc tends to be more readily sorbed at pH 7.0 than at lower pH. A small fraction of zinc may partition into the aquatic phase through speciation into soluble zinc compounds with organic or inorganic ligands in surface water) at neutral and acidic pH values. For example $ZnCl_2$ and $ZnSO_4$ are very soluble in water. As a result, zinc is one of the most mobile heavy metals. Precipitation of zinc compounds is important in reducing environments and highly polluted sites. Precipitation of ZnS is an important control on the mobility of zinc in reducing environments.

Toxicity and Regulatory Limits

Zinc is also an essential dietary element with a recommended daily intake of 15-12 mg. Harmful doses lead to pancreal damage and anaemia. It is not a known carcinogen. Regulatory limits for zinc in drinking water have been set at 3 mg/l.

2.3.2 Trace Element Occurrence in Coal

Elements present in coal may be classified into three broad groups. Major elements, present in quantities greater than 10,000 ppm, minor elements at levels of 1000 to 10000 ppm and trace elements, usually present in quantities of less than 1000 ppm. Major elements in coals are commonly Si, Al, Fe, Mg, Ca, Na, K and P and minor elements are typically Ba, Sr, S, Cl and N. Most other elements are present in trace quantities in coal.

Trace elements were categorised by V.M. Goldschmidt in 1922 as chalcophile, lithophile or siderophile. Chalcophile elements are sulphur loving, lithophile elements have an affinity to silicon whilst siderophile elements are often associated with iron. Table 2.3.1 below shows which elements fall into which category.

CLASSIFICATION	ELEMENT
Chalcophile	Ag, As, Bi, Cd, Cu, Ga, Hg, In, Pb, Po, S, Sb, Se, Te, Tl, Zn
Lithophile	Al, At B, Ba, Be, Br, Ca, Cl, Cr, Cs, F, I, Hf, K, Li, Mg, Mn, Na, Nb, O, Rb, Sc,,Sr, Ta, Th, Ti, U, V, Y, Zr, W, Lanthanides
Siderophile	Au, C, Co, Fe, Ge, Ir, Mo, Ni, Os, P, Pd, Pt, Re, Rh, Ru, Sn

Table 2.3.1 Trace Element Affinities to Sulphur, Silicon and Iron

Figure 2.3.1 below categorises trace metal occurrence in coal. Trace metals can exist either organically or inorganically. It is not yet clear which elements have the propensity to be bound organically or inorganically. Results in several studies e.g. Finkelman (1989), Swaine (1990), Palmer & Lyons (1990) showed that in the case of most elements there could be either an organic or inorganic association depending on the fuel being studied. Low rank coals for example are likely to have a higher degree of organically bound trace elements than high rank coals (Der Flir-Keller and Fyfe, (1998)).

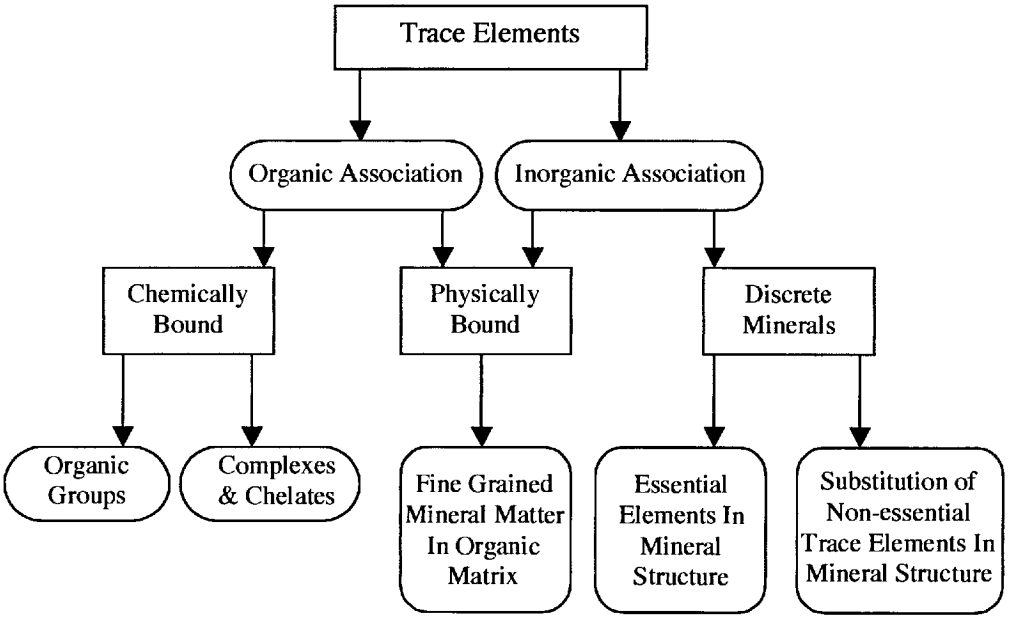


Figure 2.3.1 Modes of Occurrence of Trace Elements in Coal[37]

Elements which occur organically may be either chemically bound in chelates, complexes and organic groups e.g. carboxylic acid or physically (ionically) bound in fine mineral matter of the organic matrix. The greatest proportion of trace elements however are generally found in the inorganic part of the fuel. Direct analysis of mode of occurrence is difficult to achieve. Research into mode of occurrence has generally involved the coal being separated by density and analysing the resulting fraction. Trace element quantities may therefore be correlated to the presence of minerals and organic matter in the fractions.

The primary mineral phases found in coal are aluminosilicates and silicates, carbonates and sulphides, although a very wide variety of other minerals are present eg. oxides, chlorides, and sulphates.

Alluminosilicates associated with coal include kaolinite ($Al_2Si_2O_5(OH)_4$, illite ($(K,H3O)(Al,Mg,Fe)_2(Si,Al)4O_{10}[(OH)_2,(H_2O)]$), and chlorite($(Fe, Mg, Al)_6(Si, Al)4O_{10}(OH)_8$). Trace metals which are associated with these clays include Be, Cr, Cs, Ga, Li, Rb, Ti, and V (Finkleman (1981)).

Carbonates in coals include calcite ($CaCO_3$) and siderite ($FeCO_3$) and certain trace elements can make subustitutions in these minerals e.g. Sr, Ba, Co, and Zn have been found to substitute Ca in calcite and Mn for Fe in Siderite.

Pyrite (FeS_2) is the primary sulphide to be found in coal, whilst sphalerite (ZnS), chalcopyrite ($CuFeS_2$), galena (PbS) and occasionally cinnabar (HgS) have also been noted in small quantitites (Swain (1994)). The Elements As, Cd, Co, CU, Hg, Mo, Ni, Pb, Se and Zn have all been reported to associate with pyrite (Norton and Markuszewski, (1989). Sphalerite sees associations with Cd, Zn, Cu, Ag, Sb and Bi, whilst M, Co, Ni, Cu, As and Pb have been found in iron sulphides (Wiese (1990)).

The quantities of trace elements in coals vary greatly between coals from different locations and also with areas of a particular coal seam. Trace elements concentrations do fall within broad ranges however. For the trace elements being considered in this study the table below shows the concentration ranges which may be found in coal.

Element	**Typical Concentration Range found in Coals (ppm)**
Arsenic	0.5 – 80
Barium	20 – 1000
Beryllium	0.1 – 15
Cadmium	0.1 – 3
Chromium	0.5 – 60
Lead	2 – 80
Mercury	0.02 – 1
Selenium	0.2 – 10
Vanadium	2 – 100
Zinc	5 – 300

Table 2.3.2 Typical Concentration Ranges for Trace Elements in Coal

2.3.3 Trace Element Partitioning in Combustion

The fate of trace elements during combustion depends primarily on the combustion temperature and the mode of occurrence of the elements in the fuel. Many elements in the initial fuel are partially or totally vaporised but their ultimate fate depends upon temperature profile, operating conditions, composition of the gas, their chemistry, and the presence of fly ash.

The fate of trace elements may be in any of the three product streams of combustion. They may be emitted into the gaseous phase, escaping with the flue gas, they may be found in the fly ash or they may exist in the slag or bottom ash. It is possible to predict which group the elements belong based on the boiling points of the elements and their compounds and the temperatures at which phase change occurs.

The elements have been categorised into three groups of increasing volatility as shown in Venn diagram below. Group I elements are those which, after combustion, are present in the bottom ash or slag (although elutriated fines will carry some away). These are typically the least volatile, lithophile elements as described in Table 2.3.1 above e.g. Ba, Be, Cr & V. Group I elements are usually equally distributed between coarser residues and the combustor fly ash.

Group II elements are typically the chalcophile elements given in Table 2.3.1 above. These elements may exist in the bottom ash or slag but are more prevalent in the combustion fly ash. Most elements fall into Group II of the classification. Group III elements are those which volatilise most readily, and these may be found in the flue gas. There is a significant overlap between the groups and this may be attributed to varying operating temperatures which control volatility. The figure below may be obtained by using different methods. Some authors use theoretical data such as thermodynamic properties and typical operating conditions, whilst others use empirical data such as enrichment factors.

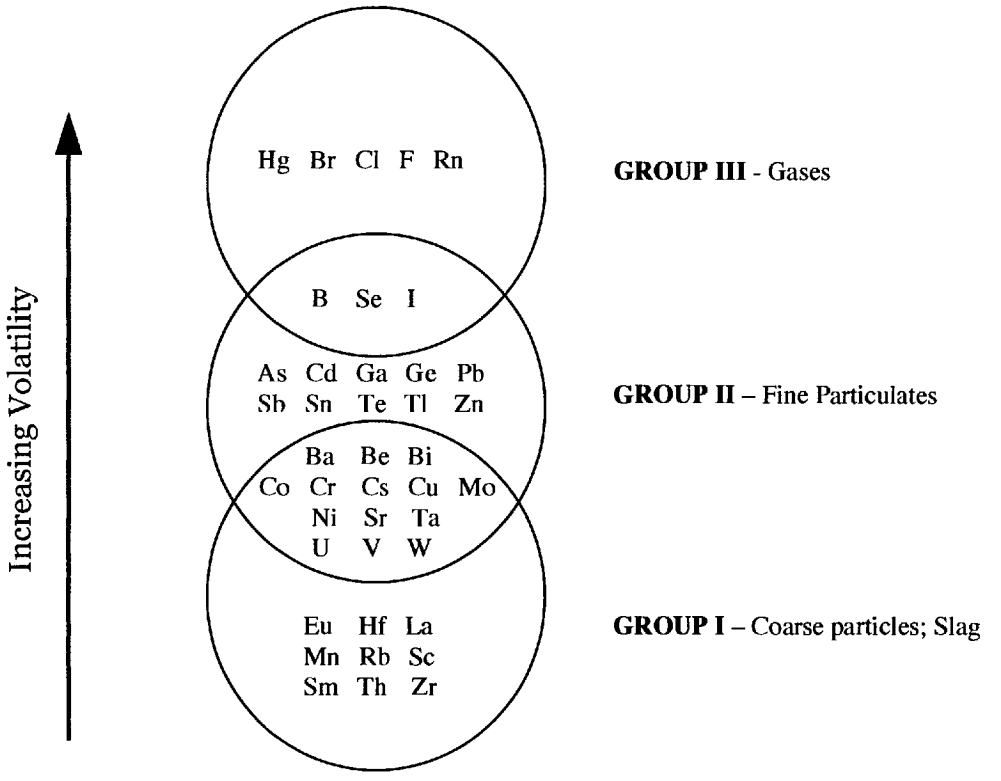


Figure 2.3.2 Classification of Trace Elements by Their Partitioning Behaviour During Combustion (CERCHAR 1985, Clarke 1991, Conzemius 1984, Klein 1975)

The majority of trace elements are present in combustion residues in the same relative proportions as in the feed coal but are enriched in the ash by a factor equivalent to material emitted in the flue gases. Chadwick et al (1987) noted that Group I elements are evenly distributed between different particle sizes, whilst enrichment in the chalcophile Group II elements was inversely proportional to particle size. In Group III elements mass balance equations which remained unresolved for elements such as Se and Hg, showed that these elements partially existed in the vapour phase.

Partitioning behaviour varies depending on the combustion system and operating conditions. Trace elements are more likely to be contained in fluidised bed systems than pulverised fuel systems due to the higher operating temperatures of the latter process. However, the longer residence time of the fuel in PF combustion will increase volatilisation.

It has been shown that in fluidised bed combustion increasing the bed depth increases the emission of elements. This has been attributed to an increase in smaller ash particulates with a higher bed depth.

2.4 LEACHING

2.4.1 Leaching of Combustion Residues

Leaching is the process by which soluble constituents are dissolved from a solid material into a fluid by percolation or diffusion. Thus when combustion residues in landfills or construction materials come in contact with the aqueous environment (precipitation, surface water or groundwater), soluble matter will be removed into the leachate. Figure 2.4.1 below shows a water balance for a land-fill site[59]. The degree to which constituents dissolve into the aqueous phase is a function of not only material properties but the conditions of the site (chemical, physical and biological).

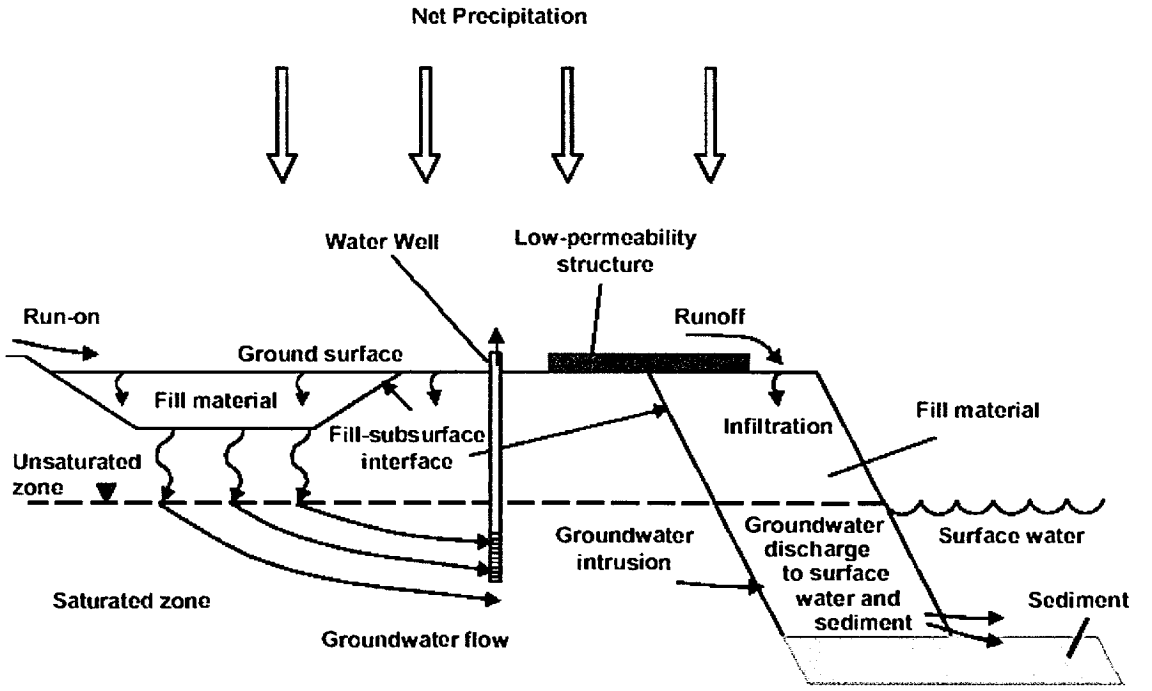


Figure 2.4.1 Conceptual Model of Water Balance at Land-fill Site.

2.4.2 Factors and Mechanisms Controlling Release

Numerous physical, chemical and biological factors influence leaching from combustion waste and soil. These factors are either specific to the fill material or to the characteristics of the deposition site.

Factors specific to the combustion residue itself include the following (adapted from van der Sloot (1995)):

- the release potential of the species being considered - which is the fraction of trace element ultimately available for leaching. This is affected by particle size and shape, and surface area exposed to leaching.

- solubility or sorption reactions of the species being considered – this is affected by changes in leaching conditions for example by the pH or redox status of the system.

- mass transfer limitations for example diffusion rates out of the solid matrix into pore water and from pore water to the environment. This is affected by the permeability of the solid matrix and flow rate of the leaching fluid.

- temperature of the system

- chemical speciation in the solid and in the solution

- biological factors that influence leaching include the presence of micro-organisms that, through the process of biodegradation, can change redox and pH conditions with in the fill material, affecting the solubility of contaminants.

The site-specific factors affecting leaching are as follows[60]:

- *Climate and meteorological conditions.* The amount of net precipitation (precipitation minus evapotranspiration) at a fill site will influence the amount of water available for infiltration through the site.

- *Design and configuration of the land-fill site.* The depth of the land-fill site will affect the quality of the leachate. Water entering the top surface of the fill material will travel through it downwards via interconnected void spaces until it eventually reaches the bottom of the unit as leachate. Dissolution from the solid phase to the water will occur until solubility limits are reached. The deeper the unit, the greater the contact time between the percolate and the fill material and thus there will be a greater opportunity for the leachate to reach saturation limits (Lu et al., (1995)). Also, the deeper the unit, the longer it will take for contaminants to be depleted. The presence of a cap or other low permeability structure will reduce the opportunity for infiltration and leachate generation. Topography will affect the site's runoff pattern and the amount of water entering (via run-on) and leaving (via run-off) of the site.

- *Vegetation.* Vegetation limits infiltration by intercepting precipitation directly (thereby improving evaporation from the surface) and by taking up soil moisture and transpiring it back to the atmosphere (i.e. via evapotranspiration).

- *Hydrological Conditions:* Subsurface geological conditions and depth to groundwater at a fill site can impact the generation of leachate. For materials that are placed at or below the water table, ground water flowing through the material can provide a source of water that is in addition to precipitation and run-on.

2.4.3 Leaching Tests

The increasing impetus to dispose or re-use combustion waste in an environmentally sound manner has also promoted the development of leaching tests, in order to assess the impact of the various methods of managing this waste. Due to the large variety of applications of combustion ash many tests have been developed and it is not possible for one test to address all leaching scenarios. Leaching tests have however in the past been applied somewhat arbitrarily without proper consideration of the applicability of the test to the particular case in question. It is therefore important to carefully define the nature and aim of the leaching characterisation required before the type of leaching test or combination of tests is decided upon.

In the broadest sense, leaching tests fall into two categories: monolith tests apply to bound applications of ash, such as construction applications, and percolation tests to all other applications. The main difference between these two tests are the mechanisms governing release. Due to these differences the system to be subjected to leaching must first be defined. Once it has been decided weather a monolith or percolation test is to be used the specific test appointed depends upon the aim of research. The four aims of research are categorised below[61].

- *As a regulatory tool.* In this case a *compliance* test is required which is generally of short duration, one or two days, and often aims at a direct comparison with threshold values, taking into account both short and long term environmental effects.

- *For environmental impact.* This aim would require a *characterisation* test which would aim to understand the precise nature of leaching behaviour of the material under a variety of exposure conditions to be found in the environment. These tests are generally of greater duration and complexity.

- *For scientific evaluation.* In this instance again a characterisation test would be used. The aim however would be to precisely model processes under controlled conditions which are not likely to occur in the environment, solely to understand the phenomena governing leaching.

- *As a management tool for daily practice.* For day to day waste management *on-site verification tests* are required to, for example, screen for compliance of a material to be disposed or verify a previous evaluation of a system. These tests which should last typically an hour or two are still being developed.

Leaching tests may either be carried out on-site via field experiments or in the laboratory. Field experiments involve the use of controlled land-fill cells or field lysimetres. A field lysimeter is a container usually installed in the unsaturated zone used to measure percolation, leaching and evapotranspiration losses from the contained material. Field lysimeter tests address different aspects of leaching such as the physical mechanisms involved, chemical interactions between the waste and the leaching fluid, the kinetics of leaching, and leaching as a function of pH, time and liquid-to-solid ratio (L/S). Figure 2.4.2 below shows an example of a field lysimeter.

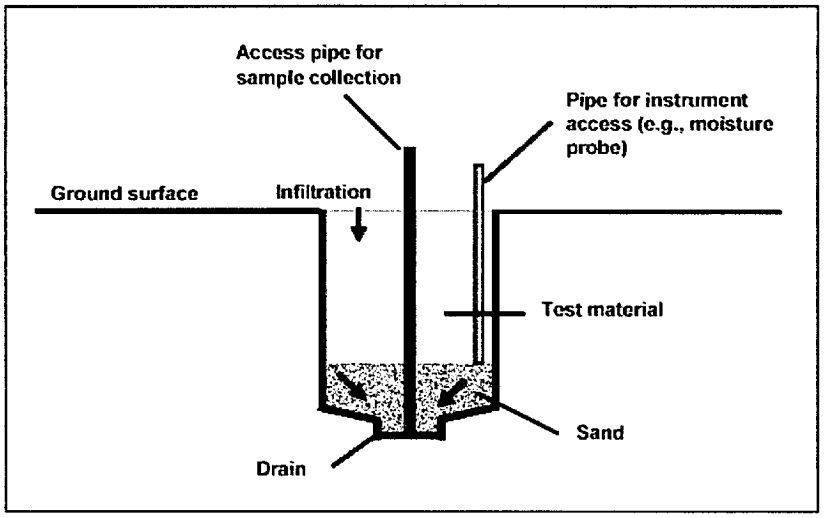


Figure 2.4.2 Example of Field Lysimeter[60]

Laboratory leaching tests involve contacting samples of the study material with liquid to determine which constituents of the sample will be dissolved into the liquid. Laboratory tests may either be batch tests or multiple extraction (dynamic) tests. Batch extraction tests generally involve mixing the sample with a specific amount of leaching solution without renewal of the leaching solution. The sample is agitated for comparatively short periods of time (hours to days) until equilibrium is reached. The sample is then filtered and the resulting leachate analysed. An example of batch leaching apparatus, used in this study, is shown in Figure 3.3.2, Section 3.3.2.1.

Dynamic tests generally investigate an aspect of the leaching which is a strong function of time. In dynamic tests the sample is place in a column and the leaching solution is periodically removed and replaced, or continuously removed. The leaching in this instance is generally performed over a long period of time. A simplified schematic of the apparatus used in a dynamic leaching test is given below in Figure 2.4.3.

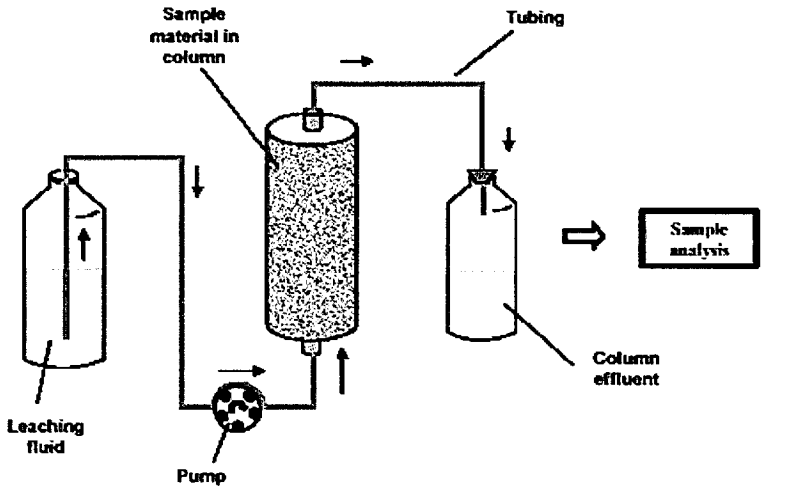


Figure 2.4.3 Basic Column Leaching Test Apparatus

2.4.4 Equilibrium Speciation Modelling – MINTEQA2

As part of this study, simulations were carried out to model the leaching behaviour of the ashes in question, by means of an equilibrium speciation model. Comparisons could therefore be made between empirical and theoretical results. For a given set of chemical components in a sample system, an equilibrium speciation model calculates the equilibrium distribution among dissolved, sorbed and precipitated fractions as well as the concentrations of individual species within each fraction. Two methods are generally used to define and solve multi-component equilibrium problems as follows[62]:

1. Minimisation of the system free energy under mass balance constraints.
2. Simultaneous solution of linear mass balance relationships and non linear mass balance expressions.

Van Zeggeren and Storey[63] have shown the two approaches to be mathematically equivalent. Several computer programs exist which rapidly perform chemical speciation calculations (e.g. MINEQL, PHREEQC, GEOCHEM[64]). The equilibrium model used in this study was a Windows version of the U.S EPA developed and distributed MINTEQA2, and its corresponding user interface PRODEFA2. This model uses the latter mathematical approach to solve the equilibrium problems posed. It is capable of performing a wide variety of calculations such as equilibrium aqueous speciation, adsorption, gas phase partition, solid phase saturation states and precipitation-dissolution of metals.

MINTEQA2 uses an extensive thermodynamic database which contains a pre-defined set of components and their corresponding equilibrium constants. Chemical species present in the system are defined in terms of these components. For example the species Al_2O_3 does not exist in the database as a component but Al^{3+} does.

Therefore 0.01 mol/l of the species Al_2O_3 would be defined as follows:

$$Al_2O_3 \Rightarrow 2Al^{3+} + 3H_2O - 6H^+$$

Thus to represent this quantity using MINTEQA2 components, 0.02 mol/l Al^{3+} , 0.03 mol/l H_2O and – 0.06 mol/l H^+.

MINTEQA2 uses the component concentrations calculated by the user as shown above along with estimates for the activity of each component, and parameters such as pH to solve calculations. A flow diagram of the general methodology used by MINTEQA2 to solve the defined problems is described in Figure 2.4.4 below. Where degrees of freedom are referred to an expression modified from the usual phase rule is shown below:

$$F = C - P$$

Where: F = Number of Degrees of Freedom

C = Number of Components as defined above

P = $X_i + X_j$

X_i = Species with fixed activity (infinite solids constrained to be present at equilibrium)

X_j = Finite solid species (species assumed to be initially present initially or may precipitate from the solution)

This modified phase rule has two less degrees of freedom than usual due to the system having been defined to be at constant temperature and pressure.

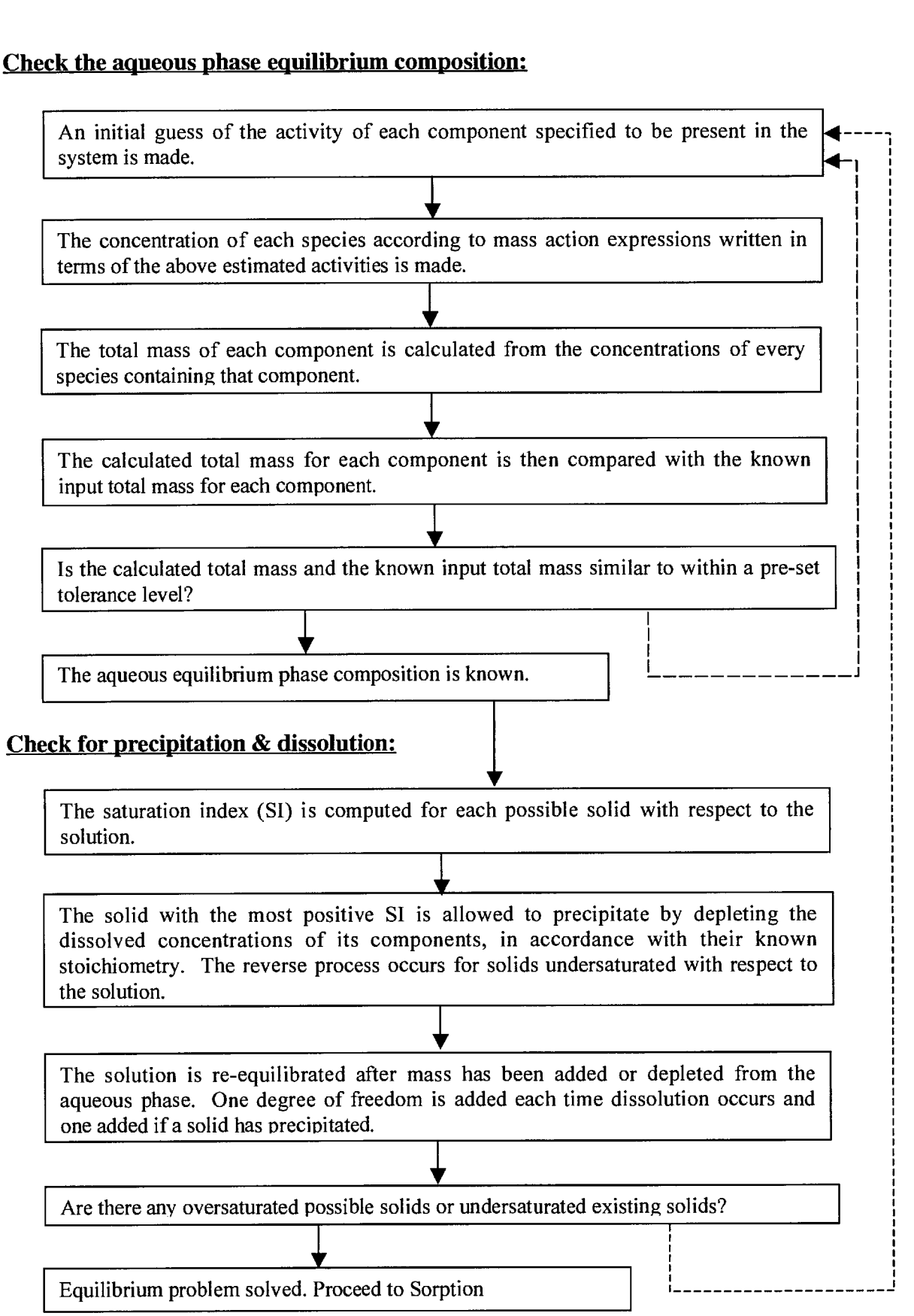


Figure 2.4.4 Flow Diagram of General MINTEQA2 Methodology

Due to non-ideal effects, the thermodynamic activity of a species in solution differs from its actual concentration. For any particular species i, the activity coefficient is a proportionality factor relating the activity of the species {Si} to the concentration of the species [Si]:

MINTEQA2 allows the user to choose from two available methods to estimate activity coefficients for ionic species: the Davies[65] equation or the modified Debye-Hückel[66] equation.

Davies equation :

$$\log\gamma_i = -Az_i^2\left[\frac{\sqrt{I}}{1+\sqrt{I}} + 0.3I\right]$$

γ_i = Activity coefficient of component i

A = Temperature dependent constant

z_i = ionic charge of species i,

I = ionic strength (M)

Extended Debye-Hückel Equation (as modified in WATEQ) :

$$\log\gamma_i = \frac{-Az_i^2\sqrt{I}}{1+Ba_i\sqrt{I}} + b_iI$$

A, B = temperature dependent constants

If the value of bi is zero for a species, then a_i is the ion size parameter and this equation is the extended Debye-Hückel equation. If the b_i is non-zero for a species, both a_i and b_i are ion-specific fitting parameters and the equation is called the modified form of the WATEQ extended Debye-Hückel equation.

2.4.4.1 Adsorption Models

Adsorption may be considered in MINTEQA2 using a variety of algorithms. There are seven models which may be used for modelling surface reactions:

1. Activity K_d Model
2. Activity Langmuir Model
3. Activity Freundlich Model
4. Ion Exchange Model
5. Constant Capacitance model
6. Triple Layer Model
7. Diffuse Layer Model

These fall into the two categories of electrostatic and non-electrostatic . Non-electrostatic models neglect the influence of charged surfaces on the solution and the influences of solution composition on surface charges. Models 1- 4 above fall into this category, whilst Models 5 – 7 are electrostatic.

Electrostatic models take account of the fact that particles in suspension carry a surface charge capable of creating electrostatic potentials extending into the solution. Ions in solution which have the same charge as the surface are repelled and those with opposite polarities are attracted. These polarised systems may have a significant effect on the adsorptive behaviour of species in solution, therefore these effects are incorporated in electrostatic models. This is done by modifying the activities of sorbate ions near charged surfaces by means of the electrical work necessary to penetrate the zone of electrostatic potentials, extending away from the surface.

In order to formulate the problem definition for sorption in MINTEQA2, databases of surface reactions and their equilbrium constants must be provided. Unlike for aqueous and solid species MINTEQA2 does not provide this information and the user must formulate the relevant input files. MINTEQA2 does however provide a database

containing a large set of surface reactions and equilibrium constants for use with the Diffuse-layer model for trace metal adsorption onto an iron oxide surface obtained from work carried out by Dzombak and Morel[67].

3.0 EXPERIMENTAL PROTOCOL, APPARATUS & ANALYTICAL PROCEDURES

3.1 SAMPLE CHARACTERISATION

The proximate and ultimate analysis of the fuel samples used is shown below. Proximate analysis is a standard characterisation test traditionally used by the coal industry to determine the content of ash, moisture, volatile matter and fixed carbon in the fuel[68]. The operating conditions of the test however generally vary greatly from those in PF combustion. When fuels are blended, proximate analysis shows both additive and synergistic effects[69]. However, it has not yet been ascertained weather synergistic effects are exhibited due to inherent properties of the coal blend, or if they result from the test itself. The differences between predicted additive results and experimental results where synergy is exhibited may be considered negligible.

Ultimate analysis is a standard test used to determine the elemental composition of coal. Quantities of carbon, hydrogen, nitrogen, sulphur and oxygen are determined. The accuracy of ultimate analysis test is hampered by several factors. The quantity of hydrogen may be determined inaccurately due to residual moisture in coal or dehydration of mineral matter. Similarly carbon and sulphur measurements may be affected by the presence of carbonates and sulphides or sulphates in the mineral matter[70]. As ultimate analysis gives elemental results synergistic effects in blends do not exist and given a homogenous sample results will be additive.

The experiments carried out may be categorised into 3 sets and three sets of samples were used. The first sample set was used in conjunction with reference materials to verify the validity of the modified TCLP test and other analytical procedures. These samples were polish coal, South Africa coal, pulp sludge and two sets of woods. Their analyses are listed in Figure 3.1.1.1 The second sample set was supplied by the project partners CERCHAR.

The samples were used for the main body of the experiments and are listed in Figure 3.1.2.1 along with the proportions in each blend. Figures 3.1.2.2 and 3.1.2.3 show their compositions. Finally a suite of fuel blends was used in the third set of experiments, to study synergistic effects of leaching as well as high temperature effects on leaching. These fuels were supplied by GENER power station in Chile and their proximate and ultimate analysis is given in Figure 3.1.3.1.

3.1.1 Fuel Set 1 - Samples Used to Verify Validity of Modified TCLP test and Analytical Procedures

A preliminary set of samples was used to carry out combustion experiments via the hot-rod reactor. The purpose of these experiments was threefold; firstly to ensure that the reactor was performing to specification, secondly to ensure that the results obtained for analytical techniques performed on the combustion ashes concurred with previous results. Finally these samples were used, along with standard reference materials for the TCLP test, in order to verify the validity of the test modified for this study. The samples used therefore were samples which had been used by previous operators and experimental parameters were replicated.

Material	Polish Coal	Columbian Coal	Pulp Sludge	Wood/Bark	Bark
Moisture	2.9	3.4	6.5	8.7	3.0
Ash	16.2	12.9	50.6	4.4	6.9
Volatile Matter	-	32.6	35.5	66.8	-
Sulphur	0.9	0.9	0.2	0.2	0.07
Chlorine	0.1	0.06	0.02	0.03	0.01
Carbon	85.0	83.4	43.0	52.8	53.1
Hydrogen	4.8	4.2	4.8	5.3	6.00
Nitrogen	1.2	1.9	0.7	0.7	0.5

Figure 3.1.1.1 Fuel Set 1 – Samples Used To Verify Validity of Analytical Techniques

Polish coal was supplied by Chalmers University, Sweden and is a blend of coal from seams around Krakow, Poland. Columbian coal was supplied by Midkraft, the Danish power station. The pulp sludge was supplied from a paper mill at Grena Denmark whilst

the two wood fuels were supplied by UPM-Kaipola paper mills in Finland. The wood bark mixture was taken directly from the de-barking plant and mixed with spruce wood.

3.1.2 Samples Provided by CERCHAR

The fuels were supplied by the project partners CERCHAR (Centre d'Etudes et de Recherches de la Combustion), France. The fuels fall into three categories: coal alone, coal and secondary fuel blends, secondary fuel blends alone. One of the secondary fuels used is referred to as schlamms. Schlamms is a term used to define fine tailings obtained from coal preparation. Water obtained from de-ashing coal for commercial preparation is decanted and filtered and the high water content residue remaining is referred to as schlamms. The product has a higher ash content than commercial coal and a fine particle size of less than 300 μm.

Fuel No.	Fuel Type	Relative Proportions (Ratio)
1	South Africa Coal 1997	-
2	South Africa Coal 1999	-
3	Freyming Coal Slurry / South Africa Coal 1999	7:3
4	Freyming Schlamms /Freyming Coal Slurry	4:1
5	South Africa Coal 1997 / Wet Saw Dust	3:1
6	Freyming Coal Slurry / Dry Saw Dust	3:7
7	South Africa Coal 1997 /Un-dried Bark	1:3
8	Freyming Schlamms / Freyming Coal Slurry/ Petroleum Coke	2:7:1

Figure 3.1.2.1 Fuels Supplied by CERCHAR & Ratios of Mixtures Used

Fuel No.	1	2	3	4
Material	South Africa Coal 1997	South Africa Coal 1999	Freyming Coal Slurry/South Africa Coal 1999	Freyming Schlamms/Freyming Coal Slurry
Moisture	3.2	5.0	2.4	2.7
Ash	15.9	14.9	40.7	30.5
Volatile Matter	22.3	21.8	17.8	23.3
Sulphur	0.7	0.6	0.6	0.9
Chlorine	0.02	0.03	0.07	0.2
Carbon	66.9	66.7	46.0	54.5
Hydrogen	3.3	3.2	2.4	3.1
Nitrogen	1.6	1.6	1.0	0.7

Figure 3.1.2.2 Proximate and Ultimate Analysis of Fuels Provided by CERCHAR

Fuel No.	5	6	7	8
Material	South Africa Coal 1997/ Wet Saw Dust	Freyming Coal Slurry/Dry Saw Dust	South Africa Coal 1997/ Un-dried Bark	Freyming Schlamms/ Freyming Coal Slurry/ Petroleum Coke
Moisture	5.2	2.5	5.2	2.0
Ash	11.7	38.9	19.0	40.3
Volatile Matter	33.6	20.5	29.2	16.8
Sulphur	0.4	0.5	0.5	1.48
Chlorine	0.03	0.07	0.04	0.1
Carbon	63.4	45.9	55.9	45.6
Hydrogen	3.6	2.6	3.3	2.5
Nitrogen	1.3	1.0	1.2	0.9

Figure 3.1.2.4 Proximate and Ultimate Analysis of Fuels Provided by CERCHAR

3.1.3 Fuels Supplied by GENER Power Station, Chile

GENER provided three sets of coals, namely Kideco, Lemington and Allied, and two sets of blends. The first blend was a blend of Kideco and Lemington whilst the second was Lemington blended with Allied Coal. Each blend was created in ratios of 25-75 50-50 and 75-25. The ultimate analysis of the coals is given below in Figure 3.1.3.1. These

samples were provided as pulverised fuel. Ashes of these fuels were produced in an 135 MW of the power station at a temperature of 1500°C.

The fuels were blended mechanically by measuring the quantities in a flask and rotating the flask for 30 minutes between two rollers at a rate of 150 revolutions per minute. The samples size range, ascertained by sieving, was 106-150 μm.

Material	Kideco Coal	Lemington Coal	Allied Coal
Volatile Matter(% daf)	49.1	45.7	44.1
Ash (% db)	2.1	11.1	11.6
Moisture (%ad)	5.4	1.1	1.1
Carbon (% daf)	70.0	81.1	81.0
Sulphur (% daf)	5.5	5.7	5.5
Hydrogen (% daf)	1.0	1.5	1.6
Nitrogen (% daf)	0.1	2.0	1.5

Figure 3.1.3.1 Proximate and ultimate analysis of fuels provided by GENER, Chile.

3.2 COMBUSTION APPARATUS

In this study ashes from 4 sources were used as follows:

- a hot-rod reactor
- a muffle furnace
- a supension reactor
- power station ash supplied by GENER, Chile

Combustion experiments were carried out in the hot-rod reactor and the muffle furnace and these are described in detail below. Ashes produced in the suspension reactor were supplied by a co-worker, whilst GENER power station also supplied a set of ashes. General characteristics rather than detailed descriptions of the latter two reactors are given

3.2.1 The Hot-Rod Reactor

Use of a hot-rod style reactor was first documented at the U.S Bureaus of Mines in order to study the hyro-pyrolysis of coal by Hiteshue, Andersen and Madden[73,-77] in the early sixties, and subsequently by Finn, Fynes and Ladner[11] at NCB a decade later. The reactor was a tubular reactor which contained the sample between two wire mesh plugs. The reactor acts as both a pressure vessel and an electrical resistance heater. In the above design a flow of gas was passed through the reactor in order to remove the pyrolysis products produced from the reaction zone. The design used in this study was first developed by O'Brien (1986)[79] and then modified by, Gonenc Z. S[81] and Pindoria (1997).[80] The O'Brien design was initially developed to quantify yields of pyrolysis products and temperature was controlled by attaching thermocouples to the external reactor walls. Gonenc added a thermocouple to the inside of the reactor at the sample point, whilst Pindoria's modifications included the control system which was used in this study. A description of the hot-rod reactor may be found below.

3.2.1.1 Reactor Body Construction Material and Specifications

The hot rod reactor is a tubular design and is essentially a rod, 350 mm in length and 10 mm internal diameter. The initial material used by Pindoria was Nimoic 80 A alloy chosen above stainless steel which is liable to undergo creep at temperatures higher than 500°C. This was replaced by Nimonic 105 alloy and subsequently by Incoloy 800 HT. Both these materials are highly resilient to temperatures up to 1050 °C, however the latter is far easier to machine. Therefore the material used in this study was Incoloy 800 HT. Incoloy 800 HT is a wrought nickel-iron-chromium base alloy strengthened by the addition of molybdenum, aluminium and titanium. Its composition may be seen in Figure 3.2.1.1 This material had received an annealing treatment at 1150°C. It is this treatment along with the Incoloy composition which gives the alloy high creep resistance and rupture strength. The maximum allowable pressures was calculated in previous studies to be 57.5 bar, the temperature to not exceed 1000°C and the working life no more than 1000 hours of operation.

Element	% w/w
Ni	30.0-35.0
Cr	19.0-23.0
Fe	39.5 min
C	0.1 max
Mn	1.5 max
Si	1.0 max
S	0.015 max
Cu	0.75 max
Al	0.15-0.6
Ti	0.15-0.6

Figure 3.2.1.1 Chemical Composition of Incoloy 800 HT alloy

The fittings used to connect the various parts of the reactor were Swagelock Stainless Steel 316. The main reactor length was increased to 350 mm from 250 mm in order to keep these fittings away from the hottest part of the reactor, as they are not temperature resistant above 500°C and exhibited the tendency to become welded to the reactor.

The elemental content in the reactor construction material, shown in Figure 3.2.1.1 affords the potential for contamination of the ash produced. As it is the trace element content in the ash produced which was to be determined, it was necessary to isolate the reactor walls from the sample fuel undergoing combustion. This was done by the insertion of a quartz tube, internal diameter 6mm, into the reactor. A Saffil kaowool plug (high quality quartz wool) was placed in the centre of the quartz tube in order to hold the sample in place. In order to prevent gas seepage from around the edges of the quartz reactor a spring was placed inside the top of the tee to seal the perimeter of the reactor. Figure 3.2.1. is a schematic of the hot-rod reactor showing all the main components, along with the quartz lining and sample placement.

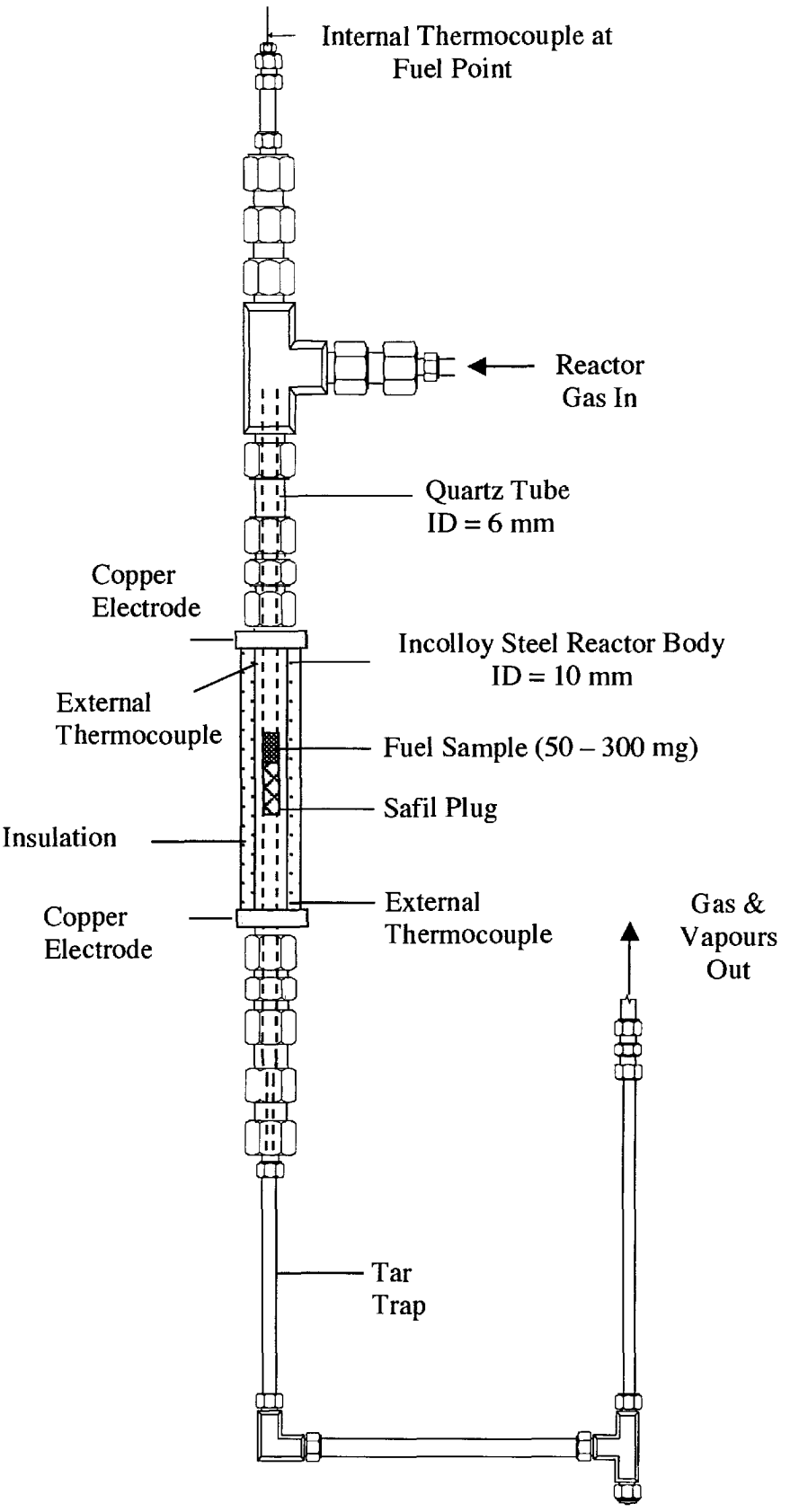


Figure 3.2.1.2 Schematic of the Hot-Rod Reactor, Kaowool Lining and Sample Placement

3.2.1.2 Reactor Gas Circuit

The gas supply circuit to the reactor was designed by O'Brien[12] and modified to suit the individual requirements of subsequent operators. The gas used first fills a buffer tank, which ensures a steady flow through the reactor system with minimal disturbance. A bursting disk is mounted on the buffer tank for safety. Two automatic valves are set up along the circuit, controlled electronically and operating on compressed air. The compressed air is switched off, in cases of over-pressure, thus venting the gas supply through the system. In the case of the combustion experiments carried out in this study the operating pressure was 2.6 bar. This was because the target experiment pressure was atmospheric pressure and the pressure drop throughout the system was 1.6 bar. A pressure gauge situated very close to the reactor gave accurate pressure measurements, whilst a needle valve and calibrated rotameter are used to control gas flow. Figure 3.2.1.3 below depicts a schematic of the gas supply circuit.

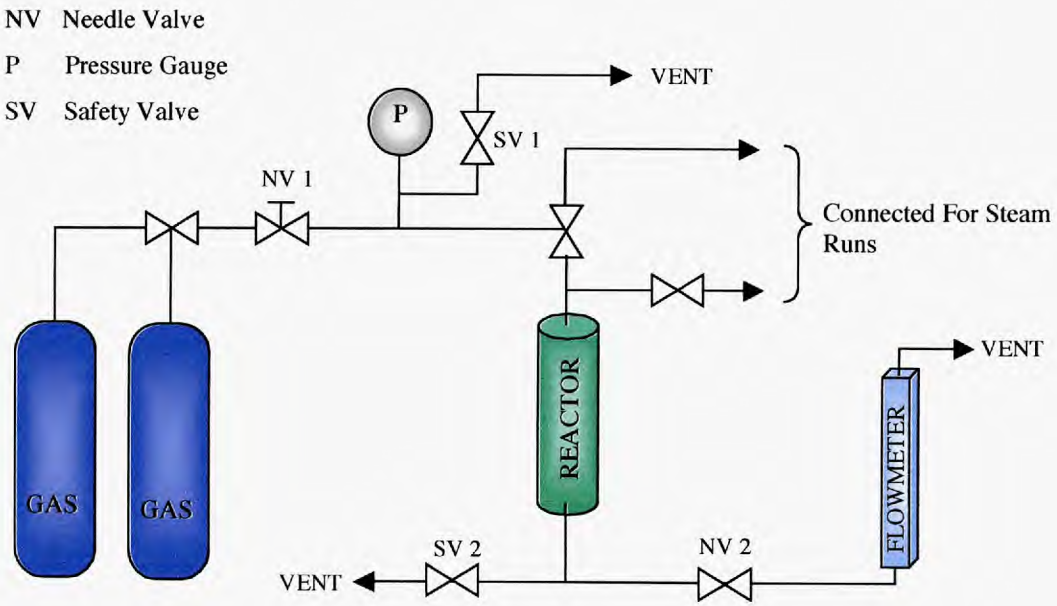


Figure 3.2.1.3 Gas Supply Circuit For Hot-Rod Reactor

3.2.1.3 Heating and Temperature Control System

Energy is supplied to the reactor via two water cooled copper electrodes, which are clamped in place to the reactor wall. The sample is placed equidistantly between the two electrodes. Temperature is measured via two external thermocouples placed at the extremities of the reactor body, just above the electrodes, as shown in Figure 3.2.1.4 below. The external thermocouples are placed directly on the reactor wall and the reactor is insulated, although for clarity this is not depicted in the figure. An other thermocouple exists inside of the reactor at the sample point.

O'Brien's design of control system consisted of a Newbrain Model, A microcomputer with an MFI data logger, used for driving the reactor temperature. The data logger sent a signal to a thyristor which in turn fired two high output transformers. The transformers were capable of delivering up to 1000 A at 2.5 V. Pindoria modified the system to incorporate a DOS based system. An Intel based 486 SX20 microcomputer with a PC30AT digital to analogue/analogue to digital card is now used for the data acquisition and control[80].

The software for temperature control was written in Turbo Pascal 6.0. As a high level language, Turbo Pascal is capable of communicated with most of the hardware directly, therefore allowing a fast response. The timing for the control program is provided by the mains power source operating at 50 Hz (50 Hz mains synchroniser). Temperature readings are recorded and plotted at 0.1s intervals. The controlling of the temperature is programmed to be at every 1s interval. Figure 3.2.1.5 shows is an over view of the control program. The programme can be terminated at any point if an unexpected even occurs, and at various stages in the program, sub routines are present to ensure that the temperatures and power output are in the operating range[81].

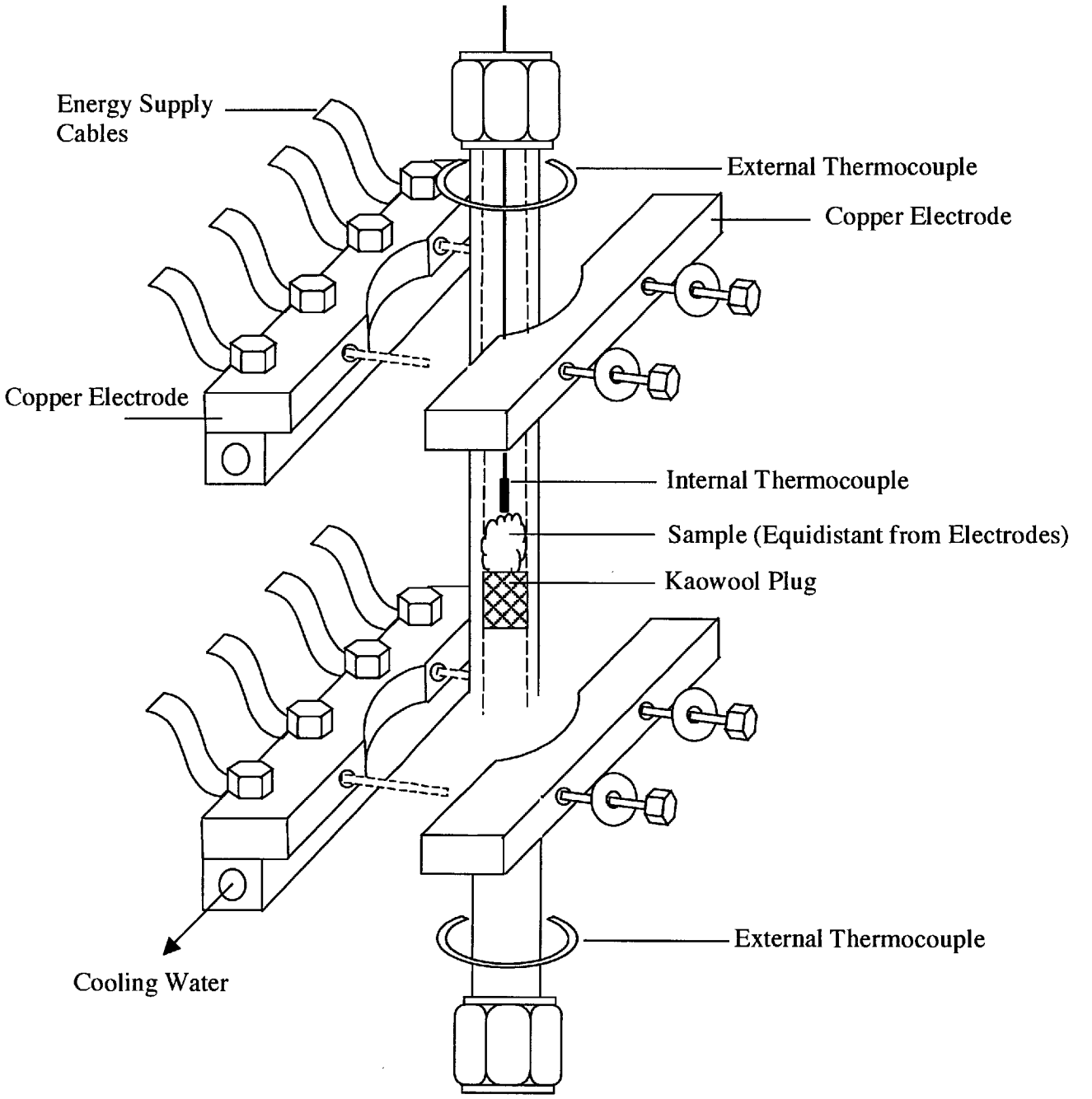


Figure 3.2.1.4 Hot-Rod Reactor Thermocouples and Heating Elements

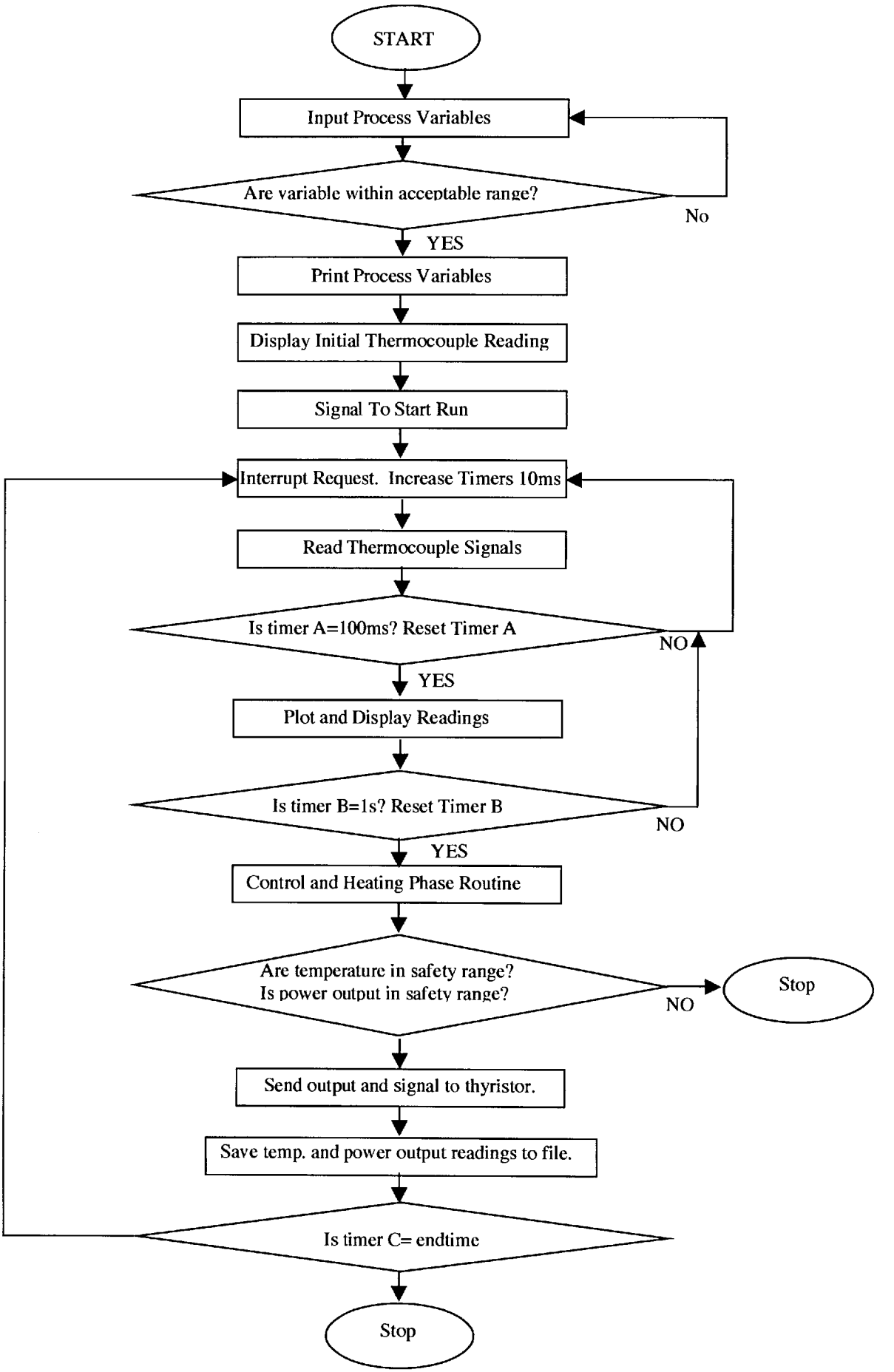


Figure 3.2.1.5 Overview of reactor control programme.

3.2.1.4 Hot-Rod Operating Parameters Used and Reactor Output

The experiments carried out using the hot-rod reactor were combustion experiments on the Fuel Set 1 and on the fuels supplied by CERCHAR. Figure 3.2.1.6 below shows typical operating parameters for the experiments conducted, and the range of parameters which the reactor is capable of operating within.

OPERATING PARAMETER	RANGE	TYPICAL VALUES USED
Sample Mass	50 – 300 mg	100 mg
Temperature	< 1050 °C	850 & 950 °C
Pressure	75 Bar Max	2.6 bar (ΔP = 1.6 bar)
Heating Rate	100 Ks^{-1}	10 Ks^{-1}
Sweep Velocity	0 – 0.3 ms^{-1}	0.1 ms^{-1}
Temperature Hold Time	-	100 s

Figure 3.2.1.6 Hot-rod Reactor Operating Parameters

As depicted in the control diagram in Figure 3.2.1.5 once an experiment is ready the operator is asked for the input variables. These variables, shown in Figure 3.2.1.6 are the temperature, pressure, heating rate, sweep velocity and temperature hold time. The pressure is controlled manually. If the variables are within the acceptable range the operator signals the run to commence. Thermocouple signals are read ever 10 ms, and readings displayed and plotted. The control and heating routine commences, until the hold time stipulated has elapsed, or in the event that the power and temperature exceeds safety limits. If the run has been completed correctly the out put signals are sent to the thyristor and the temperature and output readings are saved to file. The procedure is thus complete. Figure 3.2.1.7. below is a representation of the output file produced in a combustion run, indicating the temperature and power profiles with time.

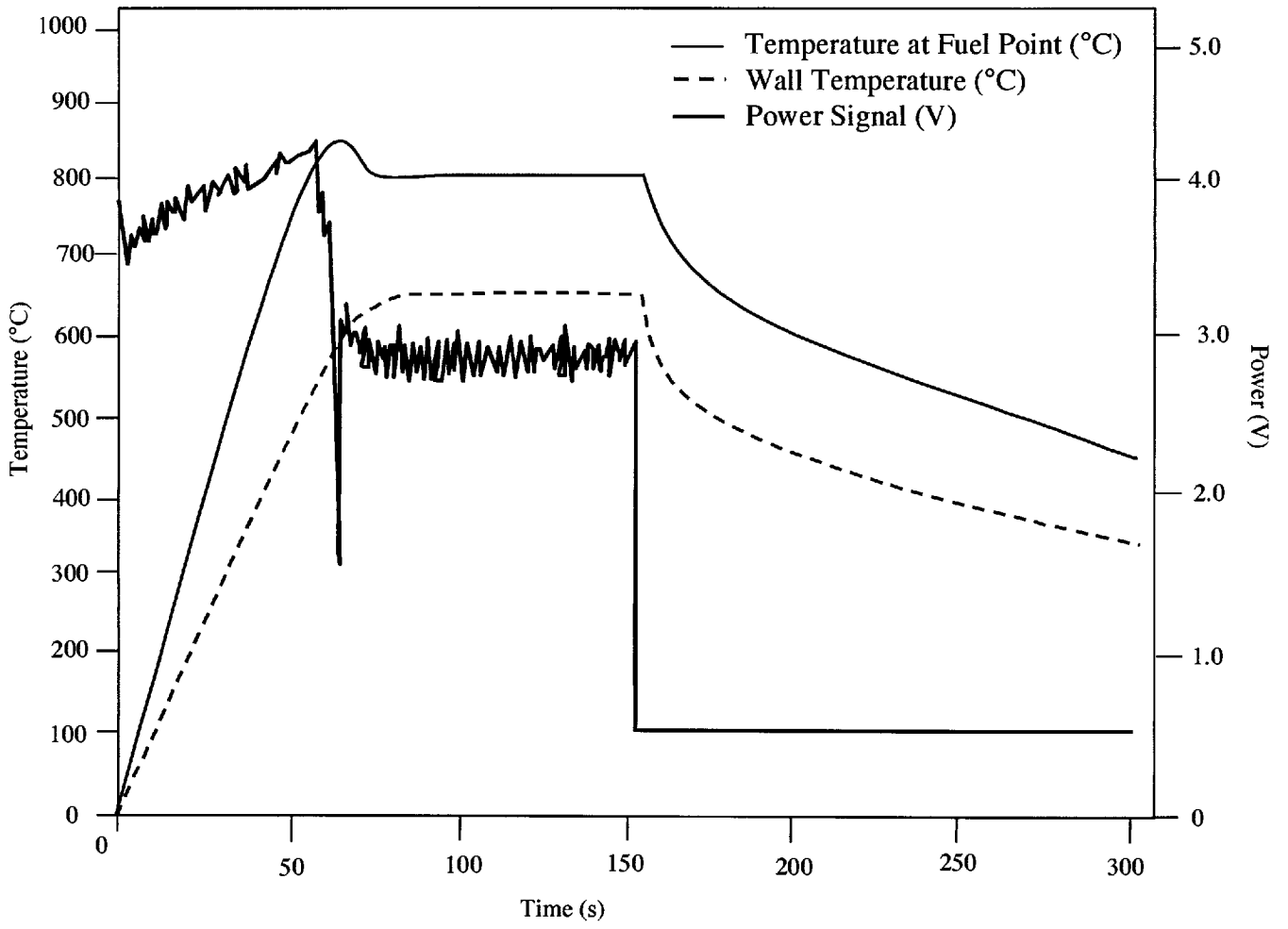


Figure 3.2.1.7 Temperature & Power Output From Typical Hot-Rod Combustion Run

3.2.2 The Muffle Furnace

The experiments carried out in the Hot-rod Reactor were replicated in a muffle furnace, operated at atmospheric pressure and the same temperatures as the fixed bed reactor. This was in order to ascertain weather results obtained were a function of reactor type. It was possible to have sample sizes as large as 2 g undergoing combustion in the furnace. The absence of a gas flow in the muffle furnace is the main difference between the two reactors used. However, sample heating rate also varied, being 1 Ks^{-1} in the muffle furnace and 10 Ks^{-1} in the hot-rod reactor.

3.3 LEACHING EXPERIMENTS

3.3.1 The Toxicity Characteristic Leaching Procedure (TCLP)

Below follows a description of the standard TCLP method as designed by the US-EPA[82]. This method was modified in order to enable the leaching of samples sizes of 100 mg. Therefore the method is firstly described in its entirety, without taking account any of the modifications made in this study or of points which are not pertinent to this study. The modified method used in this study followed the theory of the standard procedure and the modifications made are described in section 3.3.2.

For liquid wastes (i.e., those containing less than 0.5% dry solid material), the waste, after filtration through a 0.6 to 0.8 μm glass fiber filter, is defined as the TCLP extract.

For wastes containing greater than or equal to 0.5% solids, the liquid, if any, is separated from the solid phase and stored for later analysis; the particle size of the solid phase is reduced, if necessary. In this instance the waste is combustion ash and is therefore entirely in the solid phase. The solid phase is extracted with an amount of extraction fluid equal to 20 times the weight of the solid phase. The extraction fluid employed is a function of the alkalinity of the solid phase of the waste. A special extractor vessel is used when testing for volatile analytes. Following extraction, the liquid extract is separated from the solid phase by filtration through a 0.6 to 0.8 μm glass fibre filter.

If compatible (i.e., multiple phases will not form on combination), the initial liquid phase of the waste is added to the liquid extract, and these are analyzed together. If incompatible, the liquids are analyzed separately and the results are mathematically combined to yield a volume-weighted average concentration.

Potential interferences that may be encountered during analysis are discussed in the individual analytical methods.

3.3.1.1 Apparatus and Materials

Extraction Vessels

The agitation apparatus must be capable of rotating the extraction vessel in an end-over-end fashion (see Figure 1) at 30 + 2 rpm.

Zero-Headspace Extraction Vessel (ZHE).

This device is for use when the waste is being tested for the mobility of volatile analytes. The ZHE allows for liquid/solid separation within the device, and effectively precludes headspace. This type of vessel allows for initial liquid/solid separation, extraction, and final extract filtration without opening the vessel. The vessels must have an internal volume of 500-600 mL, and be equipped to accommodate a 90-110 mm filter. The devices contain O-rings which should be replaced frequently. For the ZHE to be acceptable for use, the piston within the ZHE should be able to be moved with approximately 15 psi or less. If it takes more pressure to move the piston, the O-rings in the device should be replaced. If this does not solve the problem, the ZHE is unacceptable for TCLP analyses and the manufacturer should be contacted.

The ZHE should be checked for leaks after every extraction. If the device contains a built-in pressure gauge, the device must be pressurised to 50 psi, allowed to stand unattended for 1 hour, and the pressure reassessed. If the device does not have a built-in pressure gauge, the device must be pressurised to 50 psi, submerged in water, and checked for the presence of air bubbles escaping from any of the fittings. If pressure is lost, fittings must be inspected and O-rings replaced, if necessary.

Bottle Extraction Vessel.

When the waste is being evaluated using the non-volatile extraction, as in this case, a receptacle with sufficient capacity to hold the sample and the extraction fluid is required. Headspace is required in this vessel and should not be less than 40% volume.

The extraction vessel may be constructed from various materials, depending on the analytes to be analyzed and the nature of the waste. It is recommended that borosilicate glass bottles be used instead of other types of glass, especially when inorganics are of concern. In this instance polytetrafluoroethylene (PTFE) conical test tubes were used.

Filter Holder

When the waste is evaluated for other than volatile analytes, any filter holder capable of supporting a glass fibre filter and able to withstand the pressure needed to accomplish separation may be used. Suitable filter holders range from simple vacuum units to relatively complex systems capable of exerting pressures of up to 50 psi or more. The type of filter holder used depends on the properties of the material to be filtered. These devices shall have a minimum internal volume of 300 mL and be equipped to accommodate a minimum filter size of 47 mm (filter holders having an internal capacity of 1.5 L or greater, and equipped to accommodate a 142 mm diameter filter, are recommended). Vacuum filtration can only be used for wastes with low solids content (<10%) and for highly granular, liquid-containing wastes. All other types of wastes should be filtered using positive pressure filtration. The above parameters were modified for the small sample masses used in this study as described in Section 3.3.2.

Materials of Construction

Extraction vessels and filtration devices should be made of inert materials which do not leach or absorb waste components, or in any way contaminate the analyte. Glass, polytetrafluoroethylene (PTFE), or type 316 stainless steel equipment may be used when

evaluating the mobility of both organic and inorganic components. Devices made of high density polyethylene (HDPE), polypropylene (PP), or polyvinyl chloride (PVC) may be used only when evaluating the mobility of metals. Borosiliúcate glass bottles are recommended for use over other types of glass bottles, especially when inorganics are analytes of concern.

Filters

Filters should be made of borosilicate glass fiber, shall contain no binder materials, and shall have an effective pore size of 0.6 to 0.8 μm, or equivalent. Pre-filters should not be used. When evaluating the mobility of metals, filters should be acid-washed prior to use by rinsing with 1N nitric acid followed by three consecutive rinses with deionized distilled water (a minimum of 1 L per rinse is recommended).

pH Meters

The meter should be accurate to + 0.05 units at standard conditions and must not contaminate the analyte. In this study a Technika 8400 series micro pH meter was used, accurate to 0.01 pH units. The probe diameter of 5 mm was suitable for the narrow aperture of the extraction vessels.

If a waste contains an aqueous liquid phase or if a waste does not contain a significant amount of nonaqueous liquid (i.e., <1% of total waste), a 600 mL syringe should be used to collect and combine the initial liquid and solid extract.

If the waste contains no initial liquid phase (is 100% solid) or has no significant solid phase (is 100% liquid), the 600 ml syringe may be used. If the syringe is used, discard the first 5 mL of liquid expressed from the device. The remaining aliquots are used for analysis.

ZHE Extraction Fluid Transfer Devices: Any device capable of transferring the extraction fluid into the ZHE without changing the nature of the extraction fluid is acceptable (e.g., a positive displacement or peristaltic pump, a gas tight syringe, pressure filtration unit)

Laboratory Balance: Any laboratory balance accurate to within + 0.01 grams may be used (all weight measurements are to be within + 0.1 grams). In this study a balance accurate to 0.001 grams was used.

3.3.1.2 Reagents

Reagent grade chemicals (ARISTAR) should be used in all tests. Other grades may be used, provided it is first ascertained that the reagent is of sufficiently high purity to permit its use without lessening the accuracy of the determination. In this study glacial acetic acid (1N), CH3CH2OOH, was used.

Reagent water is defined as water in which an interferant is not observed at or above the method's detection limit of the analyte(s) of interest. For non-volatile extractions, as in this case distilled deionised water (milli-Q micropore grade) was used throughout.

Extraction fluid.

To prepare the extraction fluid 5.7 mL glacial CHCH2OOH was diluted with reagent water to a volume of 1 litre. When correctly prepared, the pH of this fluid will be 2.88 + 0.05. If the pH deviates from this value, the solution contains impurities or was incorrectly made and must be freshly prepared.

3.3.1.3 Sample Collection Preservation and Handling

The TCLP places requirements on the minimal size of the field sample, depending upon the physical state or states of the waste and the analytes of concern. A minimum sample size of 100 g is stipulated. An aliquot is needed for preliminary evaluation of which

extraction fluid is to be used for the nonvolatile analyte extraction procedure. Another aliquot may be needed to actually conduct the nonvolatile extraction. Quality control measures may require additional aliquots

Preservatives should not be added to samples before extraction. Samples should be refrigerated unless refrigeration results in irreversible physical change to the waste. If precipitation occurs, the entire sample (including precipitate) should be extracted.

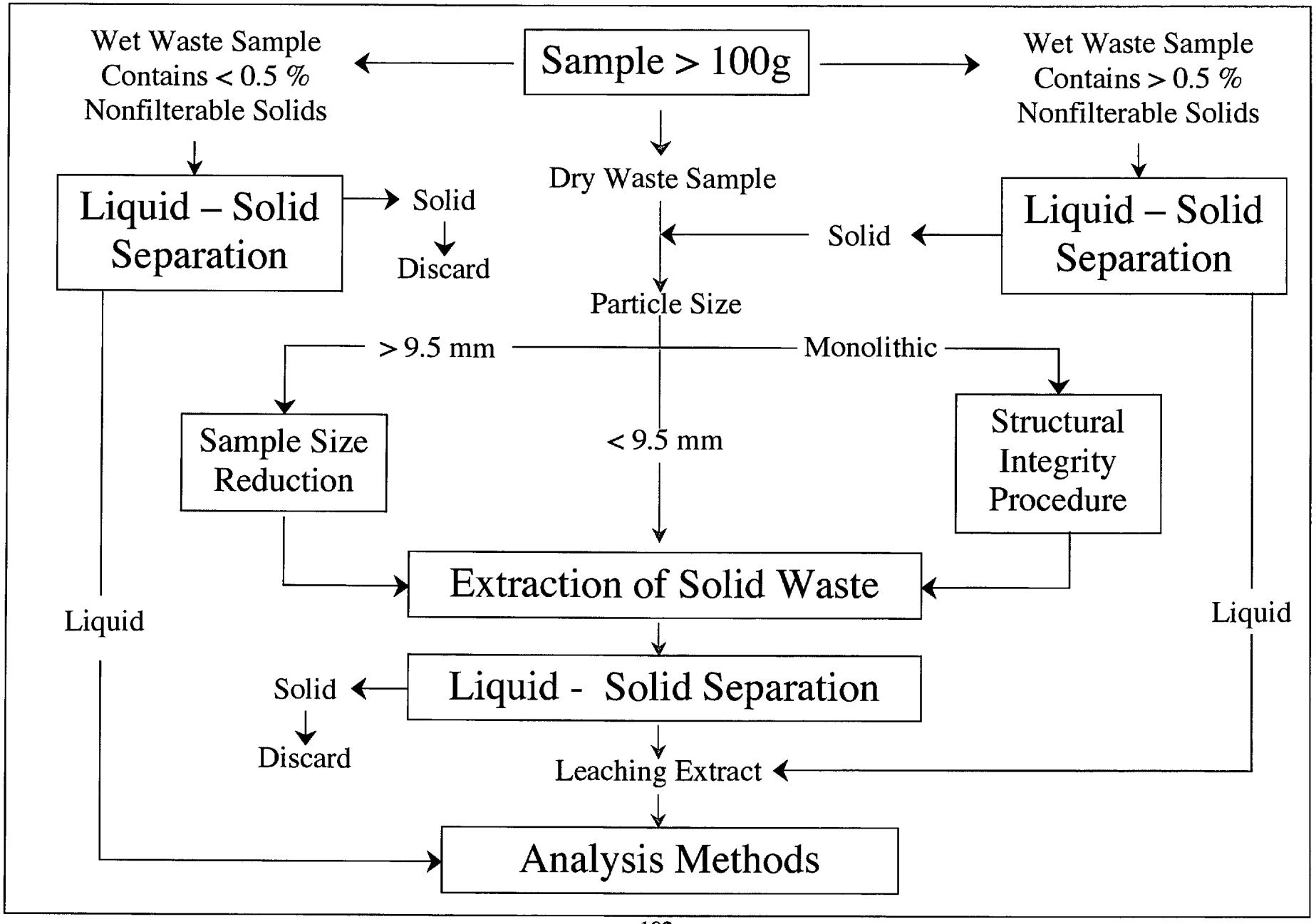
When the waste is to be evaluated for volatile analytes, care should be taken to minimize the loss of volatiles. Samples must be collected and stored in a manner intended to prevent the loss of volatile analytes. Samples should be opened only immediately prior to extraction).

TCLP extracts should be prepared for analysis and analyzed as soon as possible following extraction. Extracts or portions of extracts for metallic analyte determinations must be acidified with nitric acid to a pH < 2, unless precipitation occurs. Extracts or portions of extracts for organic analyte determinations shall not be allowed to come into contact with the atmosphere (i.e., no headspace) to prevent losses..

3.3.1.4 Procedure

The following section describes the procedure followed. The entire procedure may be represented by the flow diagram in Figure 3.3.1. The red line in the figure depicts the method followed for this study.

Figure 3.3.1 Flow Diagram of US – EPA TCLP Test Procedure[82]



Preliminary Sample Evaluation

Preliminary TCLP evaluations on a minimum 100 gram aliquot of waste must be performed. This aliquot may not actually undergo TCLP extraction. These preliminary evaluations must include:

- determination of the percent solids
- determination of whether the waste contains insignificant solids and is, therefore, its own extract after filtration
- determination of whether the solid portion of the waste requires particle size reduction

Preliminary determination of percent solids

Percent solids is defined as that fraction of a waste sample (as a percentage of the total sample) from which no liquid may be forced out by an applied pressure, as described below. If the waste will obviously yield no liquid when subjected to pressure filtration (i.e., is 100% solids) no pre-filtration is required. If the sample is liquid or multiphasic, liquid/solid separation to make a preliminary determination of percent solids is required. This involves the filtration method described below.

- Pre-weigh the filter and the container that will receive the filtrate.

- Assemble the filter holder and filter following the manufacturer's instructions. Place the filter on the support screen and secure.

- Weigh out a subsample of the waste (100 gram minimum) and record the weight.

- Allow slurries to stand to permit the solid phase to settle. Wastes that settle slowly may be centrifuged prior to filtration. Centrifugation is to be used only as an aid

to filtration. If used, the liquid should be decanted and filtered followed by filtration of the solid portion of the waste through the same filtration system.

- Quantitatively transfer the waste sample to the filter holder (liquid and solid phases). Spread the waste sample evenly over the surface of the filter. If filtration of the waste reduces the amount of expressed liquid over what would be expressed at room temperature then allow the sample to warm up to room temperature in the device before filtering.

- Gradually apply vacuum or gentle pressure of 1-10 psi, until air or pressurising gas moves through the filter. If this point is not reached under 10 psi, and if no additional liquid has passed through the filter in any 2 minute interval, slowly increase the pressure in 10 psi increments to a maximum of 50 psi. After each incremental increase of 10 psi, if the pressurising gas has not moved through the filter, and if no additional liquid has passed through the filter in any 2 minute interval, proceed to the next 10 psi increment. When the pressurising gas begins to move through the filter, or when liquid flow has ceased at 50 psi (i.e., filtration does not result in any additional filtrate within any 2 minute period), stop the filtration.

- Determine the weight of the liquid phase by subtracting the weight of the filtrate container from the total weight of the filtrate-filled container. Determine the weight of the solid phase of the waste sample by subtracting the weight of the liquid phase from the weight of the total waste sample, as determined previously.

- Record the weight of the liquid and solid phases. Calculate the percent solids.

- Remove the solid phase and filter from the filtration apparatus.

- Dry the filter and solid phase until two successive weighing yield the same value within + 1%. Record the final weight.

3.3.2 MODIFIED TCLP

3.3.2.1 TCLP Method For Small Sample Masses

The general procedure followed is shown in the flow diagram in Figure 3.3.1 The red line indicates the procedure relevant for the samples in this study which effectively involved four steps:

- Particle size determination of ash
- Extraction of ash using the appropriate leaching apparatus
- Solid-liquid separation
- Leachate Analysis

This modified procedure conforms to the theory of the TCLP procedure, which has remained unaltered, and the apparatus and materials used are described in the previous section. It does deviate in the manner in which the four stages of the test are practically carried out as described below.

Each combustion experiment in the hot-rod reactor produced approximately 10 mg of ash, depending on the fuel, so 12 combustion experiments were carried out in order to obtain sufficient ash for one leaching experiment. The ashes produced from each combustion run were mixed together thoroughly in order to produce one sample. The muffle furnace produced 1 g of ash per experiment, so enough matter was present for several leaching runs.

To carry out the TCLP test, first a mass of ash sample of 100 mg is taken. and added to receptacle which was of the correct size to allow for a void space of at least 60% and which could later be centrifuged. In this instance a 10 ml conical based PTFE test tube was used. 1M acetic acid is made and 2 ml added to the ash as the extraction fluid, so that the solid to liquid ratio is 1:20 and the pH of the mixture is 2.88 ± 0.05. The mixture is then agitated in an overhead extractor, shown in Figure 3.4 at a rate of 30 revolutions

per minute for 18 hours. After this period of time, 3 ml of 10% nitric acid is added to the leachate in order to increase the volume available for ICP-MS analysis, reduce the error involved in separating the solid from the liquid phase and to create a correctly acidified environment for introduction to the ICP-MS apparatus. The pH of this solution is checked to be less than 2.00. The sample is then centrifuged at 1500 rev/min for 3 mins to separate the liquid from the solid phases and allow the liquid phase to be syringed off. This liquid phase is then further filtered and is refrigerated until ICP-MS analysis. Samples were prepared such that no more than 24 hours passed before a prepared sample and its introduction into the ICP-MS apparatus.

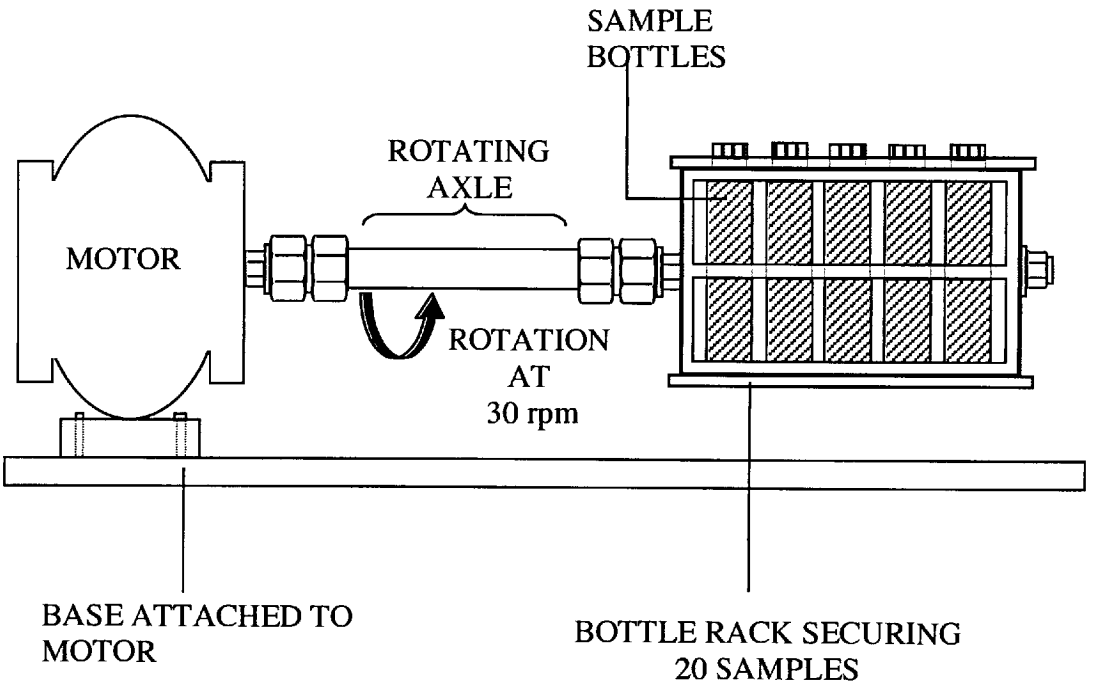


Figure 3.3.2 Agitator Designed to Carry Out Leaching

3.3.2.2 Verifying the validity of the modified test

In order to ascertain if the above method was valid for the small sample sizes used, experiments were first carried out using the standard reference material produced for the TCLP test. Two standard reference materials are provided with stipulated quantities of trace element content. If the TCLP method is carried out correctly then the trace element quantity in the leachate would be a fixed amount. The modified TCLP tests was carried out with smaller masses and altered apparatus as described above using the standard reference materials. If the trace element quantity leached was the same for the modified test as that for the standard TCLP method, using these reference materials then it could be deduced that the test for smaller samples was valid. The standard reference materials used were combustion ashes EPA RM-203 and EPA RM-205.

Ashes were also leached using the standard TCLP method at 100g, and these same ashes were leached using the modified TCLP test at 100 mg. Concurrence of results could therefore also show that the modified test could be carried out at 100 mg. The samples used in this instance were polish coal ash, wood bark and pulp sludge, produced in a muffle furnace.

Smaller sample sizes of 50 mg and 10 mg were also attempted but variance in results indicated that the smallest samples size to yield reliable data was in the 100 mg range. This is described in greater detail in the results section of this study.

3.4 ANAYLTICAL TECHNIQUES

The trace element content in the fuels was measured using ICP-MS for all elements other than mercury, where the spectrophotometric method described below was used. For ICP-MS analysis the analyte must be in solution therefore the ash must be first undergo digestion. This is achieved via two methods, an open and a closed digestion method.

3.4.1 Wet-Ashing Digestion Method

Raw fuels and ashes are treated slightly differently in this method. Raw fuels first undergo an initial ashing followed by a digestion of the resulting ashes. The basis of the method for raw fuels is as follows:

- 10 mg of sample is placed in a platinum crucible and 100 µl of concentrated sulphuric acid (98% w/w) added and placed on a hot plate at 150 °C for 3 hours. The sulphuric acid reacts with the organometallic links in the sample to form sulphate salts and the organic compounds are removed as CO_2. The samples are the placed over night in a muffle furnace at 500 °C leaving a completely ashed sample by the end of the procedure.

- 300µl of perchloric acid (60% w/w) and 500 µl hydrofluoric acid (40% w/w) were added to the remaining residue and the crucible heated for approximately 45 mins to incipient dryness, such the all the HF is removed as gas and all the Cl ions as HCl gas, as these would be deleterious to the ICP-MS analysis. This process dissolves the refractory silicates in the ash.

- The dry residue remaining in the crucibles was then dissolved by reheating in 2% nitric acid (made up from 69 %w/w) which was the background matrix required for ICP-MS and the final analyte made up to 10 ml.

A 10% solution of nitric acid was preferable for solution stability however this would require redilution for introduction into the ICP-MS and the trace element concentration in the analyte would be excessively reduced.

Ashes from combustion experiments were digested following the same method but omitting the initial, redundant, ashing step and by adding a 10% solution of nitric acid to maintain a stable solution. Each time a batch of digestions was performed a certified standard reference material was also included to verify the lack of error in the experimental procedure and accuracy of results. In order to identify contamination of the prepared samples, a blank sample is also produced in each experimental batch, which is treated in exactly the same way as the other samples but contains no ash or fuel. In this way any error from trace elements present due to reagent contamination may be eliminated by subtracting the spectrum of the blanks from that of each sample in the ICP MS analysis.

3.4.2 Microwave Digestion Method

This method developed for small masses is designed to prevent the escape of the more volatile elements and is described below:

- 10 mg of sample is placed in a 7ml PTFE vessel, and 1 ml of concentrated nitric acid is added. This vessel is closed loosely and introduced into a 120 ml vessel. 10 ml of nitric acid is added to this vessel to maintain pressure and this is sealed and placed on a carousel capable of containing 10 such vessels. The carousel is placed in a microwave oven, in this instance an MLS-1200 Milestone model. The samples are then subjected to a heating programme which is dependent upon the nature of the sample.

- Once the heating programme is completed and the samples have undergone 5 mins of ventilations the carousel is cooled at -18°C for 1 hour to minimize loss of volatiles upon opening.

- Final the sample is poured into 10 ml volumetric flasks and made up to 10 ml. It is then further filtered to eliminate undissolved mineral matter which, if introduced to the ICP-MS, would clog the nebuliser and extinguish the plasma.

As with the wet ashing method, each time a batch of samples undergoes a microwave digestion, a standard reference material of the same nature as the samples, and a blank sample, are produced.

3.4.3 Mercury Analysis

During combustion, it is estimated that between 79 and 87 % of mercury is emitted in the flue gas. It is not possible to measure mercury content in the remaining ash using ICP-MS as any mercury not volatilised during the combustion process is lost during the ash digestion methods. It is therefore measured directly using a dedicated analyser via the "LECO AMA 254" mercury analyser. The instrument allows the analysis of solid as well as liquid samples, without pre-treatment, via a spectrophotometric method, based on the fact that mercury absorbs at a wavelength of 254 nm. The premise of the method is combustion and decomposition of the sample causing mercury to be released and trapped on a gold amalgam. The mercury is subsequently released and absorption at 254nm measured through two consecutive cells.

3.4.3.1 Procedure

The LECO AMA 254 instrument releases the mercury from the sample via thermal decomposition in oxygen, where a catalytic stage ensures complete oxidation of combustion products. The gaseous combustion products then flow over a gold amalgamator to an exhaust, whilst the mercury is trapped on the amalgam. The amalgamator, which is surrounded by a heating coil, is then heated to enable thermal release of the mercury for quantitative detection. This is achieved using a spectrophotometer and passing the mercury through a two cell chamber. The absorbance

at 254 nm was measured in the first cell and if this exceeded 0.8 AU, the second cell was also used.

A known mass of sample, typically 100 mg is placed in a nickel crucible and introduced, using a mechanical arm, into the reactor. Oxygen flows through the reactor at 2 bar (to allow a pressure drop of 1 bar) and the sample undergoes a thermal programme of four stages:

- a drying phase to remove moisture and volatile compounds
- a combustion decomposition phase
- a phase whereby all the mercury and combustion products are swept from the reaction chamber through the catalyst bed to the gold amalgamator
- a thermal desorption phase where the mercury is released from the gold amalgamator and flows through the test cells for quantification

Typical times for the first three stages above are 100, 180 45 seconds respectively but these may be altered according the sample. As with the other analytical techniques a certified reference material is used at the beginning and end of each batch run to verify accuracy of results and a blank run with no sample in the crucible is made in between each sample run to correct for background levels.

The lower detection limits were considered to be 0.05ng Hg, with quantification limits of 4-5 ng. With a special preconcentration programme, the above technique can determine concentrations as low as 6-7 ppb.

3.4.4. Inductively Couple Plasma-Mass Spectrometry

3.4.4.1 Theory and Instrumentation

Plasma has been described as the fourth state of matter and is a highly ionised substance, existing at very high temperatures; the sun is in an example of a plasma. The atoms present in the plasma state are nearly all fully ionised and the substance consists of electrons and atomic nuclei. An inductively coupled plasma is an electrodeless discharge in a gas at atmospheric pressure, maintained by energy coupled to it from a radio frequency generator.

ICP-MS was developed from the work of Gray (1975) who showed that isotope ratios can be ascertained when a solution is introduced into a d.c. plasma (DCP) at atmospheric pressure and the ions formed are extracted into a mass spectrometer, yielding good detection limits. However in a DCP significant interferences occur and for elements with an ionization energy above 9eV a low ion yield is obtained. Houk and co-workers therefore began investigations into an inductively coupled system which proved to greatly improve the ion yield (1980), and the first commercially available ICP-MS was launched a decade later.[83]

In ICP-MS the sample is introduced into the plasma in a stream of argon as an aerosol obtained by pneumatic nebulisation of the solution. The argon stream punctures the plasma, forming a channel where atomisation and ionization take place. Ions are obtained 10 mm from the induction coil where the ionization temperature is 7200-7500°C. Figure 3.4.4.1 shows the sample aerosol and temperature profile in the plasma region.

At this temperature more than 50 elements are more than 90% ionized to the M^+ state. The ionization of metal atoms in a plasma ($M \leftrightarrow M^+ + e^-$) may be described by the Saha equation, where the ionization constant is given by:

$$K_i = \frac{n_{M^+} + n_e}{n_M}$$

where: n_e = Number of free electrons per cm^3

n_{M+}= Number of M^+ ions per cm^3

n_M = Number of M atoms per cm^3

and is given by:

$$K_i = 4.83 \times 10^{15} T^{3/2} \frac{Z_{M^+}(T)}{Z_M(T)} \exp\left[-\frac{E_{ion}}{kT}\right]$$

where Z_M and Z_{M+} are partition functions for the atomic and ionic states respectively i.e. the weighted sum of the number of energy states available given by:

$$Z(T) = \sum_{i=0}^{\infty} g_i e^{-E_i/kT}$$

where: g_i=statistical weight of the i-th level (2J+1)

J = Total angular moment quantum number

T = Absolute temperature

E_i= Ionisation energy (EV)

The ions are then extracted from the plasma at atmospheric pressure to the mass spectrometer which requires a vacuum less than 10^{-5} mbar. This is done via a water cooled, high conductivity nickel cone placed directly in the ICP with a 1mm sampling orifice at its top. The pressure differential carries the gas through the cone along with the ions. This supersonic jet then passes through a hole in a second cone, a skimmer, (set 7mm from the primary cone) into the vacuum. In this way the mean free path is long enough to allow extraction and focusing of the ions by electrostatic lenses.

The ion stream then passes through a lens assembly. Firstly an electrostatic lens (extraction diode) extracts positive ions which are then transported to supsequent lenses. This is done via a negative voltage. Any negative ions are replled and neutral particles diffuse to a vacuum pump. A metal disc is then set in place to prevent photons and energetic neutral species from escaping the plasma to the detector. The lens assembly conducts the ions around the photon stop from the second vacuum stage into a third vacuum (10^{-6}mbar) and into the mass spectrometer where ions of the selected mass to charge ratio are transmitted.

The ICP-MS analyses in this study were performed using a PQ 2+ STE instrument from Fisons Instruments. It was equipped with a Galan V-groove nebuliser and a Gilson Minipuls 3 peristaltic pump. A standard Pentium II PC provided overall system control.

3.4.4.2 Procedure and Operating Conditions

All the samples taken for ICP-MS analysis were acidified to 10% nitric acid in order to stabilise the solution and prevent trace element escape. The ICP-MS instrument required a 2% HNO_3 concentration therefore the samples were diluted prior to analysis. Dilution of the sample was also useful in order to prevent ionisation suppression and enhancement effects. These effects are exhibited as some of the elements which are easily ionised, such as Na and Al, will occur at too high a concentration. This has the effect of highly increasing the electron density in the plasma, causing the ionisation equilibrium to shift. This, in turn, causes the analyte elements to be ionised to a lesser extent. ICP-MS results required correction for this dilution using a dilution factor (DF) parameter defined as follows:

$$DF = \frac{V_s D}{M_s}$$

where: V_s = Volume of Sample (ml)

D = Dilution Multiple

M_s = Mass of Sample (g)

Once the ICP-MS instrument has been set up blank runs are made. The blank sample matrix consists of a solution of all the reagents used in preparing the experimental samples, in the same proportion with out containing the substance requiring analysis. In this way interferences from the reagents added during sample preparation could be eliminated. In this instance the blank analyte was a 2% nitric acid solution and five blank sample runs were conducted. Following the sample blanks, standard multi-elemental solutions were analysed to calibrate the instrument. These solutions were at concentrations of 1, 5, 10, 20 and 100 ppb and three runs of each was made.

Runs of the experimental samples could then be made. Each sample was analysed three times and the mean of the three runs taken as the final result. Each sample run was consisted of 45 seconds of uptake, for the sample to reach ionization, 90 seconds of analysis followed by 60 seconds of "washing" the system with a 2% HNO_3 wash solution, before the next sample could be introduced. After each set of 5 sample runs the 10 ppb multi element solution was introduced in order to correct for signal drift. This is because the signal weakens over the period of analysis, lowering the element count.

Figure 3.4.4.5 below show the typical operating parameters for the ICP-MS runs undertaken in this study. Figure 3.4.4.6 indicates the parameters related to data acquisition whilst Figure 3.4.4.7 depicts the operating parameters concerning data quality.

ICP-MS	
Instrument	Plasma Quad 2+ STE VG Elemental Set up following manufacturers guidelins.
Optimisation	Ion lenses turned for maximum sensitivity at ^{115}In. Optimised using a 10ng/ml multi- element tune solution
Forward Power	1350 W
Reflected Power	< 3W
Nebulizer Gas Flow	0.900 l/min
Auxilary Gas Flow	1.5 l/miin
Coolant Gas Flow	14.0 l/min
Sampling Cone	Ni 1 mm Orifice
Skimmer	Ni 0.7 mm Orifice
Nebulizer Type	Cross Flow
Solution Uptake Rate	0.8 ml/min

Figure 3.4.4.5 Instrumental Operating Parameters

Data Acquisition	
Mode	Scanning
Scan Regions	6.6-13.6, 22.4-27.6, 42.4-79.4, 80.6-97.8, 108.5-142.8, 179.9-188.6, 201.4-211.3, 228.2-241
Dwell Time	300 μs
Channels per amu	20
Total Acquisition Time	45.0 s
Number of Repeats	3 standards and samples, 5 blanks, 1 drift

Figure 3.4.4.6 Operating Parameters Governing ICP-MS Data Acquistion

Data Quality	
Calibration Via:	Multi element standards Spex USA ISP 9001 Certified
Standard Matrix	2 % HNO_3
Standard Concentrations	0, 1, 5, 10, 20, 100 ppb
Drift Monitor	10 ppb multi-element solution
Reference Materials Used	Fuel dependent

Figure3.4.4.7 ICP-MS Operating Parameters Relating to Data Quality

Once the results have been obtained and corrected using the blank values, limits of detection and quantification (LOD and LOQ) are calculated. The limit of detection of a concentration is the lowest value at which one can confidently say the element exists in the sample. The limit of quantification is the lowest value at which one can confidently attribute a quantitative value to the concentration of an element in a sample. In this instance the LOD may be defined as follows:

$$LOD = 3 \cdot \frac{[Std_{100ppb}]}{(RC_{100ppb} - RC_B)} \cdot RC_B \cdot DF$$

where: $[Std_{100ppb}]$ = Concentration of Standard 100ppb Solution

RC_{100ppb} = Raw Count of 100 ppb Solution

RC_B = Raw Count of Blank Solution

DF = Dilution Factor

For the LOQ the multiple of the above equation is 10 rather than 3 as follows:

$$LOD = 10 \cdot \frac{[Std_{100ppb}]}{(RC_{100ppb} - RC_B)} \cdot RC_B \cdot DF$$

When interpreting the results, values of different isotopes of an element should be the same, as the software corrects for an isotopes naturally occurring abundance. Occasionally however unequal isotope values occur. This could be for a number of reasons the must common of which is the occurrence of doubly charged ions. The Figure

3.4.4.8 below shows for the elements where unequal isotope values were obtained, which isotope should be used as the reliable value.

Element	Atomic Mass of Isotopes Yielding Unequal Values	Reliable Isotope
Mg	24, 26	26
Ca	43, 44	44
Ti	47, 49	47
Cr	52, 53	53
Fe	56, 57	-
Zn	66, 67, 80	67
Se	77, 82	77
Cd	111, 114	111
Ba	137, 138	137
Pb	204, 207, 208	208

Figure 3.4.4.8 Isotope Values to Be Used in Instances of "Unequal Isotope" Behaviour

Before the data is analysed the spectra of each run should also be investigated for collapsed peaks. These occur when the abundance of an element is too high. The effect of a collapsed peak not only under estimates the concentration of the element to which the peak belongs, but also has an impact on neighbouring peaks. In the experiments carried out in this instance the value of Fe was often too high, causing its peak to collapse and overlap on the manganese peak. This yielded a value for iron which was too low (due to the collapsed peak) and a manganese concentration which was too high (due to impingement from the Fe peak).

4.0 RESULTS

This section presents the results of the experiments defined in the previous chapter. Although data is presented to three decimal places, mercury results are correct to two significant figures. All other data are correct to three significant figures, unless otherwise specified.

4.1 Developing the Modified TCLP Test

The results obtained for determining whether small sample masses may be used in the TCLP , using the methodology described in the previous section, are given below.

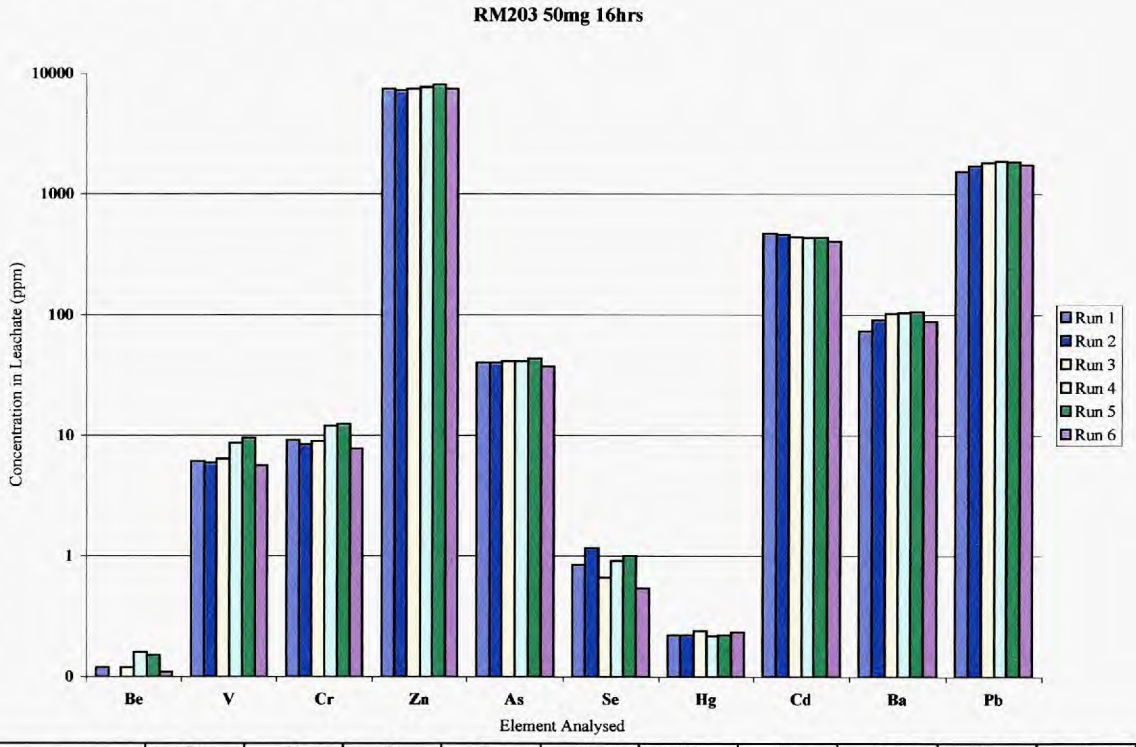
4.1.1 Ascertaining Reproducibility of Modified TCLP Test with Reduced Sample Mass

As described in the previous chapter the TCLP test was carried out using modified apparatus, three different samples and sample masses 50, 75, 100, and 125mg. In the first instance, experiments were carried out to ascertain if results were reproducible at these small sample masses (reproducibility would also imply homogeneity with regard to leaching of the sample at small masses). To this end, the figures below show the results obtained for the above masses, for each of the three sample types using agitation times of 16 and 18 hours

To ascertain reproducibility each experiment was repeated six times. The figures show the trace element concentration (ppm) of ten elements found in the modified TCLP test leachate, for each of the six runs. After each figure, a table shows the 6-experiment mean of the concentration, the standard deviation and the relative standard deviation for each trace element studied. The relative standard deviation was then taken as the criterion of reproducibility.

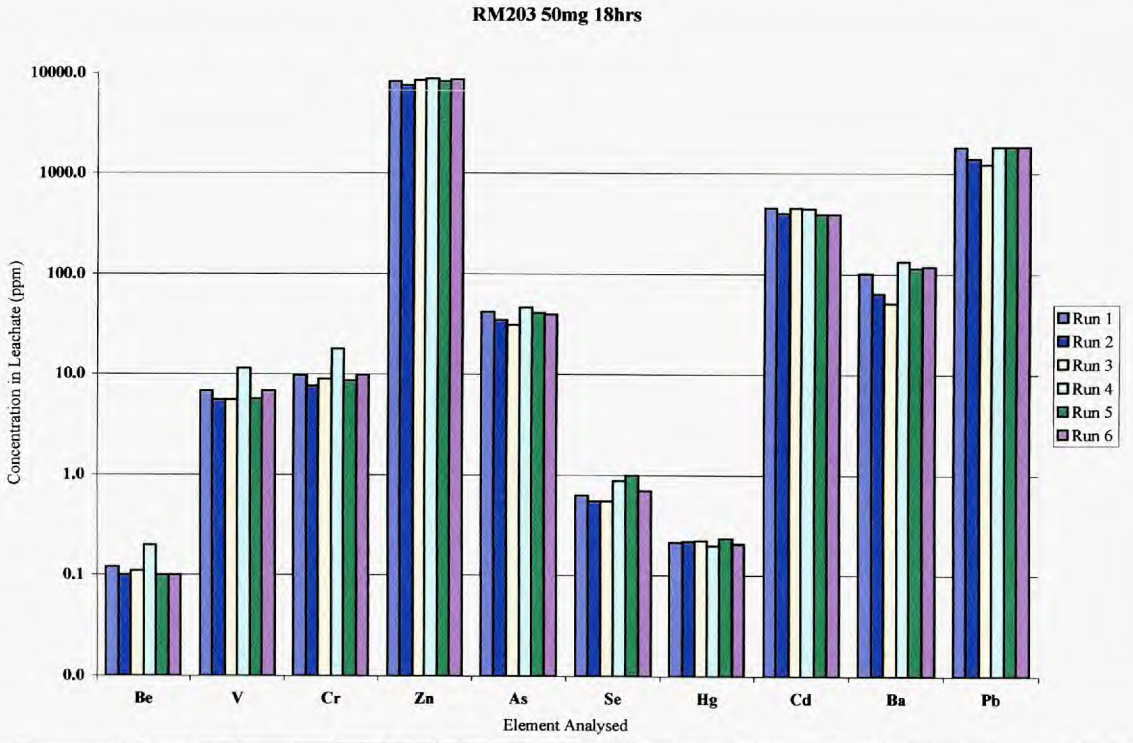
The fuels used were standard references materials, RM 203 and RM 205, provided for use with the TCLP test. The above experiments were also carried out using Polish Coal ash, produced at 900°C in the hot rod reactor. This was done in order obtain results using a material typical of the actual project samples. The Polish Coal results are shown concurrently with those obtained from the reference materials.

4.4.1.1 Results For Sample RM203



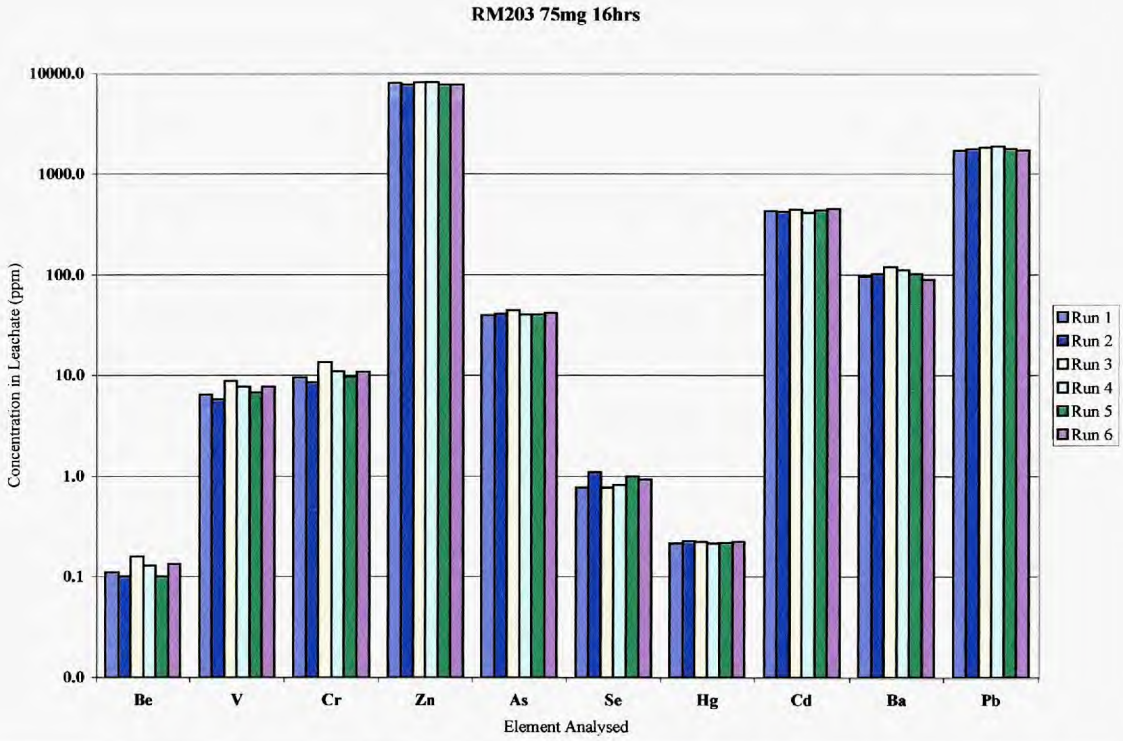
	Be	V	Cr	Zn	As	Se	Hg	Cd	Ba	Pb
Standard Deviation	0.023	1.628	1.945	279.265	1.959	0.230	0.009	23.681	12.699	120.734
% Standard Deviation	18.459	23.180	19.784	3.720	4.854	26.799	4.038	5.364	13.491	6.843
6 Experiment Mean	0.127	7.023	9.830	7507.055	40.360	0.857	0.227	441.443	94.127	1764.223

Figure 4.1.1 Reproducibility of Modified TCLP Test for Sample RM203, 50mg & 16hrs



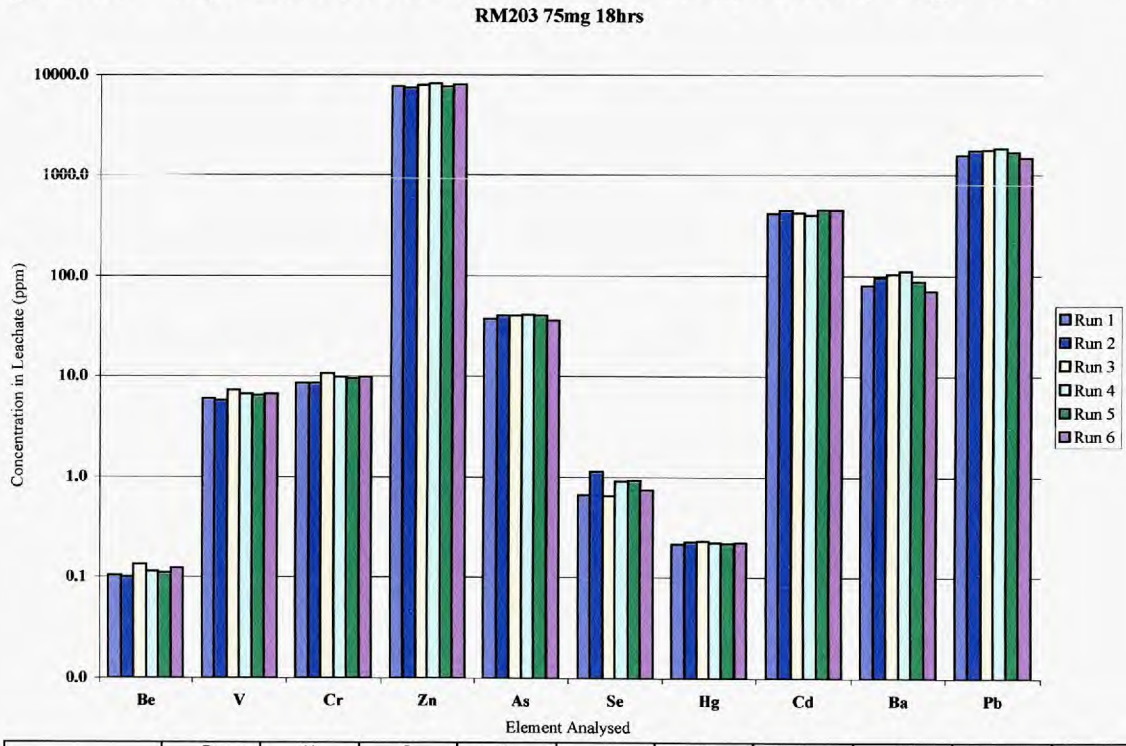
	Be	V	Cr	Zn	As	Se	Hg	Cd	Ba	Pb
Standard Deviation	0.039	2.266	3.763	419.100	5.571	0.185	0.012	32.449	32.801	279.324
% Standard Deviation	32.219	32.655	36.094	5.062	14.232	25.691	5.399	7.703	33.745	16.679
6 Experiment Mean	0.122	6.938	10.427	8279.887	39.147	0.718	0.216	421.278	97.205	1674.722

Figure 4.1.2 Reproducibility of Modified TCLP Test for Sample RM203, 50mg & 18hrs



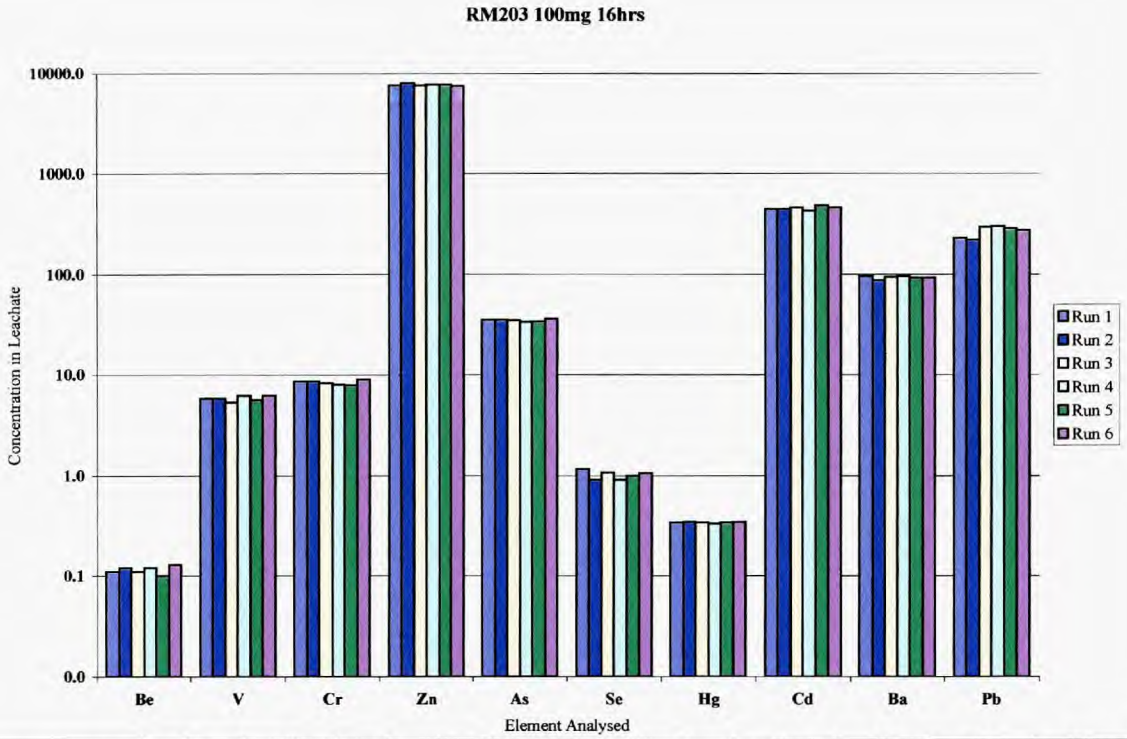
	Be	V	Cr	Zn	As	Se	Hg	Cd	Ba	Pb
Standard Deviation	0.024	1.119	1.706	202.004	1.509	0.130	0.005	13.900	10.462	68.465
% Standard Deviation	19.275	15.482	16.243	2.570	3.677	14.526	2.493	3.206	10.150	3.833
6 Experiment Mean	0.123	7.231	10.504	7859.068	41.032	0.892	0.220	433.610	103.074	1786.376

Figure 4.1.3 Reproducibility of Modified TCLP Test for Sample RM203, 75mg & 16hrs



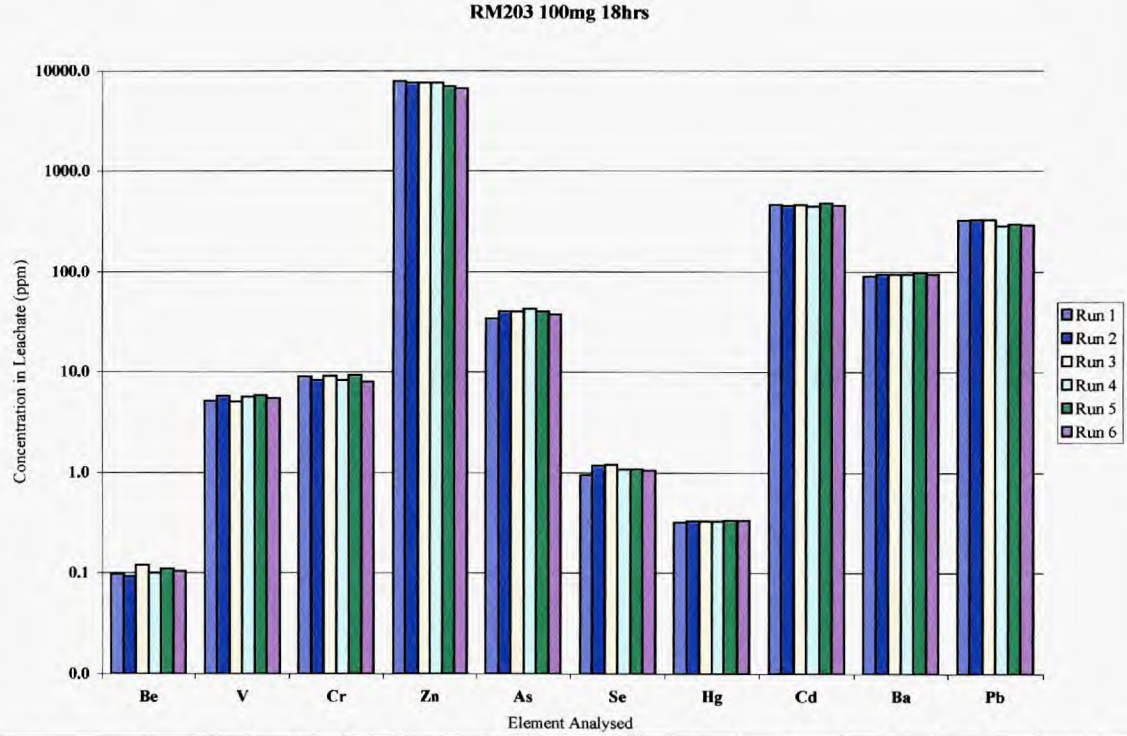
	Be	V	Cr	Zn	As	Se	Hg	Cd	Ba	Pb
Standard Deviation	0.013	0.529	0.830	288.374	1.972	0.183	0.004	22.207	15.419	149.332
% Standard Deviation	11.075	8.169	8.770	3.708	5.033	21.989	1.999	5.149	16.844	8.855
6 Experiment Mean	0.115	6.474	9.468	7777.728	39.174	0.834	0.223	431.277	91.537	1686.438

Figure 4.1.4 Reproducibility of Modified TCLO Test for Sample RM 203 75 mg & 18hrs



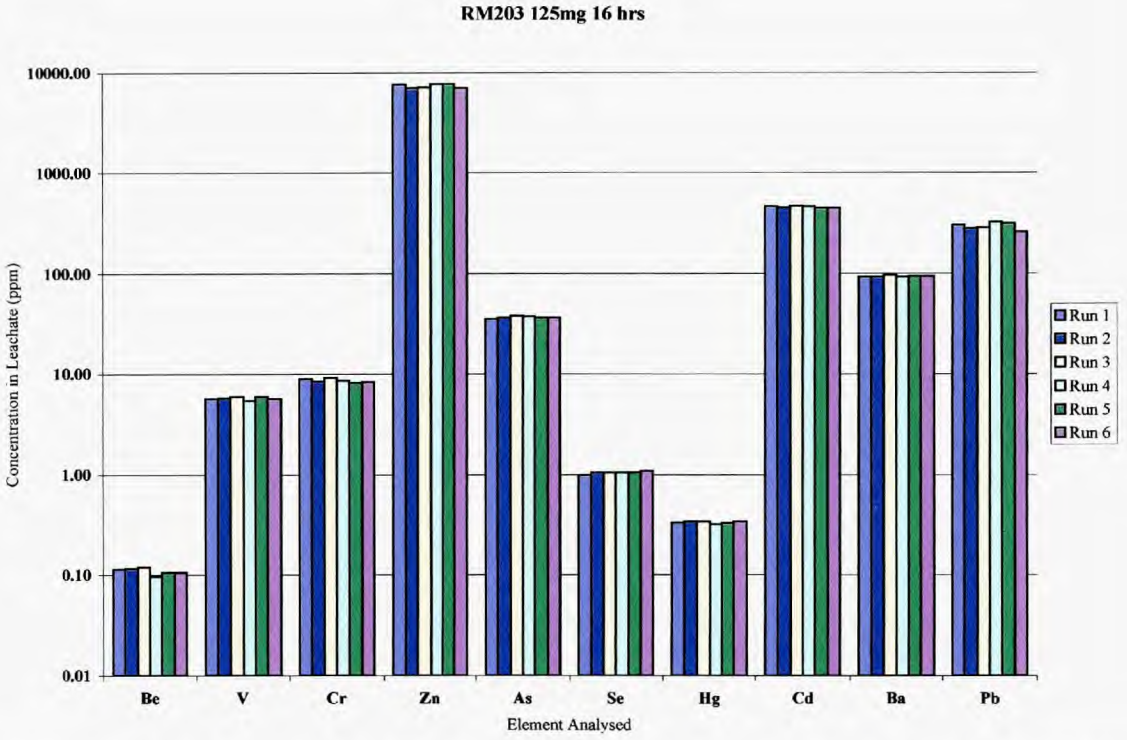
	Be	V	Cr	Zn	As	Se	Hg	Cd	Ba	Pb
Standard Deviation	0.010	0.329	0.396	200.950	1.003	0.095	0.004	20.438	3.030	34.802
% Standard Deviation	9.120	5.596	4.705	2.629	2.870	9.376	1.261	4.483	3.249	12.968
6 Experiment Mean	0.115	5.878	8.415	7642.833	34.947	1.013	0.342	455.885	93.253	268.374

Figure 4.1.5 Reproducibility of Modified TCLP Test for Sample RM203, 100mg & 16hrs



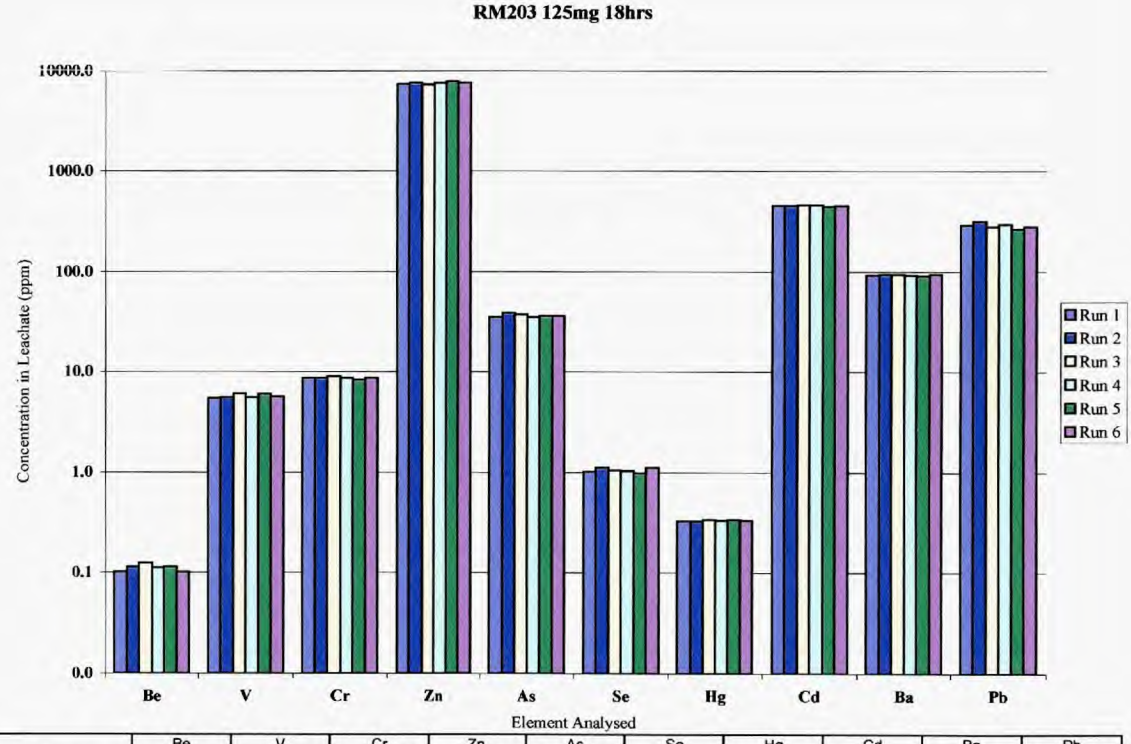
	Be	V	Cr	Zn	As	Se	Hg	Cd	Ba	Pb
Standard Deviation	0.009	0.336	0.493	461.264	2.880	0.092	0.005	12.457	2.414	20.909
% Standard Deviation	9.025	6.097	5.684	6.272	7.354	8.502	1.420	2.707	2.567	6.774
6 Experiment Mean	0.104	5.512	8.675	7354.888	39.162	1.085	0.329	460.272	94.040	308.649

Figure 4.1.6 Reproducibility of Modified TCLP Test for Sample RM203, 100mg & 18hrs



	Be	V	Cr	Zn	As	Se	Hg	Cd	Ba	Pb
Standard Deviation	0.009	0.216	0.349	329.911	1.018	0.034	0.006	10.099	1.530	24.136
% Standard Deviation	7.901	3.741	4.043	4.478	2.767	3.220	1.814	2.210	1.632	8.194
6 Experiment Mean	0.110	5.779	8.639	7367.471	36.800	1.052	0.335	457.001	93.738	294.546

Figure 4.1.7 Reproducibility of Modified TCLP Test for Sample RM203, 125mg & 16hrs



	Be	V	Cr	Zn	As	Se	Hg	Cd	Ba	Pb
Standard Deviation	0.008	0.270	0.216	173.572	1.329	0.053	0.005	7.664	1.190	19.118
% Standard Deviation	7.430	4.720	2.486	2.298	3.645	5.044	1.355	1.679	1.276	6.601
6 Experiment Mean	0.112	5.710	8.670	7551.915	36.470	1.051	0.335	456.332	93.287	289.603

Figure 4.1.8 Reproducibility of Modified TCLP Test for Sample RM203, 125mg & 18hrs

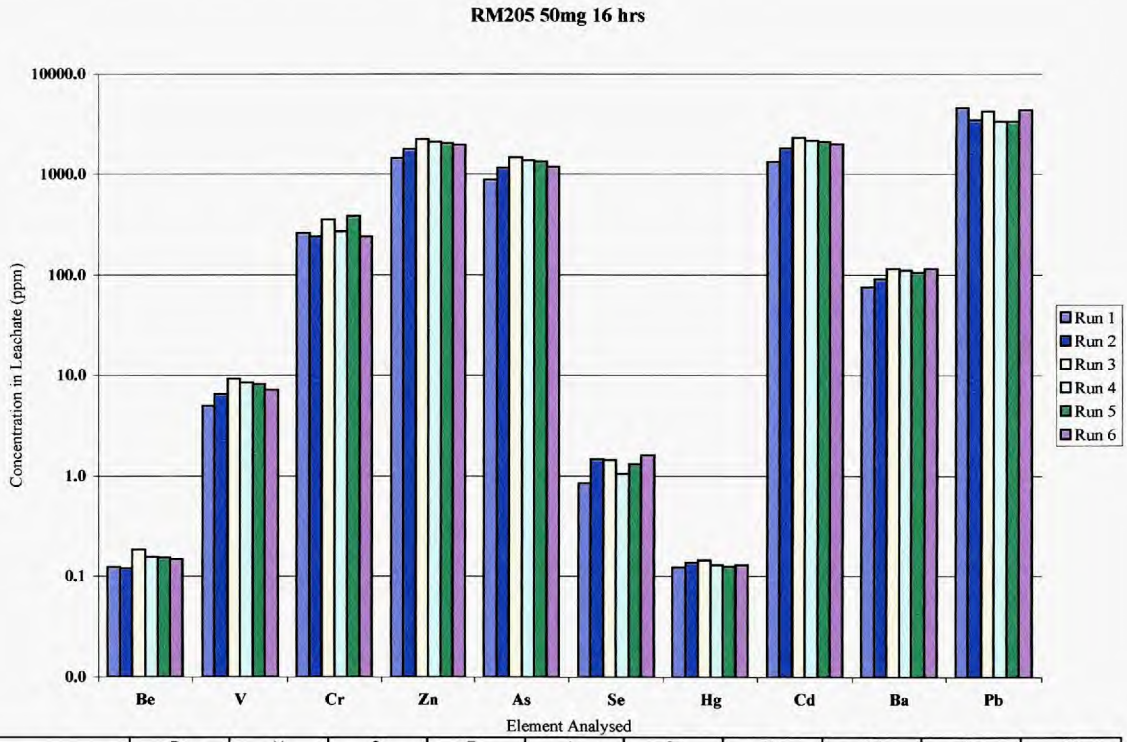
The relative standard deviation (RSD) of each set of experiments was used as the criterion of whether an experiment was reproducible. The RSD for experiments carried out for 50mg varied with trace element. For the elements Be, V, Cr and Se the RSD was above 18.4% with a maximum of 36.0 % for Cr. This was the case at both the 16 and 18 hour time spans. The RSD for the remaining elements - Zn, As, Hg, Cd and Pb, the RSD was always under 16% and mostly under 10% for both times. In conclusion the RSD values for this sample mass were deemed too high to consider the 50mg sample mass possible for use in the modified TCLP test.

For a sample mass of 75 mg the RSD's obtained were greatly reduced compared with those yielded by the 50mg experiments. Zn, As, Hg, Cd and Pb all fell below 6% for both time periods (with the exception of Pb at 18 hrs being 8.8%), whilst Be, V, Cr, Se and Ba were between 8 and 20% for both times.

When a sample mass of 100 mg was used the RSD for the six-experiment set fell below 10% for all elements, and both time periods, with the exception of Pb at 16 hrs being 12.9%. RSD's for Hg, Cd and Ba were in the region of 3 % for both times and As and Zn at 16 hrs. The RSD was in the region of 5% for V and Cr at both times and Zn, As, and Pb at 18hrs. Be and Se however were closer to 10% for both time periods.

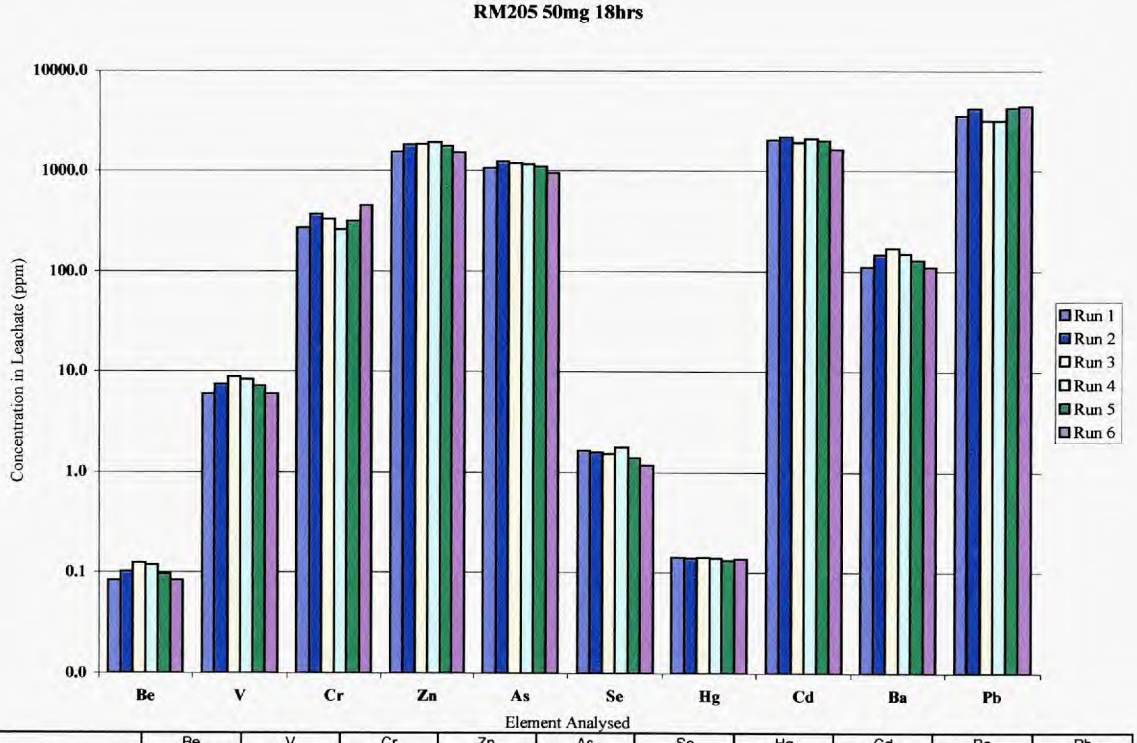
At 125 mg sample mass the RSD for all elements fell below 5% except for Be and Pb which were in the regions of 7 & 8% respectively.

4.1.1.2 Results for Sample RM205



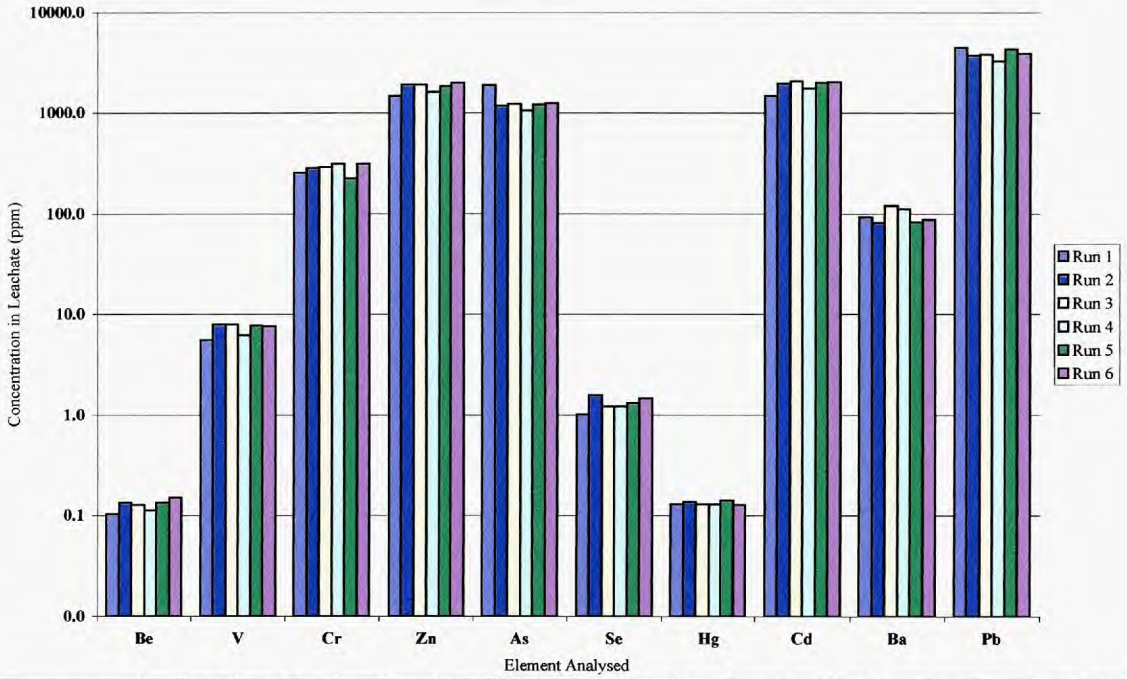
	Be	V	Cr	Zn	As	Se	Hg	Cd	Ba	Pb
Standard Deviation	0.024	1.543	61.726	271.881	208.261	0.290	0.008	343.893	16.294	579.829
% Standard Deviation	16.193	20.715	21.124	14.099	16.818	22.469	6.201	17.621	15.899	14.910
6 Experiment Mean	0.148	7.451	292.204	1928.315	1238.315	1.289	0.132	1951.574	102.481	3888.815

Figure 4.1.9 Reproducibility of Modified TCLP Test for Sample RM205, 50mg & 16hrs



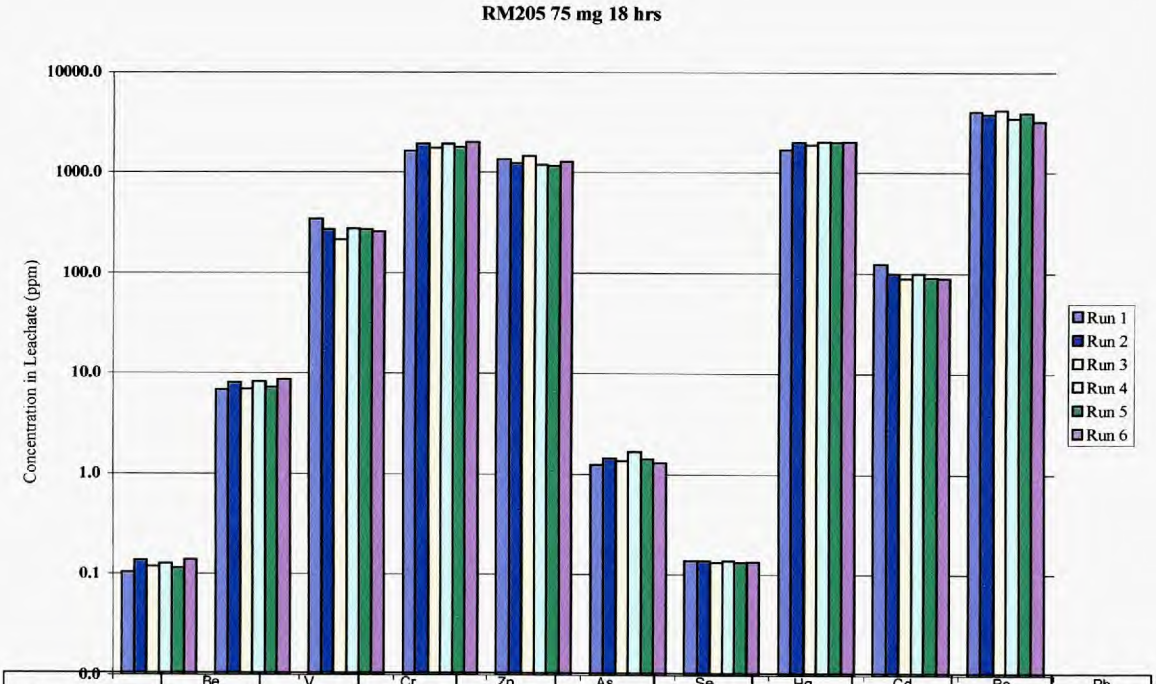
	Be	V	Cr	Zn	As	Se	Hg	Cd	Ba	Pb
Standard Deviation	0.017	1.146	70.034	171.423	107.506	0.201	0.004	191.555	23.695	563.804
% Standard Deviation	17.056	15.638	21.063	9.904	9.628	13.334	2.748	9.663	17.423	14.944
6 Experiment Mean	0.101	7.327	332.500	1730.778	1116.556	1.511	0.140	1982.389	136.000	3772.833

Figure 4.1.10 Reproducibility of Modified TCLP Test for Sample RM203, 50mg & 18hrs



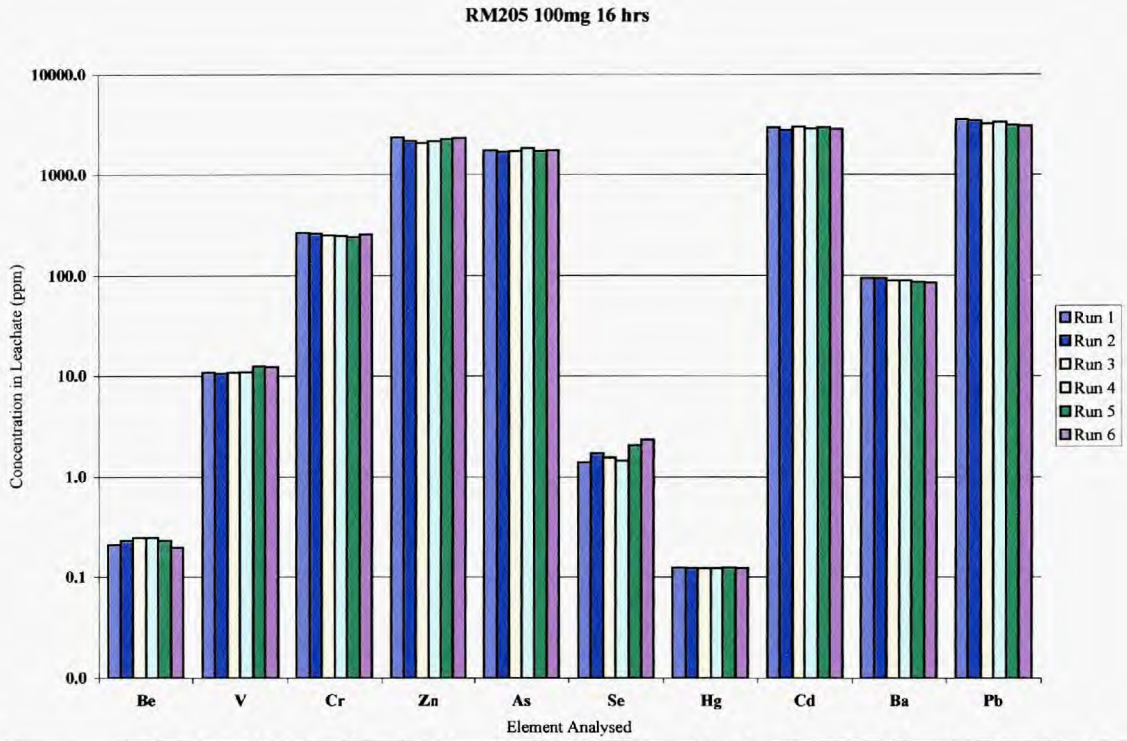
	Be	V	Cr	Zn	As	Se	Hg	Cd	Ba	Pb
Standard Deviation	0.017	1.014	35.124	201.131	289.008	0.199	0.005	224.881	16.189	442.043
% Standard Deviation	13.528	14.160	12.539	11.159	22.118	15.315	3.738	11.938	16.886	11.302
6 Experiment Mean	0.127	7.160	280.129	1802.352	1306.654	1.296	0.133	1883.787	95.876	3911.056

Figure 4.1.11 Reproducibility of Modified TCLP Test for Sample RM205, 75mg & 16hrs



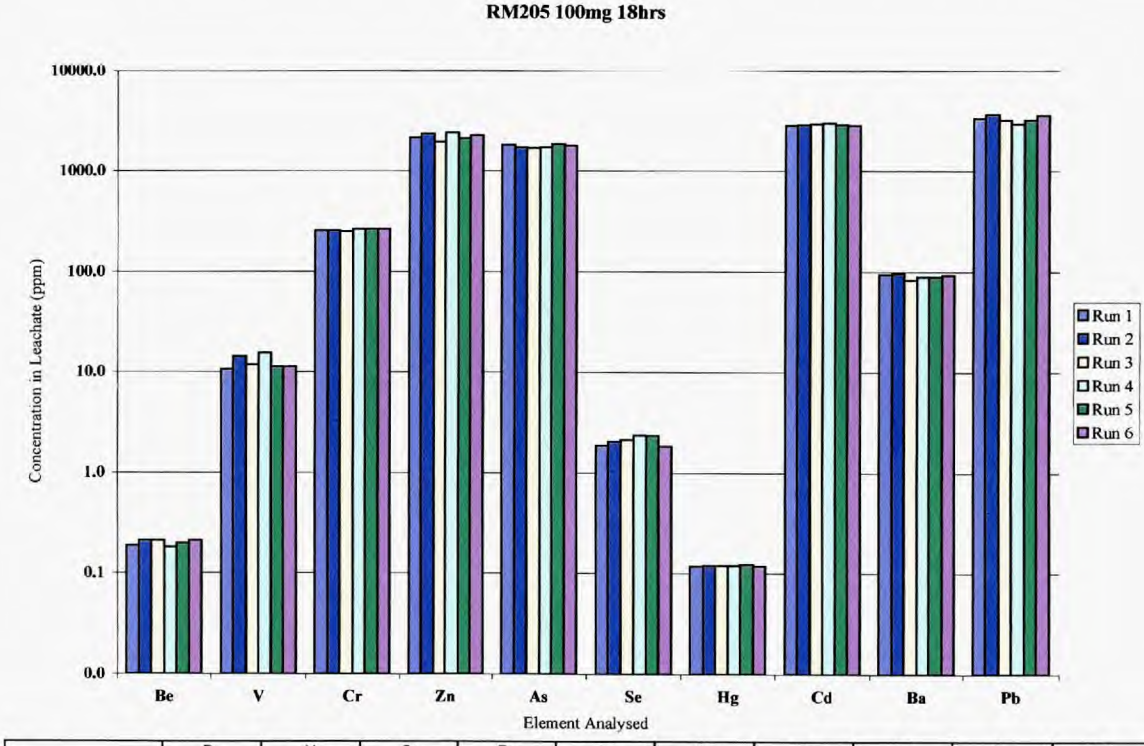
	Be	V	Cr	Zn	As	Se	Hg	Cd	Ba	Pb
Standard Deviation	0.014	0.762	42.893	132.510	112.996	0.147	0.003	180.444	13.154	352.189
% Standard Deviation	11.258	10.006	15.852	7.240	8.793	10.539	1.855	7.026	13.287	9.372
6 Experiment Mean	0.124	7.612	270.581	1831.647	1274.799	1.397	0.136	1942.059	99.000	3758.081

Figure 4.1.12 Reproducibility of Modified TCLP Test for Sample RM205, 75mg & 18hrs



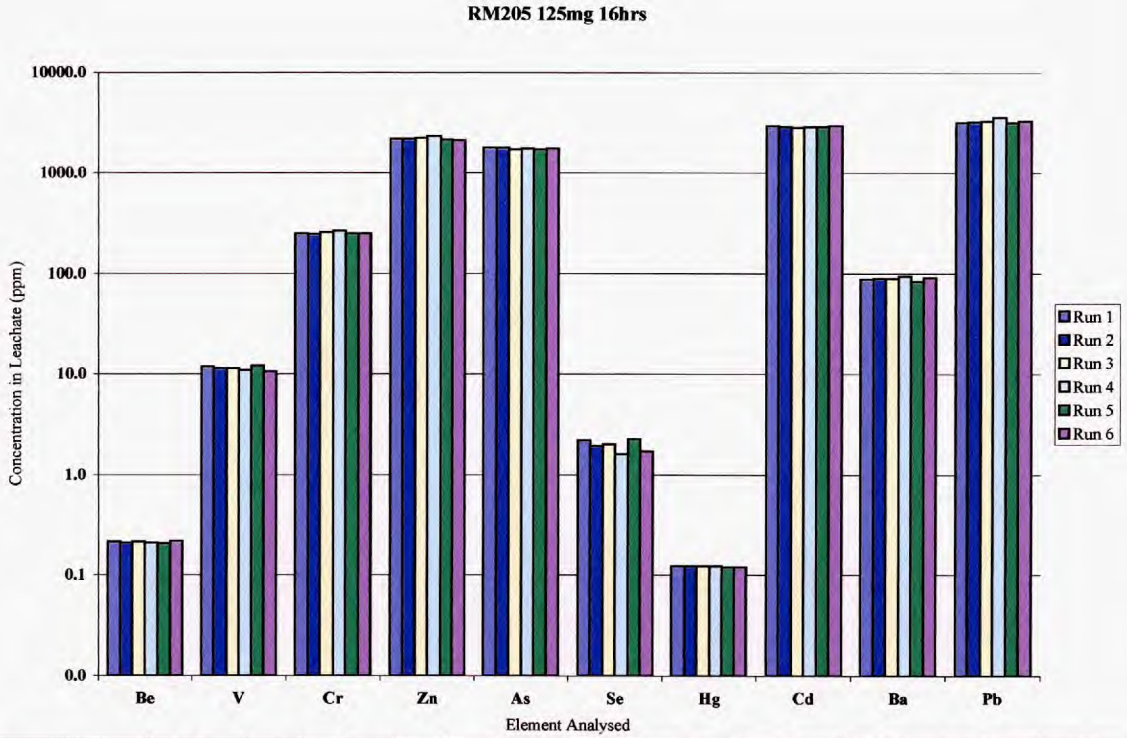
	Be	V	Cr	Zn	As	Se	Hg	Cd	Ba	Pb
Standard Deviation	0.020	0.844	9.718	93.725	52.065	0.371	0.002	74.700	4.179	200.830
% Standard Deviation	8.940	7.433	3.840	4.231	2.987	21.303	1.320	2.574	4.676	6.096
6 Experiment Mean	0.228	11.357	253.057	2214.945	1743.112	1.742	0.124	2902.500	89.367	3294.332

Figure 4.1.13 Reproducibility of Modified TCLP Test for Sample RM205, 100mg & 16hrs



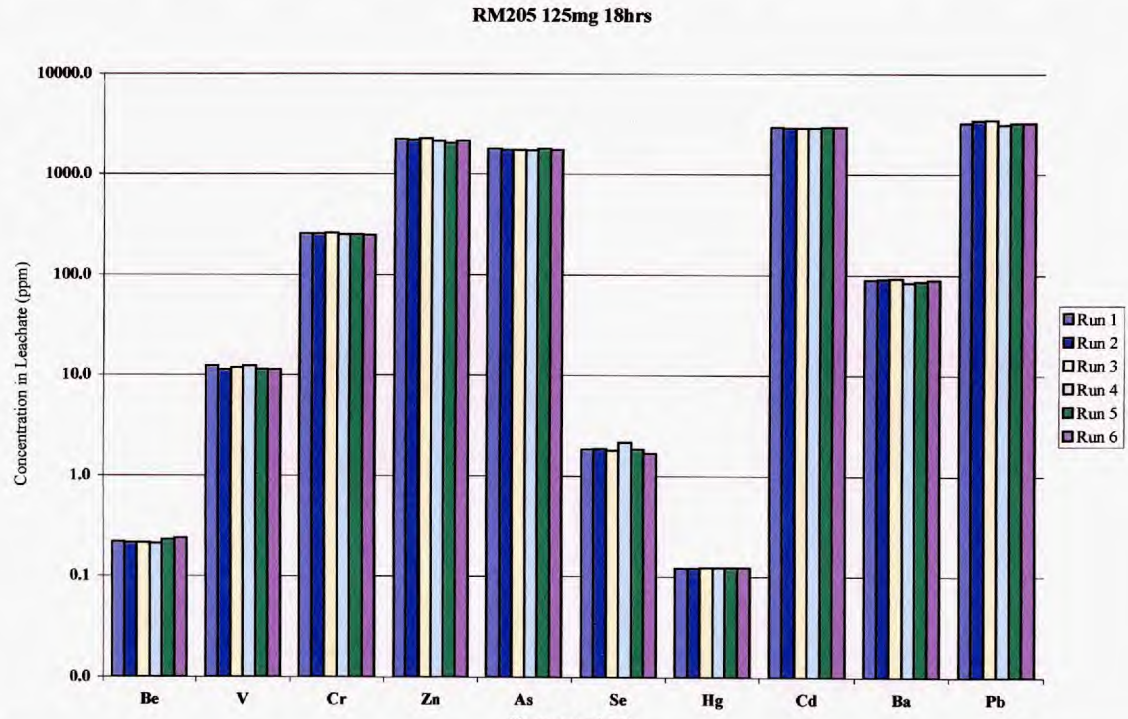
	Be	V	Cr	Zn	As	Se	Hg	Cd	Ba	Pb
Standard Deviation	0.013	2.007	6.052	165.012	61.169	0.236	0.001	57.406	4.909	264.951
% Standard Deviation	6.325	16.143	2.336	7.460	3.466	11.269	1.006	1.980	5.414	7.934
6 Experiment Mean	0.200	12.433	259.110	2211.890	1764.888	2.097	0.120	2899.002	90.675	3339.278

Figure 4.1.14 Reproducibility of Modified TCLP Test for Sample RM205, 100mg & 18hrs



	Be	V	Cr	Zn	As	Se	Hg	Cd	Ba	Pb
Standard Deviation	0.005	0.534	6.289	72.353	30.515	0.251	0.001	37.092	3.457	163.062
% Standard Deviation	2.468	4.663	2.470	3.295	1.741	12.883	0.620	1.284	3.881	4.975
6 Experiment Mean	0.213	11.443	254.639	2196.139	1753.138	1.948	0.122	2889.167	89.070	3277.804

Figure 4.1.15 Reproducibility of Modified TCLP Test for Sample RM205, 125mg & 16hrs



	Be	V	Cr	Zn	As	Se	Hg	Cd	Ba	Pb
Standard Deviation	0.010	0.521	4.627	80.341	32.961	0.168	0.001	37.318	3.258	118.356
% Standard Deviation	4.714	4.450	1.830	3.709	1.875	8.987	0.647	1.279	3.676	3.617
6 Experiment Mean	0.221	11.711	252.841	2166.123	1757.701	1.865	0.122	2916.783	88.626	3271.879

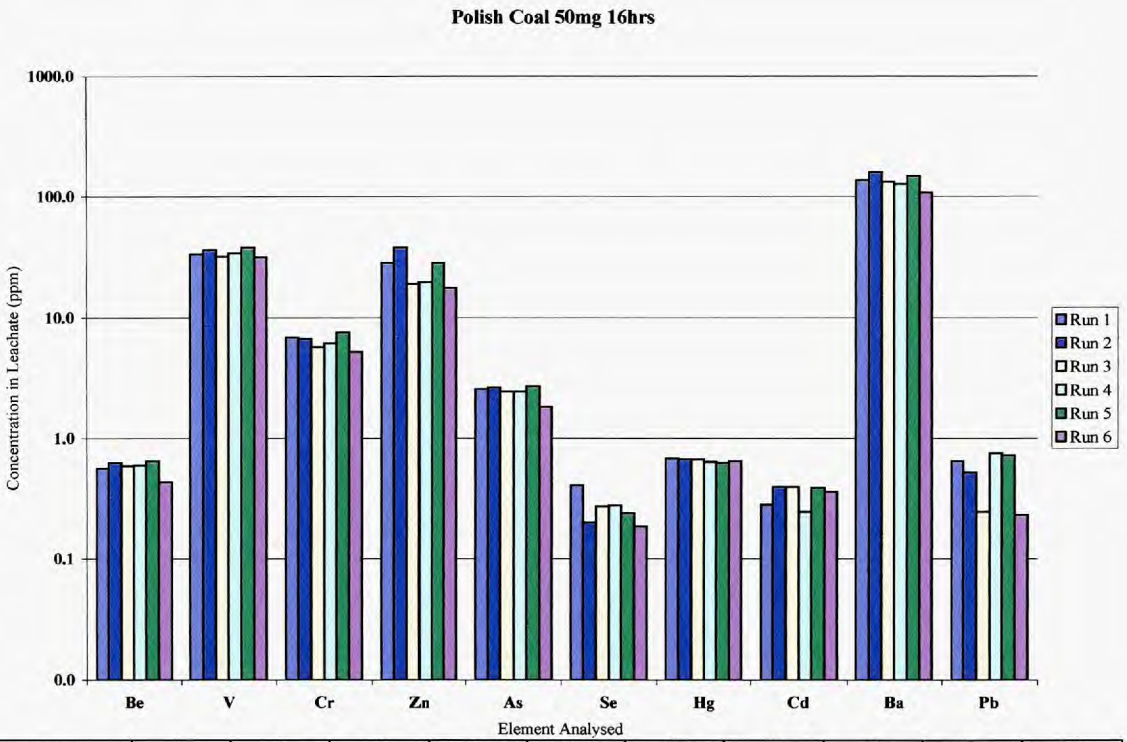
Figure 4.1.16 Reproducibility of Modified TCLP Test for Sample RM205, 125mg & 18hrs

For the sample RM205 experiments carried out using 50mg RSDs were all higher then 14..1% at 16 hrs, with the exception of Hg. At 18hrs the RSD for each set of results was lower than for 16 hrs, however all were between than 9.6% and 21.1% once more with the exception of Hg. For sample RM205 there did not seem to be an obvioius trend for which elements yielded results with high RSD's and which lower, as in the case of RM203, however the RSD for Hg results were consistently lower than for all other elements.

Experiments carried out using 75 mg saw the RSD fall slightly when compared to 50mg experiments. With the exception of Hg all RSD values were higher than 11.2% for 16 hrs reaching a maximum of 22.1% with As. At 18hrs Zn, As and Cd results were subject to RSD's of approximately 8%, whilst those of all other elements were higher than 10%. Once again the RSD for these results could not be correlated to element type or length of experiment.

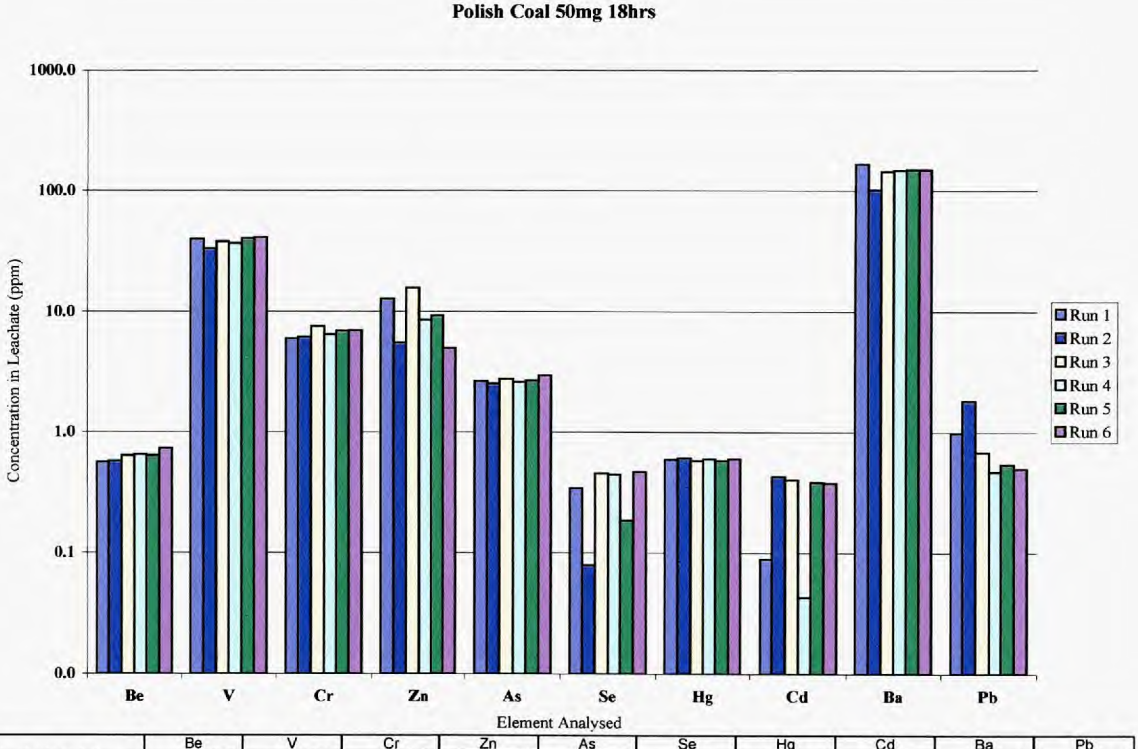
As with sample RM203 at the 100mg sample size all results begin to converge with RSDs for all elements falling below 5% (except Be and Pb which are in the region of 8% and Se and V). When the sample size is increased to 125 mg, again the RSDs for all results again fall below 5% with the exception of Se which is 12.8% and 8.9% at 16 and 18 hrs respectively.

4.1.1.4 Results for Sample Polish Coal



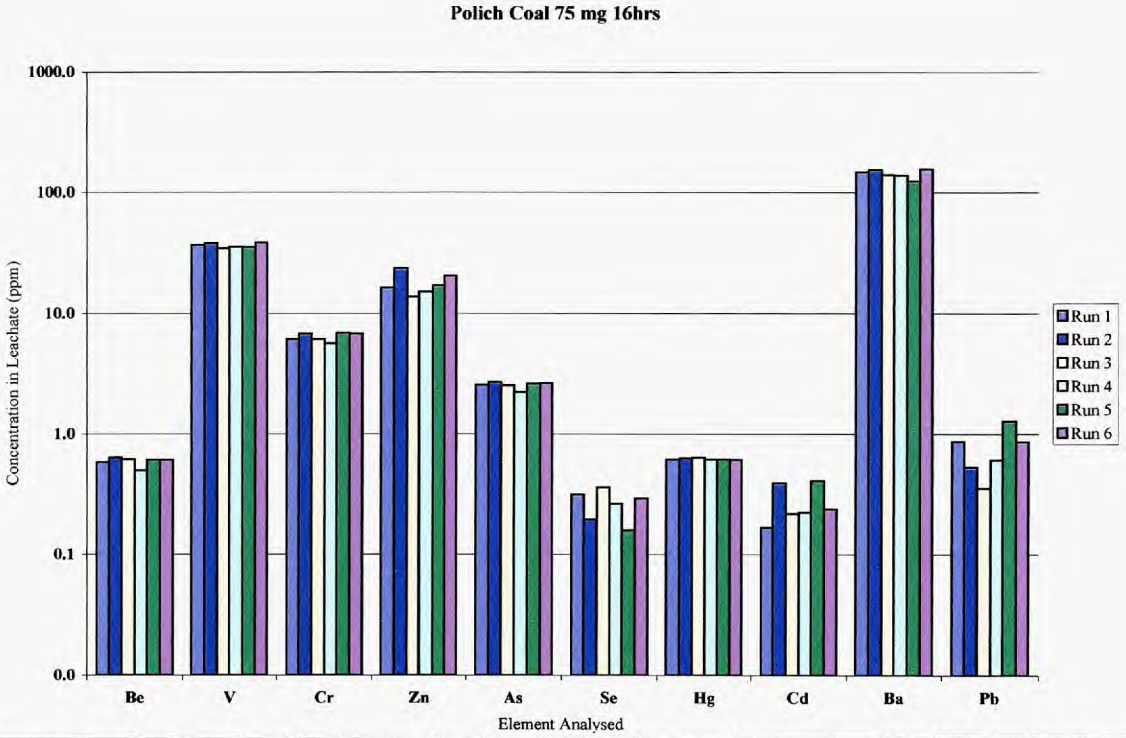
	Be	V	Cr	Zn	As	Se	Hg	Cd	Ba	Pb
Standard Deviation	0.076	2.386	0.849	7.937	0.312	0.079	0.018	0.065	17.690	0.233
% Standard Deviation	13.121	6.981	13.364	31.580	12.821	29.883	2.799	18.725	13.085	44.800
6 Experiment Mean	0.579	34.172	6.349	25.132	2.437	0.264	0.656	0.345	135.197	0.521

Figure 4.1.17 Reproducibility of Modified TCLP Test for Polish Coal, 50mg & 16hrs



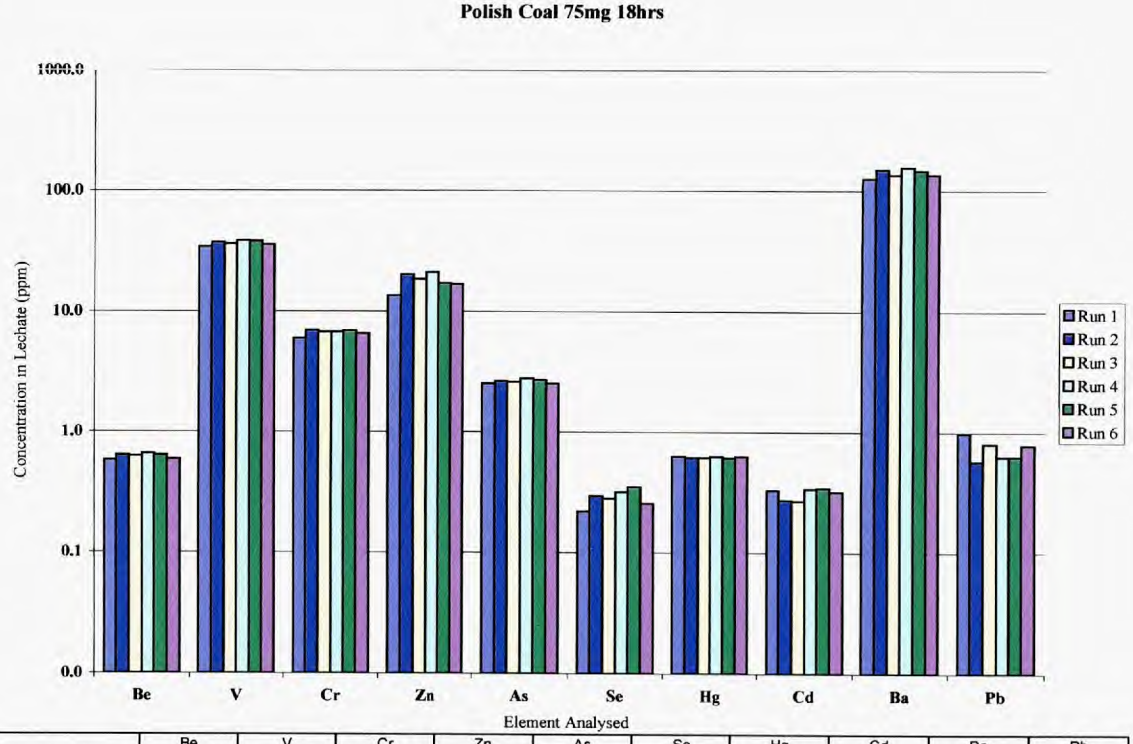
	Be	V	Cr	Zn	As	Se	Hg	Cd	Ba	Pb
Standard Deviation	0.063	2.994	0.547	4.174	0.155	0.163	0.011	0.173	22.213	0.524
% Standard Deviation	9.886	7.853	8.223	44.255	5.764	49.237	1.821	60.135	15.462	62.753
6 Experiment Mean	0.633	38.124	6.654	9.432	2.694	0.332	0.595	0.288	143.661	0.834

Figure 4.1.18 Reproducibility of Modified TCLP Test for Polish Coal, 50mg & 18hrs



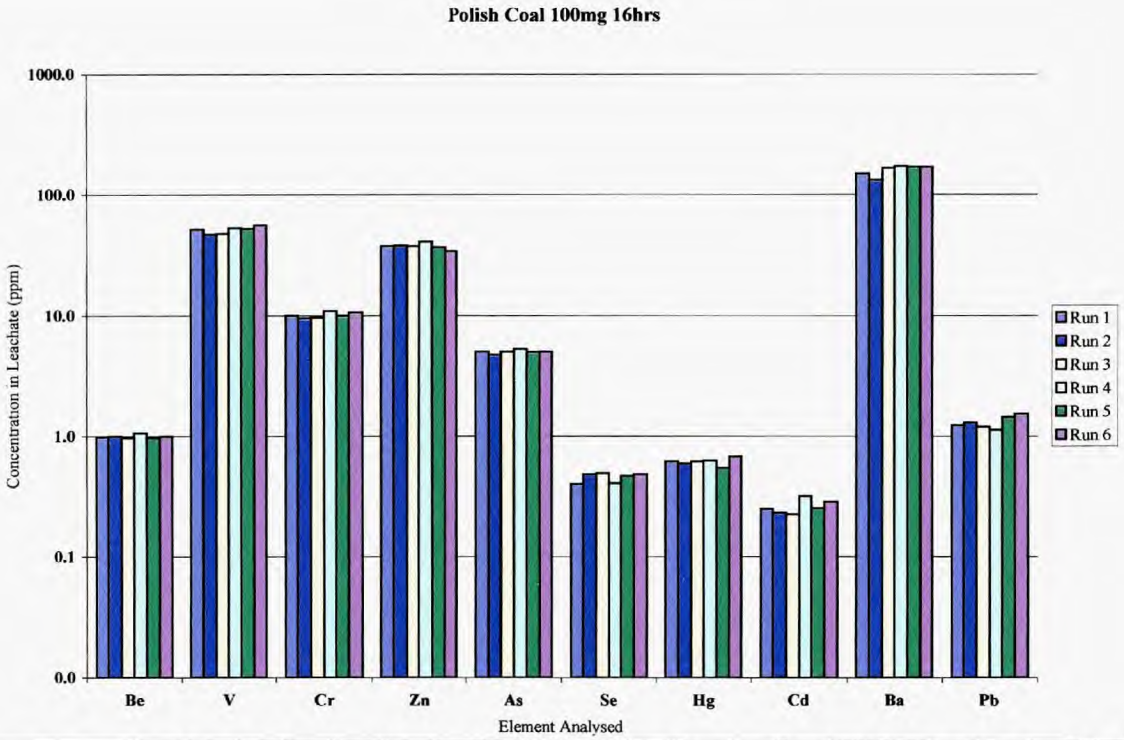
	Be	V	Cr	Zn	As	Se	Hg	Cd	Ba	Pb
Standard Deviation	0.049	1.690	0.512	3.703	0.159	0.075	0.009	0.099	12.192	0.324
% Standard Deviation	8.255	4.622	8.051	20.934	6.273	28.494	1.526	36.155	8.490	43.175
6 Experiment Mean	0.592	36.564	6.354	17.687	2.537	0.264	0.621	0.275	143.607	0.750

Figure 4.1.19 Reproducibility of Modified TCLP Test for Polish Coal, 75mg & 16hrs



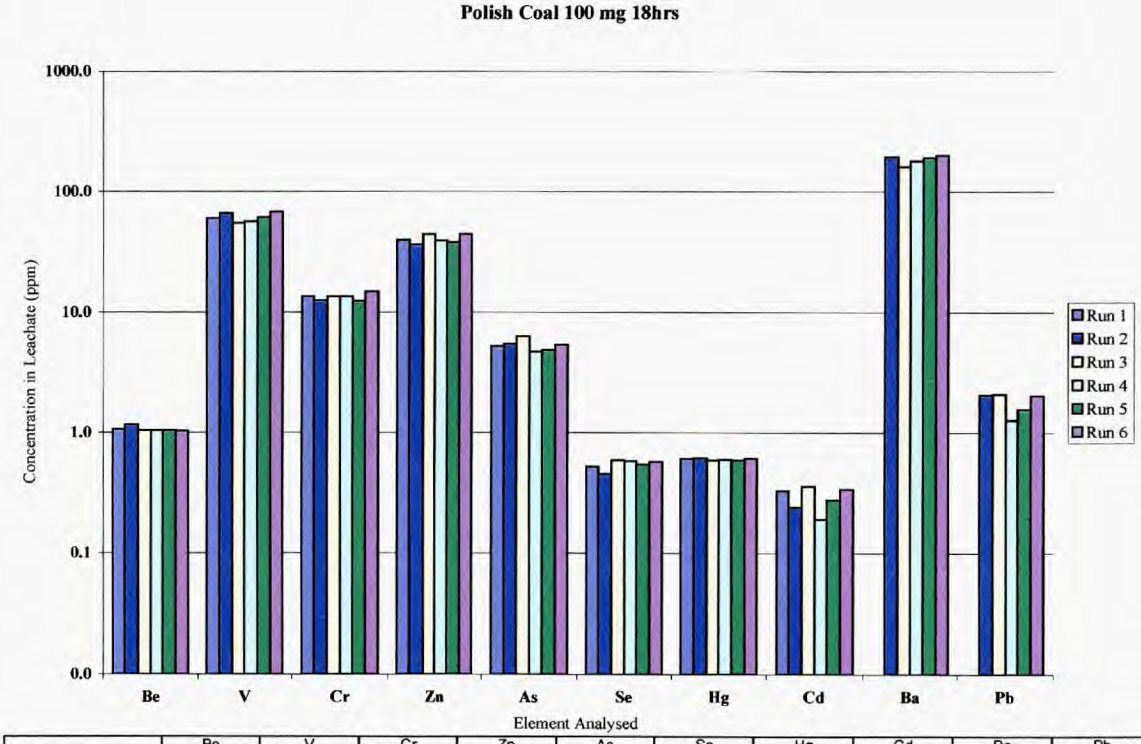
	Be	V	Cr	Zn	As	Se	Hg	Cd	Ba	Pb
Standard Deviation	0.031	1.764	0.352	2.725	0.095	0.046	0.007	0.033	10.931	0.153
% Standard Deviation	4.943	4.805	5.308	15.278	3.631	15.953	1.174	10.511	7.696	20.854
6 Experiment Mean	0.622	36.706	6.638	17.837	2.616	0.287	0.622	0.314	142.035	0.734

Figure 4.1.20 Reproducibility of Modified TCLP Test for Polish Coal, 75mg & 18hrs



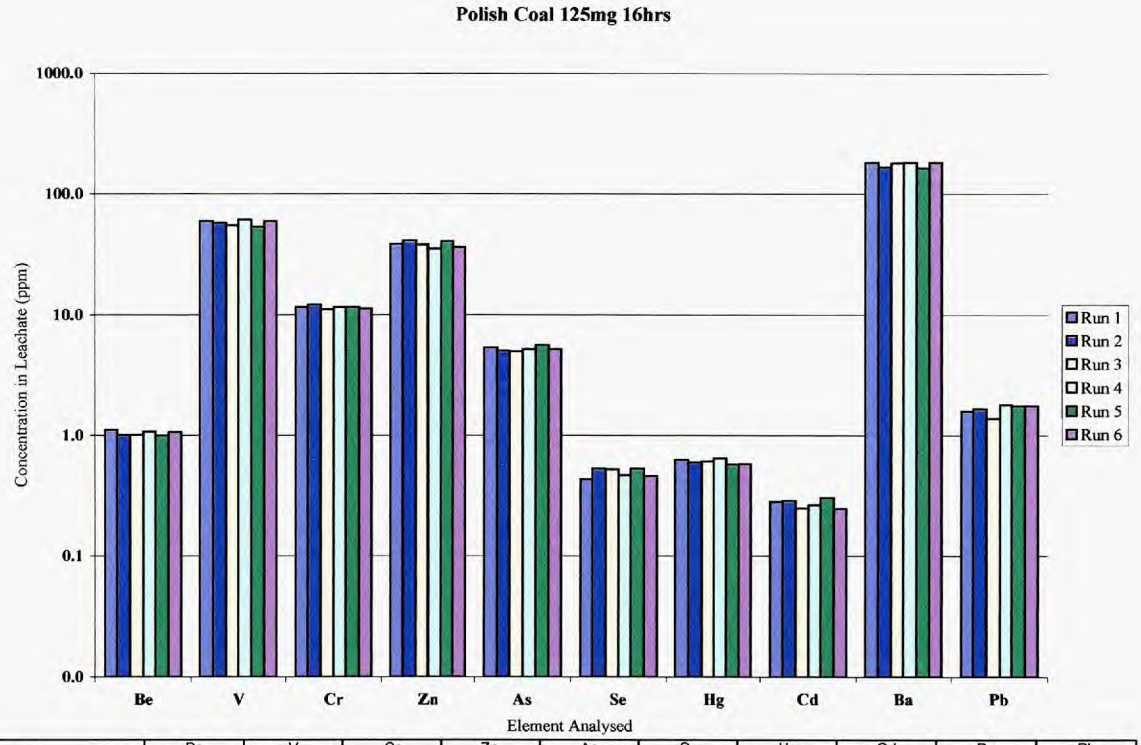
	Be	V	Cr	Zn	As	Se	Hg	Cd	Ba	Pb
Standard Deviation	0.036	3.165	0.579	2.203	0.178	0.040	0.043	0.037	15.271	0.160
% Standard Deviation	3.600	6.172	5.744	5.889	3.552	8.783	7.030	14.056	9.558	12.216
6 Experiment Mean	1.000	51.272	10.075	37.409	5.015	0.458	0.615	0.260	159.780	1.308

Figure 4.1.21 Reproducibility of Modified TCLP Test for Polish Coal, 100mg & 16hrs



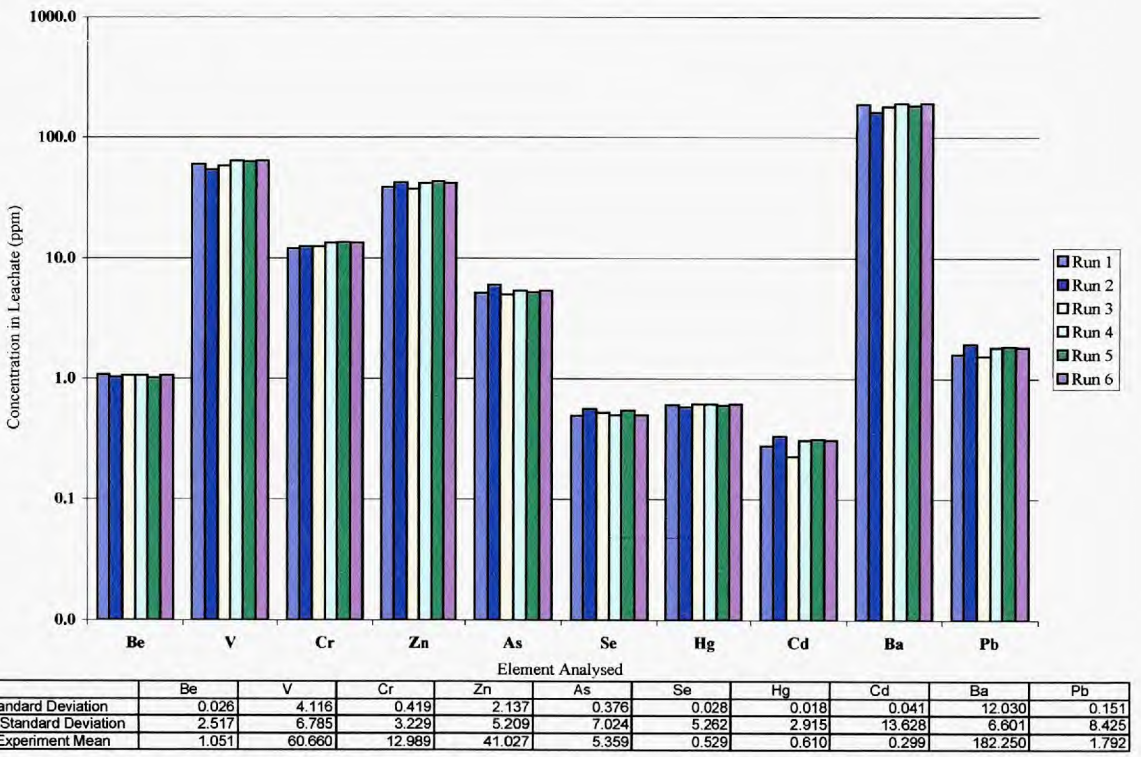
	Be	V	Cr	Zn	As	Se	Hg	Cd	Ba	Pb
Standard Deviation	0.050	5.048	0.884	3.193	0.573	0.052	0.013	0.065	16.027	0.374
% Standard Deviation	4.719	6.869	5.519	6.593	9.025	7.985	1.840	18.672	8.635	20.658
6 Experiment Mean	1.067	73.491	16.024	48.426	6.347	0.655	0.726	0.348	185.600	1.809

Figure 4.1.22 Reproducibility of Modified TCLP Test for Polish Coal, 100mg & 18hrs



	Be	V	Cr	Zn	As	Se	Hg	Cd	Ba	Pb
Standard Deviation	0.037	2.977	0.435	2.497	0.272	0.034	0.030	0.025	8.506	0.176
% Standard Deviation	3.559	5.207	3.787	6.534	5.219	6.774	4.986	9.218	4.862	10.507
6 Experiment Mean	1.035	57.173	11.486	38.217	5.206	0.503	0.602	0.271	174.967	1.677

Figure 4.1.23 Reproducibility of Modified TCLP Test for Polish Coal, 125mg & 16hrs



	Be	V	Cr	Zn	As	Se	Hg	Cd	Ba	Pb
Standard Deviation	0.026	4.116	0.419	2.137	0.376	0.028	0.018	0.041	12.030	0.151
% Standard Deviation	2.517	6.785	3.229	5.209	7.024	5.262	2.915	13.628	6.601	8.425
6 Experiment Mean	1.051	60.660	12.989	41.027	5.359	0.529	0.610	0.299	182.250	1.792

Figure 4.1.24 Reproducibility of Modified TCLP Test for Polish Coal, 125mg & 18hrs

4.1.2 Comparison of Certified Values with Modified TCLP test Results

The modified TCLP test yielded consistent results at small sample masses and experiments were reproducible at 100mg. Therefore the next stage of the test's development was to determine whether the results obtained concurred with the certified values given by the reference materials. Table 4.1.1 below shows the certified values which should be obtained when the TCLP test is correctly applied to the reference materials RM203 and RM205.

Material	RM203		RM205				
Element	Cd	Pb	Cr	As	Cd	Ba	Pb
Certified Concentration (ppm)	450.0	286.0	254.0	1790.6	2938.0	88.0	3292.0

Table 4.1.1 Certified Values of Elements in TCLP Reference Materials

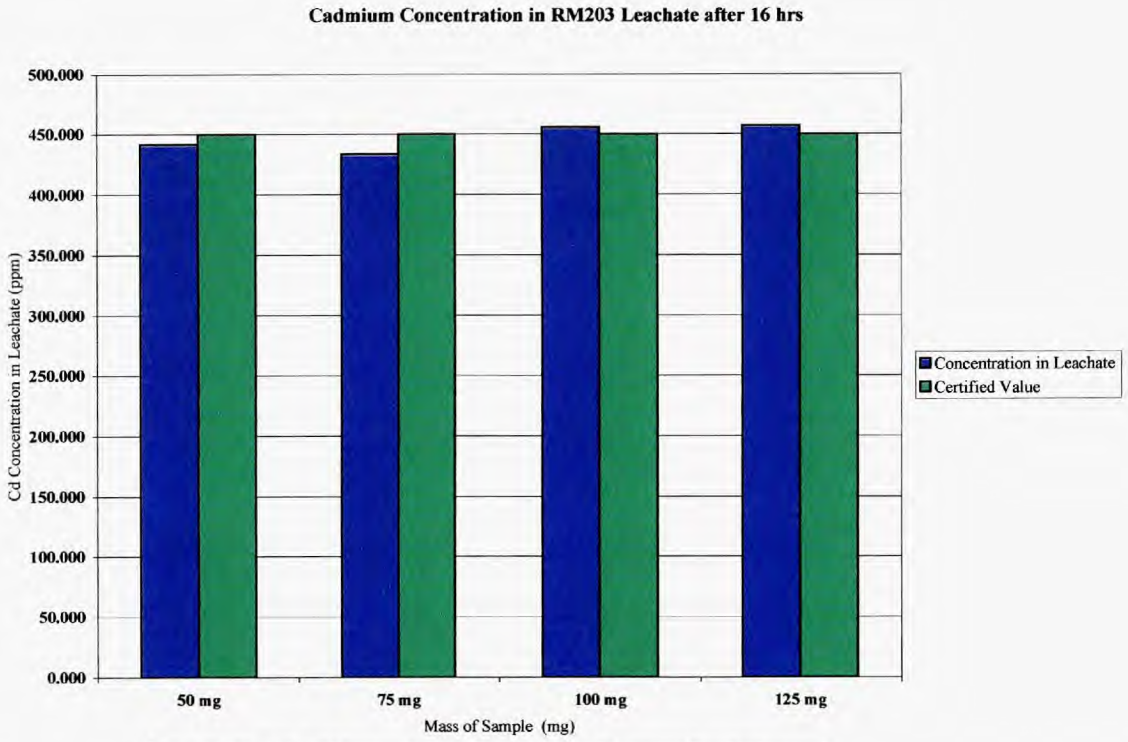
TCLP experiments were carried out with no modification, using the standard reference materials and a mass of 100 g as specified in the standard test method and the results are shown in the Table 4.1.2 below, with the error when compared to the certified value.

Material	RM203		RM205				
Element	Cd	Pb	Cr	As	Cd	Ba	Pb
Concentration (ppm)	453.4	279.0	249.0	1820.6	2967.6	84.3	3362.0
% Error	0.76	2.45	1.97	1.67	1.0	4.2	2.12

Table 4.1.2. Concentrations Obtained Using TCLP Test and Deviation from Certified Values

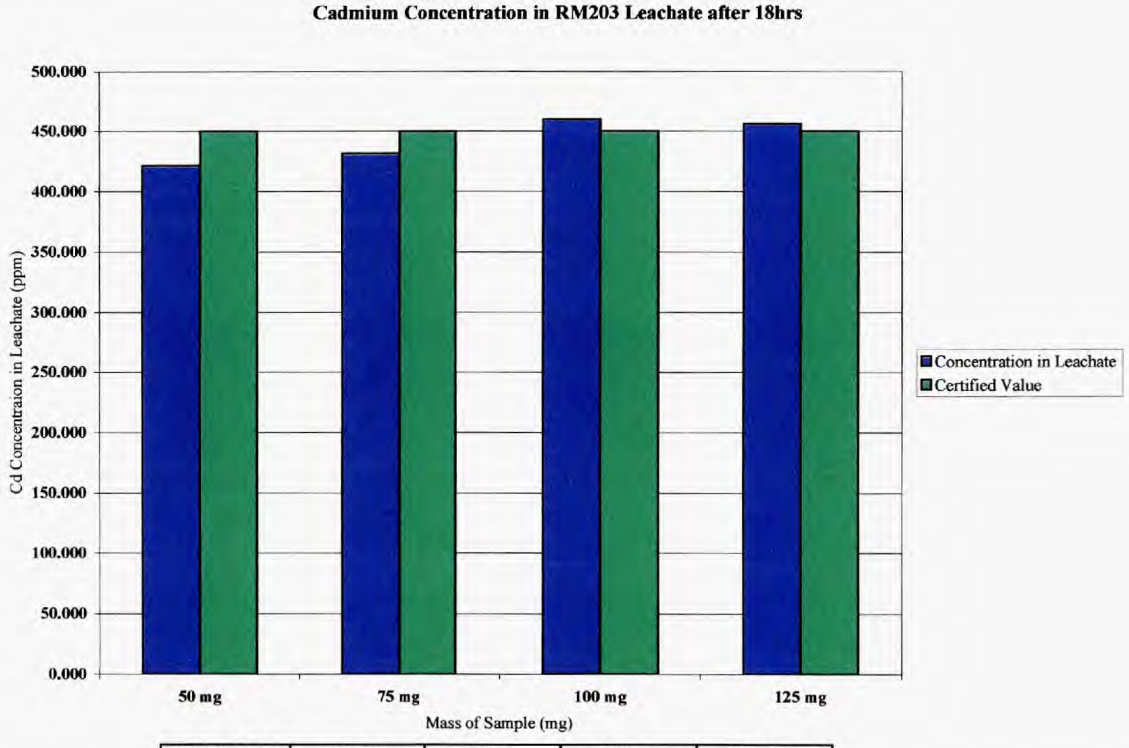
The figures in the following pages show a comparison between the verified value of trace element concentration obtained from TCLP leachate using certified reference materials and the value obtained when conducting the modified TCLP test. The figures also show how the concentrations varied for each of the 4 masses used at a specific agitation time. Below each figure is a table showing how much each empirical concentration varies from the certified value.

The difference between the certified value and the empirical value is given as a percentage of the certified value. Each experimental value given is the mean of six experiments as described in the previous section. These experimental values therefore become less meaningful if the RSD of a six experiment sample set was high. In instances where this was the case, it has been specified in the ensuing discussion of results.



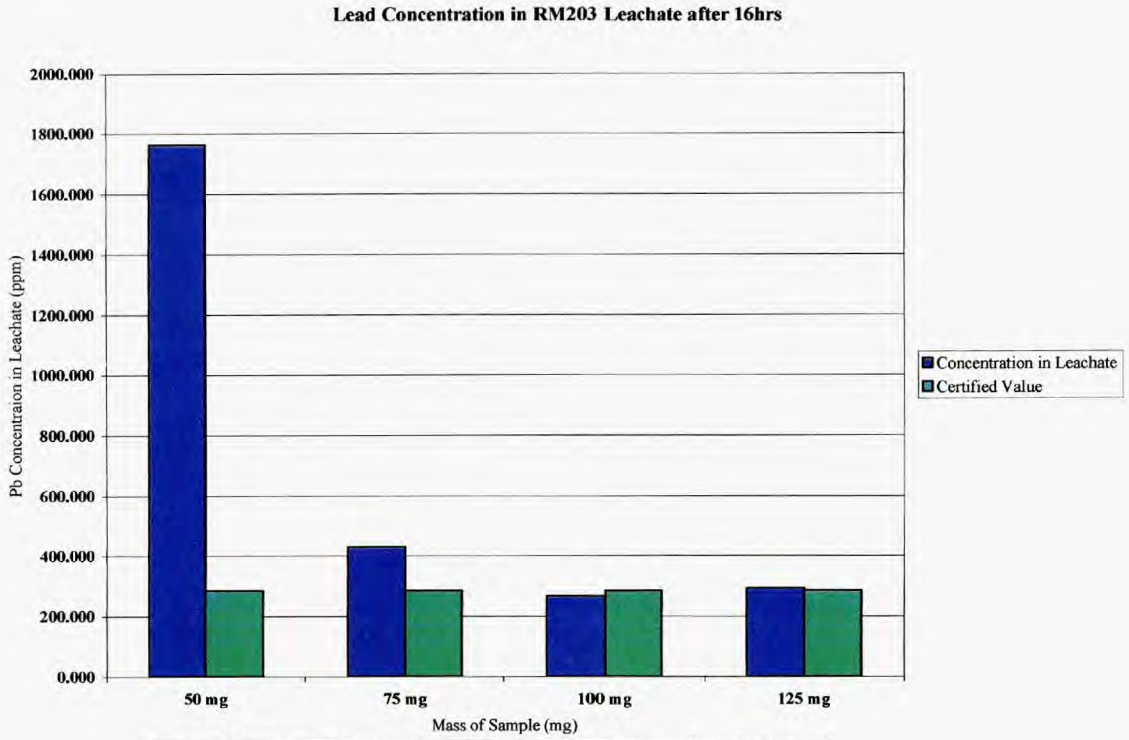
Sample Mass	50 mg	75 mg	100 mg	125 mg
% Error	1.901	3.642	1.308	1.556

Figure 4.1.25 Effect of Sample Mass on Certified Cadmium Concentration after 16hrs – Sample RM203



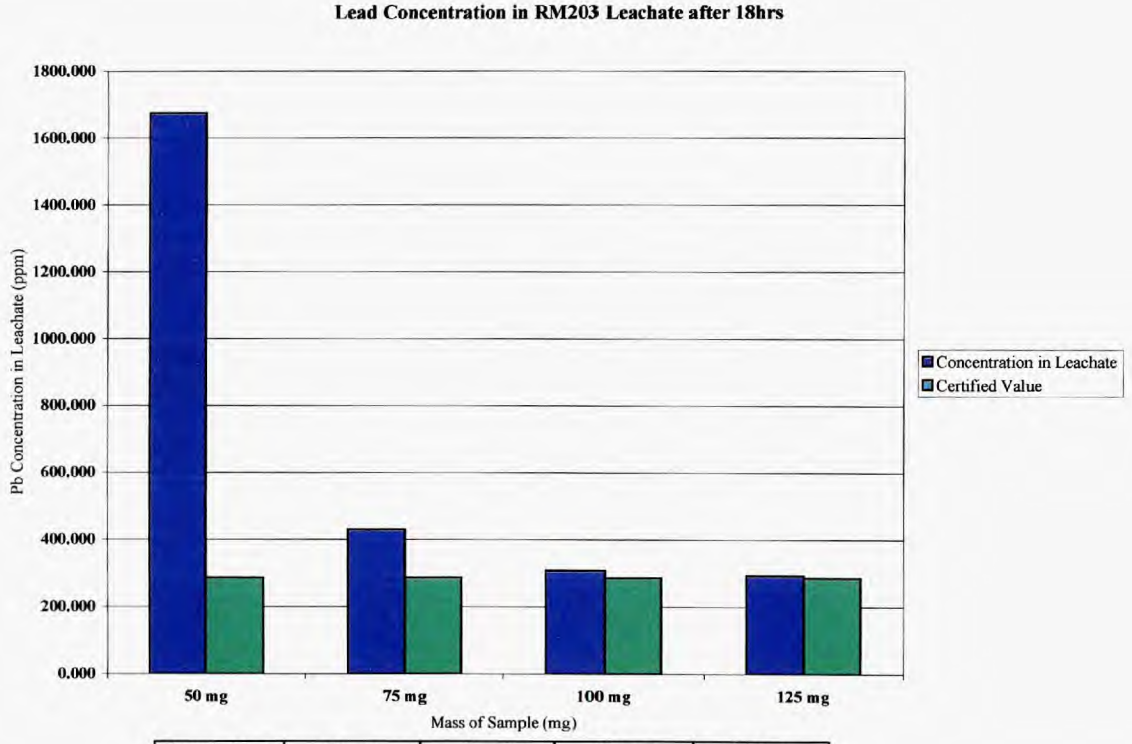
Sample Mass	50 mg	75 mg	100 mg	125 mg
% Error	6.383	4.161	2.283	1.407

Figure 4.1.26 Effect of Sample Mass on Certified Cadmium Concentration after 18hrs – Sample RM203



Sample Mass	50 mg	75 mg	100 mg	125 mg
% Error	516.861	50.670	6.163	2.988

Figure 4.1.27 Effect of Sample Mass on Certified Lead Concentration after 16 hrs – Sample RM203

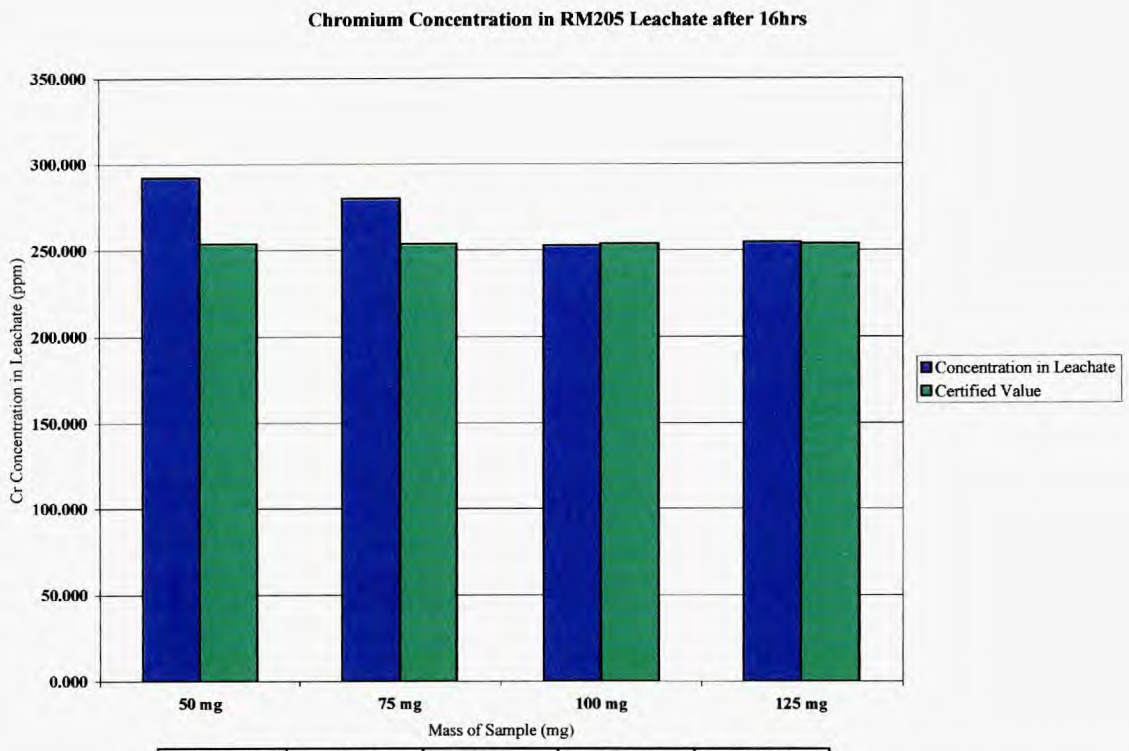


Sample Mass	50 mg	75 mg	100 mg	125 mg
% Error	485.567	50.564	7.919	2.988

Figure 4.1.28 Effect of Sample Mass on Certified Lead Concentration after 18 hrs – Sample RM203

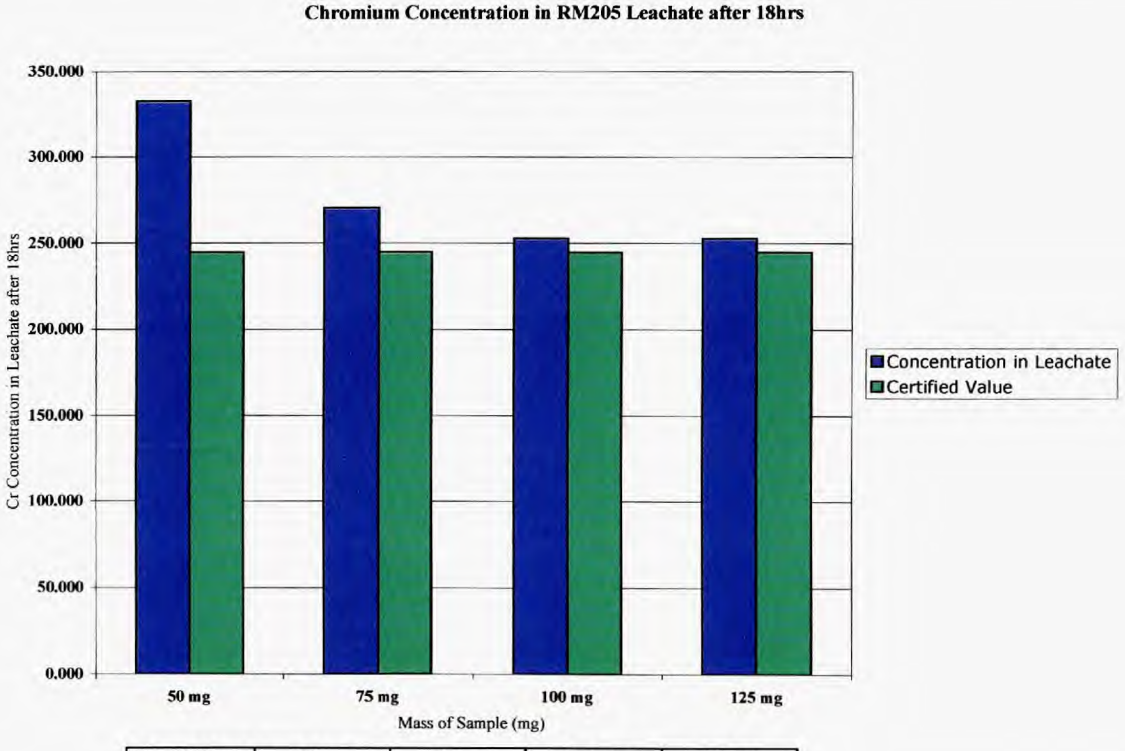
For certified reference material RM203 the results obtained for Cd concentration were close to the verified valued of 450 ppm. At 16 hrs the deviation from the certified value varied from 1.3% to 3.6%. At 18hrs the error was greatest for the smallest sample mass at 6.3 % and decreased with increasing mass to an error of 1.4%. It could therefore be stated that sample mass did not have an effect on the accuracy of results for Cd concentrations could be ascertained with confidence for even the smallest sample mass tested. In order to minimise error however it would be advantageous to use the larger sample masses.

Regarding the Pb concentration, the results obtained showed a far greater deviation from the certified value and were shown to be much more mass dependent. The percentage error at 50mg was exceedingly large for both the 16 and the 18 hour time spans, being 516.9 and 485.7 % respectively. These large error values were obtained despite the fact that the RSD, for the six experiment set used to obtain each mean final value, was comparatively small. The error decreased with increasing sample mass, giving a 10 fold drop from 50 to 75 mg and then again from 75 to 100mg. At 100mg the error was small enough to deem results obtained in this instance reliable.



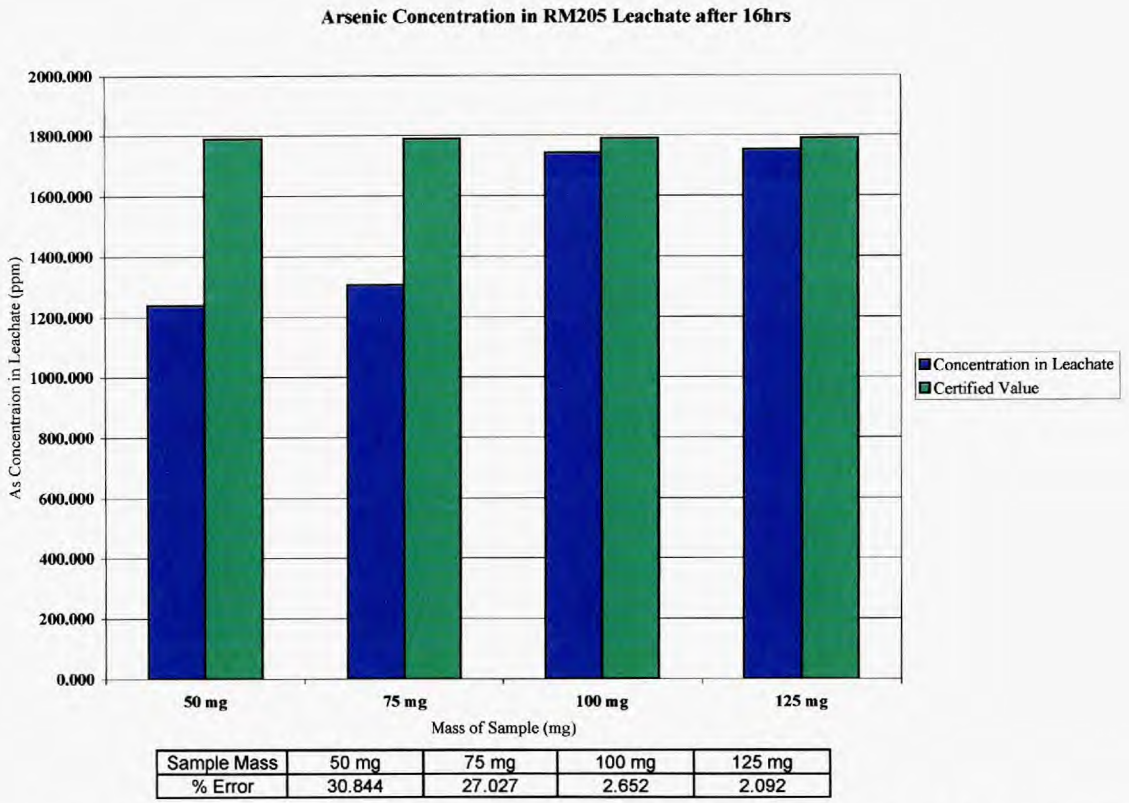
Sample Mass	50 mg	75 mg	100 mg	125 mg
% Error	15.041	10.287	0.371	0.252

Figure 4.1.29 Effect of Sample Mass on Certified Chromium Concentration after 16 hrs – Sample RM205



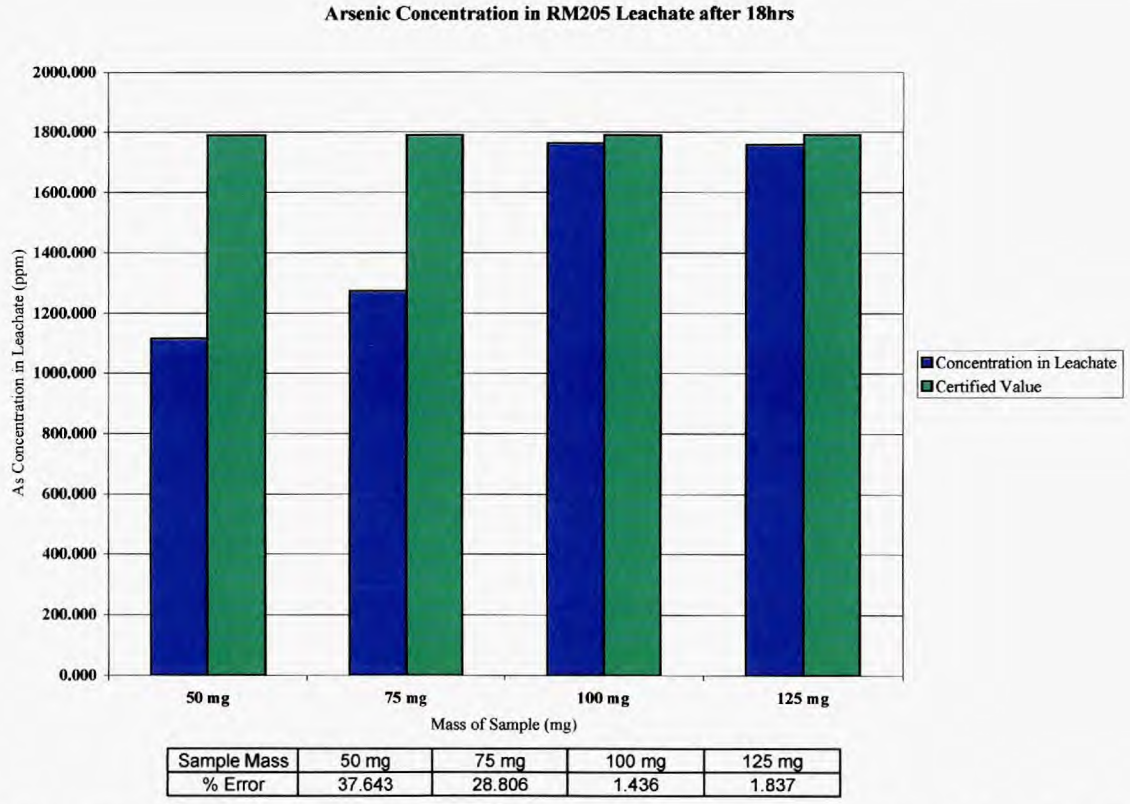
Sample Mass	50 mg	75 mg	100 mg	125 mg
% Error	35.714	10.441	3.288	3.200

Figure 4.1.30 Effect of Sample Mass on Certified Chromium Concentration after 18 hrs – Sample RM205



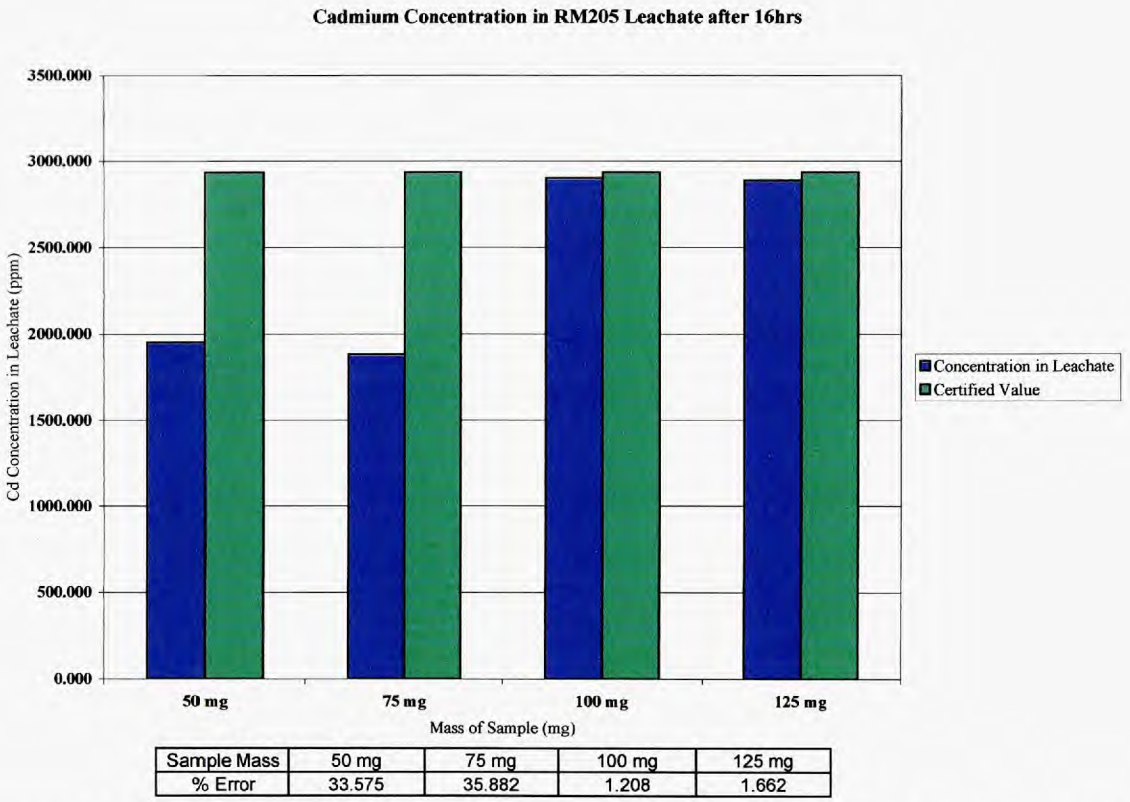
Sample Mass	50 mg	75 mg	100 mg	125 mg
% Error	30.844	27.027	2.652	2.092

Figure 4.1.31 Effect of Sample Mass on Certified Arsenic Concentration after 16 hrs – Sample 205



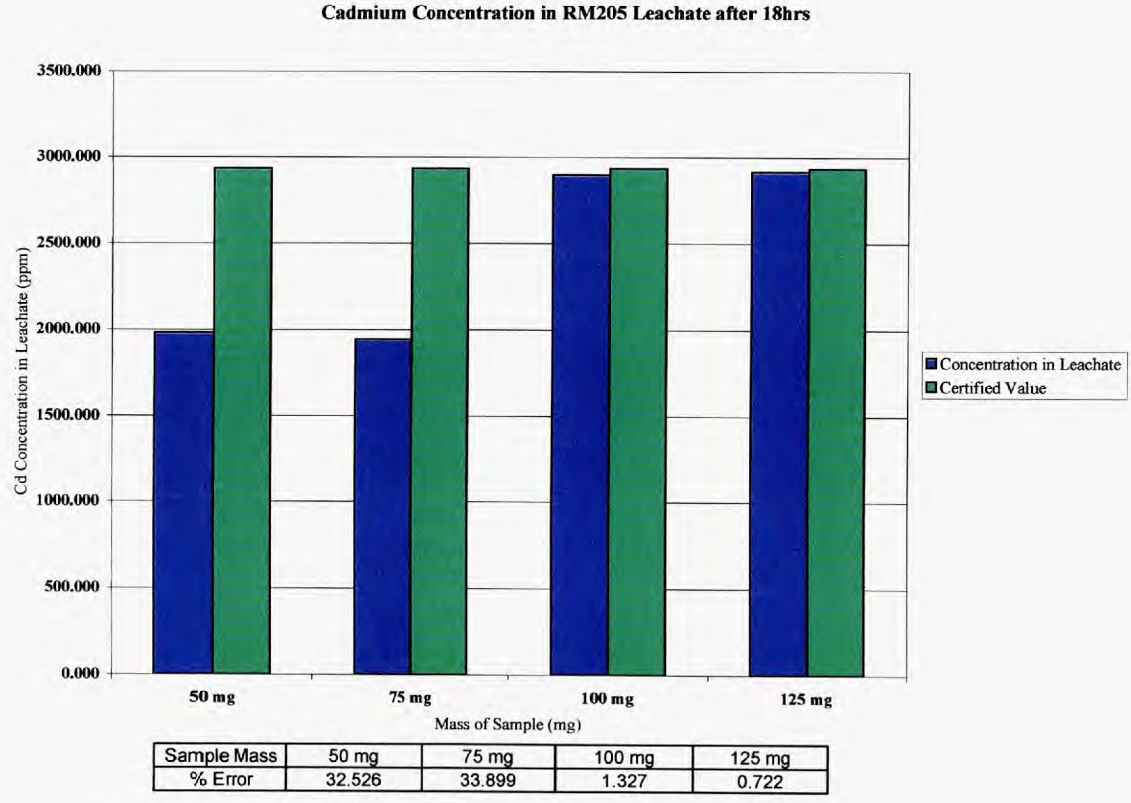
Sample Mass	50 mg	75 mg	100 mg	125 mg
% Error	37.643	28.806	1.436	1.837

Figure 4.1.32 Effect of Sample Mass on Certified Arsenic Concentration after 18 hrs – Sample 205



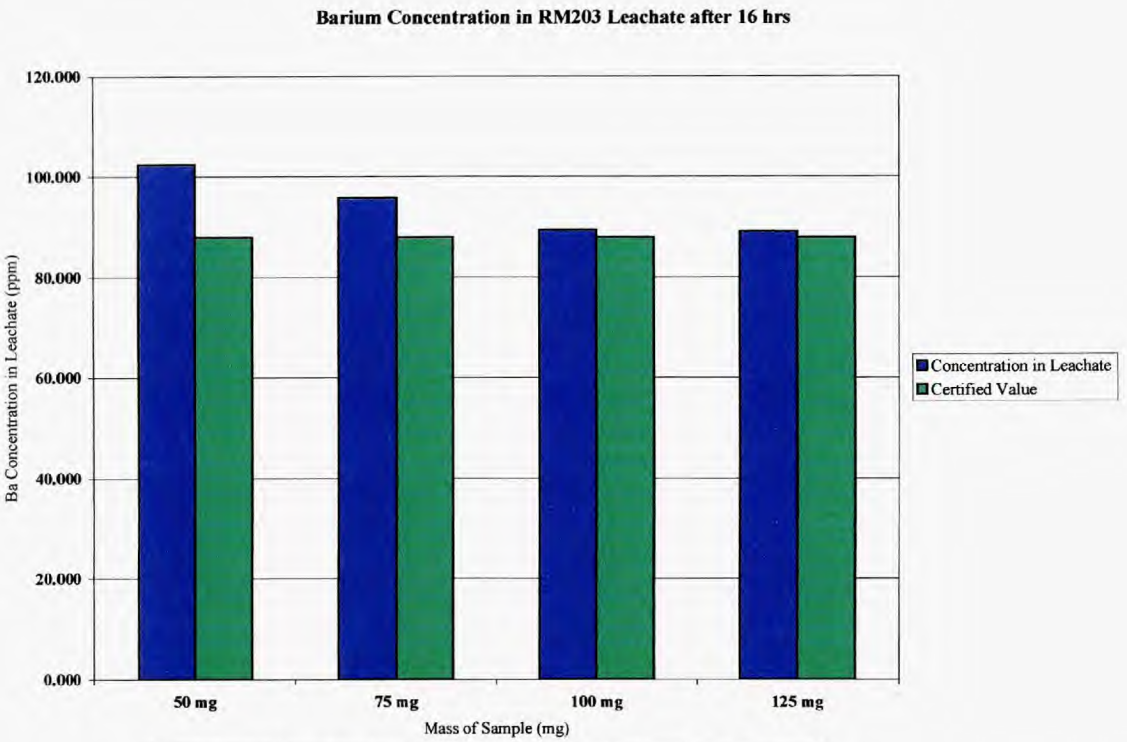
Sample Mass	50 mg	75 mg	100 mg	125 mg
% Error	33.575	35.882	1.208	1.662

Figure 4.1.33 Effect of Sample Mass on Certified Cadmium Concentration after 16 hrs – Sample RM205



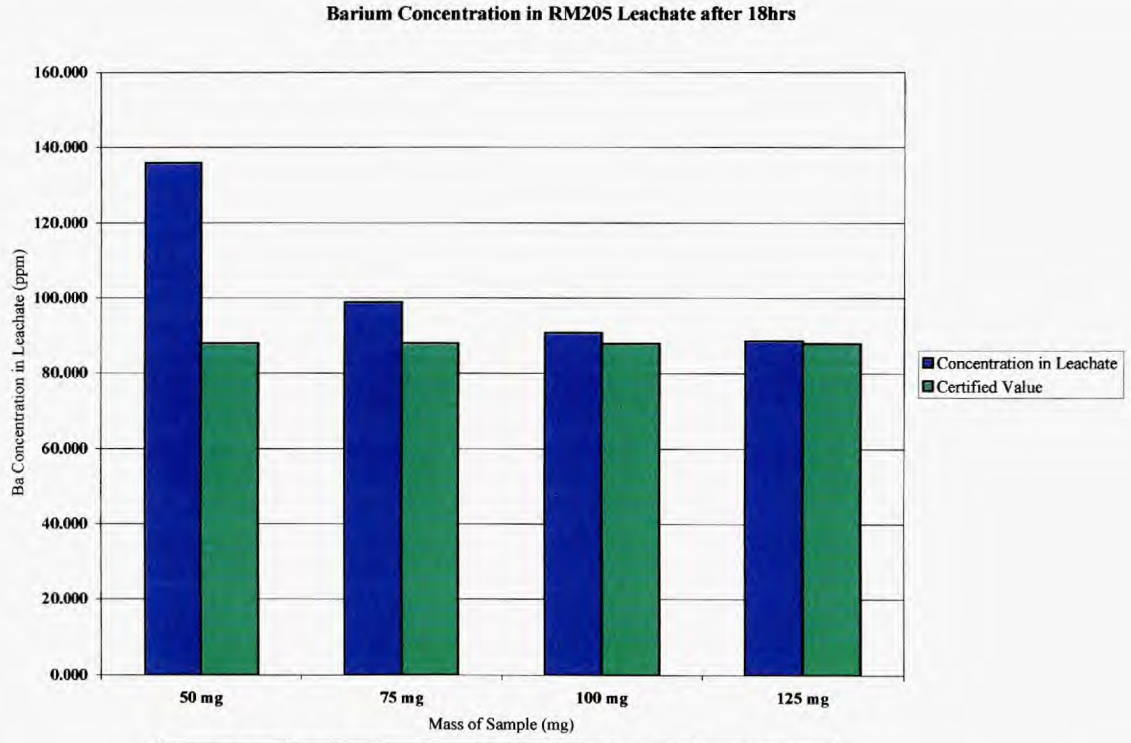
Sample Mass	50 mg	75 mg	100 mg	125 mg
% Error	32.526	33.899	1.327	0.722

Figure 4.1.34 Effect of Sample Mass on Certified Cadmium Concentration after 18 hrs – Sample RM205



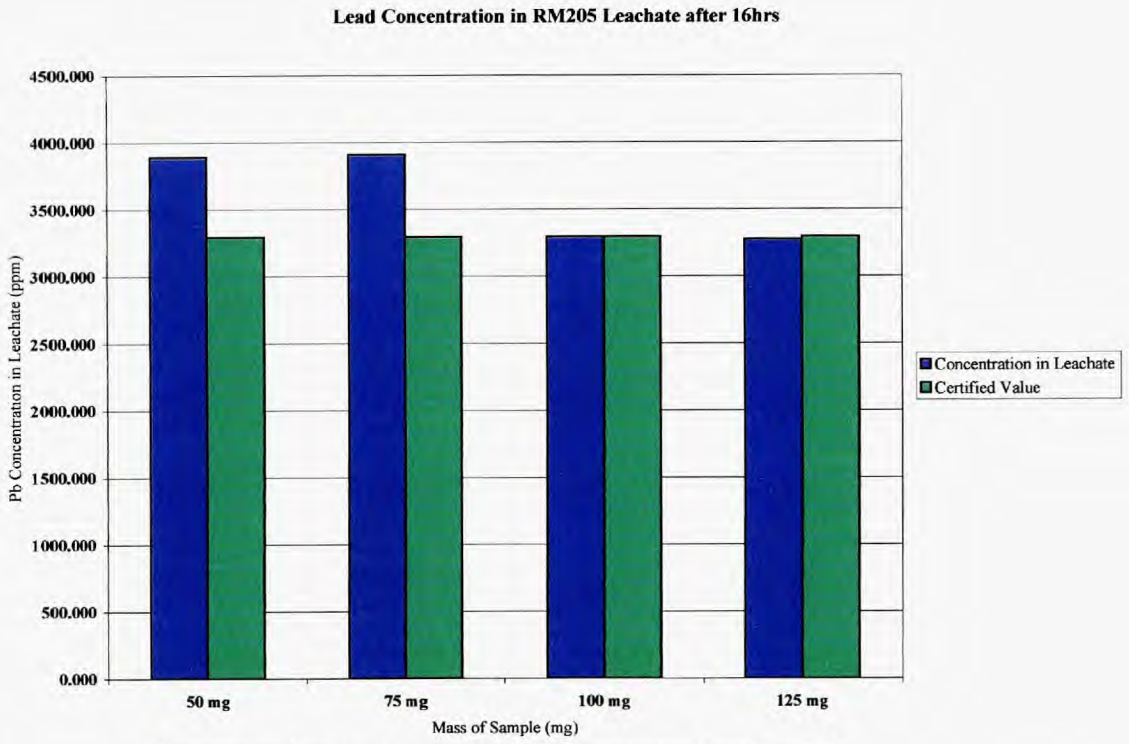
Sample Mass	50 mg	75 mg	100 mg	125 mg
% Error	16.456	8.950	1.553	1.216

Figure 4.1.35 Effect of Sample Mass on Certified Barium Concentration after 16 hrs – Sample RM205



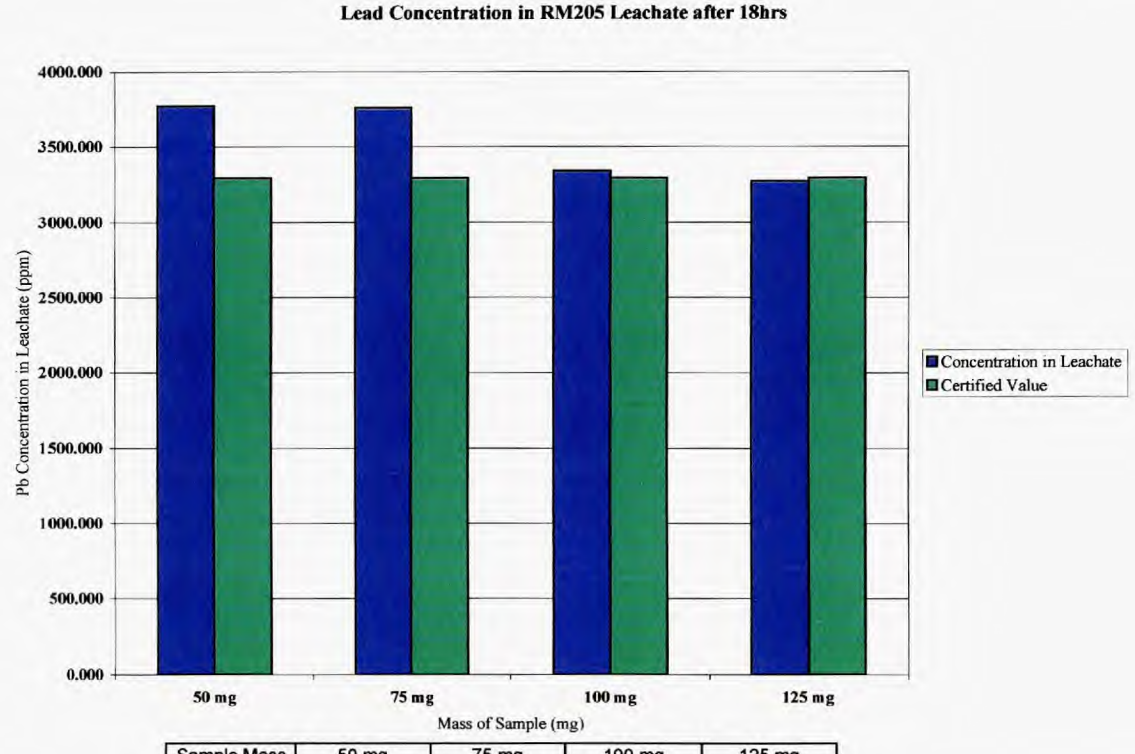
Sample Mass	50 mg	75 mg	100 mg	125 mg
% Error	54.545	12.500	3.040	0.712

Figure 4.1.36 Effect of Sample Mass on Certified Barium Concentration after 18 hrs – Sample RM205



Sample Mass	50 mg	75 mg	100 mg	125 mg
% Error	18.093	18.769	0.040	0.461

Figure 4.1.37 Effect of Sample Mass on Certified Lead Concentration after 16 hrs – Sample RM205



Sample Mass	50 mg	75 mg	100 mg	125 mg
% Error	14.571	14.123	1.405	0.641

Figure 4.1.38 Effect of Sample Mass on Certified Lead Concentration after 16 hrs – Sample RM205

The Cr concentration obtained in sample RM205 should have been 250 ppm if it agreed with the certified value. The errors involved when experiments were carried out at 16 hrs decreased with increasing mass of sample, in a non-linear manner. This was also the case for experiments conducted at 18 hrs. For both time spans there seems to be a steep drop in error from the 75 to the 100mg sample size. In the instance of Cr this could be attributed to the large standard deviation in the sample set used to determine the mean. This large standard deviation could in turn be attributed to experimental error or sample in-homogeneity. At 100mg the error was 0.37 and 3.2% for the 16 and 18hr time spans respectively. This was deemed small enough to make the assumption that results at this mass were reliable.

Arsenic once more showed the characteristics typical of the previous elements considered. The percentage error for the 50mg and 75 mg sample masses was around 30% for both masses and time spans, dropping to around 2% for the 100 and 125mg masses, at both time spans. The higher relative standard deviations of the original sample set for the lower masses explain the high error to a degree, but a consistent experimental error may have contributed to the lower than expected concentration. As with the other elements at 100mg and 125mg, there is good agreement between the certified value and the experimental value, with the empirical mean value being in all instances within 2% of the certified value.

The Cd concentration in RM205 exhibits the same trend as the other elements. There is a sharp decline in difference between empirical and certified value from 75mg to 100mg. For sample masses of 100mg and 125 mg the error is a maximum of 1.7%. Ba and Pb concentrations for RM205 show the same trends as all other elements.

4.1.2.1 Conclusions

It was necessary for the concentrations in the reference materials, leached at small sample masses, to concur with certified values obtained when the reference materials were leached using the standard TCLP test. At 50 mg and 75 mg there was a large discrepancy between the certified and the empirical value, such that results could not be deemed reliable. The error improved greatly when a mass of 100 mg was used. The errors obtained when using the modified TCLP were comparable to errors obtained when carrying out the TCLP with standard apparatus and the required mass of 100 g. It may concluded therefore, that the modified test may be used with as much confidence as the standard TCLP test for masses no smaller than 100 mg.

A mass of 100 mg was chosen to carry out all subsequent leaching tests using the TCLP method. The mass of 100 mg rather than 125 mg was chosen due to constraints in acquiring large quantities of ash in the Hot-Rod reactor. A time span of 16 hours was also chosen for all further experiments.

4.2 Trace Element Contents In Raw Fuels

Before any combustion and leaching experiments were conducted the trace element content in all the fuels to be used was determined. The sections below show the trace element content in the fuels used for the CERCHAR fuels and the Chilean Power station fuels.

4.2.1 Experimental Error and Error Calculations

Errors in the results may be defined as falling into two categories, human and instrumental. Human errors include, for example, mishandling and contamination of the samples and reagents or incorrect collection of the ash from the reactor. These are usually apparent from anomalous results, which may, in turn, be disregarded. In order to identify and eliminate these errors an experiment is conducted several times as discussed below.

Systematic errors due to instrumentation are either factored into the final error calculations if they are significant, or are ignored if they are deemed negligible when compared to other much larger experimental errors. Possible instrumentation errors in this study were contributed by:

- Balances used to measure masses
- Gas flow pressure gauges to the hot rod reactor and the AMA 254 Hg analyser
- Temperature sensors to the reactor

In order to minimise these errors the instruments were regularly calibrated. The balances used gave gram measurements to four significant figures and the temperature sensors degrees Celsius to two significant figures. Therefore, errors given by the above apparatus was deemed insignificant in comparison with the errors yielded by the trace element determination and could be discounted.

In order to measure the trace element concentration in the un-combusted fuels each experiment was conducted 7 times. The student t-distribution was then used, with a 95 % confidence interval in order to calculate the error involved in these concentration measurements. The experimental error was then converted to a percentage and rounded up to the nearest 5 %. Values for the percentage errors calculated for the CERCHAR fuels and the CHILEAN fuels are discussed separately below.

4.2.2 CERCHAR Fuels

The eight CERCHAR fuels studied have been labelled Fuel 1 to Fuel 8 and the materials contained in each fuel and their relative proportions are given in Section 3.1.2 (Figure 3.1.2). In order to gain greater insight into the relationship between the fuels and trace element content and to understand any correlations which may be present, the trace element concentrations are presented firstly by element e.g. beryllium concentration in CERCHAR Fuels 1- 8 and then by fuel e.g. the concentration of all the trace elements studied for Fuel 1.

The results for the eight Cerchar fuels studied all had errors of below 5%, for all elements, except selenium and arsenic. Consistency of results for arsenic was found to be below 10% for all fuels except Fuel 6 and Fuel 8 where the error was found to be 12.4 and 13.2 % respectively. Errors for Arsenic are therefore given as 15%. In the case of selenium the error was found to be in the region of 12 % for all fuels, so this has once more been rounded to 15%. Errors are presented as Y-error bars for each data set and data tables are presented for clearer depiction of results.

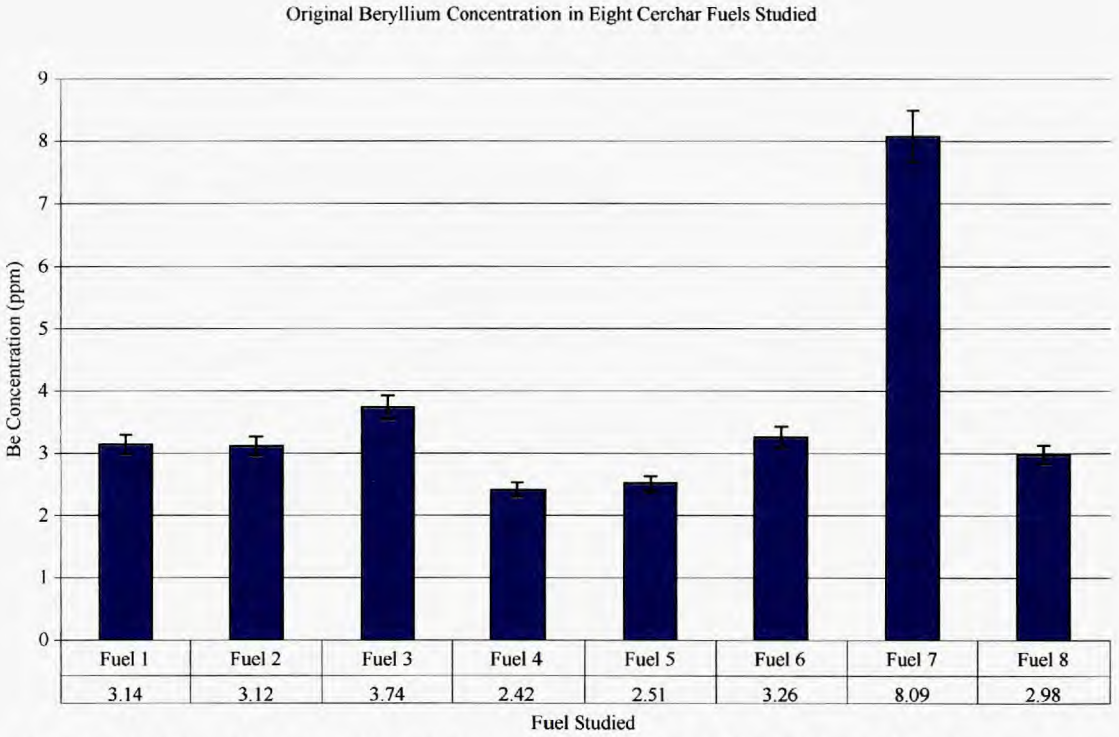


Figure 4.2.1 Beryllium Concentration in Eight CERCHAR fuels Studied

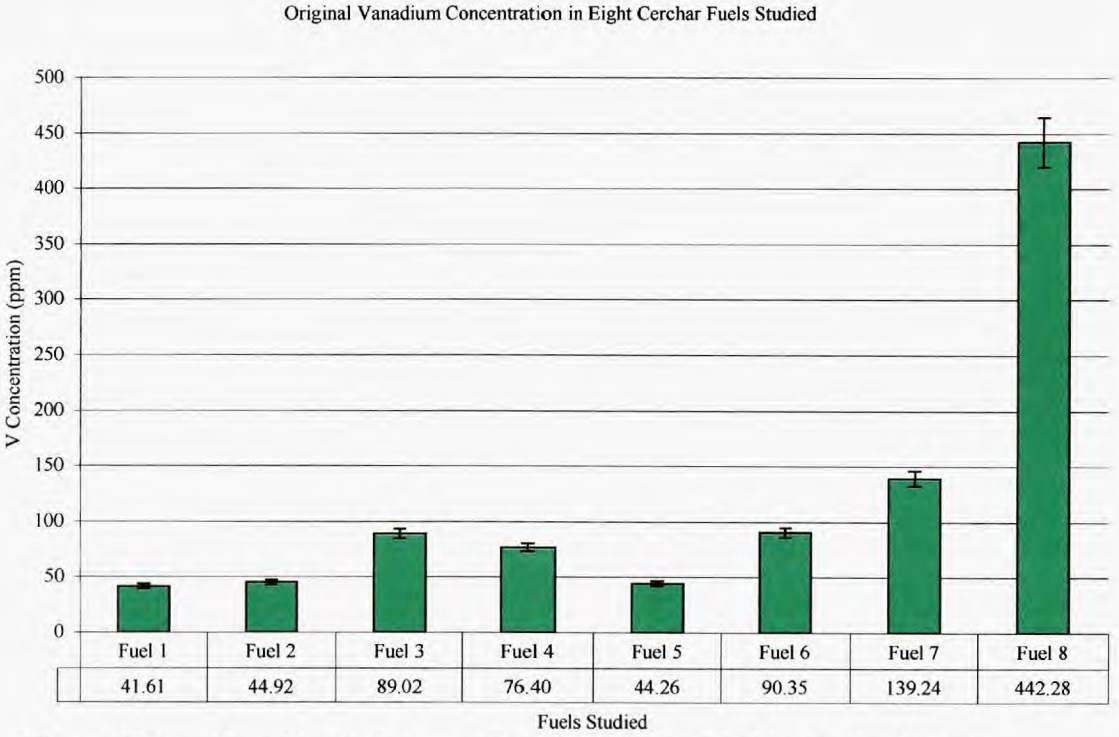


Figure 4.2.2 Vanadium Concentration in Eight CERCHAR fuels Studied

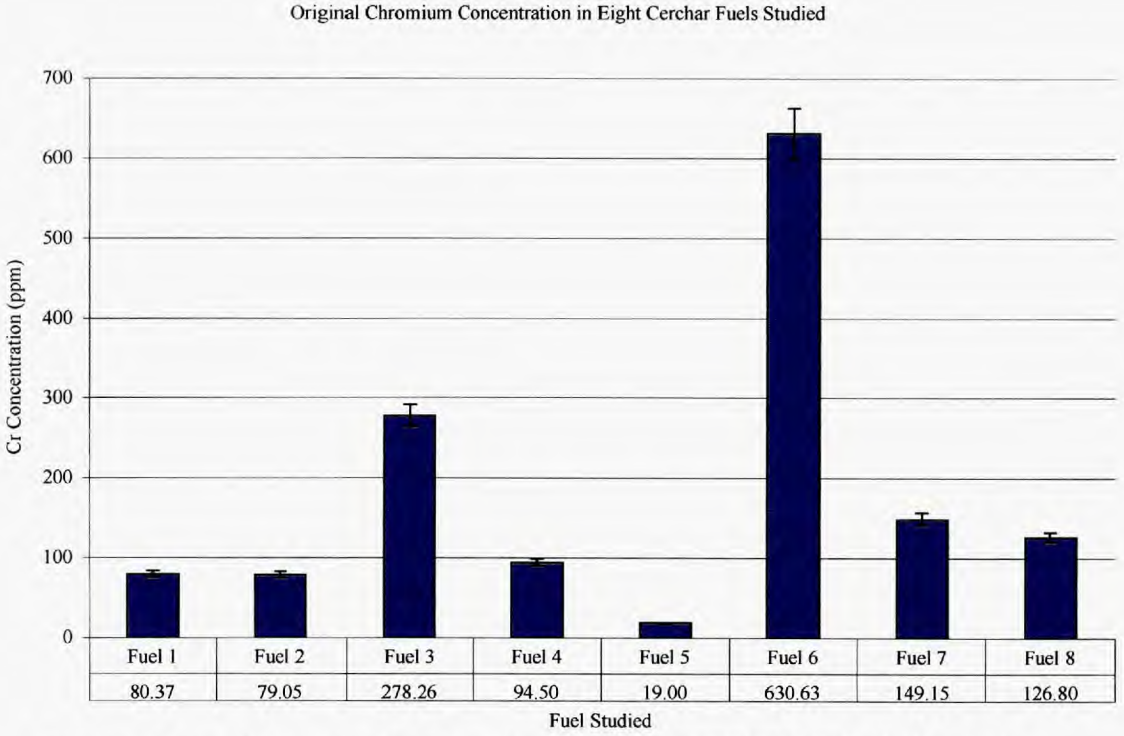


Figure 4.2.3 Chromium Concentration in Eight CERCHAR fuels Studied

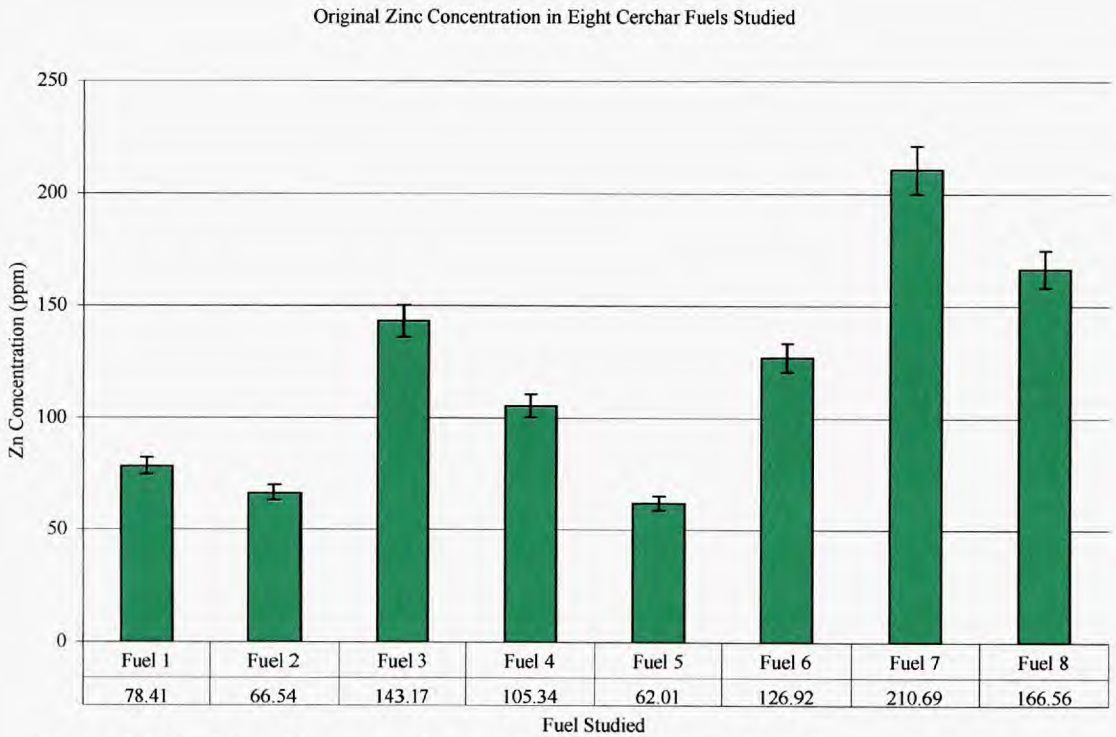


Figure 4.2.4 Zinc Concentration in Eight CERCHAR fuels Studied

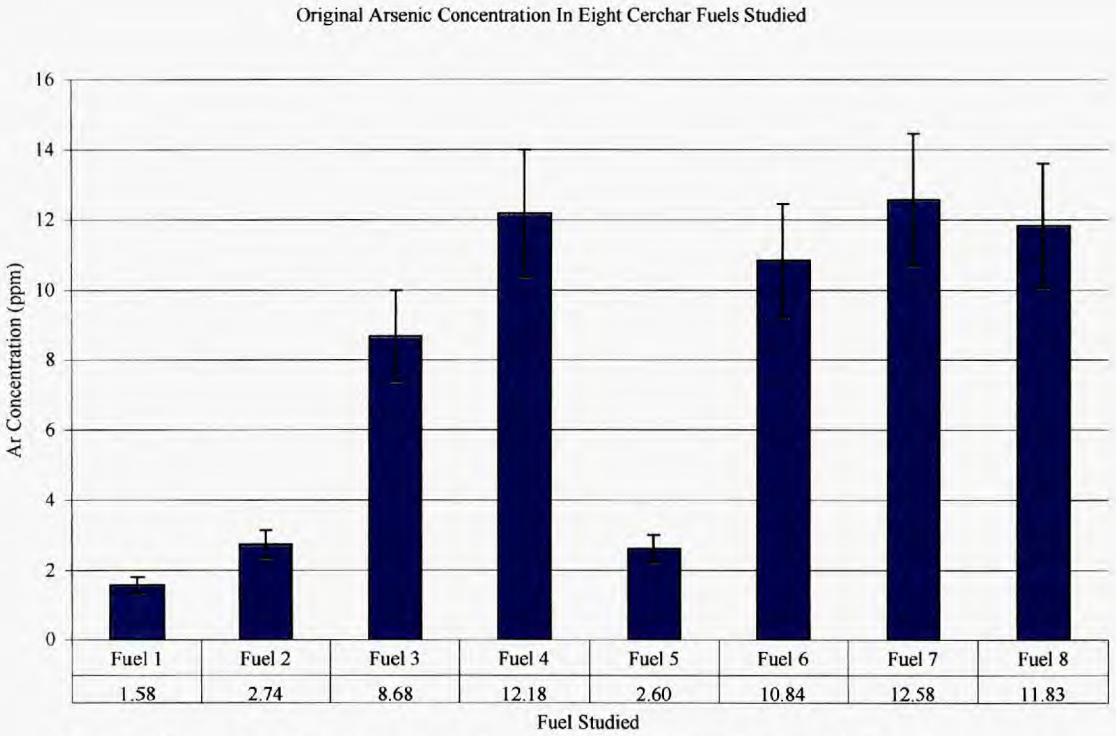


Figure 4.2.5 Arsenic Concentration in Eight CERCHAR fuels Studied

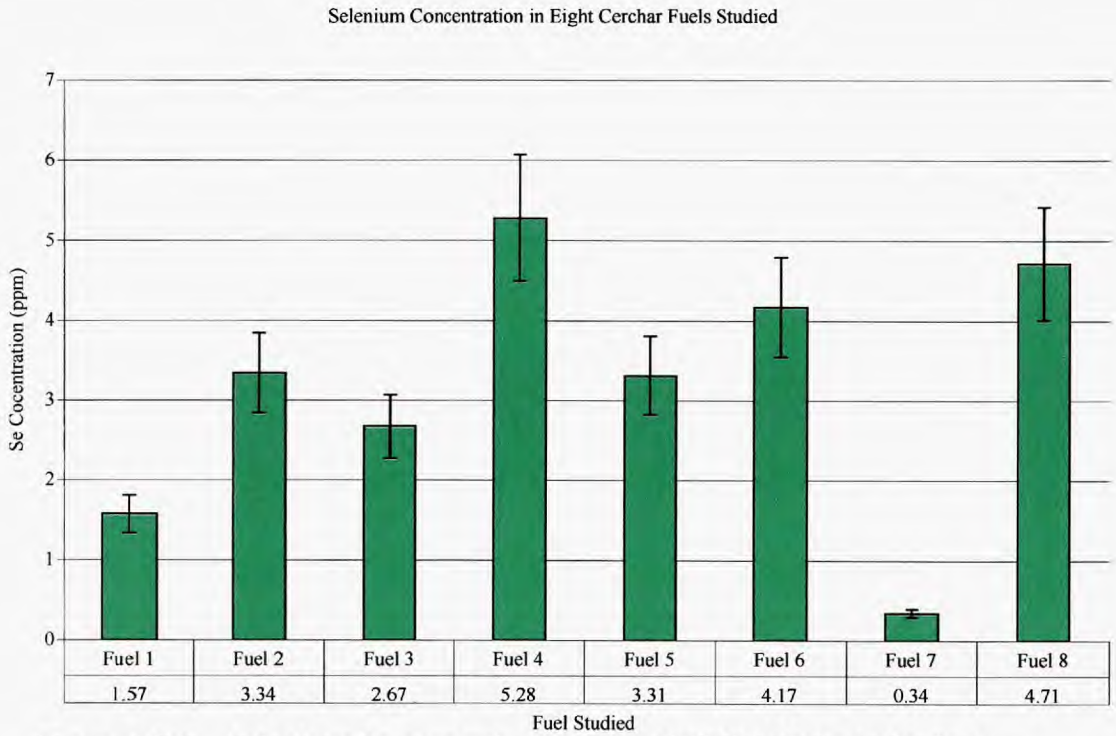


Figure 4.2.6 Selenium Concentration in Eight CERCHAR fuels Studied

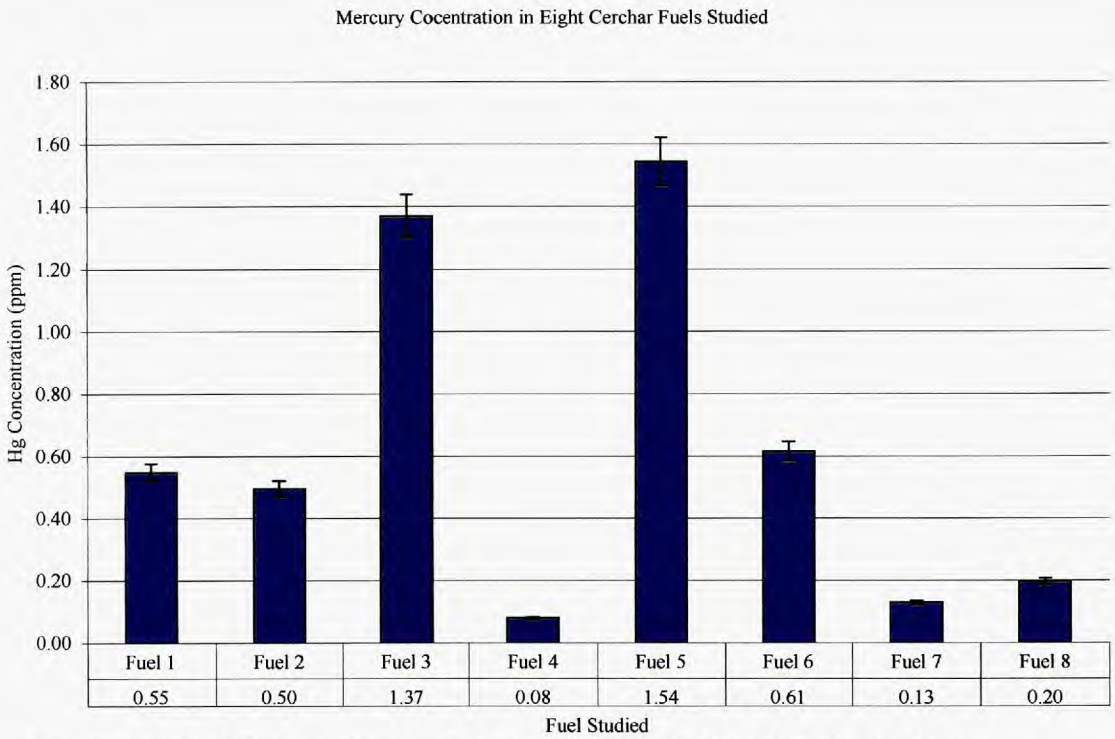


Figure 4.2.7 Mercury Concentration in Eight CERCHAR fuels Studied

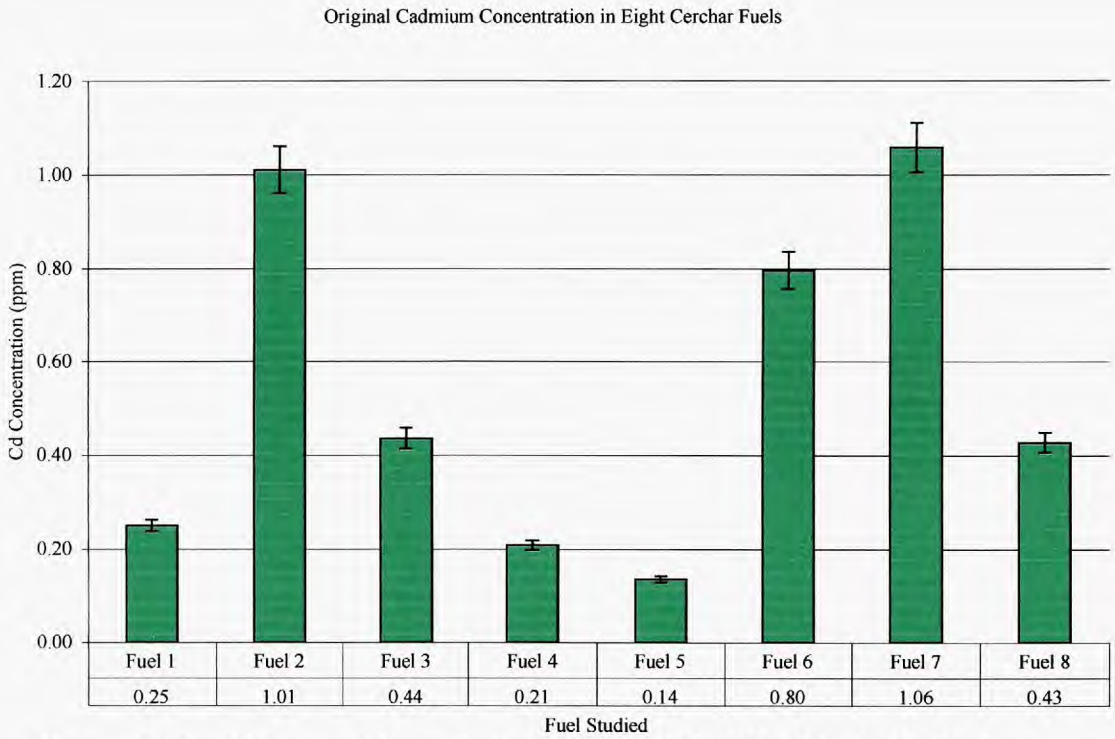


Figure 4.2.8 Cadmium Concentration in Eight CERCHAR fuels Studied

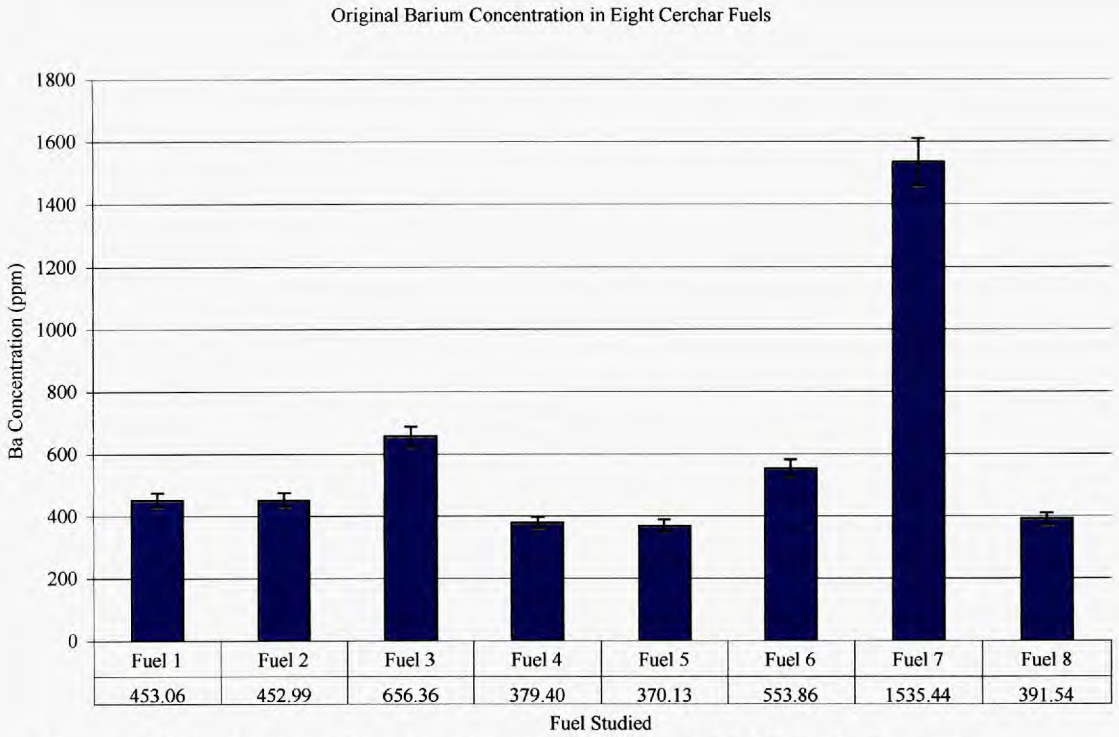


Figure 4.2.9 Barium Concentration in Eight CERCHAR fuels Studied

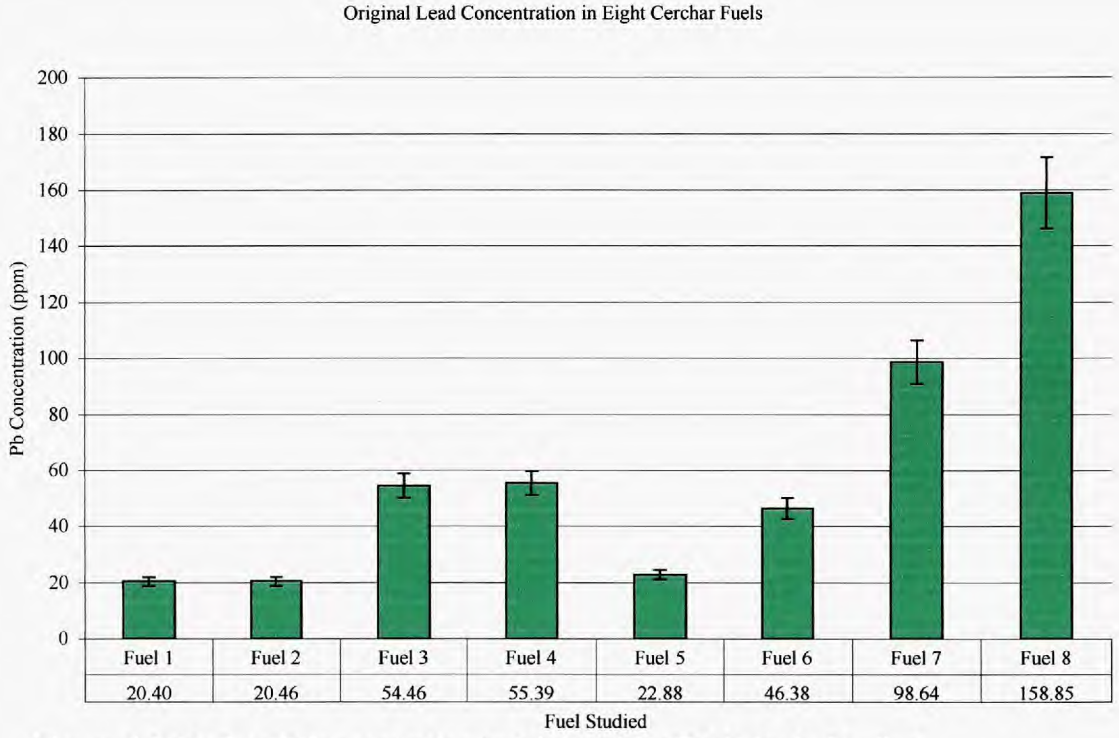


Figure 4.2.10 Lead Concentration in Eight CERCHAR fuels Studied

All the fuels contained approximately the same quantity of Be i.e. between 2.5 & 4 ppm with the exception of Fuel 7. Fuel 7 being a mixture of South African Coal 1997 (Fuel1) and un-dried bark leads to the conclusion that the bark makes a disproportionately high contribution to the Be content in Fuel 7. Fuel 1 and 2, being South Africa Coal '97 and '99 contained the same quantity of Be to a 0.02 ppm difference, which is what would be expected of fuels of such similar characteristics.

Vanadium concentrations between fuels varied by an order of magnitude between Fuels 1-7 and Fuel 8. From this it may be inferred that the petroleum coke portion of the fuel blend contributes to the higher vanadium concentration. Once more, Fuel 1 and Fuel 2 concentrations were very similar due to the similarity of the fuels.

In the case of chromium, again there is parity between the concentrations in Fuel 1 and 2. The degree of magnitude of chromium concentration for all the fuels is the same except for Fuel 3 and Fuel 6. Both of these fuel blends contain Freyming Coal Slurry, so it may be inferred that it is this fuel which contributes to the higher proportion of Chromium in these fuels. Fuel 5 contains the least chromium and it may be noted that this fuel, containing South Africa coal and wet saw dust, has the lowest trace element concentration for nearly all the elements studied.

Zinc concentration shows a higher variation between Fuel 1 and Fuel 2 at 78.41 and 66.54 ppm respectively. The lowest Zinc concentration is contained in Fuel 5 and the zinc concentration when viewed across the fuel range is within the same order of magnitude, with Fuel 7 having the highest concentration at 210.1 ppm.

The quantities of Arsenic range from 1.6 to 12.2 ppm. Fuel 4 and 7 which contained the higher concentrations of arsenic also showed the highest degree of error. Arsenic concentrations for Fuel 1 and 2 were similar taking account of the higher error involved in the arsenic results.

Selenium errors were also higher with a maximum error for fuel 8 of 12.0%. The variation between fuels was ten fold, there being a 5ppm difference between the highest and lowest selenium concentration. The highest concentrations were found in the fuels containing Freyming Schlamms. The difference in Selenium concentration in Fuel 1 and Fuel 2 is larger than for the other elements, even after considering the increased error involved.

Mercury was not found in great abundance in any of the fuels. However fuel 3 and 5 both showed levels in of 1ppm (1.37 & 1.54ppm respectively) which are high compared with typical coal value of a few tenths of a ppm. Mercury was present in equal proportions in Fuels 1 and 2 given the errors involved.

As with mercury, cadmium concentrations were also small in all the fuels, concentrations ranging from 0.14 ppm for Fuel 5 to 1.05 ppm for Fuel 7. There was a four-fold difference between the cadmium concentration in Fuel 1 and Fuel 2 but in absolute terms and accounting for errors, this is small, represented by a concentration of 0.76 ppm.

Barium was by far, the most abundant trace elements studied, with a concentration range of 370.13 ppm to 1535 ppm. Fuel 5 and Fuel 8 contained similar quantities of barium as did Fuel 1 and Fuel 2.

Lead occurrences followed the same general tendencies as the other trace elements. Lead quantities were in the same order of magnitude for all elements, Fuels 7 and 8 exhibiting the highest concentrations, Fuels 1 and 2 concentrations reflecting the similarity of the fuels and Fuel 5 showing concentrations at the lower end of the range.

The following graphs show the results obtained on a fuel by fuel basis. Results have been presented in logarithmic scale, with data tables showing the precise concentration value. Precise errors bar values may be seen in Figures 4.2.2.1-4.2.2.10 above.

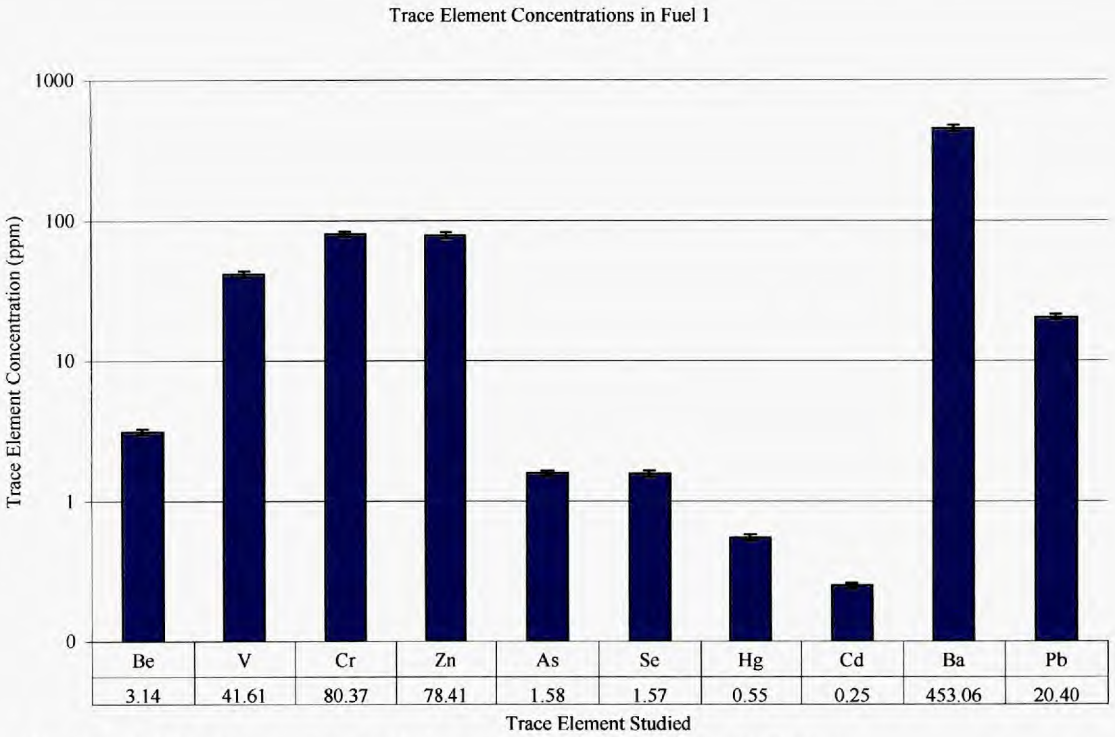


Figure 4.2.11 Trace Element Occurrence in CERCHAR Fuel 1

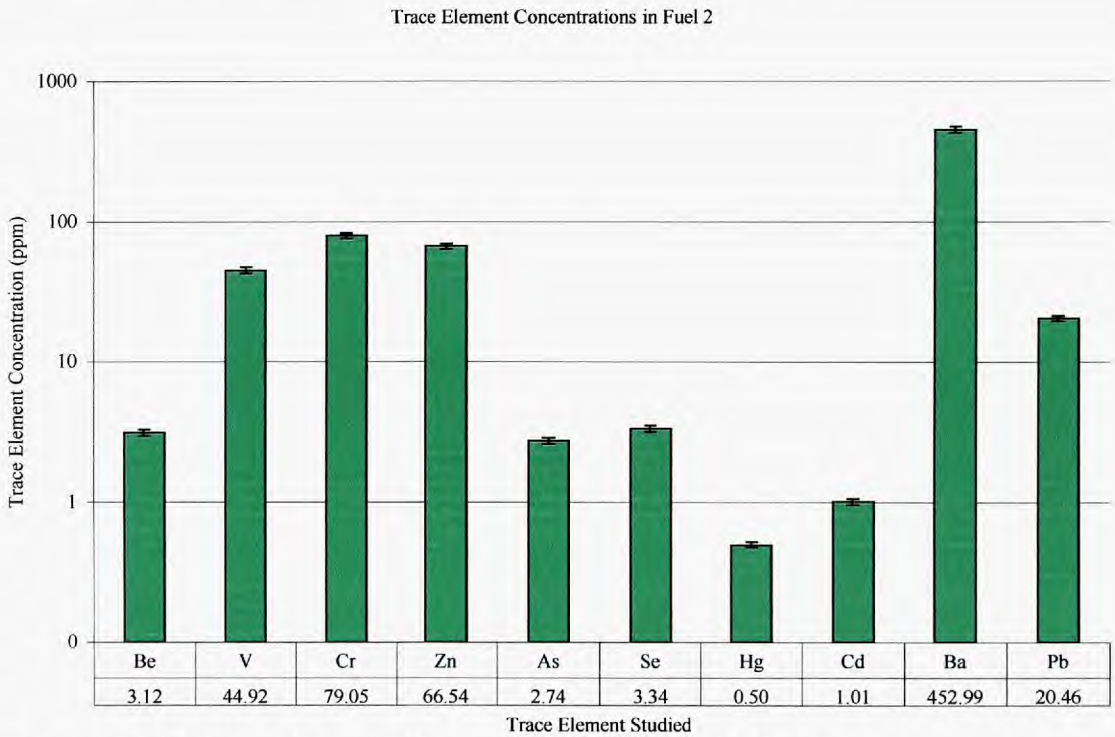


Figure 4.2.12 Trace Element Occurrence in CERCHAR Fuel 2

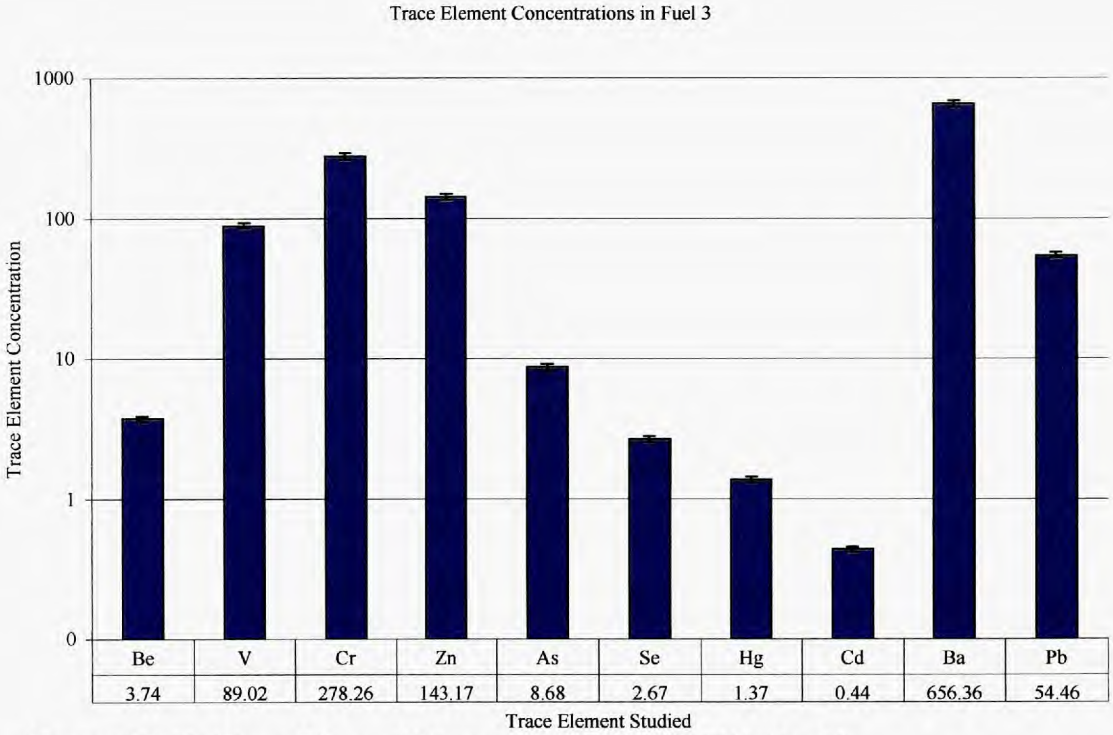


Figure 4.2.13 Trace Element Occurrence in CERCHAR Fuel 3

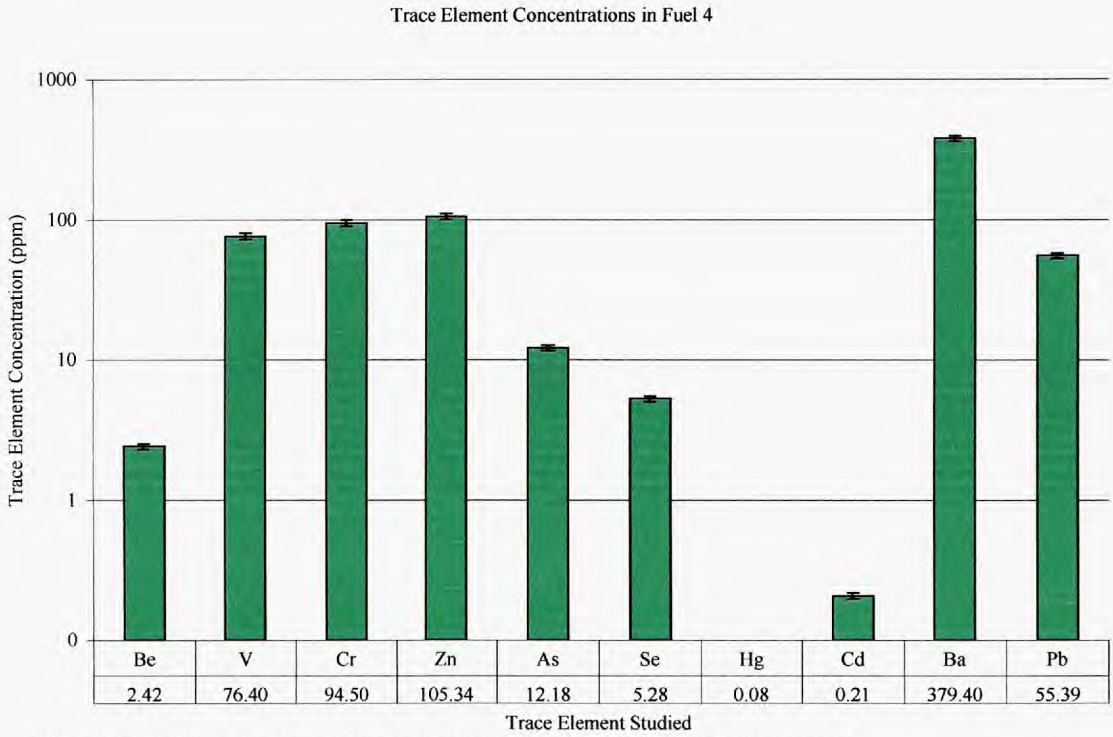


Figure 4.2.14 Trace Element Occurrence in CERCHAR Fuel 4

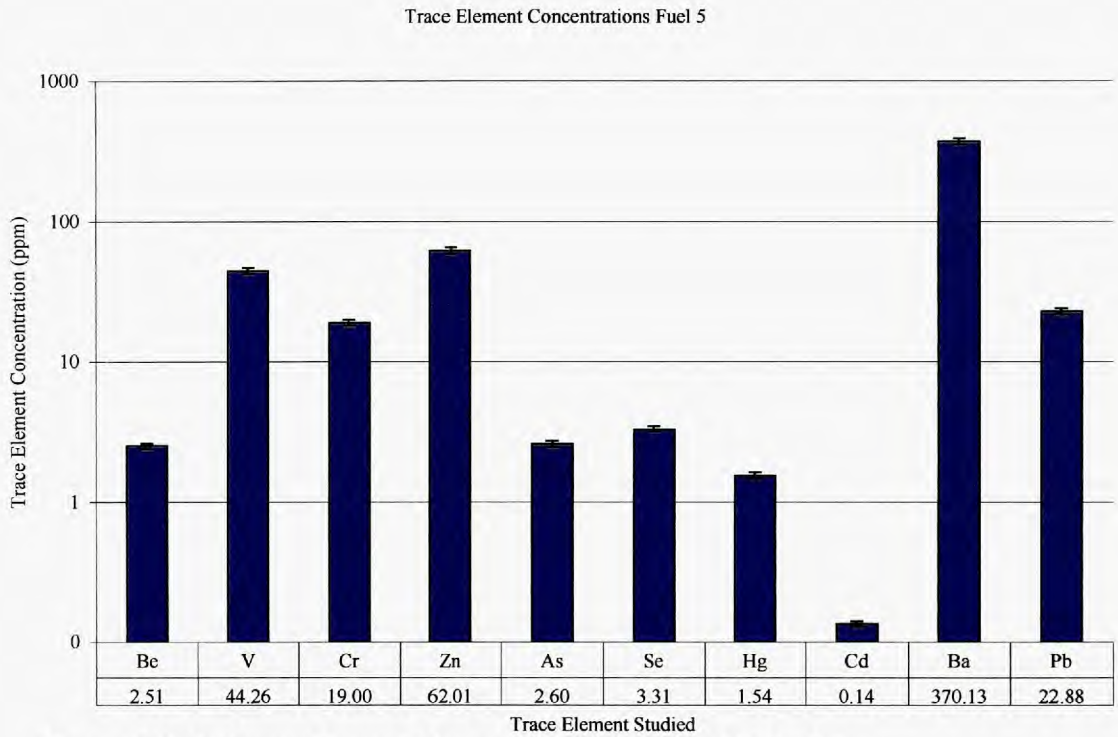


Figure 4.2.15 Trace Element Occurrence in CERCHAR Fuel 5

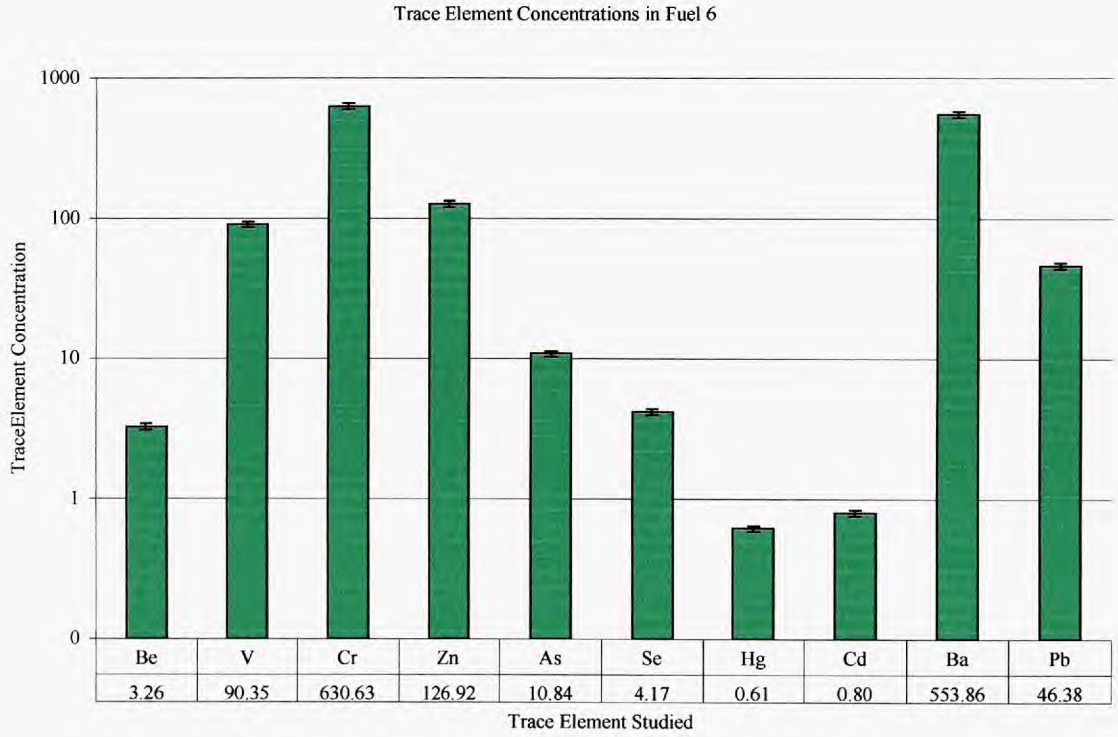


Figure 4.2.16 Trace Element Occurrence in CERCHAR Fuel 6

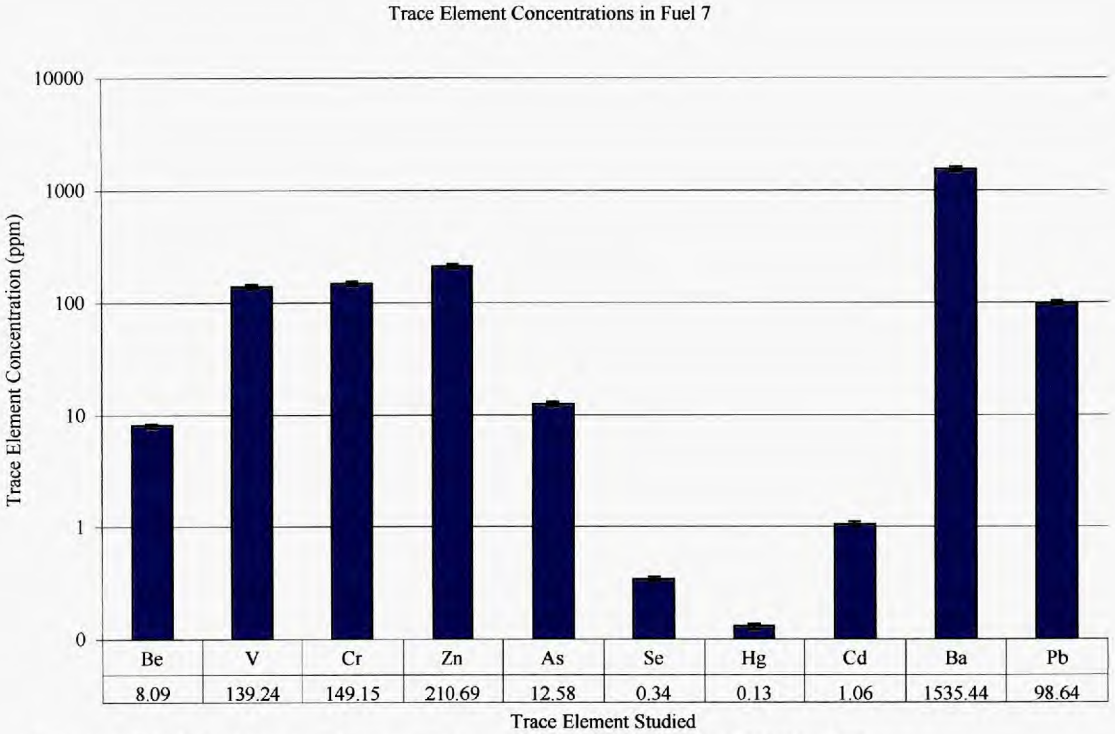


Figure 4.2.17 Trace Element Occurrence in CERCHAR Fuel 7

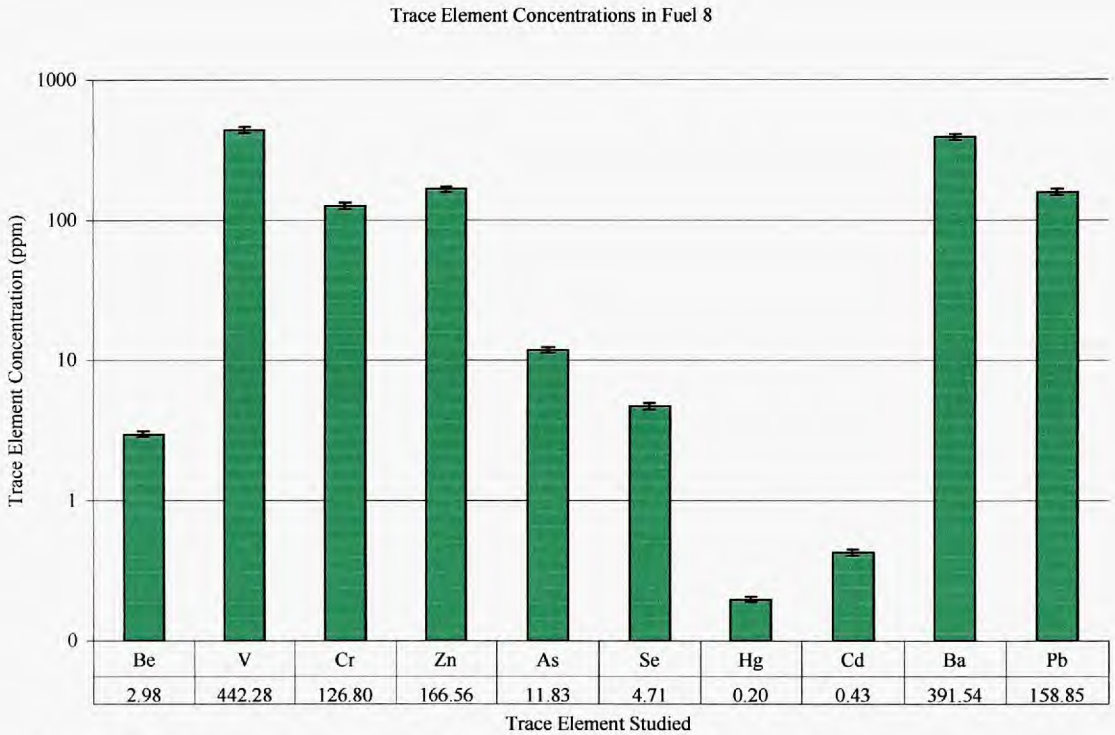


Figure 4.2.18 Trace Element Occurrence in CERCHAR Fuel 8

4.2.3 Chilean Fuels

The proximate and ultimate analysis of the Chilean fuels is given in Section 3.1.3, whilst the trace element composition is shown below. Experiments to determine the trace element content in the raw fuel were carried out in the same manner as those for the CERCHAR fuels. In order to measure the trace element concentration in the un-combusted fuels each experiment was conducted 7 times. The student t-distribution was then used, with a 95 % confidence interval. The experimental error was then converted to a percentage and rounded up to the nearest 5 %. Errors calculated were calculated to be less than 5% for all the trace elements for the 5 Chilean fuels studied, and are therefore given as 5%.

Results are given by element and then by fuel. As stated in Section 3.1.3 the Chilean fuels consisted of three coals – Kideco, Lemington and Allied. For each element the fuels are given in two groups. First Kideco coal, Kideco-Lemington mixture and Lemington coal are shown, followed by Lemington, Lemington-Allied and Allied Coal.

Kideco and Lemington were mixed in equal proportions as were the Lemington and Allied Coals. It therefore follows that the trace element concentration in each mixtures should be an average of that in its pure constituent fuels. For a given trace element, if the mixture showed a lower value than the theoretical mean, this would indicate that some of the trace element had been lost during blending. If the mixture showed a significantly higher value than the theoretical mean, two possibilities may have occurred. Either the fuel blend was contaminated or one of the constituent fuels became degraded before analysis artificially lowering the value of the theoretical mean. Figures 4.2.29 & 4.2.30 show by how much the trace element quantity deviated from the mean quantity in the constituent fuels, for the Kideco-Lemington and Lemington-Allied fuel blends respectively.

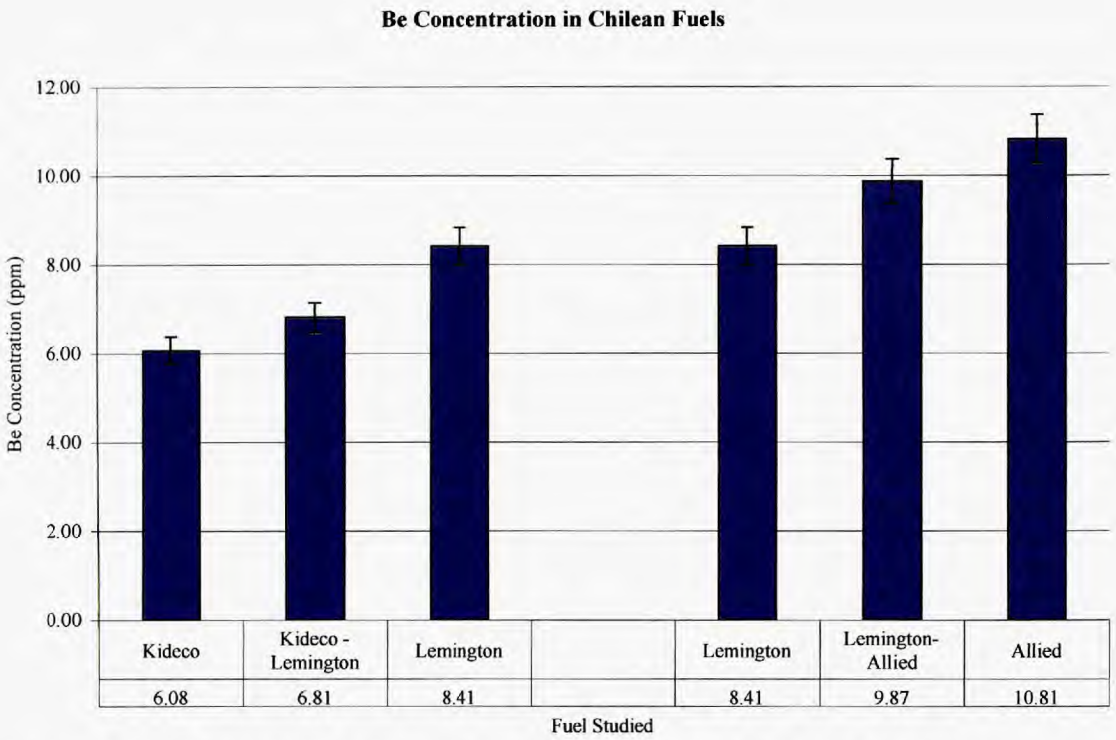


Figure 4.2.19 Beryllium Concentration in Chilean Fuels & Fuel Blends

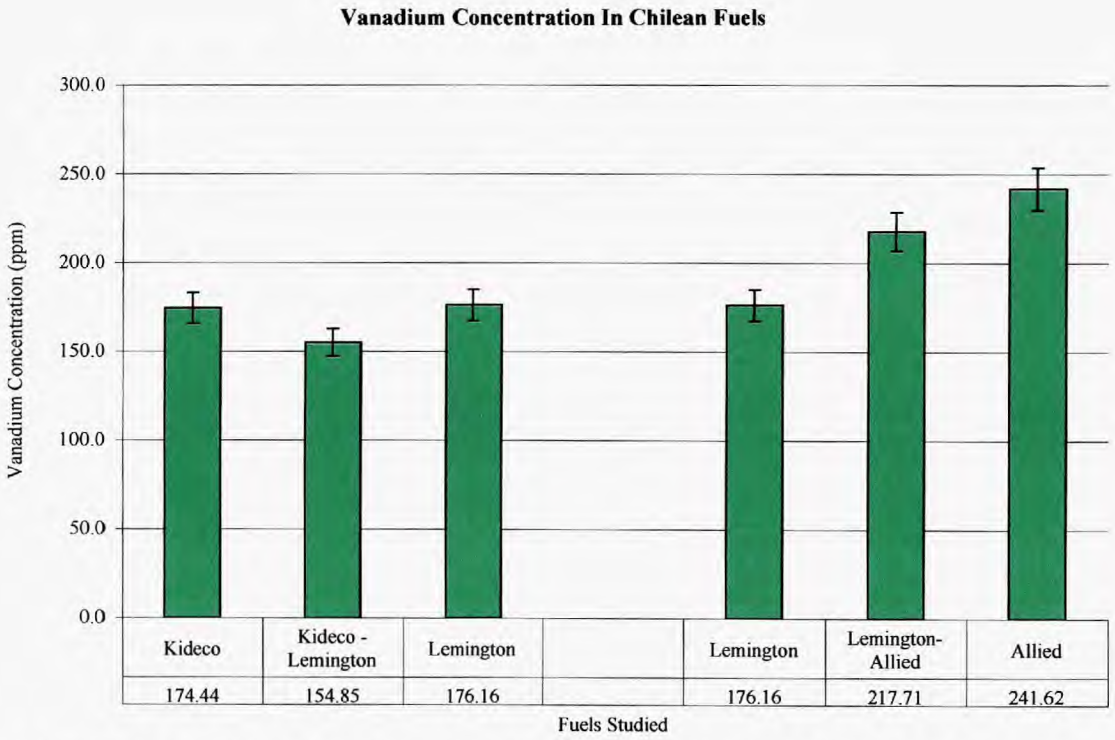


Figure 4.2.20 Vanadium Concentration in Chilean Fuels & Fuel Blends

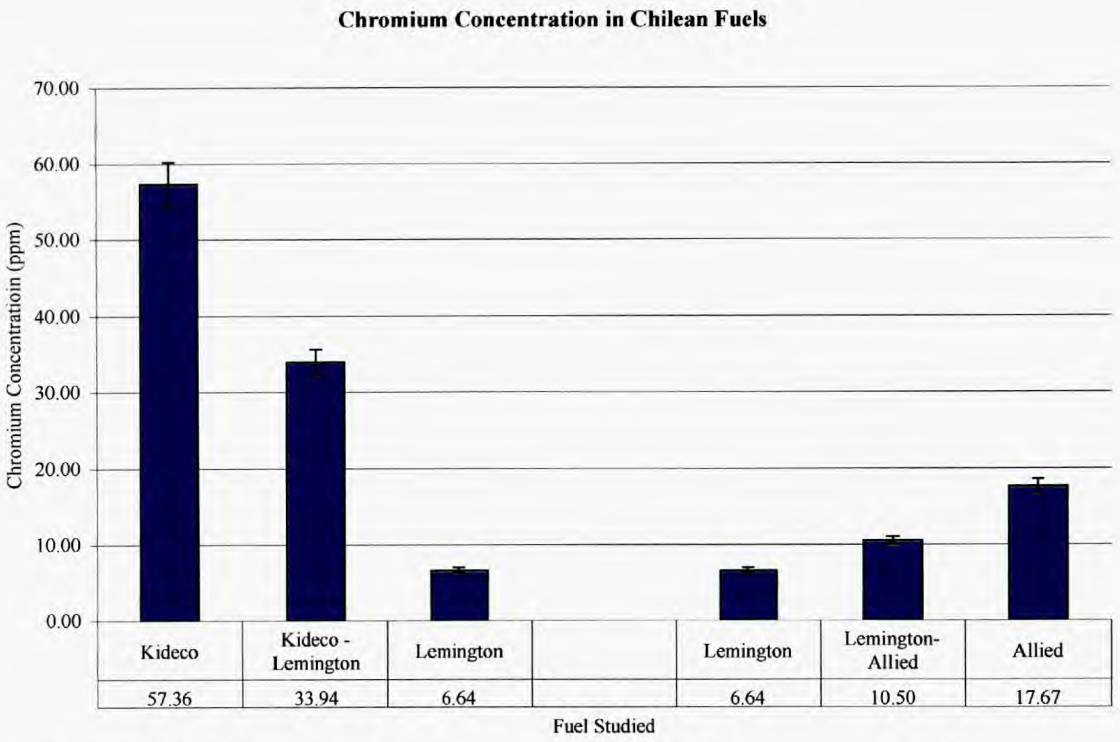


Figure 4.2.21 Chromium Concentration in Chilean Fuels & Fuel Blends

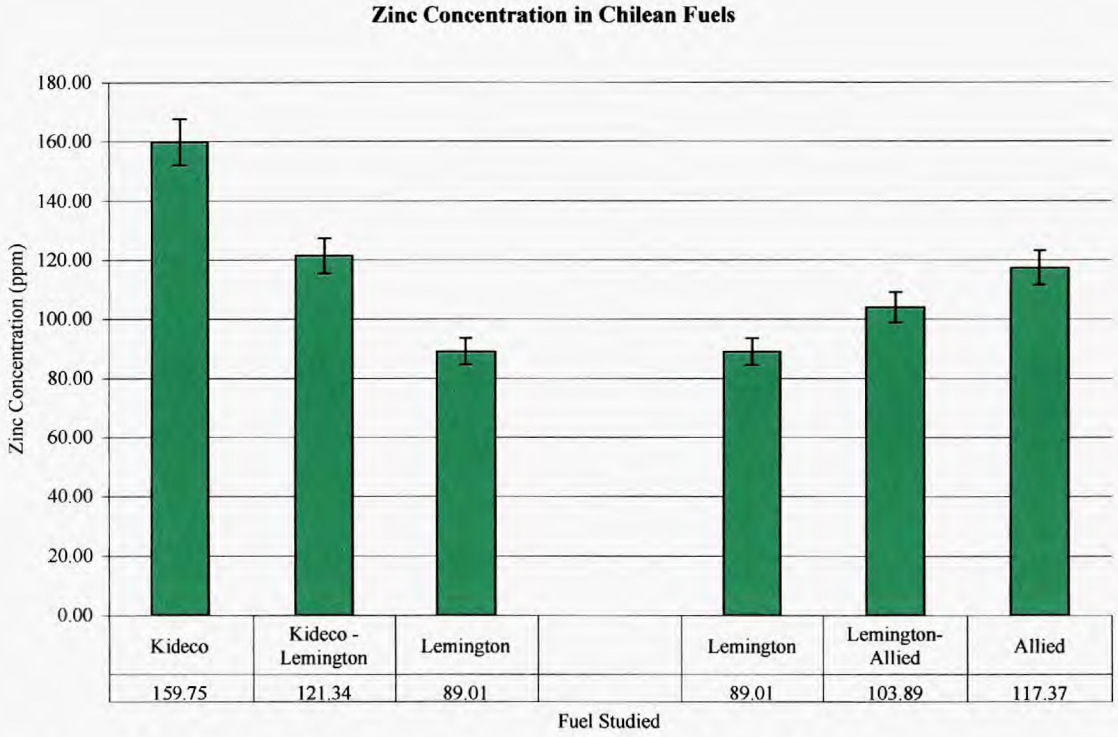


Figure 4.2.22 Zinc Concentration in Chilean Fuels & Fuel Blends

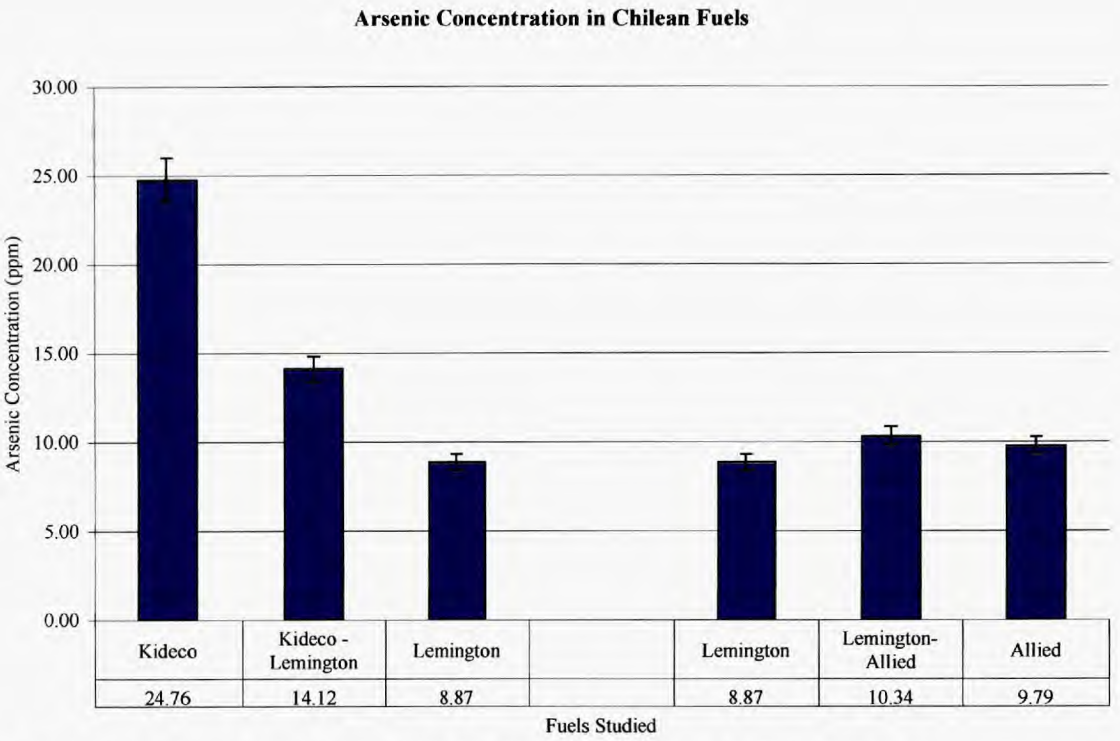


Figure 4.2.23 Arsenic Concentration in Chilean Fuels & Fuel Blends

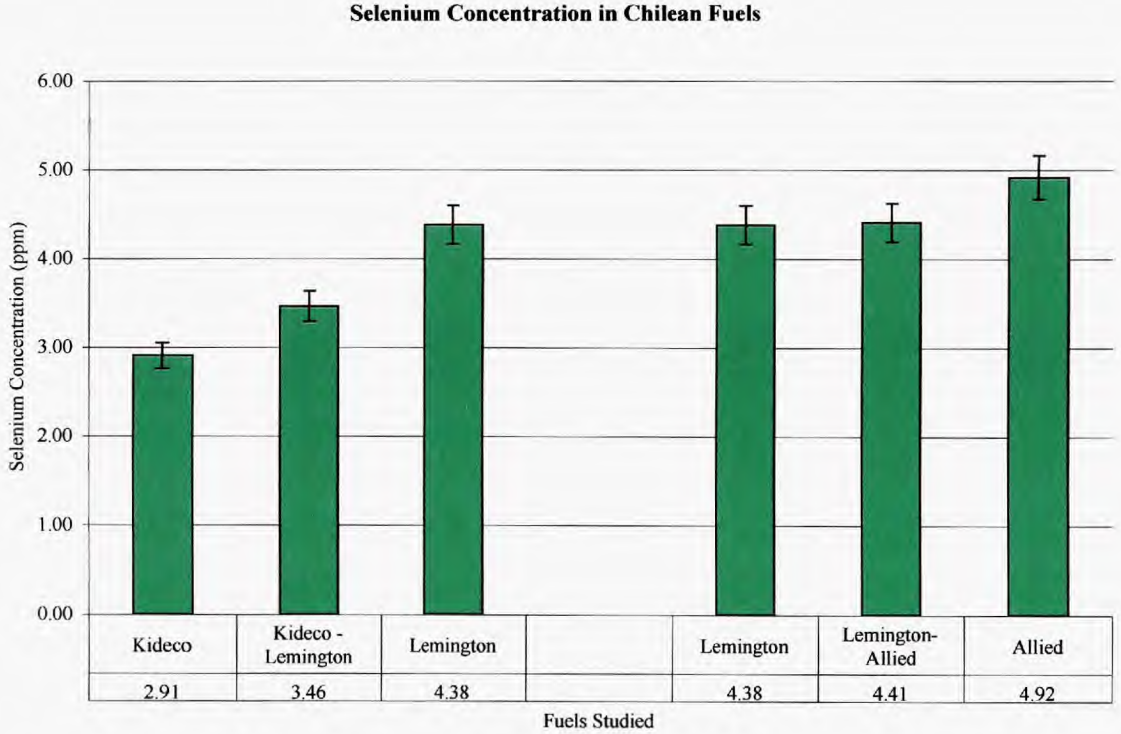


Figure 4.2.24 Selenium Concentration in Chilean Fuels & Fuel Blends

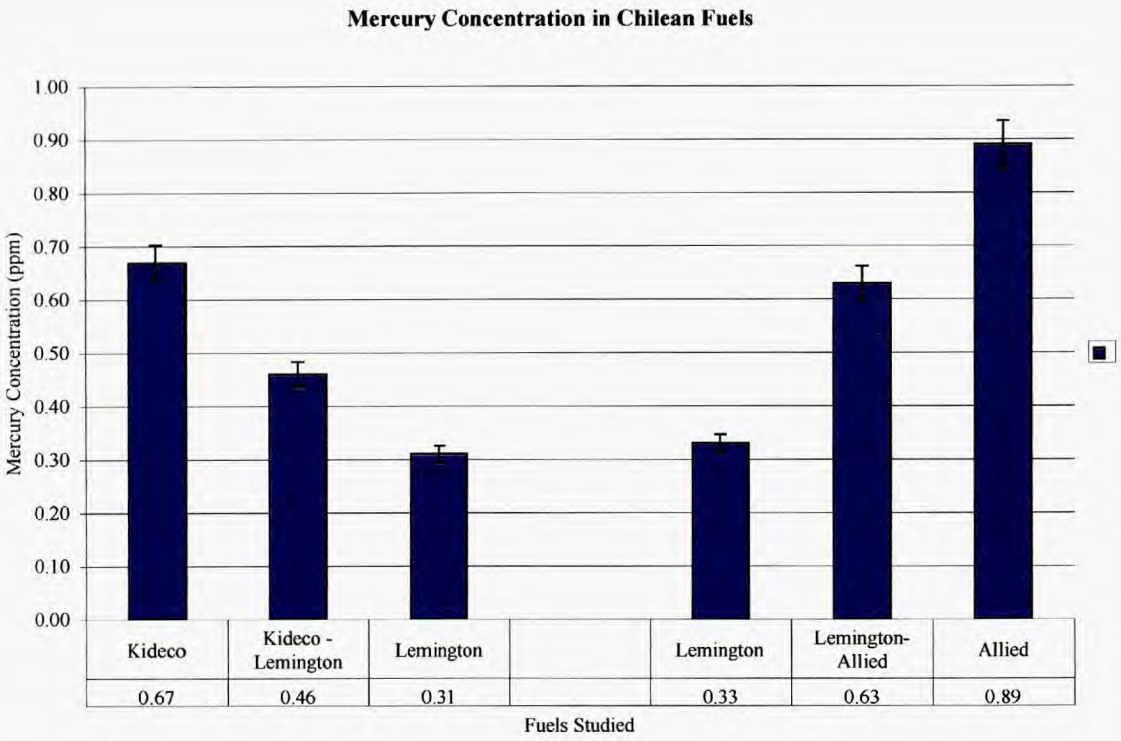


Figure 4.2.25 Mercury Concentration in Chilean Fuels & Fuel Blends

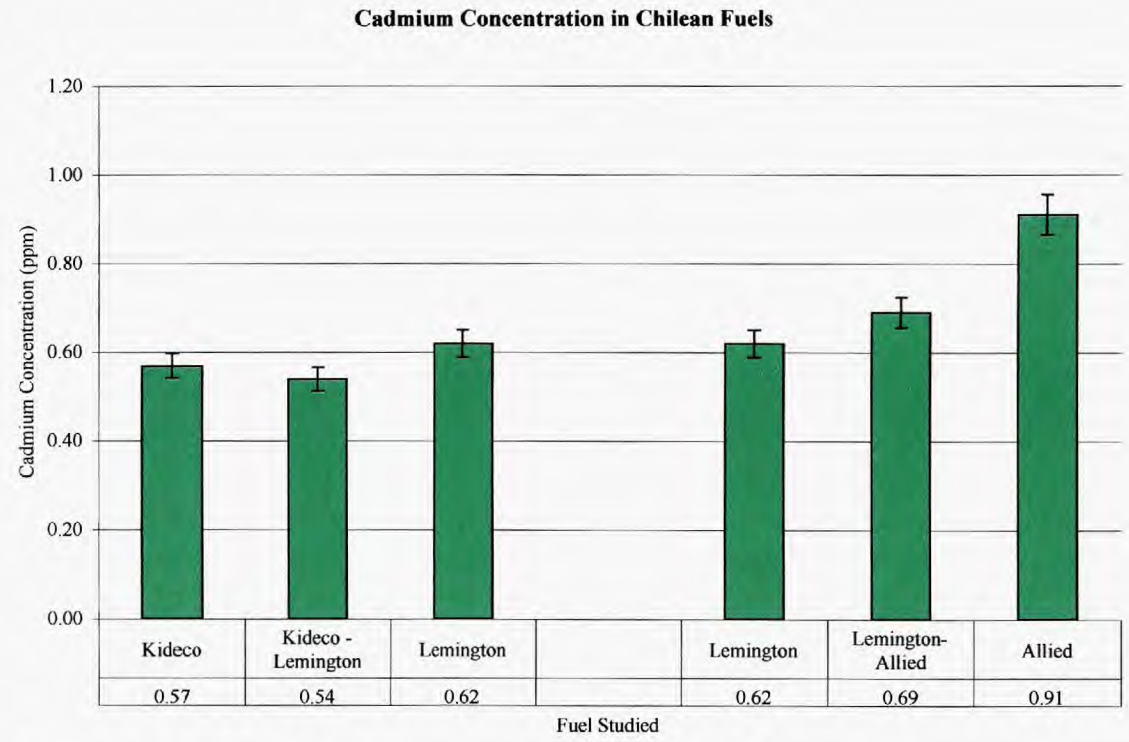


Figure 4.2.26 Cadmium Concentration in Chilean Fuels & Fuel Blends

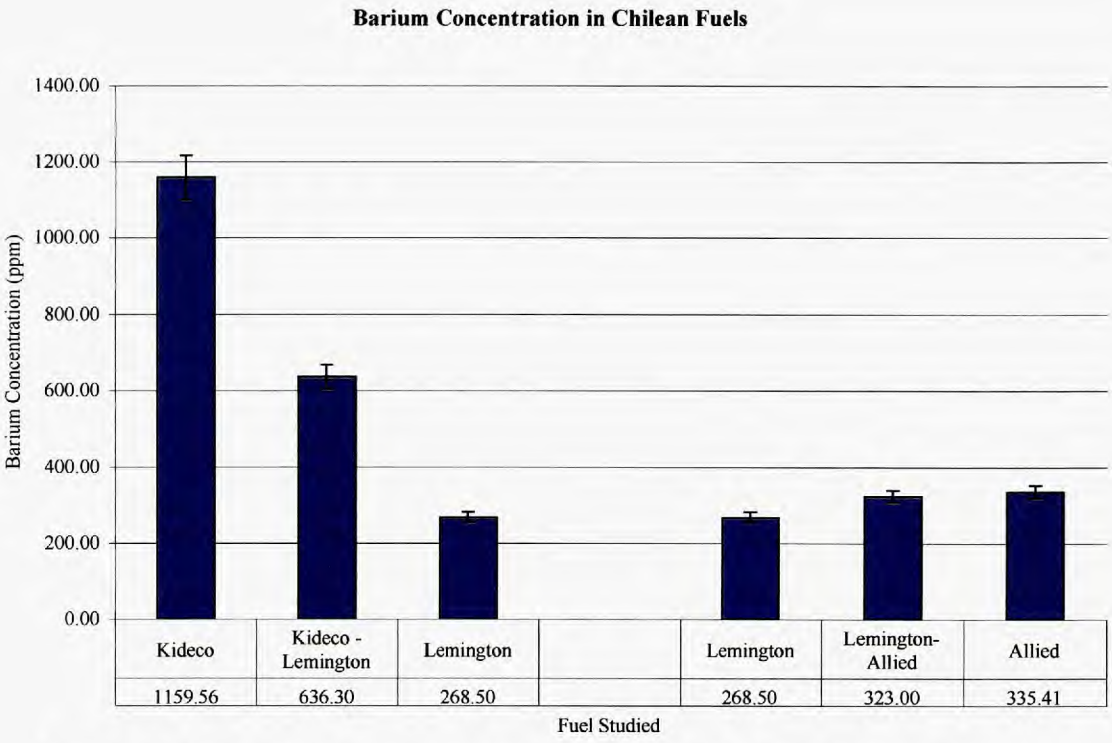


Figure 4.2.27 Barium Concentration in Chilean Fuels & Fuel Blends

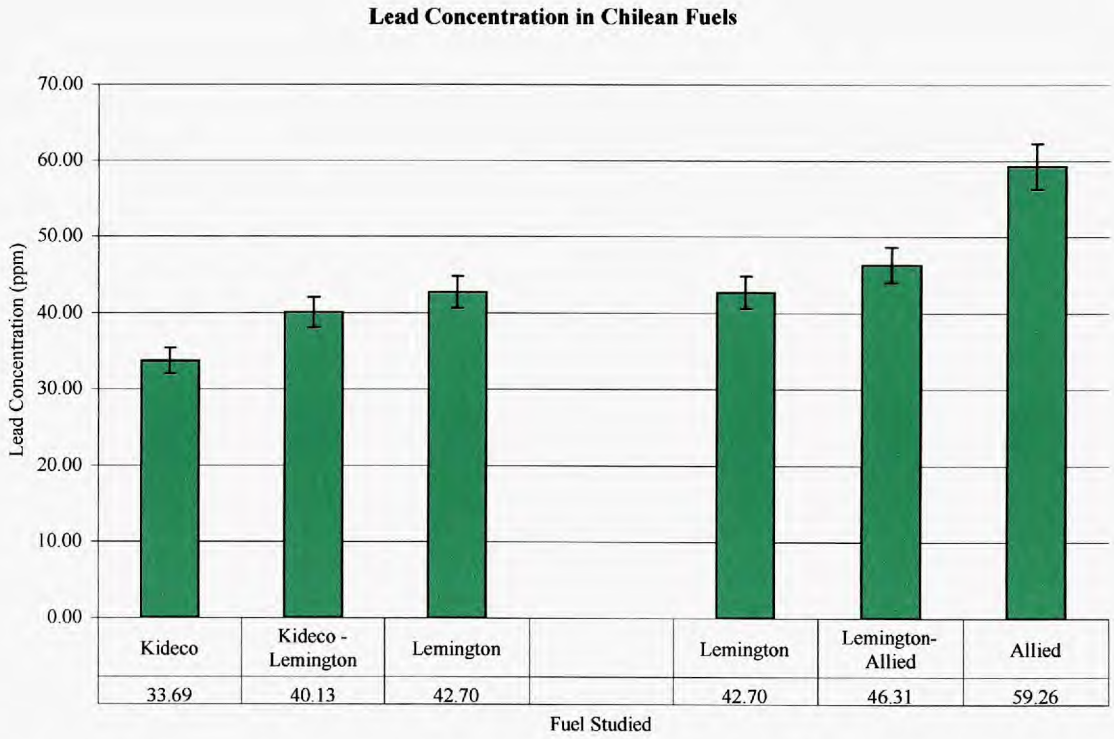


Figure 4.2.28 Lead Concentration in Chilean Fuels & Fuel Blends

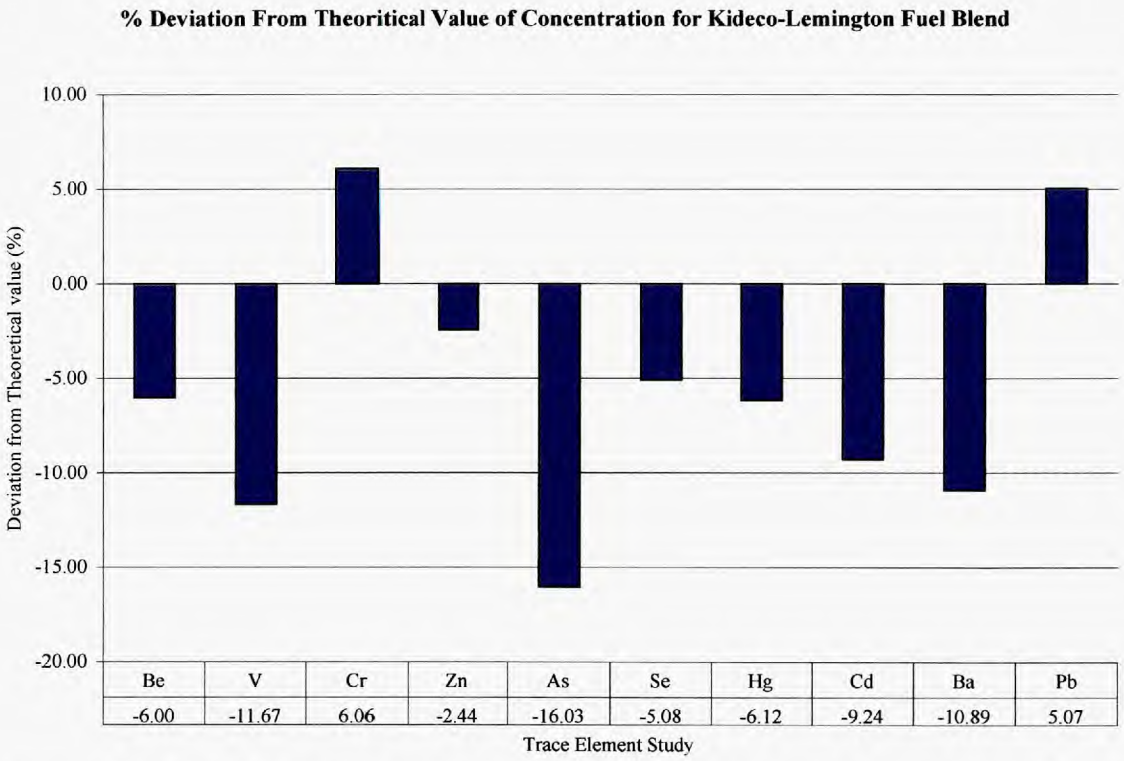


Figure 4.2.29 % Deviation from Theoretical Value of Concentration in Kideco-Lemington

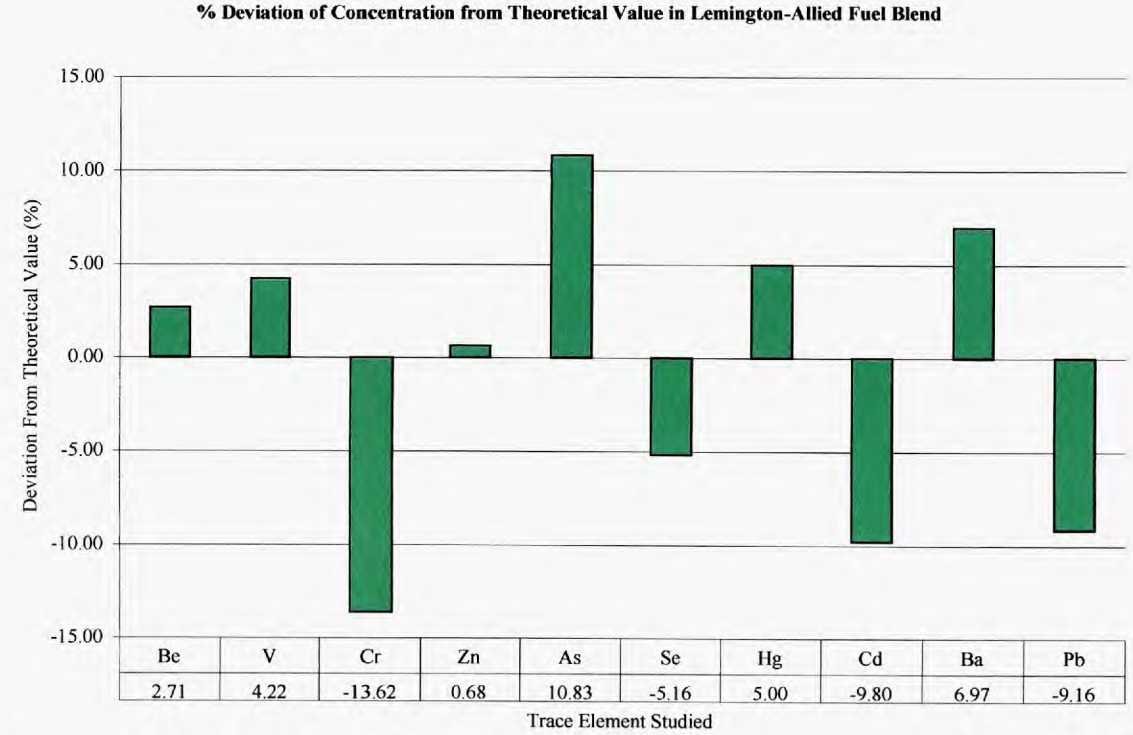


Figure 4.2.30 % Deviation from Theoretical Value of Concentration in Lemington-Allied

Beryllium

The beryllium concentration range for all the fuels was small, increasing from 6.08 ppm for Kideco coal to a maximum of 10.81 ppm for Allied coal. Figure 4.2.3.11 shows that for the Kideco-Lemington mixture the beryllium concentration is close to the mean of the concentrations of its constituent fuels, being 6.0 % lower. For the Lemington-Allied mixture the concentration is 2.71% higher than expected. Both of these values are within the bounds of experimental error given, and therefore may be discounted.

Vanadium

The vanadium concentrations in the fuels are also within the same order of magnitude increasing from 174.44 ppm for Kideco Coal to 241.62 for Allied. The vanadium concentration for the Kideco-Lemington mixture is lower than would be expected and shows one of the largest deviations from the mean value at 11.6 %. The reduced level of vanadium may be attributed to loss during blending. For the Lemington- Allied blend there is less than a 5% difference between the theoretical and actual value.

Chromium

The chromium concentration was one of the most varied between the five fuels studied, although it remained within the same order of magnitude, being 57.36 ppm for the Kideco coal and 6.64 for the Lemington. The experimental Kideco-Lemington chromium concentration was tolerably close to the theoretical value, although the Lemington-Allied concentration was 13.6 % lower than predicted. Again this is only slightly lower than the limits set by experimental error and may be due to loss during fuel blend preparation.

Zinc

Zinc concentrations varied from 89.01 for the Lemington fuel to a maximum of 159.75 for Kideco. The zinc concentrations in both mixtures were proportional to the ratios in which they were mixed.

Experimental values were very close to the theoretical value being 2.44% and 0.68% away for the Kideco-Lemington and Lemington-Allied mixtures respectively.

Arsenic

Arsenic concentration for the Lemington/Allied group of fuels was similar varying from 8.87 to 10.34 ppm. For the Kideco/Lemington fuel group it decreased from 24.7 ppm for Kideco coal to the Lemington coal value of 9.87 ppm. The mixtures showed the greatest deviation from the mean theoretical value for arsenic. The Lemington-Allied mixture was higher than predicted but within the range of experimental error. The Kideco/Lemington mixture was 16% too low. Arsenic being one of the more thermally unstable elements studied may be lost during the fuel blending process.

Selenium

Selenium concentrations were in the lower ranges of concentrations of the trace elements studied, and the concentration range was narrow. Selenium abundance varied from 2.9 to 4.9 ppm. The selenium concentration for the fuel blends were close to the theoretical mean of their constituent fuels to within 5%.

Mercury

Mercury concentrations for all the fuels were the lowest of all the elements studied, all being below 1 ppm, the lowest being Lemington coal at 0.31 ppm. The concentrations for the Kideco-Lemington and Lemington-Allied mixtures were 6.1 and 5.0% away from the theoretical means respectively, well within the limits set by experimental error.

Cadmium

Cadmium had a very similar concentration profile to lead. Cadmium concentrations were low in comparison to other trace metals studied being below 1ppm for all fuels. The lowest cadmium concentration was exhibited by the Kideco-Lemington mixture at 0.54 %. The cadmium concentration for the mixture was found to be nearly 10% below the theoretical value for both fuel blends.

Barium

Barium exhibited the highest concentrations with Kideco coal containing 1156 ppm as a maximum amongst the fuels and Lemington 269 ppm as a minimum. The Lemington/Allied fuel group exhibited similar barium concentrations, when compared to the Kideco Lemington fuel group. The Kideco-Lemington blend barium concentration was 10.8 % below the mean of its constituent fuels, whilst for the Lemington allied there was a 6.9 % deviation from the mean. These values were not outside the limits set by experimental error.

Lead

Lead concentrations were similar for all the fuels and as with all the other elements were within the same order of magnitude. Kideco coal contained the least lead (33.7 ppm) whilst Allied coal the most 59.26 ppm. The lead concentrations for the fuel blends were also within the bounds set by experimental error.

In summary the trace elements where concentration deviated the most from the theoretical value are arsenic in the Kideco-Lemington blend and chromium in the Lemington-Allied blend.

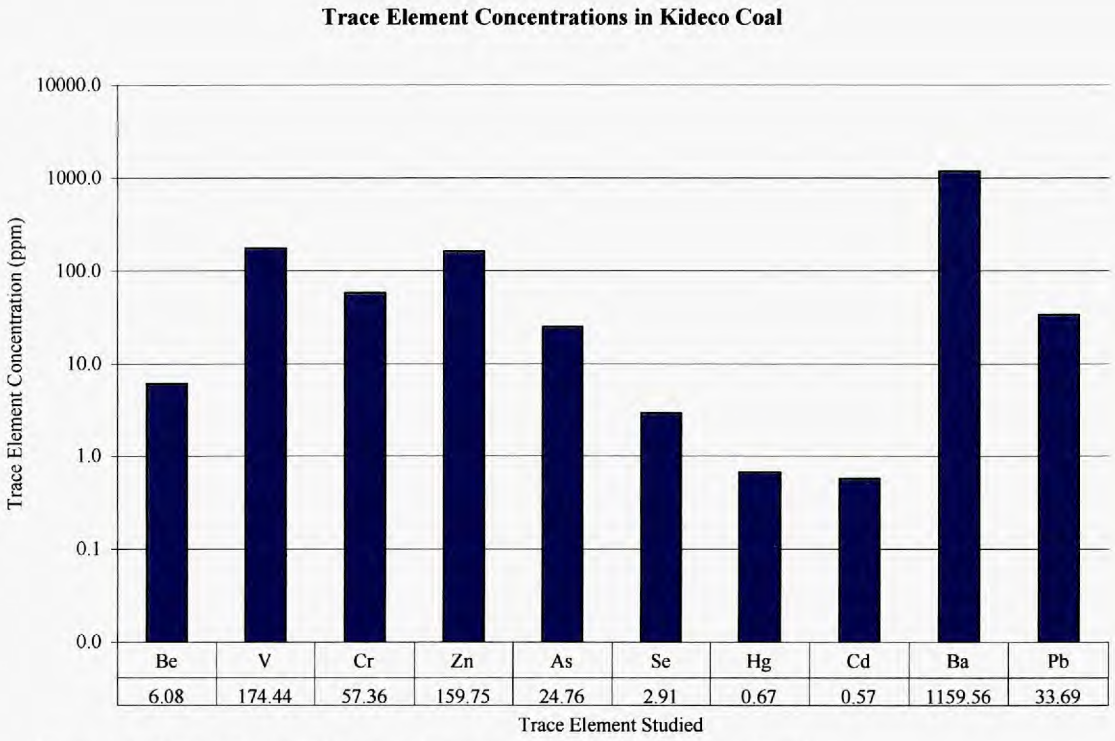


Figure 4.2.31 Trace Element Concentrations in Kideco Coal

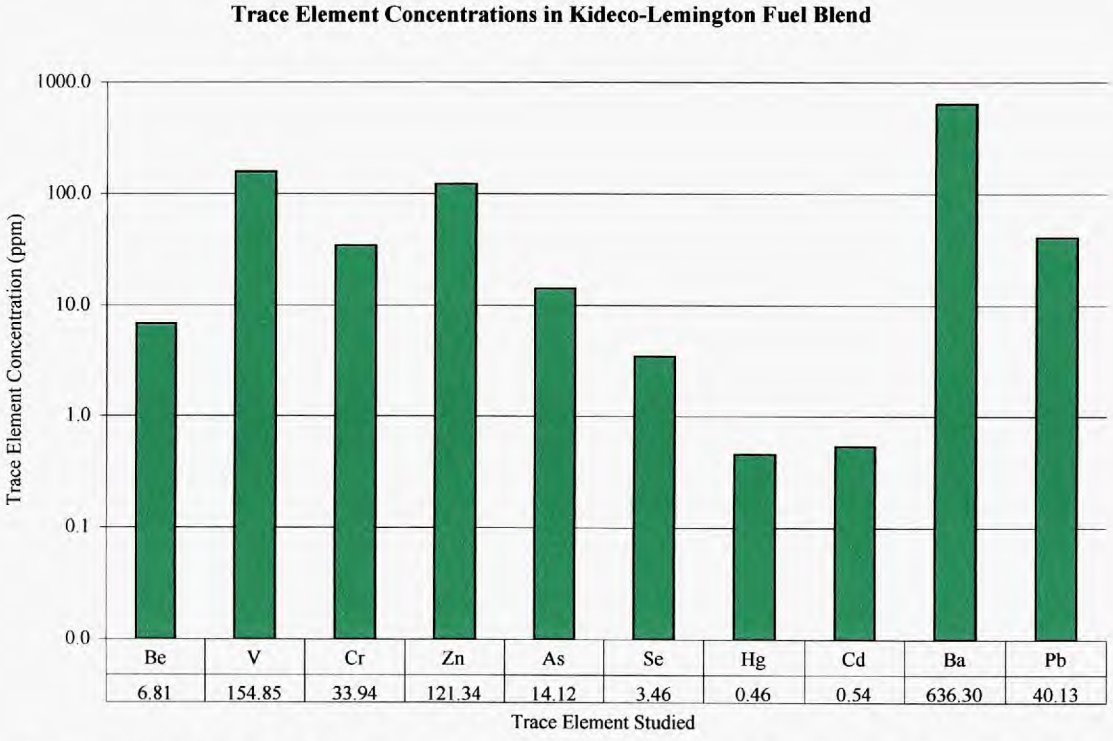


Figure 4.2.32 Trace Element Concentrations in Kideco-Lemington Coal Fuel Blend

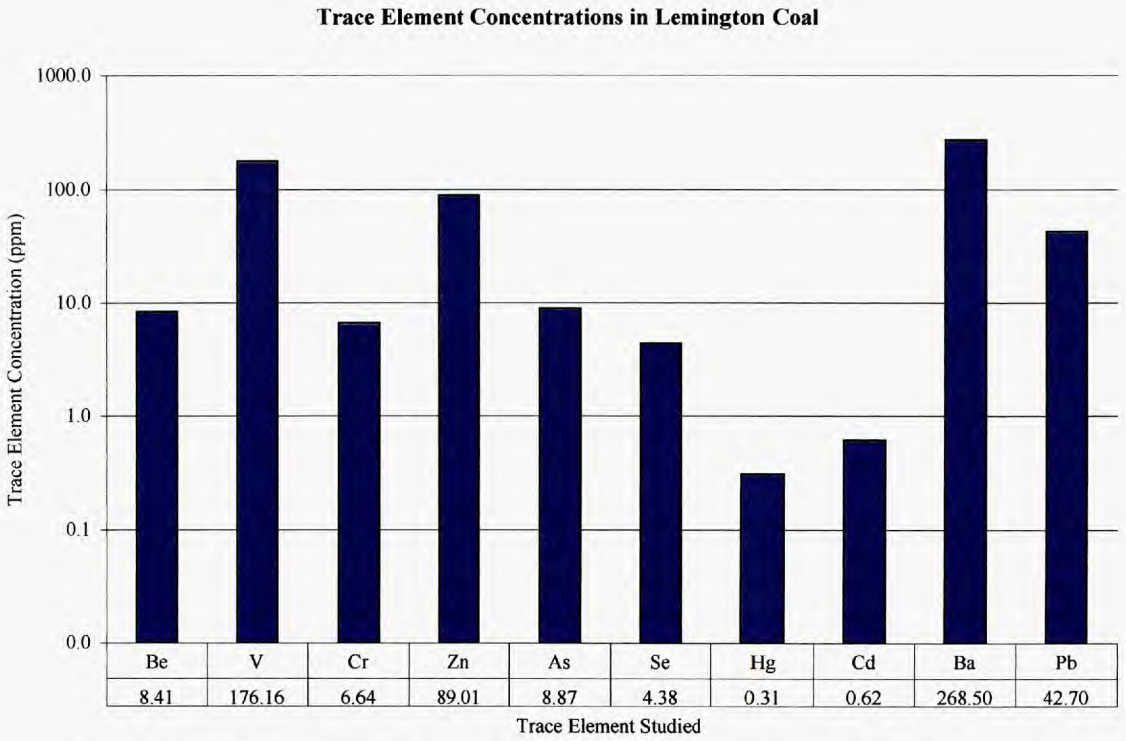


Figure 4.2.33 Trace Element Concentrations in Lemington Coal

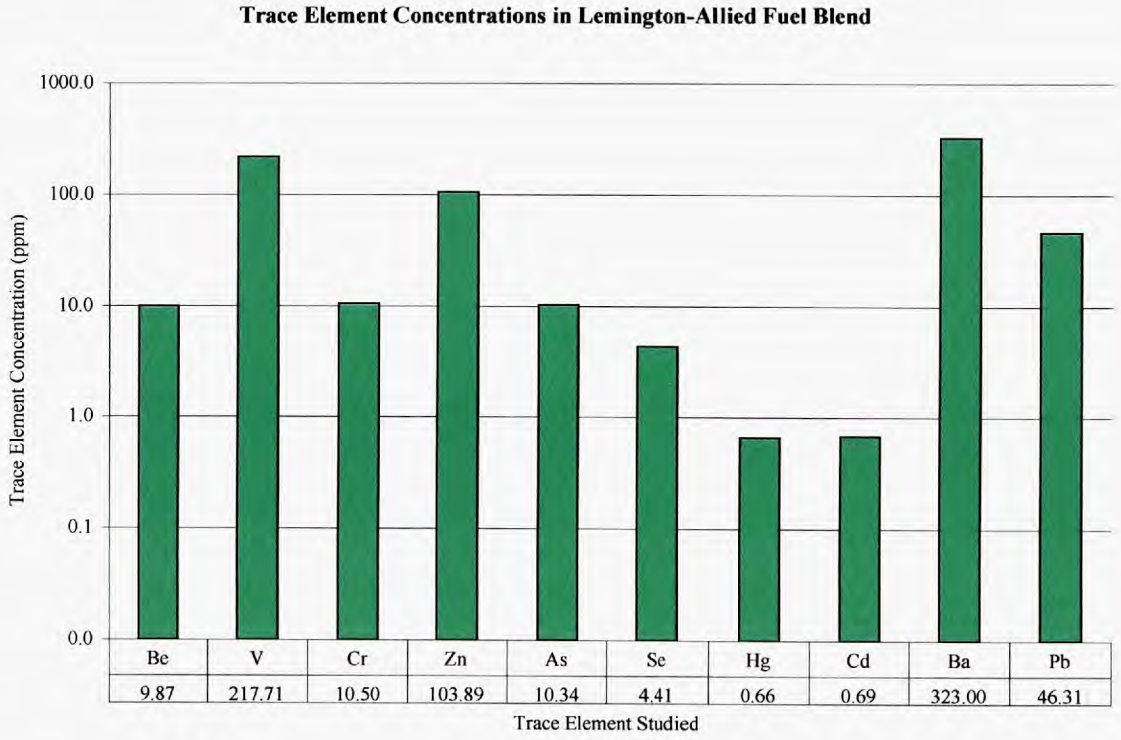


Figure 4.2.34 Trace Element Concentrations in Lemington-Allied Coal Fuel Blend

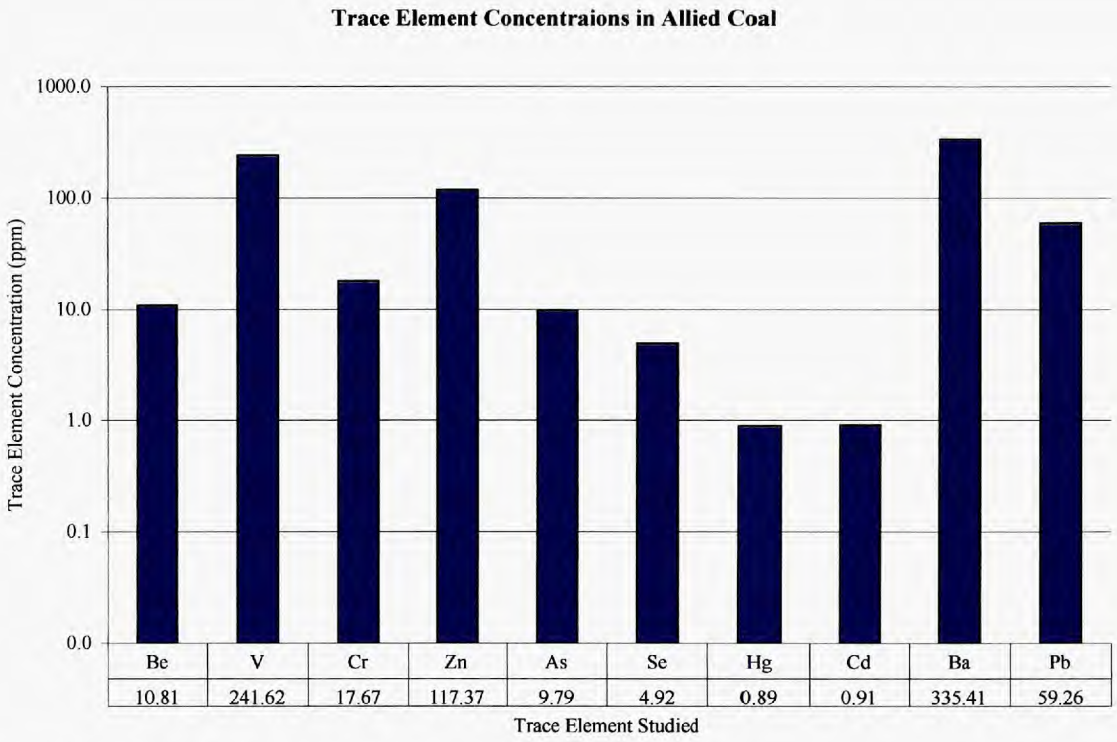


Figure 4.2.35 Trace Element Concentrations in Allied Coal

From the above figures a general view of the relative abundances of the trace elements studied may be formed. The magnitude of trace element content in the fuels has a bearing on the accuracy with which measurements maybe made when calculating the concentrations in the ash and resulting leachate, as well as availability for leaching and potential toxicity of leachate.

Mercury and cadmium are the least abundant elements (less than 1 part per million of fuel) followed by Arsenic, Selenium and Beryllium all of which are around 10 ppm or below. Lead and chromium tend to be below 100 ppm, for all fuels whilst Vanadium, Zinc and Barium show the same order of magnitude in the hundreds (with the exception of Kideco Coal where barium concentration is 1160 ppm).

4.3 Trace Element Retention in Ashes

Overview: The results presented in the section give the trace element content determined in ashes after combustion for the CERCHAR and Chilean fuels. Combustion of the CERCHAR fuels was carried out in a muffle furnace and a hot-rod reactor, at 850 °C and 950 °C. The effect of temperature variation within this range and combustion configurations could then be studied. For the Chilean fuels, trace element content obtained from power station ashes which saw temperatures in the region of 1500 °C were compared with ashes produced in a laboratory suspension firing reactor at 900 °C. This would enable the study of high temperature effects on trace element retention.

4.3.1 Trace Element Retention in CERCHAR Ashes

This section presents the trace element content in the CERCHAR ashes obtained from various combustion experiments. Experiments were carried out at 850 and 950 ° C using the hot-rod reactor and a muffle furnace, as described in Section 3.1. Experiments were repeated 6 times in order to facilitate the error calculations, as described in Section 4.2.1. Results are presented as percentage retention i.e. the trace element retained in the ash as a proportion of the original amount present in the fuel.

In order to calculate the error involved in percentage retention, the error in the original fuel and the error in the ash concentrations had to be considered. Therefore, the error in the percentage retention was calculated as the square root of the sum of the squares of the trace element concentration in the fuel and the concentration in the ash.

Appendix I shows the results given as absolute concentrations, rather than percentage retentions. Each figure in the appendix shows the trace element concentration for the eight fuels, for a particular combustion method at the two combustion temperatures studied e.g. the beryllium concentration to be found in the ashes of the CERCHAR Fuels 1-8 at 850 and 950 °C in the hot-rod reactor. These figures are relevant to the availability for leaching, calculations for percentage of trace element leached, and regulatory constraints which are discussed in following sections.

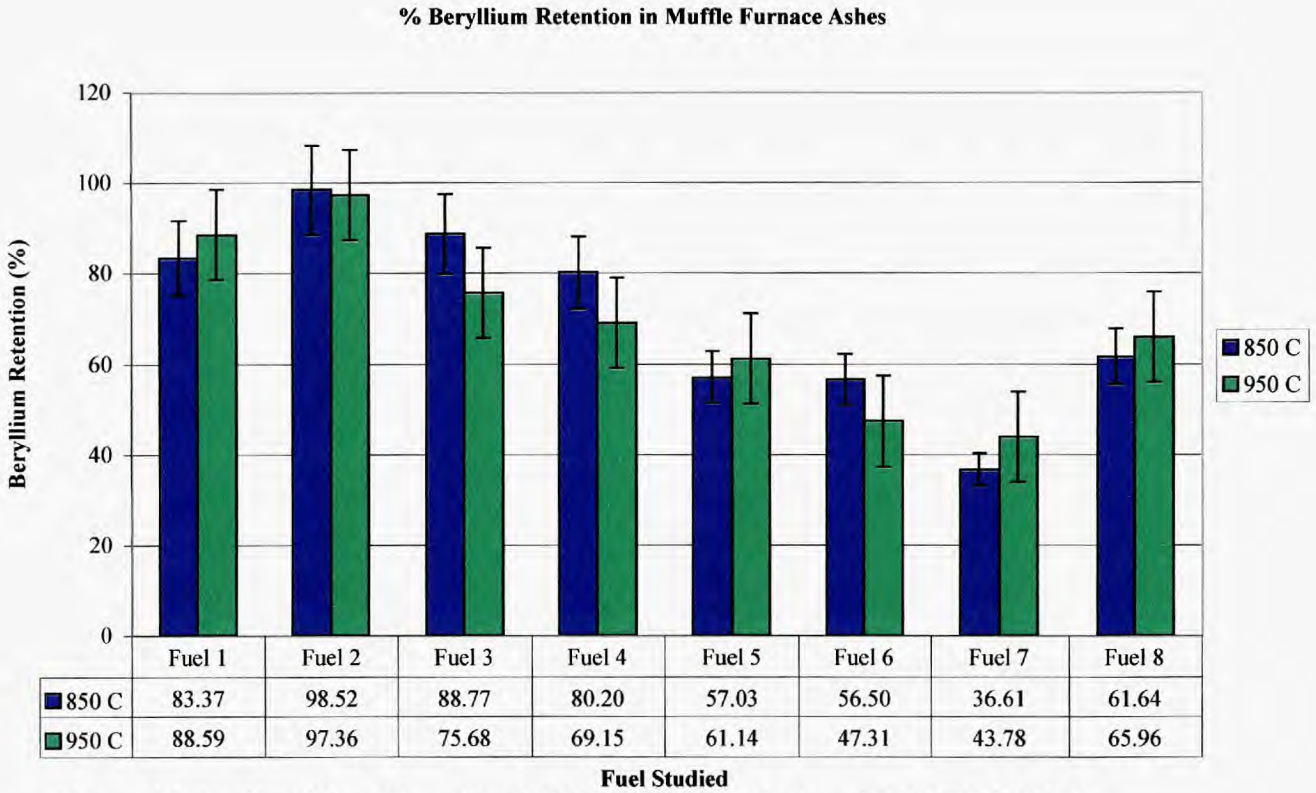
The are presented in such a way that the following influences may be investigated:

- The effect of temperature on trace element retention in muffle furnace produced ash
- The effect of temperature on trace element retention in hot-rod produced ash
- The effect of combustion method on trace element retention at 850 °C.
- The effect of combustion method on trace element retention at 950 °C.
- The effect of fuel on trace element retention in ashes produced at the above conditions.

In order to facilitate this investigation the results are presented in three ways. First graphical representations are made of the retention of a particular trace element as a function of fuel and temperature, for a particular combustion method. Secondly, trace element retention is given as a function of fuel and combustion method, at a particular temperature. Discussion is made in Section 4.3.2 and figures are shown in Appendix II. When discussing the results as a function of combustion method it may be noted that there are three differences between the two methods. The hot-rod reactor has a carrier gas flow, whilst the muffle furnace environment does not; the time at which the reactants remain at a particular temperature is greater for the muffle furnace (by an order of magnitude) Finally results are discussed on a fuel by fuel basis, as a function of temperature and combustion method.

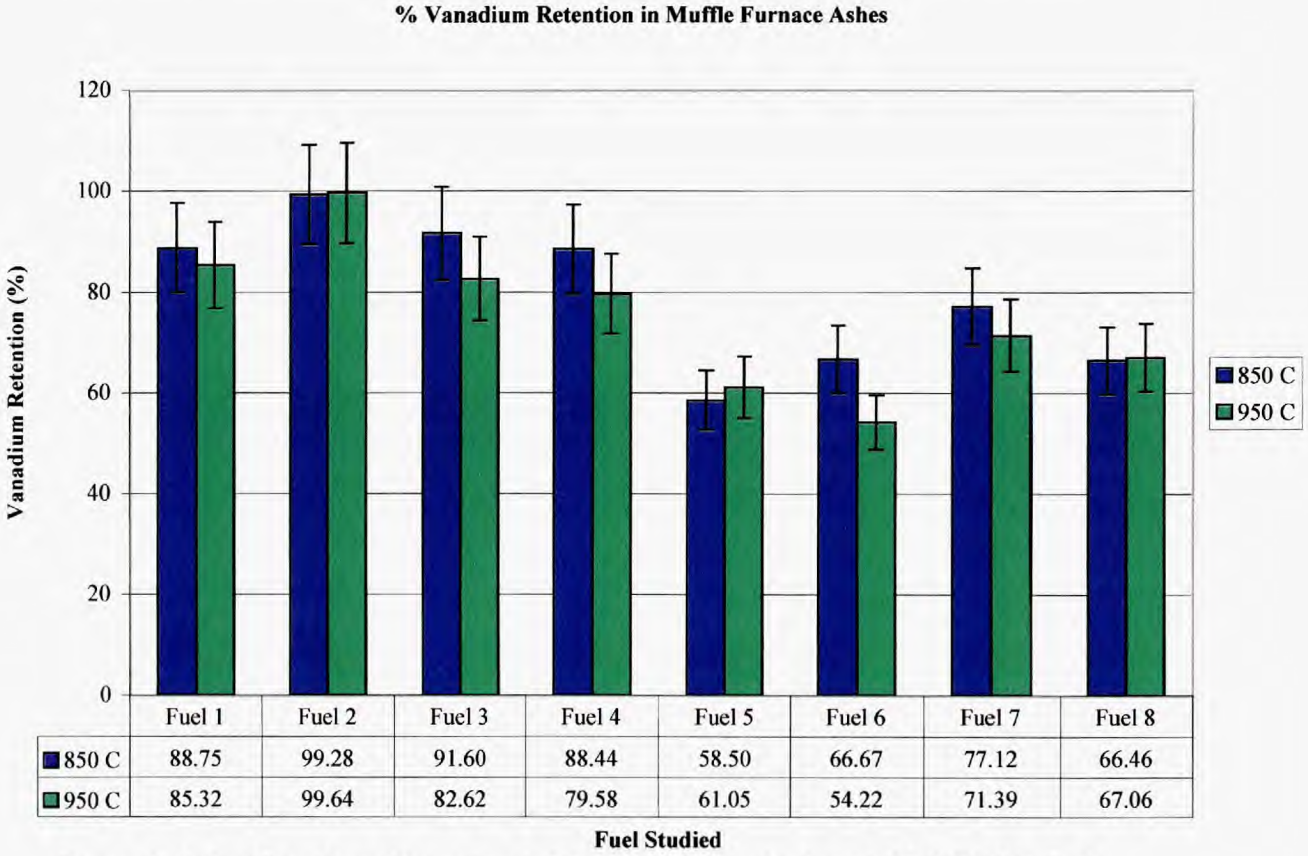
Discussion of thermodynamic equilibrium modelling, and the mode of occurrence of the trace elements after combustion is made in the first sections (Section 4.3.1 & 4.3.2) discussing temperature dependence.

4.3.1 The Effect of Temperature on Muffle Furnace Produced Ash



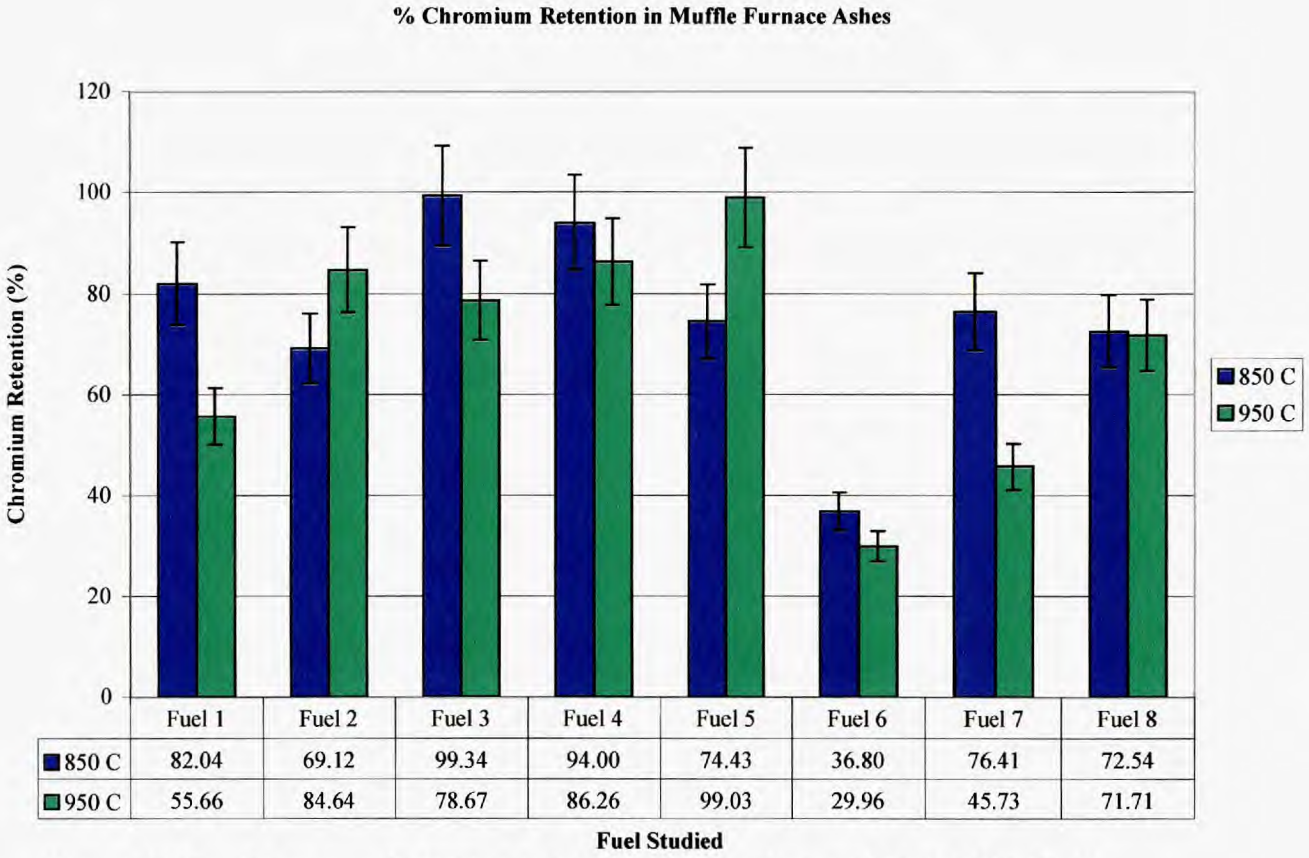
	Fuel 1	Fuel 2	Fuel 3	Fuel 4	Fuel 5	Fuel 6	Fuel 7	Fuel 8
850 C	83.37	98.52	88.77	80.20	57.03	56.50	36.61	61.64
950 C	88.59	97.36	75.68	69.15	61.14	47.31	43.78	65.96

Figure 4.3.1 Beryllium Retention in Muffle Furnace Ashes of CERCHAR fuels



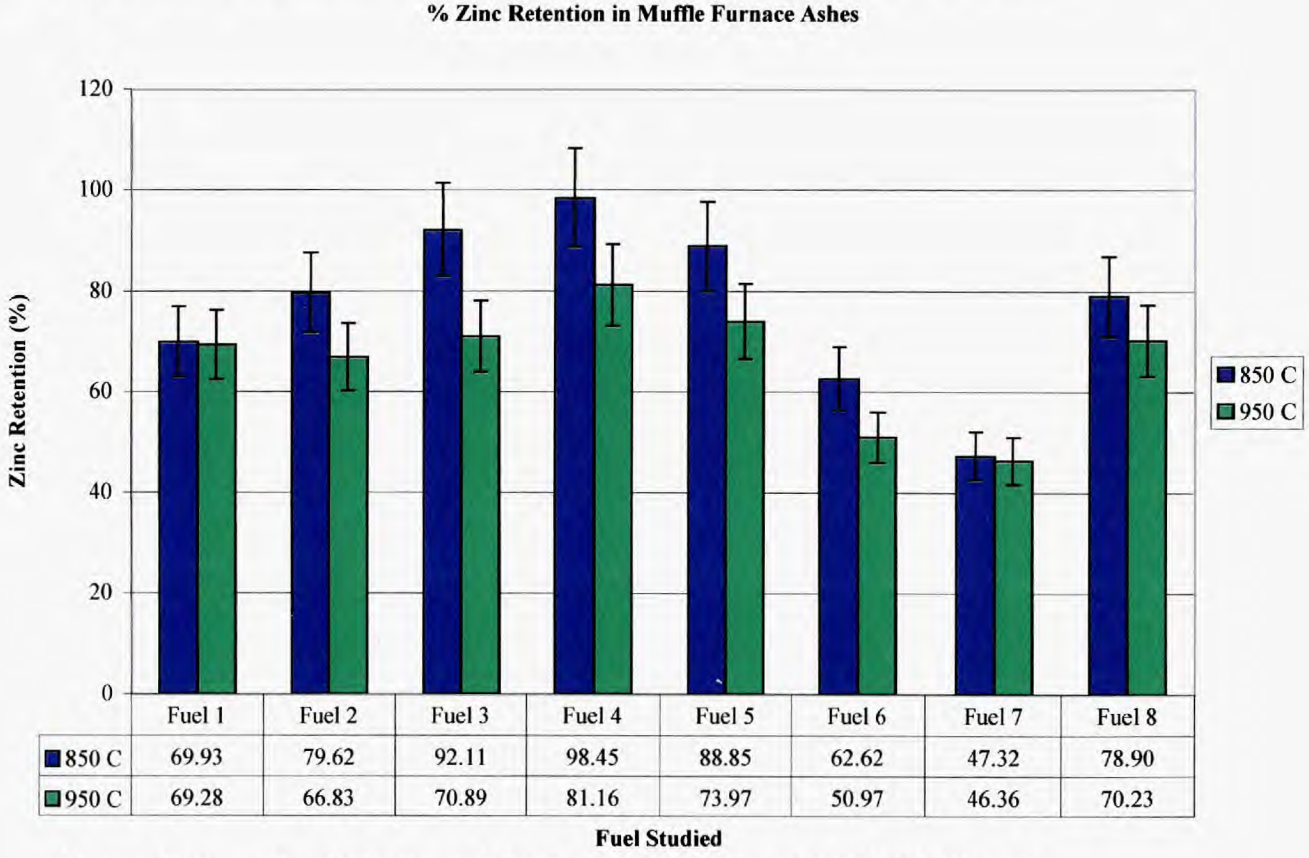
	Fuel 1	Fuel 2	Fuel 3	Fuel 4	Fuel 5	Fuel 6	Fuel 7	Fuel 8
850 C	88.75	99.28	91.60	88.44	58.50	66.67	77.12	66.46
950 C	85.32	99.64	82.62	79.58	61.05	54.22	71.39	67.06

Figure 4.3.2 Vanadium Retention in Muffle Furnace Ashes of CERCHAR fuels



	Fuel 1	Fuel 2	Fuel 3	Fuel 4	Fuel 5	Fuel 6	Fuel 7	Fuel 8
850 C	82.04	69.12	99.34	94.00	74.43	36.80	76.41	72.54
950 C	55.66	84.64	78.67	86.26	99.03	29.96	45.73	71.71

Figure 4.3.3 Chromium Retention in Muffle Furnace Ashes of CERCHAR fuels



	Fuel 1	Fuel 2	Fuel 3	Fuel 4	Fuel 5	Fuel 6	Fuel 7	Fuel 8
850 C	69.93	79.62	92.11	98.45	88.85	62.62	47.32	78.90
950 C	69.28	66.83	70.89	81.16	73.97	50.97	46.36	70.23

Figure 4.3.4 Zinc Retention in Muffle Furnace Ashes of CERCHAR fuels

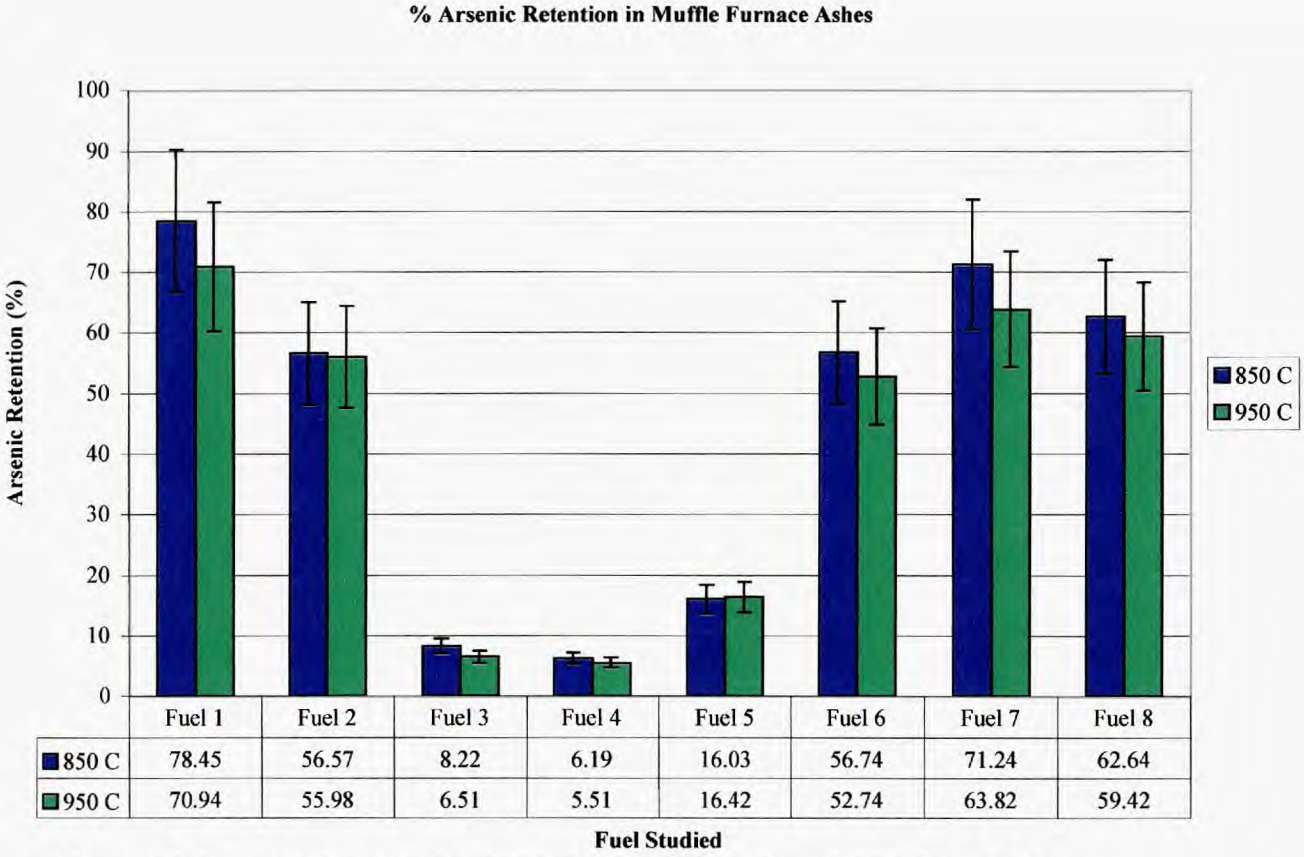


Figure 4.3.5 Arsenic Retention in Muffle Furnace Ashes of CERCHAR fuels

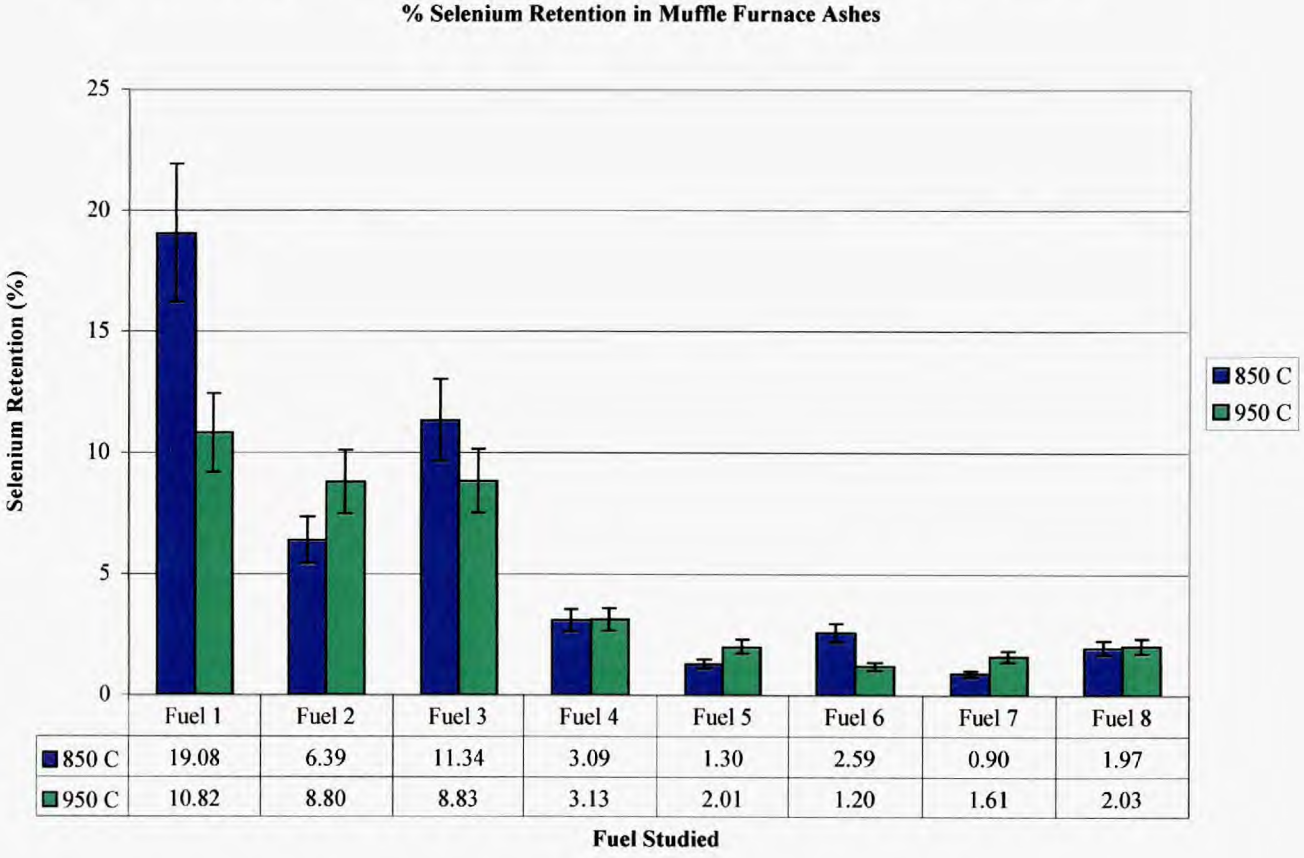
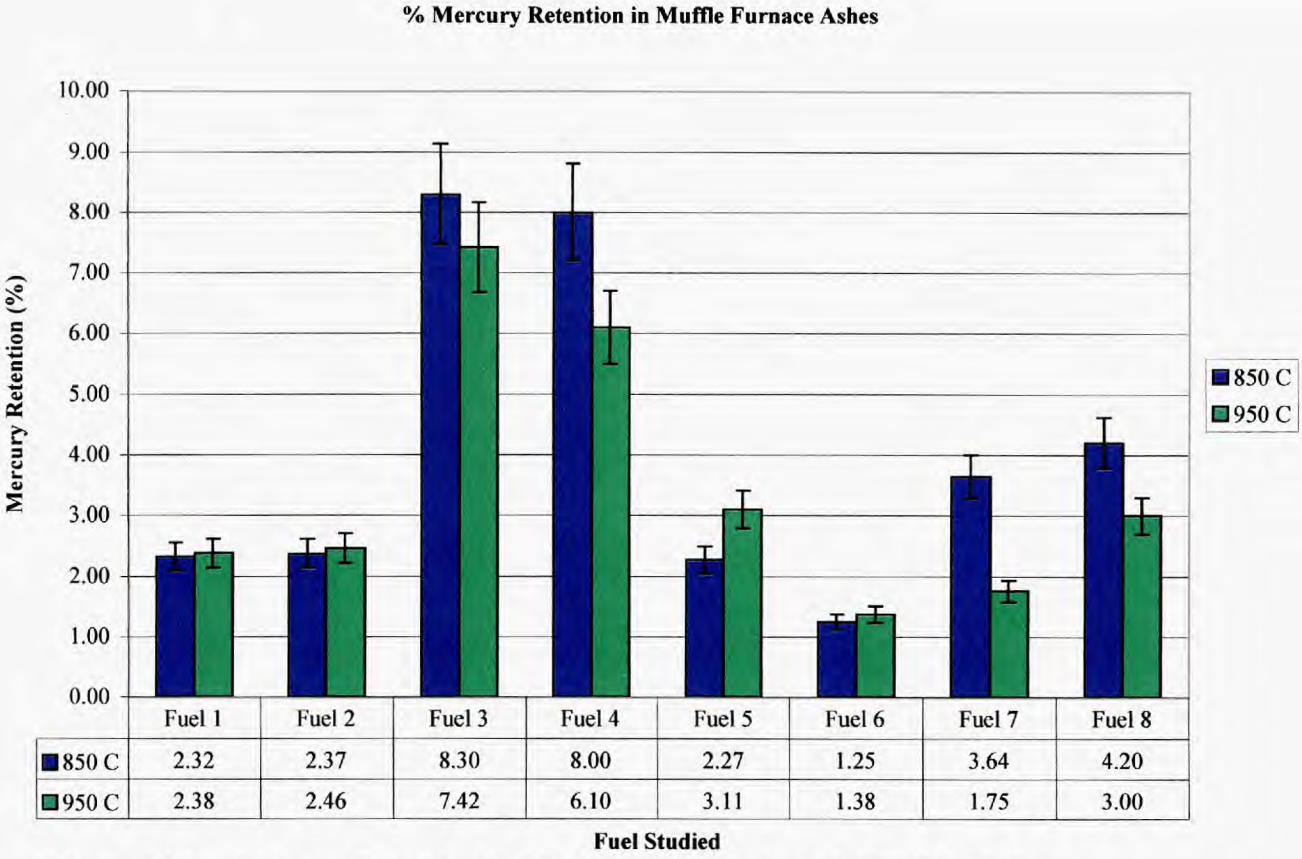
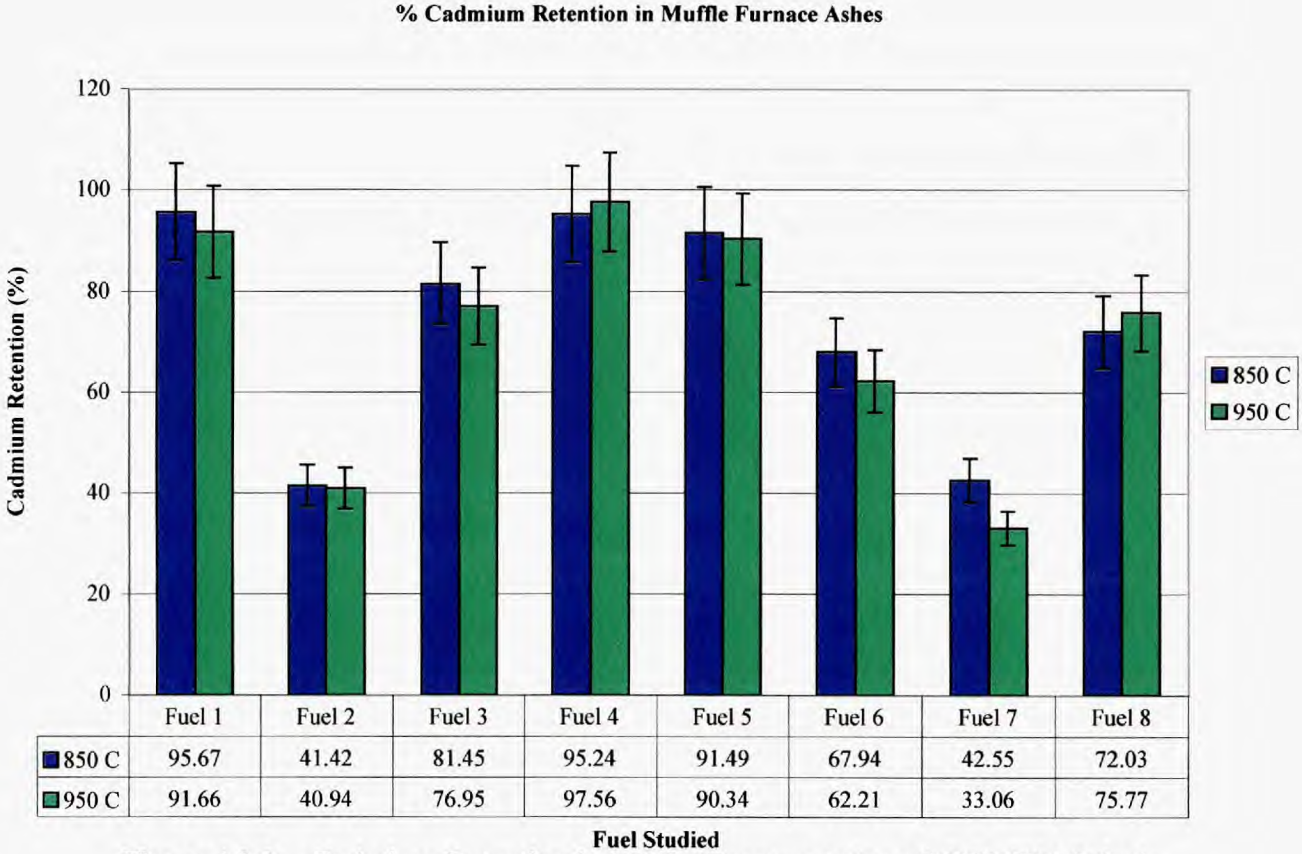


Figure 4.3.6 Selenium Retention in Muffle Furnace Ashes of CERCHAR fuels



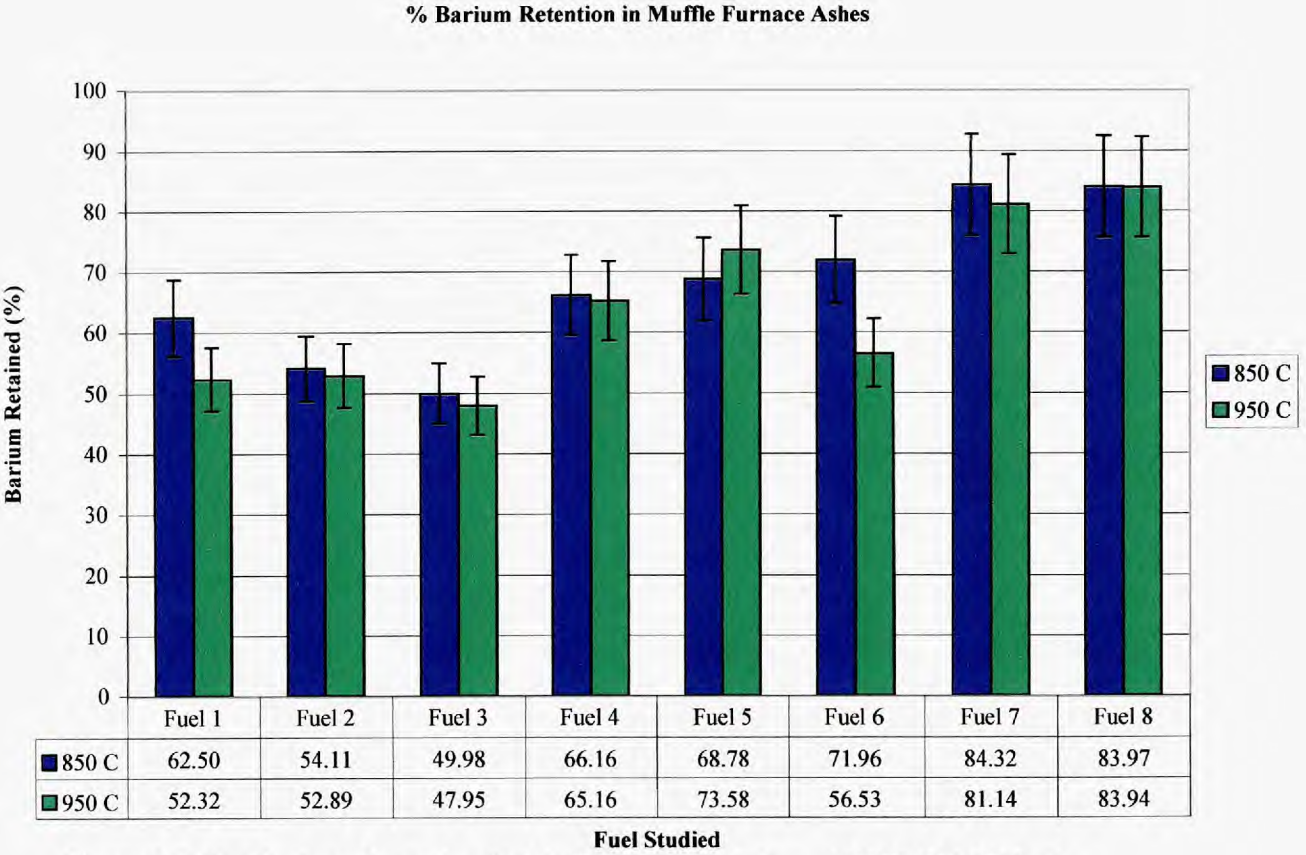
	Fuel 1	Fuel 2	Fuel 3	Fuel 4	Fuel 5	Fuel 6	Fuel 7	Fuel 8
850 C	2.32	2.37	8.30	8.00	2.27	1.25	3.64	4.20
950 C	2.38	2.46	7.42	6.10	3.11	1.38	1.75	3.00

Figure 4.3.7 Mercury Retention in Muffle Furnace Ashes of CERCHAR fuels



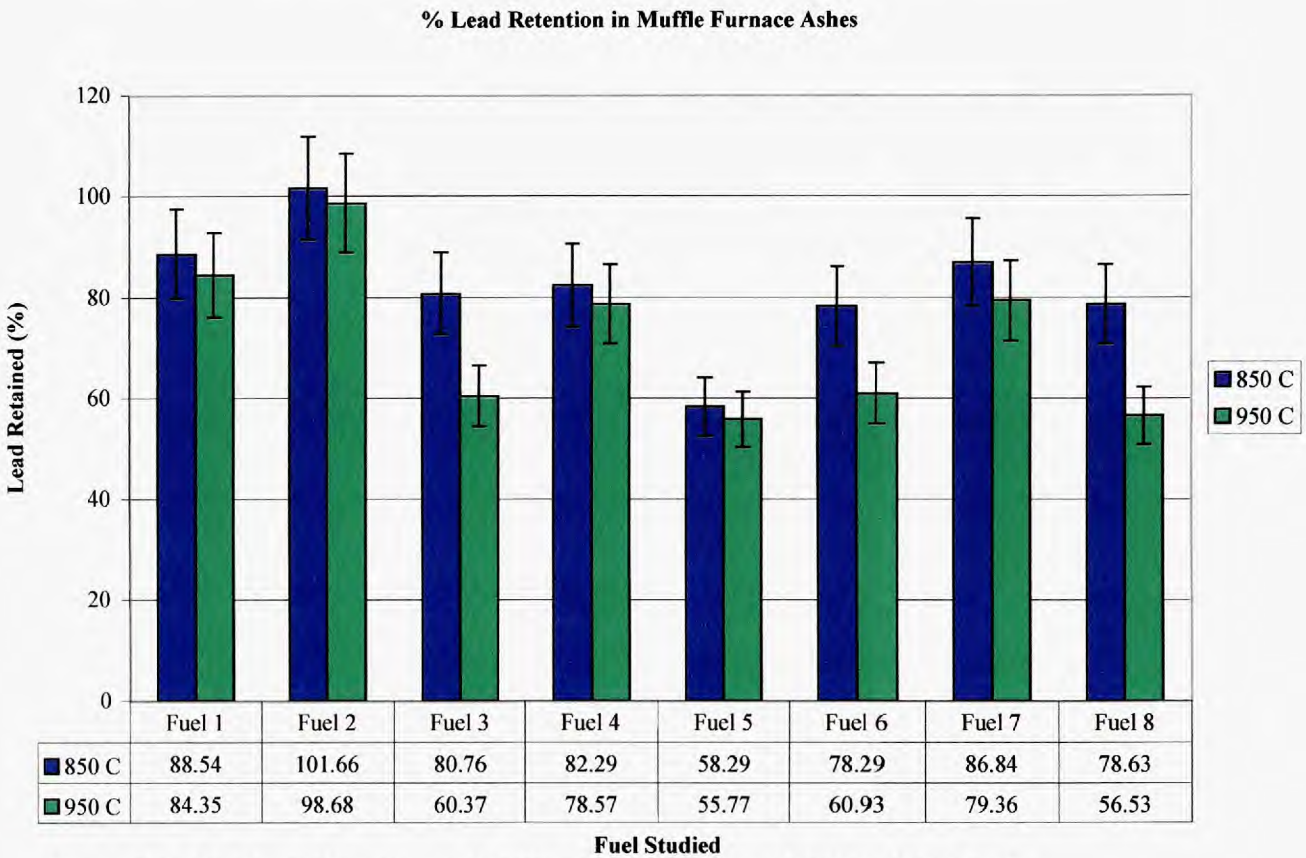
	Fuel 1	Fuel 2	Fuel 3	Fuel 4	Fuel 5	Fuel 6	Fuel 7	Fuel 8
850 C	95.67	41.42	81.45	95.24	91.49	67.94	42.55	72.03
950 C	91.66	40.94	76.95	97.56	90.34	62.21	33.06	75.77

Figure 4.3.8 Cadmium Retention in Muffle Furnace Ashes of CERCHAR fuels



	Fuel 1	Fuel 2	Fuel 3	Fuel 4	Fuel 5	Fuel 6	Fuel 7	Fuel 8
850 C	62.50	54.11	49.98	66.16	68.78	71.96	84.32	83.97
950 C	52.32	52.89	47.95	65.16	73.58	56.53	81.14	83.94

Figure 4.3.9 Barium Retention in Muffle Furnace Ashes of CERCHAR fuels



	Fuel 1	Fuel 2	Fuel 3	Fuel 4	Fuel 5	Fuel 6	Fuel 7	Fuel 8
850 C	88.54	101.66	80.76	82.29	58.29	78.29	86.84	78.63
950 C	84.35	98.68	60.37	78.57	55.77	60.93	79.36	56.53

Figure 4.3.10 Lead Retention in Muffle Furnace Ashes of CERCHAR fuels

4.3.1 The Effect of Temperature on Muffle Furnace Produced Ash

Beryllium

Beryllium retention in the ashes produced in the muffle furnace varied from being completely retained to a minimum of 45% retention. Thermodynamic modelling predicted that retention would not vary between 850 & 950 °C. For the unblended coals, Fuel 1 & 2, nearly 100% retention was predicted, with the formation of beryllium oxides and silicates, BeO, $BeO{\cdot}AL_2O_3$ & $BeO{\cdot}Si0_2$. Taking errors into account this is in agreement with the results obtained. For fuels where woody material has been added, beryllium retention is predicted to decrease significantly, where 100% woody fuel would cause 100% beryllium volatilisation via the formation of $Be(OH)_2$ (g). For Fuels 5 & 7 beryllium is volatilised at 40 and 60 % respectively and this is accurately predicted. For Fuel 6 however which contains 70% dry saw dust the beryllium retained is higher than anticipated. This may be due to the small amount of BeO forming in the gaseous phase re-condensing due to lack of carrier gas in the muffle furnace. For Fuels 3, 4, and 8 it was predicted that beryllium would be almost completely retained (95%). This was the case for Fuels 3 & 4 but not for Fuel 8 where experiments showed approximately 65% retention for both temperatures.

From the results obtained both experimentally and through modelling it may be concluded that in the muffle furnace, for the temperature ranges studied no effect on temperature on beryllium retention was observed.

Vanadium

The predicted profile for vanadium retention was similar to that of beryllium. Vanadium was predicted to be 95-100% retained for the South African Coals in Fuel 1 & 2. The solid oxides of vanadium predicted to form were VO_2, V_2O_5, $FeO{\cdot}V_2O_5$, $CaO{\cdot}V_2O_5$, $2CaO{\cdot}V_2O_5$. Experimental results concurred with these predictions. For the non-woody fuel blends, predictions also showed that vanadium would be retained to a slightly lesser extent (80-95%) and this was bourn out experimentally.

For Fuels 5-7, showed vanadium retentions from 55 to 80 %; modelling showed that vanadium could be more mobile due to its different mode of occurence in the wood. The 100 °C temperature differential did not seem to affect the proportion of Vanadium retained for any of the eight fuels.

Chromium

Thermodynamic modelling predicts that solid Cr_2O_3 will form at the temperatures studied (up to a temperature of 1100 °C) with small quantities of CrO_3 gas forming (from 830 °C) for the unblended Fuels 1 and 2, giving a retention in the 60-80% region. The results concur with these predictions. For Fuels 5, 6 & 7 CrO_3 gas was predicted to form at 870 °C, thus reducing the Chromium retention to the region of 60 %. Fuel 5 chromium concentrations were anomalous with predictions in that the retention increased at 950 °C.

As with the other elements, chromium retention did not appear to be a function of temperature for any of the fuels ecept for Fuels 1 & 7 (South Africa Coal 97 and a blend of South Africa Coal 97 and Wood bark). This was not predicted by thermodynamic modelling. In these instances it appeared that there was a 30 % decrease in chromium retention when the combustion temperature was increased. For Fuel 7 this may be explained by the fact that more CrO_3 gas is expected to form as temperature increases. For Fuel 1 the reduced retention may be due to the fact that CrO_2 gas formed does not re-condense to form Cr_2O_3 as predicted due to the low levels of chromium present, eliminating the opportunity for molecules to meet and react. It is unclear however why this lower retention occurs in Fuel 1, but not in Fuel 2.

Zinc

The zinc compounds predicted to form after combustion were ZnO in both solid and gas phase and $ZnO{\cdot}Al_2O_3$ and $2ZnO{\cdot}SiO_2$ in the solid phase. $ZnO{\cdot}Al_2O_3$ and ZnO are predominantly predicted to form at temperatures of up to 950 °C. Retention was predicted to be near 100 % for all the fuels. As may be seen this is not the case as retentions vary from 46% for Fuel 7 to nearly 100% for Fuel 4 only . This lower-than-predicted retention is particularly pronounced for fuels with higher organic content. An explanation for these lower retentions may be that most of the Zinc present in the blended fuels is present in the organic matrix. This concurs with previous studies (Kendric et Al (1992), Pendias et al (1982)) where it was stated that zinc is bound to lighter organic enzymes and vitamins present in woody material. Contrary to this, thermodynamic predictions and previous studies, state that in these instances the Zinc released (in this instance as ZnO gas) will recondense on the ash particles and form a solid compound. For the fuels where there is a large degree of volatilisation not all of the ZnO gas predicted to recondense may do so.

The results for zinc retention at 950 °C are lower than the results for 850 °C for all the fuels except Fuel 1 and Fuel 7. This is borne out to some extent by thermodynamic predictions which state that between 850 °C and 950 °C retention falls from 100% to approximately 90%. However when experimental errors are taken into account temperature dependence on zinc retention, within the range studied, may not be confidently stated.

Arsenic

Thermodynamic modelling predicted that between 60 & 100% of the arsenic would be retained as calcium and magnesium arsenates ($Ca_3(AsO_4)$ and $Mg_3(AsO_4)$) at the temperatures studied with AsO and AsO_2 gases forming at temperatures above 1050 °C. This did not agree with the results obtained where arsenic was shown to be volatilised by as much as 95 % for Fuels 3 & 4 (although most other fuels showed arsenic volatilisation to be above 50%).

These fuels contain high quantities of Freyming coal slurry. It may be suggested that most of the arsenic is present in organic form in this fuel, thus contributing to a high degree of arsenic volatility.

Temperature dependence in the temperature range studied was not predicted by thermodynamic modelling and it is not exhibited empirically.

Selenium

Selenium was present in small amounts in the original fuel and selenium retention was low for all the fuels studied. For Fuels 4 – 8 more than 96% of selenium was volatilised at both temperatures studied. Fuels 1-3 showed a selenium retention of between 6 & 10 %, with the exception of Fuel 1 exhibiting a selenium retention of 19% after combustion at 850 °C. Thermodynamic predictions suggest that all of the selenium should be emitted after combustion as SeO or SeO_2 after 650 °C for all the fuels studied. The results obtained for Fuel 1, and to a lesser extent Fuels 2 & 3 do not concur with this prediction. Possible modes of occurrence of selenium in coals are in pyrites or sulphides. It is possible that selenium is not released from this mode of occurrence.

Reasons for this may either be due to the mode of occurrence in the fuels or that a compound is formed which may not be included in the model databases. The existence of an unaccounted for compound would also explain the fact that temperature appears to have an affect on selenium retention between 850 & 950 °C. Other than the results obtained for Fuel 1 temperature does not influence Selenium volatility at the combustion temperatures studied.

Mercury

Trace element concentrations for mercury were comparatively low in all the fuels studied ranging from 0.1 to 1.5 ppm. Retention of mercury was also low for all the fuels with a maximum of 8 % for Fuels 3 & 4. For the remaining fuels mercury volatility was higher than 96%.

Thermodynamic predictions showed mercury volatilisation to be 100 % for all fuels at temperatures above 650 °C, 98% being elemental mercury, with a maximum of 2% in HgO form. The higher values of mercury retention for Fuels 3 & 4 are not predicted in simulations. In previous studies (Miller 2001) a mercury retention of 20% was found for Polish Coal during combustion in a suspension reactor. It was postulated in this instance that the mercury was retained due to capture by unburnt carbon (Hassett and Eylands, 1999). In the case of Miller this theory was rebutted after investigation using TGA analysis of the ash showed no unburnt carbon present. In this investigation the sample was shown to be 100 ± 0.1% ash. Although the quantity of carbon seems negligible even a few tens of percent of carbon will give a large excess of carbon relative to the few atoms of mercury, allowing the mercury to be recaptured.

Temperature dependence, within the range studied, is not exhibited with regard to mercury release for the Fuels 1, 2, 5 & 6. Temperature effects on mercury retention do appear to exist for Fuels 3, 4 , 7 & 8. As these were the four fuels which showed a higher degree of mercury retention, the hypothesis for an unknown compound forming, which is released to a greater extent at the higher temperature, is strengthened.

Cadmium

Cadmium was the element which deviated most from the predictions of thermodynamic modelling. For all the fuels studied no cadmium species in the solid phase were predicted to exist above 850 °C. $CdSO_4$ solid was predicted to exist up to temperatures of 710°C for Fuels 1, 2, 3, 4 and 8, and $CdO{\cdot}SiO_2$ from 690 – 750°C. For the remaining fuels it was predicted that $CdO{\cdot}SiO_2$ would form to temperatures up to 850°C. Above this temperatures it was predicted that the gases Cd, CdOH, $CdCl_2$ and $Cd(OH)_2$ would form to various proportions depending on temperature. These predictions also concurred with those from previous studies (Miller 2001, Lachas 1999, Scotto 1993).

Given that chorine concentrations were low in the fuels, simulations were conducted with the exclusion of chlorine. With out the possibility of Cl compounds forming it was found that sulphates were indeed favoured to form at higher temperatures of 800 °C. This therefore does not explain the existence of cadmium in the solid form at the given temperatures, and it must be concluded that this must be due to compounds forming which are not included in the databases used.

Cadmium retention was shown to be a function of temperature for fuels 3, 6, and 8, but no temperature dependence was shown for the other fuels at the temperatures studied.

Barium

Barium was predicted to be completely retained for Fuels 1, 2 3, 4 and 8., with the production of $BaSO_4$, $BaO{\cdot}SiO_2$ or $BaO{\cdot}Al_2O_3$. The addition of woody material to the fuels reduced the $BaO{\cdot}Al_2O_3$ content, but around 85% of barium should be retained. It is shown that there were high retentions of barium for Fuels 7 and 8 up to 95% taking into account the experimental error range, but reduced amounts for the remaining fuels, in the range of 50-80%. This decrease indicates that the mode of occurrence of barium in petroleum coke and bark must favour its retention, whilst for the other fuels barium is predicted to possibly re-condense but does not do so.

For ash produced in the muffle furnace there does not seem to be any temperature dependence, for any of the fuels, on the degree of barium release.

Lead

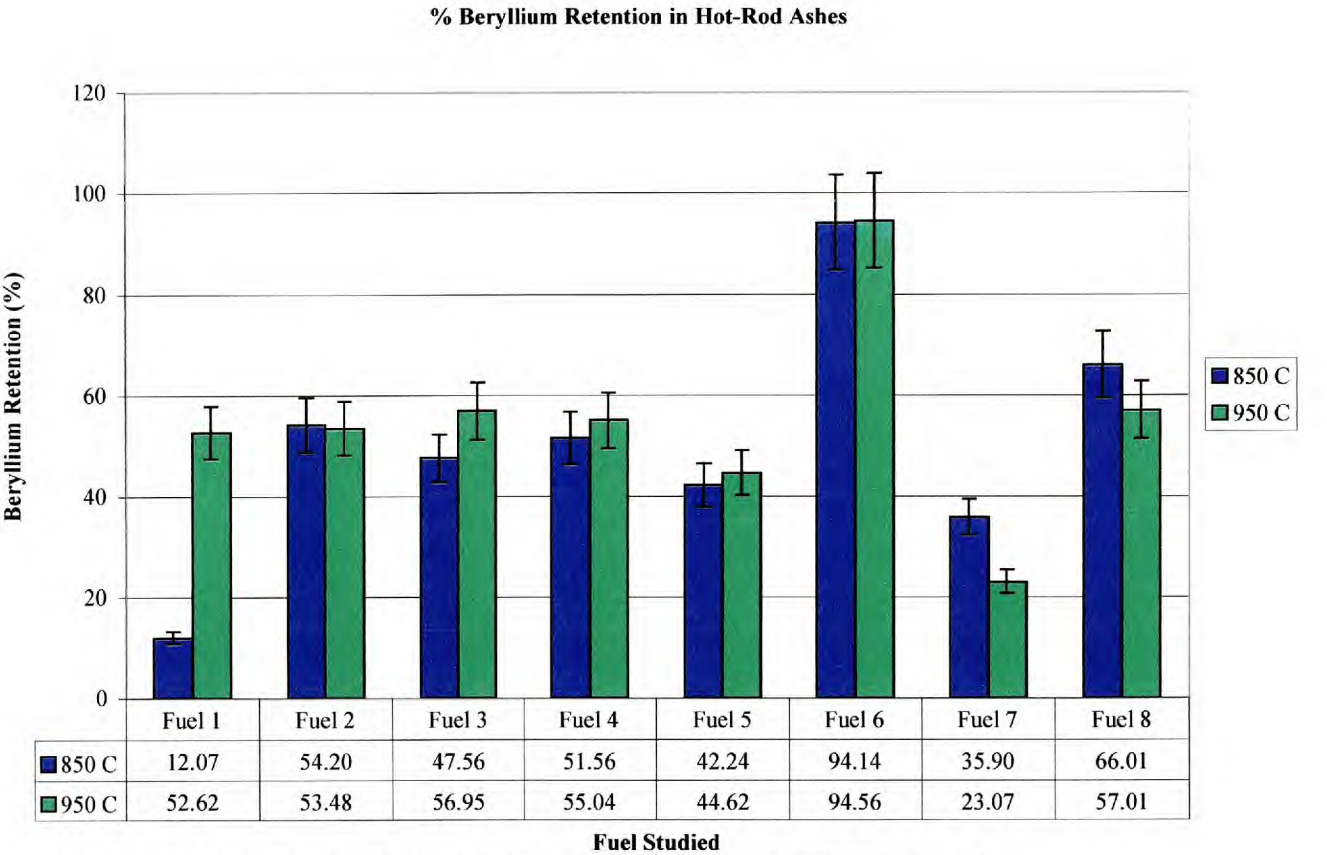
For the unblended fuels it was determined via thermodynamic modelling that lead should be completely retained for temperatures up to 870 °C after which PbCl and PbO gases were favoured to form. In the solid state lead was predicted to form as mostly $PbSO_4$. For the blended fuels which included woody matter it was predicted that a far smaller percentage of $PbSO_4$ would form (in the region of 60-70%) and that lead dichloride gas would be predominantly favoured at temperatures up to 1000 °C.

The results at 850 °C concur with predictions for all fuels, however at 950 °C where it would be expected that there would be a significant drop in lead concentration in the ash and this was only the case for some fuels. Fuels 3, 6 and 8 show the predicted lead release whilst all the other fuels show a higher level of enrichment than expected. This may be explained by low levels of chlorine present in the fuels (< 0.035% in all fuels) hindering the formation of lead chlorides (volatile) and favouring the formation of the solid lead sulphate (non-volatile). Simulations were carried restricting chlorine presence and this showed $PbSO_4$ to be favoured up to 900 °C.

Lead retention was predicted to be a function of temperature over the range studied; this was shown to be the case in Fuels 3, 6, and 8, i.e. the fuels containing Freyming coal slurry, but not in any other instance.

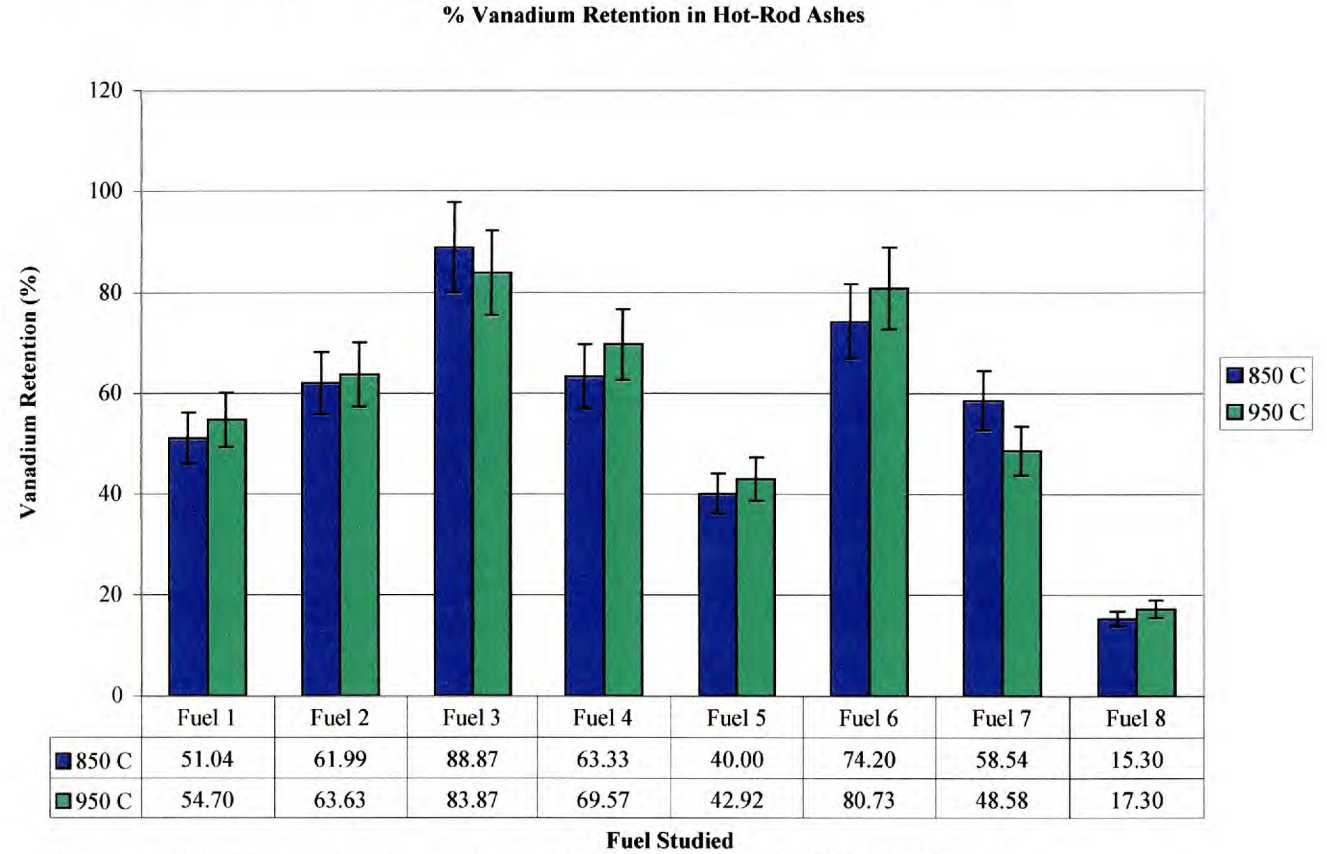
4.3.2.1 The Effect of Temperature on Hot-Rod Reactor Produced Ash

Below follow results to depict the effect of temperature of trace element retention in hot-rod ash.



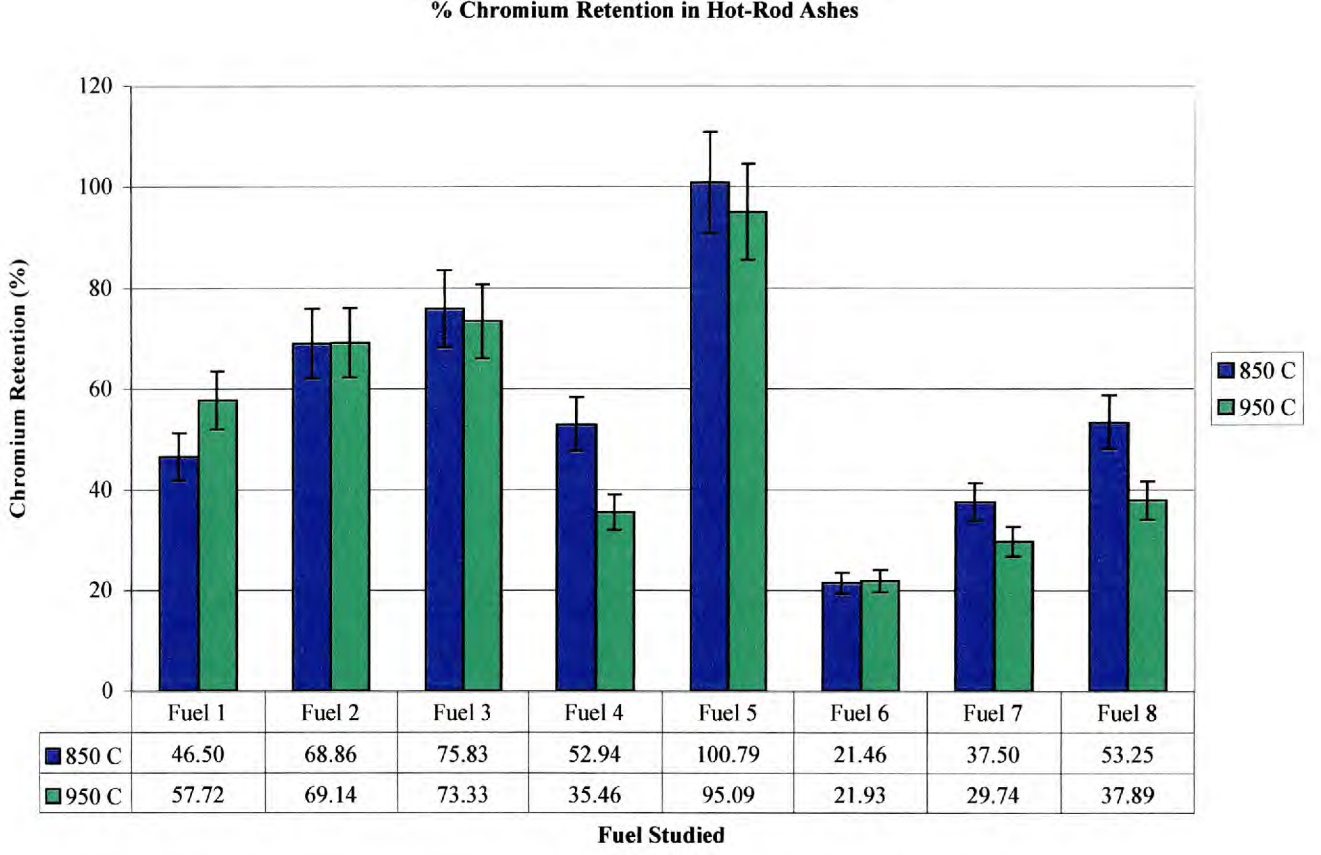
	Fuel 1	Fuel 2	Fuel 3	Fuel 4	Fuel 5	Fuel 6	Fuel 7	Fuel 8
850 C	12.07	54.20	47.56	51.56	42.24	94.14	35.90	66.01
950 C	52.62	53.48	56.95	55.04	44.62	94.56	23.07	57.01

Figure 4.3.11 Beryllium Retention in Hot-Rod Ashes of CERCHAR fuels



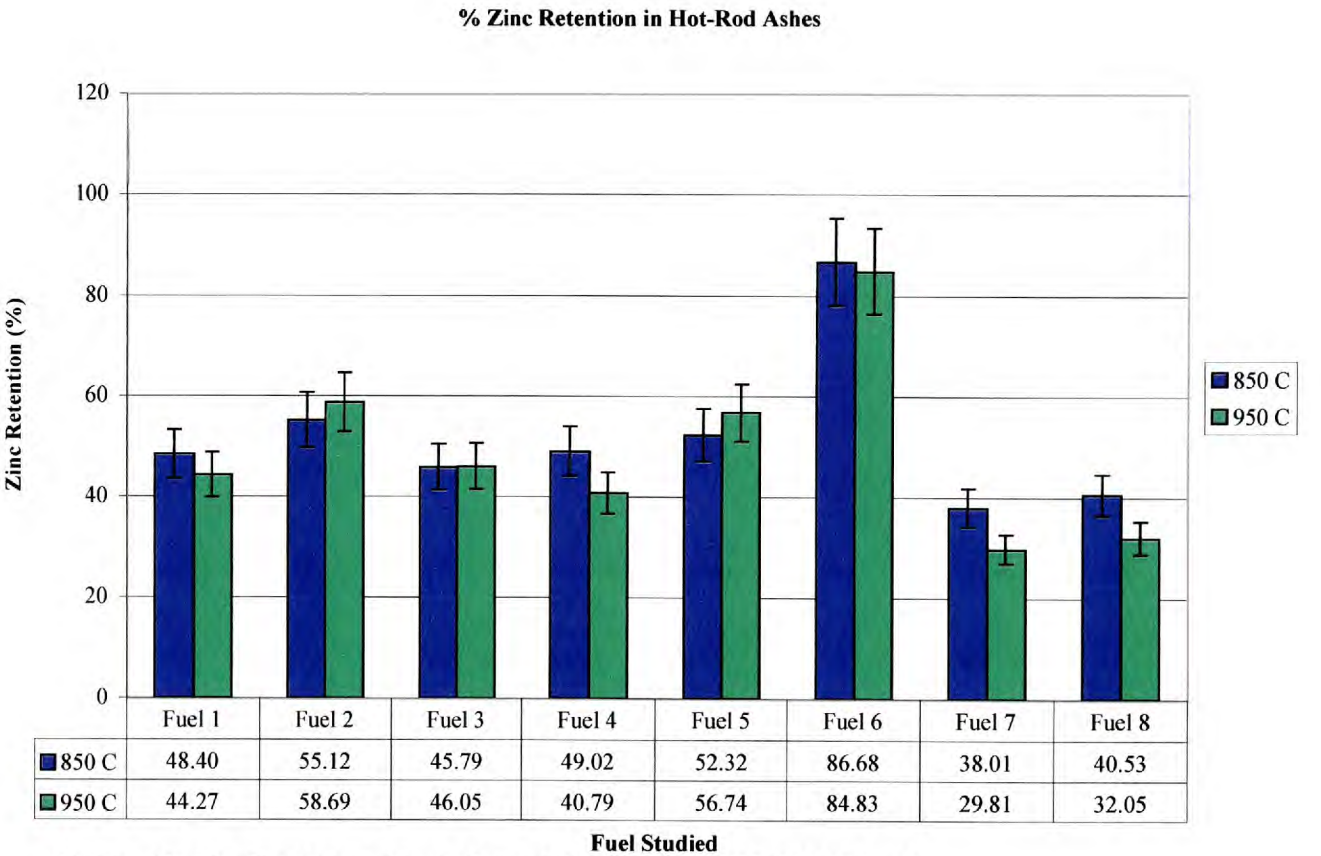
	Fuel 1	Fuel 2	Fuel 3	Fuel 4	Fuel 5	Fuel 6	Fuel 7	Fuel 8
850 C	51.04	61.99	88.87	63.33	40.00	74.20	58.54	15.30
950 C	54.70	63.63	83.87	69.57	42.92	80.73	48.58	17.30

Figure 4.3.12 Vanadium Retention in Hot-Rod Ashes of CERCHAR fuels



	Fuel 1	Fuel 2	Fuel 3	Fuel 4	Fuel 5	Fuel 6	Fuel 7	Fuel 8
850 C	46.50	68.86	75.83	52.94	100.79	21.46	37.50	53.25
950 C	57.72	69.14	73.33	35.46	95.09	21.93	29.74	37.89

Figure 4.3.13 Chromium Retention in Hot-Rod Ashes of CERCHAR fuels



	Fuel 1	Fuel 2	Fuel 3	Fuel 4	Fuel 5	Fuel 6	Fuel 7	Fuel 8
850 C	48.40	55.12	45.79	49.02	52.32	86.68	38.01	40.53
950 C	44.27	58.69	46.05	40.79	56.74	84.83	29.81	32.05

Figure 4.3.14 Zinc Retention in Hot-Rod Ashes of CERCHAR fuels

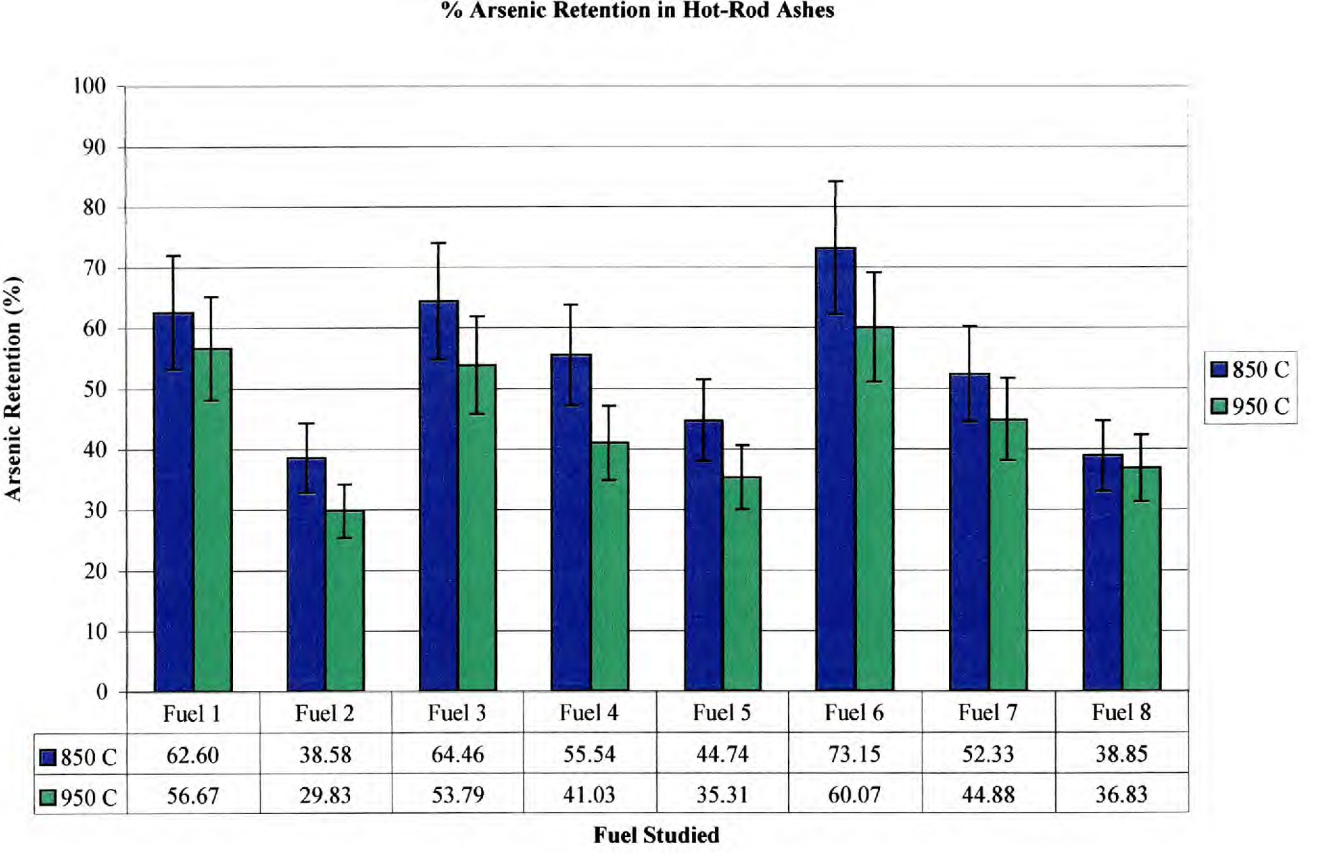


Figure 4.3.15 Arsenic Retention in Hot-Rod Ashes of CERCHAR fuels

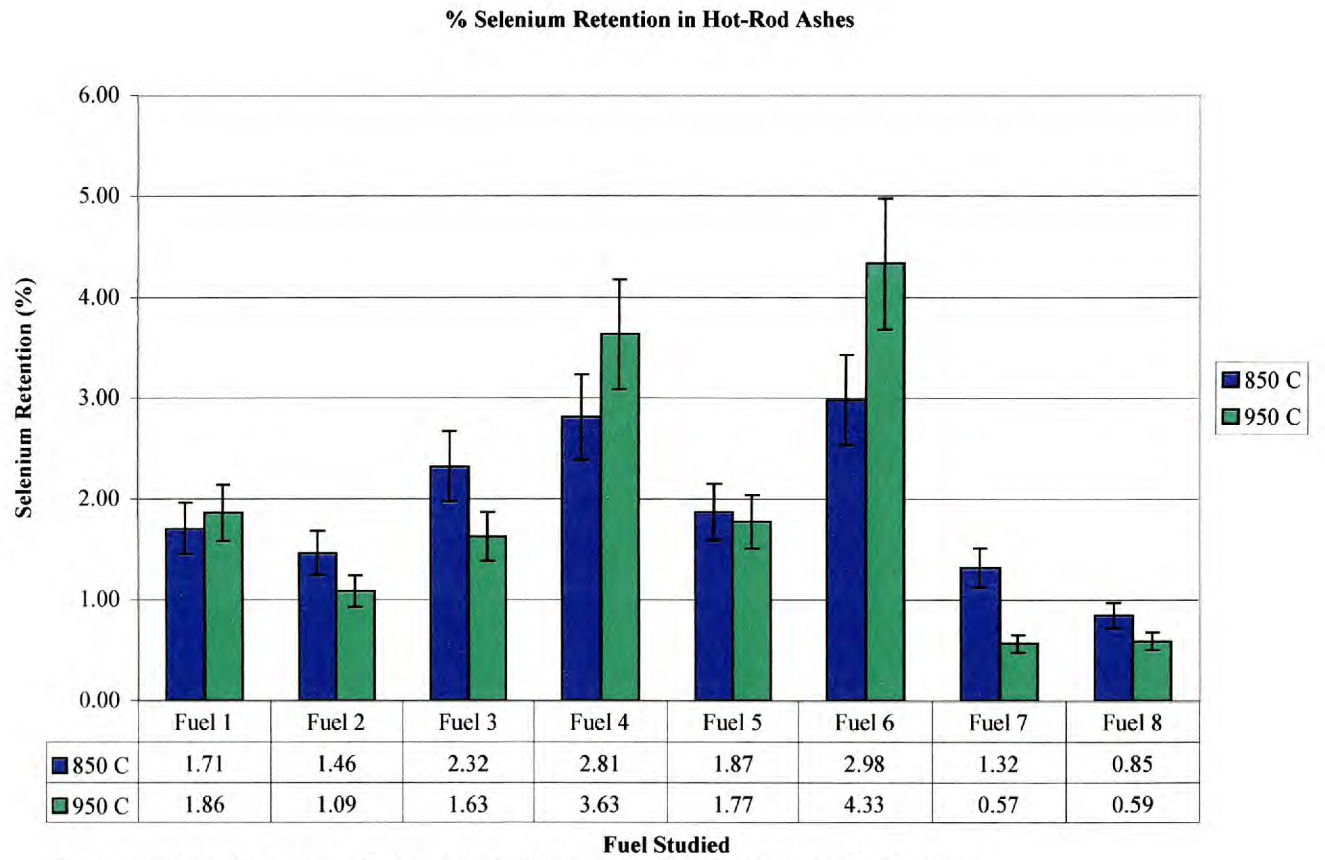


Figure 4.3.16 Selenium Retention in Hot-Rod Ashes of CERCHAR fuels

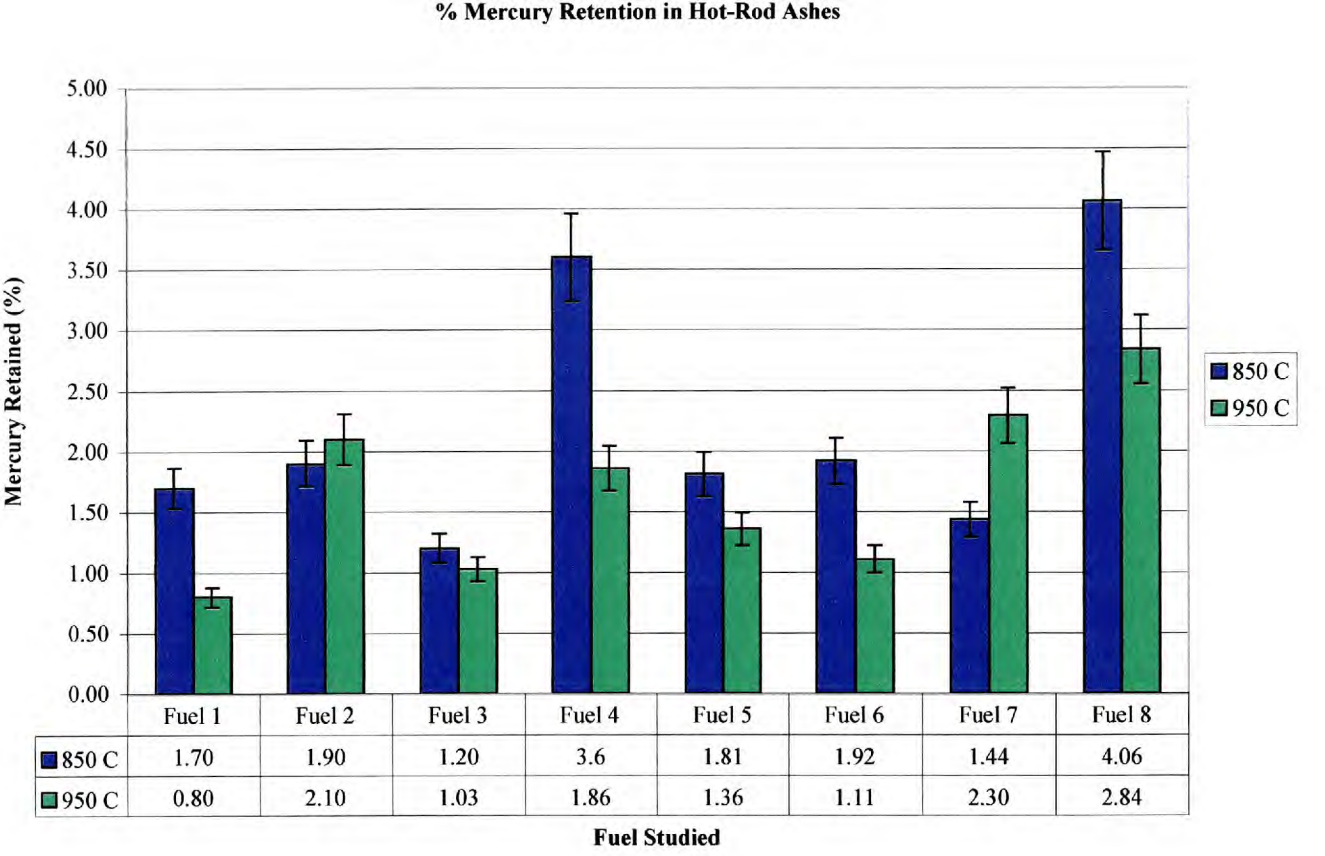


Figure 4.3.17 Mercury Retention in Hot-Rod Ashes of CERCHAR fuels

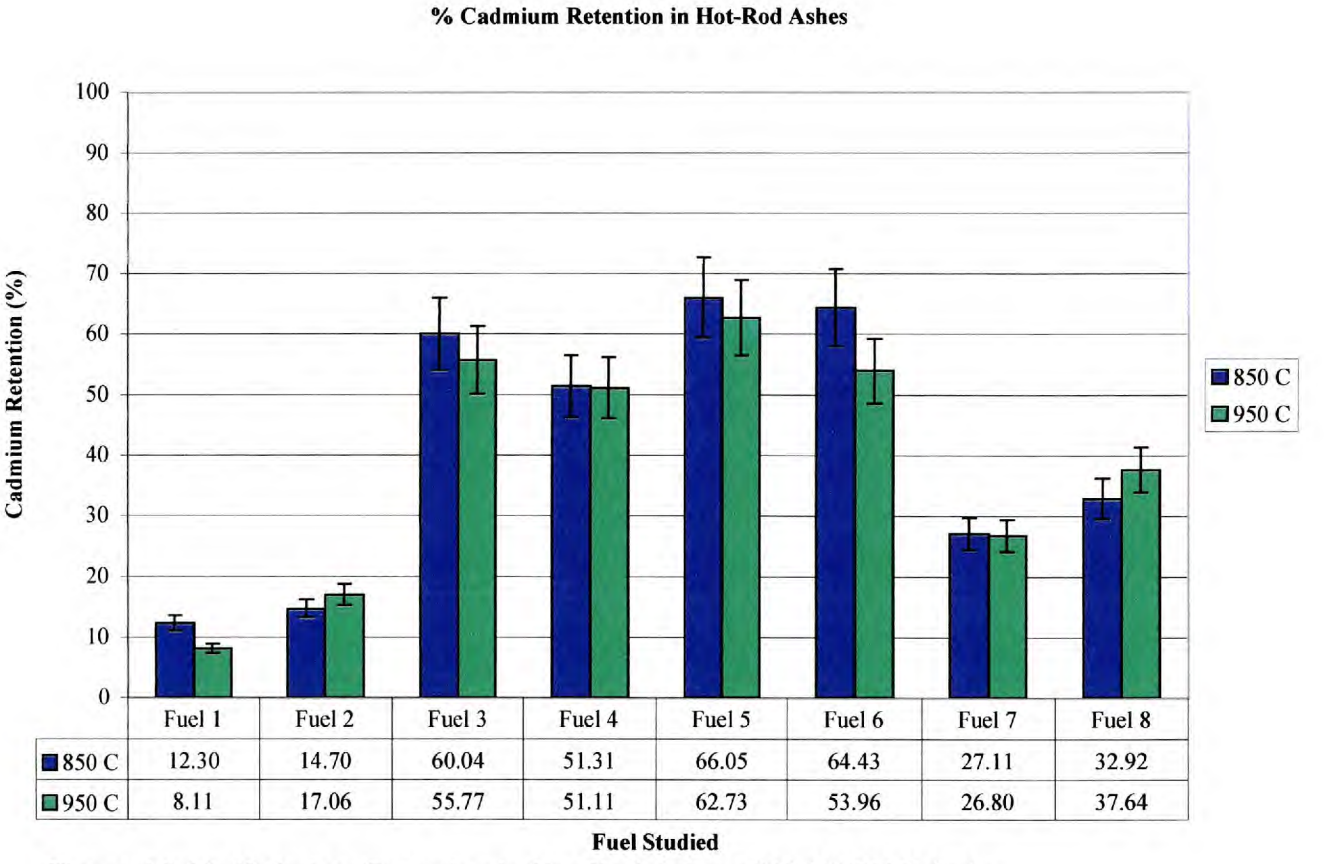
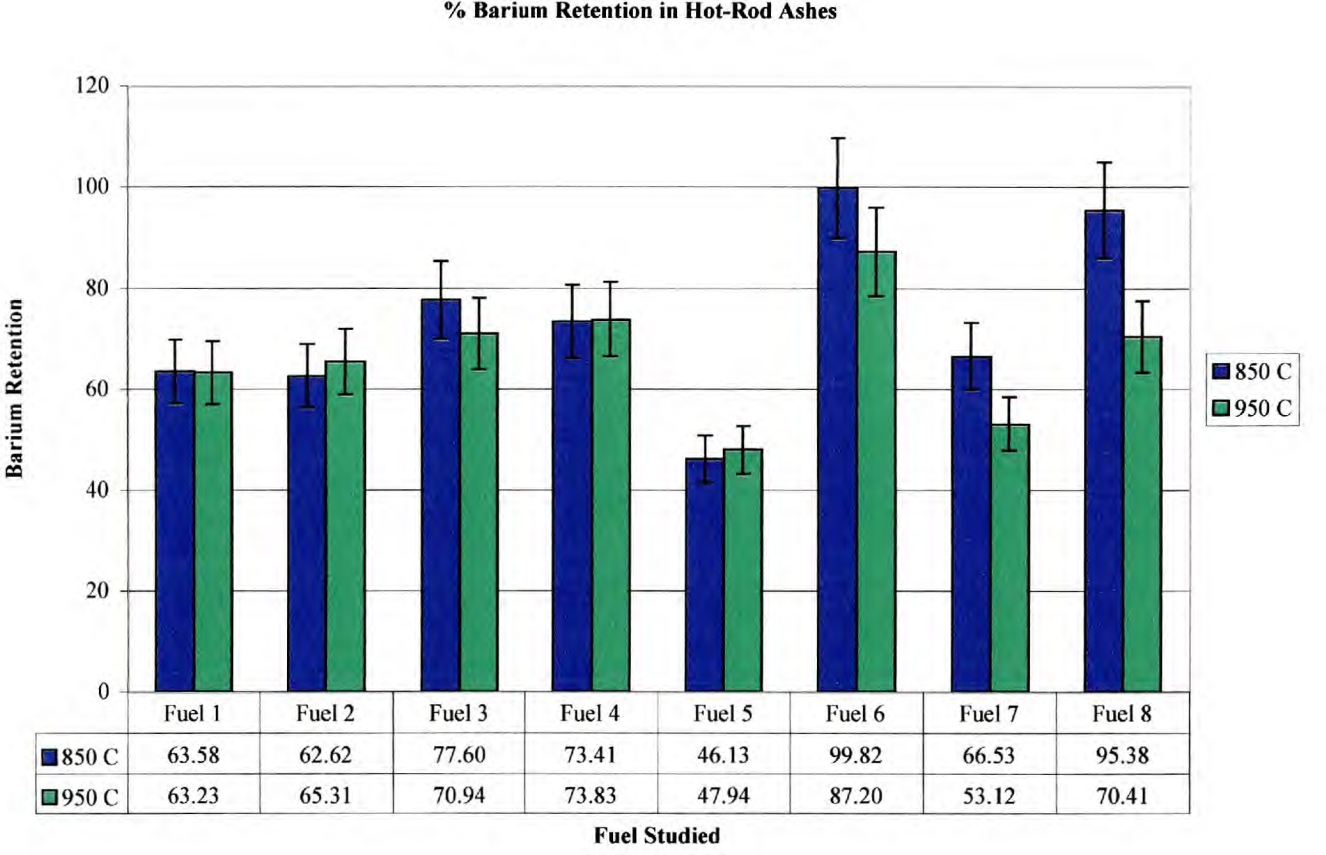
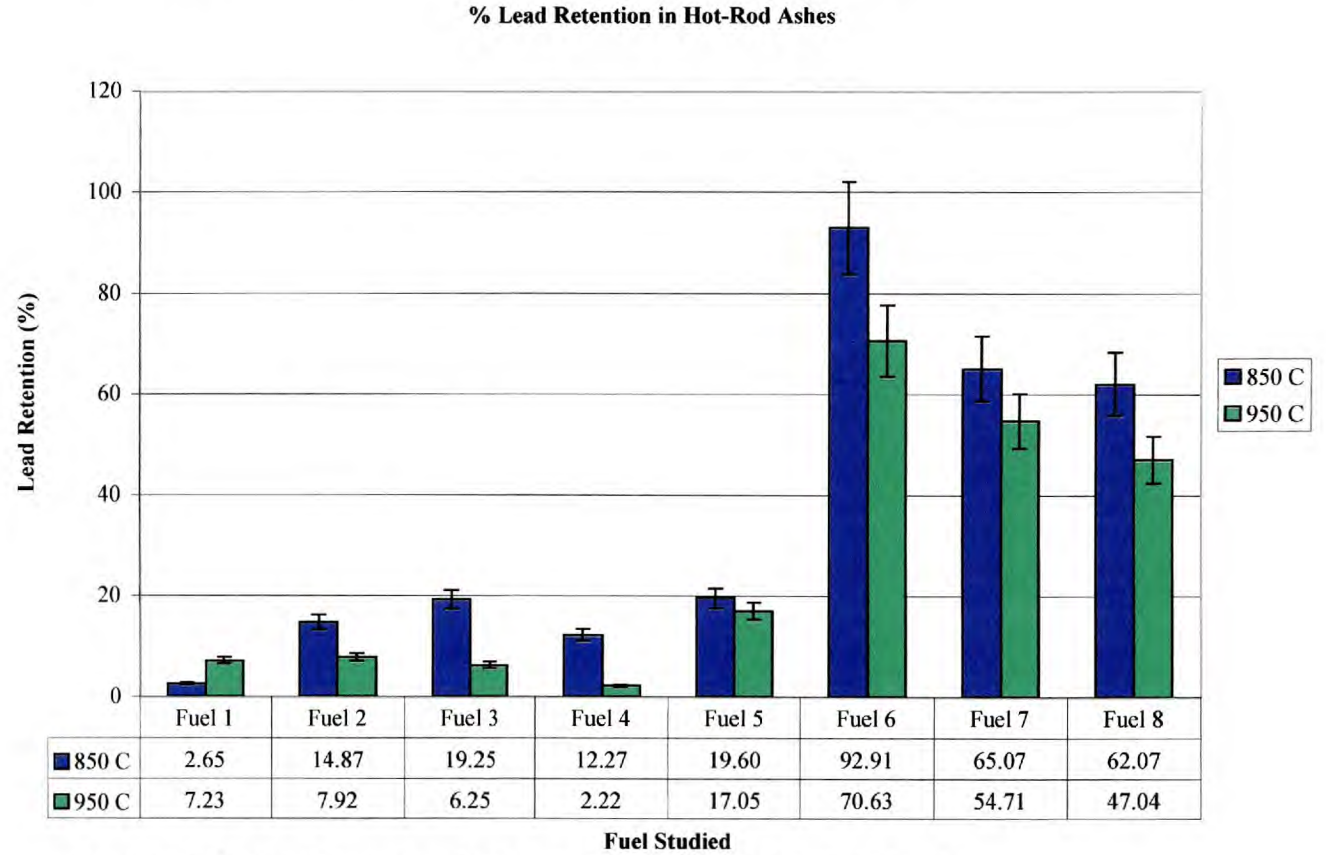


Figure 4.3.18 Cadmium Retention in Hot-Rod Ashes of CERCHAR fuels



	Fuel 1	Fuel 2	Fuel 3	Fuel 4	Fuel 5	Fuel 6	Fuel 7	Fuel 8
850 C	63.58	62.62	77.60	73.41	46.13	99.82	66.53	95.38
950 C	63.23	65.31	70.94	73.83	47.94	87.20	53.12	70.41

Figure 4.3.19 Barium Retention in Hot-Rod Ashes of CERCHAR fuels



	Fuel 1	Fuel 2	Fuel 3	Fuel 4	Fuel 5	Fuel 6	Fuel 7	Fuel 8
850 C	2.65	14.87	19.25	12.27	19.60	92.91	65.07	62.07
950 C	7.23	7.92	6.25	2.22	17.05	70.63	54.71	47.04

Figure 4.3.20 Lead Retention in Hot-Rod Ashes of CERCHAR Fuels

4.3.2.2 The Effect of Temperature on Hot-Rod Reactor Produced Ash

There are two main differences between the muffle furnace and the hot-rod reactor. The hot-rod reactor contained a flow of carrier gas, whilst the muffle furnace did not. The fuel in the muffle furnace had a longer reaction time at the specified temperature (by two orders of magnitude), in order to effect complete combustion (see section 3.3.1). After the specified hold time the muffle furnace required longer to cool from the hold temperature than the hot-rod reactor.

Beryllium

For Fuels 1 & 2 beryllium retentions in the hot-rod were much lower than predicted by thermodynamic modelling, which predicted nearly 100% retention with allumino silicate compounds forming. Beryllium retentions were in the region of 50% except for the seemingly anomalous result of 12% retention for Fuel 1 combusted at 850 °C. For Fuels 3, 4 and 8, it was predicted that 80% of the beryllium would escape from its solid state, but empirical results showed lower percentage retentions at around 50%. Fuel 6 once again showed a beryllium retention which, at 80%, was surprisingly high, given that its main component is dried saw dust. Predictions stated that beryllium concentration in this instance should be 40% at both temperatures. In summary, beryllium concentrations in the hot-rod were generally lower than from the muffle furnace and retentions were lower than thermodynamic predictions for all fuels and temperatures except Fuel 6. Fuel 6 also exhibited higher retentions in the muffle furnace. An explanation for the lower retentions may be the presence of carrier gas preventing the element from condensing on the ash. The case of Fuel 6, given higher retentions in the muffle furnace as well as the hot-rod reactor, suggests that compounds exist in the ash which were not considered in the database.

No temperature dependence of beryllium volatilisation was predicted by modelling or observed in practice, within the temperature range studied.

Vanadium

Vanadium retention was once more lower than predicted. For the unblended fuels retention was approximately 50% when 100% retention was predicted. Solid vanadium oxides were predicted to form up to 1000°C. These include VO_2, V_2O_5, $FeO{\cdot}V_2O_5$, $CaO{\cdot}V_2O_5$, $2CaO{\cdot}V_2O_5$. Above 1000°C it was predicted that various oxide gases would form eg V_4O_{10}. In reality both in the gas and solid phase the compounds likely to form are those with one vanadium atom i.e. VO_2. This is due to the low concentrations of vanadium reducing the likelihood that more than one vanadium atom meets to form the more complex compounds. For the Fuels 3, 4 and 8, it was predicted that vanadium would be more volatile at 850°C (80% retention) and this is bourn out by the results where retentions were 80, 70, and 20% respectively. The low Fuel 8 vanadium retention suggests that vanadium exists in the petroleum coke component of the fuel in modes of occurrence which promote volatility, and which are not allowed to condense, even though this behaviour is inferred by the simulations. For the woody fuel blends retention is predicted to be around 50% due to a greater proportion of vanadium being bound in organic material; this concurs with results.

Temperature dependence of vanadium retention is not predicted by the modelling for the temperatures studied, nor is it exhibited empirically.

Chromium

Chromium retentions for ashes produced in the hot-rod reactor were all lower than those produced in the muffle furnace. Modelling predicted that solid Cr_2O_3 would exist at temperatures up to 1100 °C for fuels other than 5-7 (for these fuels CrO_3 gas would begin to form above 870 °C). The retentions were therefore proven to be lower than predicted in all cases except for Fuel 5, which consisted of South African coal and un-dried sawdust. The retention her is higher than for un-blended South African coal. Therefore components in un-dried saw dust must encourage the retention of chromium, via the mode of occurrence of chromium in the un-dried sawdust.

However simulations carried out on 100% sawdust showed the retention to be very low. It may therefore be assumed that either synergistic effects govern chromium volatility in this instance, or that high degrees of chromium condensation occur which are not taken into account in the modelling.

There does not appear to be a temperature dependence when considering chromium retention in hot-rod produced ash, in any of the fuels except Fuels 4 & 8. These fuels exhibit a 33% reduction in chromium retention from 850 °C to 950 °C. Fuels 4 & 8 are both mixtures of Freyming Schlamms and Freyming coal slurry, with the addition of petroleum coke in Fuel 8. When producing ashes in the muffle furnace a temperature dependence was apparent with Fuels 1 & 7, with a reduction of 30%. When the same conditions are applied in both reactor configurations it might be assumed that fuels should the same, if any, temperature dependence. As this is not the case, it is possible that the presence of carrier gas causes temperature dependence in the hot-rod reactor. Also the increase in hold time prevents chromium re-condensation in the muffle furnace at 950 °C.

Zinc

The zinc compounds predicted to form at the temperatures studied were $ZnO{\cdot}Al_2O_3$, 2 $ZnO{\cdot}SiO_2$ and ZnO solid . ZnO gas was predicted to form at temperatures above 950 °C, with elemental gaseous zinc forming abouve 1100 °C. $ZnCl_2$ was predicted to form at around 1050 °C for unblended fuels, and zinc hydroxides for blended fuel feeds. Therefore Zinc was predicted to be 100% immobile at the temperatures studied here, however as may be seen from Figure 4.23.2.14 this is not the case. Retentions were comparatively constant, in the region of 50 % , for all fuels except for Fuel 6 (where retention was approximately 85% at both temperatures). These retentions are even lower than in the muffle furnace, where retentions were between 60-80%.

From this it may be deduced that zinc is indeed bound in the organic matrix. In the hot-rod it does not have the opportunity to condense due to the carrier gas, whereas in the muffle furnace 20% of the zinc released condenses to give the higher retentions exhibited.

The temperature difference of 100 °C, between 850 and 950 °C is not sufficient for there to be a significant change in zinc retention as with the muffle furnace and thermodynamic predictions.

Arsenic

Arsenic retention was predicted to be promoted via the formation of $FeAsO_4$, Ca_3SO_4 and Mg_3AsO_4 at temperatures up to1050 °C. Whilst arsenic retention was higher in the hot-rod than in the muffle furnace, retentions were still below predicted values. Modes of occurrence of arsenic are not widely reported in literature but the results in this study imply arsenic is largely bound to the organic matrix.

Thermodynamic modelling predicted that there would be no variation in the phase of arsenic compounds forming between 850 °C and 950 °C; this was found to be the case experimentally.

Selenium

As with the muffle furnace, selenium retention in the hot-rod reactor was the lowest of all the trace elements studied except mercury. In concurrence with the muffle furnace, more than 96 % selenium was lost from the original fuel after combustion, at both temperatures, for Fuels 4-8. In the muffle furnace retentions of between 6-10% are exhibited for Fuels 1-3, whilst in the hot-rod reactor this is reduced to 2% and under. This again may be due to condensation occurring in the muffle furnace, where there is none in the hot-rod reactor. Thermodynamic predictions suggest that nearly all of the selenium should be released as oxide gases at combustion above 650 °C, so the empirical and theoretical results concur.

Thermodynamic predictions do not suggest that selenium retention should be a function of temperature above 650 °C, and experimental results agree with these predictions.

Mercury

Trace element concentrations ranged from a high of 0.4 ppm found in Fuel 5 to a low of 0.01 ppm. The highest retention was 4% for Fuel 8 and Fuel 4 , whilst all the other fuels exhibited retentions below 2%. Thermodynamic predictions suggest that all of mercury should be released at the temperatures studied, therefore the small quantities mercury present in the ash may be attributed to volatilsed mercury, not managing to escape the system.

As with the muffle furnace, there appears to be a temperature dependence on retention for Fuels 4 and 8, although not for Fuels 3 and 7. This may either be due to less re-condensation of volatilised mercury or the formation of a compound, not present in the simulation database, that is more volatile at 950 °C than at 850 °C,

Cadmium

As with the results obtained from combustion in the muffle furnace, cadmium retention in hot-rod produced ashes was shown to be higher than predicted via modelling. No solid species were predicted to exist above 750 °C for any of the fuels studied. As previously discussed various alterations to the modelling were made in order to clarify the behaviour of cadmium without success. It must therefore be supposed, as previously stated, that cadmium either recondenses to a great extent or that its modes of occurrence in the fuel invalidate the results of the modelling.

No temperature dependence is exhibited for cadmium retention in any of the fuels combusted in the hot-rod reactor, in the temperature range studied.

4.3.3 Trace Element Retention in the Chilean Ashes

The Chilean ashes produced at 1500 °C were produced at the GENER power station, Chile, having seen nominal temperatures of 1500 °C (between 1450-1750°C). The same coal was combusted to produce the 900 °C ashes in a laboratory suspension firing reactor. Analyses were carried out in the same manner as those for the CERCHAR ashes for the purposes of error determination. In order to calculate the error involved in percentage retention, the error in the original fuel and the error in the ash concentrations had to be considered. Therefore, the error in the percentage retention was calculated as the square root of the sum of the squares of the trace element concentration in the fuel and the concentration in the ash.

The purpose of conducting the analyses with these fuels was twofold. First the effect of conducting high temperature combustion experiments could be determined. Secondly, any synergistic effects of high temperature combustion could be investigated. Trace element retentions in the mixtures should be proportional to the retentions of their constituent parts. If significant deviation occurs from the theoretical value, synergy maybe be imputed. Results are therefore presented with these goals in mind. Percentage retentions of each element are given for the five fuels at the two temperatures, followed by percentage retentions of all the elements for a given fuel at the two temperatures.

Absolute values of trace element concentrations in the various fuels are shown in Appendix III. These results give an indication of the leaching availability of each particular ash and are relevant to leaching calculations made.

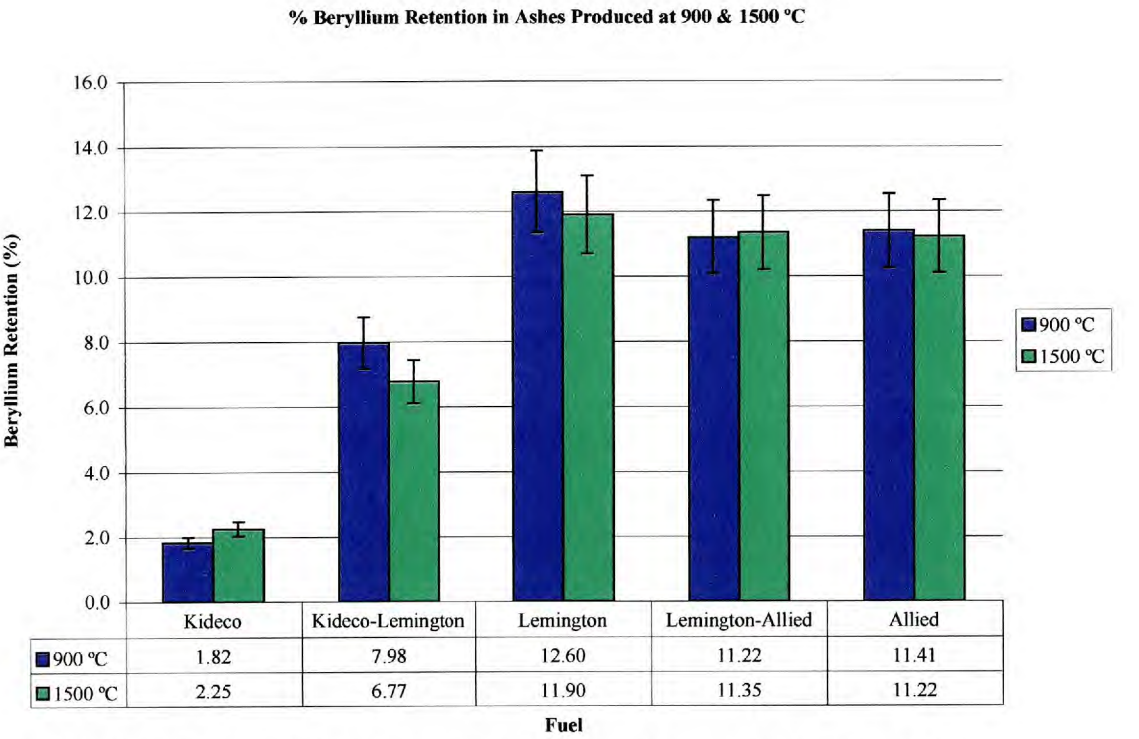


Figure 4.3.21 Beryllium Retention in Chilean Ashes Produced at 900 & 1500 °C

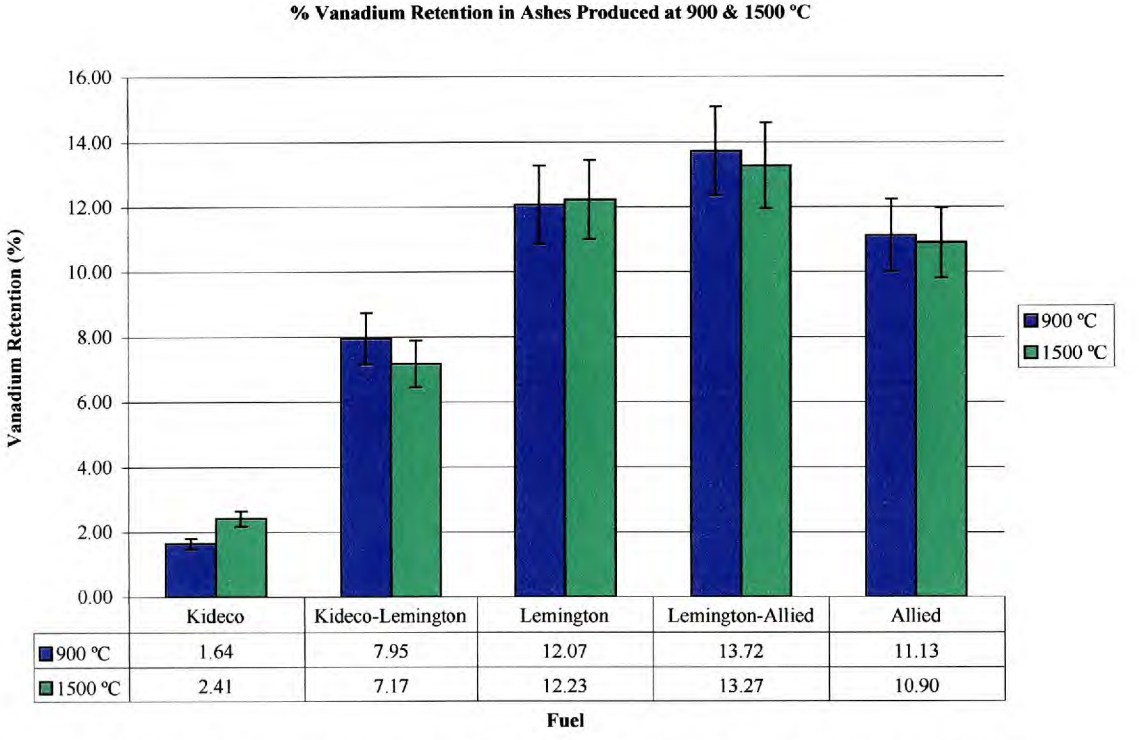


Figure 4.3.22 Vanadium Retention in Chilean Ashes Produced at 900 & 1500 °C

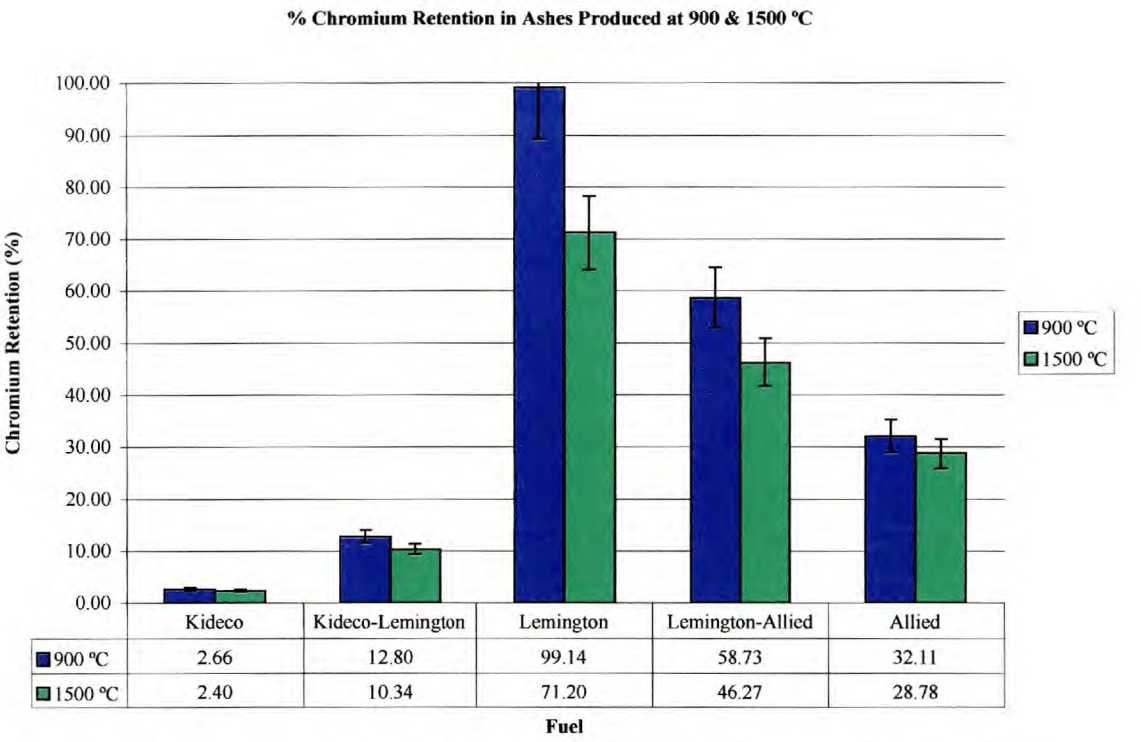


Figure 4.3.23 Chromium Retention in Chilean Ashes Produced at 900 & 1500 °C

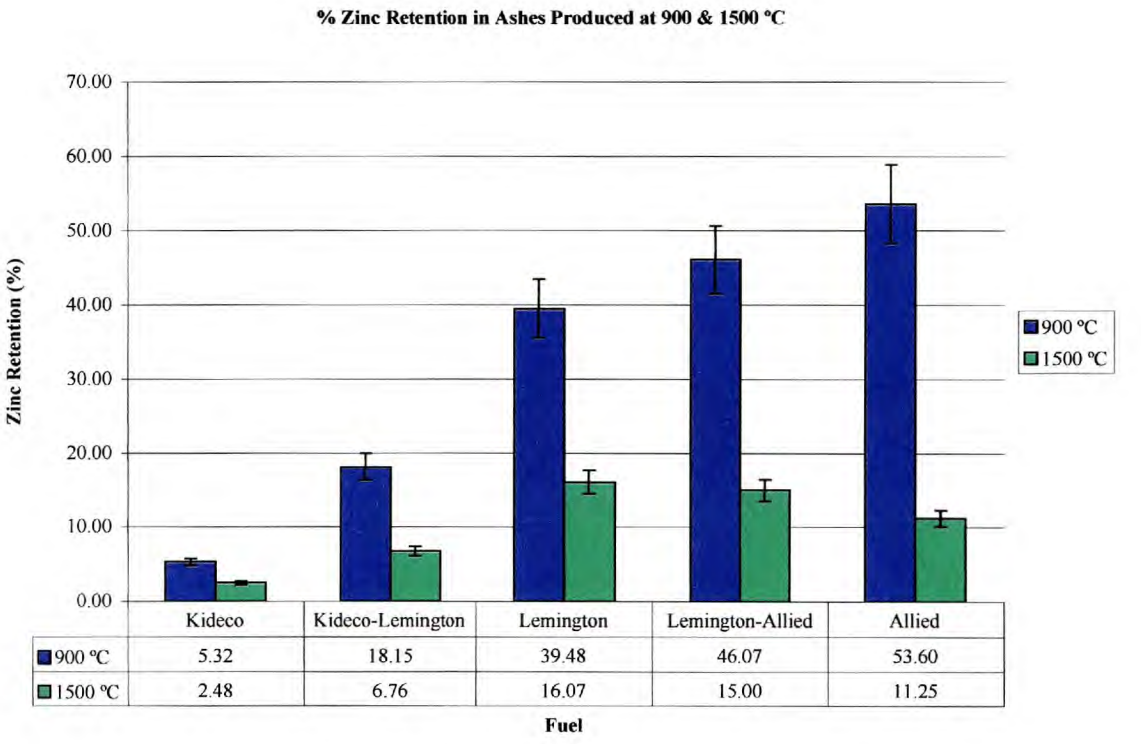


Figure 4.3.24 Zinc Retention in Chilean Ashes Produced at 900 & 1500 °C

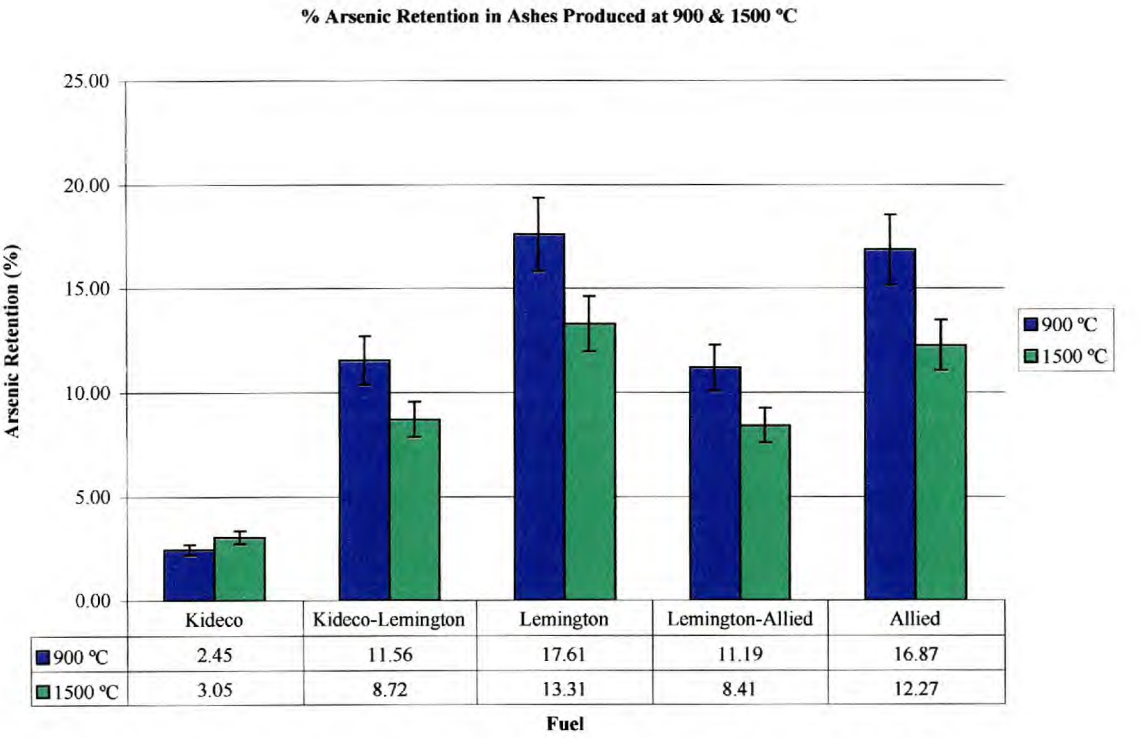


Figure 4.3.25 Arsenic Retention in Chilean Ashes Produced at 900 & 1500 °C

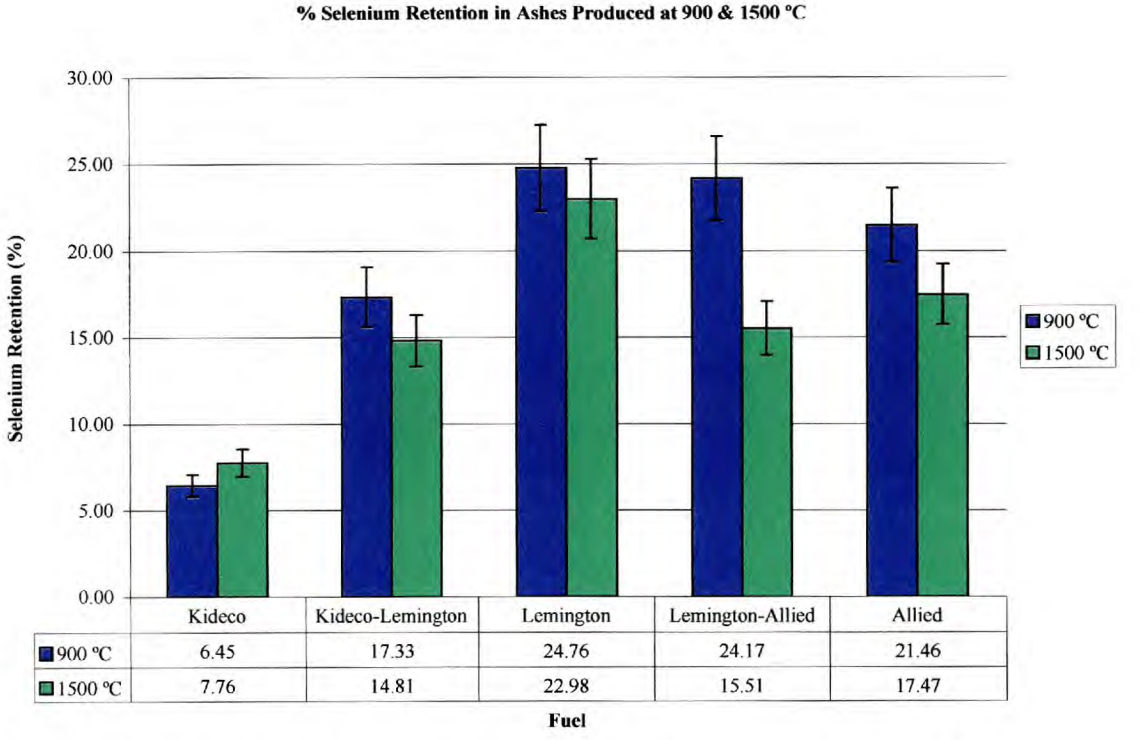


Figure 4.3.26 Selenium Retention in Chilean Ashes Produced at 900 & 1500 °C

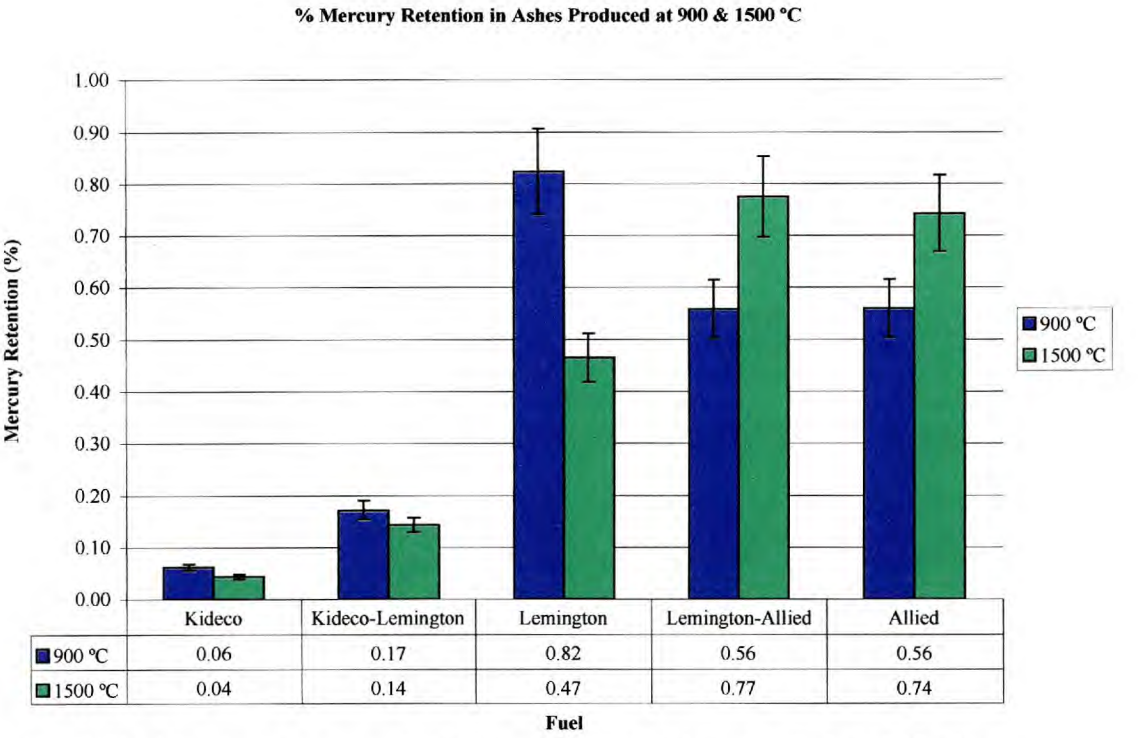


Figure 4.3.27 Mercury Retention in Chilean Ashes Produced at 900 & 1500 °C

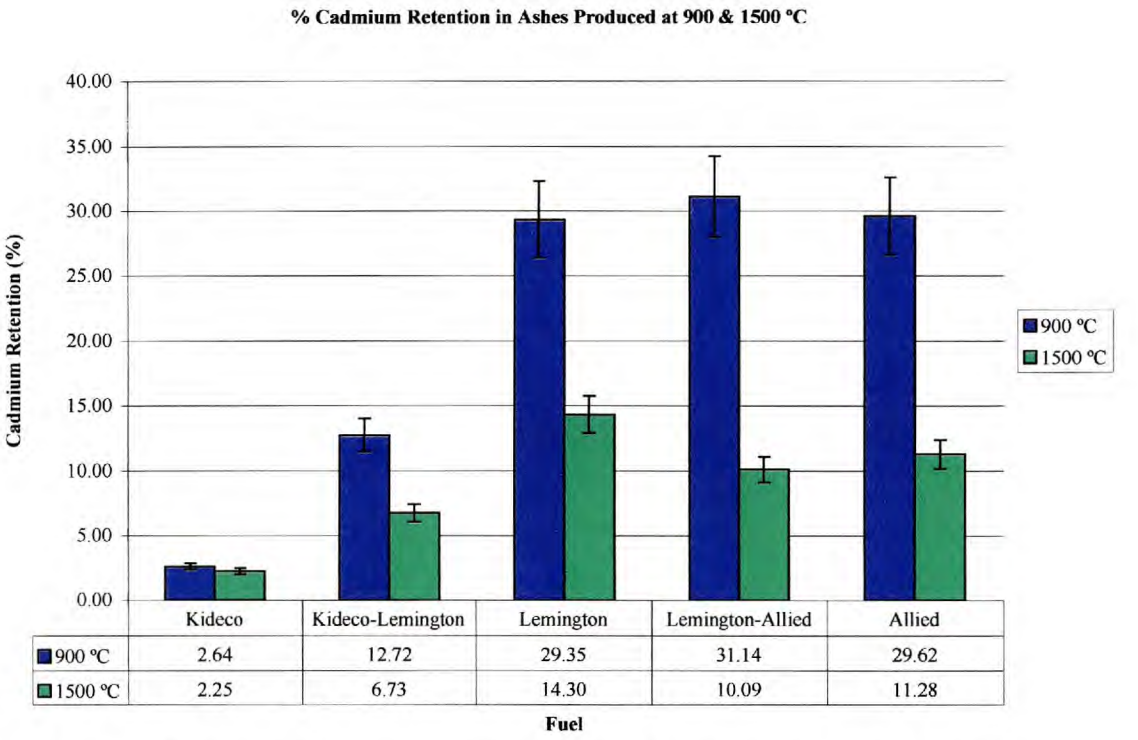


Figure 4.3.28 Cadmium Retention in Chilean Ashes Produced at 900 & 1500 °C

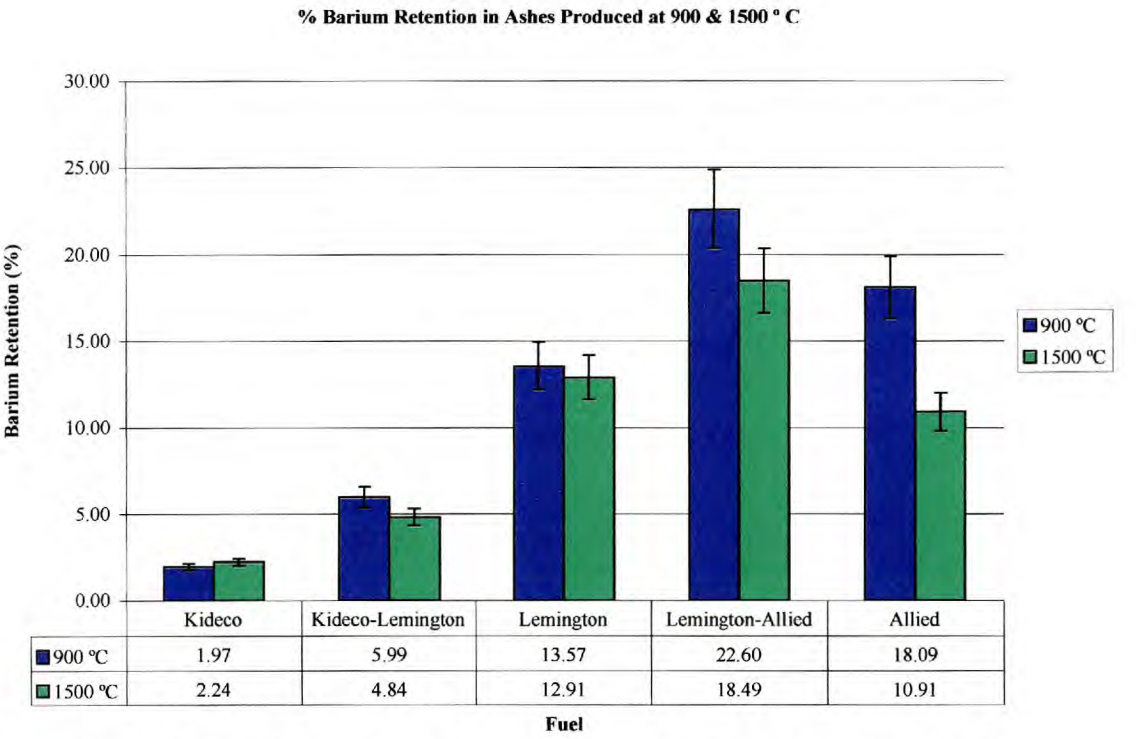


Figure 4.3.29 Barium Retention in Chilean Ashes Produced at 900 & 1500 °C

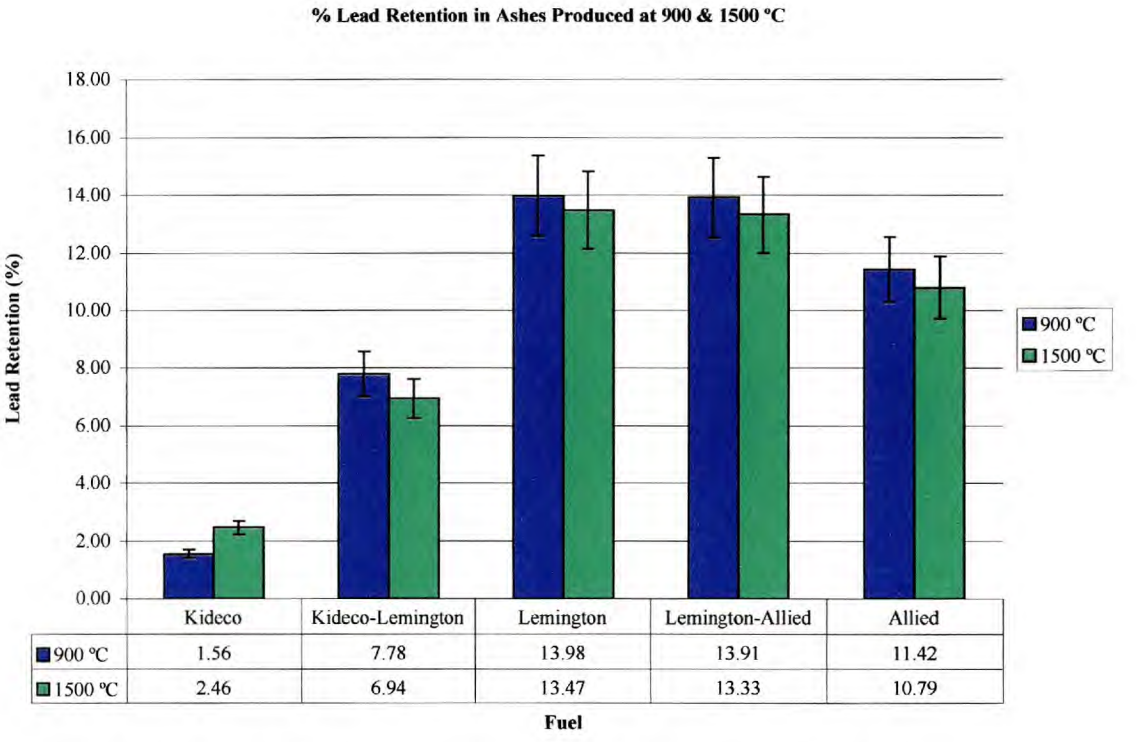
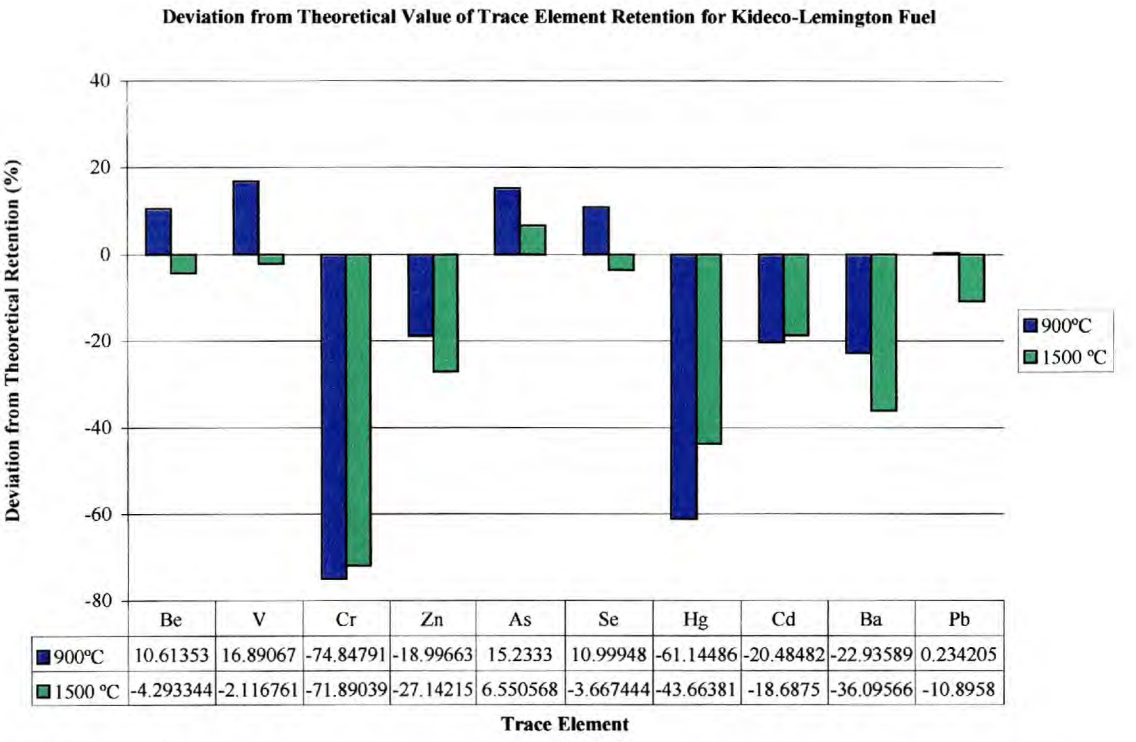
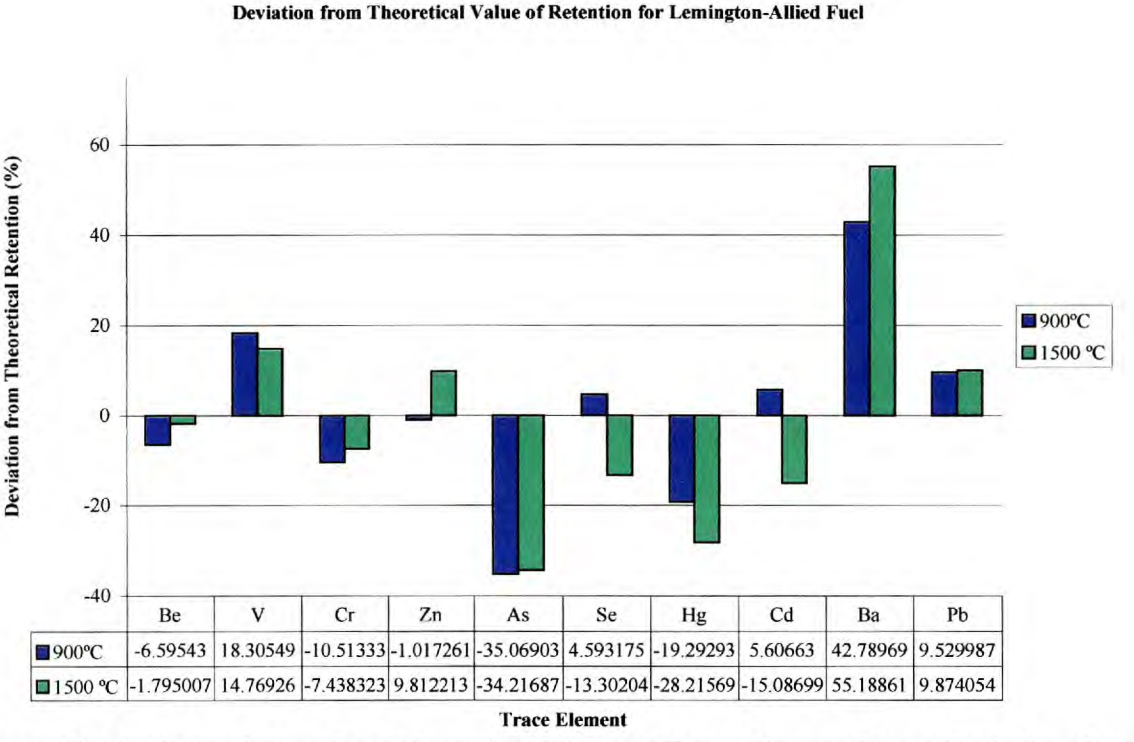


Figure 4.3.30 Lead Retention in Chilean Ashes Produced at 900 & 1500 °C



	Be	V	Cr	Zn	As	Se	Hg	Cd	Ba	Pb
900°C	10.61353	16.89067	-74.84791	-18.99663	15.2333	10.99948	-61.14486	-20.48482	-22.93589	0.234205
1500 °C	-4.293344	-2.116761	-71.89039	-27.14215	6.550568	-3.667444	-43.66381	-18.6875	-36.09566	-10.8958

Figure 4.3.31 % Deviation from Theoretical Value of Trace Element Retention in Kideco Lemington Fuel



	Be	V	Cr	Zn	As	Se	Hg	Cd	Ba	Pb
900°C	-6.59543	18.30549	-10.51333	-1.017261	-35.06903	4.593175	-19.29293	5.60663	42.78969	9.529987
1500 °C	-1.795007	14.76926	-7.438323	9.812213	-34.21687	-13.30204	-28.21569	-15.08699	55.18861	9.874054

Figure 4.3.32 % Deviation from Theoretical Value of Trace Element Retention in Lemington Allied Fuel

Beryllium

Beryllium retention showed no temperature dependence in any of the fuels, being the same at 900 °C and 1500 °C. At 1500 °C thermodynamic predictions indicated that beryllium would exist completely as the gaseous $Be(OH)_2$ compound. Small amounts of beryllium were observed in Kideco coal (2 %) ash but retentions were as high as 12.6 % in the other fuel ashes. $BeO{\cdot}Al_2O_3$ is predicted to be present until 1300 °C. The deviation from predicted beryllium quantities was far higher in combustion at 900 °C. At this temperature nearly all the beryllium should be retained as $BeO{\cdot}Al_2O_3$. The low ash content in the fuels, particularly Kideco coal suggests that most of the beryllium may be organically bound. The two fuel blends showed retentions which concurred with theoretical values, being well within the error margins. It may therefore be concluded that synergistic effects need not be considered when regarding beryllium retention.

Vanadium

The vanadium retention profile was very similar to that of beryllium. Thermodynamic predictions indicate there should be a temperature dependence, where none is observed. At 900 °C, Vanadium should be almost completely retained in the form of $CaO{\cdot}V_2O_5(s)$ and $FeO{\cdot}V_2O_5$ in equal proportions. Again the low retention of vanadium suggests that the mode of occurrence of vanadium is in organic form. At the higher temperature results concur very well with theoretical predictions. At 1500 °C most of the vanadium will have been released as VO_2 with between 2 and 10% bound to the solid iron oxide. This was also observed empirically. The Kideco-Lemington fuel blend showed a slightly higher retention than observed by its component parts individually, after combustion at 900 °C (being 16.9% higher than expected, which is slightly higher than the error margin). Synergy was also observed in the Lemington-Allied fuel blend at 900 °C, once more retention being higher than expected, by 18.3 %.

Chromium

Chromium retention was not shown to be a function of temperature for any of the fuels except for Lemington coal, where retention was seen to be 99.1 % at 900 °C and 71.2 % at 1500 °C. This was contrary to predictions which indicated that at the lower temperature Cr would be present predominantly in the form of Cr_2O_3 (s). Around 1500 °C it was predicted that 50% of the chromium would exist in equal proportions of Cr_2O_3 and Cr_2O_3·FeO (s) whilst the remaining would be gaseous CrO_2, CrO_3 and $CrO_2(OH)$. The lower than expected chromium retention could be due to its speciation in the fuel, but also to the fact that only small quantities of chromium were initially present in the fuel. Added to the fact that the reaction time in the suspension firing reactor was small, this would reduce the probability of two chromium atoms reacting with three oxygen atoms to form the solid compound. The chromium retention in the Kideco-Lemington coal fuel mixture appears to be significantly lower than the theoretical at both 900 & 1500 °C combustion temperatures (75.8 % & 71.9 % lower respectively). This suggests that this fuel blend shows a degree of synergy with regard to chromium at both temperatures. No synergy is exhibited with respect to chromium in the Lemington-Allied fuel blend.

Zinc

Zinc retention was shown to be highly temperature dependent by thermodynamic predictions and this was bourn out in practice. The retention at 900 °C varied proportionally from 5.3 to 39.5 % for the Kideco-Lemington group of fuels and from 39.5 to 53.6 for the Lemington-Allied fuels and blends. It was predicted however that at 900 °C Zinc would be predominantly present as the solids $ZnO·Al_2O_3$ and $ZnO·SiO_2$, but as seen from the above figures this is not the case. Higher zinc volatility in similar experiments was also observed in previous studies and reviews by Kenrick et al (1992) and Pendias et al (1982) who suggest that zinc may be bound to lighter organic compounds. In the case of the Kideco-Lemington mixture the zinc retention was lower than would be expected at both

combustion temperatures, being 18.9 and 27.12 % lower for combustion at 900 & 1500 °C respectively.

Arsenic

Arsenic retention did not appear to be significantly temperature dependent, and retention varied from a low of 2.45 % for the Kideco fuel to a maximum of 17.6 % for the Lemington coal. At 900 °C a retention of 60 % was expected from thermodynamic calculations for the entire suite of coals studied, therefore retentions were determined experimentally were far lower. In others studies such as by Senior et al arsenic retention in a variety of coals was also shown to be as low as 10%. The mode of occurrence of arsenic is not extensively reported in literature, but the above results suggest that arsenic is largely bound to the organic component of the fuel. The results obtained after combustion at 1500 °C indicated higher retention than that predicted by thermodynamic calculations, with a maximum retention of 13.3 % in Lemington coal. It was predicted that at temperatures of 960 °C, and higher all arsenic is released as AsO and AsO_2(g). No synergy in terms of extra arsenic retention or volatilisation was observed.

Selenium

Selenium retention in ashes produced at 900 °C varied from a maximum 24.8 % for Lemington coal to a minimum of 6.45 % for Kideco. Thermodynamic calculations suggest that at both temperatures the favoured state of selenium SeO_2. The discrepancy between experimental results and theoretical predictions was also observed in studies by Senior (2001), Thomson (2001), and by Miller (2001), and is attributed to kinetic limitations, reaction time being insufficient for the selenium to break down from its initial mode of occurrence. Selenium retention was a function of temperature for the Lemington-Allied fuel blend only. Synergy was not observed in either of the fuel mixtures.

4.3.3 Trace Element Retention in the Chilean Ashes

The Chilean ashes produced at 1500 °C were produced at the GENER power station, Chile, having seen nominal temperatures of 1500 °C (between 1450-1750°C). The same coal was combusted to produce the 900 °C ashes in a laboratory suspension firing reactor. Analyses were carried out in the same manner as those for the CERCHAR ashes for the purposes of error determination. In order to calculate the error involved in percentage retention, the error in the original fuel and the error in the ash concentrations had to be considered. Therefore, the error in the percentage retention was calculated as the square root of the sum of the squares of the trace element concentration in the fuel and the concentration in the ash.

The purpose of conducting the analyses with these fuels was twofold. First the effect of conducting high temperature combustion experiments could be determined. Secondly, any synergistic effects of high temperature combustion could be investigated. Trace element retentions in the mixtures should be proportional to the retentions of their constituent parts. If significant deviation occurs from the theoretical value, synergy maybe be imputed. Results are therefore presented with these goals in mind. Percentage retentions of each element are given for the five fuels at the two temperatures, followed by percentage retentions of all the elements for a given fuel at the two temperatures.

Absolute values of trace element concentrations in the various fuels are shown in Appendix III. These results give an indication of the leaching availability of each particular ash and are relevant to leaching calculations made.

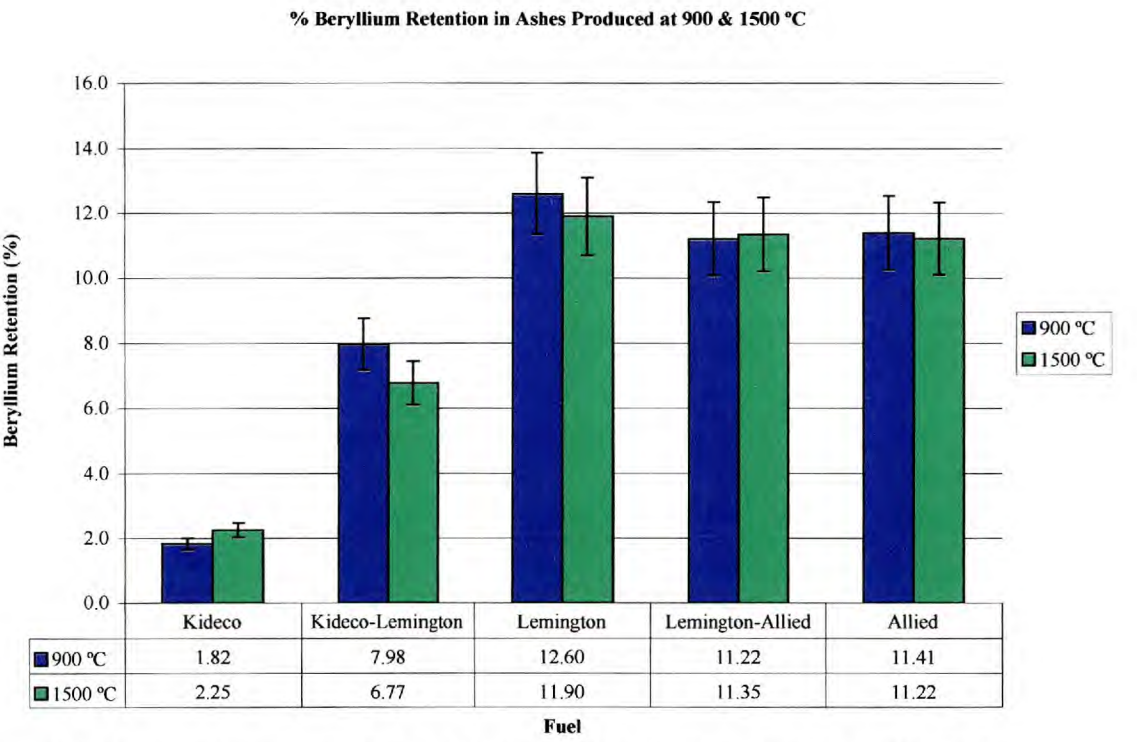


Figure 4.3.21 Beryllium Retention in Chilean Ashes Produced at 900 & 1500 °C

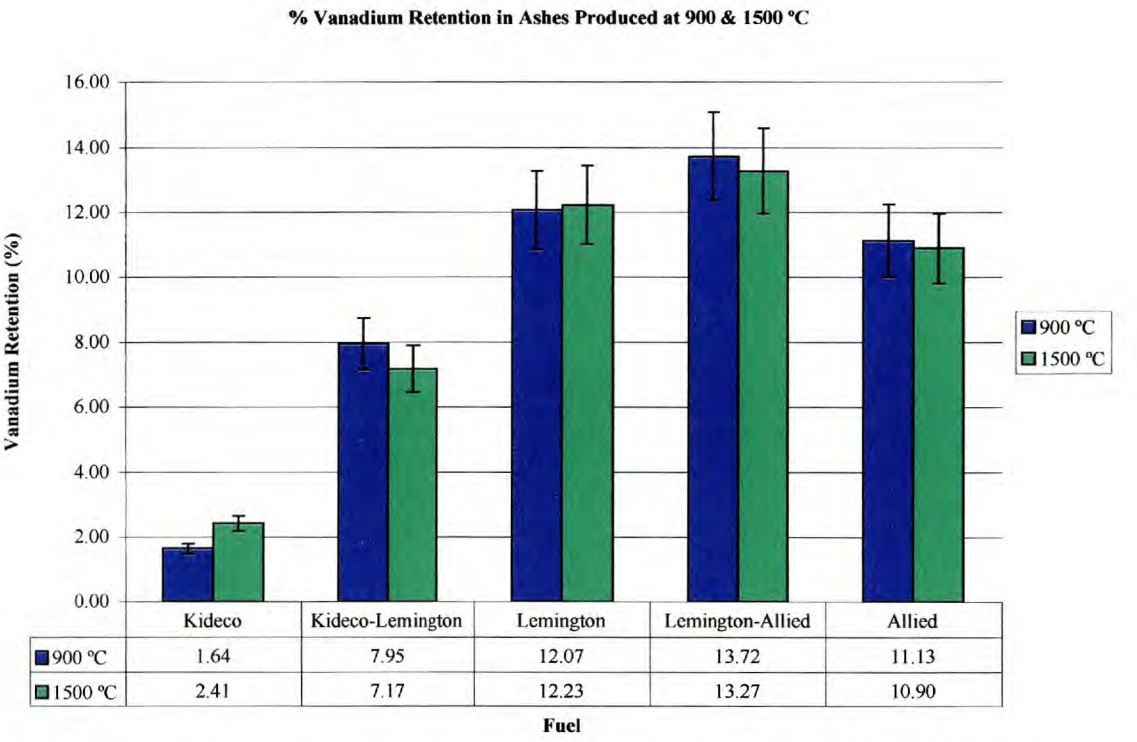


Figure 4.3.22 Vanadium Retention in Chilean Ashes Produced at 900 & 1500 °C

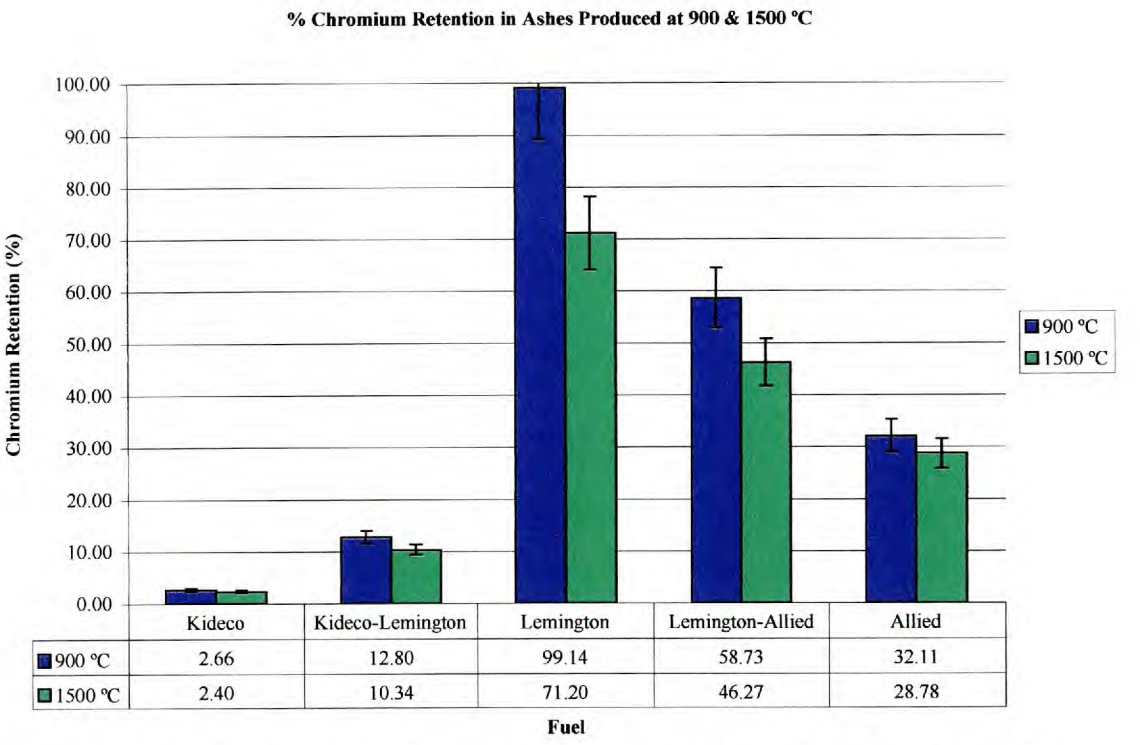


Figure 4.3.23 Chromium Retention in Chilean Ashes Produced at 900 & 1500 °C

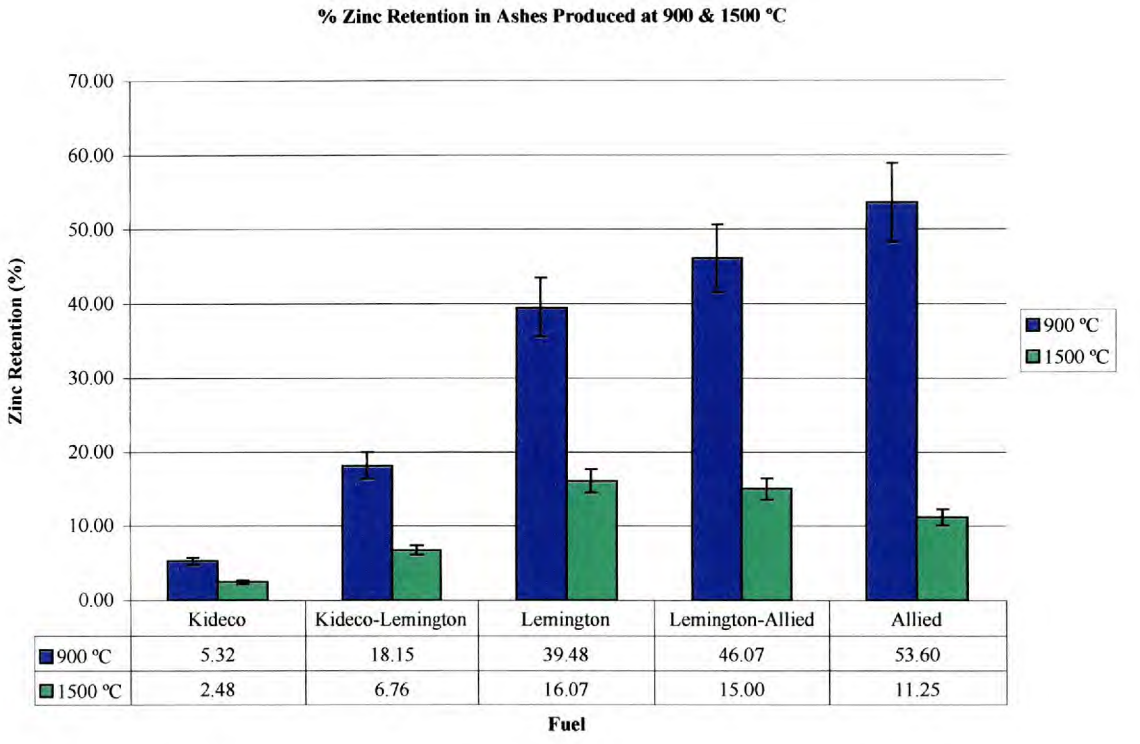


Figure 4.3.24 Zinc Retention in Chilean Ashes Produced at 900 & 1500 °C

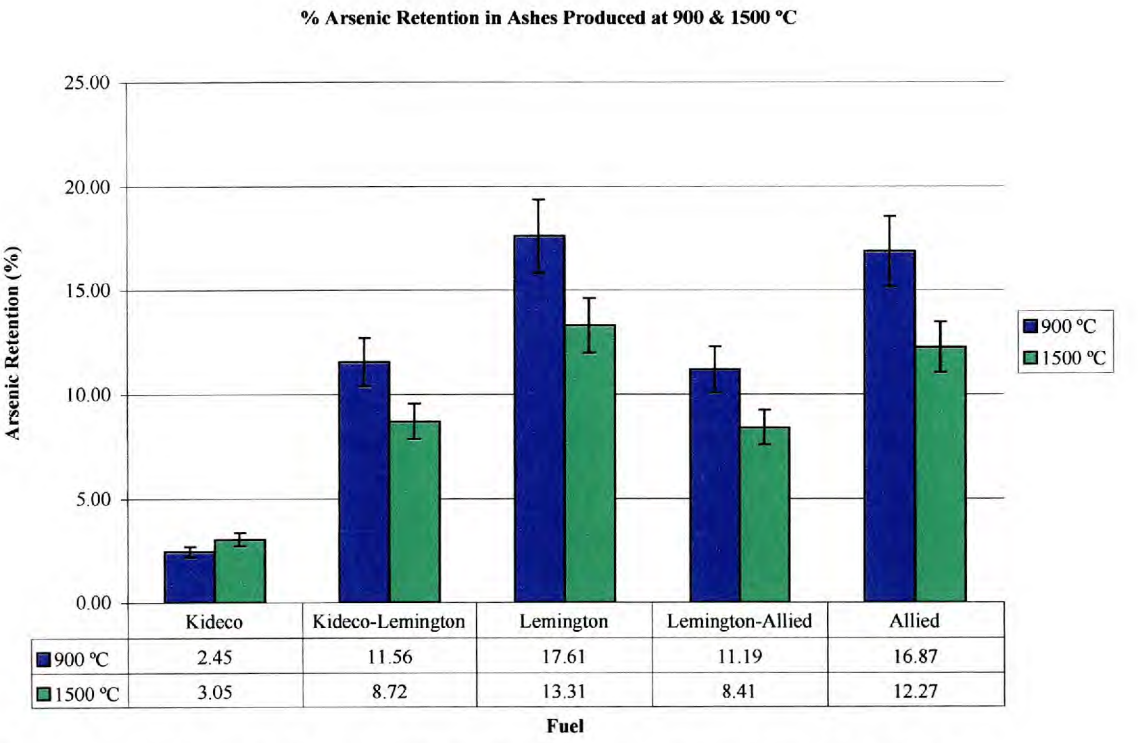


Figure 4.3.25 Arsenic Retention in Chilean Ashes Produced at 900 & 1500 °C

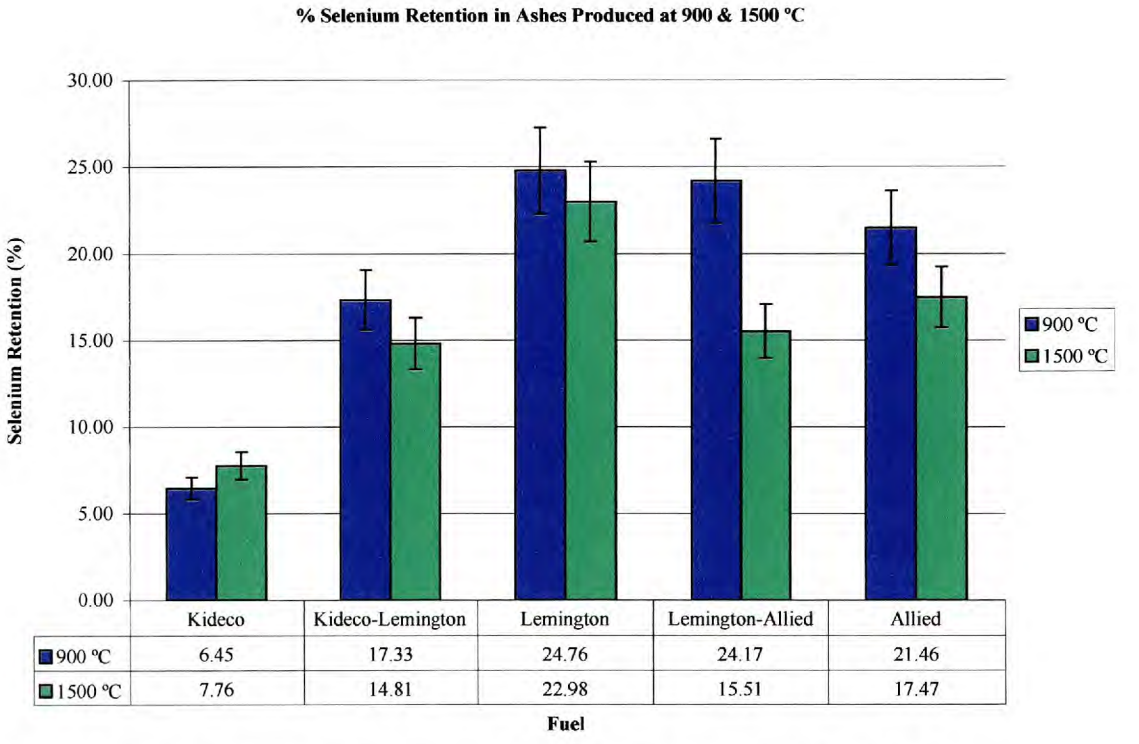


Figure 4.3.26 Selenium Retention in Chilean Ashes Produced at 900 & 1500 °C

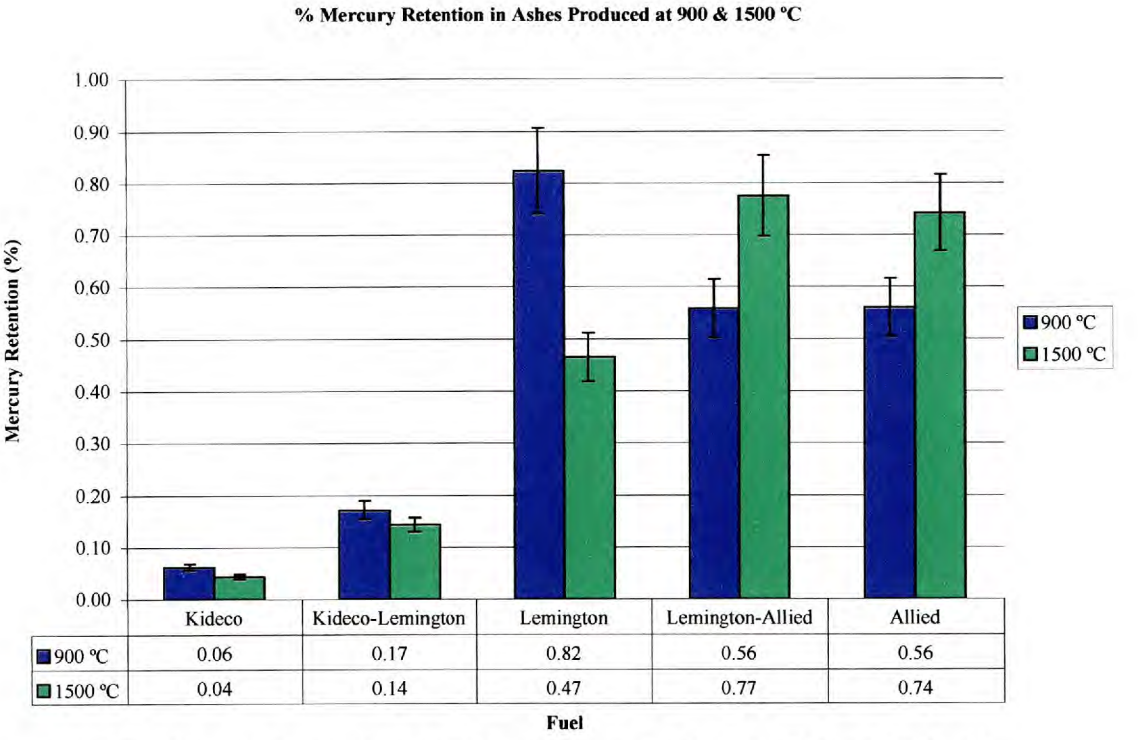


Figure 4.3.27 Mercury Retention in Chilean Ashes Produced at 900 & 1500 °C

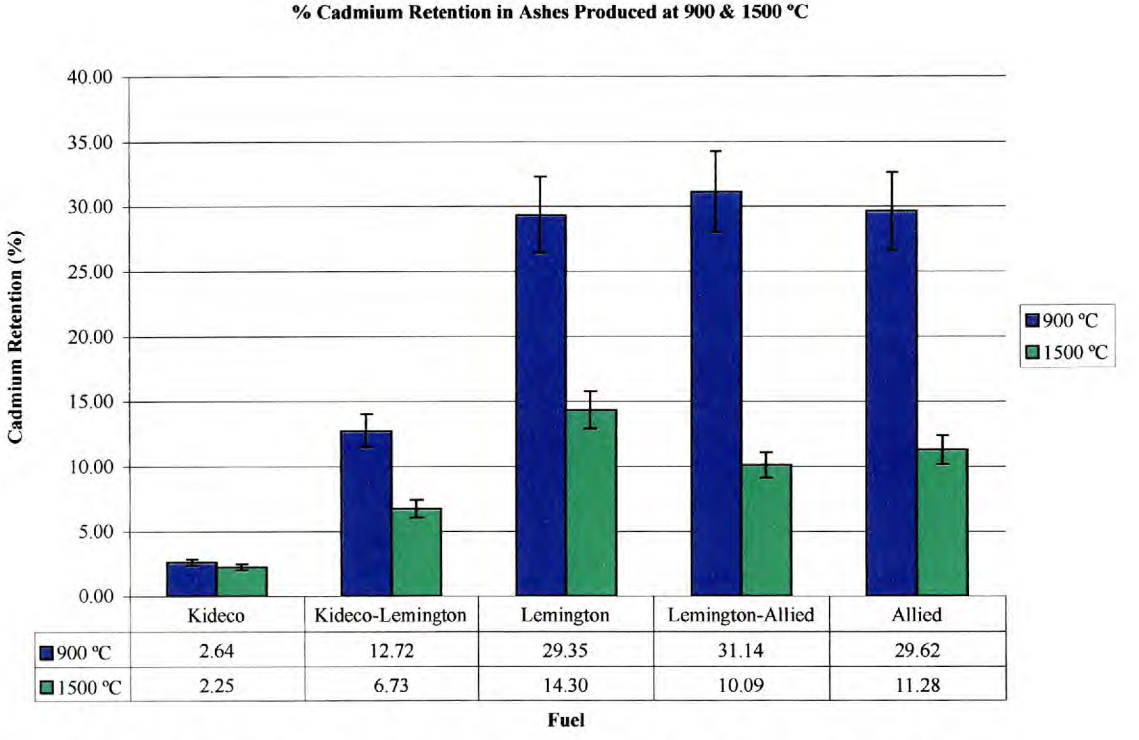


Figure 4.3.28 Cadmium Retention in Chilean Ashes Produced at 900 & 1500 °C

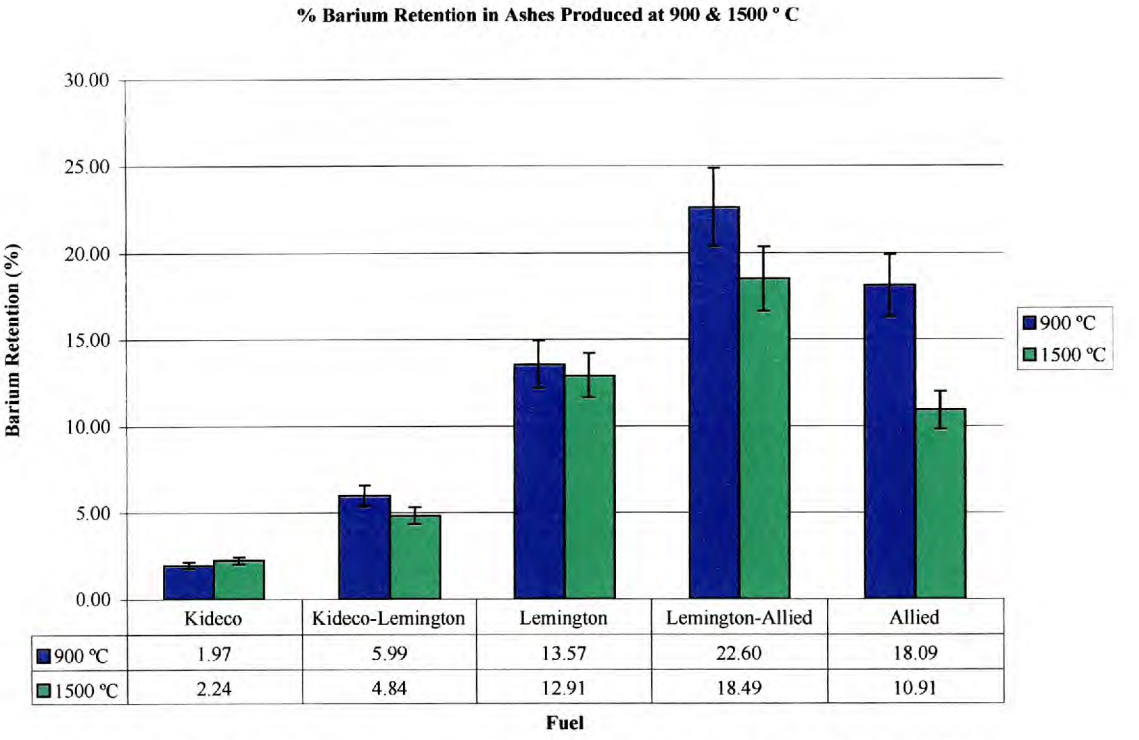


Figure 4.3.29 Barium Retention in Chilean Ashes Produced at 900 & 1500 °C

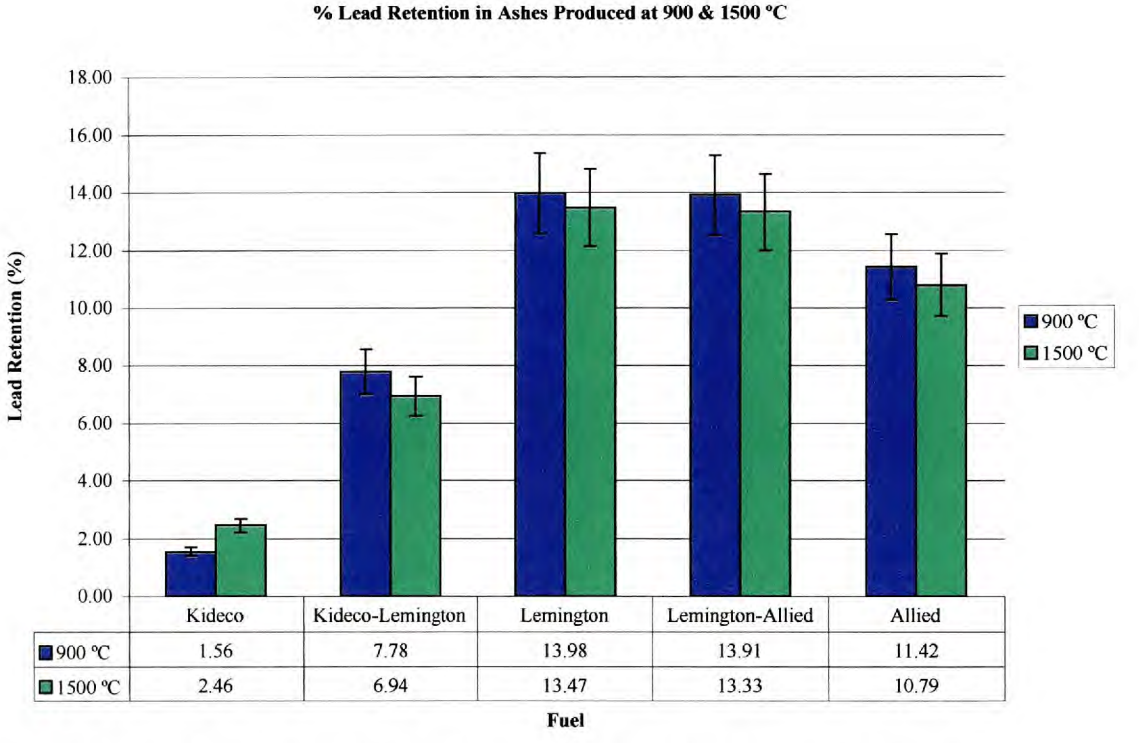
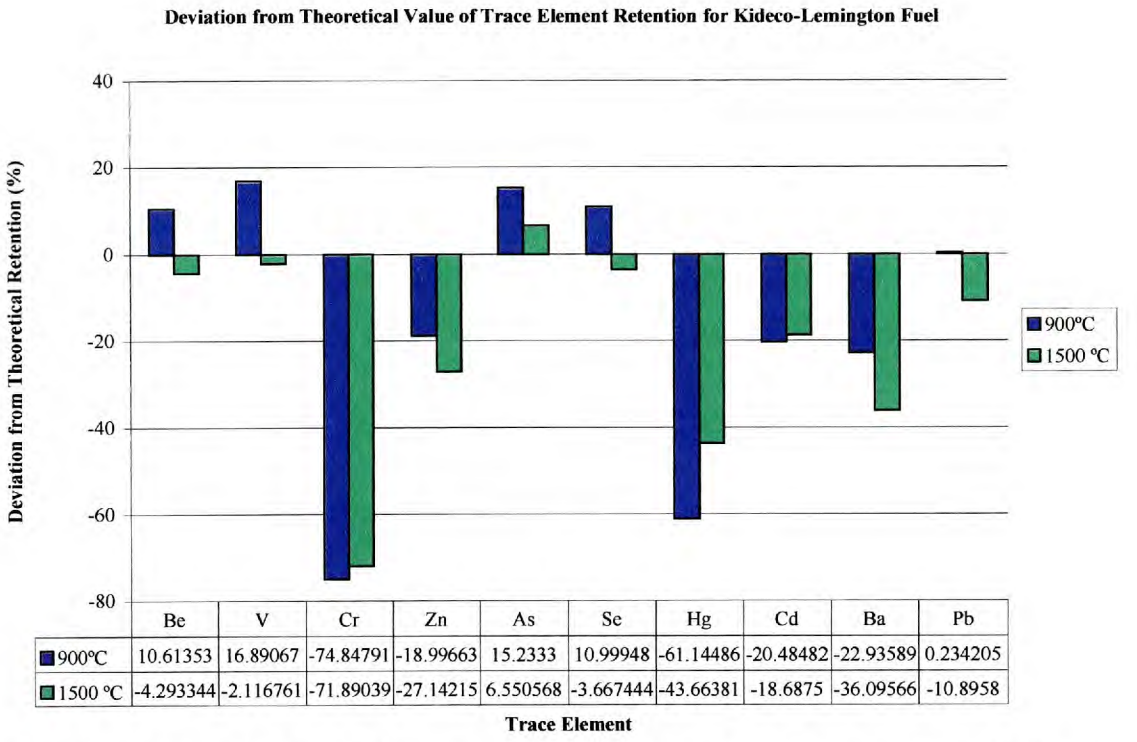
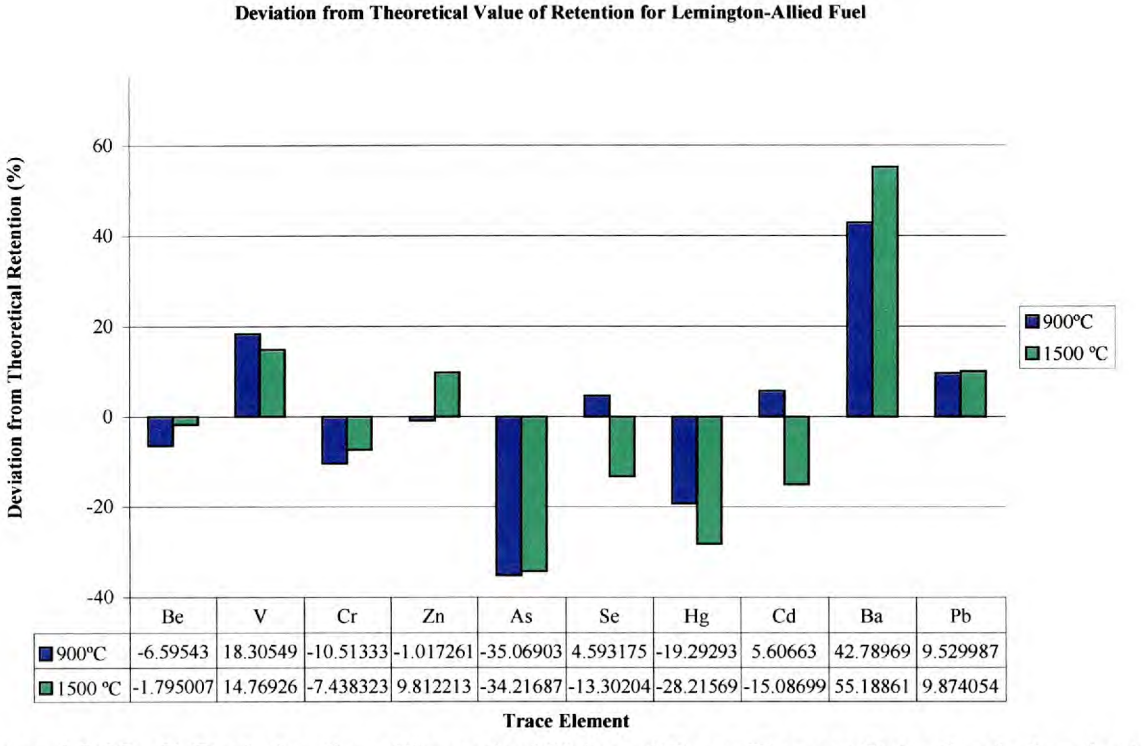


Figure 4.3.30 Lead Retention in Chilean Ashes Produced at 900 & 1500 °C



	Be	V	Cr	Zn	As	Se	Hg	Cd	Ba	Pb
900°C	10.61353	16.89067	-74.84791	-18.99663	15.2333	10.99948	-61.14486	-20.48482	-22.93589	0.234205
1500 °C	-4.293344	-2.116761	-71.89039	-27.14215	6.550568	-3.667444	-43.66381	-18.6875	-36.09566	-10.8958

Figure 4.3.31 % Deviation from Theoretical Value of Trace Element Retention in Kideco Lemington Fuel



	Be	V	Cr	Zn	As	Se	Hg	Cd	Ba	Pb
900°C	-6.59543	18.30549	-10.51333	-1.017261	-35.06903	4.593175	-19.29293	5.60663	42.78969	9.529987
1500 °C	-1.795007	14.76926	-7.438323	9.812213	-34.21687	-13.30204	-28.21569	-15.08699	55.18861	9.874054

Figure 4.3.32 % Deviation from Theoretical Value of Trace Element Retention in Lemington Allied Fuel

Beryllium

Beryllium retention showed no temperature dependence in any of the fuels, being the same at 900 °C and 1500 °C. At 1500 °C thermodynamic predictions indicated that beryllium would exist completely as the gaseous $Be(OH)_2$ compound. Small amounts of beryllium were observed in Kideco coal (2 %) ash but retentions were as high as 12.6 % in the other fuel ashes. $BeO{\cdot}Al_2O_3$ is predicted to be present until 1300 °C. The deviation from predicted beryllium quantities was far higher in combustion at 900 °C. At this temperature nearly all the beryllium should be retained as $BeO{\cdot}Al_2O_3$. The low ash content in the fuels, particularly Kideco coal suggests that most of the beryllium may be organically bound. The two fuel blends showed retentions which concurred with theoretical values, being well within the error margins. It may therefore be concluded that synergistic effects need not be considered when regarding beryllium retention.

Vanadium

The vanadium retention profile was very similar to that of beryllium. Thermodynamic predictions indicate there should be a temperature dependence, where none is observed. At 900 °C, Vanadium should be almost completely retained in the form of $CaO{\cdot}V_2O_5(s)$ and $FeO{\cdot}V_2O_5$ in equal proportions. Again the low retention of vanadium suggests that the mode of occurrence of vanadium is in organic form. At the higher temperature results concur very well with theoretical predictions. At 1500 °C most of the vanadium will have been released as VO_2 with between 2 and 10% bound to the solid iron oxide. This was also observed empirically. The Kideco-Lemington fuel blend showed a slightly higher retention than observed by its component parts individually, after combustion at 900 °C (being 16.9% higher than expected, which is slightly higher than the error margin). Synergy was also observed in the Lemington-Allied fuel blend at 900 °C, once more retention being higher than expected, by 18.3 %.

Chromium

Chromium retention was not shown to be a function of temperature for any of the fuels except for Lemington coal, where retention was seen to be 99.1 % at 900 °C and 71.2 % at 1500 °C. This was contrary to predictions which indicated that at the lower temperature Cr would be present predominantly in the form of Cr_2O_3 (s). Around 1500 °C it was predicted that 50% of the chromium would exist in equal proportions of Cr_2O_3 and Cr_2O_3·FeO (s) whilst the remaining would be gaseous CrO_2, CrO_3 and $CrO_2(OH)$. The lower than expected chromium retention could be due to its speciation in the fuel, but also to the fact that only small quantities of chromium were initially present in the fuel. Added to the fact that the reaction time in the suspension firing reactor was small, this would reduce the probability of two chromium atoms reacting with three oxygen atoms to form the solid compound. The chromium retention in the Kideco-Lemington coal fuel mixture appears to be significantly lower than the theoretical at both 900 & 1500 °C combustion temperatures (75.8 % & 71.9 % lower respectively). This suggests that this fuel blend shows a degree of synergy with regard to chromium at both temperatures. No synergy is exhibited with respect to chromium in the Lemington-Allied fuel blend.

Zinc

Zinc retention was shown to be highly temperature dependent by thermodynamic predictions and this was bourn out in practice. The retention at 900 °C varied proportionally from 5.3 to 39.5 % for the Kideco-Lemington group of fuels and from 39.5 to 53.6 for the Lemington-Allied fuels and blends. It was predicted however that at 900 °C Zinc would be predominantly present as the solids $ZnO·Al_2O_3$ and $ZnO·SiO_2$, but as seen from the above figures this is not the case. Higher zinc volatility in similar experiments was also observed in previous studies and reviews by Kenrick et al (1992) and Pendias et al (1982) who suggest that zinc may be bound to lighter organic compounds. In the case of the Kideco-Lemington mixture the zinc retention was lower than would be expected at both

combustion temperatures, being 18.9 and 27.12 % lower for combustion at 900 & 1500 °C respectively.

Arsenic

Arsenic retention did not appear to be significantly temperature dependent, and retention varied from a low of 2.45 % for the Kideco fuel to a maximum of 17.6 % for the Lemington coal. At 900 °C a retention of 60 % was expected from thermodynamic calculations for the entire suite of coals studied, therefore retentions were determined experimentally were far lower. In others studies such as by Senior et al arsenic retention in a variety of coals was also shown to be as low as 10%. The mode of occurrence of arsenic is not extensively reported in literature, but the above results suggest that arsenic is largely bound to the organic component of the fuel. The results obtained after combustion at 1500 °C indicated higher retention than that predicted by thermodynamic calculations, with a maximum retention of 13.3 % in Lemington coal. It was predicted that at temperatures of 960 °C, and higher all arsenic is released as AsO and AsO_2(g). No synergy in terms of extra arsenic retention or volatilisation was observed.

Selenium

Selenium retention in ashes produced at 900 °C varied from a maximum 24.8 % for Lemington coal to a minimum of 6.45 % for Kideco. Thermodynamic calculations suggest that at both temperatures the favoured state of selenium SeO_2. The discrepancy between experimental results and theoretical predictions was also observed in studies by Senior (2001), Thomson (2001), and by Miller (2001), and is attributed to kinetic limitations, reaction time being insufficient for the selenium to break down from its initial mode of occurrence. Selenium retention was a function of temperature for the Lemington-Allied fuel blend only. Synergy was not observed in either of the fuel mixtures.

Mercury

As predicted by thermodynamic calculations mercury was almost completely volatilised. It is predicted that the mercury volatilisation will take the form of $HgCl_2(g)$ up to temperatures of 750 °C after which formation of Hg(g) is favoured. The mercury retentions for all the fuels and blends at both combustion temperatures were shown to be less than 1 %. This coupled with the small concentrations of mercury present make deductions regarding temperature dependence and synergy less meaningful. However, mercury retention for both fuel mixtures was shown to be significantly lower than the theoretical values at both combustion temperatures. For the Kideco-Lemington fuel blend retention was lower by 61.1 % and 43.6 % for combustion at 900 °C and 1500 °C respectively. For the Lemington-Allied fuel blend retentions were less than expected by 19.2 and 28.2 % for the two combustion temperatures.

Cadmium

Cadmium as previously discussed is predicted to exist as a gaseous product at temperatures above 600 °C. Above this temperature cadmium is present in its hydroxide form up until 900 °C, where increases in temperature favour the formation of elemental cadmium. This was not observed empirically for any of the fuels except for Kideco, where cadmium was almost completely volatilised. At 900 °C, cadmium retention varied from 2 to 30%, whilst at 1500 °C the retention range was lower from 2-15%. Previous experimental studies also showed that cadmium was not completely volatilised at the temperatures in question. The disparity between theoretical and experimental results may be attributed to unknown modes of occurrence not represented in the equilibrium modelling or metal recondensation. Cadmium retention for the Lemington-Allied fuel blend was the mean of the retentions of its constituent parts. Cadmium retention was lower than expected for the Kideco-Lemington fuel blend.

Barium

Solid $BaSO_4$ was favoured to form at temperatures up to 1100 °C and barium silicates thereafter up to 1500 °C, according to thermodynamic modelling. At 900 °C therefore, barium retention was predicted to be almost complete. This was not the case for any of the Chilean fuels studied. Retentions varied from 2% for Kideco coal to 22 % for the Lemington – Allied fuel blend at 900 °C. At 1500 °C retentions varied from 2% for Kideco to 18 % for the Lemington-Allied fuel. Previous studies showed lower than predicted retentions, but only for fuels with higher organic content such as coal-wood fuel blends.

For the Kideco –Lemington blend the trace element retention for combustion at 900 & 1500 °C was lower by 22% and 36 %, respectively, than would be expected given the retentions of its constituent fuels. Conversely for the Lemington-Allied fuel blend barium retention was higher by 45 % and 55 % for combustion at 900 and 1500 °C, respectively. This indicates that synergy is relevant when considering barium retention in these fuels. As Lemington is the common fuel in these blends it may be inferred that the addition of Kideco and Allied fuels are the contributing factors, the former's properties contributing to lower barium retention and the latter's higher.

Lead

For the fuels in this study, 80-90% of lead was predicted by thermodynamic calculations to be volatilised at 900 °C. This was indeed the case for the fuels except Kideco where 98% volatilisation was observed. For the coals studied lead was predicted to exist in the solid sulphate form till 850 °C after which some $PbTiO_3$ (s) was predicted to form along with 80 –90% PbO(g). Above 1000 °C no solid lead compounds were favoured, with small quantities of elemental lead predicted to form after 1100 °C. The experimental results for ashes produced at 1500 °C show retentions which were surprisingly high at around 13%. However lead in the solid phase at these temperatures has also been found in previous

studies (Finkelman (1994)). Lead was shown to be predominantly inorganically bound in coals.

The retentions for all fuels were the same, within the bounds of error, at both combustion temperatures. Retentions were low at both the higher and lower temperature therefore lead retention was not shown to be temperature dependent. The lead retention in the fuel mixtures was as predicted from the mean of its constituent fuels, therefore synergistic effects need not be considered in this instance.

4.4 Trace Element Content In Leachates

The results presented in this section give the trace element content in leachates produced from ashes of the CERCHAR and Chilean fuels. Leaching was carried out using the TCLP method, modified for small sample masses. Results are presented firstly as percentage retentions and then as absolute concentrations. Percentage retentions indicate the propensity of a particular element to leach from ash, whilst absolute concentrations in the leachate are discussed in the context of regulatory limits.

4.4.1 Leaching Modelling

In order to model the leaching process undertaken in this study the experimental values for the elemental content of the ash in each sample were used as input values. The final pH of the leachate was measured in experiments and, due to the type of leaching test employed, was assumed to be the equilibrium pH. It was therefore specified as fixed for modelling purposes. Simulations were also carried out without a fixed input value for pH in order to compare the computed theoretical equilibrium pH with that obtained in experiments. The pH for CERCHAR ashes produced at 850 °C and those produced at 950 °C was the same ± 0.05. The pH for these ashes produced in the different reactor configurations was more significant. The results are shown in Tables 4.4.1 and 4.4.2 for the CERCHAR and Chilean Fuels. The pH of the initial extraction fluid was 2.88 ± 0.05.

pH	Fuel 1	Fuel 2	Fuel 3	Fuel 4	Fuel 5	Fuel 6	Fuel 7	Fuel 8
Experimental MF	4.18	4.18	4.3	4.62	4.85	4.9	4.87	4.53
Experimental HR	4.88	4.88	4.67	4.93	5.95	6.25	6.84	5.81
Computed	3.93	3.93	3.92	4.12	4.13	4.17	4.09	4.01

Table 4.4.1 Theoretical and computed system pH for the CERCHAR fuels.

pH	Kideco	Kideco-Lemington	Lemington	Lemington -Allied	Allied
Experimental 900 °C	4.97	5.01	5.1	4.98	4.82
Experimental 1500 °C	5.57	6.03	6.12	5.88	5.72
Computed	4.85	4.92	4.98	4.74	4.67

Table 4.4.2 Theoretical and computed system pH for the Chilean fuels

The discussion below for the CERCHAR fuels contains graphs that show how the leaching propensity of the elements varied with pH. The trends shown were similar for both the muffle furnace and hot-rod reactor ashes and are therefore only depicted for the muffle furnace ashes. Diagrams depicting pH are also shown for the Chilean fuels at 900 and 1500 °C.

The method used to compute activity coefficients used the Davies equation as described in section 2.5. Where empirically determined trace element contents in the ash varied significantly from those predicted by MTDATA a separate MINTEQA2 simulation was carried out using these theoretical trace element contents.

Modelling the sorption reactions occurring in the leachate system introduced the greatest uncertainty in the modelling process due to the lack of comprehensive and reliable sorption reactions and data available in literature. The adsorption model specified to compute sorption was the Diffuse Layer model. MINTEQA2 incorporates two databases containing sorption data. These were derived from studies by Dzombak & Morrel 1990[67] for a sorption site of hydrous ferric oxide and Mathur (1995)[84] for sorption on Geothite. Another source of uncertainty was the surface layer of the ash. As an approximation, it was assumed that hydrous ferric oxide was the predominant component on the sample surfaces. The data derived for hydrous ferric oxide were therefore used in this study.

Appendix IV illustrates a typical MINTEQA2 output file. Out put data pertinent to this study were the percentage a particular trace element sorbed, dissolved or precipitated, the speciation of the this element in solution, and the equilibrium pH.

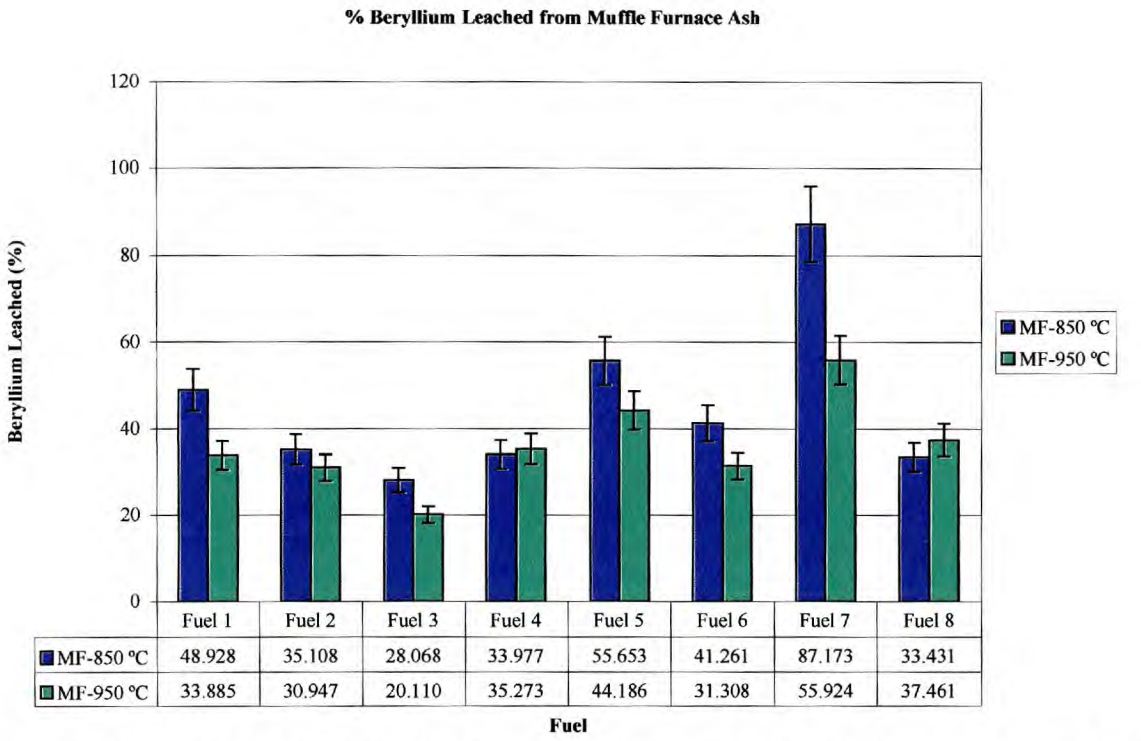
4.4.2 Trace Element Content in Leachate Produced from CERCHAR Ashes

The experiments were carried out as described in Section 3.3. In order to measure the trace element concentration in the leachate each experiment was conducted seven times. The student t-distribution was then used, with a 95 % confidence interval, in order to calculate the error involved in these concentration measurements. The experimental error was then converted to a percentage and rounded up to the nearest five %. In the majority of instances the error was below 5% indicating consistent experimental method and homogeneity of sample. Specific values for the percentage errors calculated for the CERCHAR ashes are discussed below.

The errors involved in percentage leached took into account the errors in measuring the trace element content in the ash and the error calculated for the leachate measurements. The final error obtained for the percentage retention was the square root of the sum of the squares of the errors in the leachates and ashes.

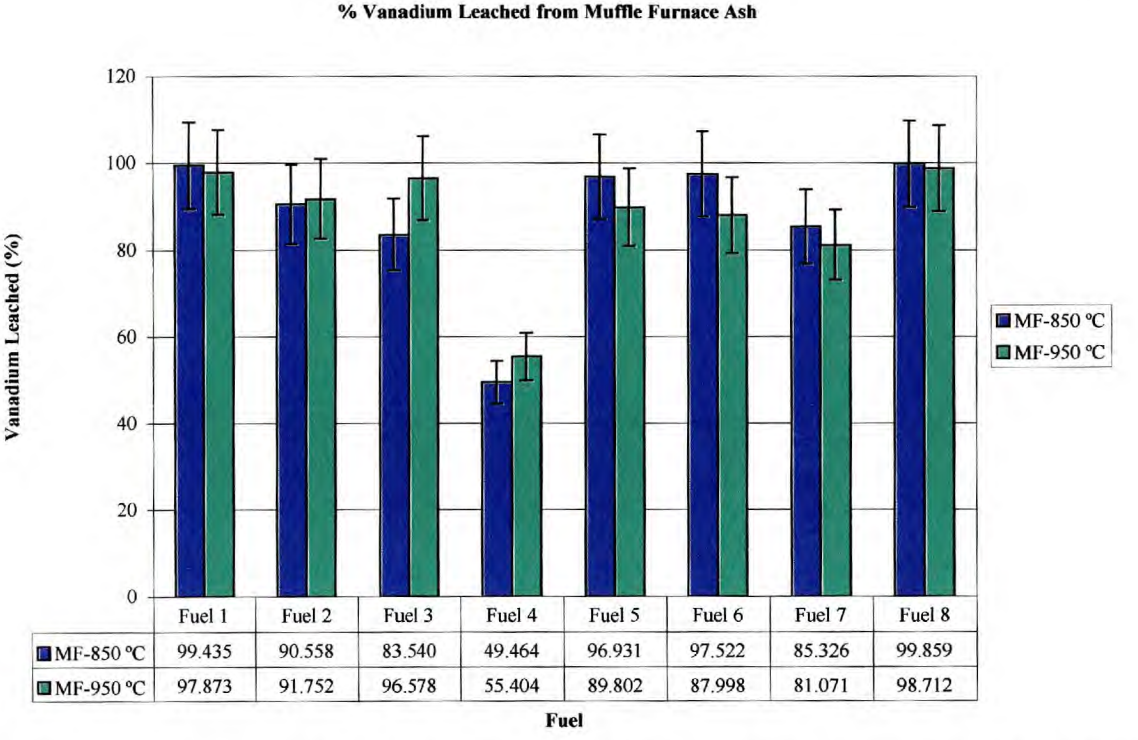
Results are presented firstly by percent trace element leached at a particular reactor configuration and two temperatures e.g. % beryllium leached for all the CERCHAR ashes produced in the muffle furnace at 850 and 950 °C. Concentrations are then presented in the same format. For a particular fuel combusted in the muffle furnace and the hot-rod reactor, the bulk composition (primary elements) of the resulting ash is the same. Therefore when modelling the system for a particular fuel, only the quantity of trace elements was changed when computing separate runs for the hot-rod and muffle furnace. The variation of concentration with pH was the same for a particular element from a hot-rod run and for the muffle furnace. Therefore pH-concentration diagrams are only given for the muffle furnace results and reference to them made in the hot-rod results.

4.4.2.1 Trace Element Content in Leachate from CERCHAR Ash produced in Muffle



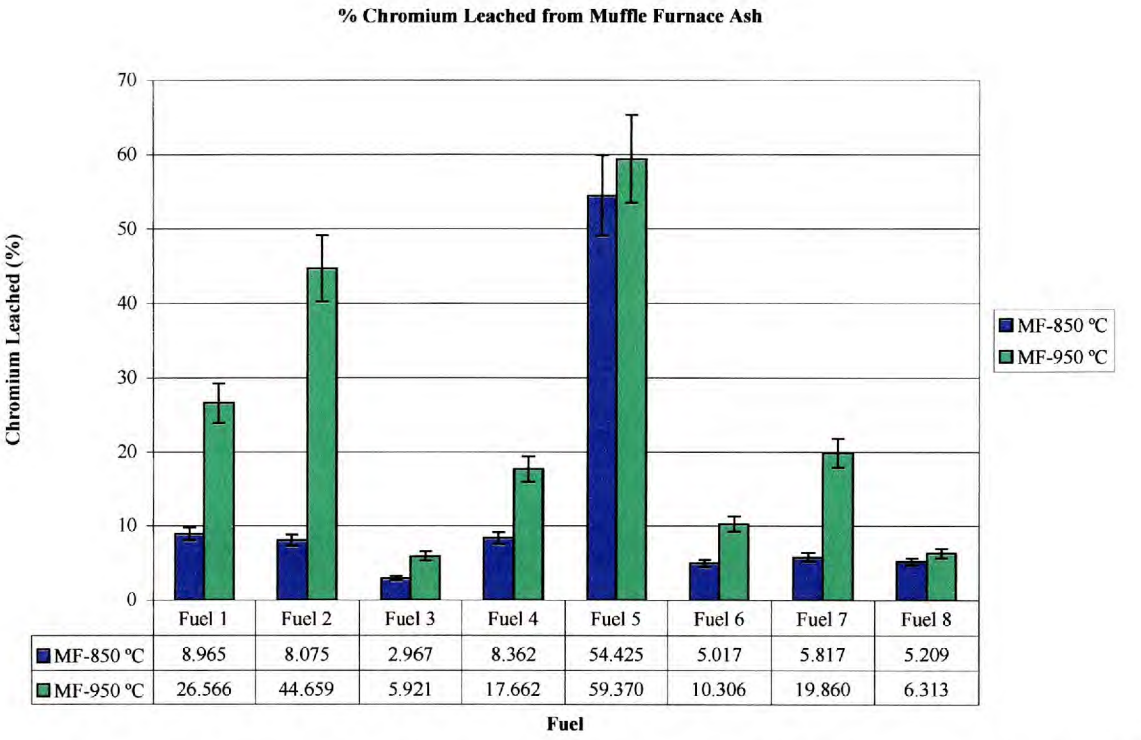
	Fuel 1	Fuel 2	Fuel 3	Fuel 4	Fuel 5	Fuel 6	Fuel 7	Fuel 8
MF-850 °C	48.928	35.108	28.068	33.977	55.653	41.261	87.173	33.431
MF-950 °C	33.885	30.947	20.110	35.273	44.186	31.308	55.924	37.461

Figure 4.4.1 % Beryllium Leached from Ash Produced in Muffle Furnace at 850 & 950 °C



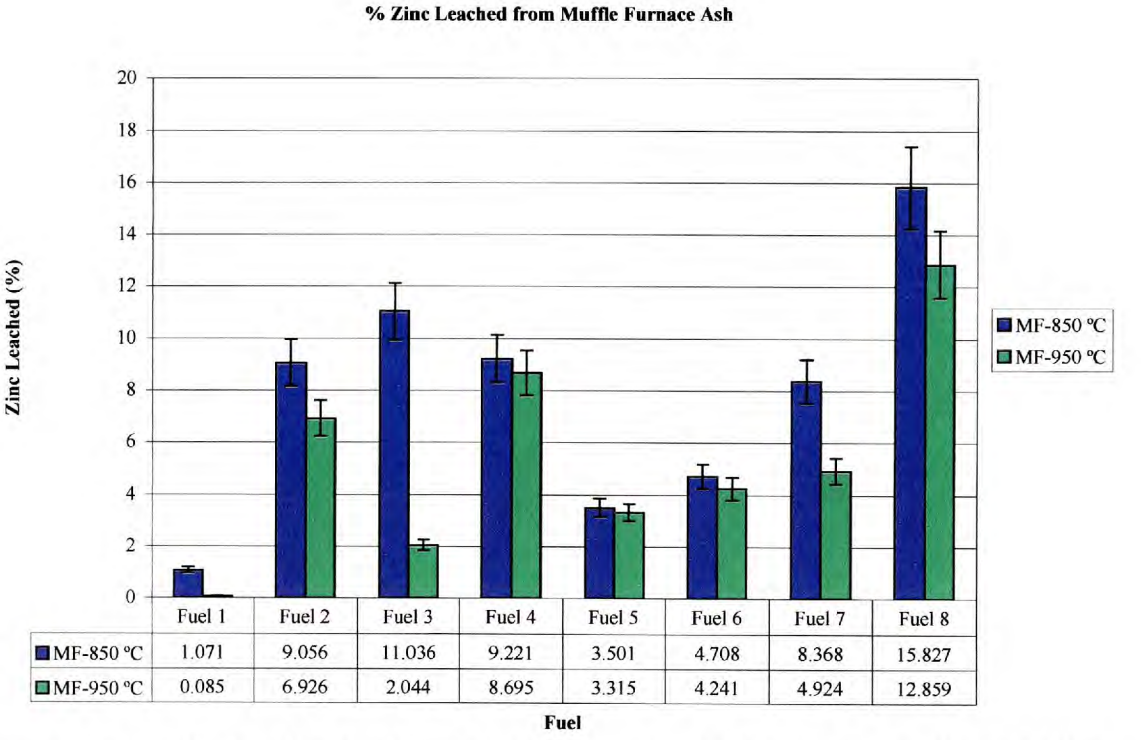
	Fuel 1	Fuel 2	Fuel 3	Fuel 4	Fuel 5	Fuel 6	Fuel 7	Fuel 8
MF-850 °C	99.435	90.558	83.540	49.464	96.931	97.522	85.326	99.859
MF-950 °C	97.873	91.752	96.578	55.404	89.802	87.998	81.071	98.712

Figure 4.4.2 % Vanadium Leached from Ash Produced in Muffle Furnace at 850 & 950 °C



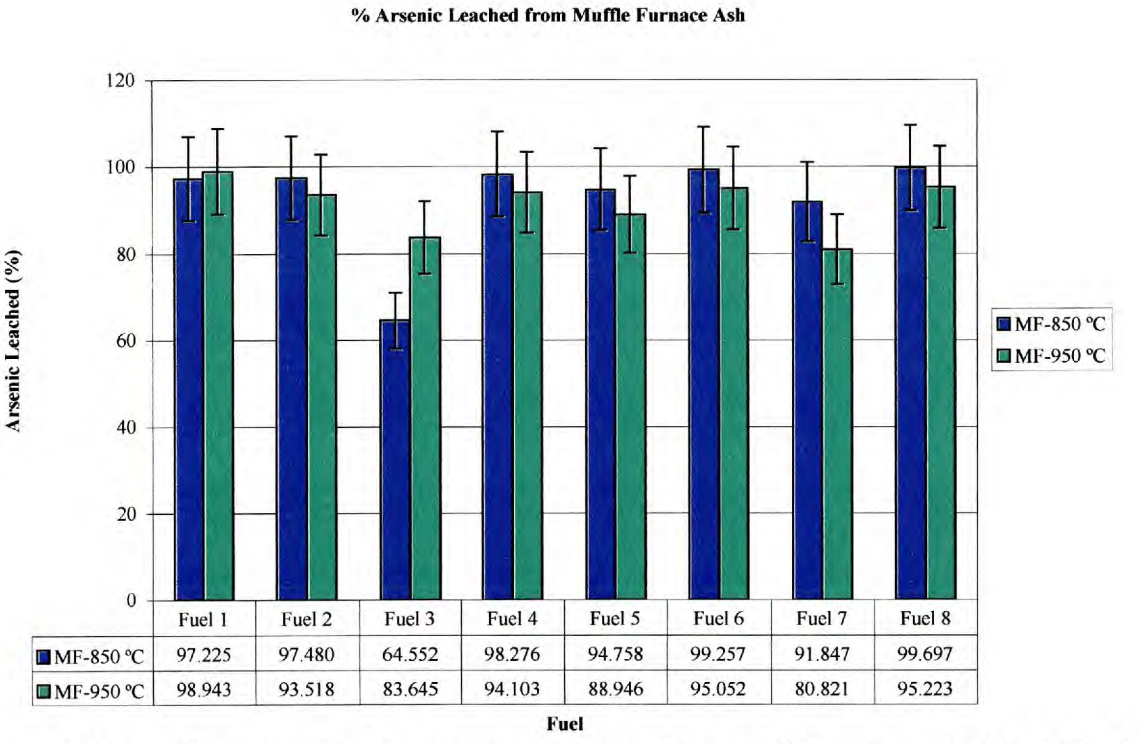
	Fuel 1	Fuel 2	Fuel 3	Fuel 4	Fuel 5	Fuel 6	Fuel 7	Fuel 8
MF-850 °C	8.965	8.075	2.967	8.362	54.425	5.017	5.817	5.209
MF-950 °C	26.566	44.659	5.921	17.662	59.370	10.306	19.860	6.313

Figure 4.4.3 % Chromium Leached from Ash Produced in Muffle Furnace at 850 & 950 °C



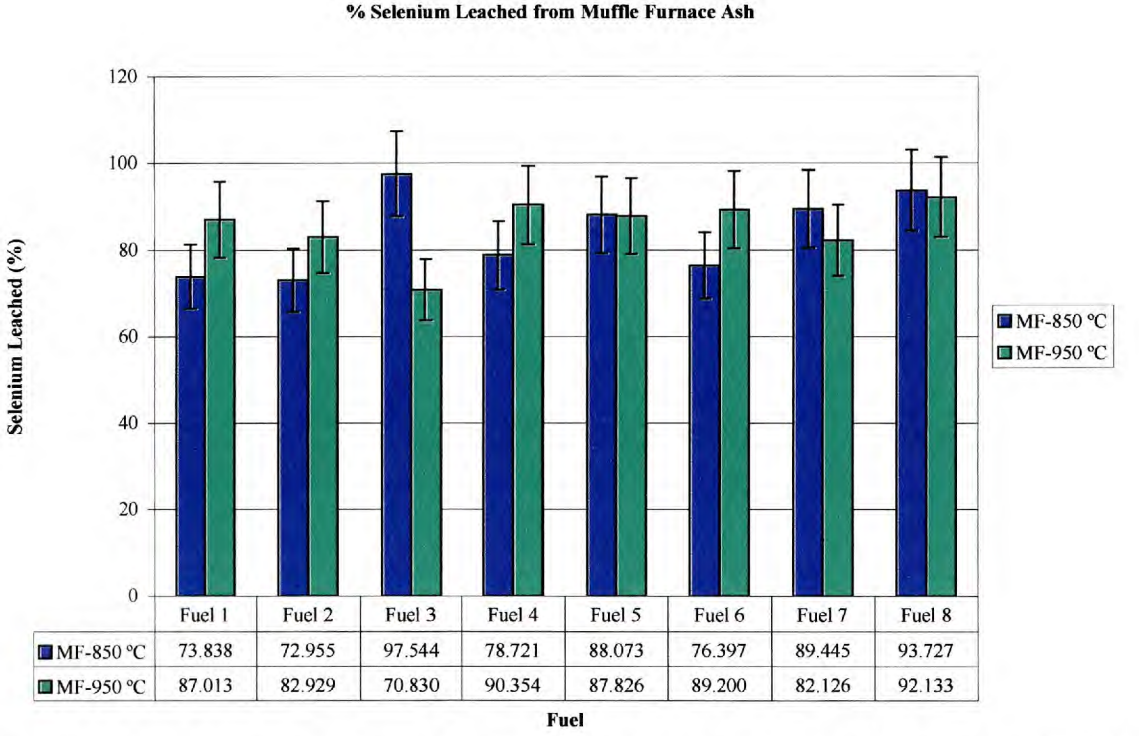
	Fuel 1	Fuel 2	Fuel 3	Fuel 4	Fuel 5	Fuel 6	Fuel 7	Fuel 8
MF-850 °C	1.071	9.056	11.036	9.221	3.501	4.708	8.368	15.827
MF-950 °C	0.085	6.926	2.044	8.695	3.315	4.241	4.924	12.859

Figure 4.4.4 % Zinc Leached from Ash Produced in Muffle Furnace at 850 & 950 °C



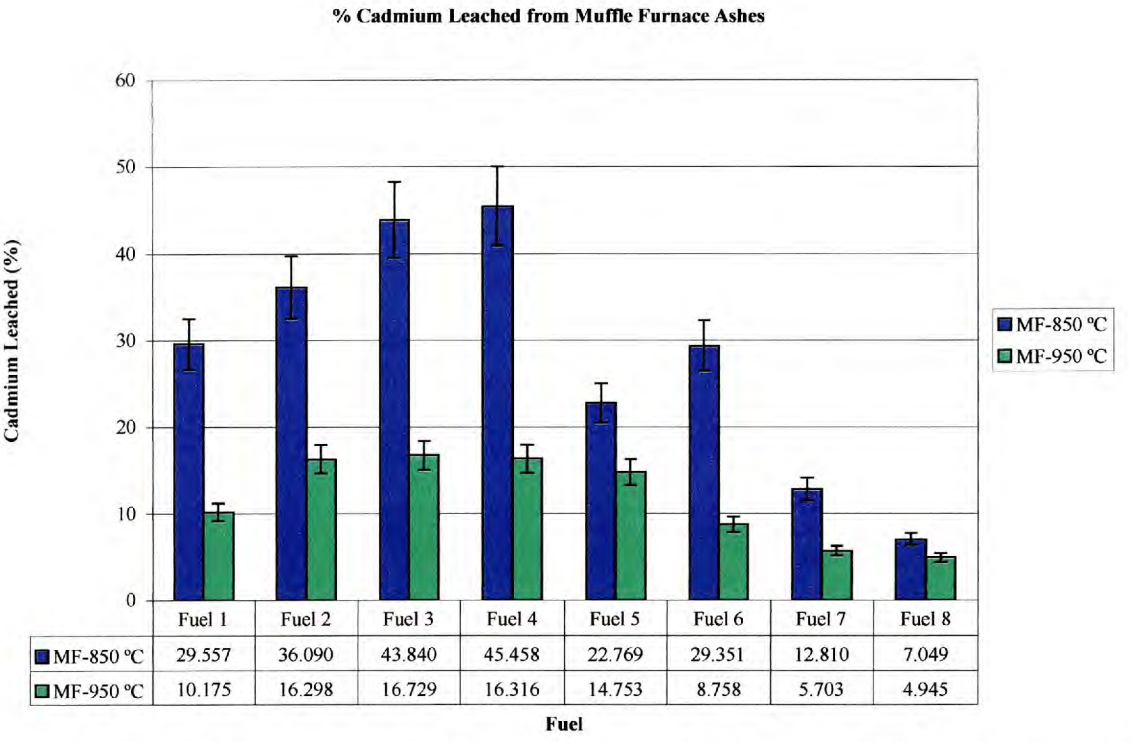
	Fuel 1	Fuel 2	Fuel 3	Fuel 4	Fuel 5	Fuel 6	Fuel 7	Fuel 8
MF-850 °C	97.225	97.480	64.552	98.276	94.758	99.257	91.847	99.697
MF-950 °C	98.943	93.518	83.645	94.103	88.946	95.052	80.821	95.223

Figure 4.4.5 % Arsenic Leached from Ash Produced in Muffle Furnace at 850 & 950 °C



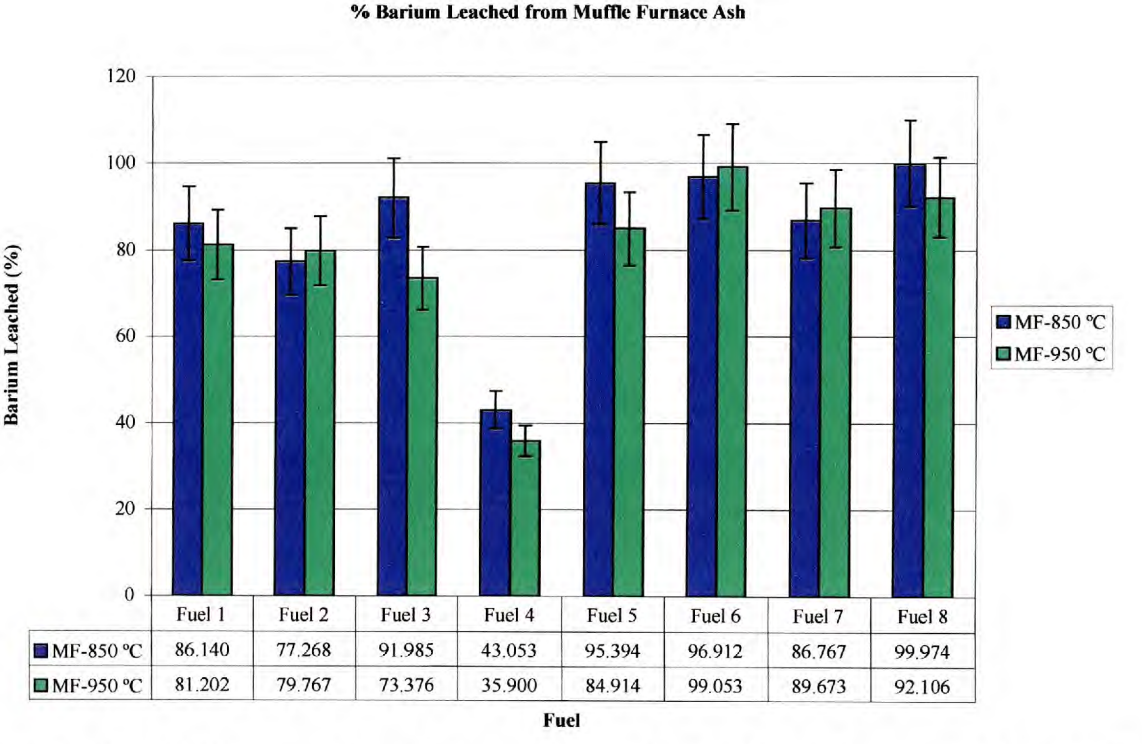
	Fuel 1	Fuel 2	Fuel 3	Fuel 4	Fuel 5	Fuel 6	Fuel 7	Fuel 8
MF-850 °C	73.838	72.955	97.544	78.721	88.073	76.397	89.445	93.727
MF-950 °C	87.013	82.929	70.830	90.354	87.826	89.200	82.126	92.133

Figure 4.4.6 % Selenium Leached from Ash Produced in Muffle Furnace at 850 & 950 °C



	Fuel 1	Fuel 2	Fuel 3	Fuel 4	Fuel 5	Fuel 6	Fuel 7	Fuel 8
MF-850 °C	29.557	36.090	43.840	45.458	22.769	29.351	12.810	7.049
MF-950 °C	10.175	16.298	16.729	16.316	14.753	8.758	5.703	4.945

Figure 4.4.7 % Cadmium Leached from Ash Produced in Muffle Furnace at 850 & 950 °C



	Fuel 1	Fuel 2	Fuel 3	Fuel 4	Fuel 5	Fuel 6	Fuel 7	Fuel 8
MF-850 °C	86.140	77.268	91.985	43.053	95.394	96.912	86.767	99.974
MF-950 °C	81.202	79.767	73.376	35.900	84.914	99.053	89.673	92.106

Figure 4.4.8 % Barium Leached from Ash Produced in Muffle Furnace at 850 & 950 °C

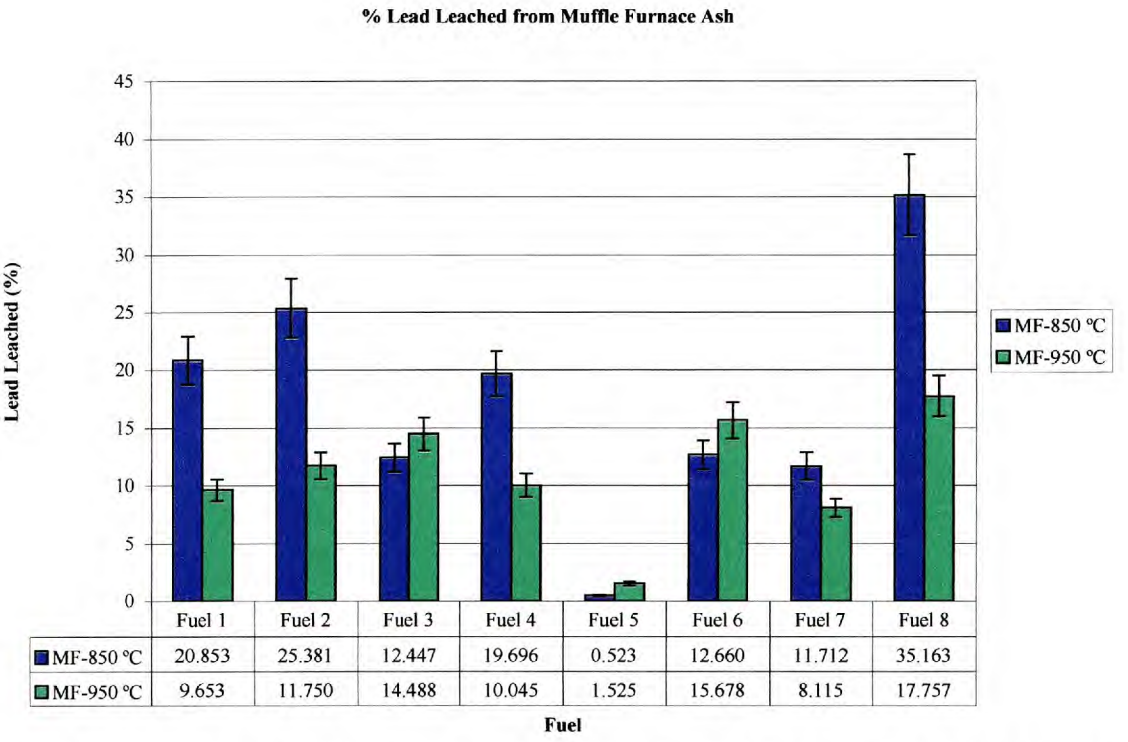


Figure 4.4.9 % Lead Leached from Ash Produced in Muffle Furnace at 850 & 950 °C

Beryllium in Leachate

The quantity of beryllium leached from muffle furnace ashes was in the region of 20-50% of the original amount present in the ash. Beryllium leached from ashes produced at 950 °C did not appear to vary significantly from that of ashes produced at 850 °C for Fuels 2, 4 and 8, but a slight temperature dependence did seem significant for the remaining fuels. The leaching propensity decreased with increasing temperature. There was no temperature dependence in the trace element content in the ashes. This implies that at 950 °C beryllium is bound to the ash matrix in such a way as to hinder leaching.

Modelling predicted that beryllium would be nearly 100% leached, with no precipitation and no sorption when the system was allowed to calculate the equilibrium pH. It was predicted, in this instance, that beryllium existed as the species Be^{2+}, $BeOH^{+}$, $BeSO_4$ and beryllium acetate for all the fuels studied in varying proportions. The predominant species for all fuels and temperatures were Be^{2+} and beryllium acetate, with the other species being present in quantities between two and five percent, for the eight fuels. The difference between computed and experimental values for beryllium leached reflected the difference between computed and experimental pH. The figure below shows a pH-concentration profile for beryllium, calculated by the model.

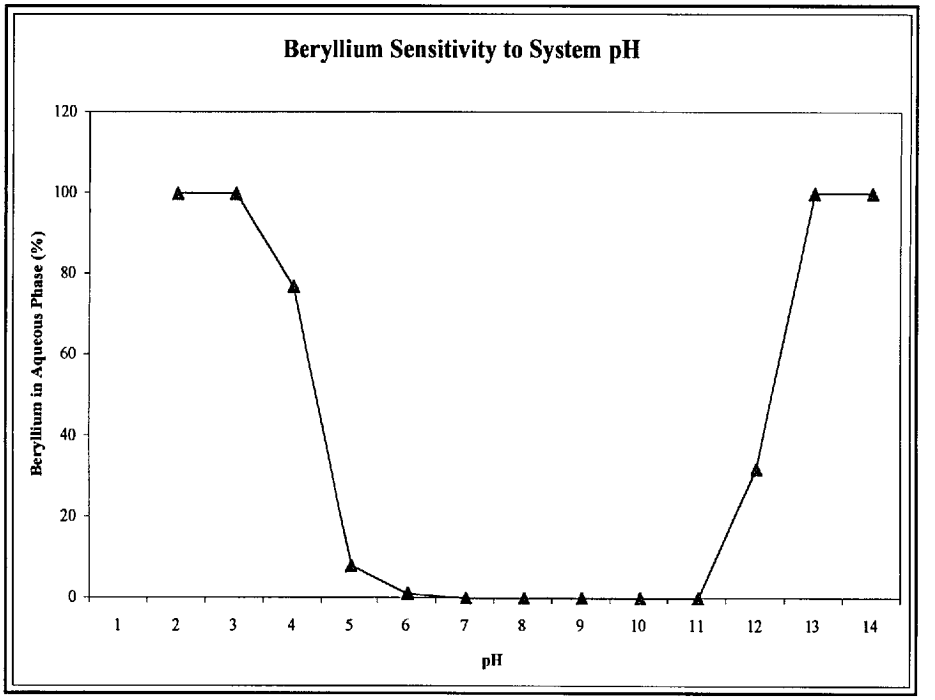


Figure 4.4.10 Beryllium Leached as a Function of System pH

It may be seen from Figure 4.4.10 that at a pH of between 3 and 4 over 80% of beryllium present is expected to leach. The beryllium leached is a function of a steep pH gradient in this range. The experimental pH varied between 4.2 and 5 and the beryllium leached in this range more accurately represents the empirical findings.

Vanadium in Leachate

Vanadium was shown to be greatly susceptible to leaching under the conditions studied. All the fuels showed more than 80% of vanadium would be leached except for an anomalous Fuel 4 where it was unclear why the leaching was in the region of 50-60%. None of the fuels exhibited temperature dependence for vanadium leaching.

Modelling predicted that at the equilibrium pH calculated (a range of 3-4 for all the fuels) over 98% of vanadium would exist in solution. At this pH range vanadium would typically exist in solution in species $H_3V_2O_7^-$, H_3VO_4 (aq), $H_2VO_4^-$, and VO_2^+, in varying proportions. The former two species were the dominant species with minor quantities of $H_2VO_4^-$, and VO_2^+. This was the case up to a pH of 4.8 which was the maximum pH determined experimentally for the 8 fuels. After this system pH the vanadium concentration in solution is predicted to drop rapidly with increasing pH as shown in Figure 4.4.11 below.

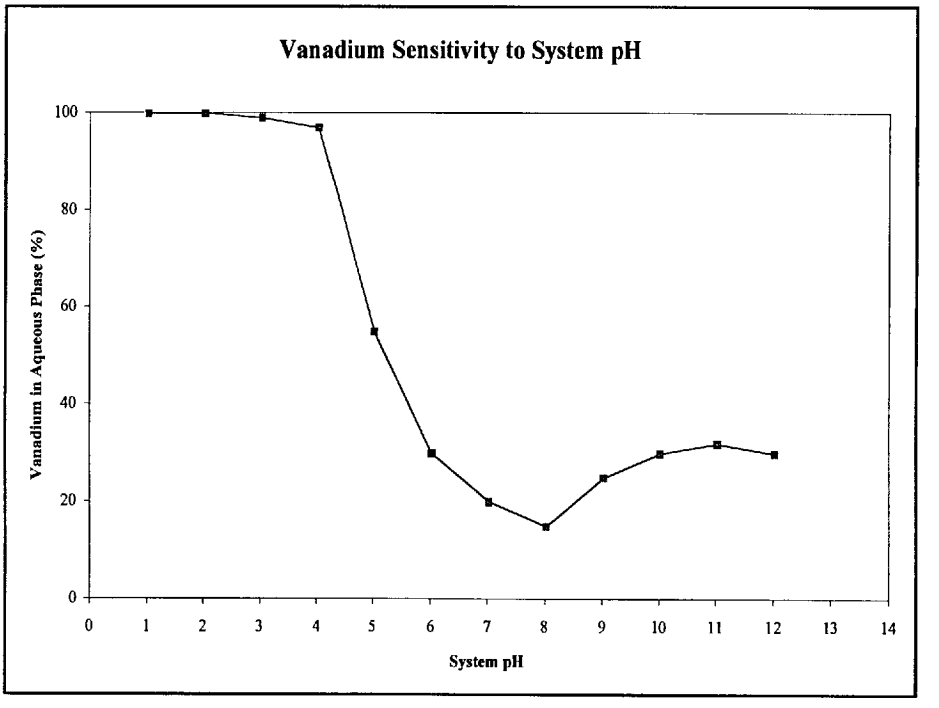


Figure 4.4.11 Vanadium Leached as a Function of System pH

Chromium in Leachate

The chromium leaching profile showed characteristics which differed from the other trace elements. The quantity of chromium leached was between 2.9 and 8.3 % for ashes produced at 850 °C, and with the exception of Fuel 5 where 54.4% of the chromium leached. With an increase in ash production temperature the quantity of chromium leached also increased in all fuels, again with the exception of Fuel 5. The increase in chromium leaching may be due to the fact that in the muffle furnace chromium is released at the higher temperature but not carried away.

Modelling predicted that chromium would be leached in higher quantities than determined experimentally at the equilibrium pH calculated by MINTEQA2. Modelling predicted that between a pH of 3 & 4 chromium leaching would occur in the range of 75-35%. When the runs were carried out specifying the pH to be that determined experimentally i.e. a pH range of 4.19 to 4.9 leaching was expected to occur at approximately 35%. In the leachate solution at a pH of approximately 4, chromium was expected to exist as predominantly $HCrO_4^-$, with other species such as CrO_4^{2-} making up the remaining 1%. No chromium was predicted to precipitate and sorbed species would be present as $=FeCrO_4^-$ and $=FeOHCrO_4^{2-}$. The Figure 4.4.12 below shows a typical curve for chromium dissolved in leachate as a function of pH.

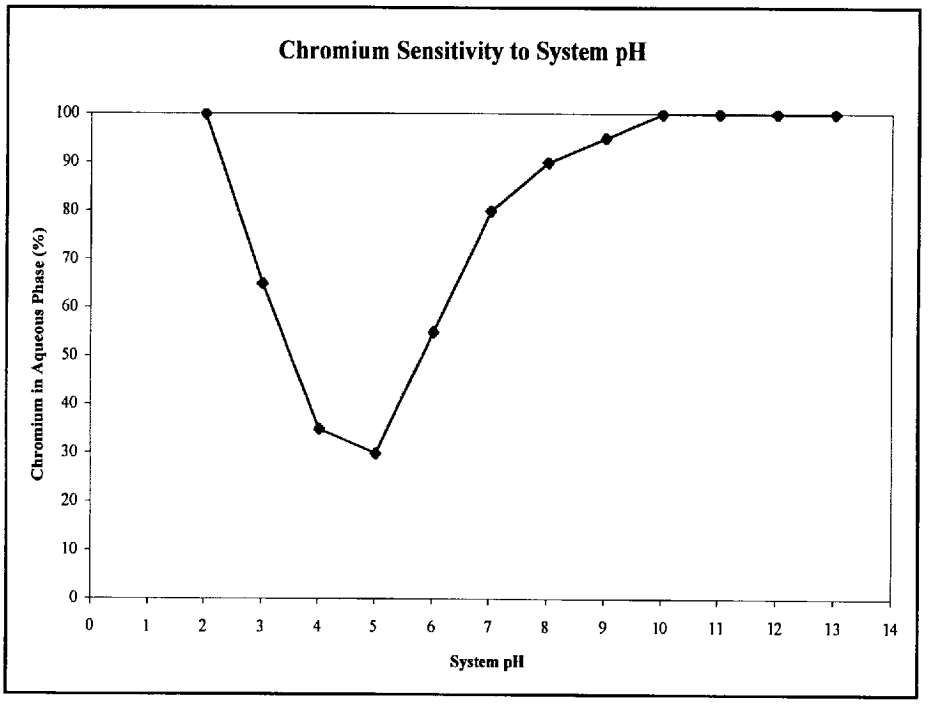


Figure 4.4.12 Chromium Leached as a Function of System pH

Zinc in Leachate

Zinc present in muffle furnace ashes was found to be strongly retained after leaching experiments, with a maximum of 15% zinc leached for Fuel 8 ash produced at 850 °C. Leaching was found to be dependent upon temperature for all fuels except Fuel 4, 5 and 6. For ash produced at 950 °C leaching ranged from 0.01 – 12.8 %. The decreased leaching propensity in this instance may be due to the fact that there was slightly less zinc in the ash obtained at 950 °C. There is therefore less zinc available for leaching and at the higher temperature zinc which has not been released due to combustion may be more strongly bound to its host material.

Modelling quite accurately predicted that most of the zinc would be retained in the ash, at both temperatures. At the pH range of 3-4 predicted as the equilibrium pH through modelling runs, zinc was predicted to leach from 100% a pH of 3 to 10% at a pH of 4. In this instance the zinc would be present in solution as a variety of species. The predominant species would be zinc acetates (in the region of 60%) whilst Zn^{2+}, and $ZnSO^4(aq)$ would make up the remainder. At the pH range obtained experimentally, modelling predicted that the sorped species $=FeOZn^{+}$ would be formed. Higher pH would see the formation of various zinc hydroxides ($Zn(OH)^{3-}$, $Zn(OH)_4^{2-}$ and $Zn(OH)_2(aq)$). Figure 4.4.13 below shows how the concentration in the aqueous phase varies with pH.

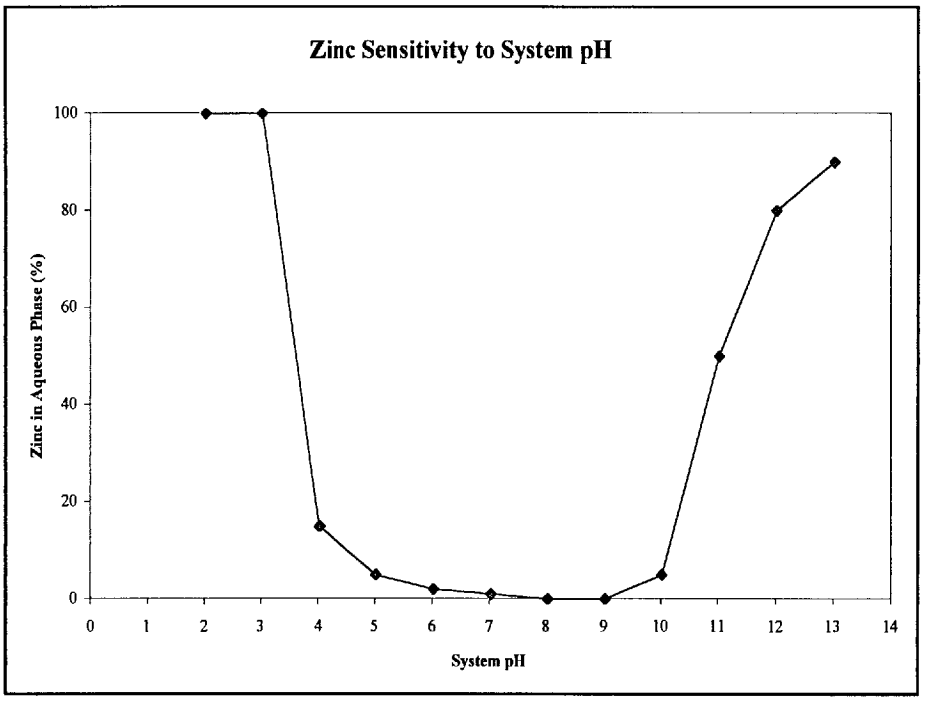


Figure 4.4.13 Zinc Leached as a Function of System pH

Arsenic in Leachate

For ashes produced in the muffle furnace arsenic showed a high propensity to be leached. It was nearly 100 % leached for all fuels for ashes produced at both 850 and 950 °C and no temperature dependence on arsenic leaching was evident. Fuel 3 showed a slightly lower Arsenic retention but still retained the trend.

Modelling agreed well with experimental results. At the computed pH range of 3 to 4% for the suite of fuels arsenic was predicted to be 100% in solution. At the pH range of 4.19-5 obtained experimentally arsenic was also predicted to be 100% but at a higher pH, 6-13, the leaching propensity dropped to 0%. It was predicted that in this instance Arsenic would be 100% precipitated. Between a pH of 5 and 6 arsenic was predicted to exist as $H_2AsO_4^-$ and H_3AsO_4. The variation of Arsenic in solution with pH is shown Figure 4.4.14 below.

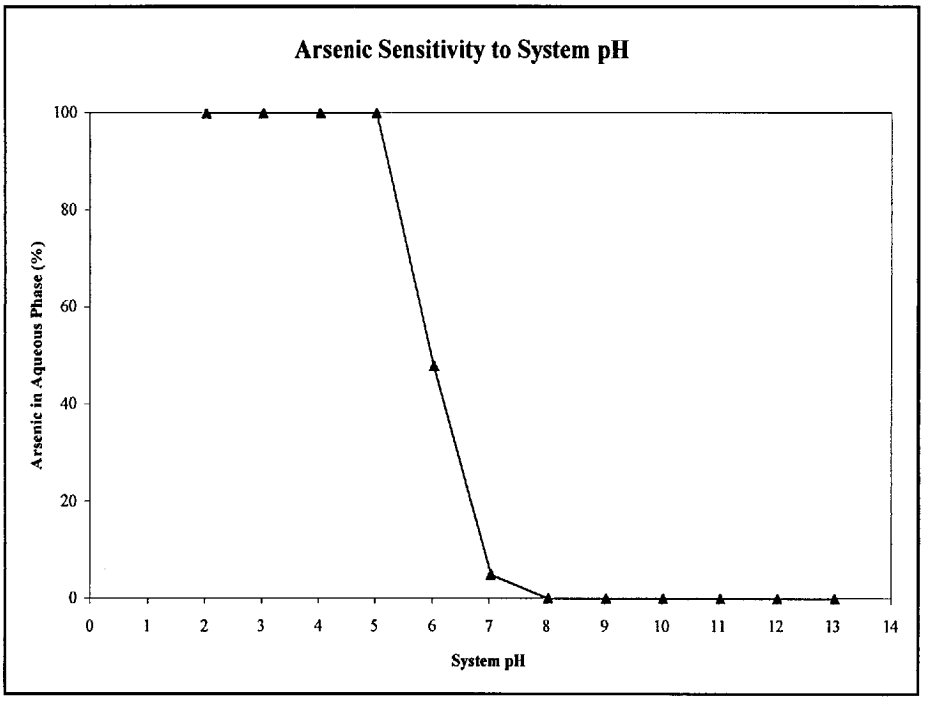


Figure 4.4.2.14 Arsenic Leached as a Function of System pH

Selenium in Leachate

The selenium profile was similar to the arsenic profile. Selenium was highly susceptible to leaching at both temperatures, with all fuels leaching to a region of 80% and over. Again Fuel 3 was an exception with a slightly lower percentage of selenium leached (70%). Other than for the lower level of selenium leached in Fuel 3, there did not appear to be a temperature dependence for selenium leaching.

Modelling selenium showed that it would be almost completely leached for all the fuels. The experimental results were overall slightly lower but concurred with the computed predictions, within the bounds of experimental error. At the computed equilibrium pH for the various fuels between 90 & 93 % of the selenium was expected to be in solution. This would primarily be present as species SeO_4^{2-} (over 90% for all fuels) with the remainder being present as $HSeO_4^-$. A small amount of selenium was expected to be sorbed as $=FeSO_4^-$. The selenium concentration/pH curve was unique in that above a pH of 4, selenium concentration in the leachate was not a function of pH. This is shown below in Figure 4.4.15.

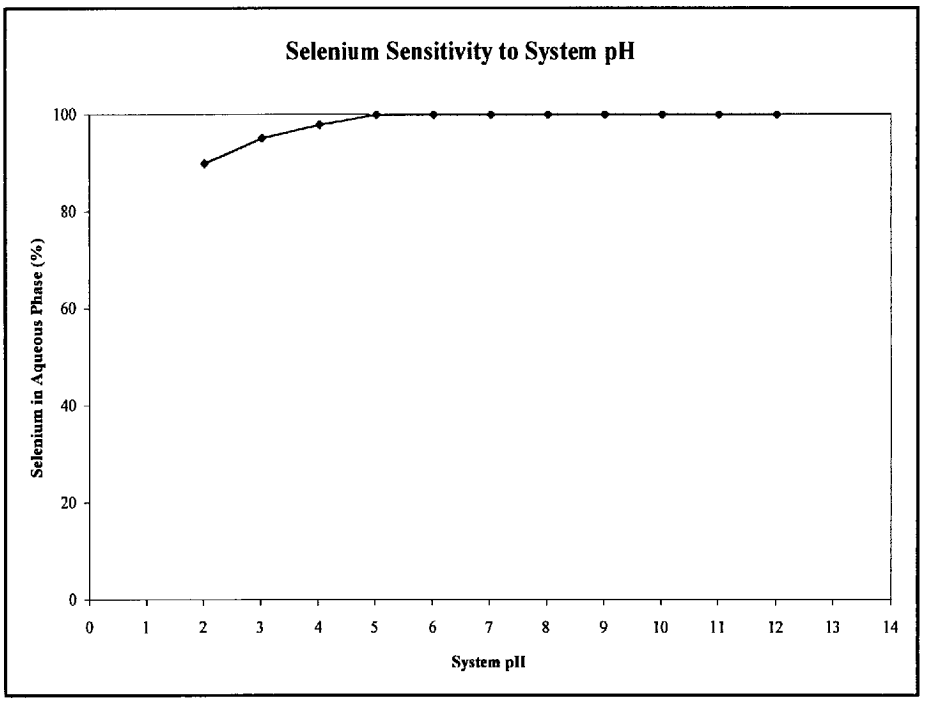


Figure 4.4.2.15 Selenium Leached as a Function of System pH

Mercury in Leachate

The mercury retention in the CERCHAR ashes was low, varying from 1-8%, with concentrations being a maximum of 0.1 ppm. Given these low values, the mercury concentration in the leachate was below the limits of detection in all instances.

Modelling predicted that mercury dissolution would be at its minimum at around the neutral pH range and as pH tended towards the two extremes of its scale the percent of mercury leached would increase with a steep gradient. This is shown in Figure 4.4.16 below. It was predicted that mercury in the leachate would exist as mercury acetate, Hg^{+} and $Hg(OH)_2$, and any sorbed mercury would be in the form $=FeOHg^{+}$.

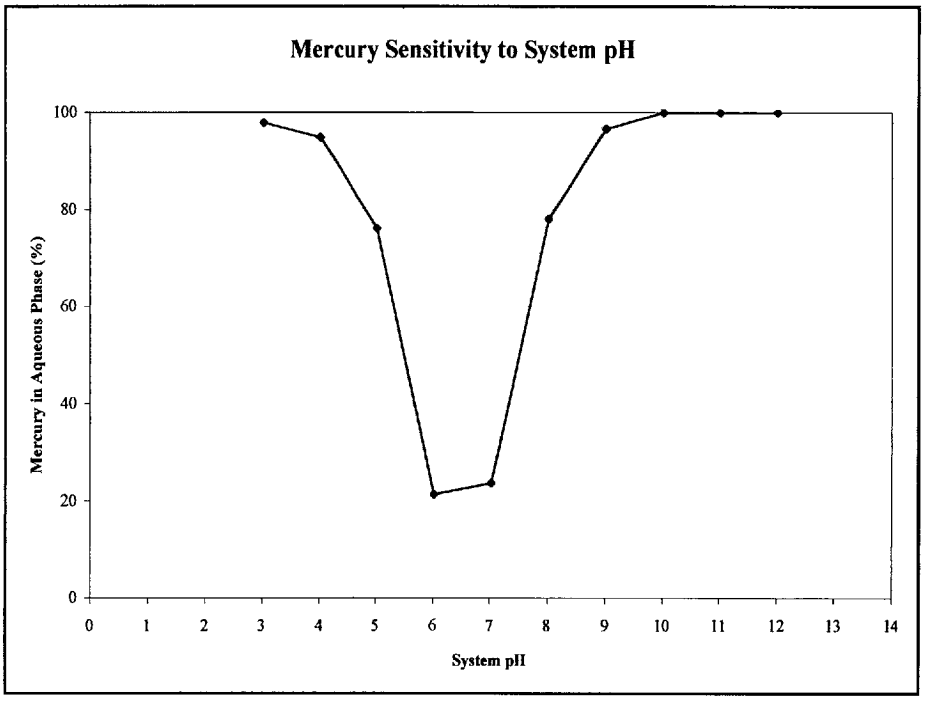


Figure 4.4.16 Mercury Leached as a Function of System pH

Cadmium in Leachate

The cadmium present in the ashes was susceptible to moderate leaching. Cadmium in ashes produced at 850 °C underwent around 36% leaching for Fuel 2, with a minimum of 7% cadmium leached for Fuel 8. Cadmium leaching did appear to be a function of ash temperature for all the fuels studied. Less cadmium was leached at ashes produced at 950 °C. As previously suggested this may be because a fraction of cadmium which could withstand higher temperatures and remain in the ash matrix, could also withstand the leaching process.

The modelling for cadmium showed that it was very sensitivity to acidic conditions and would be dissolved almost entirely up to a pH of 7, thereafter the extent of leaching would decrease to a minimum of 11.2 % at a pH of 11. At the alkaline extreme the degree of leaching would again increase. As may be seen this is contrary to what was obtained in the experimental results. At the pH ranges obtained experimentally cadmium was predicted to exist primarily as the Cd^{2+} ion, cadmium acetate with small quantities of aqueous cadmium sulphate.

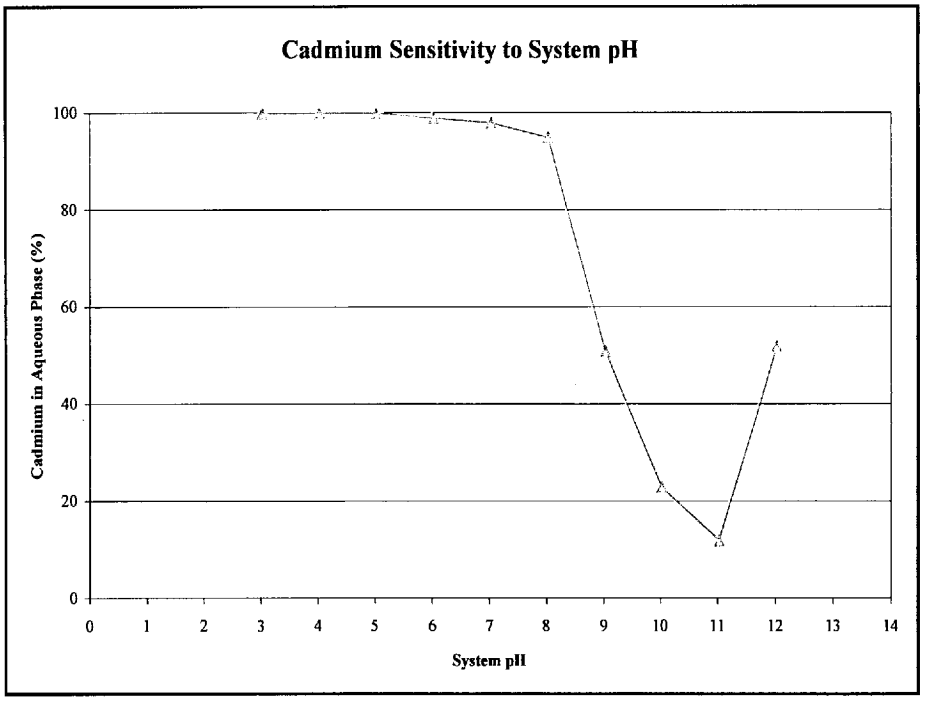


Figure 4.4.17 Cadmium Leached as a Function of System pH

Barium in Leachate

A large proportion of the barium present in the ashes was leached for all the fuels except Fuel 4. For ashes produced at both temperatures, the barium leached ranged from 73.3% to 99.9 %. Leaching of barium did not appear to be a function of the temperature at which the ash was produced.

In computing the theoretical barium leached, it was found that at the calculated equilibrium pH all the barium would be dissolved, whilst at the experimental pH (between 4.2 and 5) a drop of 10 % in barium leached was observed. Barium was primarily present in solution as the Ba^{2+} ion for all the fuels, with barium acetate making up the remainder. Above a pH of approximately 6, barium was mostly sorbed into the ash matrix. The experimental and theoretical results are therefore in good agreement except for the case of Fuel 4.

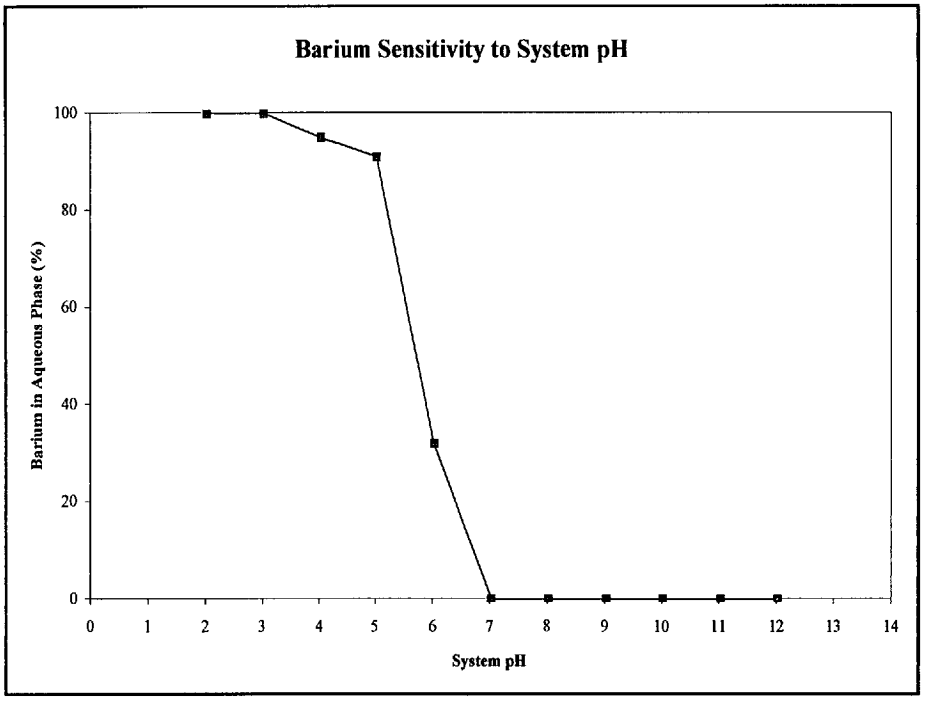


Figure 4.4.18 Barium Leached as a Function of System pH

Lead in Leachate

Lead leaching was between 35.1 and 0.5 % from the ashes produced at 850 °C and between 17.7 and 1.5 % from ashes produced at 950 °C. There appeared to be a temperature dependence for all fuels except Fuel 3 and fuel 6. Lead leaching was more fuel dependent than the other elements with a greater variation in leaching between the fuels. Again in may be postulated that the temperature dependence may be due to lead in the higher temperature ash being present in a form less susceptible to leaching..

Modelling of lead leaching broadly agreed with the results obtained experimentally as may be seen in Figure 4.4.19 below. Lead was present in solution as lead acetate and the Pb^{2+} ion with a small quantity of lead sorbed as $=FeOPb^{+}$.

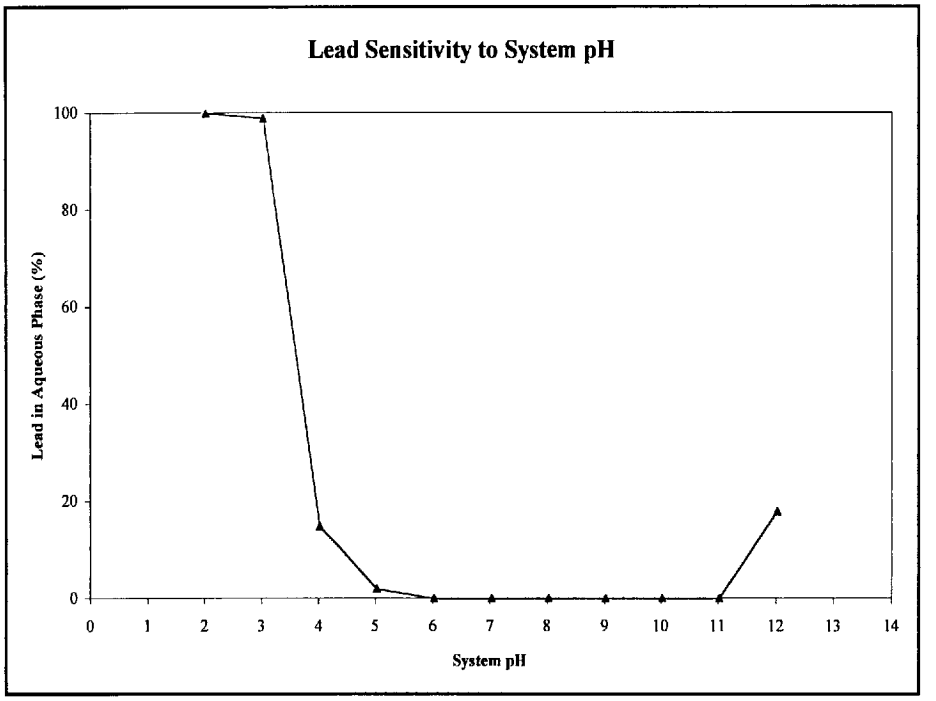
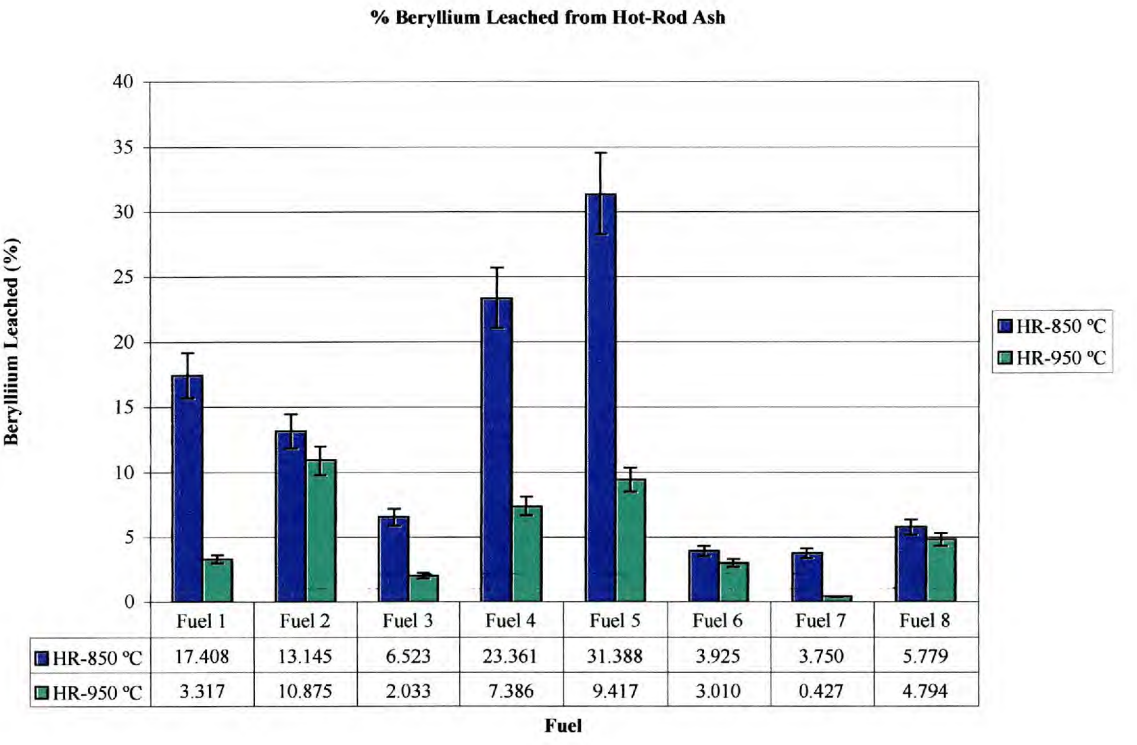


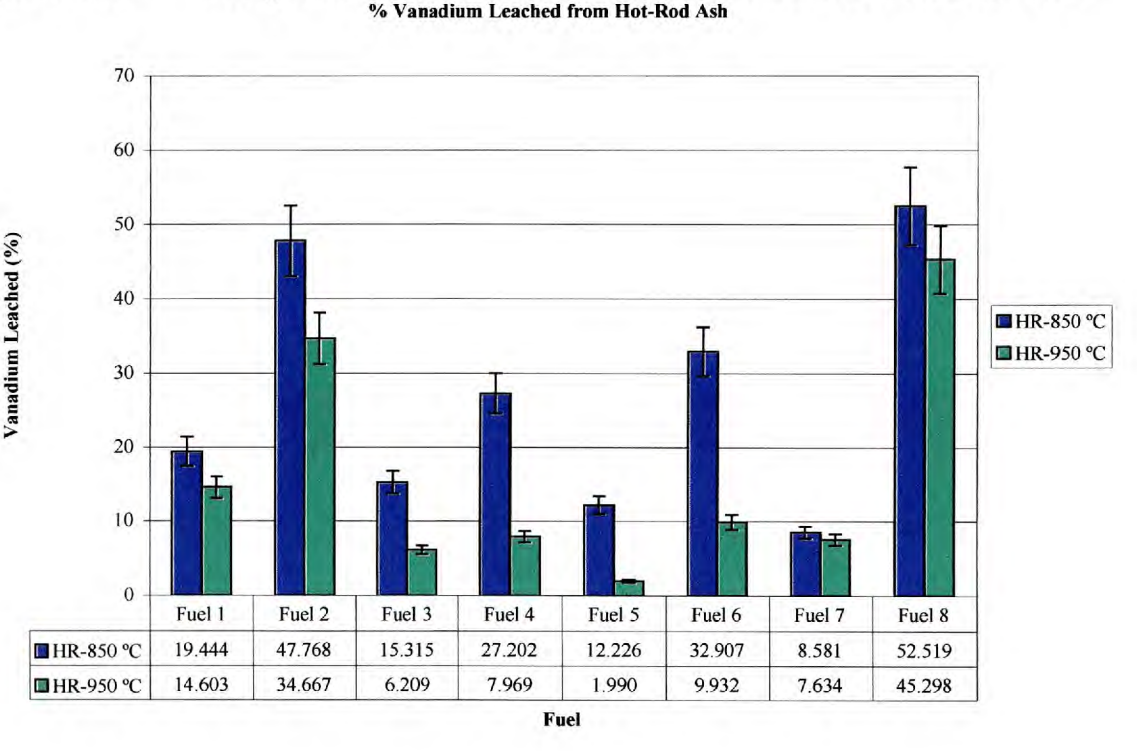
Figure 4.4.19 Lead Leached as a Function of System pH

4.4.2.2 Trace Element Content in Leachate from CERCHAR Ash produced in Hot-Rod



	Fuel 1	Fuel 2	Fuel 3	Fuel 4	Fuel 5	Fuel 6	Fuel 7	Fuel 8
HR-850 °C	17.408	13.145	6.523	23.361	31.388	3.925	3.750	5.779
HR-950 °C	3.317	10.875	2.033	7.386	9.417	3.010	0.427	4.794

Figure 4.4.20 % Beryllium Leached from Ash Produced in Hot-Rod at 850 & 950 °C



	Fuel 1	Fuel 2	Fuel 3	Fuel 4	Fuel 5	Fuel 6	Fuel 7	Fuel 8
HR-850 °C	19.444	47.768	15.315	27.202	12.226	32.907	8.581	52.519
HR-950 °C	14.603	34.667	6.209	7.969	1.990	9.932	7.634	45.298

Figure 4.4.21 % Vanadium Leached from Ash Produced in Hot-Rod at 850 & 950 °C

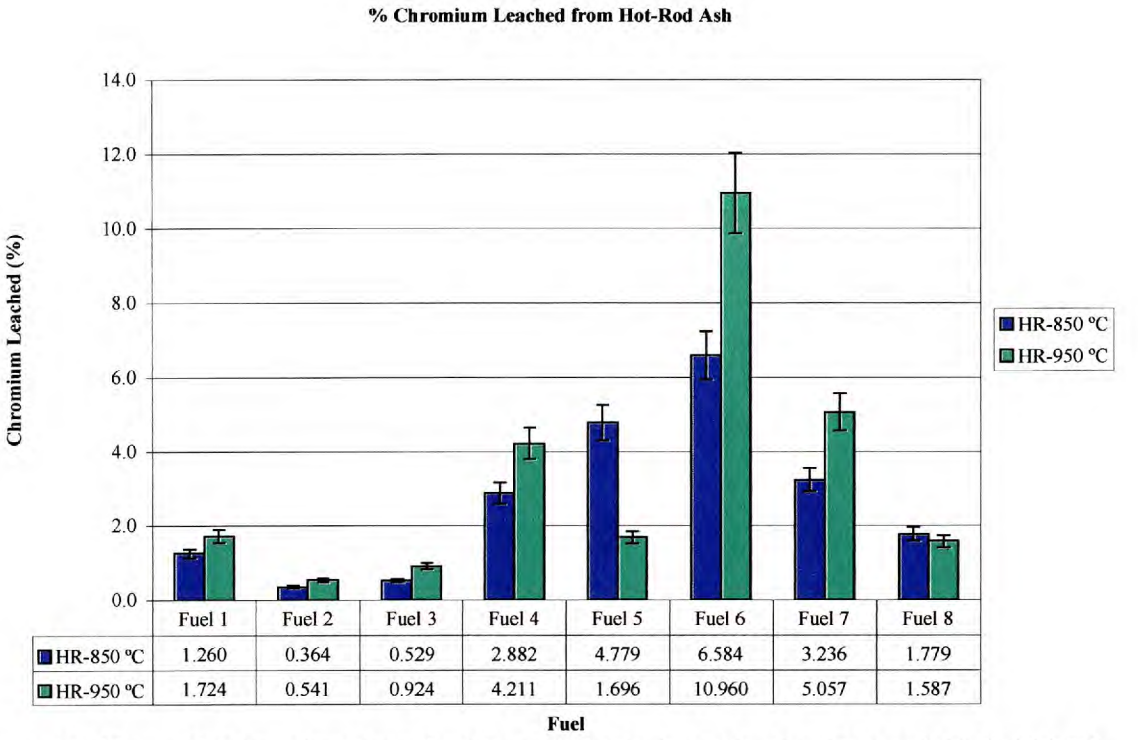


Figure 4.4.22 % Chromium Leached from Ash Produced in Hot-Rod at 850 & 950 °C

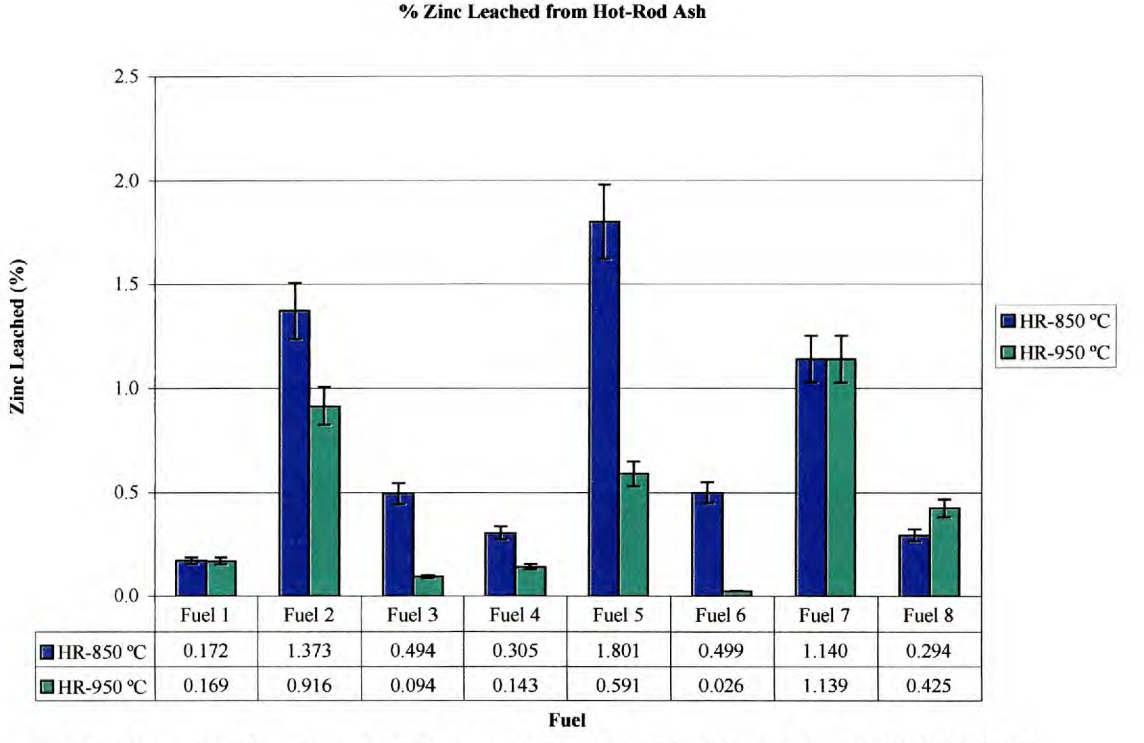
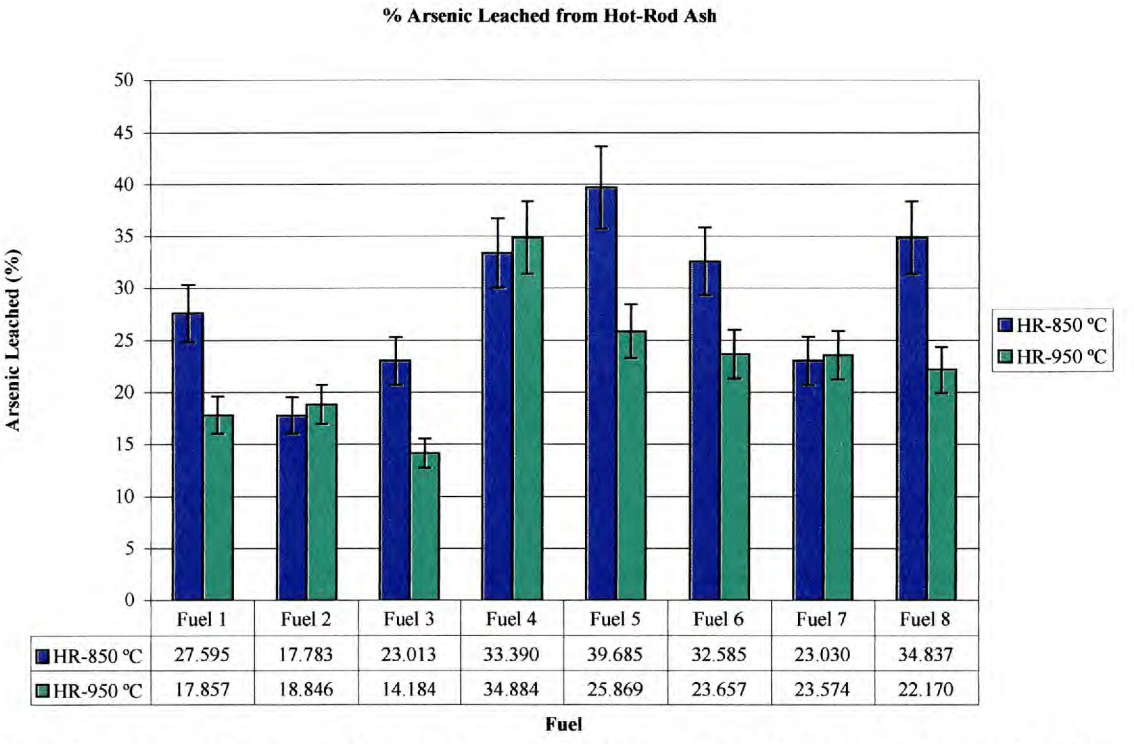
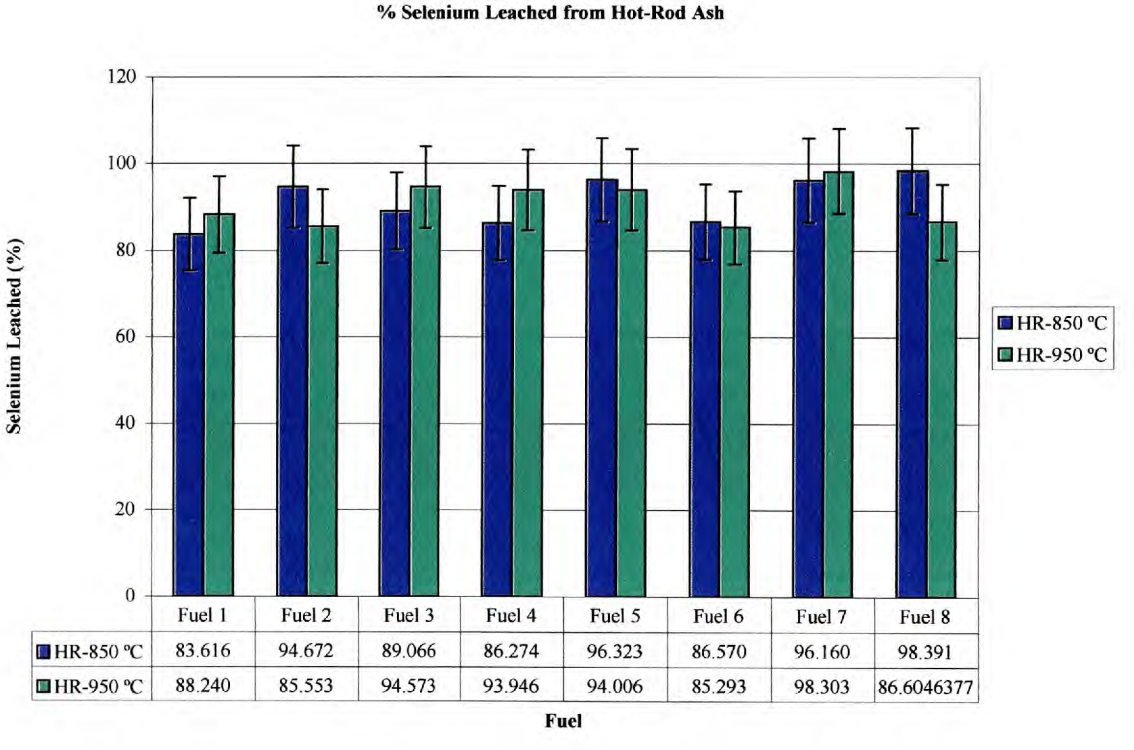


Figure 4.4.23 % Zinc Leached from Ash Produced in Hot-Rod at 850 & 950 °C



	Fuel 1	Fuel 2	Fuel 3	Fuel 4	Fuel 5	Fuel 6	Fuel 7	Fuel 8
HR-850 °C	27.595	17.783	23.013	33.390	39.685	32.585	23.030	34.837
HR-950 °C	17.857	18.846	14.184	34.884	25.869	23.657	23.574	22.170

Figure 4.4.24 % Arsenic Leached from Ash Produced in Hot-Rod at 850 & 950 °C



	Fuel 1	Fuel 2	Fuel 3	Fuel 4	Fuel 5	Fuel 6	Fuel 7	Fuel 8
HR-850 °C	83.616	94.672	89.066	86.274	96.323	86.570	96.160	98.391
HR-950 °C	88.240	85.553	94.573	93.946	94.006	85.293	98.303	86.6046377

Figure 4.4.25 % Selenium Leached from Ash Produced in Hot-Rod at 850 & 950 °C

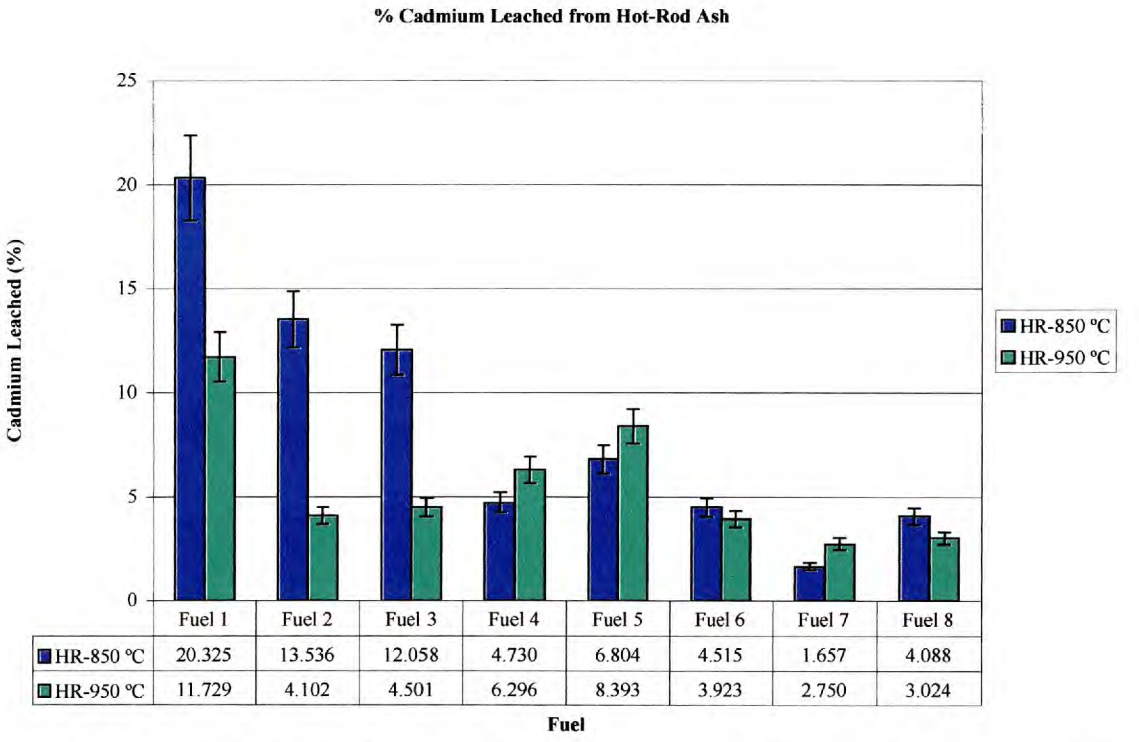


Figure 4.4.26 % Cadmium Leached from Ash Produced in Hot-Rod at 850 & 950 °C

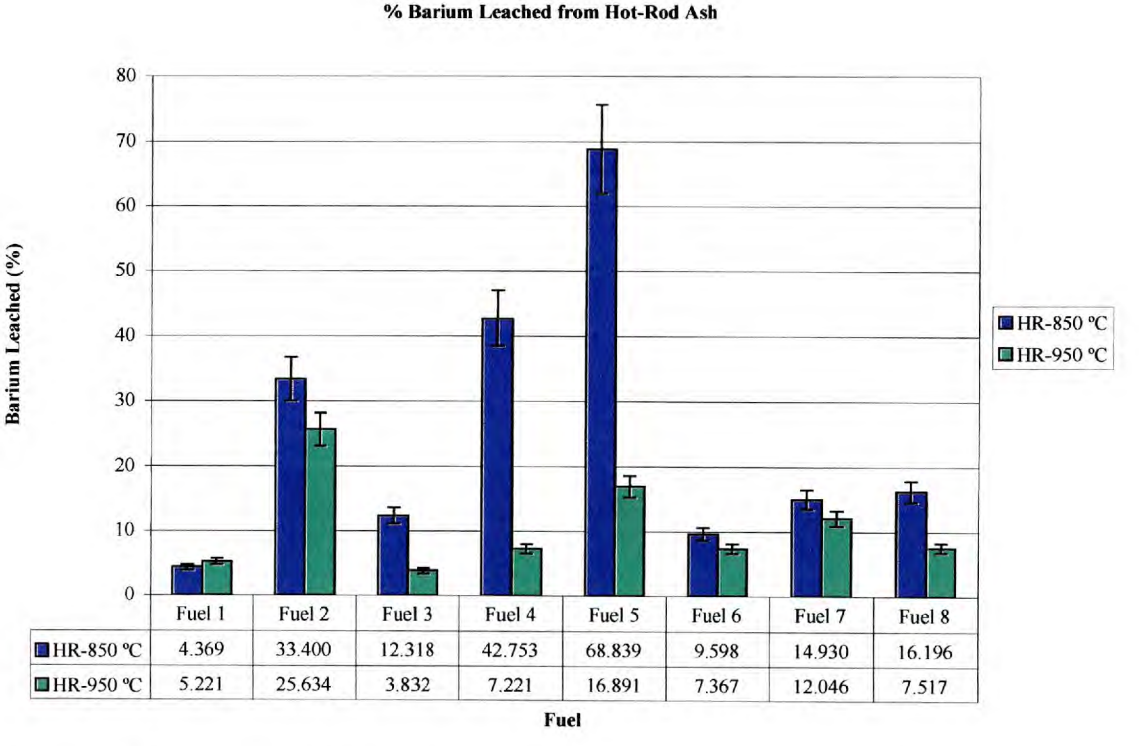


Figure 4.4.27 % Barium Leached from Ash Produced in Hot-Rod at 850 & 950 °C

4.4.2.2 Trace Element Content in Leachate from CERCHAR Ash produced in Hot-Rod

Beryllium Leached

The percentage beryllium leached from ashes produced in the hot-rod was slightly lower than that leached from muffle furnace ashes at 850 °C. At 950 °C however, the beryllium percentage leached was reduced in hot-rod ashes for all fuels. The initial quantity of beryllium in the ashes at the two different temperatures was the same. The temperature dependence may be due to beryllium still being present in the ash at 950 °C but, held in a mode of occurrence which is less susceptible to leaching.

The overall reduction in beryllium leached from the hot-rod ashes compared to those of the muffle furnace might be due to the higher pH of the leachate produced from these ashes. The general pH trend for beryllium is shown in Figure 4.1.1.10. The beryllium products formed in the leachate were computed to be Be^{2+}, $BeOH^{+}$ and $BeSO_4$. Beryllium was predicted to sorb quite strongly and to exist as $=FeBe^{+}$.

Vanadium Leached

The vanadium leached from hot rod ash was at far lower levels than for muffle furnace ash. At 850 °C the vanadium leached varied from 52.5 % for Fuel 8 to a minimum of 8.5% for Fuel 6. Ashes produced at 950 °C were subject to vanadium leaching in the range from 45.2 – 1.99 %. As with beryllium leaching in the hot-rod, vanadium leaching was dependent upon the temperature of ash production for all fuels except Fuel 7. The percentage of vanadium leached decreased with increasing temperature.

Modelling concurred with the results obtained at 850 °C but did not predict the low levels of vanadium leached when ashes were produced at 950 °C. Vanadium would be found in solution at the following species : $H_3V_2O_7^{-}$, H_3VO_4 (aq), $H_2VO_4^{-}$, and VO_2^{+}. Sorption was not predicted to occur with vanadium in any of the ash samples at any pH.

Chromium in Leachate

The chromium found in hot-rod ashes exhibited the same behaviour as that in muffle furnace ashes. Low quantities of chromium were found to leach (between 0.3 and 6.5 %) from ashes produced at 850 °C. For ashes produced at 950 °C the chromium showed a higher propensity for leaching. This behaviour is unique to chromium and cadmium found in hot rod ashes.

Modelling did not concur with experimental results. At the computed pH range for the fuels studied chromium was expected to leach between 50 and 30%. At the empirical pH from 30 to up to 60 % of the chromium was expected to leach. A small degree of sorption was computed from modelling (sorped species would be present as $=FeCrO_4^-$ and $=FeOHCrO_4^{2-}$) but literature suggests that at the pH range in question, a higher degree of sorption may be taking place. This would explain the reduced quantity of chromium to be found in the leachate.

Zinc in Leachate

When leaching occurs in hot-rod ashes the resulting leachate is a higher pH than that produced from muffle furnace ashes. This reduces the leaching propensity of some elements including in this case zinc. Zinc showed a very low leaching propensity, being almost entirely retained. The highest degree of leaching was 1.8 % for Fuel 1 ash produced at 850 °C. The fuels produced at 950 °C occasionally showed a lower percentage leaching, but at the low levels in question, this was not of significance practically.

Modelling predicted the behaviour of zinc well and a typical zinc-pH curve is shown in Figure 4.4.1.13. Modelling did not predict any precipitation of zinc, but did indicate that large quantities of the zinc present (up to 60 %) would be sorbed. The remaining zinc would be present as part of the inner ash matrix and would not available for leaching.

Arsenic in Leachate

The arsenic leached from hot-rod ashes was significantly lower than that leached in muffle furnace. For ashes produced at 850 °C arsenic leaching ranged from 39.7 to 17.8 %. For ashes produced at 950 °C the range was a maximum of 34.9% arsenic leached to a minimum of 14.2 %. Unlike the muffle furnace where arsenic leaching did not depend upon temperature of ash production, less arsenic was leached in hot-rod ashes produced at 950 °C to those produced at 850 °C. This was the case for all fuels except Fuel 2, 4 and 7. Arsenic in the hot-rod fuels is retained to the same amount at the two temperatures.

Modelling predicted an equilibrium pH of between 3.93 to 4.17 for the eight fuels. At this pH range it was predicted that all the arsenic would be leached and for all fuels would exists as predominantly $H_2AsO_4^-$, with very small quantities (between 1-2%) of H_3AsO_4. At the pH observed experimentally the arsenic leached would exist as species $H_2AsO_4^-$ H_3AsO_4 and $HAsO_4^{2-}$. Small quantities of Arsenic (< 3% for all fuels) would be sorbed as $=FeOHAsO_4^{3-}$ and the remaining arsenic would remain in the ash matrix not exposed to the leaching medium.

Selenium in Leachate

Selenium in hot-rod ashes showed a very high leaching propensity. A minimum of 85.6% of selenium was leached in the hot-rod ashes. Selenium leaching was not found to be dependent upon the temperature of ash production. The selenium leaching profile for hot-rod ashes was the same as that for muffle furnace ashes at both temperatures.

Modelling concurred with leaching results to predict that nearly all selenium would be leached. A minimum of 90% selenium was predicted to leach at a theoretical pH of 2, rising to a maximum of 100% selenium leachate after a pH of 5. This would primarily be present as species SeO_4^{2-} (over 90% for all fuels) with the remainder being present as $HSeO_4^-$.

Mercury in Leachate

As with results obtained for the muffle furnace the concentration of mercury in hot-rod ashes was low (< 0.1 ppm). No mercury was detected in the leachate of any of the ashes, at either operating temperature.

Modelling predicted that at the experimental pH range between 20-25% of Mercury would exist in the aqueous phase. The remainder was predicted to be either sorbed or retained in the ash matrix in its intital mode of occurrence.

Cadmium in Leachate

Cadmium in hot-rod ashes was shown to have a low propensity for leaching similar to that obtained by muffle furnace ashes. Cadmium leaching ranged from 20% to 2%. Temperature dependence was significant for Fuels 1, 2 and 3. The leaching decreased with increasing temperature.

As with the muffle furnace ashes, the cadmium leaching profile was the one which varied the most significantly from that predicted by modelling. At the equilibrium pH observed experimentally cadmium was expected to be present in its entirety in the aqueous phase as Cd^{+}. The disparity of experimental and computed results may be attributed to the low levels of cadmium initially present. Lower quantities of a trace element mean less is available for leaching and additionally some of this trace element is present within parts of the ash matrix not accessible to leaching. The model may not take this into account.

Barium in Leachate

Barium in leachate produced from hot-rod ashes showed variable results and was the only element whose leaching propensity was significantly fuel dependent. From ashes produced at 850 °C, 68.8 % of barium was leached at a maximum for Fuel 5 and a minimum of 4.3 % of barium was leached for Fuel 1. From ashes produced at 950 °C the Fuel 3. For all fuels except Fuel 1 and Fuel 6, it appeared that less barium leached from the higher temperature ash.

At the equilibrium pH range observed empirically for the different fuels it was predicted by modelling that between 45% and 5% of barium would be leached. This therefore reasonably reflected the results obtained. Barium was primarily present in solution as the Ba^{2+} ion for all the fuels with barium acetate making up the remainder. After a pH of approximately 6 it was predicted that the barium released would be mostly sorbed into the ash matrix.

Lead In Leachate

For hot-rod ashes produced at both temperature lead was leached below the limits of detection or quantification for all fuels. This was as predicted by modelling. Lead was predicted to be highly sorbed as $FeOPb^{+}$ at the equilibrium pH range observed.

4.4.2.3 Trace Element Concentration in CERCHAR Leachates in Relation to Regulatory Constraints

The figures below depict trace element content of leachate depicted as a concentration rather than as a retention. Recent practice would use this measure in a risk assessment to determine weather a landfill site's emissions are within regulatory limits. However, this measurement cannot be used in isolation, without considering other relevant parameters. When determining whether a waste product is suitable for landfill the following points would need to be considered in conjunction with the TCLP leaching test results

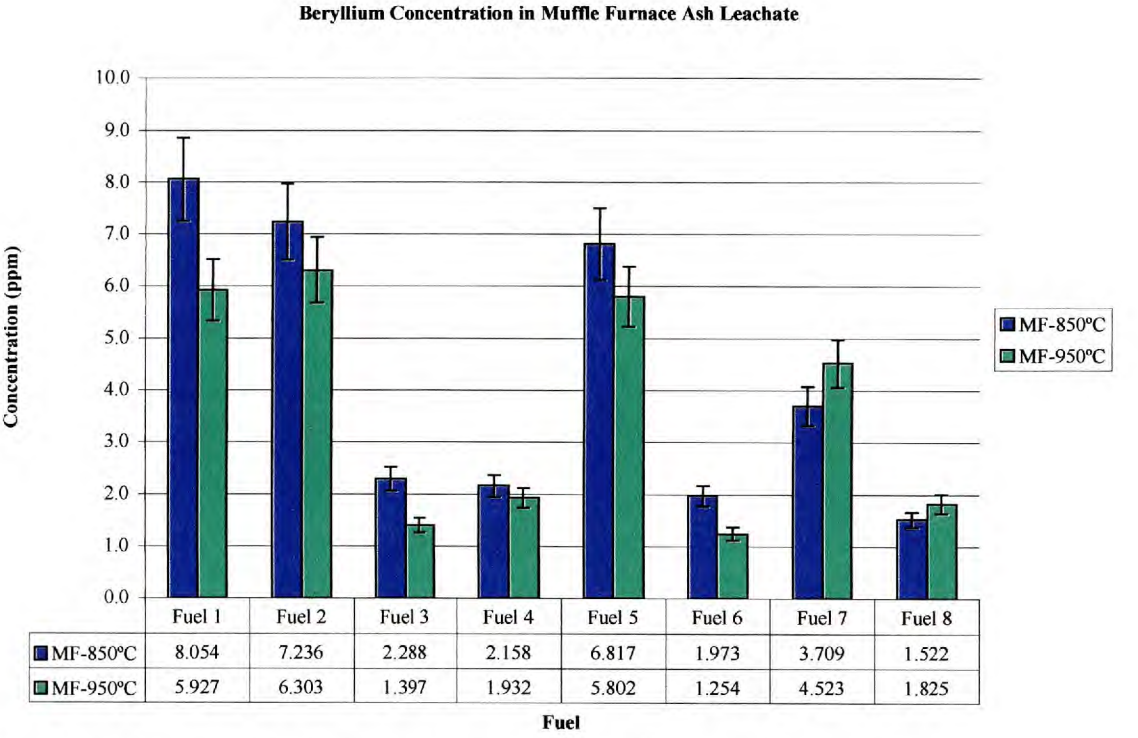
- The absolute quantity of trace element available for leaching should be considered. This is a function of the quantity of ash to be disposed in the landfill as well as the speciation of the element in the ash. Once this is known along with the results from any leaching tests carried out, dispersion models would need to be used to determine how the trace element in question would migrate in the environment.

- The type of landfill site in which the ash will be deposited should be taken into consideration. Modern landfill design is increasingly taking into account the potentially hazardous nature of substances they may emit. Landfills constructed of various materials such as membranes which reduce leaching from the site or contain it altogether and landfill covers which prevent rainwater infiltrating the site.

In order to compensate for the above factors, the US-EPA developed a "dilution-attenuation factor" (DAF). The DAF is a quantity used to relate the concentration of leachate leaving a source zone (e.g. land-fill, surface impoundment, or contaminate soils) to its impact on down gradient ground water quality[85]. The DAF is usual calculated by developing a contaminant transport model for the system being considered.

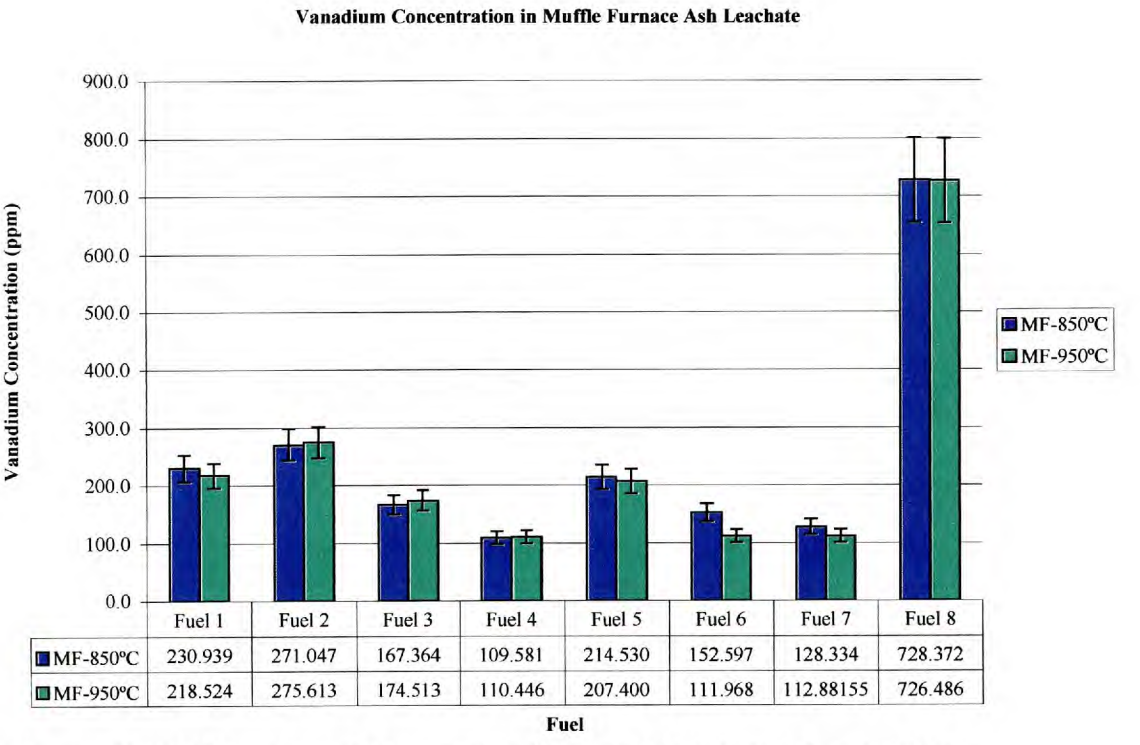
The US-EPA specifies a worst case scenario DAF for TCLP leachates of 100.[85] That is to say that each trace element concentration from TCLP leachate is divided by 100 and it is this value which is compared to regulatory limits. If this value falls below stipulated limits then the waste may be safely disposed of in the environment with regard to the trace element in question.

The figures below show the actual trace element concentrations in the CERCHAR ash leachates in the muffle furnace and the hot-rod reactor at the two temperatures studied. The DAF has not been applied to these concentrations. There then follows a discussion of whether the ashes studied could be disposed of in a landfill according to the these results, the WHO (World Health Organisation) limits given in Section 2.3.3 and with a DAF of 100 applied.



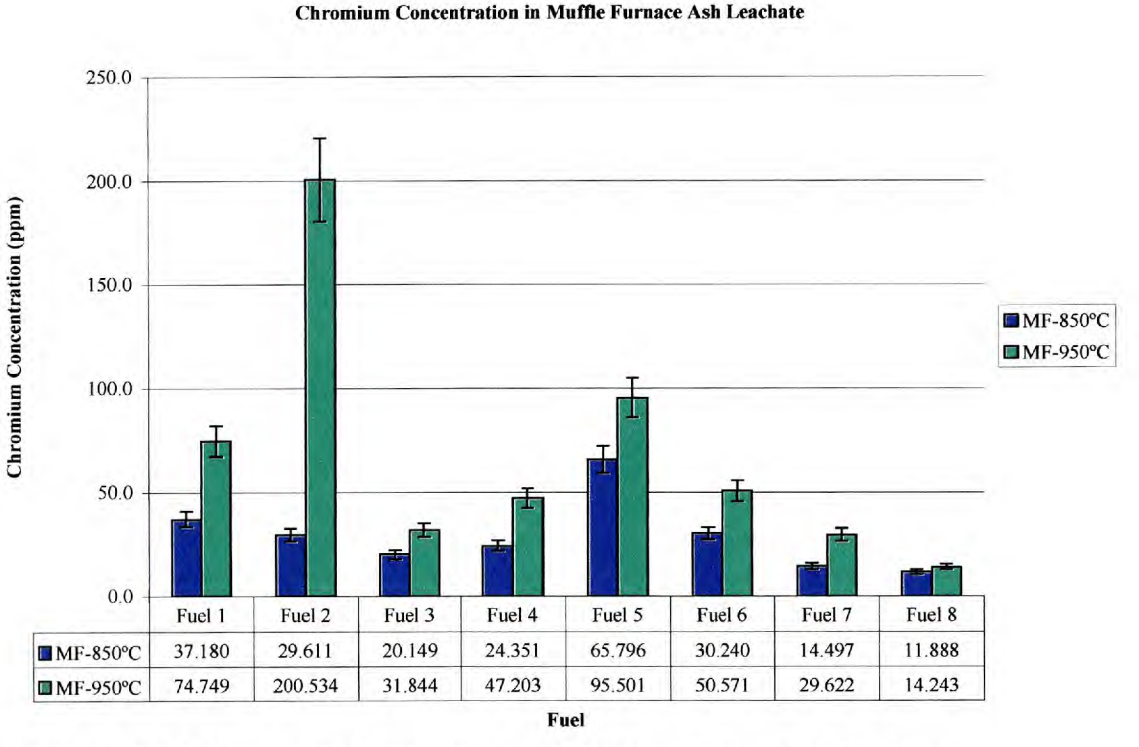
	Fuel 1	Fuel 2	Fuel 3	Fuel 4	Fuel 5	Fuel 6	Fuel 7	Fuel 8
MF-850°C	8.054	7.236	2.288	2.158	6.817	1.973	3.709	1.522
MF-950°C	5.927	6.303	1.397	1.932	5.802	1.254	4.523	1.825

Figure 4.4.28 Beryllium Concentration in Muffle Furnace Ash Leachate



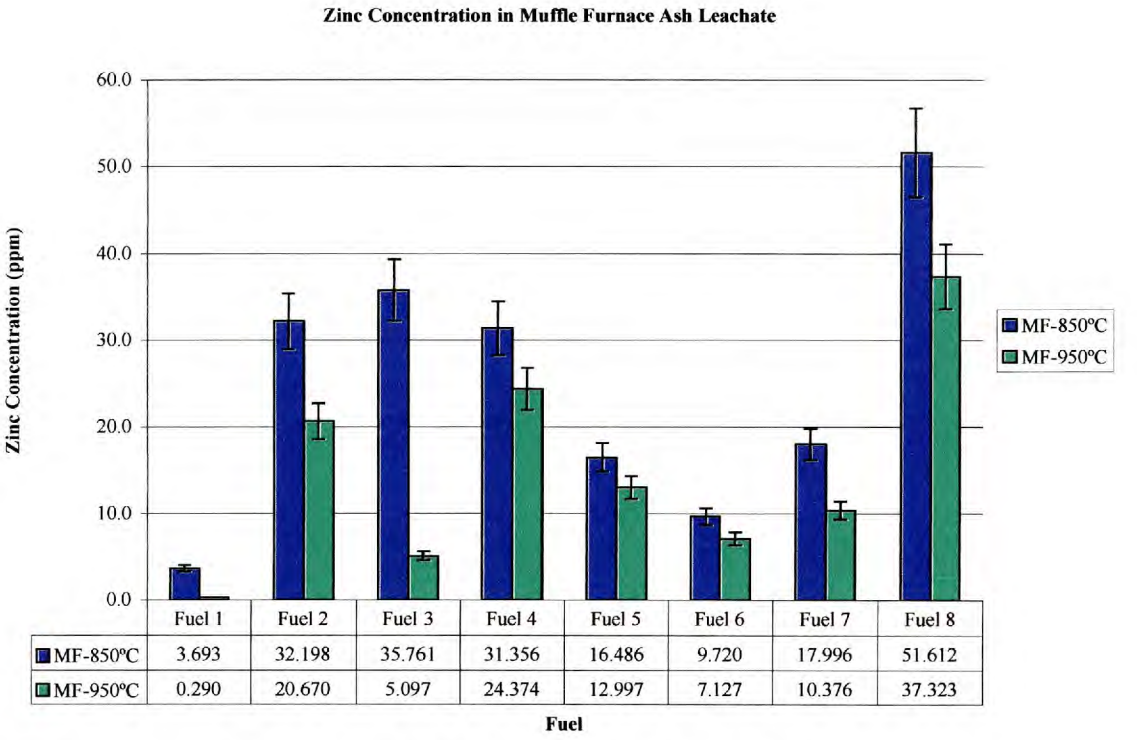
	Fuel 1	Fuel 2	Fuel 3	Fuel 4	Fuel 5	Fuel 6	Fuel 7	Fuel 8
MF-850°C	230.939	271.047	167.364	109.581	214.530	152.597	128.334	728.372
MF-950°C	218.524	275.613	174.513	110.446	207.400	111.968	112.88155	726.486

Figure 4.4.29 Vanadium Concentration in Muffle Furnace Ash Leachate



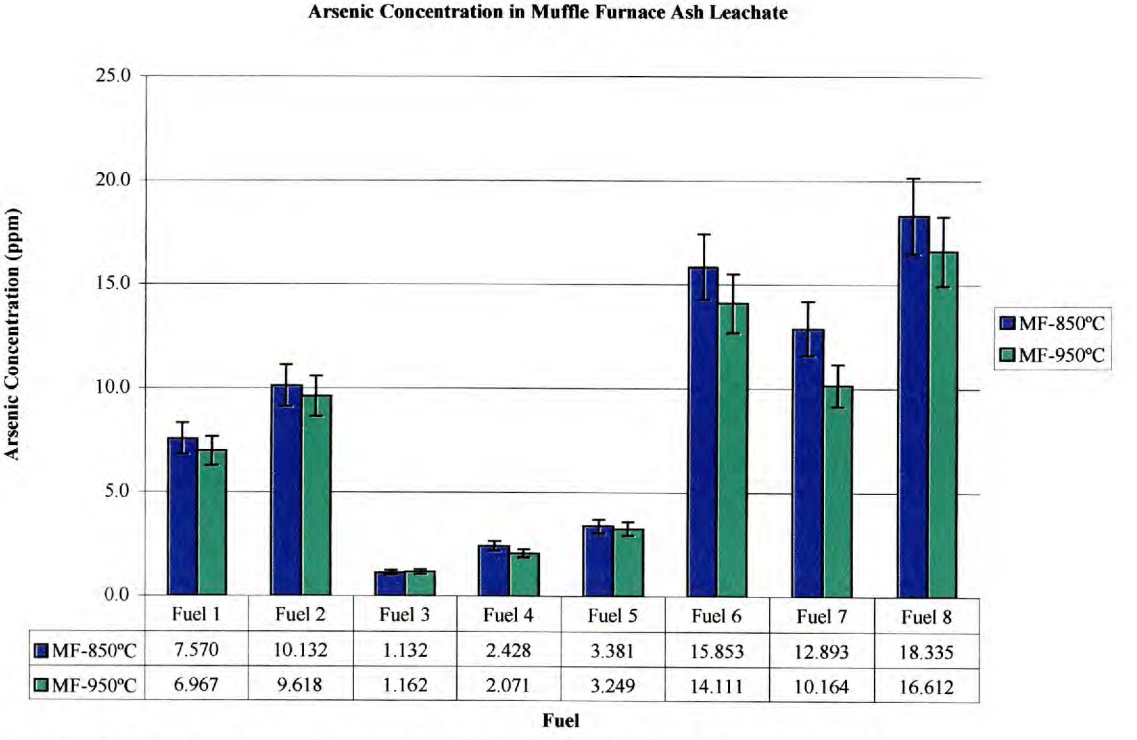
	Fuel 1	Fuel 2	Fuel 3	Fuel 4	Fuel 5	Fuel 6	Fuel 7	Fuel 8
MF-850°C	37.180	29.611	20.149	24.351	65.796	30.240	14.497	11.888
MF-950°C	74.749	200.534	31.844	47.203	95.501	50.571	29.622	14.243

Figure 4.4.30 Chromium Concentration in Muffle Furnace Ash Leachate



	Fuel 1	Fuel 2	Fuel 3	Fuel 4	Fuel 5	Fuel 6	Fuel 7	Fuel 8
MF-850°C	3.693	32.198	35.761	31.356	16.486	9.720	17.996	51.612
MF-950°C	0.290	20.670	5.097	24.374	12.997	7.127	10.376	37.323

Figure 4.4.31 Zinc Concentration in Muffle Furnace Ash Leachate



	Fuel 1	Fuel 2	Fuel 3	Fuel 4	Fuel 5	Fuel 6	Fuel 7	Fuel 8
MF-850°C	7.570	10.132	1.132	2.428	3.381	15.853	12.893	18.335
MF-950°C	6.967	9.618	1.162	2.071	3.249	14.111	10.164	16.612

Figure 4.4.32 Arsenic Concentration in Muffle Furnace Ash Leachate

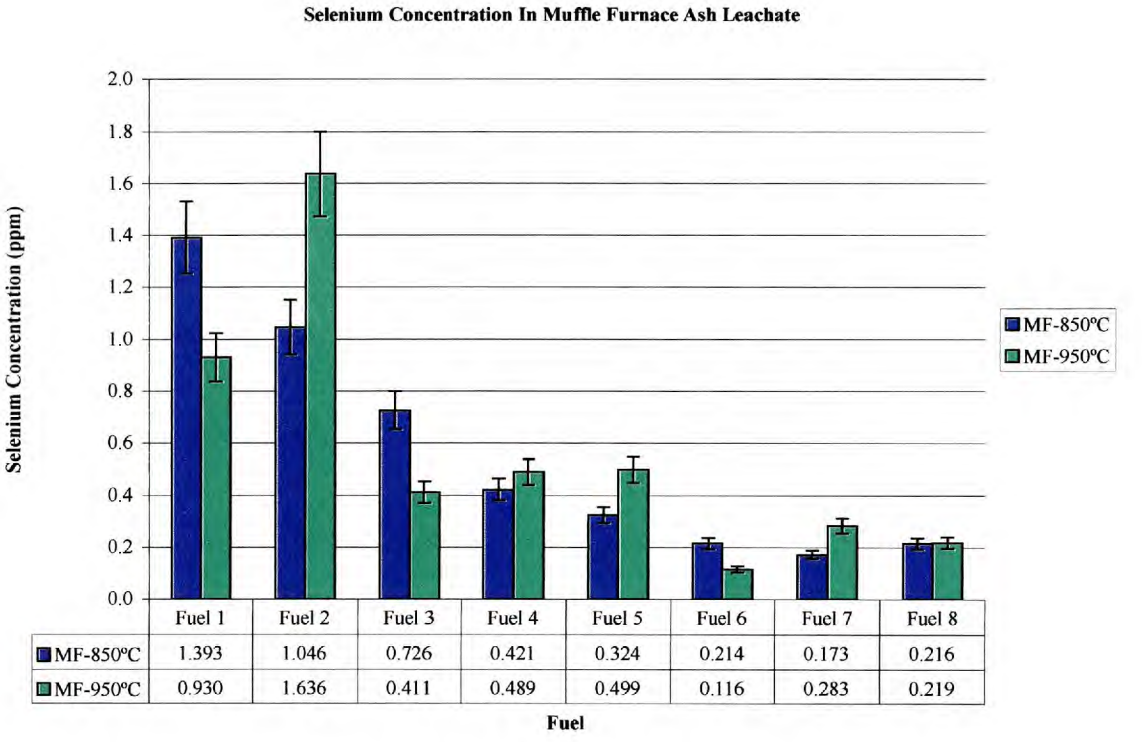


Figure 4.4.33 Selenium Concentration in Muffle Furnace Ash Leachate

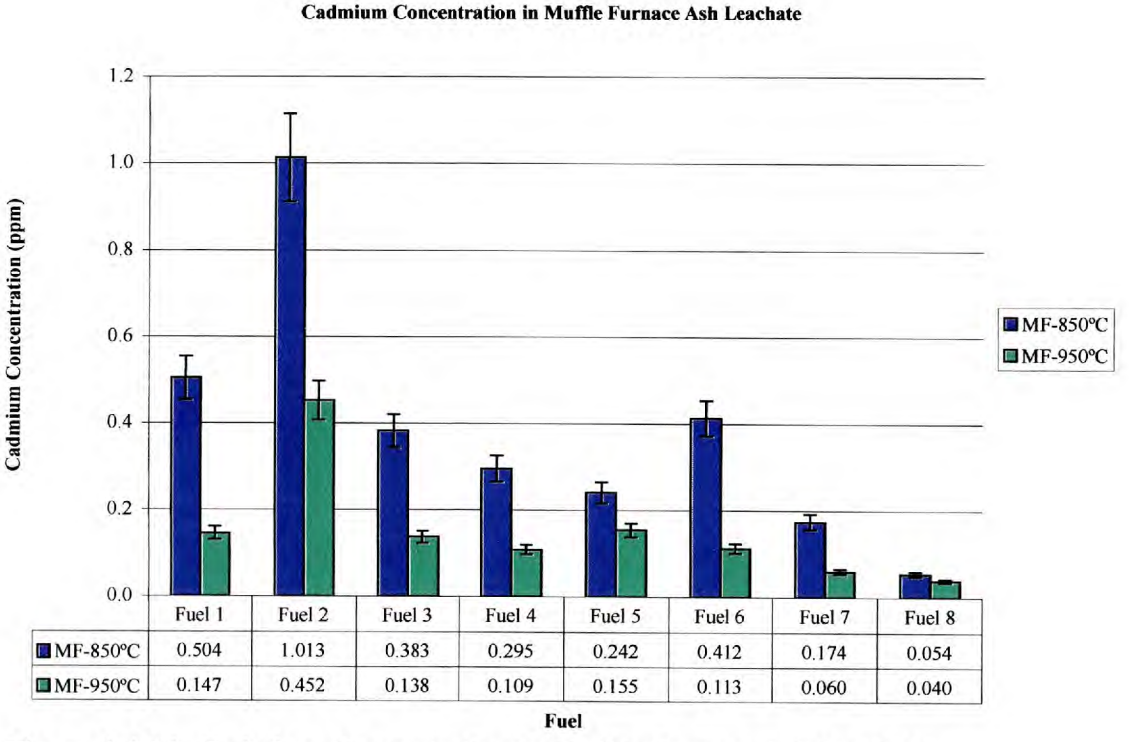
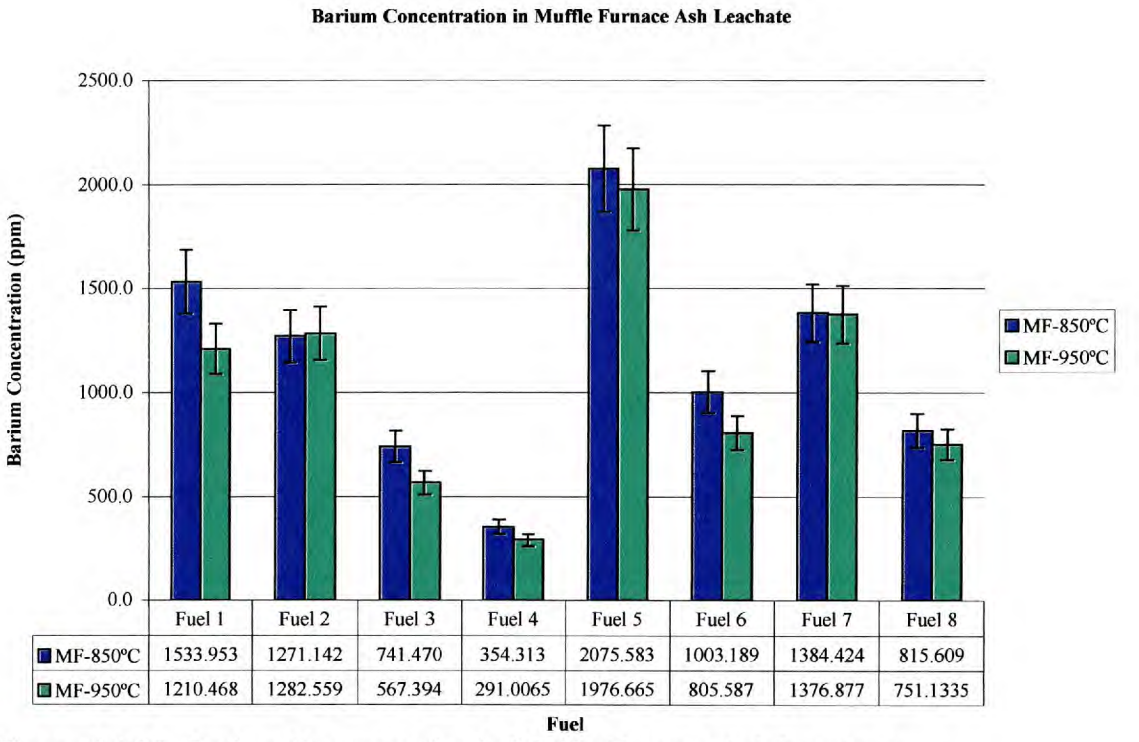
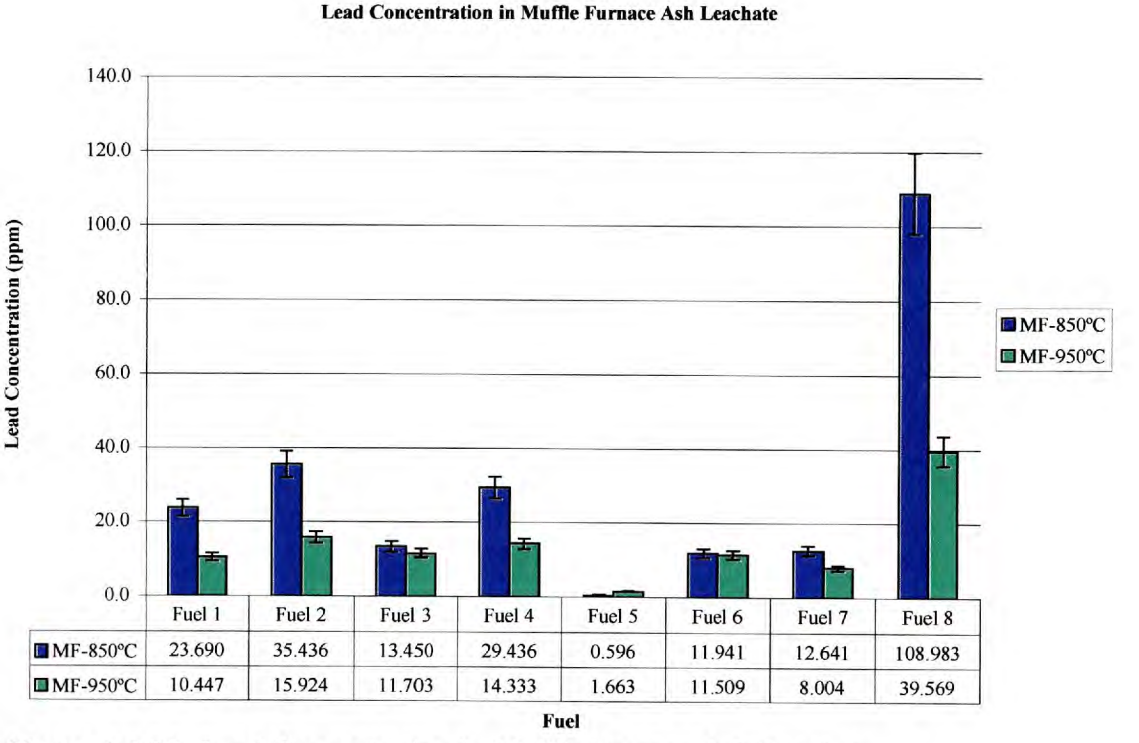


Figure 4.4.34 Cadmium Concentration in Muffle Furnace Ash Leachate



	Fuel 1	Fuel 2	Fuel 3	Fuel 4	Fuel 5	Fuel 6	Fuel 7	Fuel 8
MF-850°C	1533.953	1271.142	741.470	354.313	2075.583	1003.189	1384.424	815.609
MF-950°C	1210.468	1282.559	567.394	291.0065	1976.665	805.587	1376.877	751.1335

Figure 4.4.35 Barium Concentration in Muffle Furnace Ash Leachate



	Fuel 1	Fuel 2	Fuel 3	Fuel 4	Fuel 5	Fuel 6	Fuel 7	Fuel 8
MF-850°C	23.690	35.436	13.450	29.436	0.596	11.941	12.641	108.983
MF-950°C	10.447	15.924	11.703	14.333	1.663	11.509	8.004	39.569

Figure 4.4.36 Lead Concentration in Muffle Furnace Ash Leachate

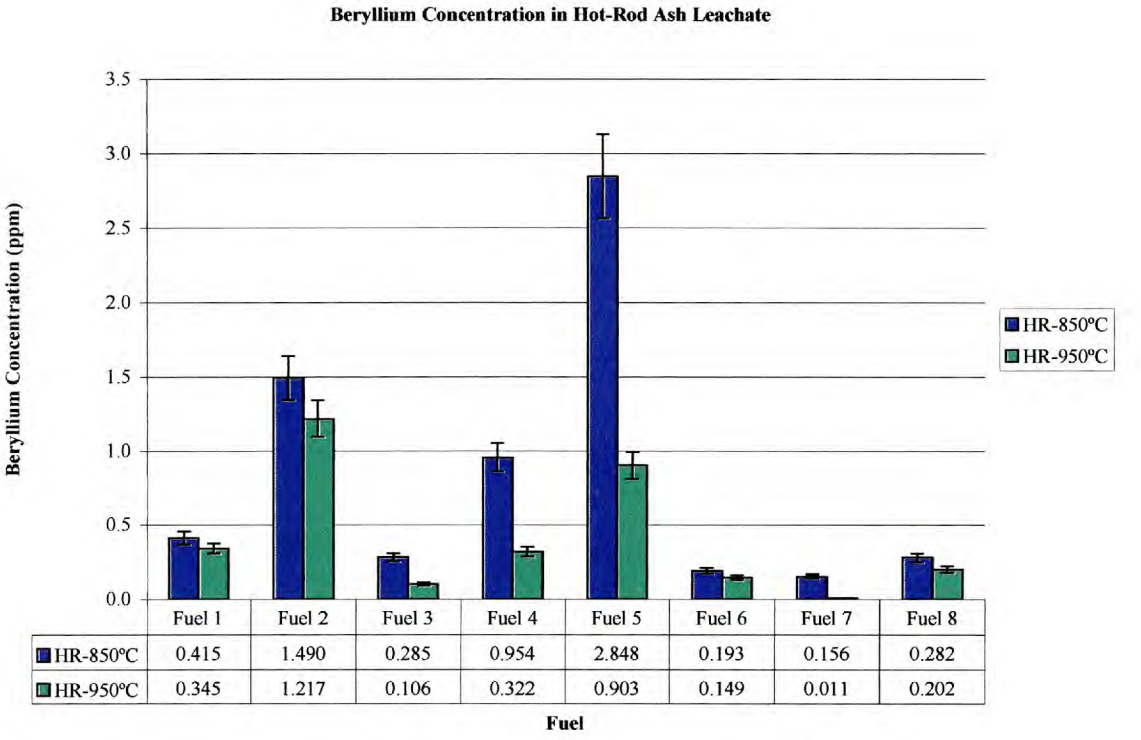


Figure 4.4.37 Beryllium Concentration in Hot-Rod Furnace Ash Leachate

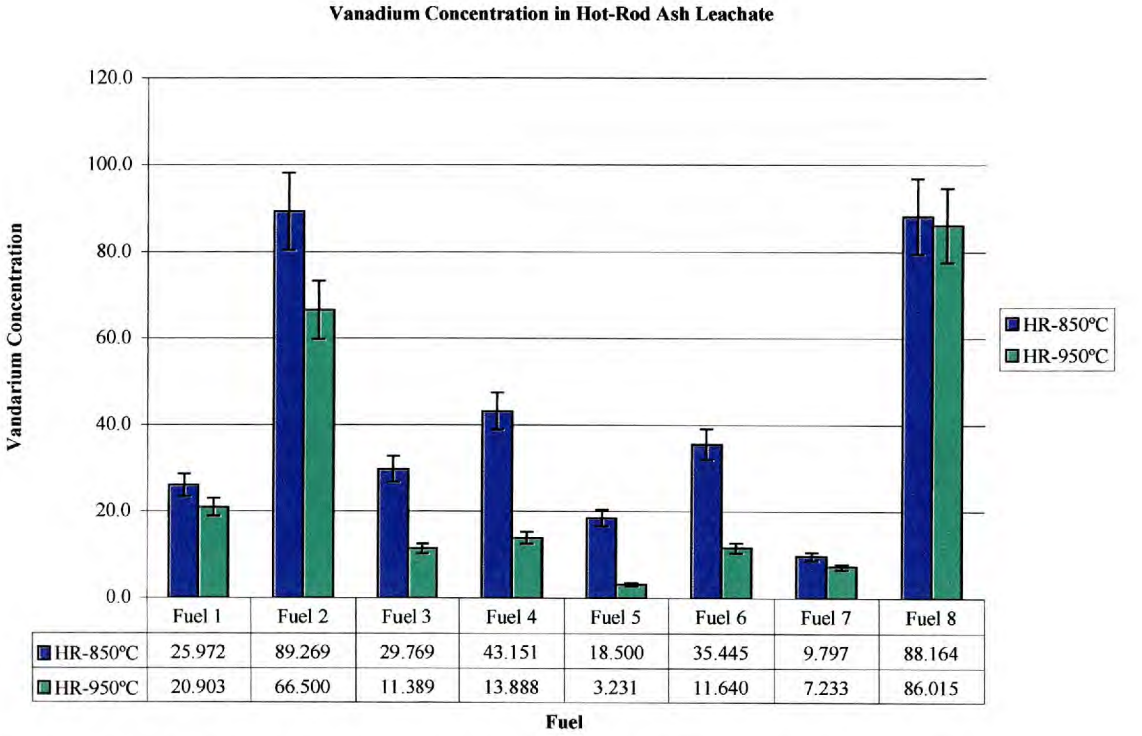
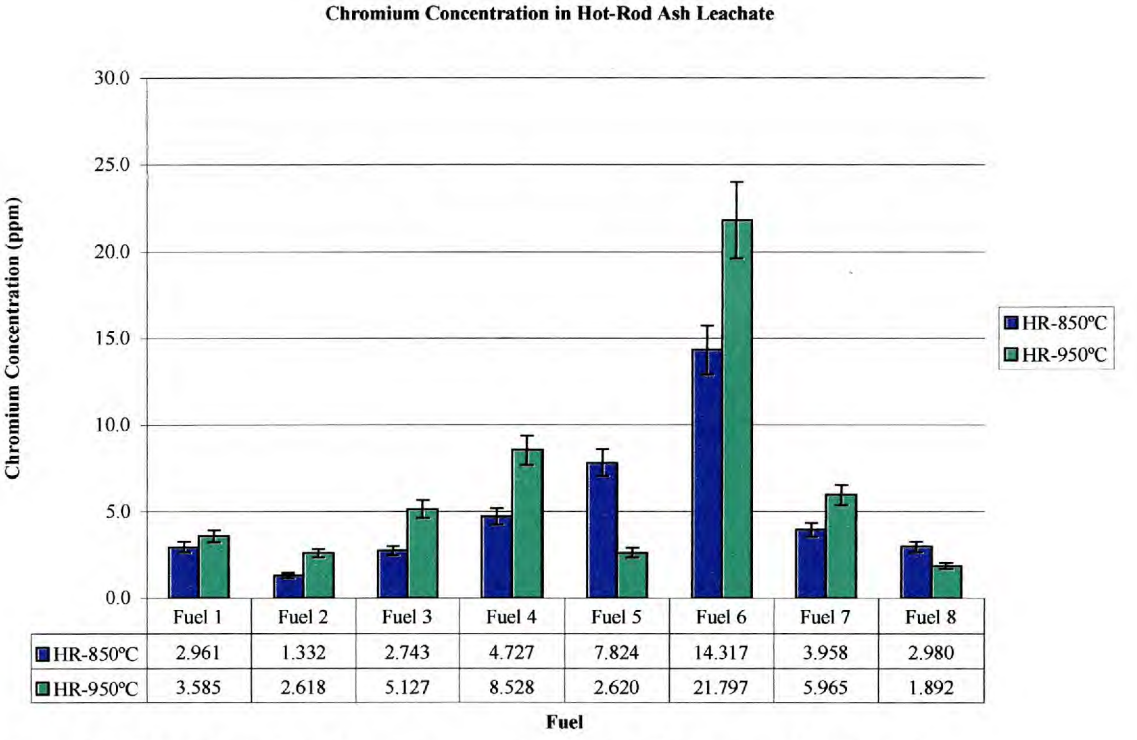
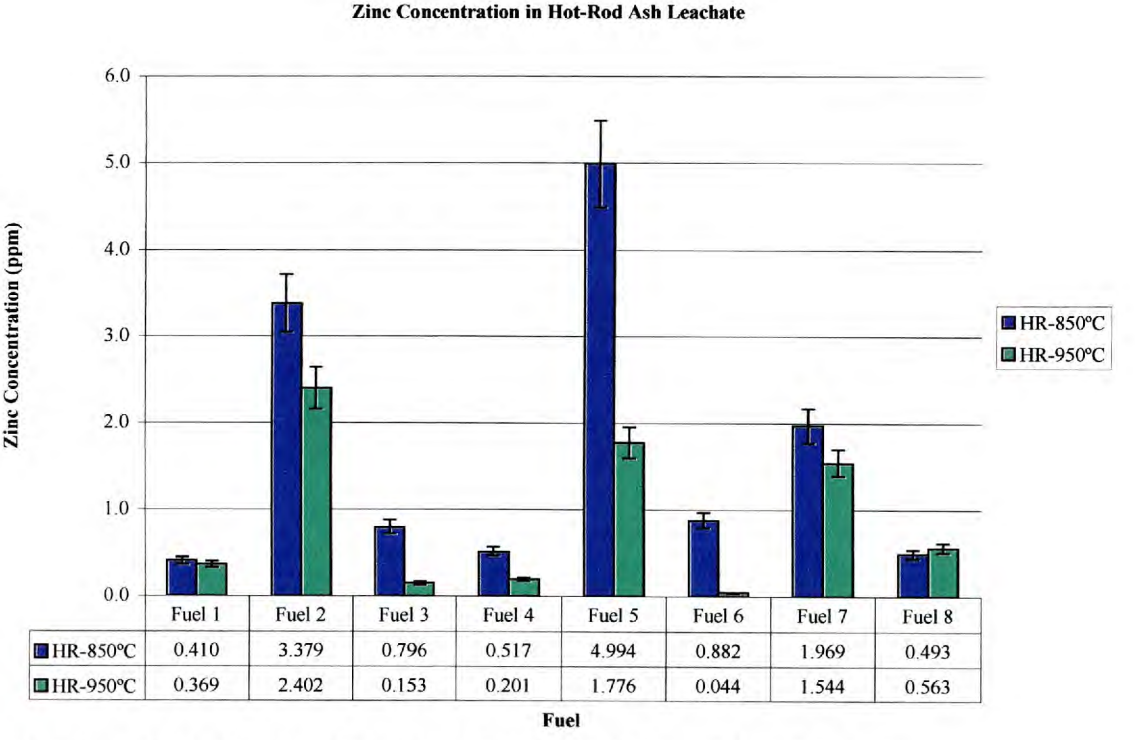


Figure 4.4.38 Vanadium Concentration in Hot-Rod Furnace Ash Leachate



	Fuel 1	Fuel 2	Fuel 3	Fuel 4	Fuel 5	Fuel 6	Fuel 7	Fuel 8
HR-850°C	2.961	1.332	2.743	4.727	7.824	14.317	3.958	2.980
HR-950°C	3.585	2.618	5.127	8.528	2.620	21.797	5.965	1.892

Figure 4.4.39 Chromium Concentration in Hot-Rod Furnace Ash Leachate



	Fuel 1	Fuel 2	Fuel 3	Fuel 4	Fuel 5	Fuel 6	Fuel 7	Fuel 8
HR-850°C	0.410	3.379	0.796	0.517	4.994	0.882	1.969	0.493
HR-950°C	0.369	2.402	0.153	0.201	1.776	0.044	1.544	0.563

Figure 4.4.40 Zinc Concentration in Hot-Rod Furnace Ash Leachate

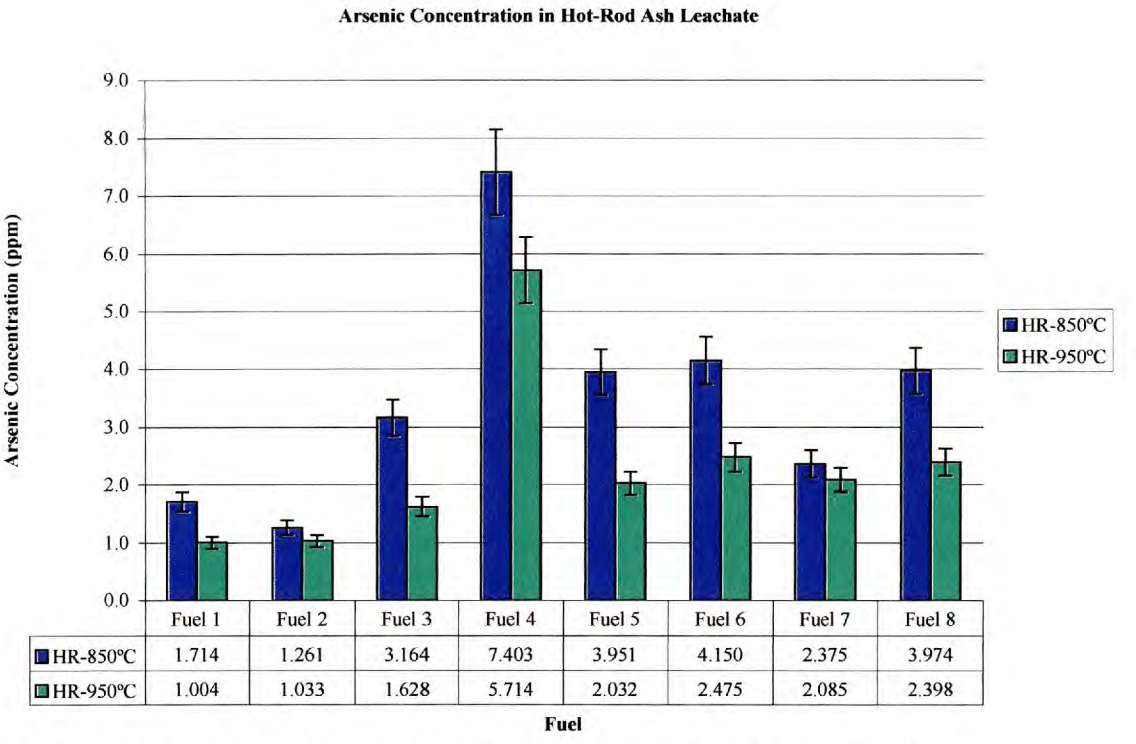


Figure 4.4.41 Arsenic Concentration in Hot-Rod Furnace Ash Leachate

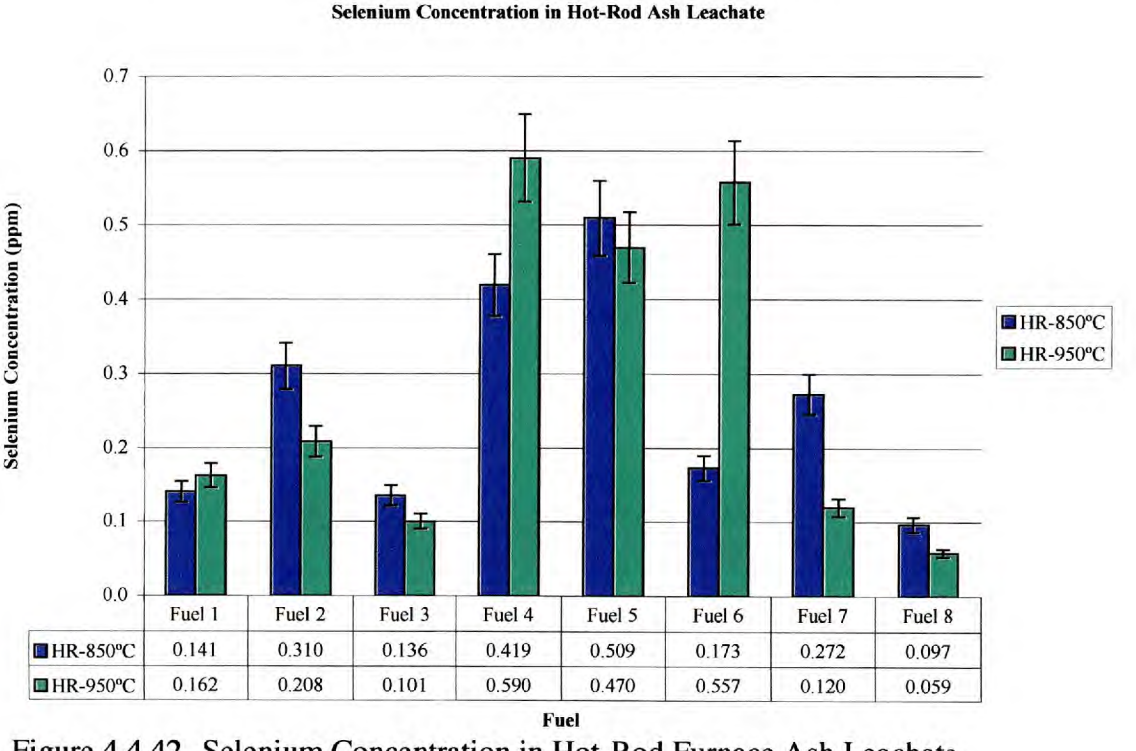
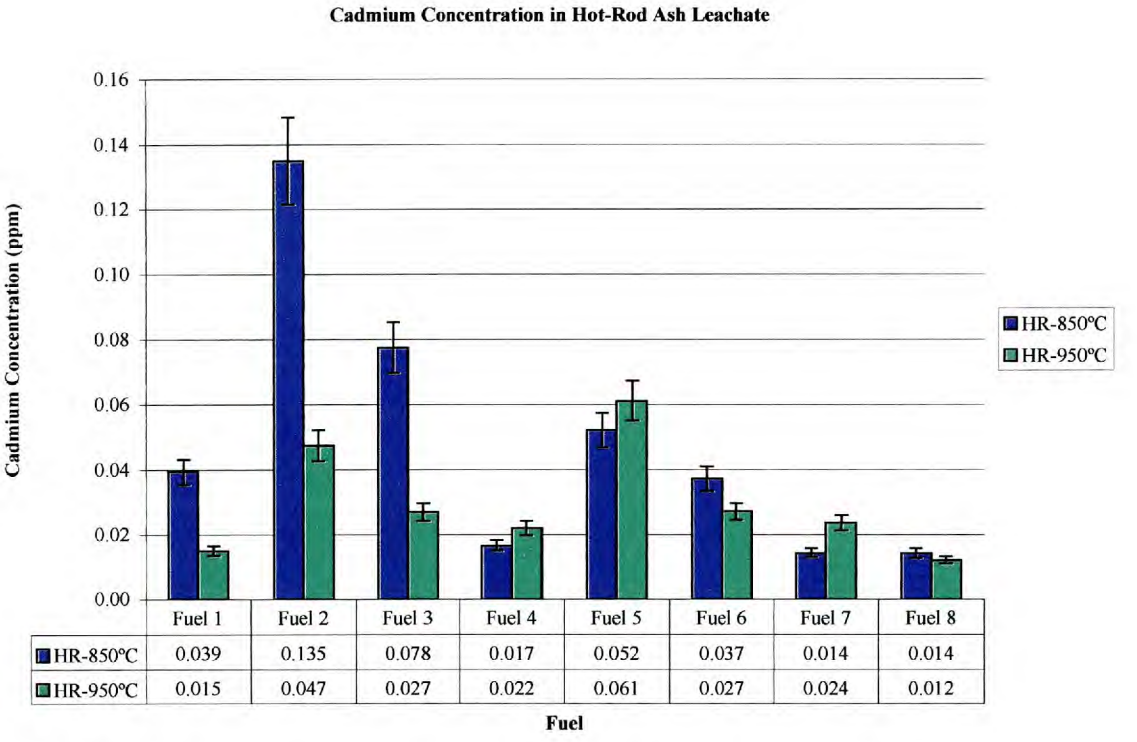
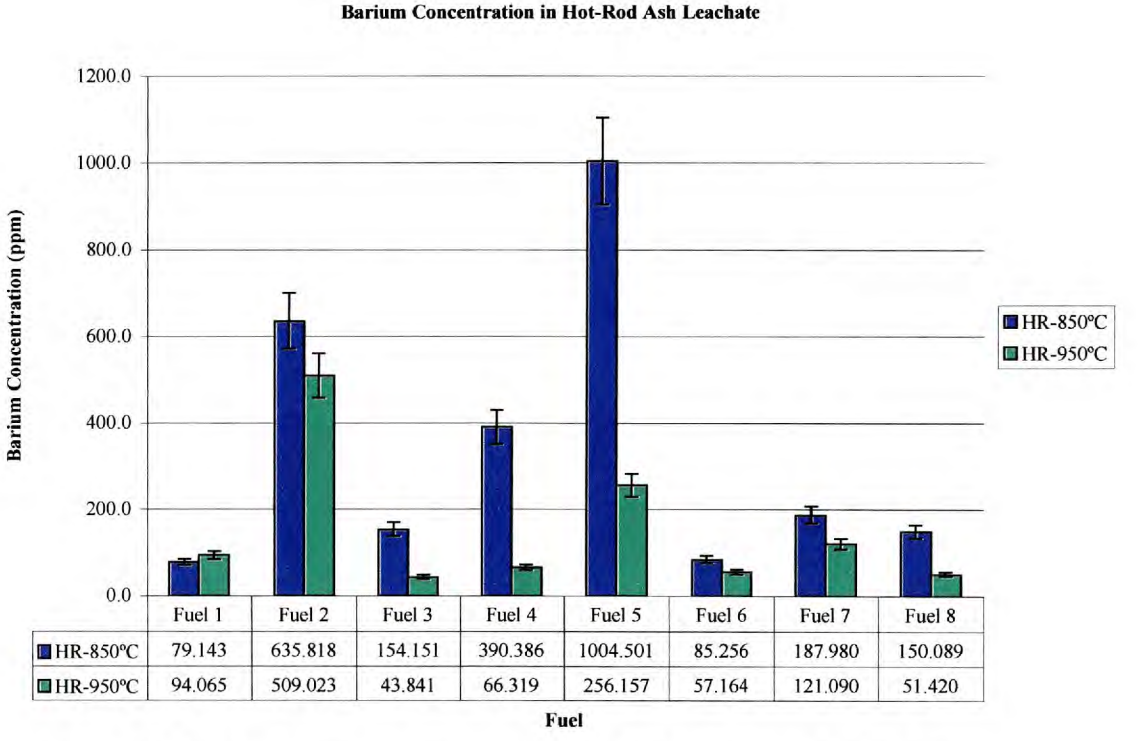


Figure 4.4.42 Selenium Concentration in Hot-Rod Furnace Ash Leachate



	Fuel 1	Fuel 2	Fuel 3	Fuel 4	Fuel 5	Fuel 6	Fuel 7	Fuel 8
HR-850°C	0.039	0.135	0.078	0.017	0.052	0.037	0.014	0.014
HR-950°C	0.015	0.047	0.027	0.022	0.061	0.027	0.024	0.012

Figure 4.4.43 Cadmium Concentration in Hot-Rod Furnace Ash Leachate



	Fuel 1	Fuel 2	Fuel 3	Fuel 4	Fuel 5	Fuel 6	Fuel 7	Fuel 8
HR-850°C	79.143	635.818	154.151	390.386	1004.501	85.256	187.980	150.089
HR-950°C	94.065	509.023	43.841	66.319	256.157	57.164	121.090	51.420

Figure 4.4.44 Barium Concentration in Hot-Rod Furnace Ash Leachate

Beryllium

Overall beryllium in the CERCHAR leachates exceeded limits 20% of the time. The concentration of beryllium in the leachate was below WHO limits for all ashes produced in the hot-rod. In the muffle furnace it exceeded regulatory limits for Fuel 1 and Fuel 2 (the two South African Coals) and for Fuel 5 (South African/Coal and Un-dried Saw Dust) by approximately a factor of 2. In these instances regulatory limits were exceeded at both temperatures. For the remaining fuels in the muffle beryllium was always in allowable concentrations.

Vanadium

Vanadium concentrations were higher than the specified limits 31% of the sample set. Vanadium concentrations in the leachate never exceed limits for hot-rod ashes. For muffle ashes limits were exceeded again for Fuels 1, 2 and 5 but also for fuels 3 & 8. Concentrations were higher by a factor of approximately 2 in all cases except Fuel 8. In this instance vanadium concentration was 4 times higher. Where limits were exceeded this occurred at both temperatures. The remaining muffle furnace leachates contained vanadium below WHO limits.

Chromium

Chromium concentrations exceeded regulatory limits 68% of the time. Chromium exceed regulatory limits in the muffle furnace for all the ashes studied at both temperatures. In the hot rod limits were exceed in Fuels 3 , 4 and 7 at 950 °C , Fuel 5 in leachate from 850 °C ash and Fuel 6 at both temperatures. The degree to which chromium exceeded regulatory limits varied with the fuel and the temperatures. At 950 °C in the muffle furnace, limits were exceed by a larger amount.

Zinc

Zinc concentrations never exceeded regulatory limits, for any temperature, combustion configuration or fuel.

Arsenic

Arsenic always exceed regulatory limits for all fuels, combustion configurations and temperatures. The DAF corrected limit for arsenic is 0.68 ppm. Arsenic concentrations varied between 1.0 ppm and 18.3 ppm for the Fuel 8 muffle furnace ash produced at 850 °C.

Selenium

Selenium exceeded regulatory limits 9.3 % of the sample set. This was for Fuel 2 ash produced in the muffle furnace at both temperatures and Fuel 1 muffle furnace ash at 850 °C. In these instances selenium exceed limits by a maximum factor of 0.5.

Cadmium

Cadmium exceeded regulatory limits on one occasion for Fuel 2 muffle furnace ash at 850 °C and did so by a very small amount (7%).

Mercury

Mercury did not undergo discernable amounts of leaching and therefore never exceeded allowable concentrations.

Barium

Barium exceeded limits 78% of instances. It always exceeded limits in leachates produced from muffle furnace ash and in the hot-rod ashes produced at 850 °C. In some cases barium exceeded limits by a factor of 10.

Lead

Lead exceed limits 48% of the time. As with the other elements this was predominantly in the leachates produced from the muffle furnace. There were no instances of limits being exceeded from hot-rod ashes as it was present below detectable limits. For the muffle furnace ashes leachates limits were exceeded for both temperatures except in the case of Fuel 5, where no limits were exceeded.

4.4.3 Trace Element Content in Leachate Produced from Chilean Ashes

The leaching experiments were carried out as described in section 3.4. Experimental error was calculated in the same manner as for the CERCHAR leachates and this is as shown in section 4.4.2. When depicting the percentage of trace element leached, error calculations were carried out in the same manner as for the CERCHAR leachates.

Results are presented by trace element. Each graph in the following pages shows how the percentage leached of a particular trace element varies with fuel type. Each graph shows the results at both 900° & 1500 °C. As with the CERCHAR fuels the bulk composition of the ashes leached was very similar at the two temperatures. Therefore only the input values for initial trace element content varied in the modelling of each system. The graphs produced to show trace element sensitivity to pH are therefore the same for ashes produced at the two combustion temperatures.

Figure 4.4.47 shows the degree to which trace element quantities of the Kideco-Lemington mixture deviate from their theoretical values. Figure 4.4.48 does so for the Lemington-Allied fuel mixture. A significant deviation from the theoretical value of trace element content would indicate synergistic effects played a part in the leaching process.

As with the CERCHAR ashes, the quantity of mercury leached was below detection limits, and may be considered negligible. Results for mercury are therefore not shown. This is not an indication of mercury's propensity to remain in the ash during leaching. It was not possible to ascertain the extent to which mercury is mobile because of the insignificant quantity of mercury in the ash.

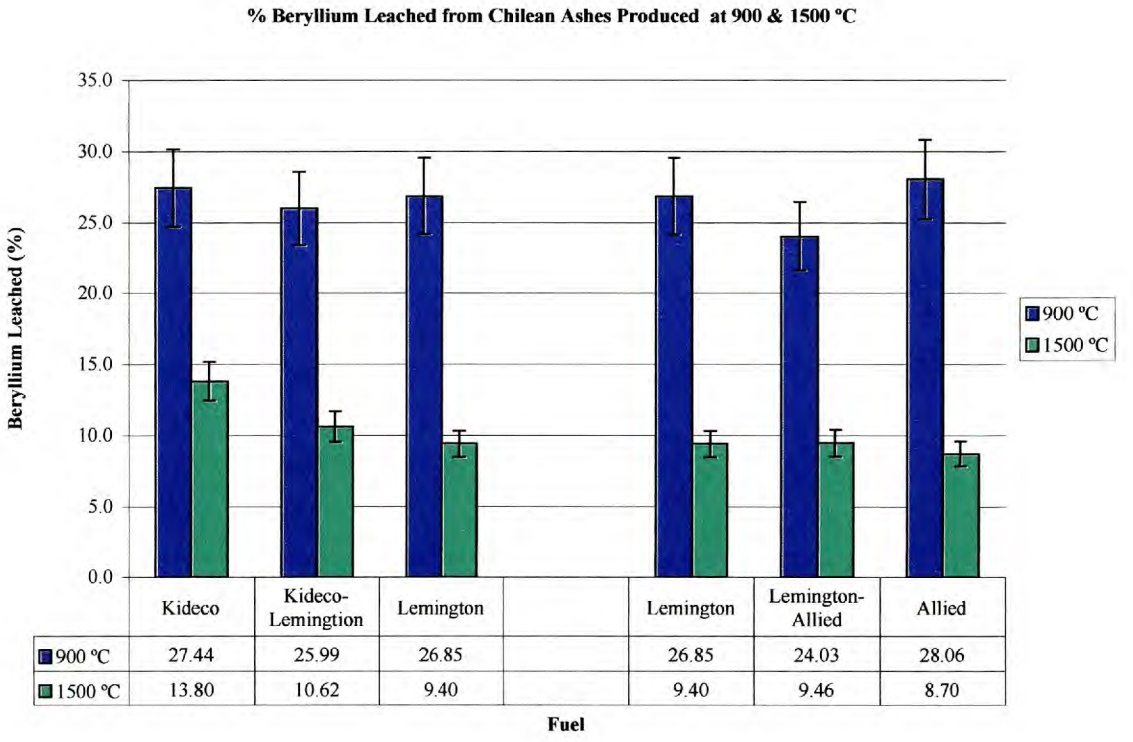


Figure 4.4.38 % Beryllium Leached from Chilean Ashes Produced at 900 & 1500 °C

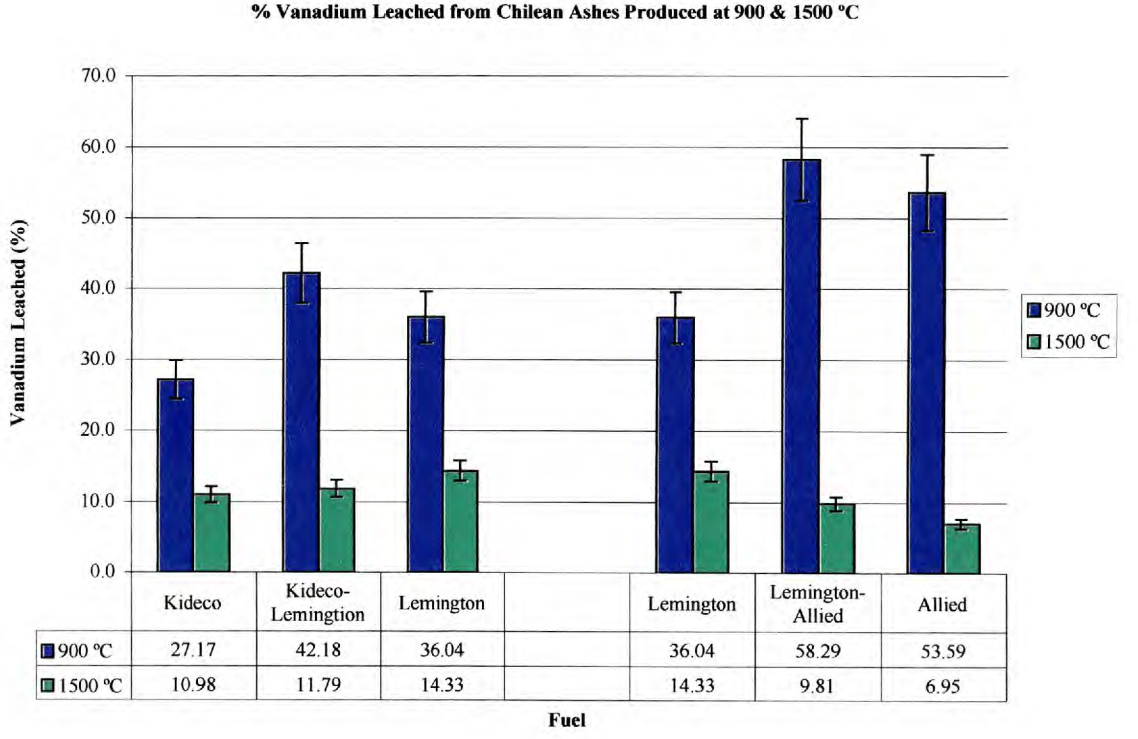


Figure 4.4.39 % Vanadium Leached from Chilean Ashes Produced at 900 & 1500 °C

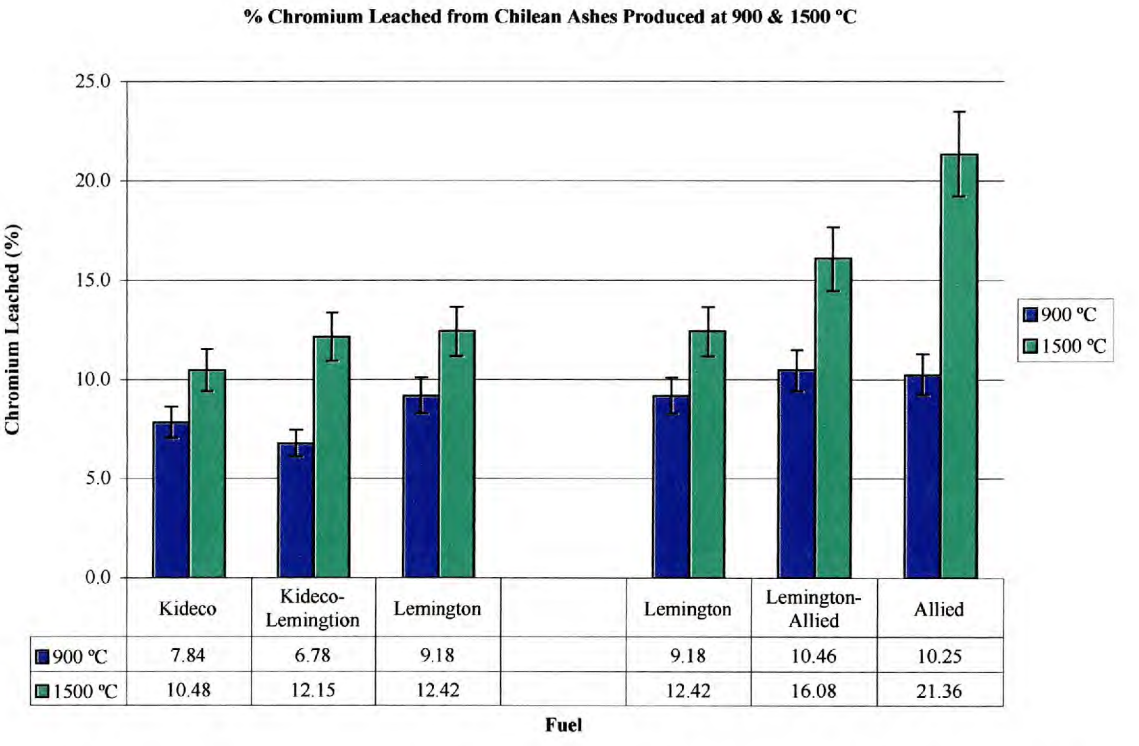


Figure 4.4.40 % Chromium Leached from Chilean Ashes Produced at 900 & 1500 °C

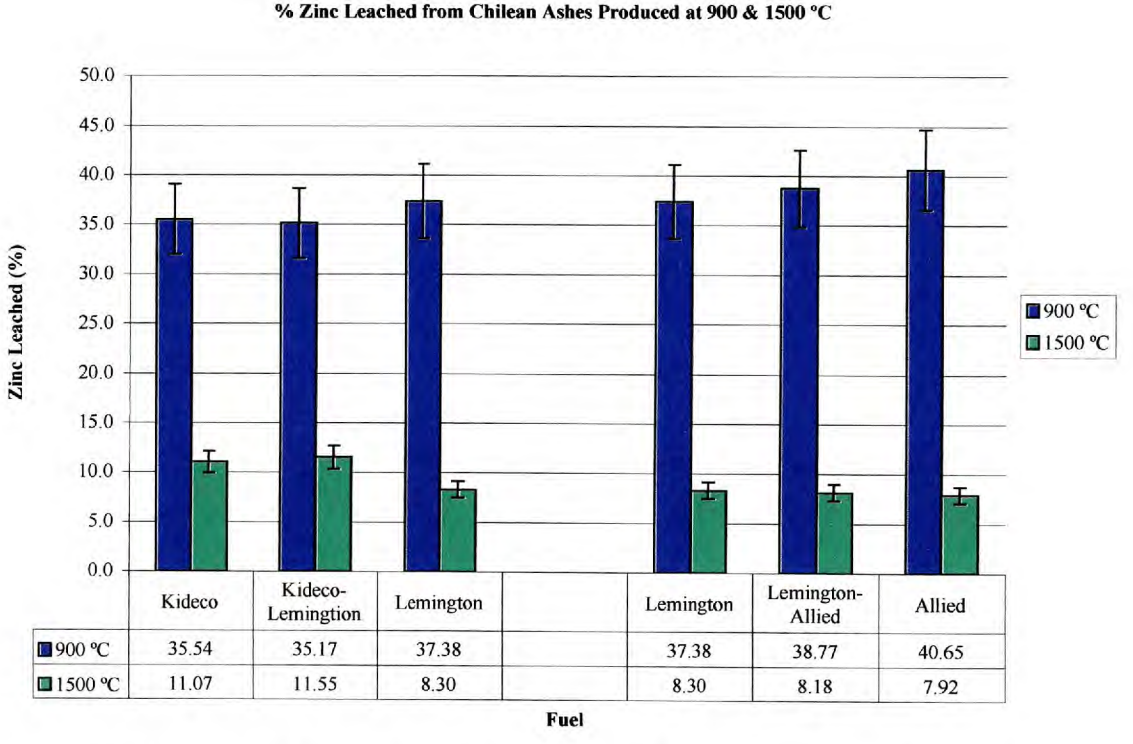


Figure 4.4.41 % Zinc Leached from Chilean Ashes Produced at 900 & 1500 °C

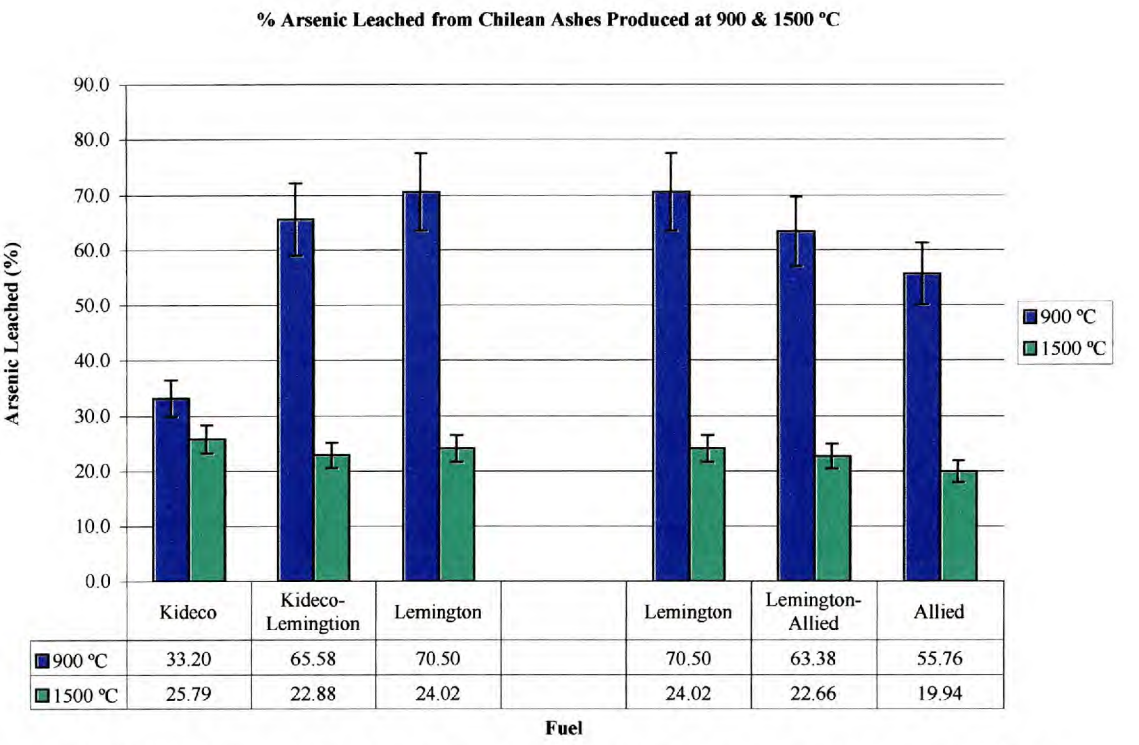


Figure 4.4.42 % Arsenic Leached from Chilean Ashes Produced at 900 & 1500 °C

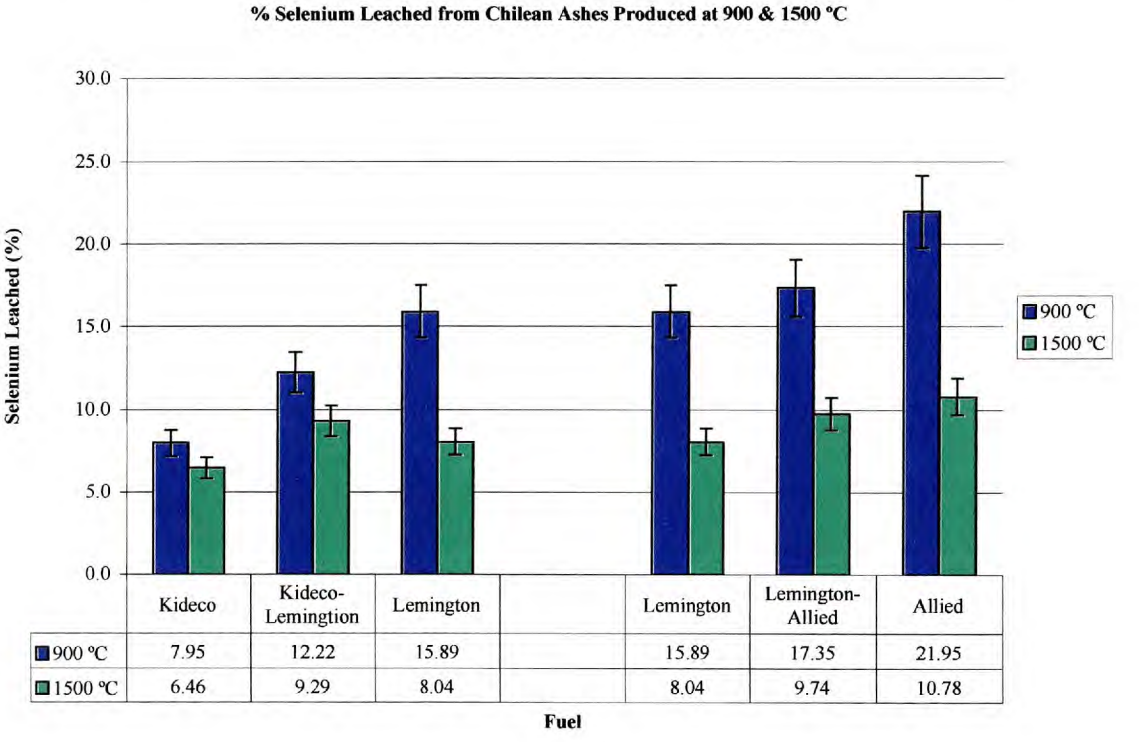


Figure 4.4.43 % Selenium Leached from Chilean Ashes Produced at 900 & 1500 °C

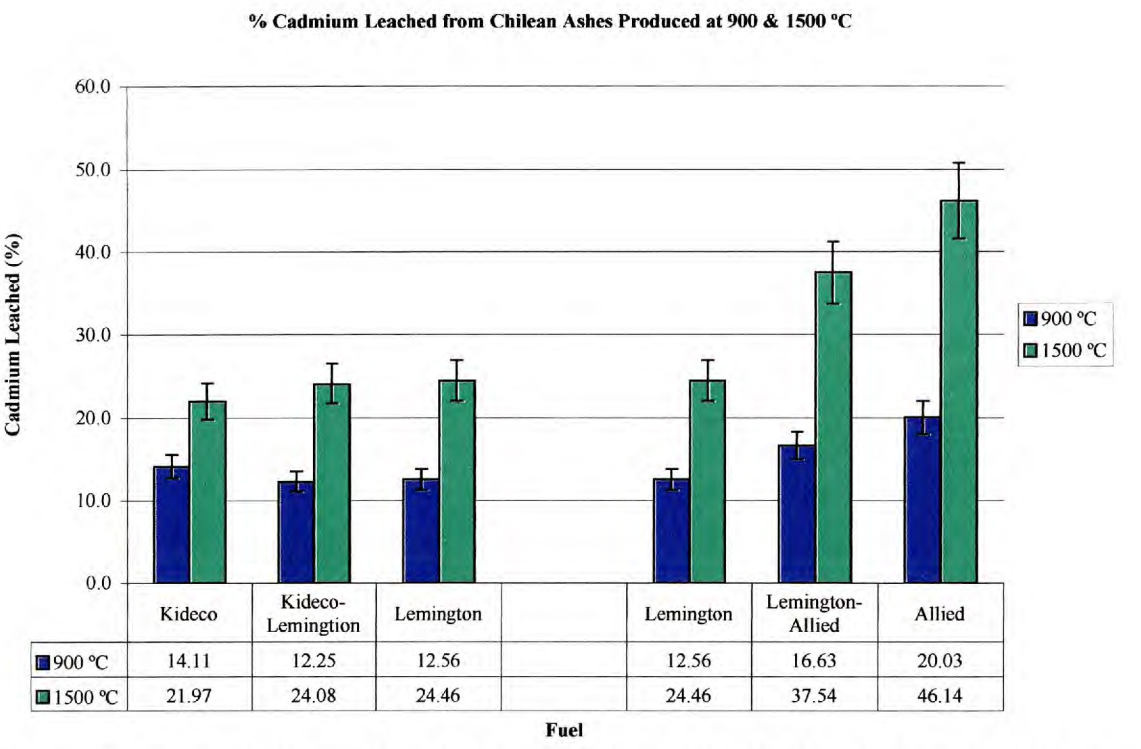


Figure 4.4.44 % Cadmium Leached from Chilean Ashes Produced at 900 & 1500 °C

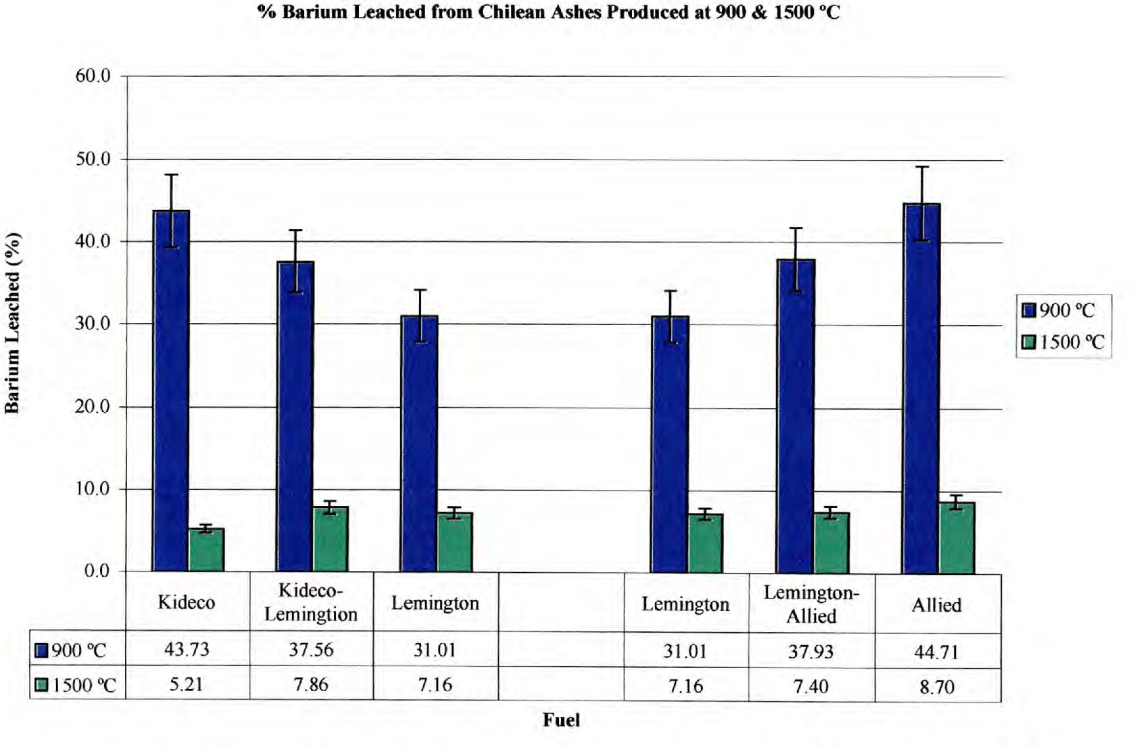


Figure 4.4.45 % Barium Leached from Chilean Ashes Produced at 900 & 1500 °C

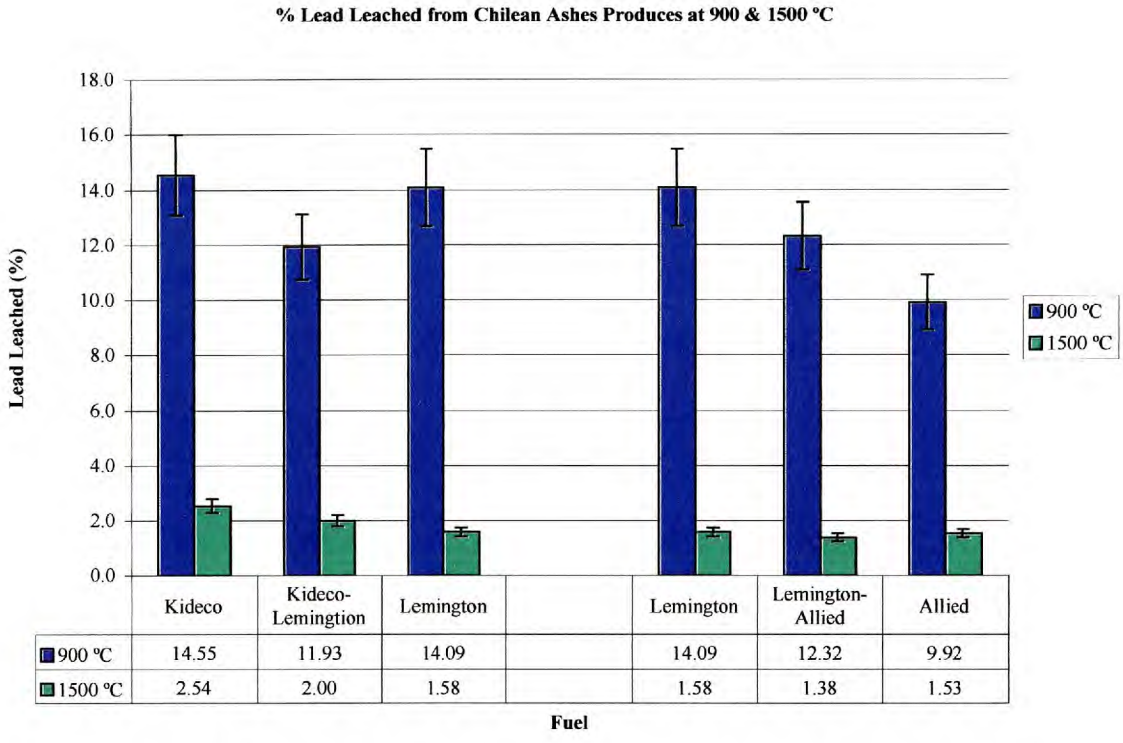


Figure 4.4.46 % Lead Leached from Chilean Ashes Produced at 900 & 1500 °C

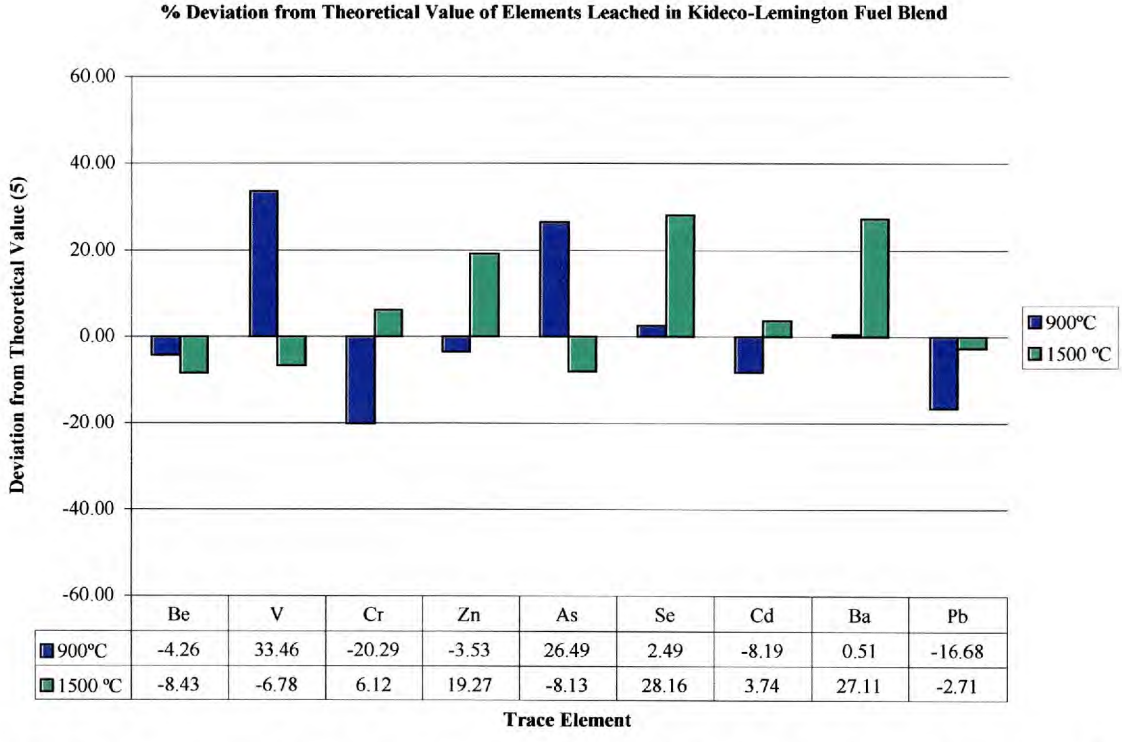
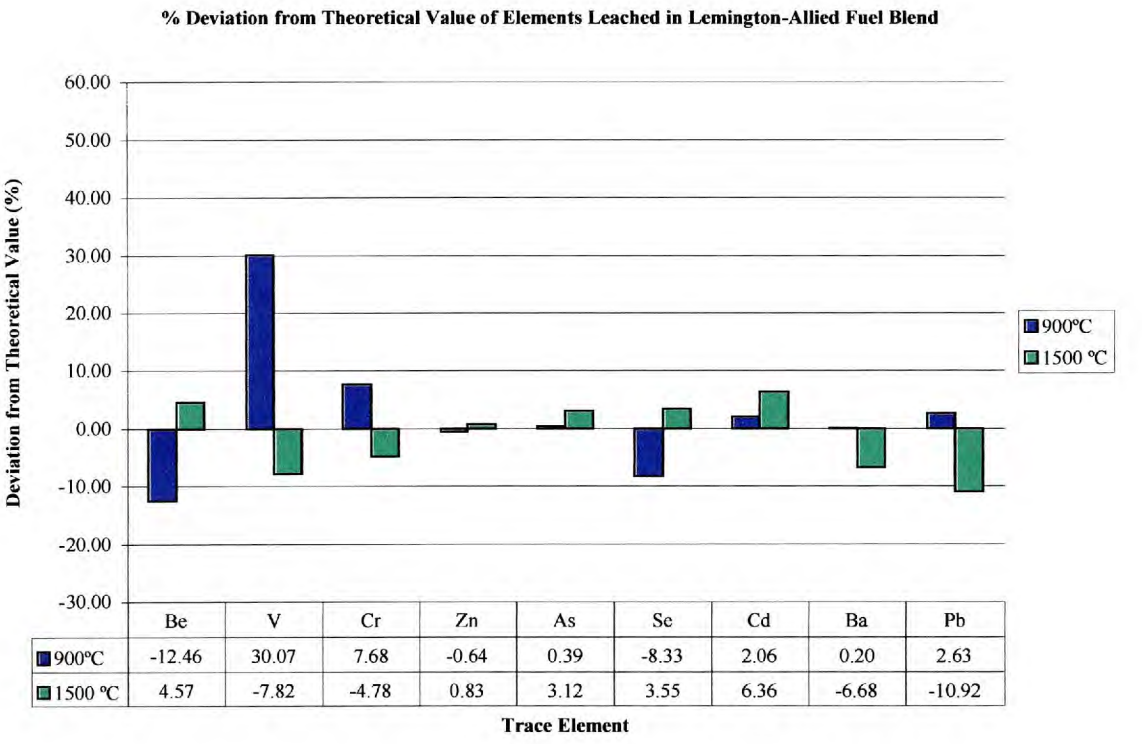


Figure 4.4.47 % Deviation from Theoretical Value for Kideco-Lemington Fuel Blend



	Be	V	Cr	Zn	As	Se	Cd	Ba	Pb
900°C	-12.46	30.07	7.68	-0.64	0.39	-8.33	2.06	0.20	2.63
1500 °C	4.57	-7.82	-4.78	0.83	3.12	3.55	6.36	-6.68	-10.92

Figure 4.4.48 % Deviation from Theoretical Value for Lemington-Allied Fuel Blend

Beryllium in Leachate

For ashes produced at 900 °C beryllium was leached at approximately 25% for each of the fuels. Synergistic effects were therefore not exhibited by mixing fuels. At 1500 °C the quantity of beryllium leached was consistently lower at around 10% for all fuels. These figures imply that the beryllium which was not lost during the combustion process is more strongly fixed/less susceptible to leaching in the 1500 °C ash than in the 900 °C. Figures 4.3.9. and 4.3.10 show the % deviation from the theoretical value of beryllium leached. The deviation in both the Kideco-Lemington mixture and the Lemington-Allied mixture is below the error involved in making the measurement. Therefore any synergistic effects may not be considered significant.

Thermodynamic modelling accurately predicted the quantity of beryllium which would be leached for each fuel, when the final pH of the leachate was an input. The beryllium products formed in the leachate were computed to be Be^{2+}, $BeOH^{+}$ and $BeSO_4$. Beryllium was predicted to sorp quite strongly, to exist as $=FeBe^{+}$.

When the model was allowed to calculate the system pH the percentage leached was slightly over estimated in all cases.

When considering all the fuels studied (CERCHAR & Chilean), at all temperatures and combustion methods, it may be noted that leaching propensity for beryllium is at the lower end of the scale, all percentages for leaching being lower than 50%.

Vanadium in Leachate

At 900 °C the percentage vanadium leached varied from a minimum of 27.17 % for Kideco coal to a maximum of 58.29 % for the Lemington-Allied mixture. At 1500 °C the percentage of vanadium leached falls significantly. The maximum percentage of vanadium leached in this instance is 14.3 % for Lemington coal, with a minimum of 6.95 % for Allied coal. Figures 4.2.9 & 4.3.10 indicate that no synergistic effects are exhibited at 1500 °C. However, at the lower temperature the vanadium leached is 33% lower than the sum of its constituent parts. This is greater than may be attributed to error.

Thermodynamic predictions predicted underestimated the degree to which vanadium would be leached at 900 °C but accurately did so for the leachates produced from 1500 °C ashes. Neither vanadium sorption nor precipitation were predicted to occur at any pH. Vanadium was predicted to occur as $H_2VO_4^-$, and VO_2^+ in solution.

Chromium in Leachate

Chromium showed a high retention level in the leachate produced from 900 °C ashes. Chromium was leached at a maximum level of 10.46 % for the Lemington-Allied fuel blend and 6.78 % for the Kideco-Lemington leachate. Chromium was unique amongst the Chilean fuels in that its propensity to leach increased with increasing temperature. This increase in leaching with increasing temperature was more predominant in the Lemington-Allied group of fuels. This behaviour is consistent with results obtained in the CERCHAR fuels. No synergistic effects were exhibited in either of the fuel blends, with regard to chromium leaching.

As with the CERCHAR fuels, chromium leaching was estimated by MINTEQA2 to be higher than the empirical values obtained. The minimum percentage of chromium leached was when the pH of the leachate was at 4.7, giving a % leached of 15%. The characteristics of chromium mobility in all the systems studied were not clearly reflected by modelling.

Zinc in Leachate

The degree to which zinc was leached from the ash was found to be constant amongst the different fuels and strongly temperature dependent. At 900 °C zinc leaching was in the range of 35-40%. This was reduced to a range of 8-11% at 1500 °C. This again indicates an increased stability of the ash matrix , with respect to leaching at the higher temperature. This may either be due to the strength with which zinc is bound to matrix at this temperature, or with the fact that there is less zinc initially present and therefore less availability for leaching. As the zinc quantities leached from each ash may be considered constant no synergistic effects of mixing fuels could be imputed.

There was excellent agreement between the values predicted for leaching by MINTEQA2 and those determined through experiments at 900 °C. The pH of the leachate in the 1500 °C ashes was 1 pH unit higher than the 900 °C ashes, with the exception of Kideco coal (exhibiting a pH difference of 0.6 units). The increased pH of the higher temperature ash corresponds to the lower leaching percentage in the region of 10%. At the pH observed for all the leachates, the predominant species would be zinc acetates (in the region of 60%) the remainder being Zn^{2+}, and $ZnSO^4$(aq).

Arsenic in Leachate

The degree of arsenic leached was shown to be strongly temperature dependent for all fuels except Kideco coal. At 900 °C the percentage of arsenic leached was within a narrow range of 33.2 % to 75.5 %. At 1500 °C the percentage of arsenic leached was more constant, being within a narrow range of 19.8% to 25.8 %. This once more indicates that leaching of high temperature ash produces consistent, non-fuel dependent results.

Thermodynamic modelling of the system agreed well at both temperatures, except for the Kideco coal at 900 °C. At a pH in the region of 5, exhibited by the 900 °C ash leachate, the it was expected that 60% of the zinc would be leached. At the pH region of 6 leaching propensity decreased to 20% with all of the beryllium expected to exist as a precipitate in the solution after a pH of 6.8. In the pH range of the leachates arsenic was predicted to form $H_2AsO_4^-$ and $H_3AsO_4^-$ in solution.

Selenium in Leachate

The leachability of selenium at both temperatures was at the lower end of the scale, with a maximum of 22.0 % selenium leached. As with the other trace metals selenium leaching was temperature dependent and showed a constant leaching propensity in the 1500 °C ash leachate (the percentage leached being within a range of 6.5 and 10.7 %.) At 900 °C the percentage leached was fuel dependent and varied from 8.0 % to 22.0 %. The Kideco-Lemington fuel mixture showed a higher than expected quantity of selenium in its leachate, given the proportions in which it was mixed. 28.2 % more selenium was leached than the expected value. No synergistic effects were exhibited by the Lemington-Allied fuel mixture. This implies that if any synergy does exist in the Kideco-Lemington fuel, this is fuel rather than trace element dependent.

Modelling results with respect to selenium were not in any concurrence with experimental results. It was predicted that selenium would be completely leached after a pH of 4.9. The inaccuracy in the results may be due to the low levels of selenium initially present in the fuel, and subsequently the ash. Selenium was predicted to exist as the $HseO_4^-$ ion in solution, with small quantities sorbed as $=FeSO_4$-.

Cadmium in Leachate

The cadmium present in the Chilean ashes underwent low levels of leaching, ranging from 12.3-20.0 % for 900 °C ashes and 22.0 –46.1 % for 1500 °C ashes. The fuel mixtures did not exhibit synergy with respect to cadmium leaching but cadmium leaching did appear to be a function of temperature. The percentage of cadmium leached increased with increasing temperature by approximately a factor of 2 in all fuels.

The only other element which exhibited this behaviour is chromium. The increase may be due to a change in speciation of the cadmium in the ash at 1500 °C which was more susceptible to leaching.

Modelling of the systems studied showed that cadmium was highly susceptible to leaching up to a pH of 4.5 after which cadmium retained was strongly a function of increasing pH. The modelling results accurately predicted the experimental results obtained for the 900 °C leachate, but slightly overestimated the 1500 °C ash cadmium retention. Cadmium was predicted to exist as the Cd^{2+} ion in solution with no precipitation and no sorption predicted.

Barium in Leachate

The barium trend was typical to most of the trace elements studied in the Chilean fuels i.e. a comparatively low percentage leached and a strong temperature dependence on the percentage leached. The percentage barium leached at 900 °C was in the range 31.0%, for lemington fuel to 44.7% for Allied fuel. There was a sharp decrease in the quantity of barium leached for 1500 °C ashes, the range being 5.21 to 8.7 %. No synergistic effects with regard to barium were observed in the fuel blends.

Modelling showed that barium was would be susceptible to high degrees of leaching at low PHS up to a pH of 4.5, with no leaching after a pH of 8. At the pH of the leachates produced from 900 °C ashes, approximately 40% of the barium was expected to leach, concurring with experimental results. Modelling also predicted the low values of barium in the leachate of the 1500 °C ashes. Modelling predicted that barium would be present in the form of Ba^{2+} ions and barium acetate. As with the CERCHAR fuels barium was predicted to be strongly sorbed and this may contribute to the low levels of barium leached.

4.4.3.1 Trace Element Content in Leachate in Relation to Regulatory Constraints

The figures below show the concentrations of trace elements found in the Chilean fuels. A discussion then follows of whether this concentrations fall beneath WHO limits for groundwater. The discussion refers to DAF corrected results as discussed in Section 4.4.2.1.

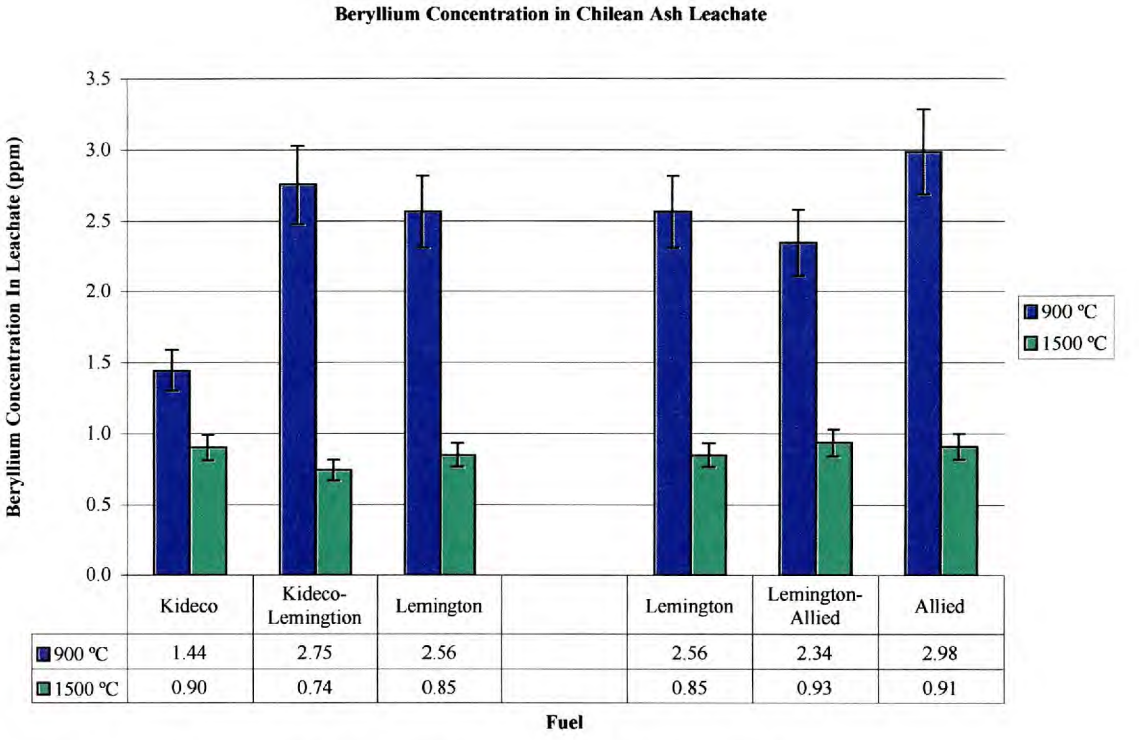


Figure 4.4.49 Beryllium Concentration in Chilean Ash Leachate

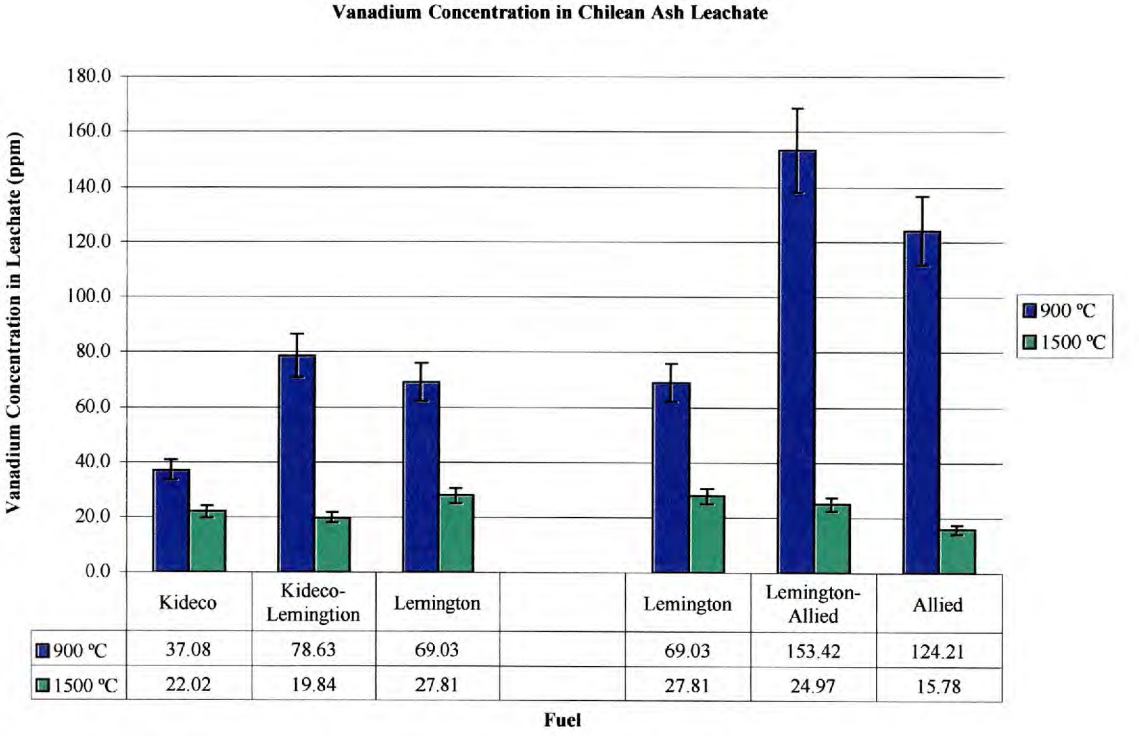
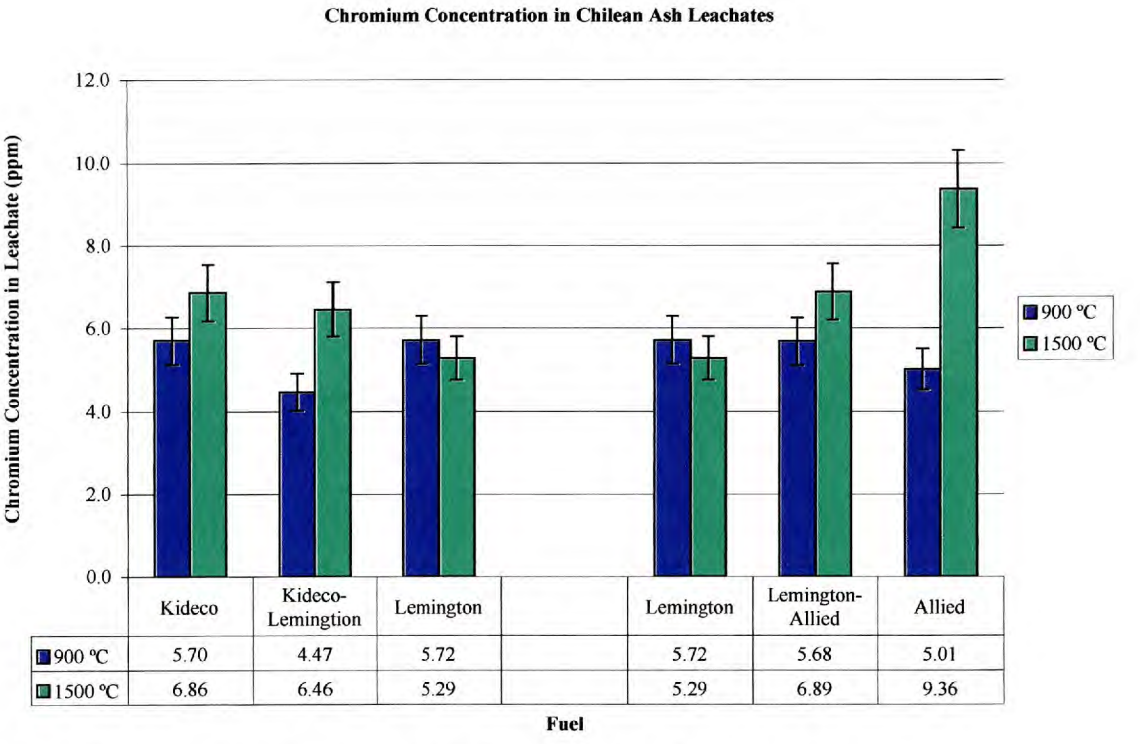


Figure 4.4.50 Vanadium Concentration in Chilean Ash Leachate



4.4.51 Chromium Concentration in Chilean Ash Leachate

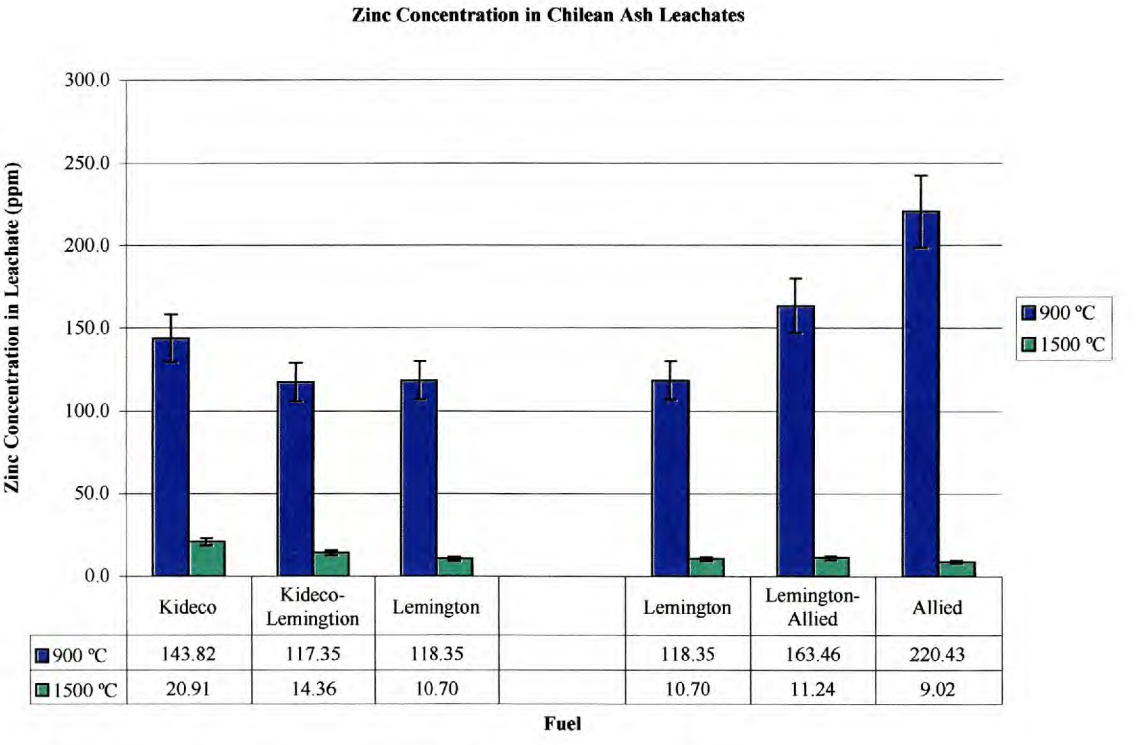


Figure 4.4.52 Zinc Concentration in Chilean Ash Leachate

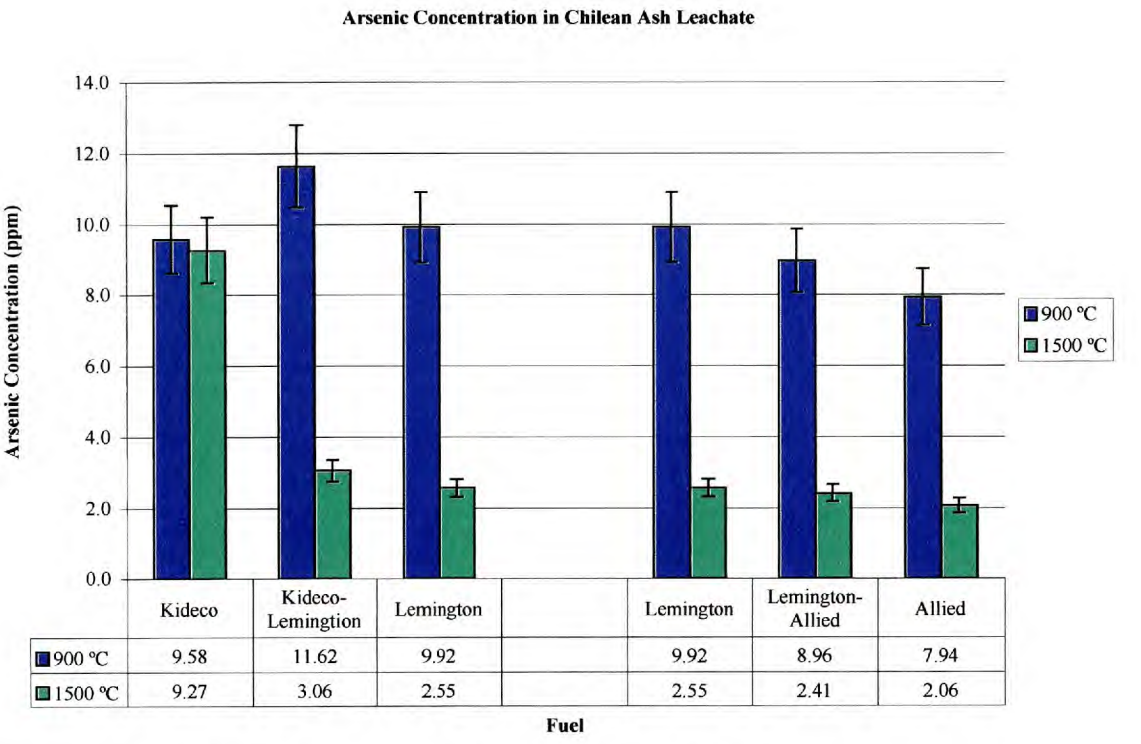


Figure 4.4.53 Arsenic Concentration in Chilean Ash Leachate

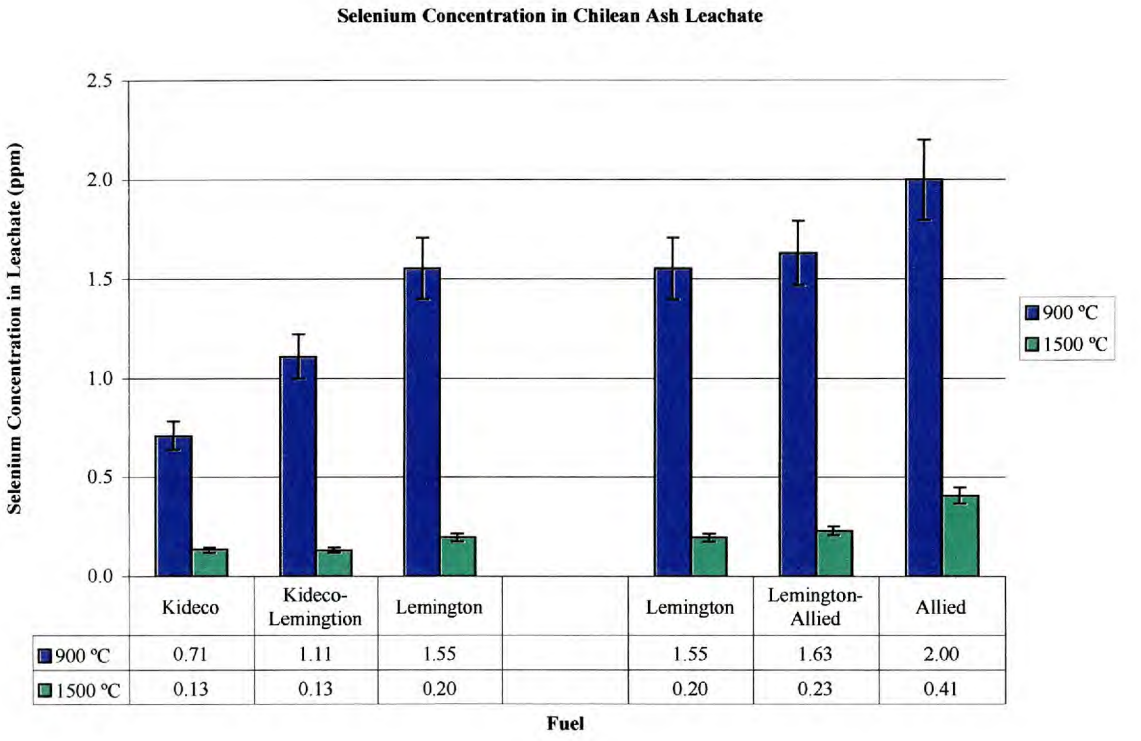


Figure 4.4.54 Selenium Concentration in Chilean Ash Leachate

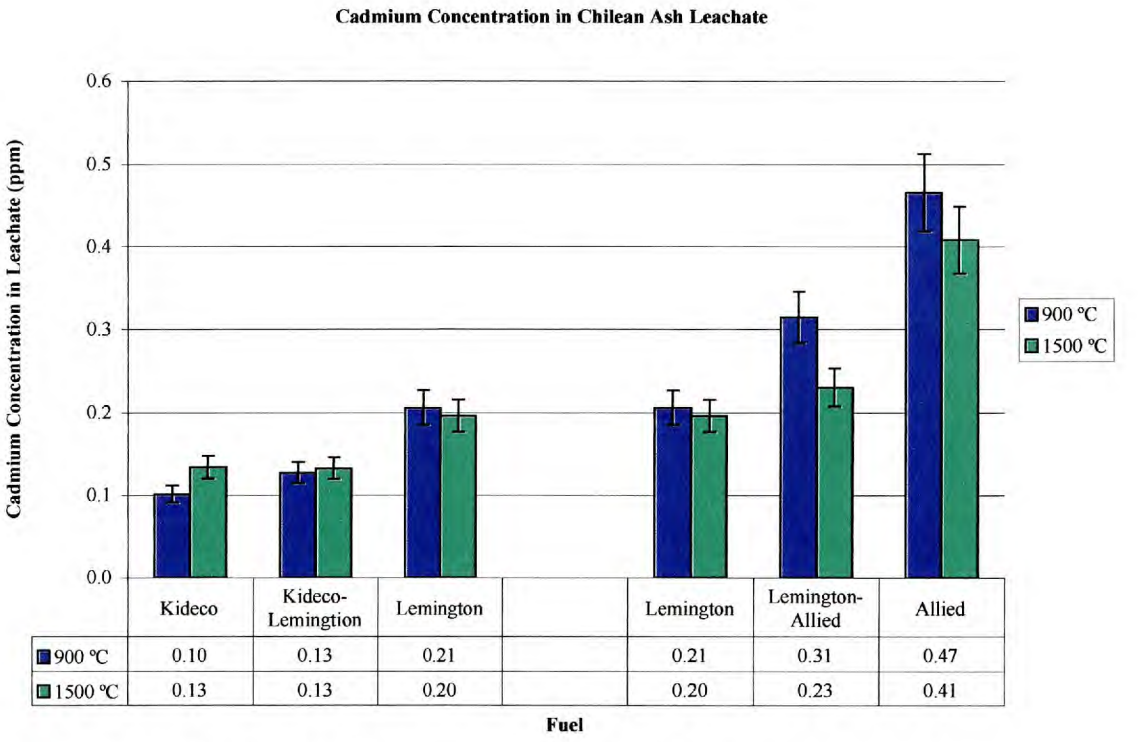


Figure 4.4.55 Cadmium Concentration in Chilean Ash Leachate

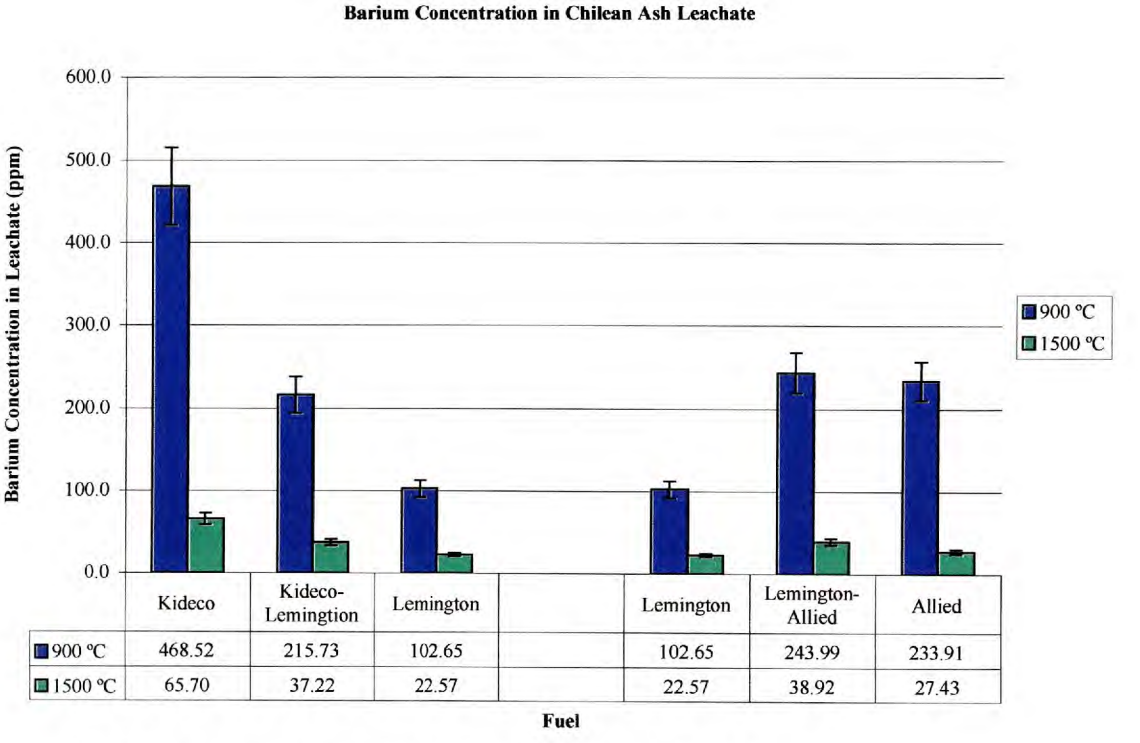


Figure 4.4.56 Barium Concentration in Chilean Ash Leachate

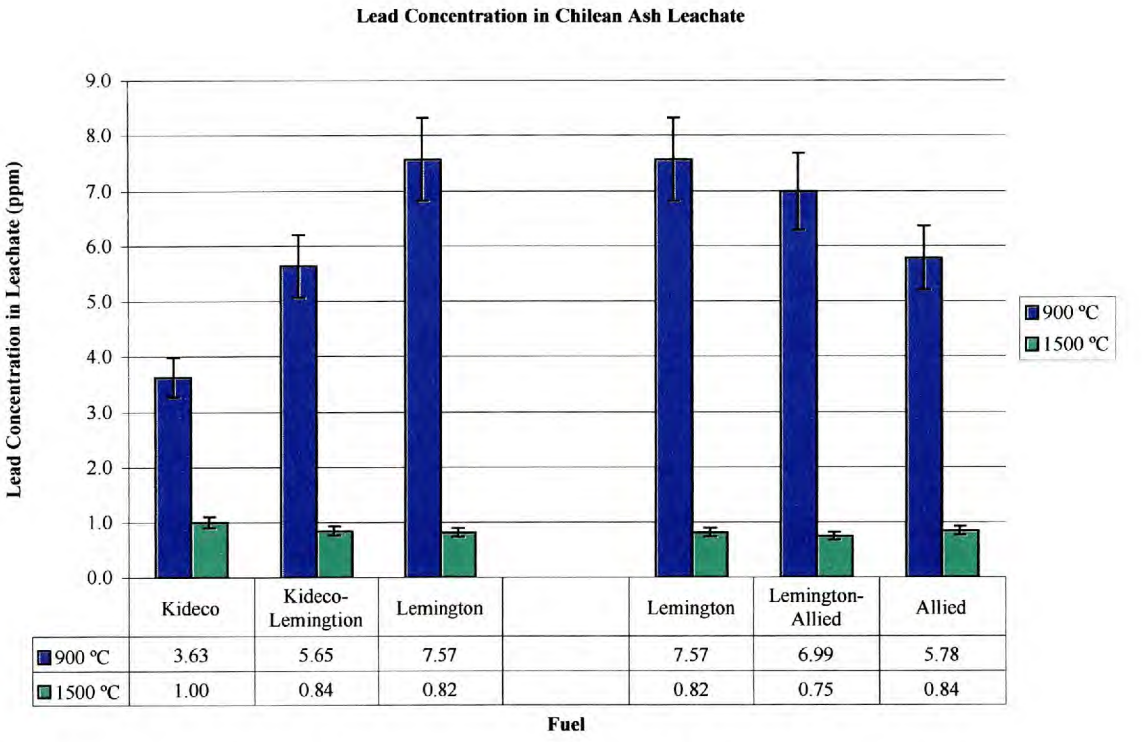


Figure 4.4.57 Lead Concentration in Chilean Ash Leachate

Beryllium

Beryllium concentrations fell below WHO limits for all the fuels studied at both temperatures.

Vanadium

Vanadium concentrations were also within regulatory limits in all cases.

Chromium

Chromium exceeded regulatory limits in all instances. In comparison to CERCHAR fuels concentrations were only marginally higher than the maximum WHO level.

Zinc

As with the previous fuel set, Zinc in leachate was below stipulated harmful levels in all the fuels studied at both temperatures.

Arsenic

As with the results for the CERCHAR fuels arsenic concentrations exceeded regulatory limits in all leachate samples studied. The degree to which arsenic exceeded limits was as high as in the CERCHAR fuels; in some instances limits were exceeded by a factor of 20. Limits were exceeded by a smaller quanity in the leachates produced from 1500 °C ashes, to those obtained from 900 °C ashes.

Selenium

Selenium exceeded limits in 40% of cases, namely in leachates from ashes which saw 900 °C. Kideco ash did not have selenium exceed regulatory limits for either temperature. Selenium concentrations exceeded limits by a maximum of a factor of 2.

Cadmium

Cadmium exhibited the must arbitrary behaviour with regard to exceeding regulatory safety limits. It exceed limits for Lemington Coal, Lemington-Allied Coal, and Allied coal at 900 °C. At 1500 °C it exceeded limits for Lemington-Allied Coal and Allied coal only. The degree to which cadmium exceeded regulatory limits was marginal, in comparison with other elements, being a maximum of 15%.

Barium

Barium exhibited a similar trend to selenium in that all the leachates produced from 900°C ash showed higher the allowed concentrations. At 1500 °C all the barium concentrations were below specified limits. Kideco coal showed the greatest quanity of chromium, being 4 times higher than limits. This was contrary to the previous fuel set where barium exceeded limits by a great amount for all fuels.

Lead

Lead also showed a tendency to exist in higher than allowable limits in leachates from 900 °C ashes. The lead levels in 1500 °C ashes were lower than stipulated limits. In the instances where lead exceeded limits this was by a maximum of 30%.

5.0 SUMMARY

The primary aim of this study was to assess how trace element retention in ash, and its subsequent leaching from the ash vary with certain parameters. These parameters were fuel type, combustion temperature and combustion method. The second aim of this study was to assess the toxicity of the leachates obtained, given accepted maximum safe limits. This section summarises and categorises the results presented in Section 4.

First the trace element content of the raw fuels is given. These results have been given with an emphasis on the order of magnitude a particular element is present in the fuel. Following this, the results of the trace element retained in the ash, after combustion are categorised to show any trends observed. Trends with regard to trace element retention as a function of fuel type, combustion temperature and combustion method are presented for the CERCHAR and Chilean fuels. This is then done for the trace element leached from the ashes. Finally the results of the absolute values of trace element leached are summarised with an emphasis on regulatory limits.

5.1 Trace Element Concentration in the Raw Fuel

The raw fuels studied contained trace elements in varying quantities but certain broad trends could be observed as shown in Tables 5.1 and 5.2 below. Table 5.1 shows the abundances of trace metals in the CERCHAR fuels and table 5.2. the Chilean fuels. These tables categorise the abundance of each trace element in each fuel, within four categories namely: elements which are present in less than 1ppm, those between 1 and 10 ppm, those between 10 & 100 ppm and finally elements which are more than 100 ppm of the fuel.

As may be seen from the tables, the trace metals show a broad trend. This trend with small exceptions holds true for both the CERCHAR and the Chilean fuels. Cadmium and mercury are present in the smallest quantities, being generally below 1 ppm. The elements beryllium, and selenium are usually present in between 1 and 10 ppm, whilst arsenic overlaps this category with the 10 to 100 ppm category. Chromium and lead are usually present in this category whilst barium is always present in quantities above 100 ppm. Zinc and vanadium always exist above 10 ppm in all the fuels. The trace element abundance generally follows this trend for the fuels studied:

$$Hg\ ,\ Cd < Be,\ Ar,\ Se < V,\ Cr,\ Pb,\ Zn < Ba$$

FUEL	[TE]<1 (ppm)			1< [TE] <10 (ppm)					10< [TE]<100 (ppm)					[TE]>100 (ppm)			
South Africa Coal '97	Hg	Cd		Be	As	Se			V	Cr	Pb	Zn		Ba			
South Africa Coal '99	Hg			Be	As	Se		Cd	V	Cr	Pb	Zn		Ba			
Frey. Coal Slurry / SA 'Coal 99		Cd		Be	As	Se	Hg		V		Pb			Ba	Zn	Cr	
Frey. Schlamms / Frey. Coal Slurry	Hg	Cd		Be		Se			V	Cr	Pb		As	Ba	Zn		
SA Coal '97 / Wet Saw Dust		Cd		Be	As	Se	Hg		V	Cr	Pb	Zn		Ba			
Frey. Coal Slurry /Saw Dust	Hg	Cd		Be	As	Se			V		Pb			Ba	Zn	Cr	
SA Coal '97/ Undried Bark	Hg		Se	Be				Cd	V	Cr				Ba			
Frey. Schlamms /Frey. Coal Slurry/ Petroleum Coke	Hg	Cd		Be		Se				Cr			As	Ba	Zn	Cr	Pb

Table 5.1 Trace Element Concentrations in the Raw CERCHAR Fuels With Emphasis on Order of Magnitude

FUEL	[TE]<1 (ppm)		1< [TE] <10 (ppm)				10< [TE]<100 (ppm)				[TE]>100 (ppm)		
Kideco Coal	Hg	Cd	Be		Se		Cr	As	Pb		V	Zn	Ba
Kideco-Lemington Coal Blend	Hg	Cd	Be		Se		Cr	As	Pb		V	Zn	Ba
Lemington Coal	Hg	Cd	Be	As	Se	Cr			Pb	Zn	V		Ba
Lemington Allied Coal Blend	Hg	Cd	Be		Se		Cr	As	Pb		V	Zn	Ba
Allied Coal	Hg	Cd	Be	As	Se		Cr		Pb		V	Zn	Ba

Table 5.2 Trace Element Concentrations in the Raw Chilean Fuels With Emphasis on Order of Magnitude

5.2 Trace Element Retention in Ashes

When assessing the trace element retention in the CERCHAR and Chilean fuels quantitatively, it was not possible to develop a hierarchy of elements based on degree of retention. Retention was very much a function of fuel. The two exceptions to this rule were selenium and mercury which were very volatile in all experiments conducted. Selenium retention was always below 24.5 % and mercury retention always less than 8.3%.

5.2.1 Trace Element Retention as a Function of Temperature

The results section 4.3 quantified the trace element retention after fuel combustion. Tables 5.3 and 5.4 show the trends which were observed from these results as a function of temperature. These tables allow the following observations to be made:

- With a temperature difference of 100 °C from 850 – 950 °C the tendency for trace element retention to vary occurs in 11.9% of the sample set. Therefore, the temperature change does not affect trace element retention to a great extent. When the temperature differential is higher, as for the Chilean fuels the change in temperature reduces the trace element retention for 25% of the sample set.

- For the CERCHAR fuels mercury, chromium and lead are the elements most affected by the temperature increase, whilst for the Chilean fuels it is zinc and cadmium. As the results are not consistent amongst the two fuel groups, this implies that the reduced retention with higher temperature is fuel dependent, rather than trace metal specific, presumably due to differing modes of occurrence of individual elements.

- No fuel shows a significantly higher propensity to retain trace metals more than any other, at different temperatures. The maximum number of trace elements which showed a variation in retention with temperature were 3 for any particular fuel.

- The combustion method does not appear to affect whether trace element retention is a function of temperature. A change in retention with temperature appears 12.5% of instances in the muffle furnace and 10.0% of instances in the Hot-rod reactor.

Fuel	Reactor	Be	V	Cr	Zn	As	Se	Hg	Cd	Ba	Pb
South Africa Coal '97	MF	-	-	↓	-	-	↓	-	-	-	-
	HR	↑	-	-	-	-	-	↓	-	-	-
South Africa Coal '99	MF	-	-	-	-	-	-	-	-	-	-
	HR	-	-	-	-	-	-	-	-	-	↓
Frey. Coal Slurry / SA 'Coal 99	MF	-	-	-	-	-	-	↓	-	-	-
	HR	-	-	-	-	-	-	-	-	-	↓
Frey. Schlamms / Frey. Coal Slurry	MF	-	-	-	-	-	-	-	-	-	-
	HR	-	-	-	-	-	-	↓	-	-	-
SA Coal '97 / Wet Saw Dust	MF	-	-	↑	-	-	-	-	-	-	-
	HR	-	-	-	-	-	-	-	-	-	-
Frey. Coal Slurry /Saw Dust	MF	-	-	-	-	-	↓	-	-	-	↓
	HR	-	-	-	-	-	-	↓	-	-	-
SA Coal '97 / Undried Bark	MF	-	-	↓	-	-	-	↓	-	-	-
	HR	-	-	-	-	-	-	-	-	-	-
Frey. Schlamms /Frey. Coal Slurry/ Petroleum Coke	MF	-	-	-	-	-	-	↓	-	-	↓
	HR	↓	-	↓	-	-	-	↓	-	-	-

" -" Depicts no change in retention from 850 °C to 950 °C. " ↑" Depicts an increase in retention from 850 °C to 950 °C and "↓" depicts a decrease in retention with increase in temperature.

Table 5.3 TE Retention Trends when Combustion Temperature Increased in CERCHAR fuels

Fuel	Be	V	Cr	Zn	As	Se	Hg	Cd	Ba	Pb
Kideco Coal	-	-	-	↓	-	-	-	-	-	-
Kideco-Lemington Coal Blend	-	-	-	↓	-	-	-	↓	-	-
Lemington Coal	-	-	↓	↓	-	-	-	↓	-	-
Lemington Allied Coal Blend	-	-	-	↓	-	↓	-	↓	-	-
Allied Coal	-	-	-	↓	-	-	-	↓	↓	-

" -" Depicts no change in retention from 900 °C to 1500 °C. " ↑" Depicts an increase in retention from 900 °C to 1500 °C and "↓" depicts a decrease in retention with increase in temperature.

Table 5.4 TE Retention Trends when Combustion Temperature Increased in Chilean fuels

5.2.2 Trace Element Retention Trends as a Function of Combustion Method

The trace element retention varied with combustion method to a high degree, as shown in Table 5.5. Trace element retentions may be categorised as follows:

- The trace element retention remained constant when combustion method was changed from muffle furnace to hot-rod reactor 28.0 % of the time. There was an increase in retention with a change from muffle furnace to hot-rod 8.7% of the time. Predominantly however there was a decrease in retention when combustion method was changed to the hot-rod reactor. This occurred in 63.3% of instances.

- An increase in retention with change in combustion method was shown predominantly by arsenic, and the Freyming coal slurry / saw dust mixture.

- No element showed consistent behaviour for all fuels and temperatures, which again shows that trace element behaviour is driven by its mode of occurrence in the fuel.

Fuel	T (°C)	Be	V	Cr	Zn	As	Se	Hg	Cd	Ba	Pb
South Africa Coal '97	850	↓	↓	↓	↓	-	↓	-	↓	-	↓
	950	↓	↓	-	↓	-	↓	↓	↓	↓	↓
South Africa Coal '99	850	↓	↓	-	↓	↓	↓	-	↓	-	↓
	950	↓	↓	↓	-	↓	↓	-	↓	↓	↓
Frey. Coal Slurry / SA 'Coal 99	850	↓	-	↓	↓	↑	↓	↓	↓	↑	↓
	950	↓	-	-	↓	↑	↓	↓	↓	-	↓
Frey. Schlamms / Frey. Coal Slurry	850	↓	↓	↓	↓	↑	-	↓	↓	-	↓
	950	↓	-	↓	↓	↑	-	↓	↓	-	↓
SA Coal '97 / Wet Saw Dust	850	↓	↓	↑	↓	↑	-	-	↓	↓	↓
	950	↓	↓	↓	↓	↑	-	↓	↓	-	↓
Frey. Coal Slurry /Saw Dust	850	↑	-	↓	-	-	-	-	-	↑	-
	950	↑	↑	↑	↑	-	↑	-	-	-	-
SA Coal '97 / Undried Bark	850	-	↓	↓	-	-	-	↓	↓	↓	↓
	950	↓	↓	-	↓	↓	↓	-	-	↓	↓
Frey. Schlamms /Frey. Coal Slurry/ Petroleum Coke	850	-	↓	↓	↓	↓	↓	↓	↓	-	↓
	950	-	↓	↓	↓	↓	↓	-	↓	↓	-

" -" Depicts no change in retention from Muffle to Hot-Rod at temperature T. " ↑" Depicts an increase in TE retention from Muffle Furnace to Hot-rod and "↓" depicts a decrease in trace element retention with change in combustion method at temperature T.

Table 5.5 Trace Element Retention Trends when Combustion Method Changed

5.3 Trace Element Leaching From Ashes

The degree to which trace elements were leached varied with combustion conditions. It was possible to broadly categorise the amount of trace element leached within specified ranges. The propensity of the different trace elements to leach showed the general trend shown below. This was in the case of the CERCHAR fuels combusted in the muffle furnace at both temperatures studied.

$$(V, As, Se, Ba,) > (Be, Cr) > (Zn, Hg, Cd, Pb)$$

The trace elements in the first group above were leached by over 70% for all CERCHAR fuels at the conditions specified. The final group was for elements which showed a weak leaching propensity (from 0 – 35%) and the middle group, in this case beryllium and chromium, was for elements which showed an intermediate degree of leaching.

For the hot-rod reactor the following trend was shown, for both the 850 °C and the 950 °C temperature:

$$(V, As, Se, Ba,) > (Be, Cd) > (Zn, Hg, Cr, Pb)$$

As may be observed the degree to which metals are leached is similar at both temperatures and combustion configurations, with the exception of chromium and cadmium. These may also be stated however to be never more than moderately leached.

For the Chilean fuels the overall leaching was less than for the CERCHAR fuels, particularly for leachates obtained from 1500 °C ashes. Leaching occurred over a far more narrow range so classification of the degree of trace element leaching was not as clear. For the Chilean fuels trace element leaching was always below 50% for all elements and conditions except arsenic and vanadium.

5.3.1 Trace Element Leaching as a Function of Temperature

Table 5.6 and table 5.7 below show how trace element leaching is affected by an increase in temperature for the CERCHAR and Chilean fuels respectively. Table 5.6 shows this variation for the muffle furnace and the hot-rod ashes. In the CERCHAR fuels there is a change in leaching quantity with a change in temperature for 43.1% of the sample set. For the Chilean fuels this increases to 90% of the time. The results may be summarised with the following points:

- For the CERCHAR fuels the quantity of trace element leached decreased in 35.6 % of instances. For the Chilean fuels this was 70 % of the sample set. These instances did not appear to be linked to a particular combustion method or indeed element. It may therefore be inferred that the mode of occurrence of an element in the fuel is the factor which affects this temperature dependency.

- In certain instances the trace element leached increased with increasing temperature. This occurred 7.5% of the time in the CERCHAR fuels and 20 % of the time in the Chilean fuels. In occasions where leaching propensity increased with increasing temperature this was dependent on the trace element. In the CERCHAR samples this trend appeared only with the element chromium and in the Chilean ashes this was the case with chromium and cadmium.

- The degree to which trace element leaching varied with temperature was not constant for a particular trace element, combustion method or fuel and there were no discernable trends.

Fuel	Reactor	Be	V	Cr	Zn	As	Se	Hg	Cd	Ba	Pb
South Africa Coal '97	MF	↓	-	↑	↓	-	-	-	↓	-	↓
	HR	↓	↓	↑	-	↓	-	-	↓	-	-
South Africa Coal '99	MF	-	-	↑	↓	-	-	-	↓	-	↓
	HR	↓	↓	↑	↓	-	-	-	↓	↓	-
Frey. Coal Slurry / SA 'Coal 99	MF	↓	-	↑	↓	-	↓	-	↓	-	-
	HR	-	↓	↑	↓	↓	-	-	↓	↓	-
Frey. Schlamms / Frey. Coal Slurry	MF	-	-	↑	-	-	-	-	↓	-	↓
	HR	↓	↓	↑	↓	-	-	-	-	↓	-
SA Coal '97 / Wet Saw Dust	MF	-	-	-	-	-	-	-	↓	-	-
	HR	↓	↓	↓	↓	↓	-	-	-	↓	-
Frey. Coal Slurry /Saw Dust	MF	↓	-	↑	-	-	-	-	↓	-	-
	HR	-	↓	↑	↓	↓	-	-	-	-	-
SA Coal '97 / Undried Bark	MF	↓	-	↑	↓	-	-	-	↓	-	↓
	HR	↓	↓	↑	-	-	-	-	-	-	-
Frey. Schlamms /Frey. Coal Slurry/ Petroleum Coke	MF	-	-	-	↓	-	-	-	↓	-	↓
	HR	↓	↓	-	-	↓	-	-	↓	↓	-

" -" Depicts no change in trace element leached from 850 °C to 950 °C. " ↑" Depicts an increase in TE leached from 850 °C to 950 °C and "↓" depicts a decrease in TE leached with increase in temperature.

Table 5.6 Trends in TE Leaching with Increasing Temperature in CERCHAR fuels

Fuel	Be	V	Cr	Zn	As	Se	Hg	Cd	Ba	Pb
Kideco Coal	↓	↓	↑	↓	↓	↓		↑	↓	↓
Kideco-Lemington Coal Blend	↓	↓	↑	↓	↓	↓		↑	↓	↓
Lemington Coal	↓	↓	↑	↓	↓	↓		↑	↓	↓
Lemington Allied Coal Blend	↓	↓	↑	↓	↓	↓		↑	↓	↓
Allied Coal	↓	↓	↑	↓	↓	↓		↑	↓	↓

" -" Depicts no change in TE leached from 900 °C to 1500 °C. " ↑" Depicts an increase in TE leached from 900 °C to 1500 °C and "↓" depicts a decrease in leaching with increase in temperature. Mercury detected was below quantification limits.

Table 5.7 Trends in TE Leaching with Increasing Temperature in Chilean fuels

5.3.2 Trace element leached as a function of Combustion Method

There was a consistent trend in the leaching of trace metals from ashes produced in the muffle furnace and hot-rod. Except for the elements selenium and Hg (which were present in very small quantities), there was always a decrease in trace element leached from muffle furnace to hot-rod. An analysis of the reasons for this are presented in the results section 4.4.1.3.

Fuel	T (°C)	Be	V	Cr	Zn	As	Se	Hg	Cd	Ba	Pb
South Africa Coal '97	850	↓	↓	↓	↓	↓	-	-	↓	↓	↓
	950	↓	↓	↓	↓	↓	-	-	↓	↓	↓
South Africa Coal '99	850	↓	↓	↓	↓	↓	-	-	↓	↓	↓
	950	↓	↓	↓	↓	↓	-	-	↓	↓	↓
Frey. Coal Slurry / SA 'Coal 99	850	↓	↓	↓	↓	↓	-	-	↓	↓	↓
	950	↓	↓	↓	↓	↓	-	-	↓	↓	↓
Frey. Schlamms / Frey. Coal Slurry	850	↓	↓	↓	↓	↓	-	-	↓	↓	↓
	950	↓	↓	↓	↓	↓	-	-	↓	↓	↓
SA Coal '97 / Wet Saw Dust	850	↓	↓	↓	↓	↓	-	-	↓	↓	↓
	950	↓	↓	↓	↓	↓	-	-	↓	↓	↓
Frey. Coal Slurry /Saw Dust	850	↓	↓	↓	↓	↓	-	-	↓	↓	↓
	950	↓	↓	↓	↓	↓	-	-	↓	↓	↓
SA Coal '97 / Undried Bark	850	↓	↓	↓	↓	↓	-	-	↓	↓	↓
	950	↓	↓	↓	↓	↓	-	-	↓	↓	↓
Frey. Schlamms /Frey. Coal Slurry/ Petroleum Coke	850	↓	↓	↓	↓	↓	-	-	↓	↓	↓
	950	↓	↓	↓	↓	↓	-	-	↓	↓	↓

" -" Depicts no change in TE leaching from Muffle to Hot-Rod at temperature T. " ↑" Depicts an increase in TE leaching from Muffle Furnace to Hot-rod and "↓" depicts a decrease in leaching with change in combustion method at temperature T.

Table 5.8 Leaching Trends in CERCHAR Fuels as a Function of Combustion Method

5.4 Toxicity of Leachates

In order to assess whether the leachates from experiments contained levels of trace metals below acceptable limits, calculation were made, as shown in section 4.4.2.3 using a dilution attenuation factor (DAF) of 100. Elements were present in the leachate above the maximum limits 47.9 % of the time for the CERCHAR fuels and 37.0 %for the Chilean fuels. The following points observed with regard to toxicity limits:

- In the CERCHAR fuels trace elements which exceeded toxicity limits were very much a function of the combustion method used. Toxicity limits were exceeded 35.0 % of the time in the muffle furnace and 12.9 % of the time in the hot-rod reactor.

- The toxicity of samples was not a function of temperature for the CERCHAR fuels. 48.6% of instances a trace metal exceed limits at 850 °C and at 950 °C this figure was 46.7%.

- For the Chilean fuels the toxicity of the leachates varied strongly with temperature. At 900 °C trace metals concentrations were higher than the regulatory limits 52.0 % of the sample set. This reduced to 22.0% when the temperature was increased to 1500 °C.

- The incidence of toxicity for the trace elements followed approximately the same trend for both the CERCHAR and Chilean fuels. This is shown in table 5.9 below. Concentrations for some elements always fell within safe limits. These were zinc and mercury for both fuel sets and additionally vanadium and beryllium for the Chilean fuels. For the CERCHAR fuels beryllium and vanadium were on the lower end of the scale for exceeding toxicity limits. Cadmium, selenium and lead were at the lower end of the range for both sets of fuels, exceeding limits less than 50 % of the time.

Barium and chromium were at the upper end of the range, for occurrences above the limit for both fuels sets. In these cases toxicity limits were exceeded 70 % of the time. The element which always exceeded the maximum level, was Arsenic for both fuel sets.

- Arsenic was the element most consistently above the limits as shown below but it was also the element which exceed limits by the greatest amount (an order of magnitude). Of the elements which exceed maximum allowable concentrations, selenium was the element which when exceeding limits by the least (20%). The amount by which the limits were exceeded did not appear to be a function of any of the variables studied.

Occurrence Above Limits	CERCHAR	Chilean
0 %	Zn, Hg	Zn, Hg, Be, V
<50 %	Pb, Cd, Se, Be, V	Pb, Cd, Se
>70%	Cr, Ba	Cr, Ba
100 %	As	As

Table 5.9 Trace Element Occurrence Above Toxicity Limits

No fuels had all trace elements below the safe limits. The results from this study therefore show that none of the fuel ashes analysed could be disposed of in a landfill without further precautions being taken.

6.0 CONCLUSIONS

6.1 Trace Element Concentration in the Raw Fuels

There was no great variation in the abundance of trace elements amongst the different fuels. Trace element concentrations were found to be similar for the pure coals, and fuel mixtures.

6.2 Trace Element Retention After Combustion

6.2.1 Influence of Temperature on Trace Element Retention

There was no temperature dependence observed with a 100 °C temperature differential from 850 – 950 °C. This was true in approximately 90% of the experiments carried out. For the Chilean fuels and a 600 °C differential (900 – 1500 °C) the temperature dependence was higher at 25%. Where a temperature dependence was observed, this was not reserved for a particular trace element.

6.2.2 Influence of Combustion Method on Trace Element Retention

Trace element retention did appear to be a function of combustion method. The trace element retention changed in 72% of cases when the combustion method was changed. Trace element retention decreased in 88 % of these cases when the combustion method was changed from the muffle furnace to the hot-rod reactor. Where an increase in trace element retention was observed, this was predominantly for arsenic.

6.2.3 Influence of Fuel Type on Trace Element Retention

No link could be established between the type of fuel used and trace element retention.

6.3.4 Possible Synergistic Effects in the Chilean Fuels

No synergistic effects could be observed in the trace metal retention of the Chilean fuels blended in varying proportions.

6.3 Trace Element Leaching

6.3.1 Influence of Temperature on Trace Element Leaching

Temperature increases affected leaching much more than they affected trace element retention. The leaching of trace elements in the CERCHAR fuels was affected by a temperature change in 43.1 % of cases and of the Chilean fuels in 90% of the sample set. The leaching propensity decreased with increasing temperature except for the elements chromium and cadmium.

6.3.2 Influence of Combustion Method on Trace Element Leaching

In the cases where combustion method was the variable studied, the trace element leached consistently decreased from the muffle furnace to the hot-rod reactor. The reduction was by a consistent amount of between 20 & 35 %. This was the case for all trace elements except selenium and mercury, at both temperatures studied.

6.3.3 Influence of Fuel Type on Trace Element Leaching

The fuel type did not discernibly affect the degree of trace element leaching.

6.3.4 Possible Synergistic Effects in the Chilean Fuels

Synergy did not appear to be an effect which affected the leaching in the Chilean ashes.

6.4 Toxicity of Leachates

All the CERCHAR and Chilean fuels study contained some trace metals in their leachate which were above the maximum allowable for emission into groundwater. Some elements however were always below the legal specified limits. These were mercury and zinc for the CERCHAR fuels and mercury, zinc, beryllium and vanadium for the Chilean samples. Arsenic was the element which was above regulatory limits in all cases studied and chromium and barium for over 70 % of cases studied. The remaining elements were above the toxic limits less than 50% of the time.

The element most drastically above regulatory limits was Arsenic (sometimes 2000% above). Of the elements which exceeded the limits, selenium exceeded these limits by the least amount (a maximum of 20%). The degree to which an element occurred above the amount deemed safe did not appear to be a function of any of the variables studied.

7.0 Recommendations for Future Work

7.1 Continuation & Changes to Experimental Work:

In this study the ten elements which were deemed to be of most concern to the environment were studied. This was in order to allow a more in-depth study of the leaching behaviour of these elements. If all available trace elements were studied, it may be possible to draw correlations between the physical and chemical properties of groups of elements, and the leaching of these elements.

Leaching was a function of temperature when the temperature differential was 600 °C (i.e. between 900 & 1500 °C). The effect when the temperature difference was 100 °C was not as pronounced. Temperatures between 900 & 1500 °C could be investigated, at increments of 100 for example, and the progression of leaching with temperature, (any linearity etc), could be ascertained.

The fuels studied were inherited from the project partners and although offered some variety did not reflect the interesting and broad variety of waste fuels available. A refined version of this study could be applied to a wider variation in fuels, currently being investigated as feasible for co-combustion.

7.2 Further Modelling:

The DAF factor used in this study was developed by the US-EPA to be applied in a universal fashion to TCLP results. This leads to results which are to be interpreted as a worst case scenario. A more pragmatic and elucidating approach would be to use dispersion modelling. This would show what the impact of the leachate would be to the environment in terms of density and volume of the polluting plume. There are several models which may be used to do this such as Multimed.

One of the most significant factors influencing leaching is pH. In the MINTEQA2 modelling the equilibrium pH was consistently miscalculated and this caused prediction errors. When the equilibrium pH was entered manually as the empirical pH, simulations provided much more accurate results. When modelling leaching, trace elements were predicted to precipitate or exist in various modes of occurrence. It is the formation of these species which change the initial pH to the equilibrium pH. Analysis of the leachate could be made in order to ascertain whether these species did exist in the leachate and to what extent. This would not only enhance the understanding of the system but would greatly increase the accuracy of the modelling simulations.

REFERENCES

1. Tillman D., "Co-firing benefits for coal and biomass," Biomass and Bio-Energy 19 (2000), 363-364.

2. Demirbas A., "Biomass Resource Facilities and Biomass Conversion Processing for Fuels and Chemicals", Energy Conversion and Management 42 (2001), 1357-1378.

3. Chiaramonti D., Grimm H.P., Bassam N.E., Cendagorta M., "Energy Crops and Bio-energy for Rescuing Deserting Coastal Area by Desalination: Feasibility Study", Bioresource Technology 72 (2000), 131-146.

4. Ekmann J.M. et al., "International survey of co-firing with biomass and other wastes", Fuel Processing Technology 54 (1998), 171 –188.

5. Kim D., Shin S., Sohn S., Choi J., Ban B., "Waste Plastics as Supplemental Fuel in the Blast Furnace Process: Improving Combustion Efficiencies", Journal of Hazardous Materials B94 (2002), 213-222.

6. Antonio C., Pelagagge P., "Waste-to-Energy Plant For Paper Industry Sludges Disposal: Technical Economic study", Journal of Hazardous Materials B81 (2001), 265-283.

7. Boie W., Wiss Z., Tech Hochsch Dresden 2 (1952/53) 687

8. Paul W., Buchele, F., "Development of Concentric Vortex Agri-Residue Furnace", Agricultural Energy 2 (1980), 349-356.

9. LePori W.A., "Fluidised Bed Combustion and Gasification of Biosolid", Agriculutural Energy 2 (1980), 623-629.

10. Mendis M.S., "Biomass Gasification: Past Experiences and Future Prospects in Developing Countries." Pyrolysis and Gasification Procedings of the International Conference in Luxumberg 23-25 May (1989), 257-263.

11. Maschio G., Lucchesi A., STOPPATO G., "Production of Syngas From Biosolid", Bioresource Technology 48 (1994), 119-126.

12. Ebling J.M., Jenkins, B.M., "Physical and Chemical Properties of Biomass", ASAE 23 (1985), 898-902.

13. Kandpal J.B., Maheshwari R.C., "Particulate Pollution from Biosolid Combustion in Three Cookstoves", International Journal of Energy Resource 19 (1995). 433-441.

14. Abbas T., Costen P., Kandamby H.H., "The Influence of Burner Injection Mode on Pulverised Coal and Biosolid Co-fired Flames", Combustion Flame 99 (1994), 617-625.

15. Aerts D.J.,Bryden K.M., Hoerning J.M., Ragland K.W., "Co-firing Switchgrass in a 50MW Pulverised Coal Boiler", Proceedings of the 1997 59th Annual American Power Conference 59 (1997), 1180-1185.

16. Saxena S.C., Jotshi C.K., "Fluidised Bed Incineration of Waste Materials", Progress in Energy Combustion Science 20 (1994), 247-252.

17. Christian R., Unsworth J., "Pilot Plant Demonstration of Used Tires Vacuum Pyrolysis", Pyrolysis and Gasification Procedings of the International Conference in Luxumberg 23-25 May (1989), 180-189.

18. "Fluidised bed combustion of alternative fuels". EPRI TR- 100547. Research Project 2190-6. Final Report, December (1993). Electric Power Research Institute

19. Hein KRG., Bemtgen JM, "EU Clean Coal Technology", Co-combustion of Coal and Biomass, Fuel Processing Technology 54 (1998), 159-169

20. Hein K., Bemtgen J., "EU Clean Coal Technology" – Co-combustion of Coal and Biomass, Fuel Processing Technology 54 (1998), 159-169

21. Spielthoff H., Hein KRG., "Effect of Co-combustion of Biomass on Emission in Pulverised Fuel Furnaces", Fuel Processing Technology 54 (1998), 189-205

22. Final Report, European Co-Combustion of Coal, Biomass and Wastes, (2000)

23. http://www.worldenergy.org/wec-geis/edc/scenario.asp

24. Williams A. et al., "Combustion of pulverised coal and biomass", Progress in Energy and Combustion Science 27 (2001), 587-610.

28. Essenhigh RH., "The influence of coal rank on the burning times of single captive particles", Journal of Engineering Power 85 (1963), 183-190.

29. Kharbat E., "Digital Image Processing Applications in the Ignition and Combustion of Coal", MS Thesis, Mechanical Engineering Department, Texas University (1992).

30. Seeker W.R., Samuelsen G.S., Heap M.P., Trolinger J.D., "The Thermal Decomposition of Pulverised Coal Particles". 18th International Symposium on Combustion (1981), 1213-1226.

31. Smoot L., Horton M.D., Williams G.A., "Propagation of Laminar Pulverised Coal-air Flames", 16th International Symposium on Combustion (1977), 375-397.

32. Baxter L.L., "Ash Depositon During Bio-solid and Coal combustion. A mechanistic Approach.", Biomass Bioenergy 4 (1993), 85-102.

33. Easterly J.L., Burnahm M., "Overview of Biomass and Waste Fuel Resources for Power Production"., Biomass Bioenergy 10 (1996), 79-92.

34. Chen Y., Charpenay S., Jensen A., Wojotowicz M.A., "Twenty Seventh Symposium on Combustion", The Combustion Institute (1998), 1327-1324.

35. Hughes E. "Biomass Co-firing: economics, policy opportunities", Biomass and Bioenergy 10 (2000), 457 – 464.

36. Tests from Greenidge Station, Sewared Generating Station and Plant Kraft

37. American Coal Ash Associatioin (1998)

38. Steenari B.M., Lindquist O., "Fly ash Characteristics in Co-combustion of Wood with Coal, Oil or Peat", Fuel 78 (1999), 479-488.

39. Mahorta & Mehta, "Pozzolanic and Cementitious Materials", Gordon & Breach (1996).

40. Sarsby R.W., "Waste Disposal By Landfill", Proceedings of the Symposium Green – Geotechinics Related to the Environment

41. Baxter L.L., "The Behaviour of Inorganic material in Biomass-fired Power Boilers: Field and Laboratory Experience", Proceedings of the Biomass Usage for Utility and Industrial Power, An Engineering foundation conference, Snowbird UT, April 28-May (1996).

42. Arvelakis S., Vourliotis P., Kakaras E., Koukios E.G., "Effect of Leaching the Ash Behaviour of What Straw and Olive Residue during Fluidised Bed Combustion", Biomass and Bioenergy 20 (2001), 459-470.

43. Skorupska, N.M., "Coal Specifications – Impact on Power Station Performance", IEA CR/52, IEA Coal Research, UK, (1993).

44. Carpenter A.M., "Coal Blending for Power Stations", IEA CR/81, IEA Coal Research UK, (1995).

45. "Methods for analysis and testing of coal and coke- Ultimate analysis BS 106-106.4.2", British Standards Institution, (1996)

46. Brown T.D., Schmidt C.E., "American Chemicial Society Division of Fuel Chemistry Preprints", (1993), 38(1), 286.

47. Richaud R., Lachas H., Herod A., Dugwell D., Kandiyoti R., "Trace Element Concentratioins in Coals and Coal Derived Material Determined by Atomic Absorption Spectrophotometry."

48. Hiteshue R.W., Andersen R.B., Schlesinger M.D., Industrial Engineering Chemistry, 1957 (47) 200-208.

49. Hiteshue R.W., Andersen R.B., Madden R., Industrial Engineering Chemistry, 1947 (52) 577-588.

50. Hiteshue R.W., Andersen R.B., Madden R., Industrial Engineering Chemistry, 1962 60-67.

51. Hiteshue R.W., Andersen R.B., Madden R., Industrial Engineering Chemistry, 1964 63-76.

52. Hiteshue R.W., Andersen R.B., Schlesinger M.D., Industrial Engineering Chemistry, 1965 (47) 64-70.

53. Finn M.J., Fynes G., Ladner W.R., and Newman J.O.H., Fuel 1980 (59) 397-402

54. O'Brien R.J., "Tar Production in Coal Pyrolysis", PhD Thesis, Department of Chemical Engineering, Imperial College (1986)

55. Pindoria R.V., "Thermochemical Upgrading of Biomass to Gaseous and Liquid Fuels", PhD Thesis, Department of Chemical Engineering, Imperial College (1997)

56. Gonec Z.S., "Coal Pyrolysis in a Fixed Bed Reactor", PhD Thesis, Department of Chemical Engineering, Imperial College (1989).

57. Method 1311 – Toxicity Characteristic Leaching Procedure US-EPA (1990).

58. Houk R.S., Fassel V.A., Flesch., G.D., Svec H.J., Gray A.L., Taylor C.E., Analytical Chemistry 52 (1980) 2283-2299.

59. "Leaching Tests for Assessing Impact on Groundwater Quality", Report to Congress, State Department of Technology (2003)

60. Townsend, T., Jang Y., " Leaching Tests for Evaluating Risk in Solid Waste Management Decision Making", Final Report 03-01, Florida Centre For Solid and Hazardous Waste Management (2003)

61. Van der Sloot, H.A., "Leaching Behaviour of Waste and Stabilised Waste Materials; Characterisation for Environmental Assessment Purposes." Waste Management and Research, pp 215-228 (1990)

62. Allison, J. D., Brown D.S., 1995, "MINTEQA2/PRODEFA2 a Geochemical Speciation Model and Interactive Preprocessor Chemical Equilibrium and Reaction Models", SSSA Special Publication Number 42, Soil Science Society of America, American Society of Agronomy, Madison, WI, pp. 241-252. (1990)

63. Van Zeggeren, Storey "Chemical Equilibrium Systems as Numerical Test Problems", ACM Transaction on Mathematical Software (TOMS) Volume 16, Issue 2 (1990)

64. Dreher G.B., "Elements of Computer Assisted Thermodynamic Chemical Equilibrium Modelling as Applied to Waste Treatment at Coal Mines." Illinois State Geological Survey (1998)

65. Davies C.W. "Ion Association" Butterworths Publications pp 190(1962)

66. Truedell, A.H., Jones, B.F., WATEQ, "A computer Program for Calculating Chemical Equilibria in Natural Waters." US Geological Survey (1974)

67. Dzombak and Morel "Surface Complexation Modelling Hyrdous Ferric Oxide" Wiley Interscience (1990)

68. Skorupska, N.M., "Coal Specifications – Impact on Power Station Performance", IEA CR/52, IEA Coal Research, UK, 1993

69. Carpenter A.M., "Coal Blending for Power Stations", IEA CR/81, IEA Coal Research UK, 1995

70. British Standards Institution., "Methods for analysis and testing of coal and coke"- Ultimate analysis BS 106-106.4.2, 1996

71. Brown T.D., Schmidt C.E., "American Chemcial Society Division of Fuel Chemistry Preprints, 1993, 38(1), 286

72. Richaud R., Lachas H., Herod A., Dugwell D., Kandiyoti R., Trace Element Concentratioins in Coals and Coal Derived Material Determeind by Atomic Absorption Spectrophotometry.

73. Hiteshue R.W., Andersen R.B., Schlesinger M.D., Industrial Engineering Chemistry, 1957 (47) 200-208

74. Hiteshue R.W., Andersen R.B., Madden R., Industrial Engineering Chemistry, 1947 (52) 577-588

75. Hiteshue R.W., Andersen R.B., Madden R., Industrial Engineering Chemistry, 1962 60-67

76. Hiteshue R.W., Andersen R.B., Madden R., Industrial Engineering Chemistry, 1964 63-76

77. Hiteshue R.W., Andersen R.B., Schlesinger M.D., Industrial Engineering Chemistry, 1965 (47) 64-70

78. Finn M.J., Fynes G., Ladner W.R., and Newman J.O.H., Fuel 1980 (59) 397-402

79. O'Brien R.J., Tar Production in Coal Pyrolysis, PhD Thesis, Department of Chemical Engineering, Imperial College 1986

80. Pindoria R.V., Thermochemical Upgrading of Biomass to Gaseous and Liquid Fuels, Department of Chemical Engineering, Imperial College 1997

81. Gonec Z.S., Coal Pyrolysis in a Fixed Bed Reactor, Department of Chemical Engineering, Imperial College 1989

82. Method 1311 – Toxicity Characteristic Leaching Procedure US-EPA 1990

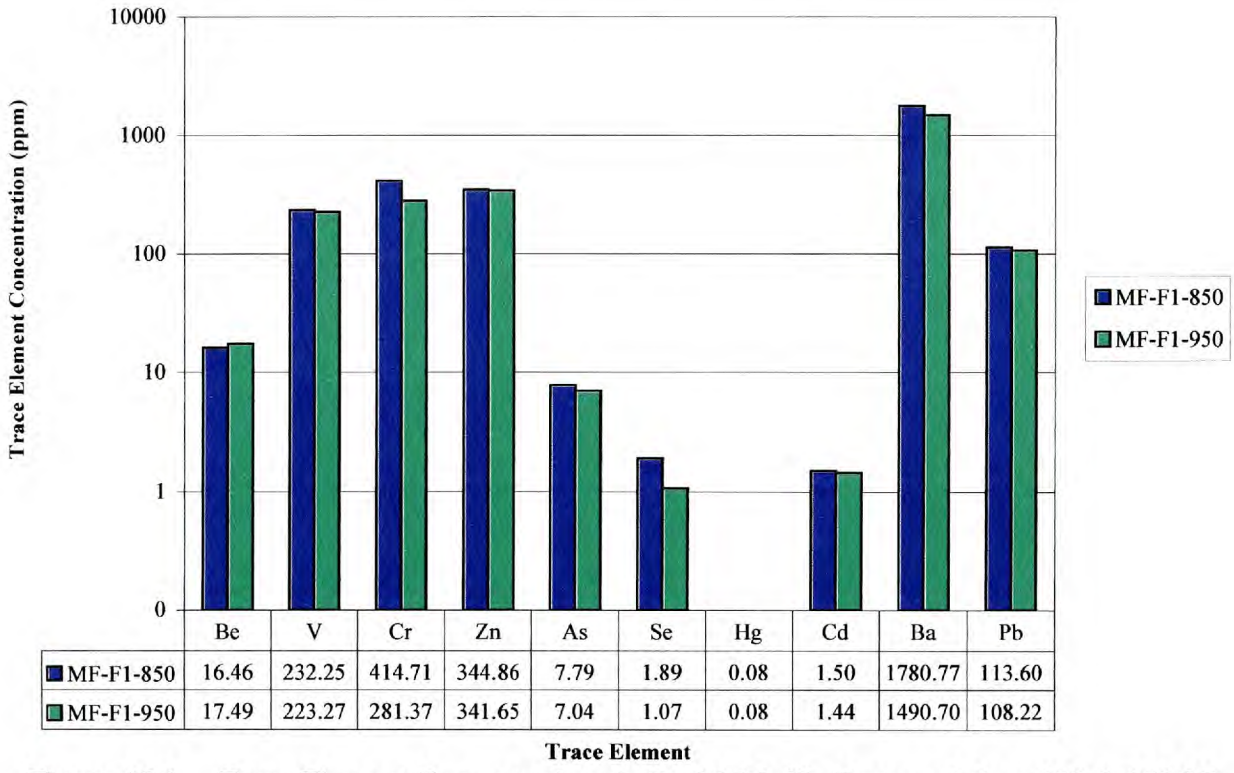
83. Houk R.S., Fassel V.A., Flesch., G.D., Svec H.J., Gray A.L., Taylor C.E., Analytical Chemistry 52 (1980) 2283-2299

84. Mathur, S. S., Development of a database for ion sorption on goethite using surface complexation modelling [MSc thesis] Carnegie Mellon Univ.(1990), 178

85. EPA Office of Solid Waste, "Determination of Groundwater Dilution Attenuation Factors For Fixed Waste Site Areas Using EPACMTP", Background Document (1994)

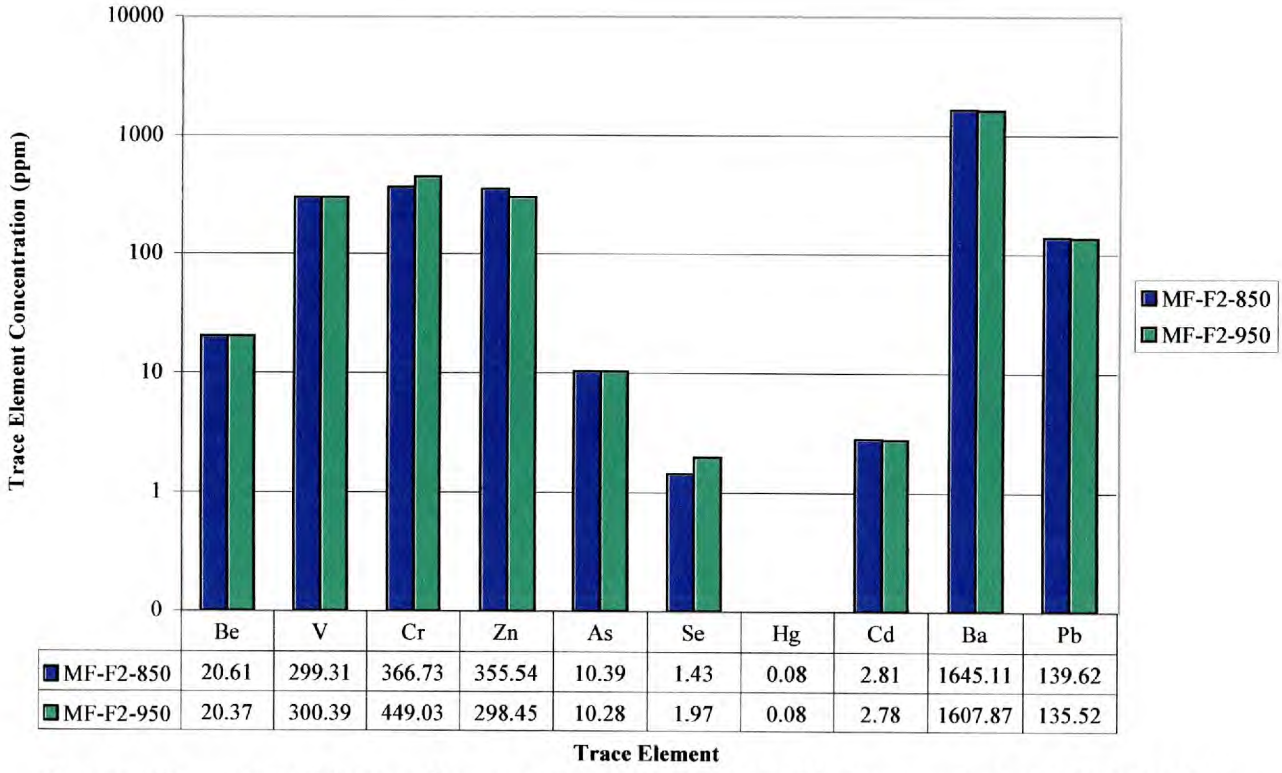
APPENDIX I

Appendix I depicts the absolute trace element concentrations in the ashes of the CERCHAR fuels. Each figure presents the trace element concentrations obtained for a particular fuel, at a particular combustion configuration at the two temperatures studied, e.g. all the trace element concentrations obtained for Fuel 1 ashes produced in the muffle furnace at 850 °C & 950 °C. The scales are logarithmic due to the large variations from one trace element another, but do nevertheless give an idea of the relative magnitudes of trace element content. Precise results are given in data tables presented with each figure. Error bars are not clearly represented on log scales; however the errors are as described in section 4.3.2.1.



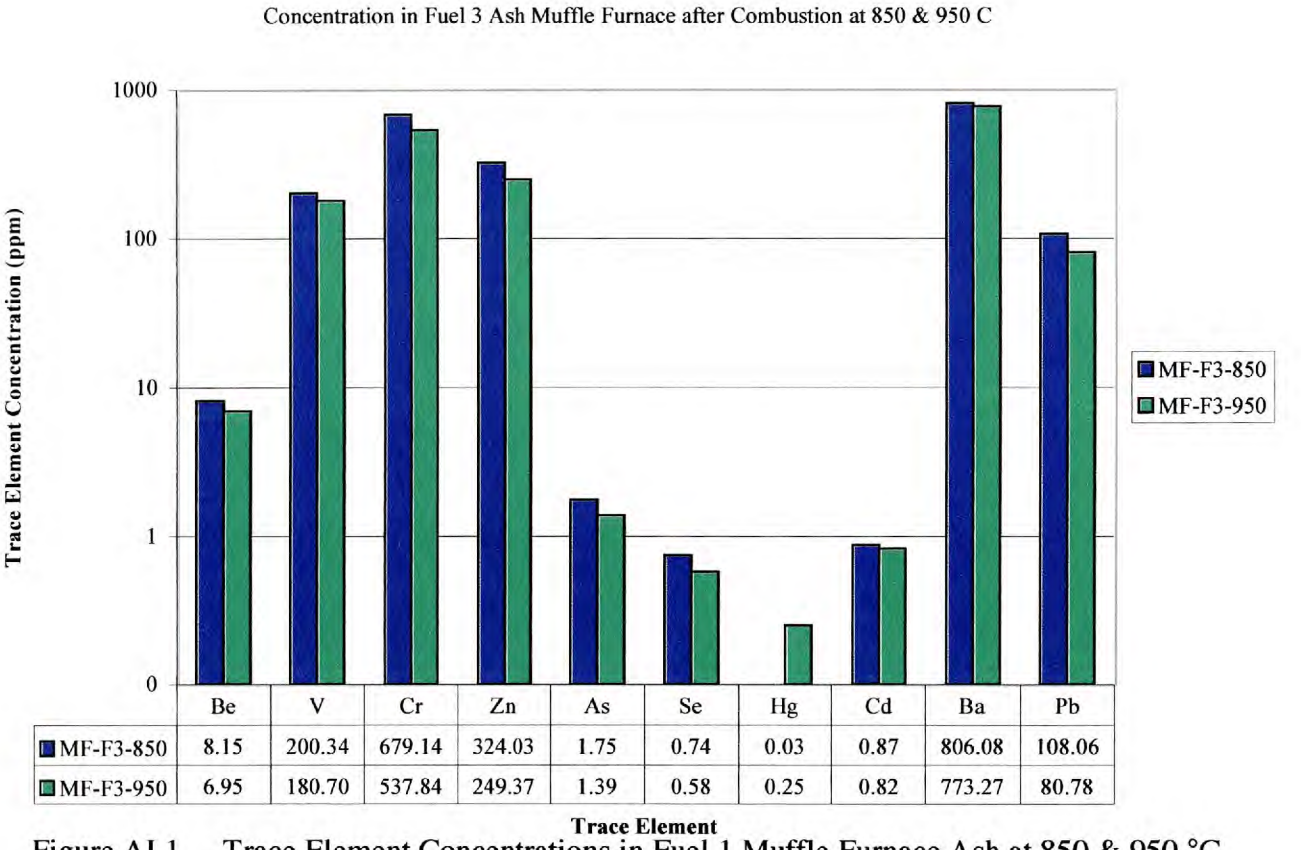
	Be	V	Cr	Zn	As	Se	Hg	Cd	Ba	Pb
MF-F1-850	16.46	232.25	414.71	344.86	7.79	1.89	0.08	1.50	1780.77	113.60
MF-F1-950	17.49	223.27	281.37	341.65	7.04	1.07	0.08	1.44	1490.70	108.22

Figure AI.1 Trace Element Concentrations in Fuel 1 Muffle Furnace Ash at 850 & 950 °C



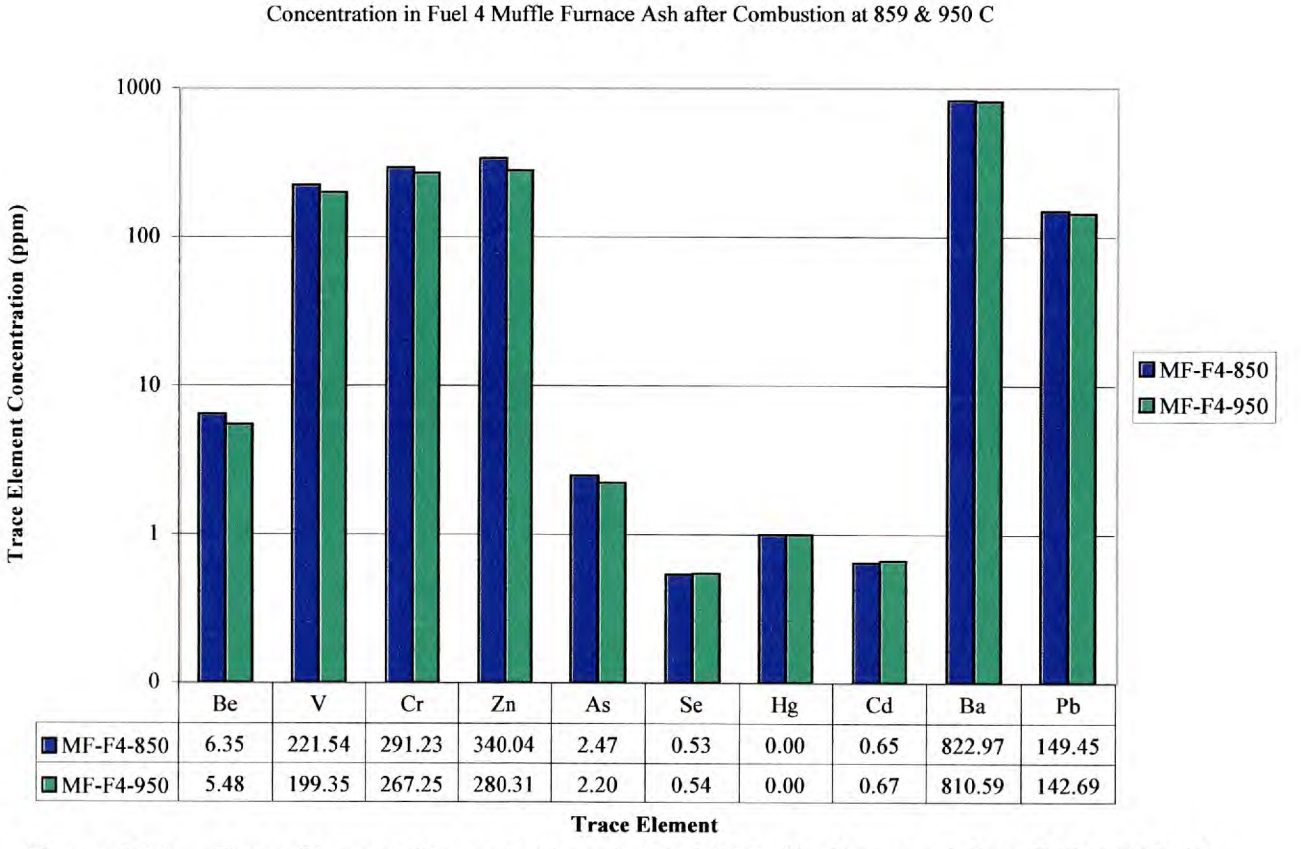
	Be	V	Cr	Zn	As	Se	Hg	Cd	Ba	Pb
MF-F2-850	20.61	299.31	366.73	355.54	10.39	1.43	0.08	2.81	1645.11	139.62
MF-F2-950	20.37	300.39	449.03	298.45	10.28	1.97	0.08	2.78	1607.87	135.52

Figure AI.2 Trace Element Concentrations in Fuel 2 Muffle Furnace Ash at 850 & 950 °C



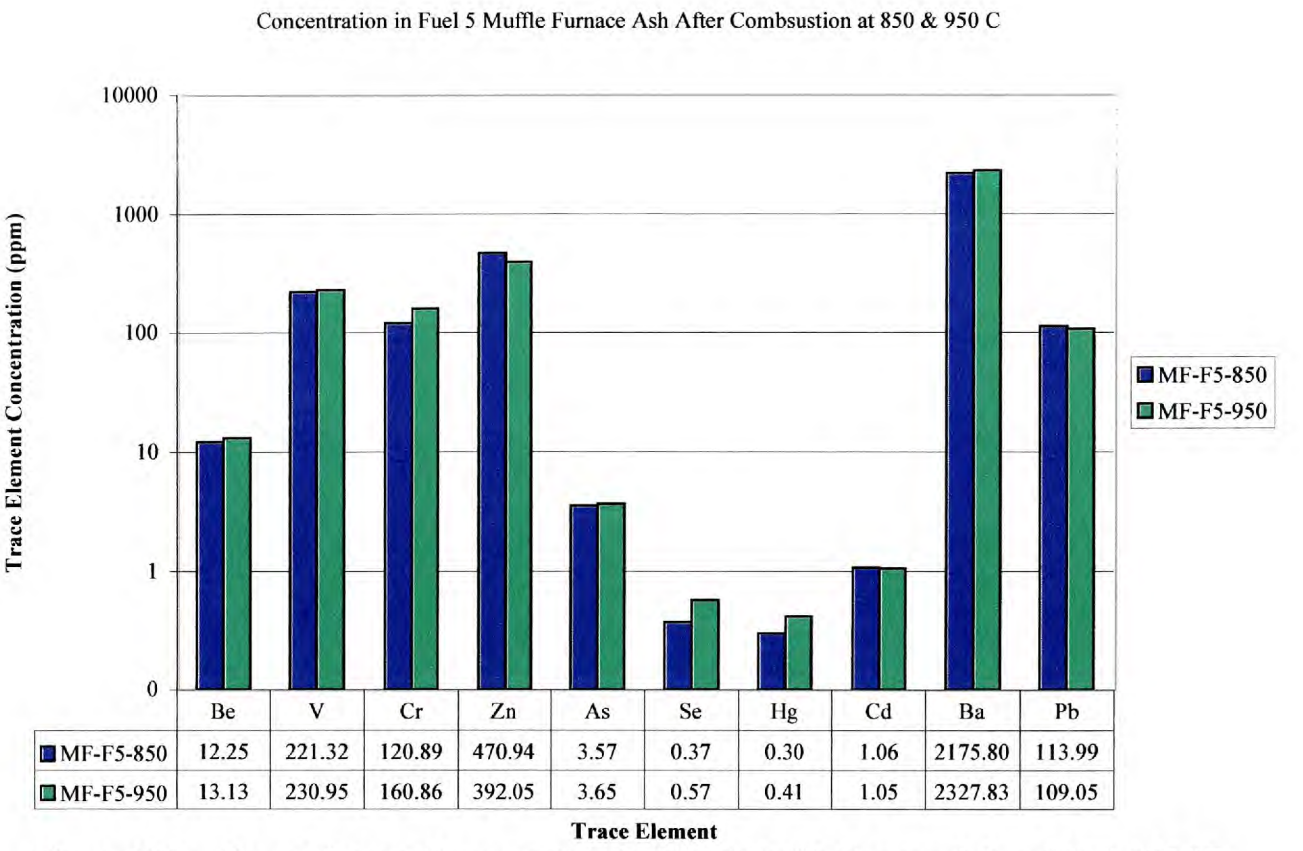
	Be	V	Cr	Zn	As	Se	Hg	Cd	Ba	Pb
MF-F3-850	8.15	200.34	679.14	324.03	1.75	0.74	0.03	0.87	806.08	108.06
MF-F3-950	6.95	180.70	537.84	249.37	1.39	0.58	0.25	0.82	773.27	80.78

Figure AI.1 Trace Element Concentrations in Fuel 1 Muffle Furnace Ash at 850 & 950 °C



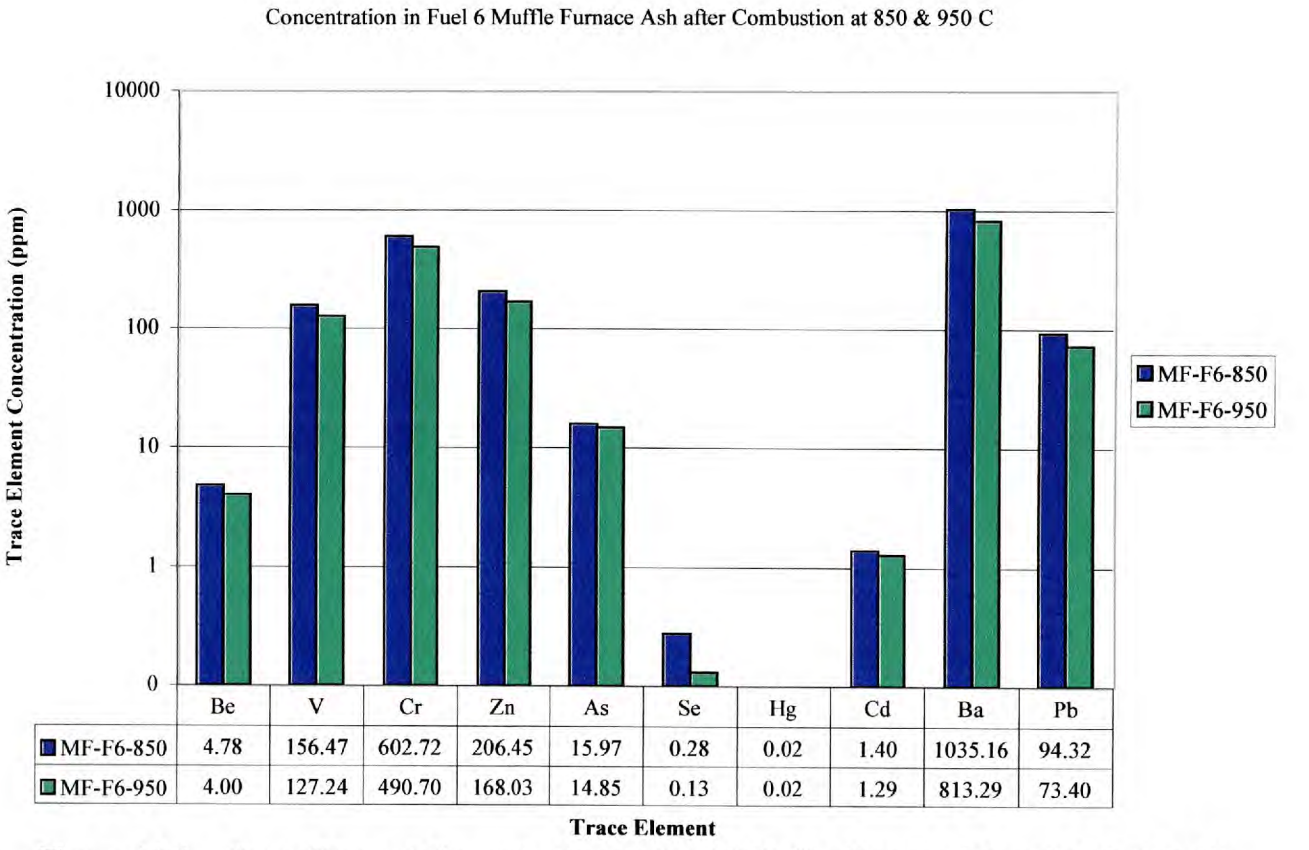
	Be	V	Cr	Zn	As	Se	Hg	Cd	Ba	Pb
MF-F4-850	6.35	221.54	291.23	340.04	2.47	0.53	0.00	0.65	822.97	149.45
MF-F4-950	5.48	199.35	267.25	280.31	2.20	0.54	0.00	0.67	810.59	142.69

Figure AI.4 Trace Element Concentrations in Fuel 4 Muffle Furnace Ash at 850 & 950 °C



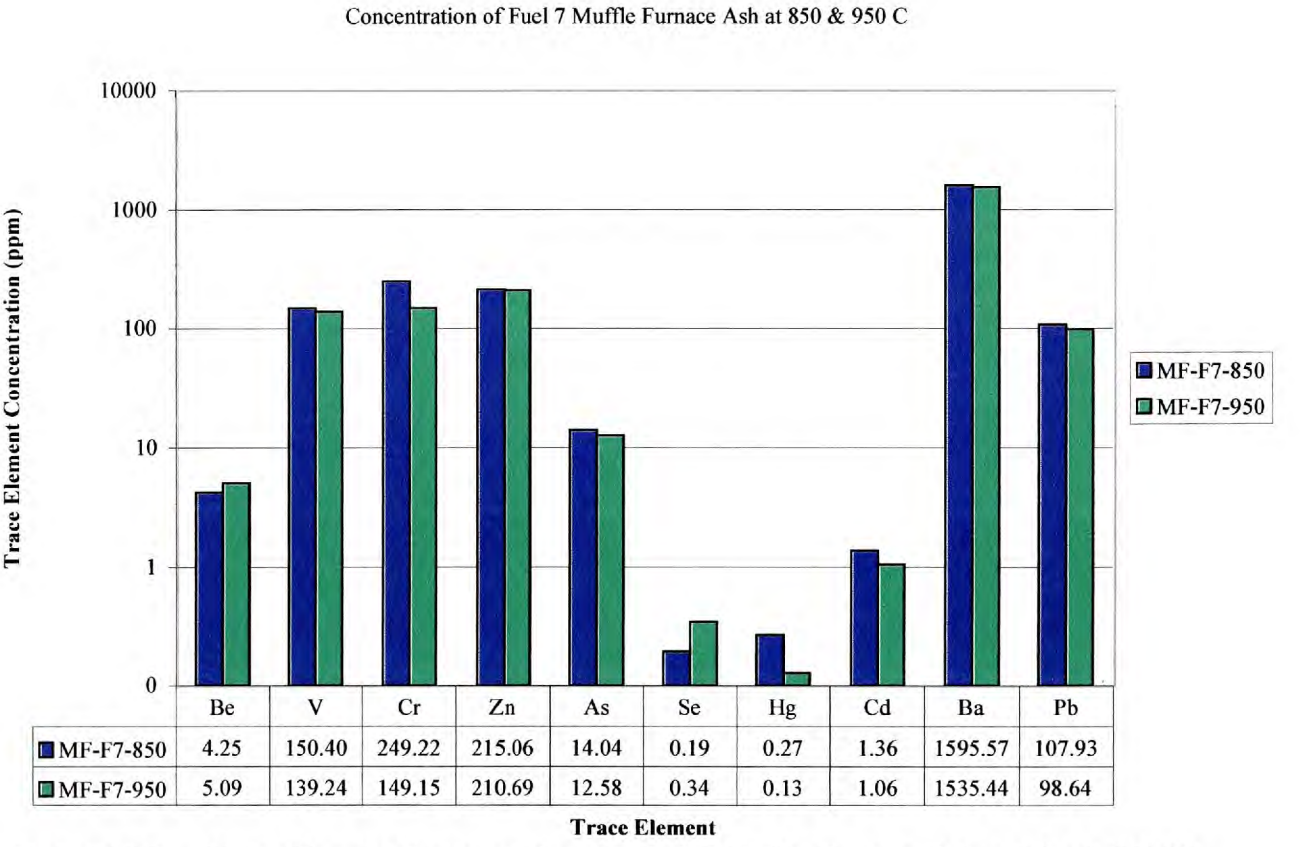
	Be	V	Cr	Zn	As	Se	Hg	Cd	Ba	Pb
MF-F5-850	12.25	221.32	120.89	470.94	3.57	0.37	0.30	1.06	2175.80	113.99
MF-F5-950	13.13	230.95	160.86	392.05	3.65	0.57	0.41	1.05	2327.83	109.05

Figure AI.5 Trace Element Concentrations in Fuel 5 Muffle Furnace Ash at 850 & 950 °C



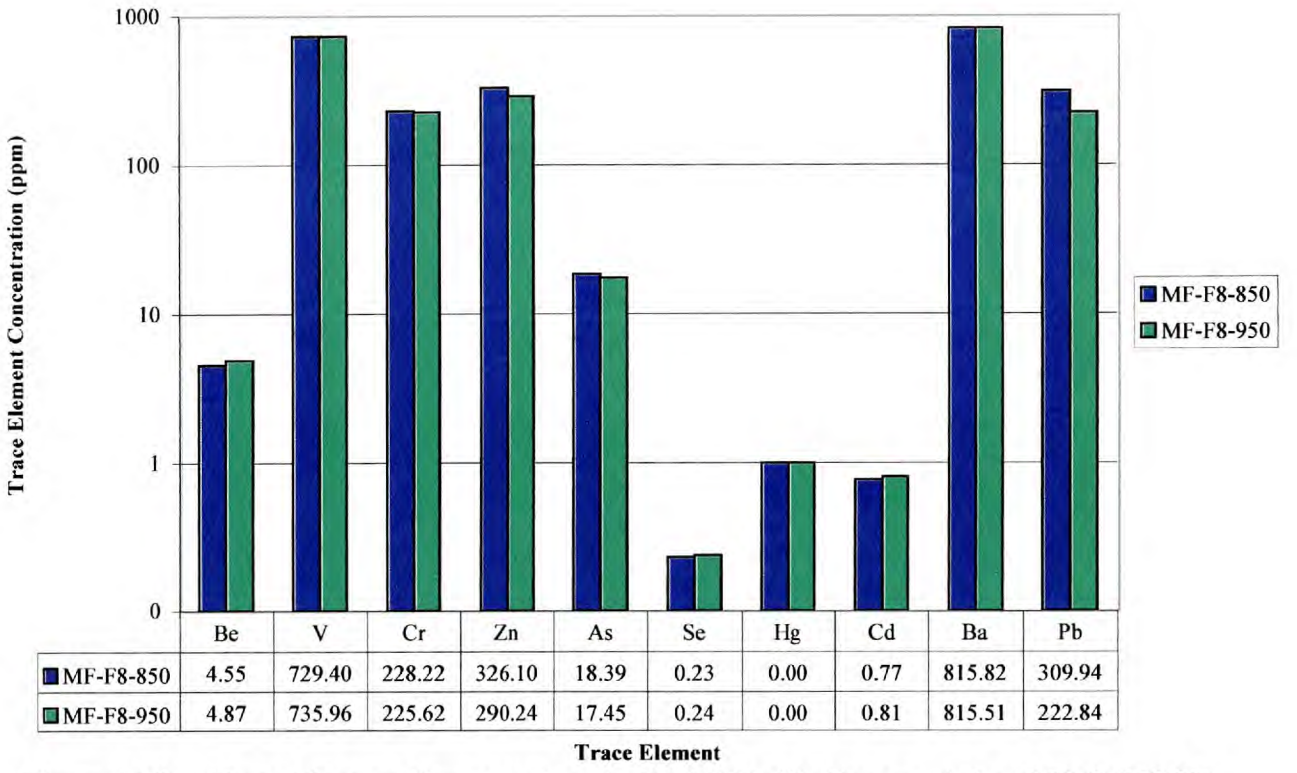
	Be	V	Cr	Zn	As	Se	Hg	Cd	Ba	Pb
MF-F6-850	4.78	156.47	602.72	206.45	15.97	0.28	0.02	1.40	1035.16	94.32
MF-F6-950	4.00	127.24	490.70	168.03	14.85	0.13	0.02	1.29	813.29	73.40

Figure AI.6 Trace Element Concentrations in Fuel 6 Muffle Furnace Ash at 850 & 950 °C



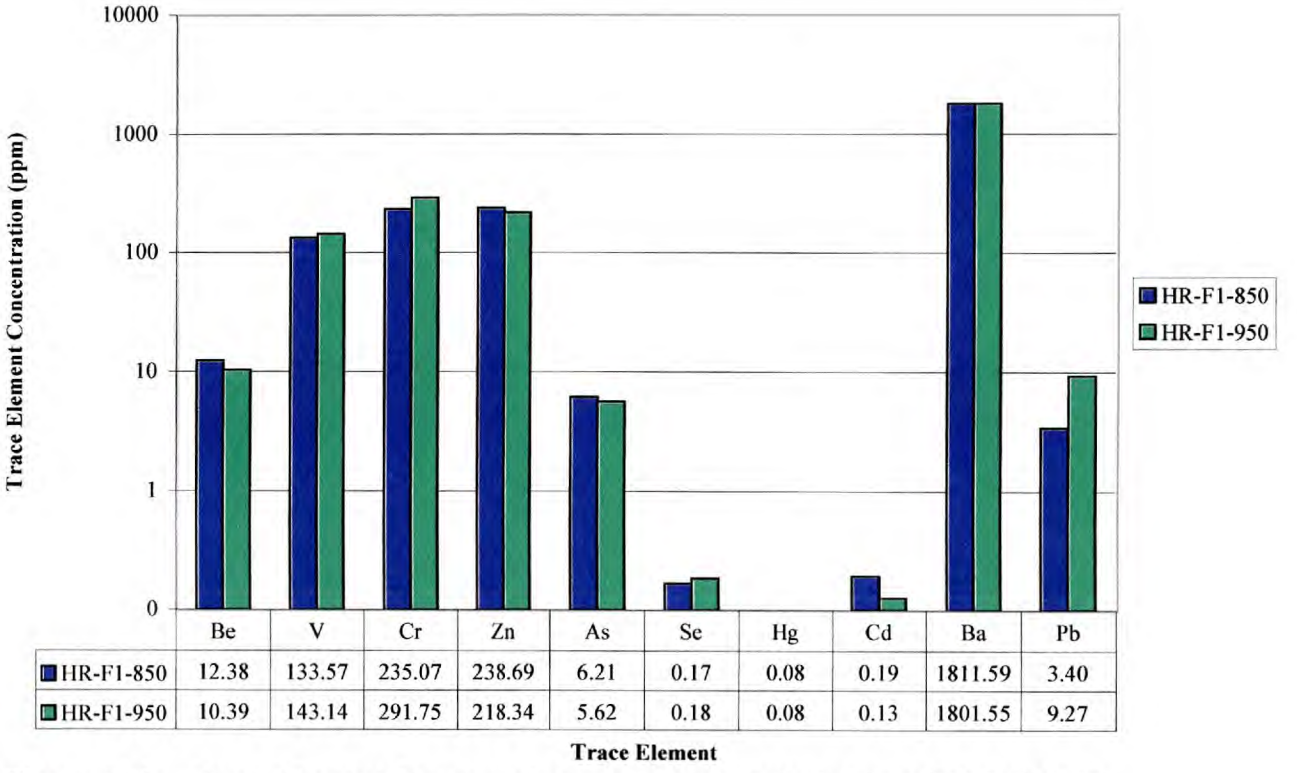
	Be	V	Cr	Zn	As	Se	Hg	Cd	Ba	Pb
MF-F7-850	4.25	150.40	249.22	215.06	14.04	0.19	0.27	1.36	1595.57	107.93
MF-F7-950	5.09	139.24	149.15	210.69	12.58	0.34	0.13	1.06	1535.44	98.64

Figure AI.7 Trace Element Concentrations in Fuel 7 Muffle Furnace Ash at 850 & 950 °C



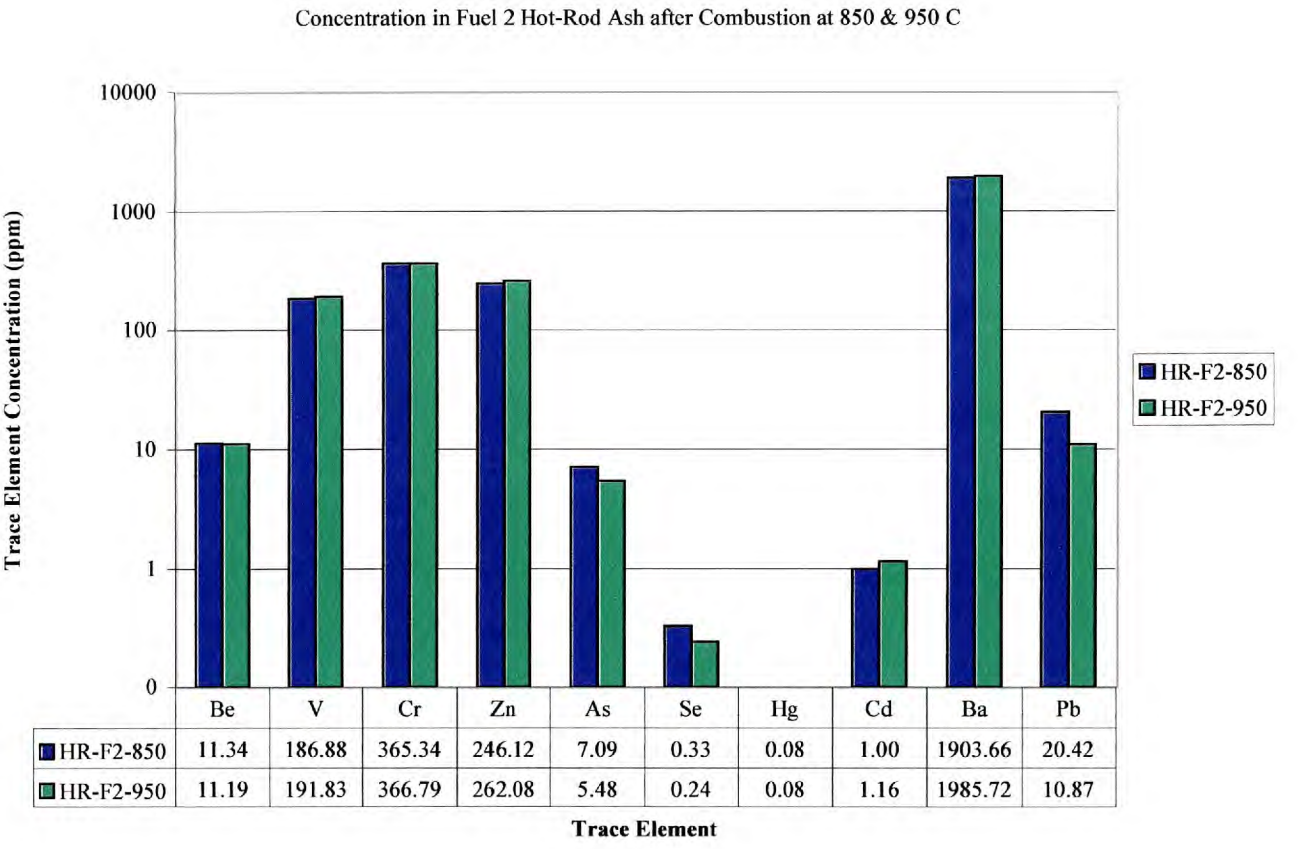
	Be	V	Cr	Zn	As	Se	Hg	Cd	Ba	Pb
MF-F8-850	4.55	729.40	228.22	326.10	18.39	0.23	0.00	0.77	815.82	309.94
MF-F8-950	4.87	735.96	225.62	290.24	17.45	0.24	0.00	0.81	815.51	222.84

Figure AI.8 Trace Element Concentrations in Fuel 8 Muffle Furnace Ash at 850 & 950 °C



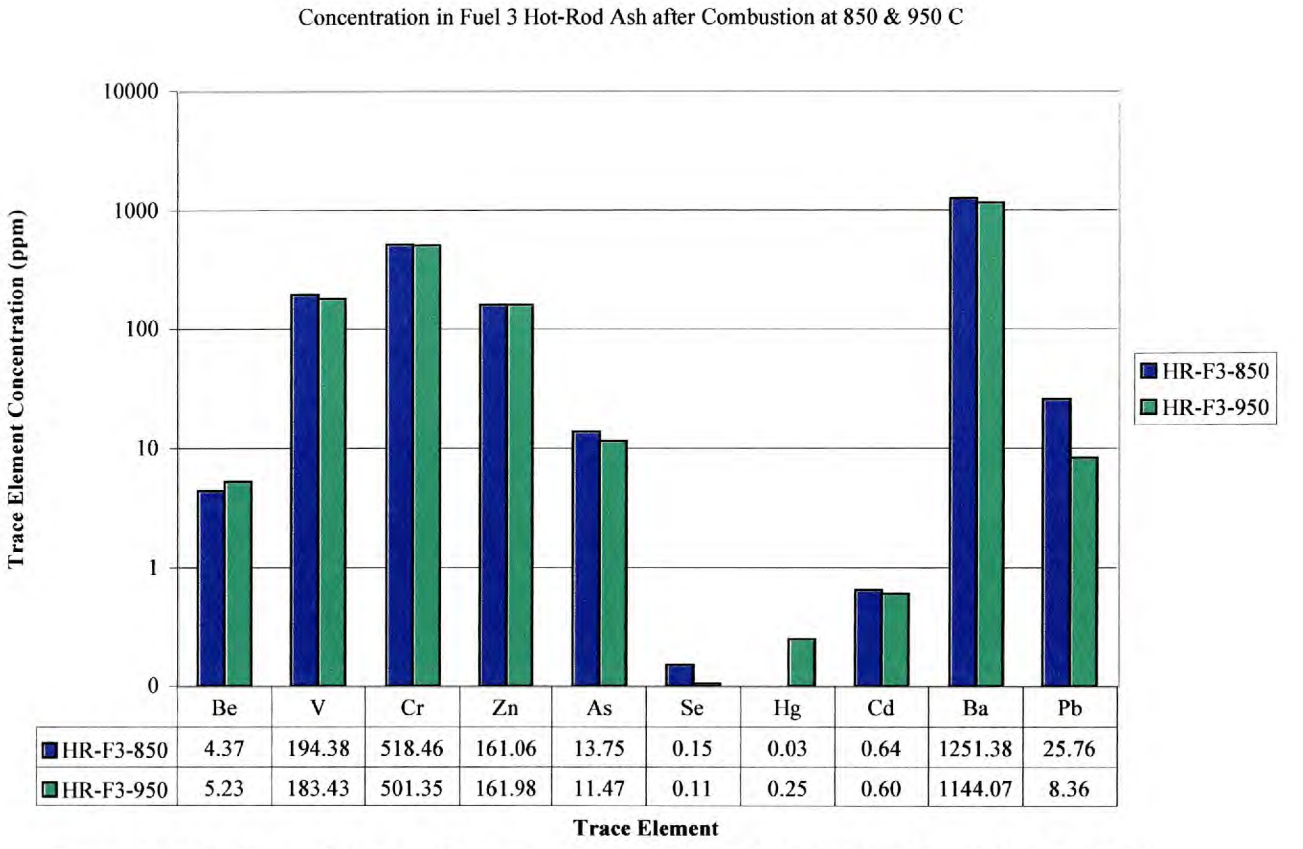
	Be	V	Cr	Zn	As	Se	Hg	Cd	Ba	Pb
HR-F1-850	12.38	133.57	235.07	238.69	6.21	0.17	0.08	0.19	1811.59	3.40
HR-F1-950	10.39	143.14	291.75	218.34	5.62	0.18	0.08	0.13	1801.55	9.27

Figure AI.9 Trace Element Concentrations in Fuel 1 Hot-Rod Ash at 850 & 950 °C



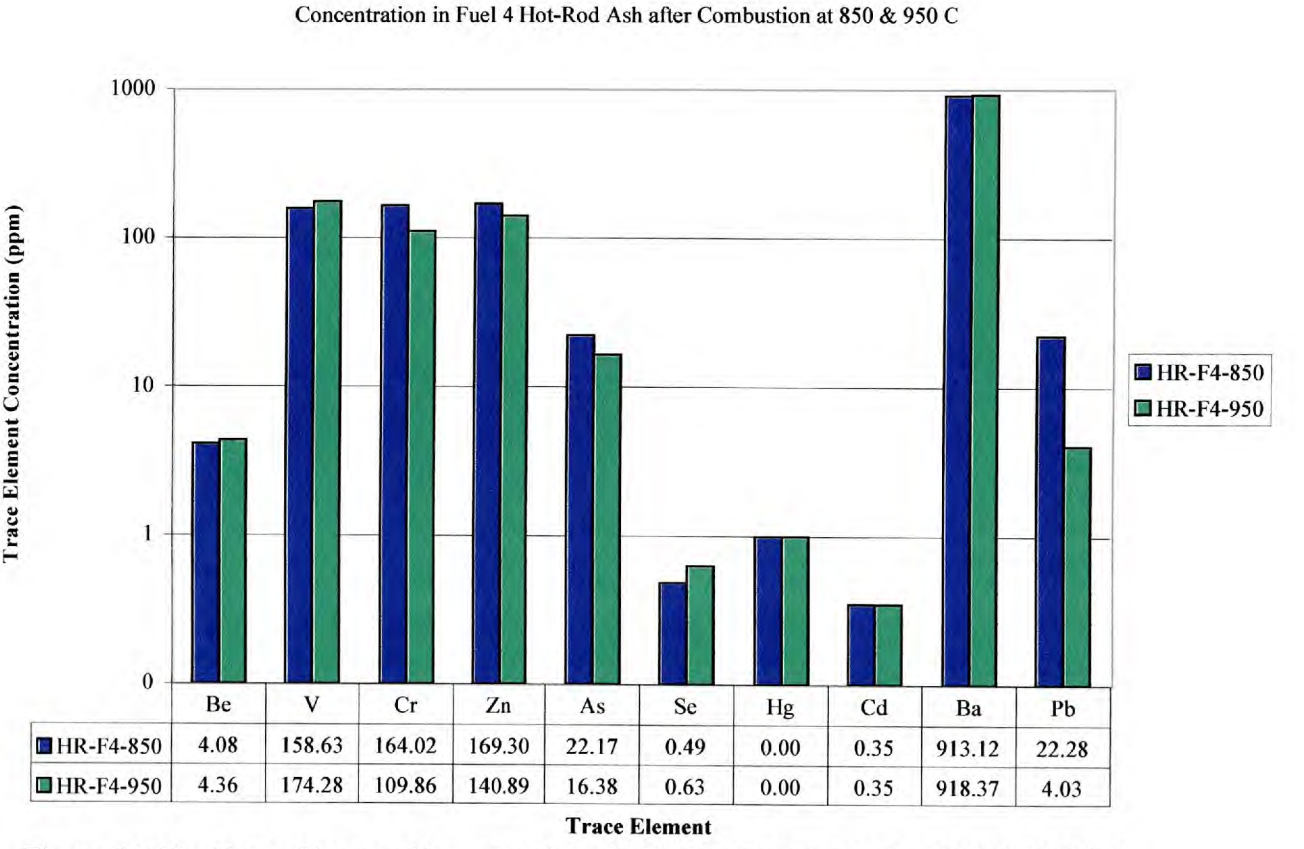
	Be	V	Cr	Zn	As	Se	Hg	Cd	Ba	Pb
HR-F2-850	11.34	186.88	365.34	246.12	7.09	0.33	0.08	1.00	1903.66	20.42
HR-F2-950	11.19	191.83	366.79	262.08	5.48	0.24	0.08	1.16	1985.72	10.87

Figure AI.10 Trace Element Concentrations in Fuel 2 Hot-Rod Ash at 850 & 950 °C



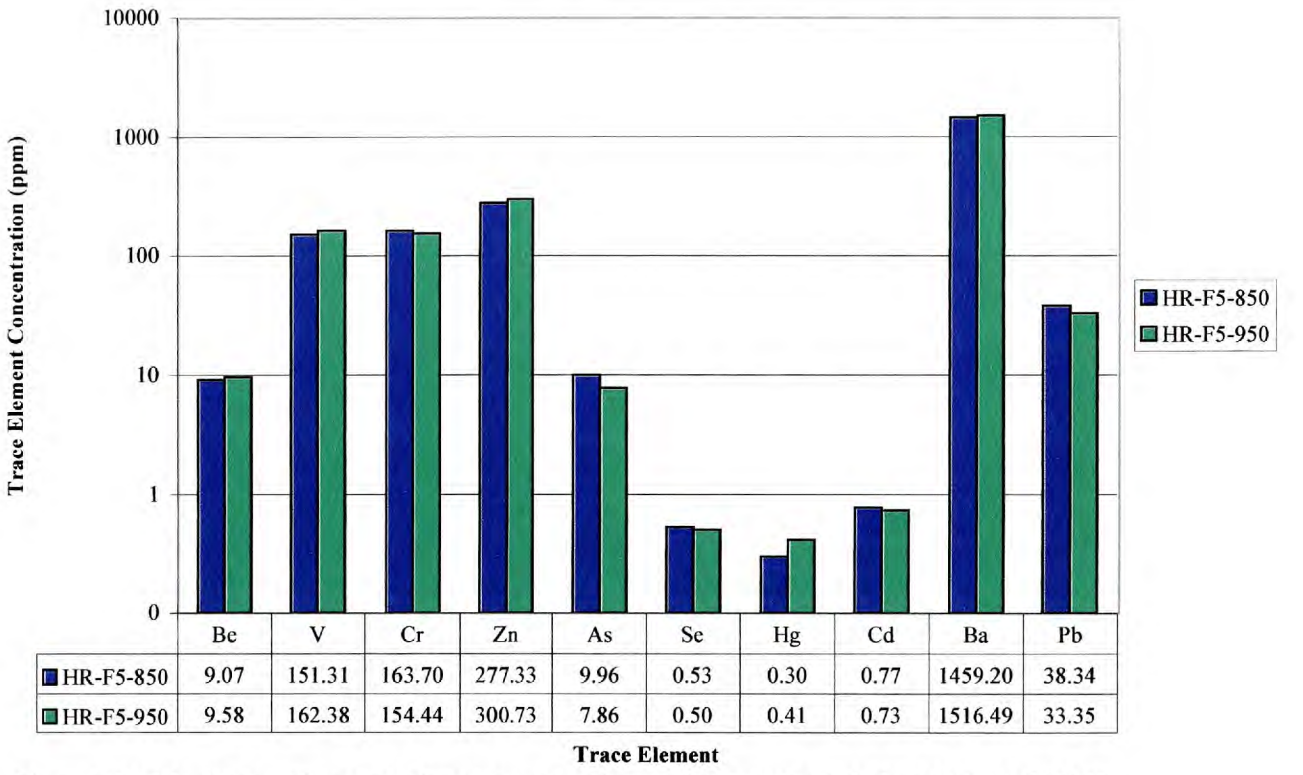
	Be	V	Cr	Zn	As	Se	Hg	Cd	Ba	Pb
HR-F3-850	4.37	194.38	518.46	161.06	13.75	0.15	0.03	0.64	1251.38	25.76
HR-F3-950	5.23	183.43	501.35	161.98	11.47	0.11	0.25	0.60	1144.07	8.36

Figure AI.11 Trace Element Concentrations in Fuel 3 Hot-Rod Ash at 850 & 950 °C



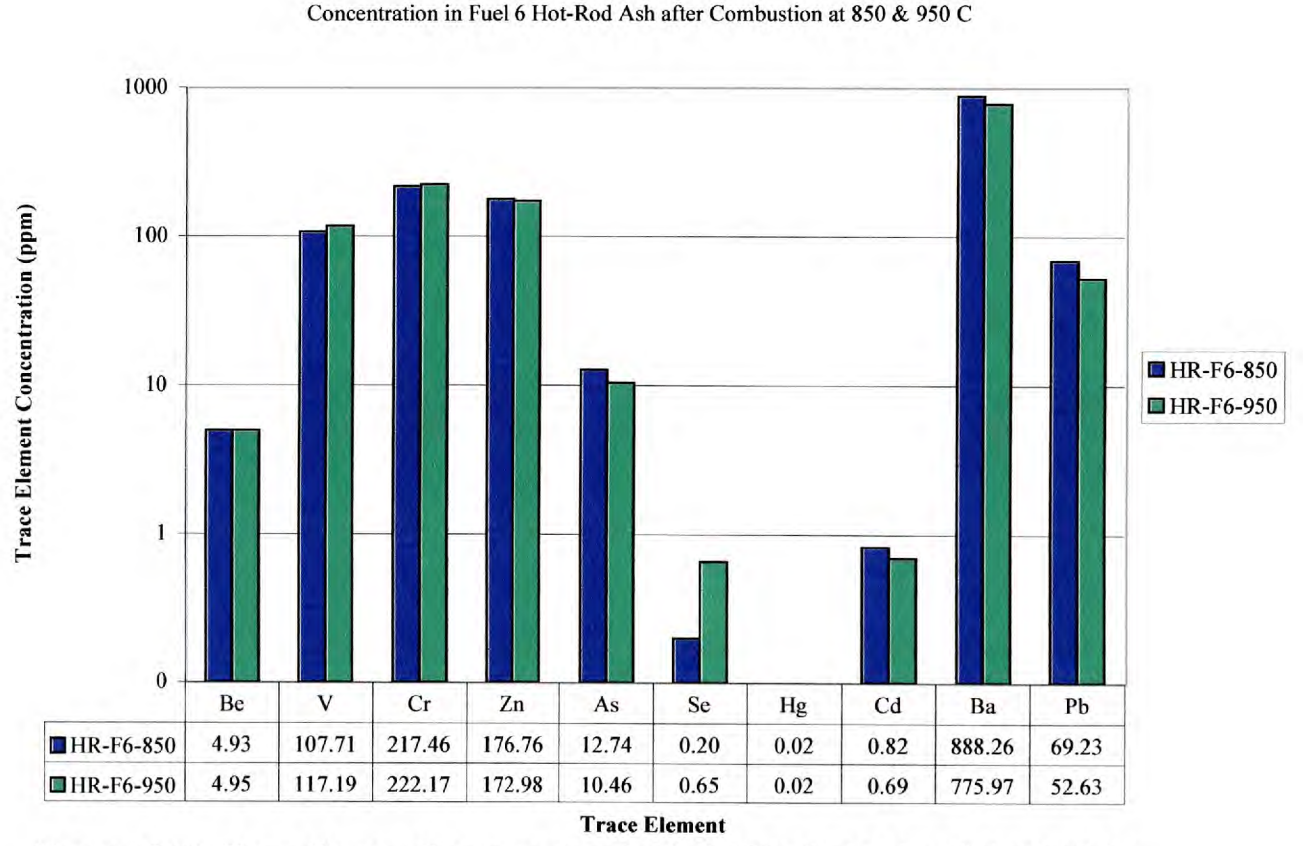
	Be	V	Cr	Zn	As	Se	Hg	Cd	Ba	Pb
HR-F4-850	4.08	158.63	164.02	169.30	22.17	0.49	0.00	0.35	913.12	22.28
HR-F4-950	4.36	174.28	109.86	140.89	16.38	0.63	0.00	0.35	918.37	4.03

Figure AI.12 Trace Element Concentrations in Fuel 4 Hot-Rod Ash at 850 & 950 °C



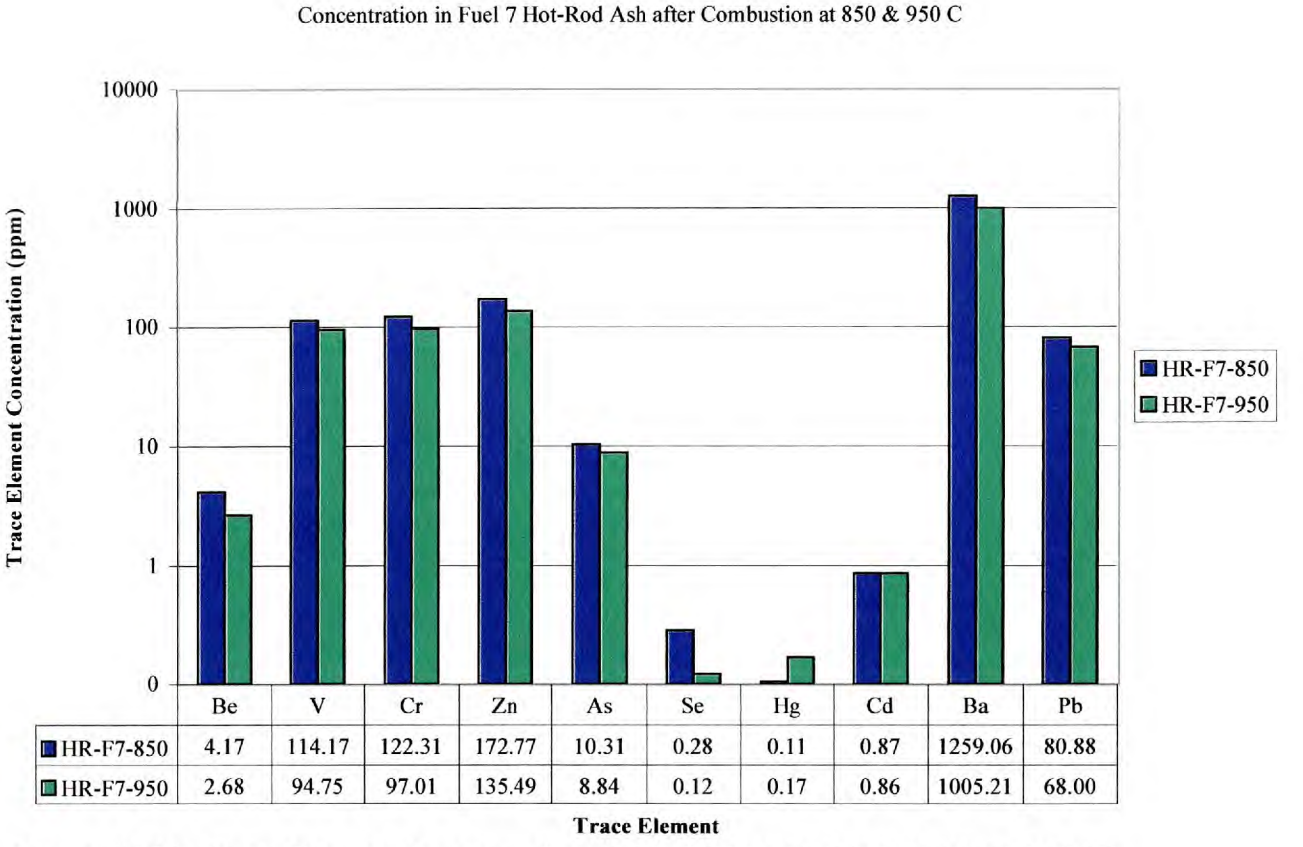
	Be	V	Cr	Zn	As	Se	Hg	Cd	Ba	Pb
HR-F5-850	9.07	151.31	163.70	277.33	9.96	0.53	0.30	0.77	1459.20	38.34
HR-F5-950	9.58	162.38	154.44	300.73	7.86	0.50	0.41	0.73	1516.49	33.35

Figure AI.13 Trace Element Concentrations in Fuel 5 Hot-Rod Ash at 850 & 950 °C



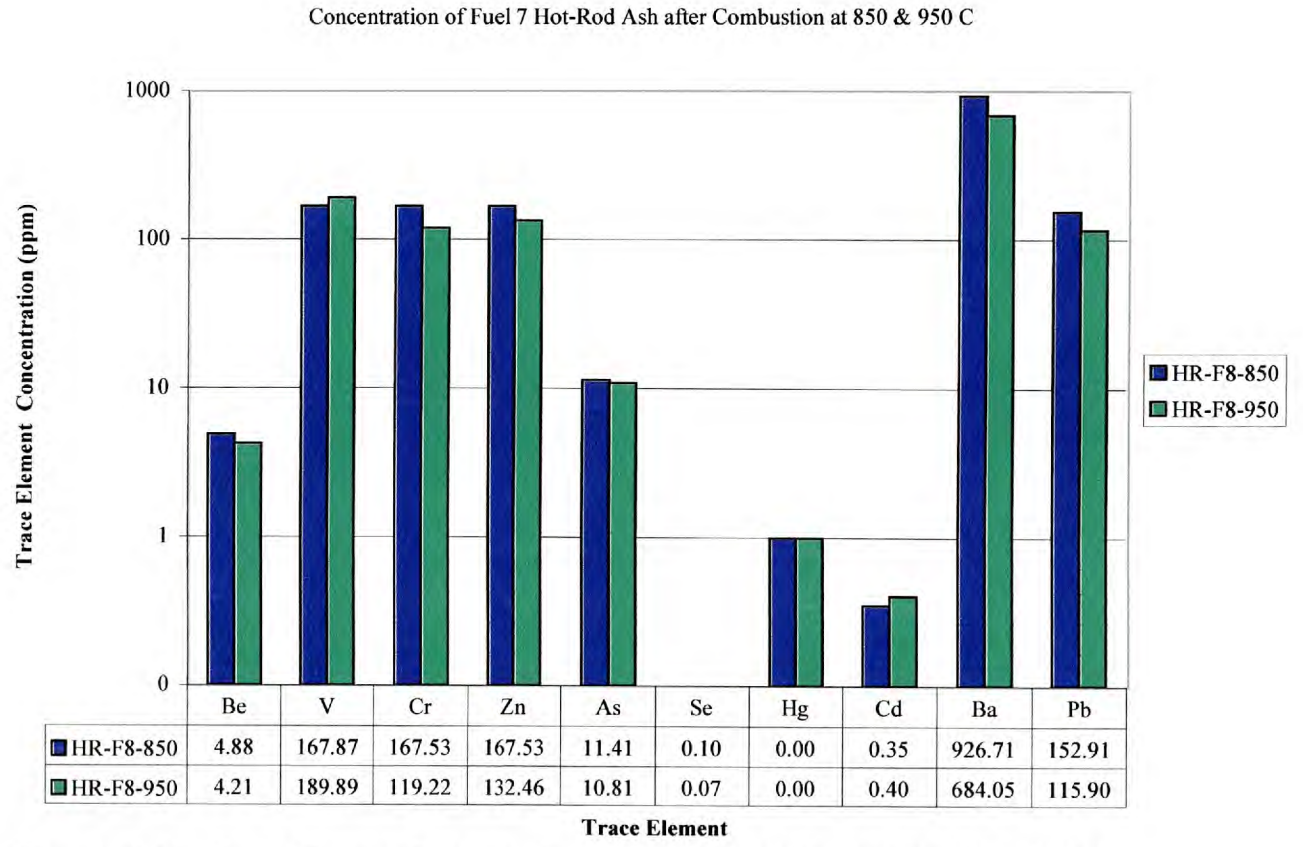
	Be	V	Cr	Zn	As	Se	Hg	Cd	Ba	Pb
HR-F6-850	4.93	107.71	217.46	176.76	12.74	0.20	0.02	0.82	888.26	69.23
HR-F6-950	4.95	117.19	222.17	172.98	10.46	0.65	0.02	0.69	775.97	52.63

Figure AI.14 Trace Element Concentrations in Fuel 6 Hot-Rod Ash at 850 & 950 °C



	Be	V	Cr	Zn	As	Se	Hg	Cd	Ba	Pb
HR-F7-850	4.17	114.17	122.31	172.77	10.31	0.28	0.11	0.87	1259.06	80.88
HR-F7-950	2.68	94.75	97.01	135.49	8.84	0.12	0.17	0.86	1005.21	68.00

Figure AI.15 Trace Element Concentrations in Fuel 7 Hot-Rod Ash at 850 & 950 °C



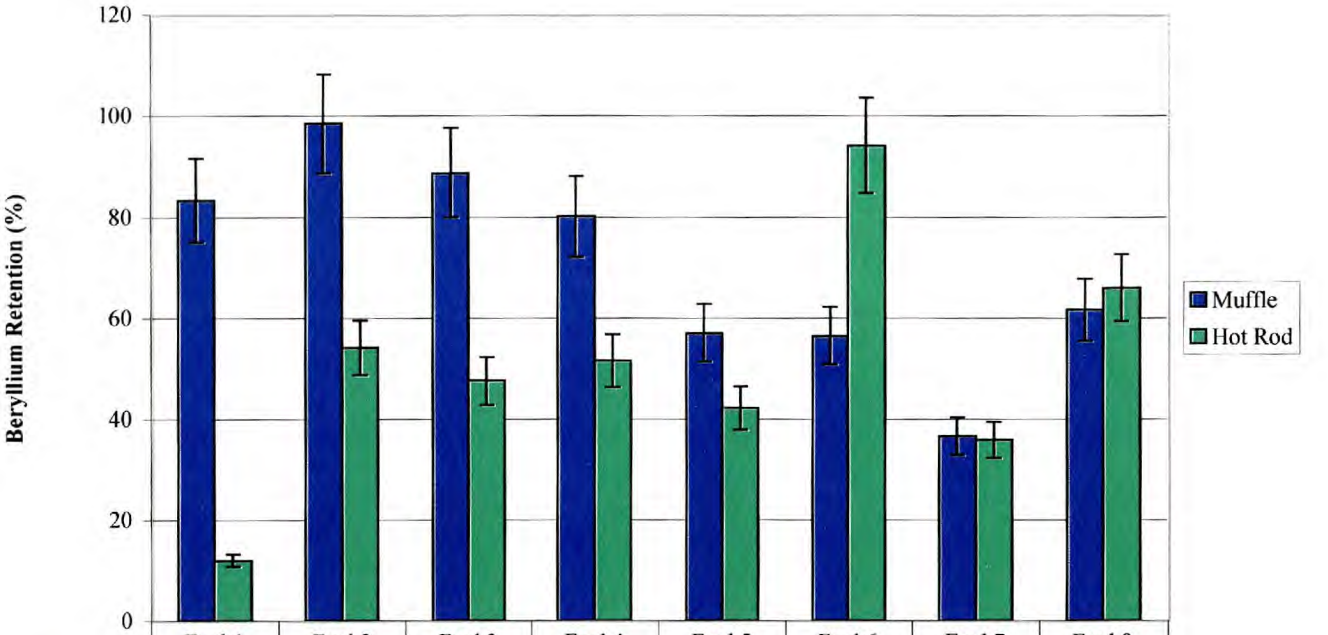
	Be	V	Cr	Zn	As	Se	Hg	Cd	Ba	Pb
HR-F8-850	4.88	167.87	167.53	167.53	11.41	0.10	0.00	0.35	926.71	152.91
HR-F8-950	4.21	189.89	119.22	132.46	10.81	0.07	0.00	0.40	684.05	115.90

Figure AI.16 Trace Element Concentrations in Fuel 8 Hot-Rod Ash at 850 & 950 °C

APPENDIX II

Appendix II depicts the trace element retentions as a function of combustion method. The results presented in this appendix are discussed in Section 5.4. Each figure presents a particular the trace element retention for a particular element, at a particular temperature for the eight fuels studied, and the two combustion methods. Precise results are given in data tables. Error bars are calculated as the square root of the sum of the squares of the trace element concentration in the fuel and the concentration in the ash.

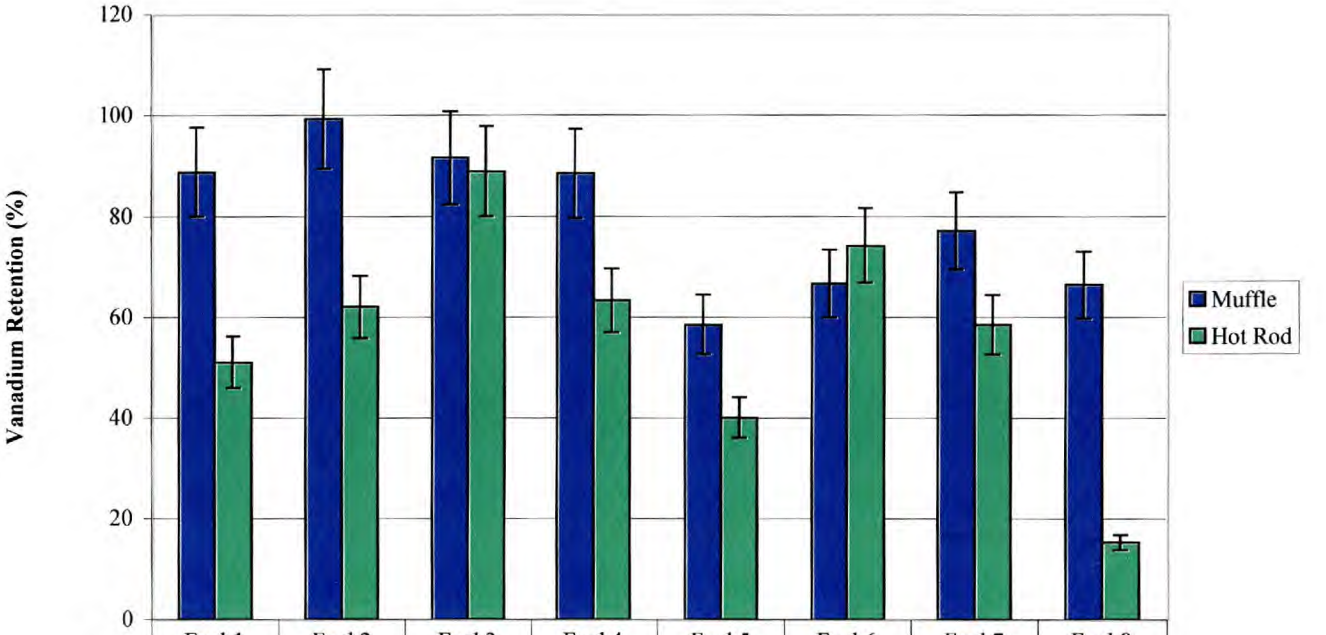
% Beryllium Retention as a Function of Combustion Method at 850 C



	Fuel 1	Fuel 2	Fuel 3	Fuel 4	Fuel 5	Fuel 6	Fuel 7	Fuel 8
Muffle	83.37	98.52	88.77	80.20	57.03	56.50	36.61	61.64
Hot Rod	12.07	54.20	47.56	51.56	42.24	94.14	35.90	66.01

Fuel Studied

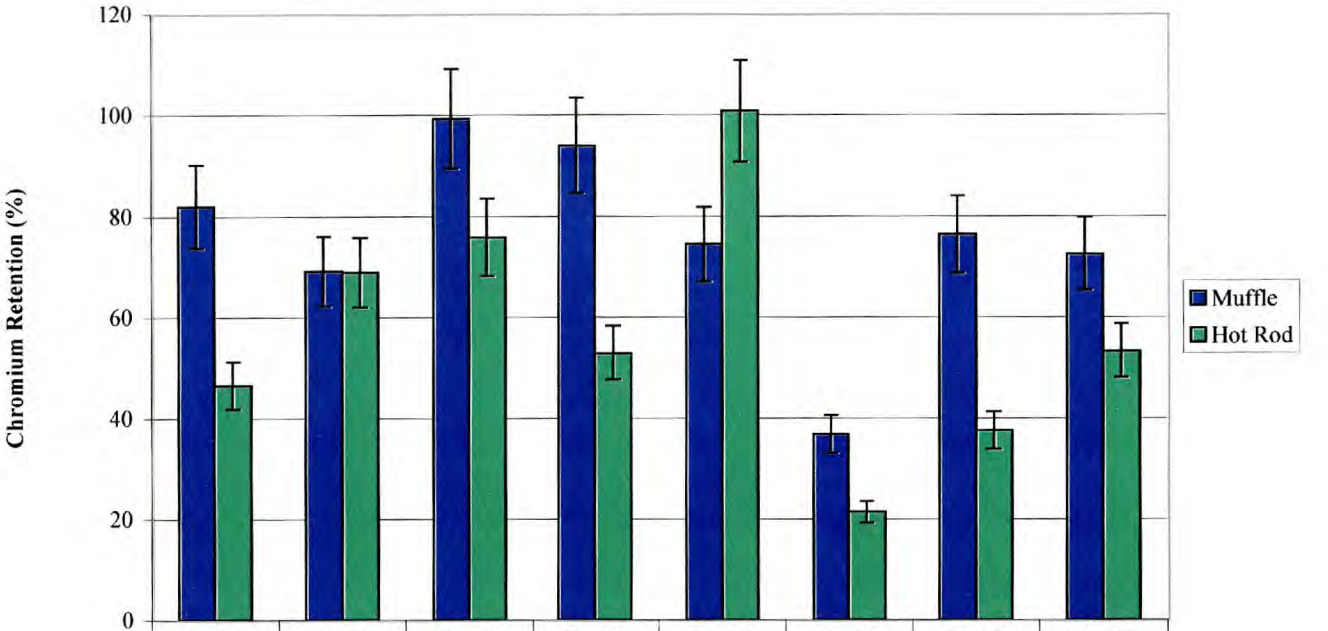
% Vanadium Retention as a Function of Combustion Method at 850 C



	Fuel 1	Fuel 2	Fuel 3	Fuel 4	Fuel 5	Fuel 6	Fuel 7	Fuel 8
Muffle	88.75	99.28	91.60	88.44	58.50	66.67	77.12	66.46
Hot Rod	51.04	61.99	88.87	63.33	40.00	74.20	58.54	15.30

Fuel Studied

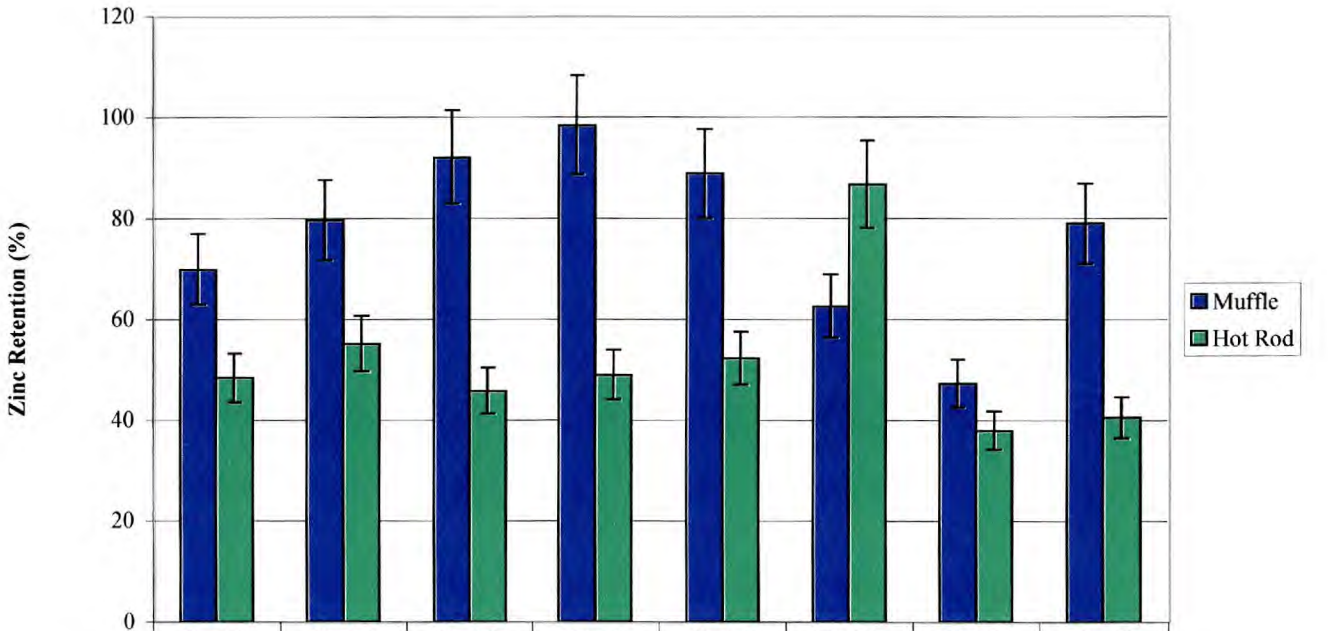
% Chromium Retention as a Function of Combustion Method at 850



	Fuel 1	Fuel 2	Fuel 3	Fuel 4	Fuel 5	Fuel 6	Fuel 7	Fuel 8
Muffle	82.04	69.12	99.34	94.00	74.43	36.80	76.41	72.54
Hot Rod	46.50	68.86	75.83	52.94	100.79	21.46	37.50	53.25

Fuel Studied

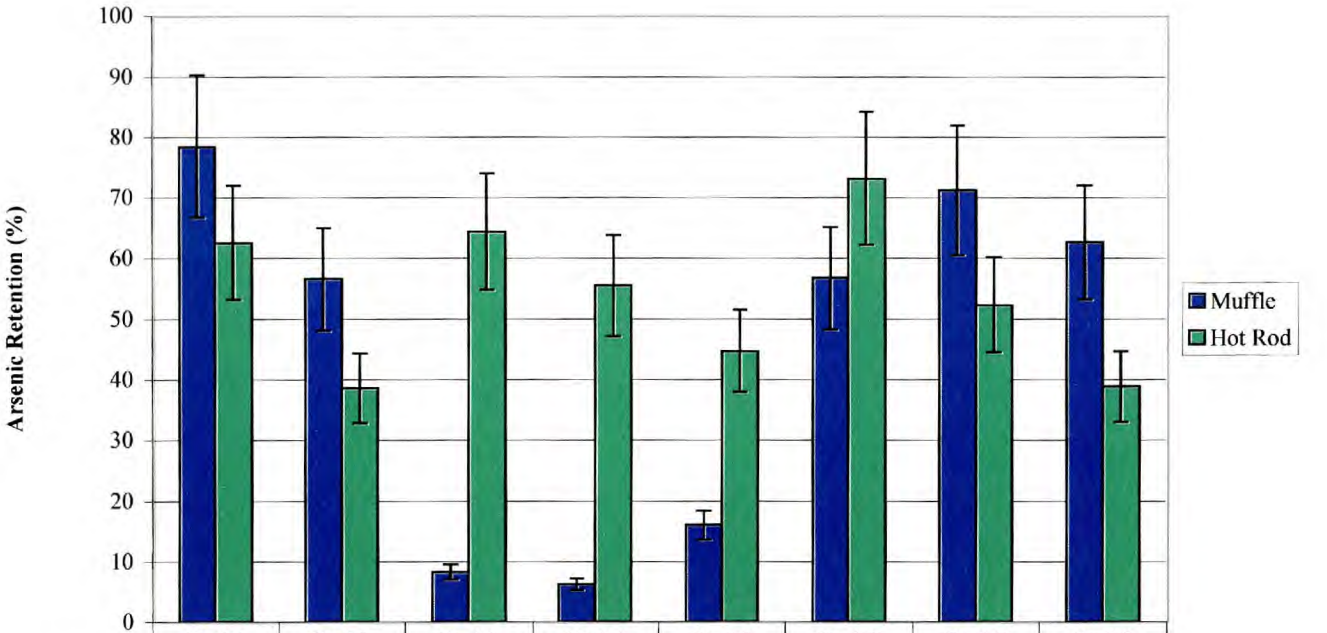
% Zinc Retention as a Function of Combustion Method at 850 C



	Fuel 1	Fuel 2	Fuel 3	Fuel 4	Fuel 5	Fuel 6	Fuel 7	Fuel 8
Muffle	69.93	79.62	92.11	98.45	88.85	62.62	47.32	78.90
Hot Rod	48.40	55.12	45.79	49.02	52.32	86.68	38.01	40.53

Fuel Studied

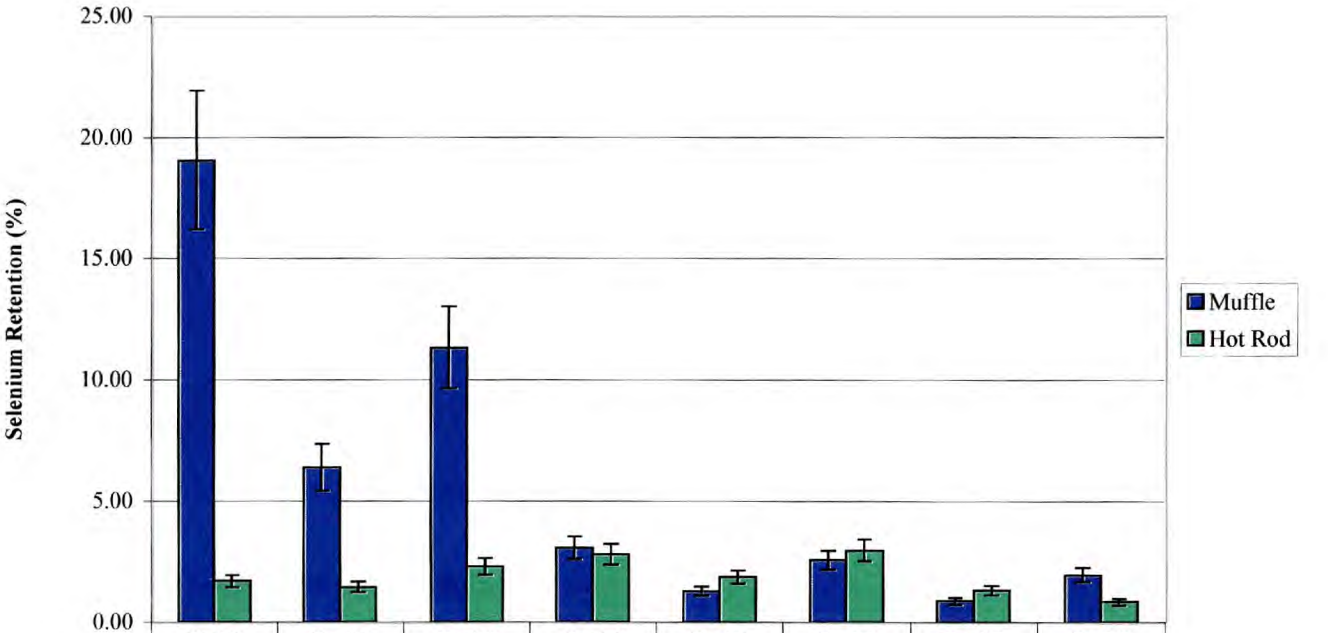
% Arsenic Retention as a Function of Combustion Method at 850 C



	Fuel 1	Fuel 2	Fuel 3	Fuel 4	Fuel 5	Fuel 6	Fuel 7	Fuel 8
Muffle	78.45	56.57	8.22	6.19	16.03	56.74	71.24	62.64
Hot Rod	62.60	38.58	64.46	55.54	44.74	73.15	52.33	38.85

Fuel Studied

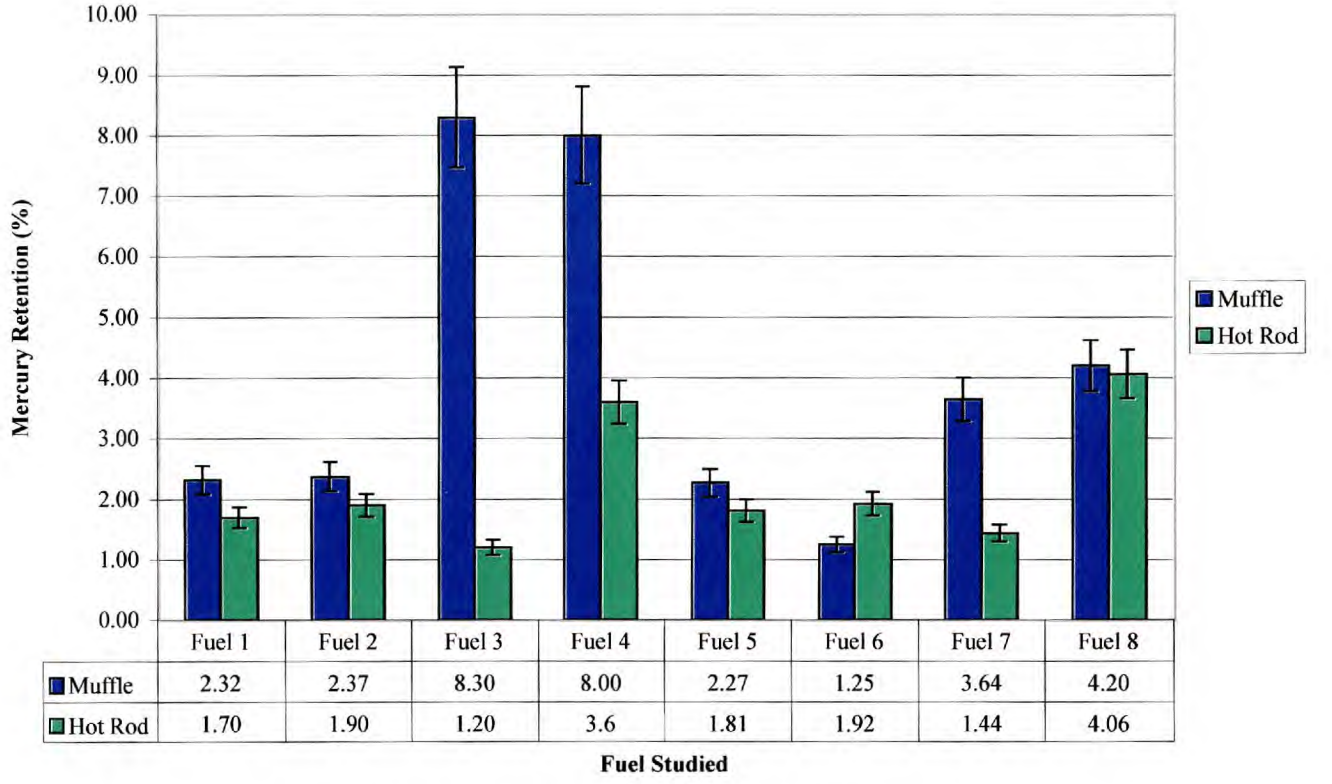
% Selenium Retention as a Function of Combustion Method at 850 C



	Fuel 1	Fuel 2	Fuel 3	Fuel 4	Fuel 5	Fuel 6	Fuel 7	Fuel 8
Muffle	19.08	6.39	11.34	3.09	1.30	2.59	0.90	1.97
Hot Rod	1.71	1.46	2.32	2.81	1.87	2.98	1.32	0.85

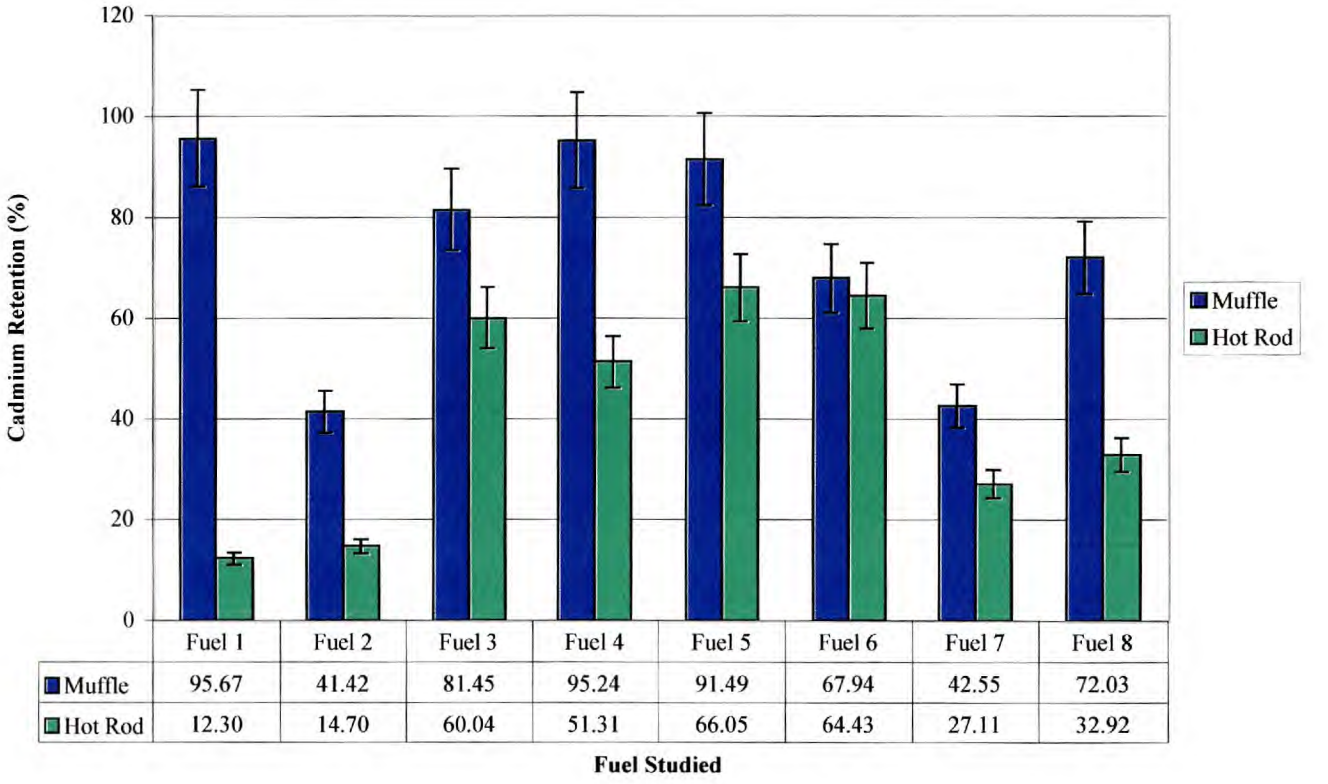
Fuel Studied

% Mercury Retention as a Function of Combustion Method at 850 C



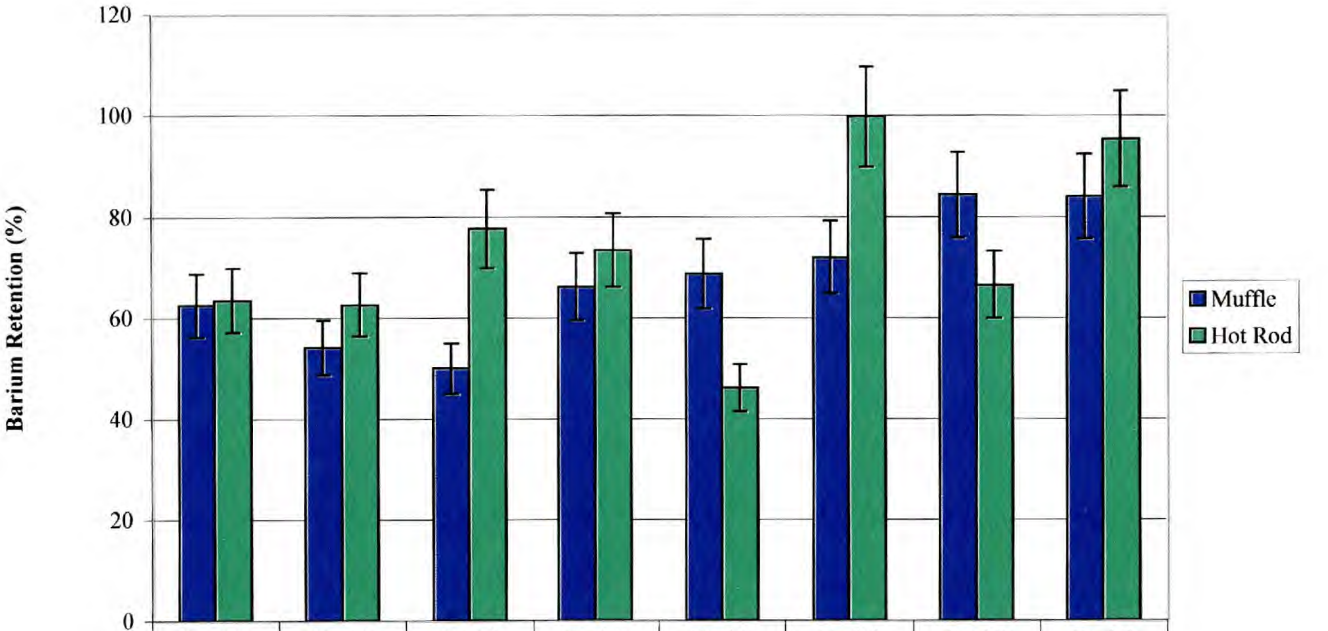
	Fuel 1	Fuel 2	Fuel 3	Fuel 4	Fuel 5	Fuel 6	Fuel 7	Fuel 8
Muffle	2.32	2.37	8.30	8.00	2.27	1.25	3.64	4.20
Hot Rod	1.70	1.90	1.20	3.6	1.81	1.92	1.44	4.06

% Cadmium Retention as a Function of Combustion Method at 850 C



	Fuel 1	Fuel 2	Fuel 3	Fuel 4	Fuel 5	Fuel 6	Fuel 7	Fuel 8
Muffle	95.67	41.42	81.45	95.24	91.49	67.94	42.55	72.03
Hot Rod	12.30	14.70	60.04	51.31	66.05	64.43	27.11	32.92

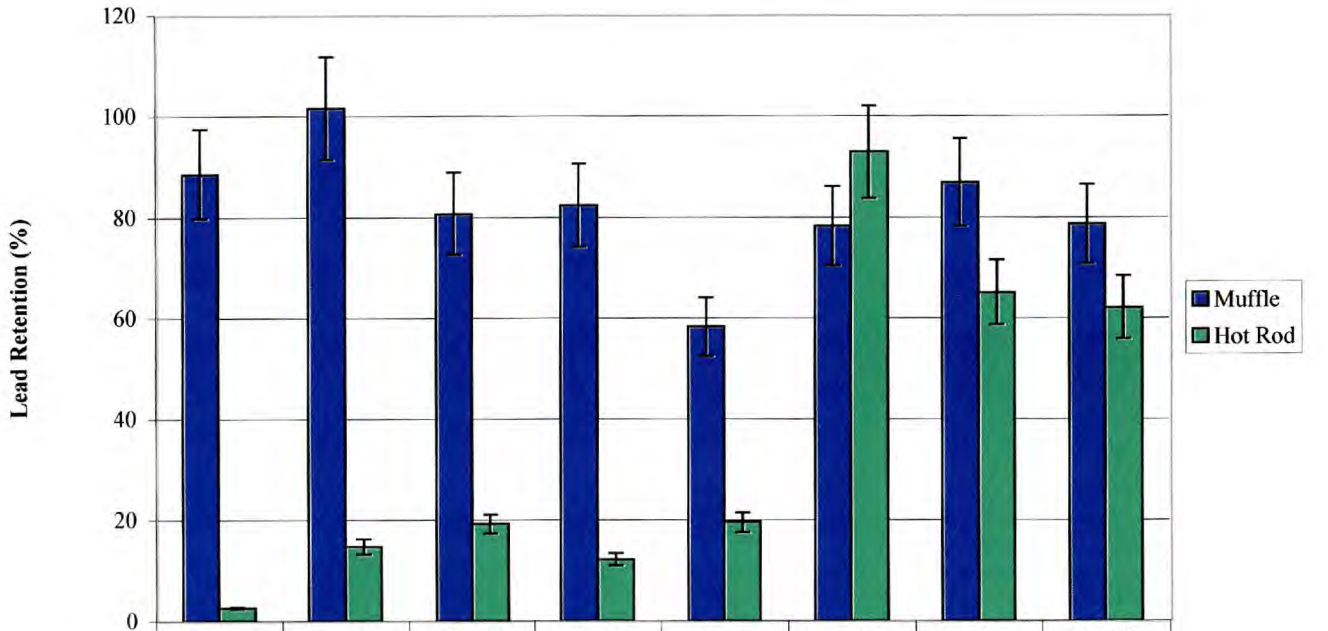
% Barium Retention as a Function of Combustion Method at 850 C



	Fuel 1	Fuel 2	Fuel 3	Fuel 4	Fuel 5	Fuel 6	Fuel 7	Fuel 8
Muffle	62.50	54.11	49.98	66.16	68.78	71.96	84.32	83.97
Hot Rod	63.58	62.62	77.60	73.41	46.13	99.82	66.53	95.38

Fuel Studied

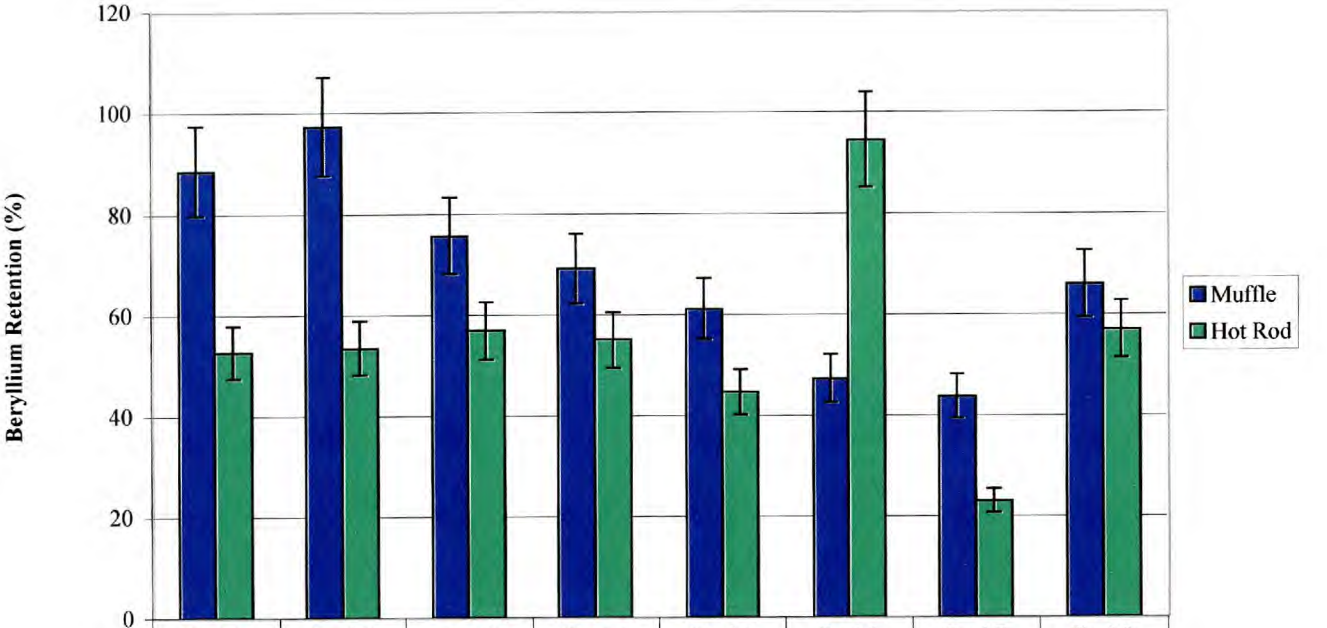
% Lead Retention as a Function of Combustion Method



	Fuel 1	Fuel 2	Fuel 3	Fuel 4	Fuel 5	Fuel 6	Fuel 7	Fuel 8
Muffle	88.54	101.66	80.76	82.29	58.29	78.29	86.84	78.63
Hot Rod	2.65	14.87	19.25	12.27	19.60	92.91	65.07	62.07

Fuel Studied

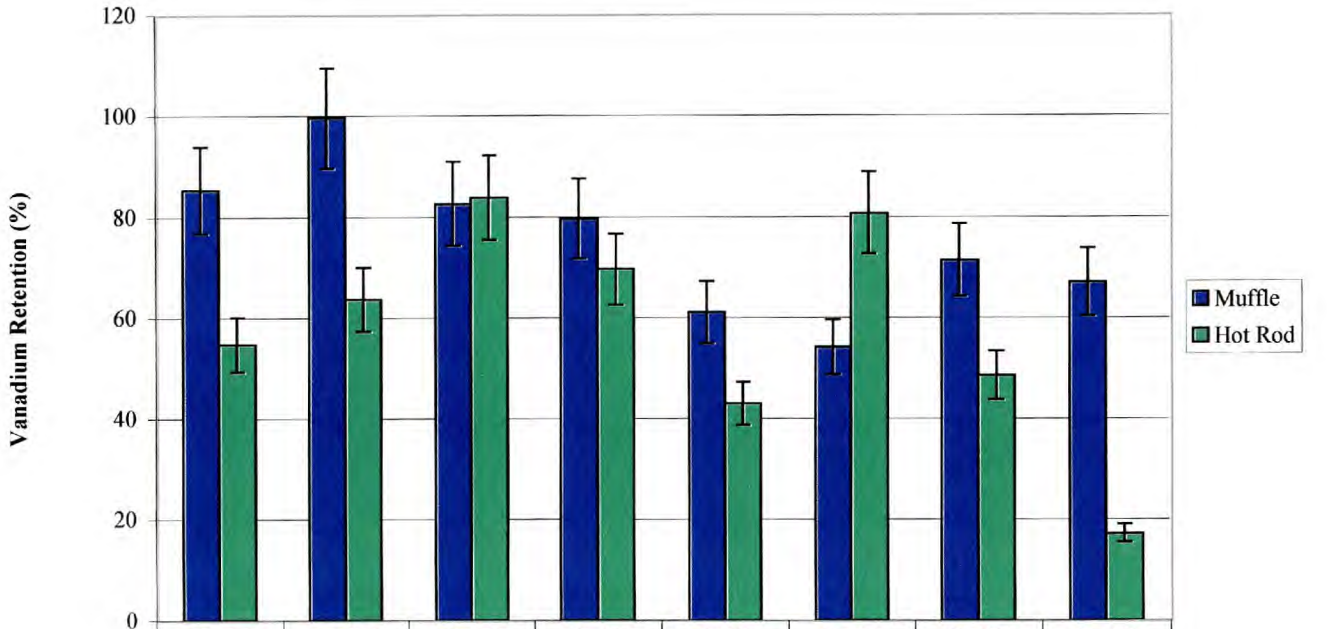
% Beryllium Retention as a Function of Combustion Method at 950 C



	Fuel 1	Fuel 2	Fuel 3	Fuel 4	Fuel 5	Fuel 6	Fuel 7	Fuel 8
Muffle	88.59	97.36	75.68	69.15	61.14	47.31	43.78	65.96
Hot Rod	52.62	53.48	56.95	55.04	44.62	94.56	23.07	57.01

Fuel Studied

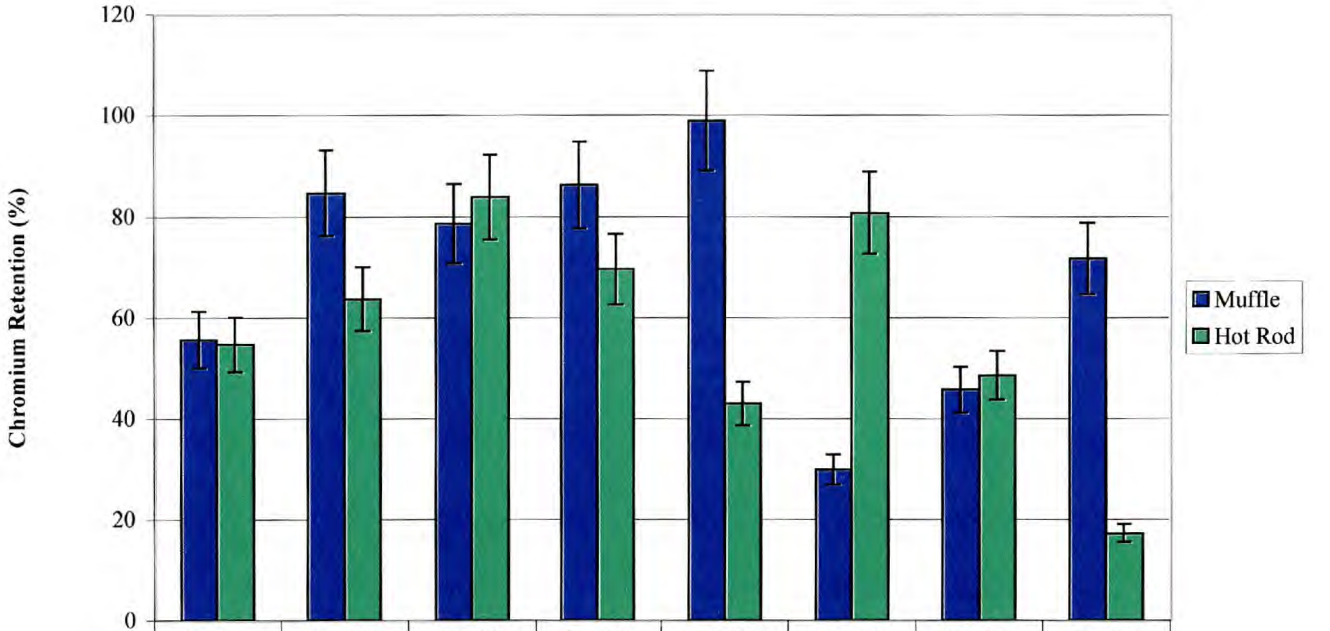
% Vanadium Retention as a Function of Combustion Method at 950 C



	Fuel 1	Fuel 2	Fuel 3	Fuel 4	Fuel 5	Fuel 6	Fuel 7	Fuel 8
Muffle	85.32	99.64	82.62	79.58	61.05	54.22	71.39	67.06
Hot Rod	54.70	63.63	83.87	69.57	42.92	80.73	48.58	17.30

Fuel Studied

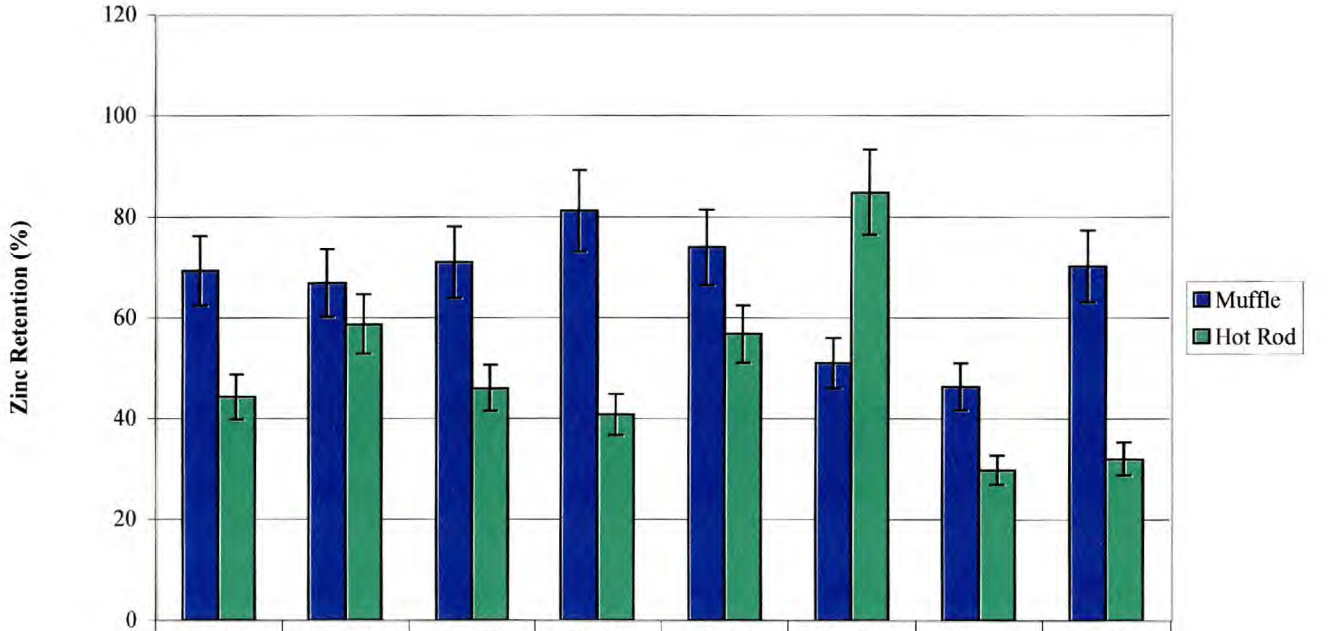
% Chromium Retention as a Function of Combustion Method at 950 C



	Fuel 1	Fuel 2	Fuel 3	Fuel 4	Fuel 5	Fuel 6	Fuel 7	Fuel 8
Muffle	55.66	84.64	78.67	86.26	99.03	29.96	45.73	71.71
Hot Rod	54.70	63.63	83.87	69.57	42.92	80.73	48.58	17.30

Fuel Studied

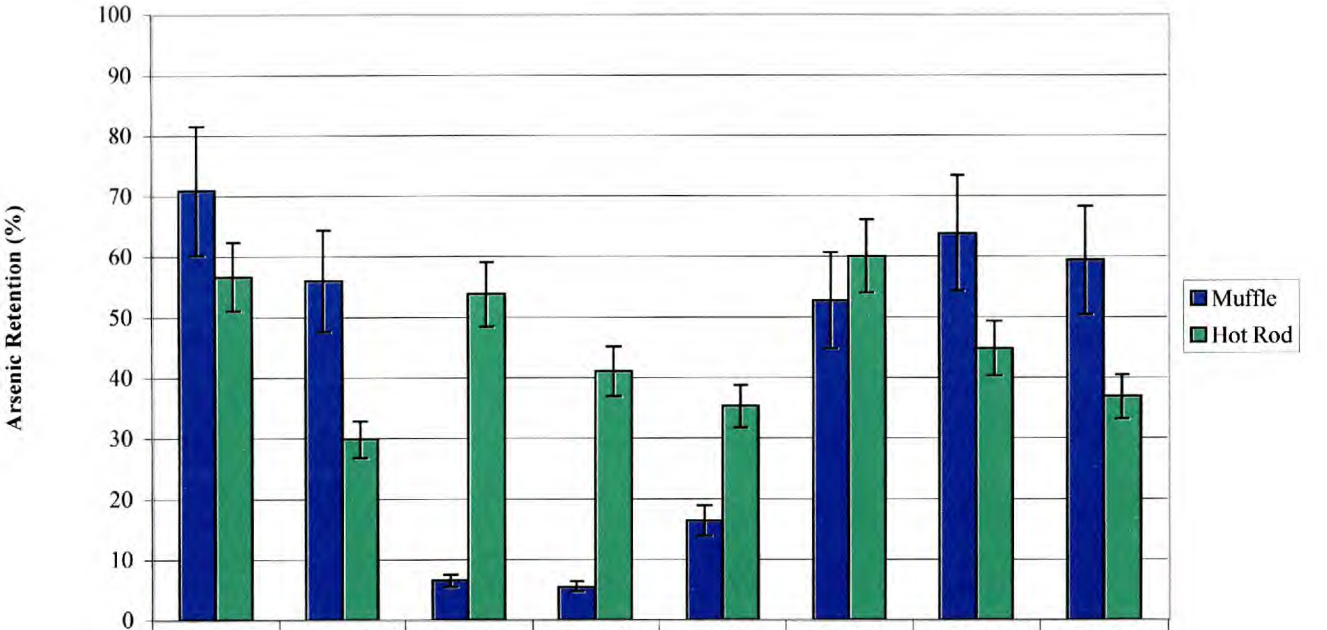
% Zinc Retention as a Funtion of Combustion Method at 950 C



	Fuel 1	Fuel 2	Fuel 3	Fuel 4	Fuel 5	Fuel 6	Fuel 7	Fuel 8
Muffle	69.28	66.83	70.89	81.16	73.97	50.97	46.36	70.23
Hot Rod	44.27	58.69	46.05	40.79	56.74	84.83	29.81	32.05

Fuel Studied

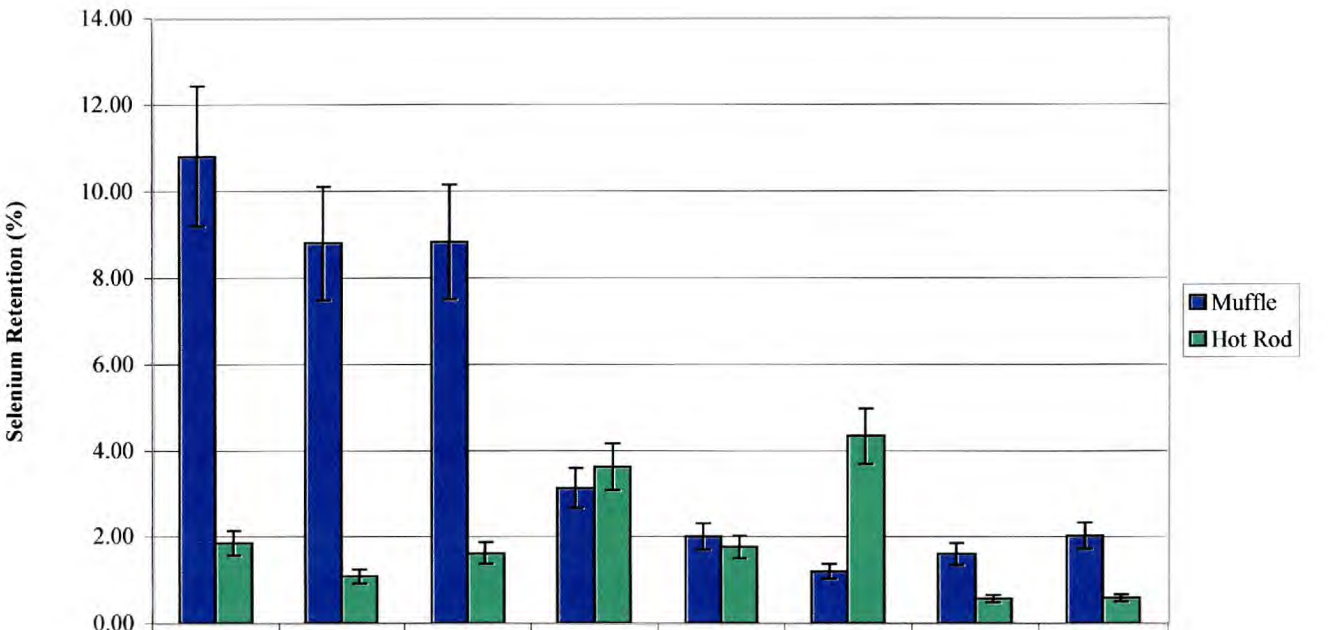
% Arsenic Retention as a Function of Combustion Method at 950 C



	Fuel 1	Fuel 2	Fuel 3	Fuel 4	Fuel 5	Fuel 6	Fuel 7	Fuel 8
Muffle	70.94	55.98	6.51	5.51	16.42	52.74	63.82	59.42
Hot Rod	56.67	29.83	53.79	41.03	35.31	60.07	44.88	36.83

Fuel Studied

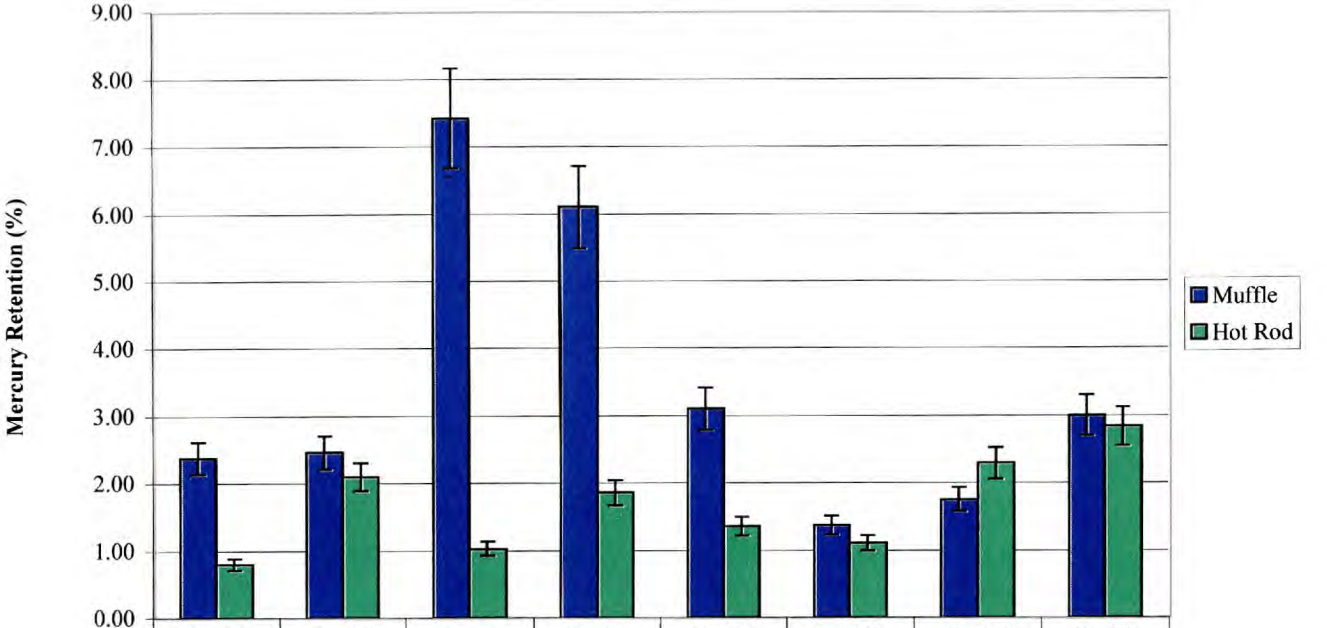
% Selenium Retention as a Function of Combustion Method at 950 C



	1	2	3	4	5	6	7	8
Muffle	10.82	8.80	8.83	3.13	2.01	1.20	1.61	2.03
Hot Rod	1.86	1.09	1.63	3.63	1.77	4.33	0.57	0.59

Fuel Studied

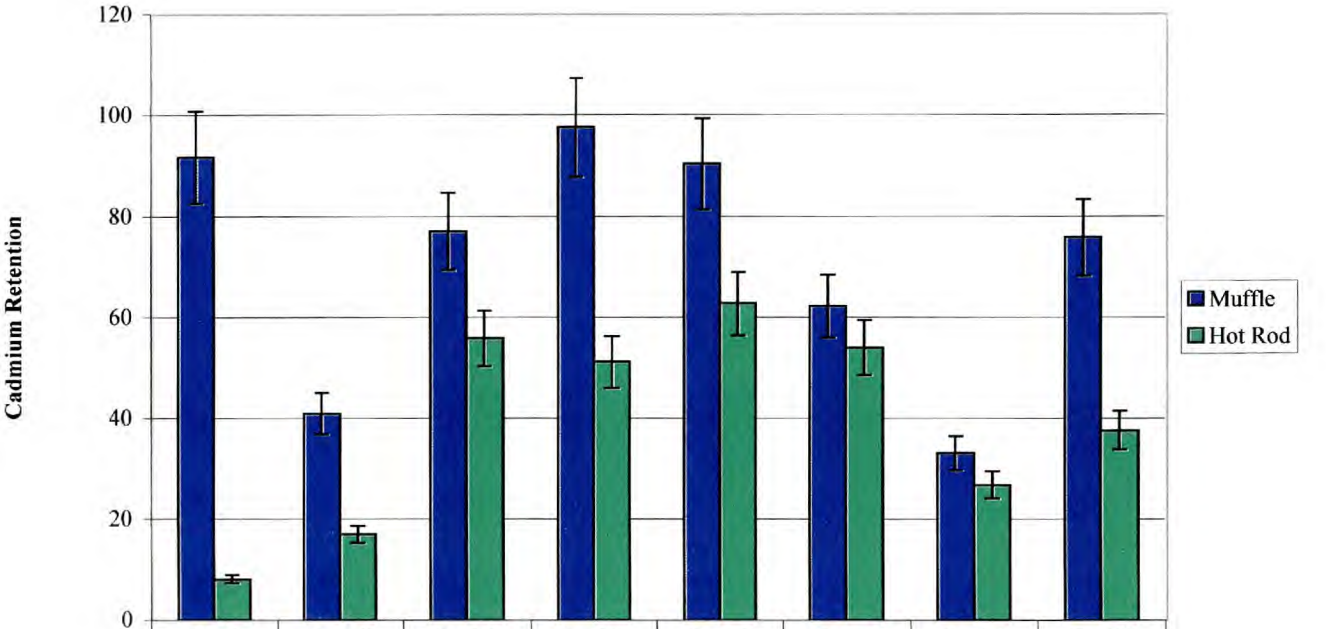
% Mercury Retention as a Function of Combustion Conditions at 950 C



	Fuel 1	Fuel 2	Fuel 3	Fuel 4	Fuel 5	Fuel 6	Fuel 7	Fuel 8
Muffle	2.38	2.46	7.42	6.10	3.11	1.38	1.75	3.00
Hot Rod	0.80	2.10	1.03	1.86	1.36	1.11	2.30	2.84

Fuel Studied

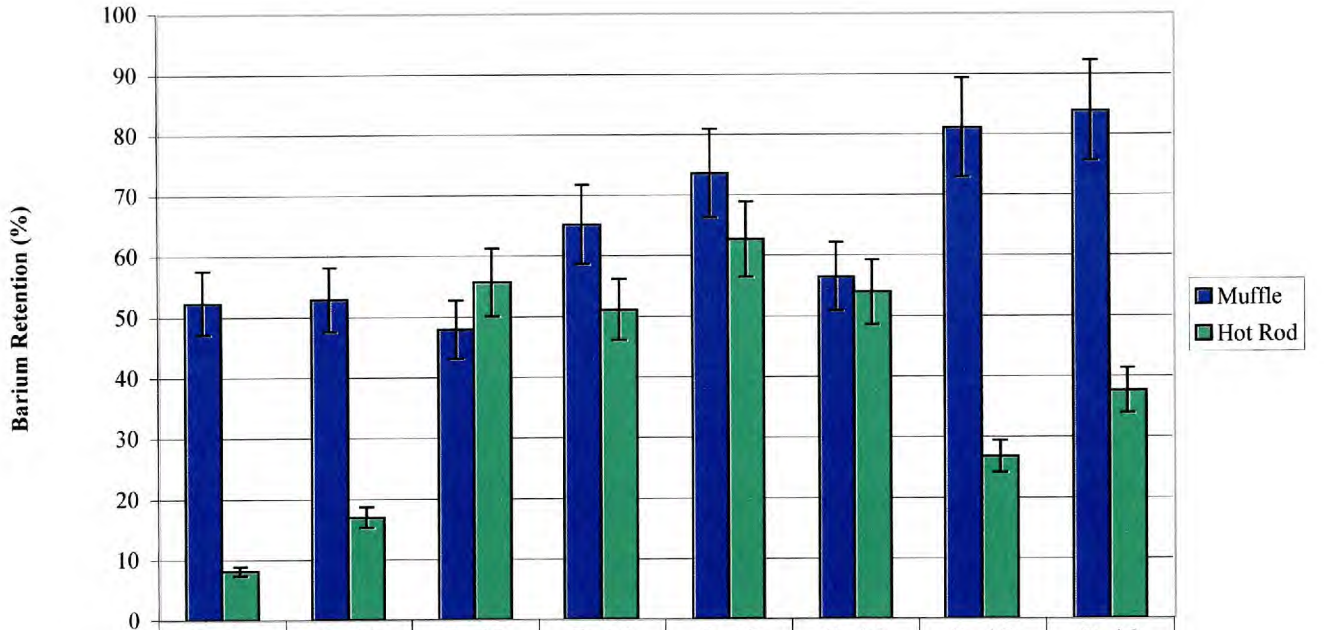
% Cadmium Retention as a Function of Combustion Method at 950 C



	Fuel 1	Fuel 2	Fuel 3	Fuel 4	Fuel 5	Fuel 6	Fuel 7	Fuel 8
Muffle	91.66	40.94	76.95	97.56	90.34	62.21	33.06	75.77
Hot Rod	8.11	17.06	55.77	51.11	62.73	53.96	26.80	37.64

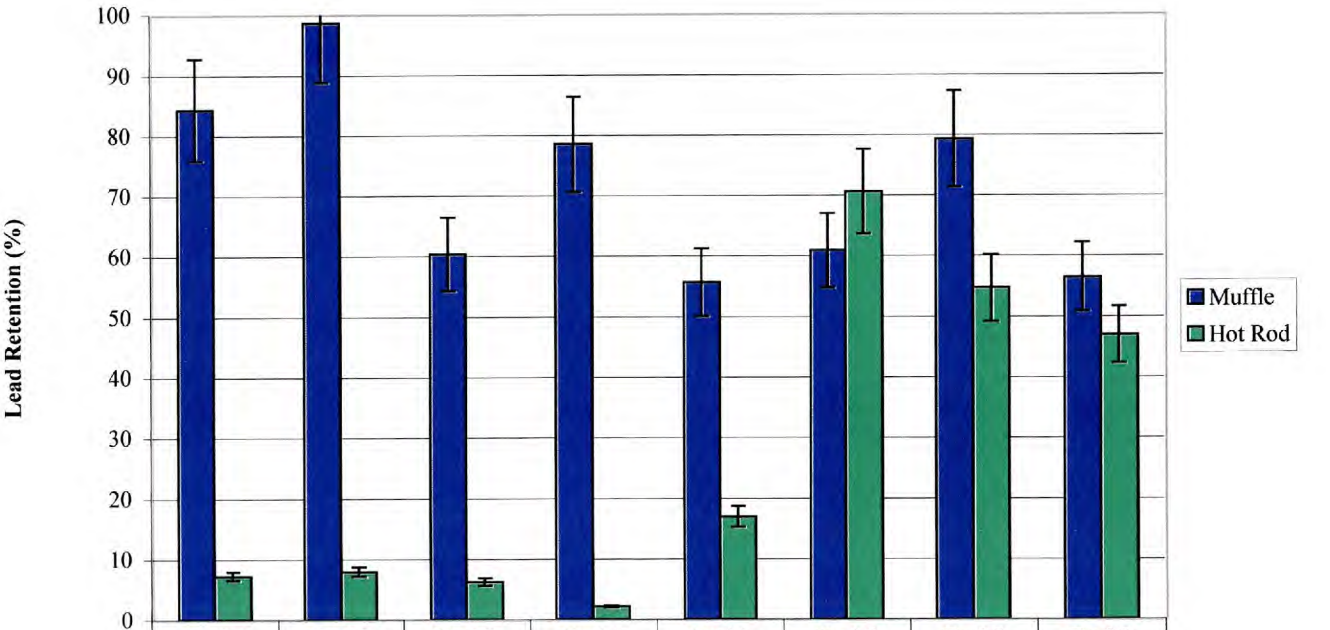
Fuel Studied

% Barium Retention as a Function of Combustion Method at 950 C



	Fuel 1	Fuel 2	Fuel 3	Fuel 4	Fuel 5	Fuel 6	Fuel 7	Fuel 8
Muffle	52.32	52.89	47.95	65.16	73.58	56.53	81.14	83.94
Hot Rod	8.11	17.06	55.77	51.11	62.73	53.96	26.80	37.64

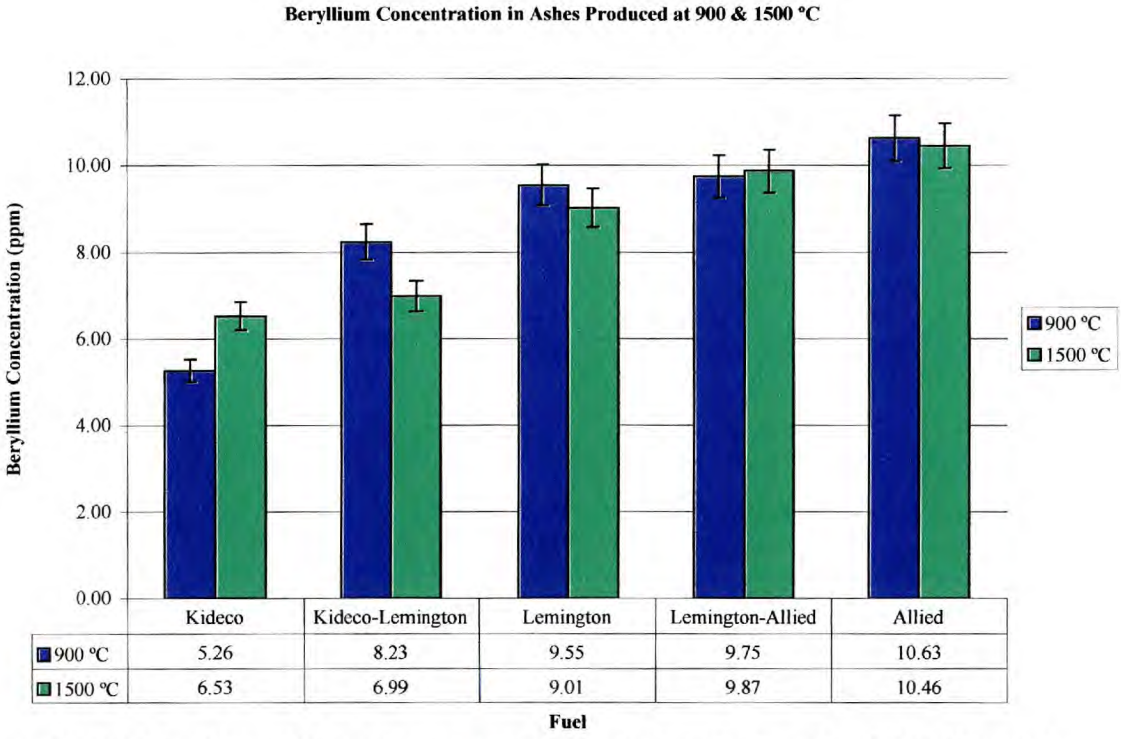
% Lead Retention as a Function of Combustion Method at 950 C



	Fuel 1	Fuel 2	Fuel 3	Fuel 4	Fuel 5	Fuel 6	Fuel 7	Fuel 8
Muffle	84.35	98.68	60.37	78.57	55.77	60.93	79.36	56.53
Hot Rod	7.23	7.92	6.25	2.22	17.05	70.63	54.71	47.04

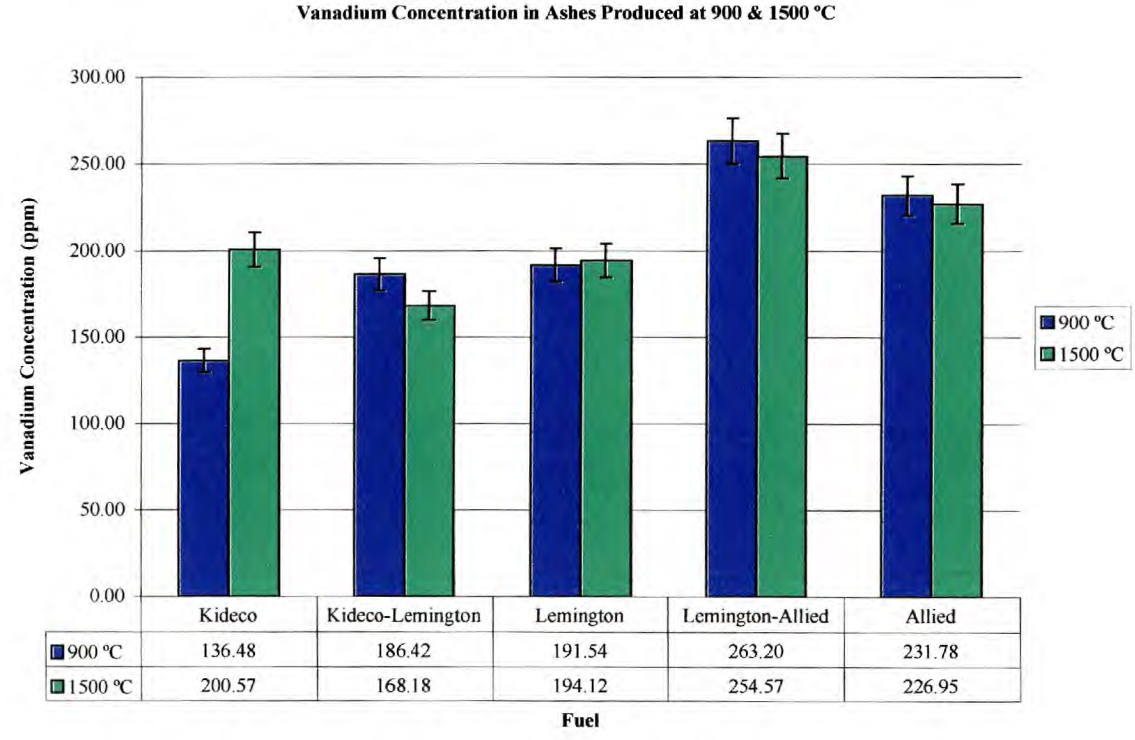
APPENDIX III

The figures below show absolute values for trace element concentrations obtained in the Chilean Ashes produced at combustion temperatures of 900 & 1500 °C. These values were used to calculate trace metal retention and percentage trace element leached.



	Kideco	Kideco-Lemington	Lemington	Lemington-Allied	Allied
900 °C	5.26	8.23	9.55	9.75	10.63
1500 °C	6.53	6.99	9.01	9.87	10.46

Figure AIV.1 Beryllium Concentration in Chilean Ashes Produced at 900 & 1500 °C



	Kideco	Kideco-Lemington	Lemington	Lemington-Allied	Allied
900 °C	136.48	186.42	191.54	263.20	231.78
1500 °C	200.57	168.18	194.12	254.57	226.95

Figure AIV.2 Vanadium Concentrations in Chilean Ashes Produced at 900 & 1500 °C

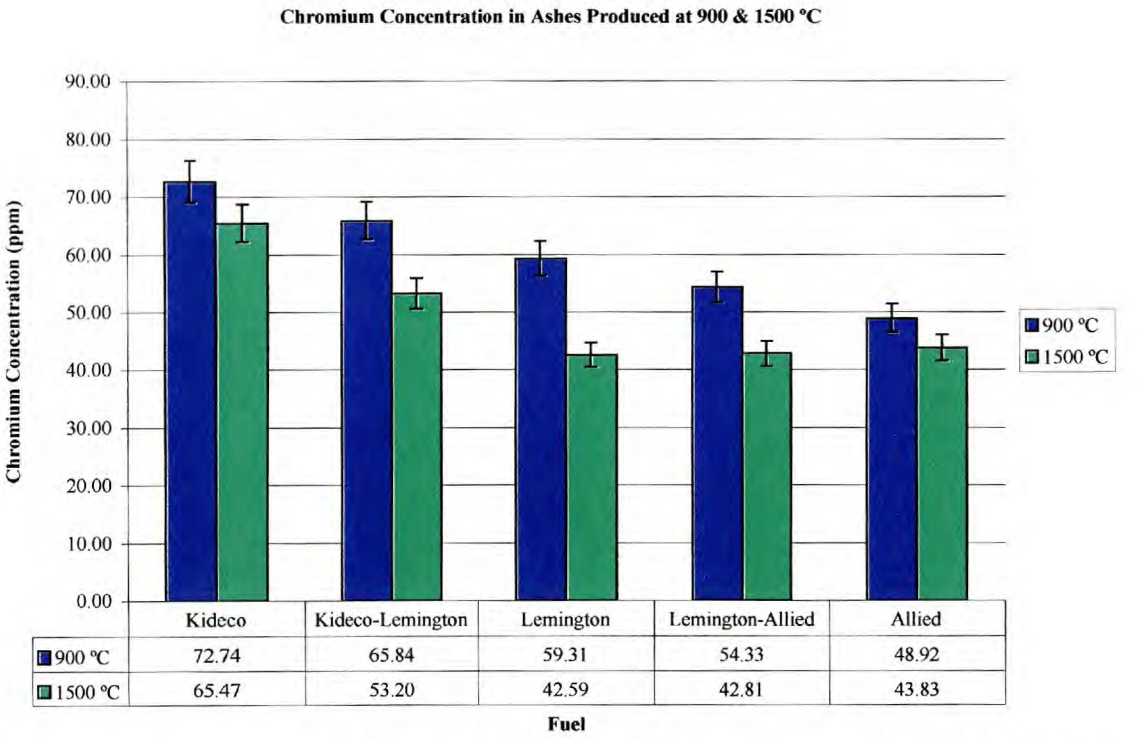


Figure AIV.3 Chromium Concentrations in Chilean Ashes Produced at 900 & 1500 °C

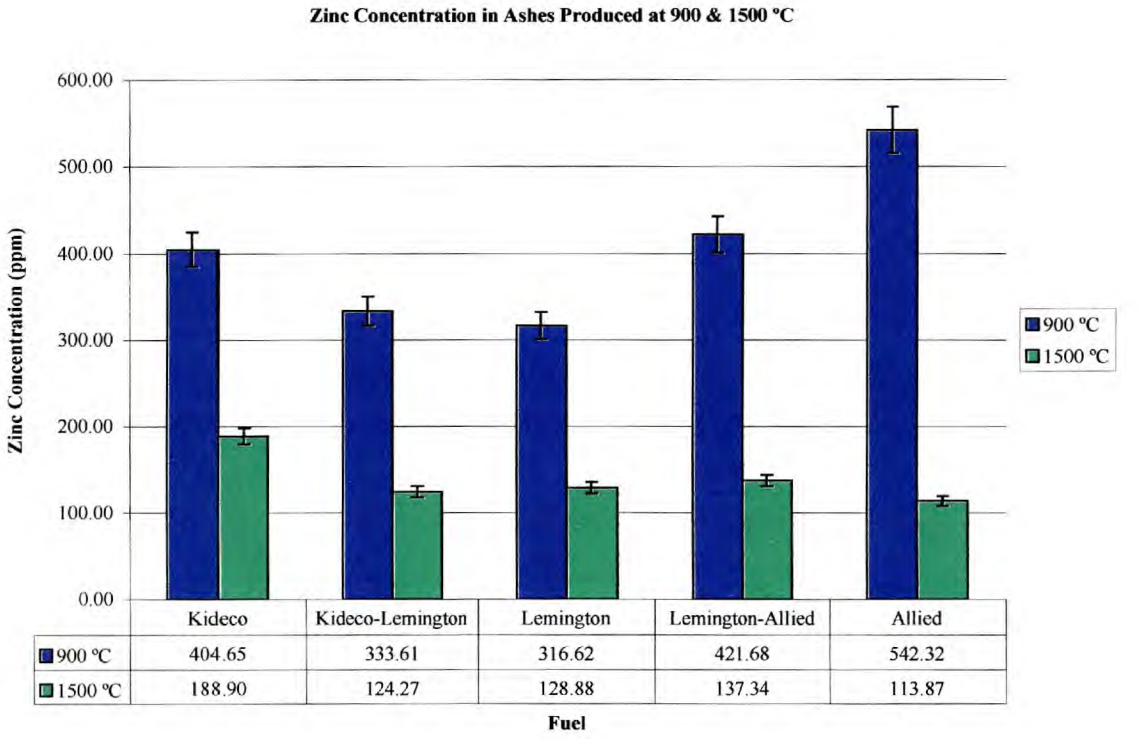
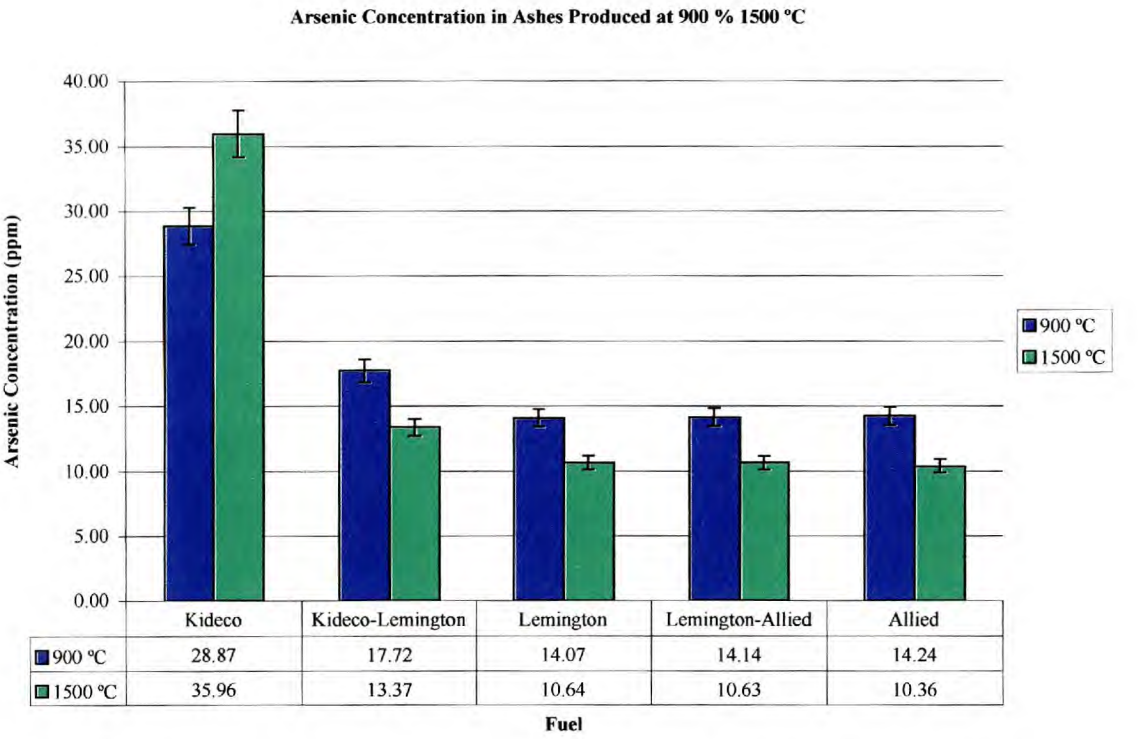
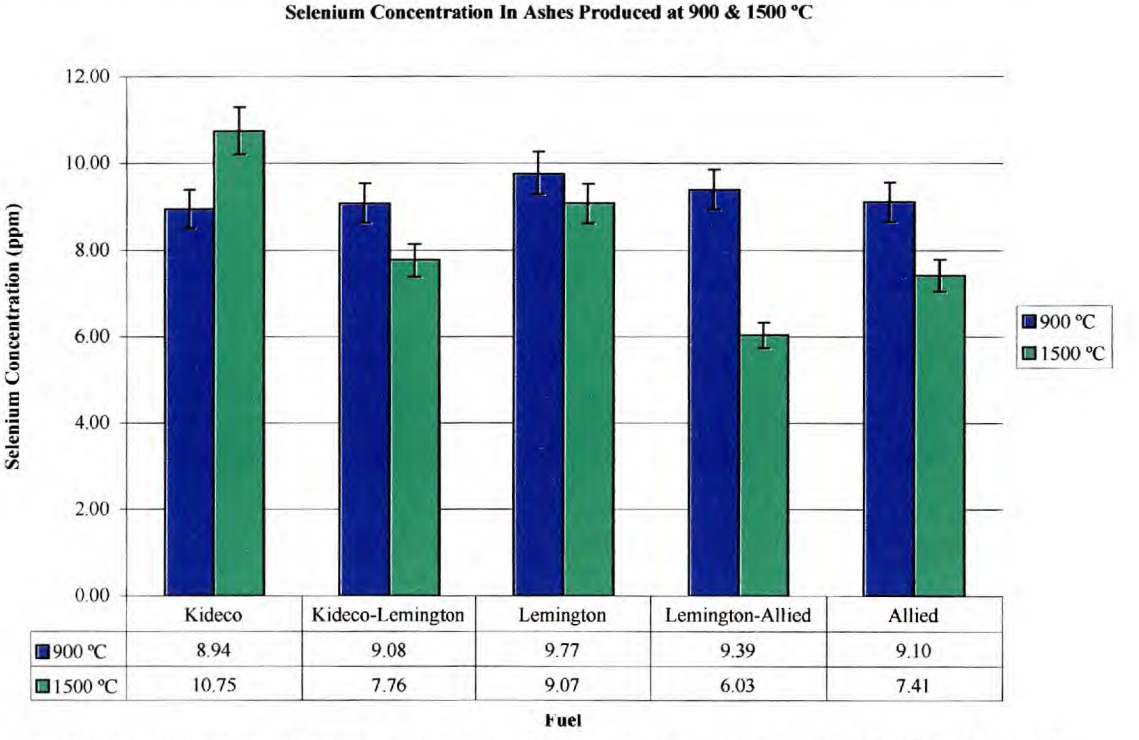


Figure AIV.4 Zinc Concentrations in Chilean Ashes Produced at 900 & 1500 °C



	Kideco	Kideco-Lemington	Lemington	Lemington-Allied	Allied
900 °C	28.87	17.72	14.07	14.14	14.24
1500 °C	35.96	13.37	10.64	10.63	10.36

Figure AIV.5 Arsenic Concentrations in Chilean Ashes Produced at 900 & 1500 °C



	Kideco	Kideco-Lemington	Lemington	Lemington-Allied	Allied
900 °C	8.94	9.08	9.77	9.39	9.10
1500 °C	10.75	7.76	9.07	6.03	7.41

Figure AIV.6 Selenium Concentrations in Chilean Ashes Produced at 900 & 1500 °C

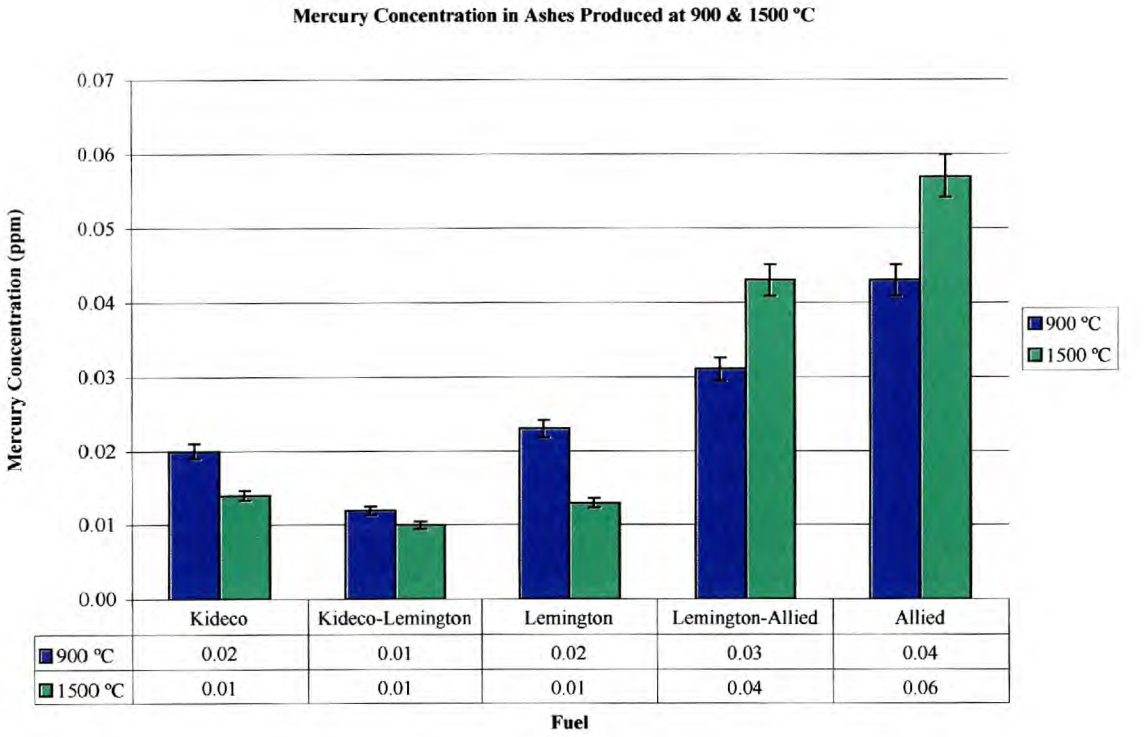


Figure AIV.7 Mercury Concentrations in Chilean Ashes Produced at 900 & 1500 °C

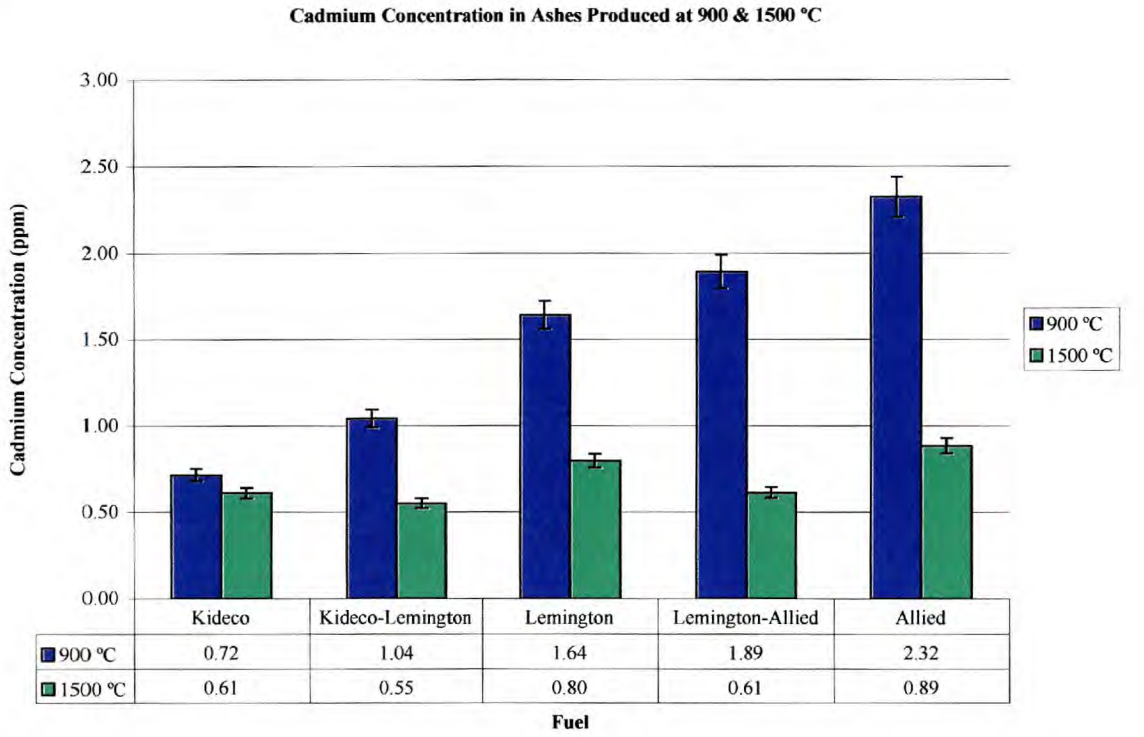


Figure AIV.8 Cadmium Concentrations in Chilean Ashes Produced at 900 & 1500 °C

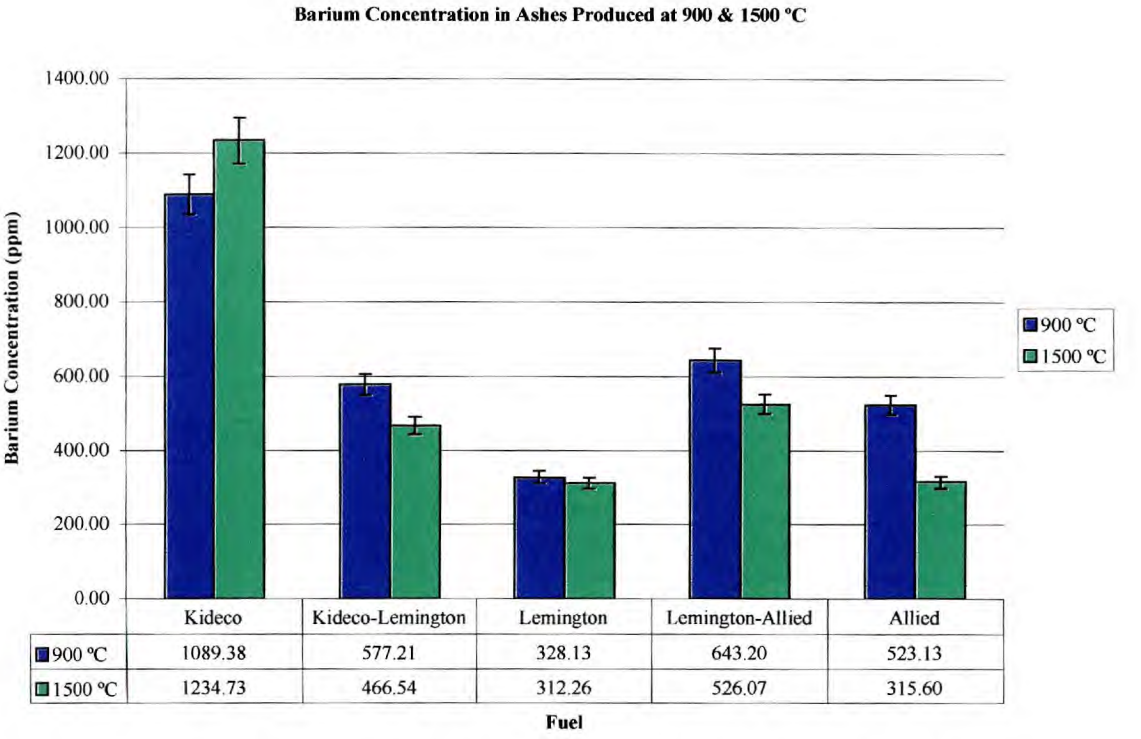


Figure AIV.9 Barium Concentrations in Chilean Ashes Produced at 900 & 1500 °C

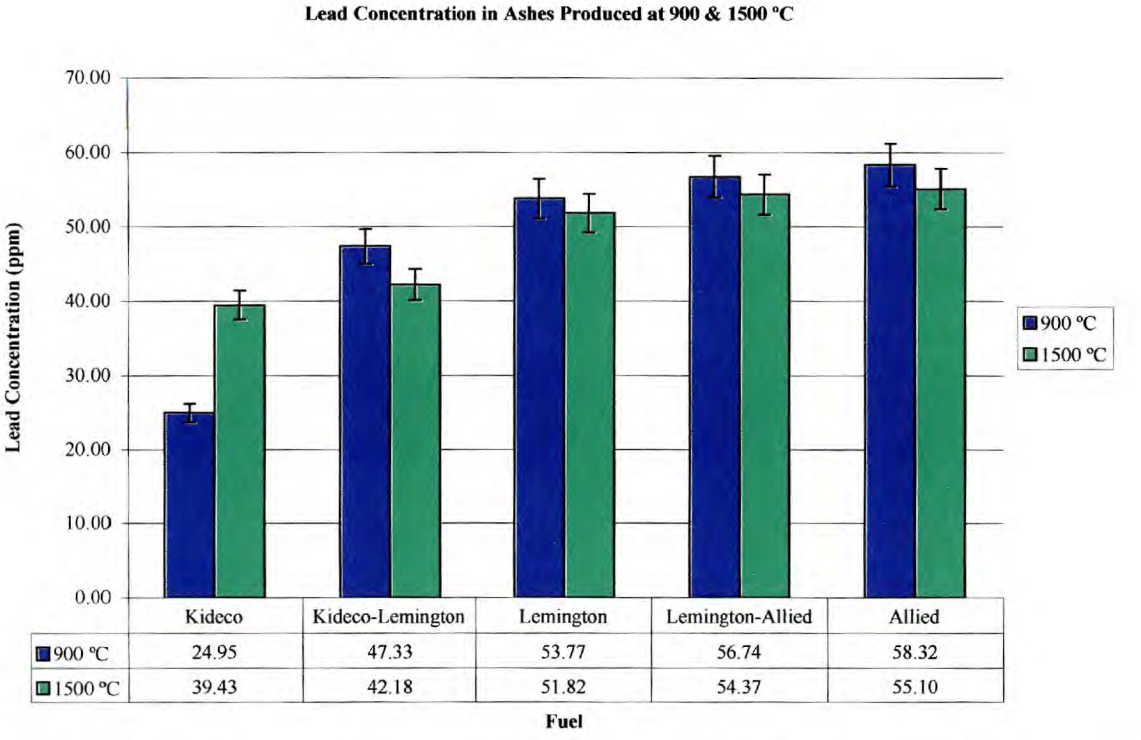
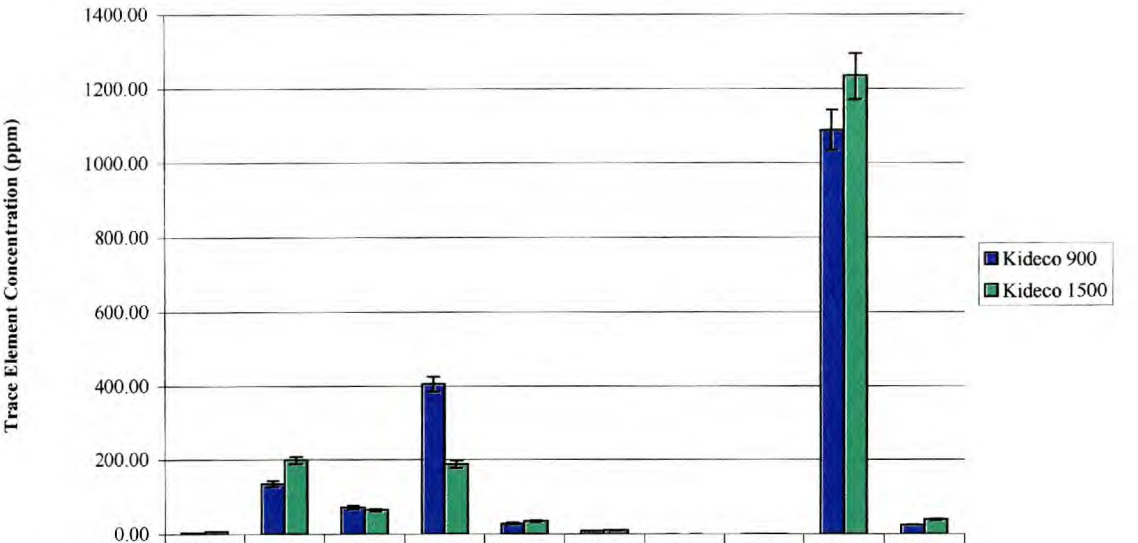


Figure AIV.10Trace Element Concentrations in Chilean Ashes Produced at 900 & 1500 °C

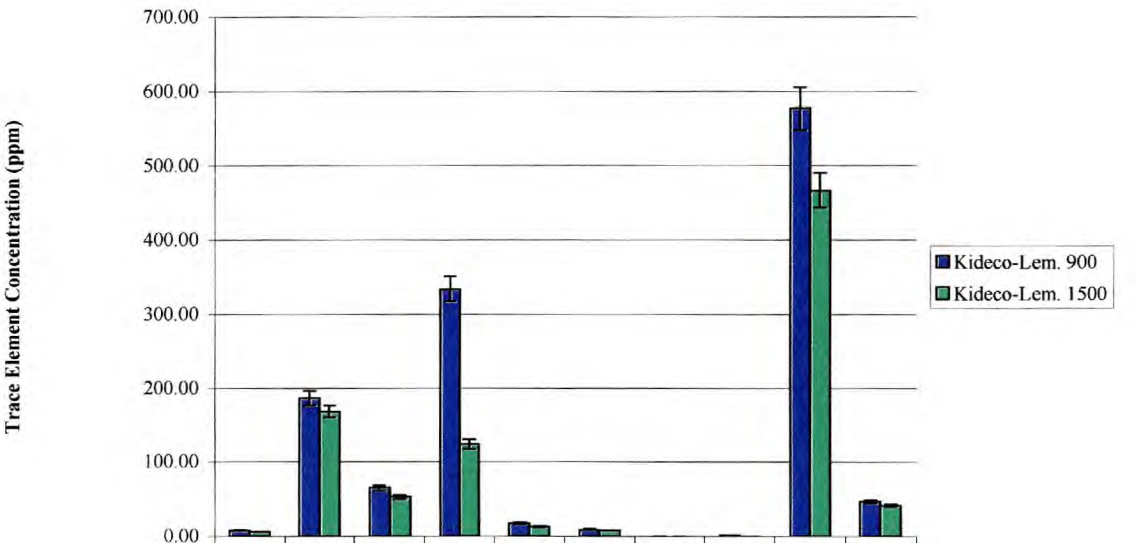
Trace Element Concentration in Kideco Ash Produced at 900 & 1500 °C



	Be	V	Cr	Zn	As	Se	Hg	Cd	Ba	Pb
Kideco 900	5.26	136.48	72.74	404.65	28.87	8.94	0.02	0.72	1089.38	24.95
Kideco 1500	6.53	200.57	65.47	188.90	35.96	10.75	0.01	0.61	1234.73	39.43

Trace Element Studied

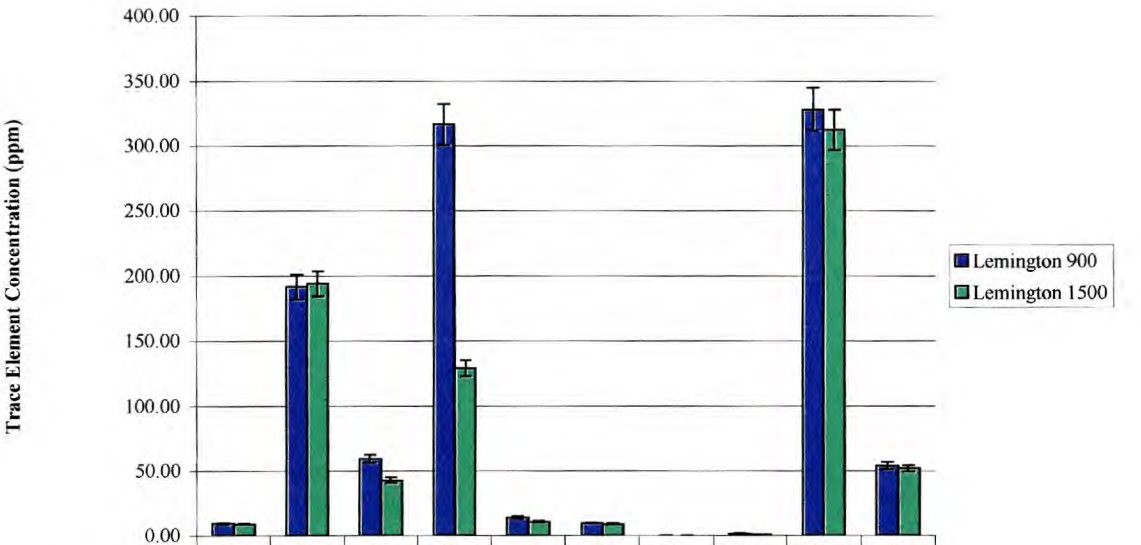
Trace Element Concentration in Kideco-Lemington Ash Produced at 900 & 1500 °C



	Be	V	Cr	Zn	As	Se	Hg	Cd	Ba	Pb
Kideco-Lem. 900	8.23	186.42	65.84	333.61	17.72	9.08	0.01	1.04	577.21	47.33
Kideco-Lem. 1500	6.99	168.18	53.20	124.27	13.37	7.76	0.01	0.55	466.54	42.18

Trace Element Studied

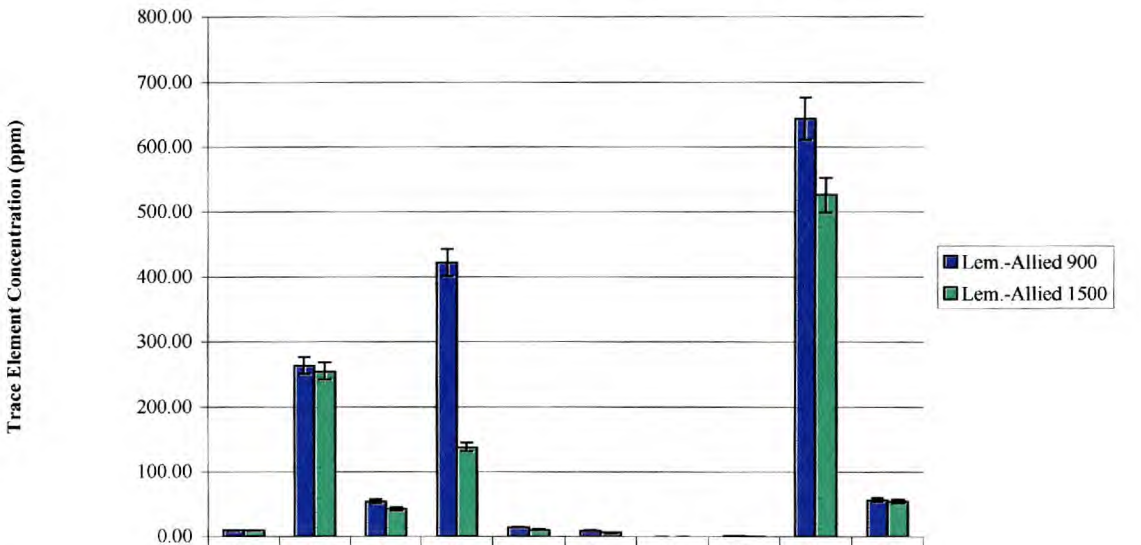
Trace Element Concentration in Lemington Ash Produced at 900 & 1500 °C



	Be	V	Cr	Zn	As	Se	Hg	Cd	Ba	Pb
Lemington 900	9.55	191.54	59.31	316.62	14.07	9.77	0.02	1.64	328.13	53.77
Lemington 1500	9.01	194.12	42.59	128.88	10.64	9.07	0.01	0.80	312.26	51.82

Trace Element Studied

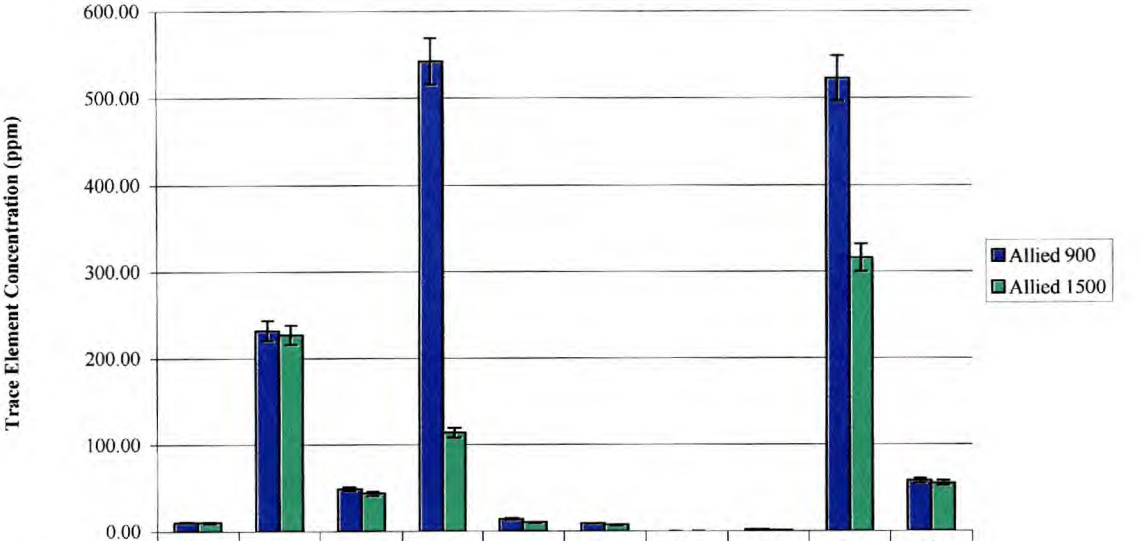
Trace Element Concentration in Lemington Allied Ash Produced at 900 & 1500 °C



	Be	V	Cr	Zn	As	Se	Hg	Cd	Ba	Pb
Lem.-Allied 900	9.75	263.20	54.33	421.68	14.14	9.39	0.03	1.89	643.20	56.74
Lem.-Allied 1500	9.87	254.57	42.81	137.34	10.63	6.03	0.04	0.61	526.07	54.37

Trace Element Studied

Trace Element Concentration in Allied Ash Produced at 900 & 1500 °C



	Be	V	Cr	Zn	As	Se	Hg	Cd	Ba	Pb
Allied 900	10.63	231.78	48.92	542.32	14.24	9.10	0.04	2.32	523.13	58.32
Allied 1500	10.46	226.95	43.83	113.87	10.36	7.41	0.06	0.89	315.60	55.10

Trace Element Studied

APPENDIX IV

This appendix is a print-out of a complete MINTEQA2 output file. Part 4 of the printo-out shows the main results output with details of trace metals in leachate and predictions of their speciation.

PART 1 of OUTPUT FILE

```
Speciate w/trace metals and sorption for Pb, Cr

Component file (COMP.DBS):           COMP.DBS     MTQWv1.50
Thermodynamic file (THERMO.UNF):     THERMO.UNF   MTQWv1.50
Gaussian DOM file (GAUSSIAN.DBS):    GAUSSIAN.DBSV1.50 MTQW
Solids file (TYPE6.UNF):             TYPE6.UNF    MTQWv1.50

--------------------------------------------------------------------------------
 Temperature (Celsius):   25.0
 Units of concentration for input data: mol/L
 (***Calculated concentrations in output are always in molar units.)
 Ionic strength to be computed.
 If specified, carbonate concentration represents total inorganic carbon.
 Precipitation is allowed for all solids in the thermodynamic database and
   the print option for solids is set to: 1
 The method used to compute activity coefficients is: Davies equation
 Intermediate output file
 Adsorption model: Diffuse Layer
 Number of adsorbing surfaces: 1

--------------------------------------------------------------------------------
2.200E-02  600.00 0.000 0.000 81
    330 -1.008E-01   -4.00 Y
    770  8.738E-02   -1.06 Y
     30  4.767E-02   -1.32 Y
    281  1.478E-02  -12.00 Y
    150  2.853E-03   -2.54 Y
    460  3.721E-03   -2.43 Y
    500  9.681E-04   -3.01 Y
    410  2.335E-03   -2.63 Y
    732  1.624E-03   -2.79 Y
    992  1.000E-01   -1.00 Y
     61  3.853E-06   -5.41 Y
    100  7.932E-05   -4.10 Y
    110  5.841E-06   -5.23 Y
    160  6.379E-08   -7.20 Y
    212  1.399E-05   -4.85 Y
    361  2.493E-08   -7.60 Y
    600  1.204E-06   -5.92 Y
    762  1.133E-06   -5.95 Y
    903  2.679E-05   -4.57 Y
    950  6.190E-05   -4.21 Y
    811  1.236E-06   -5.91 N
    812  4.944E-05   -4.31 N
    813  0.000E+00    0.00 N

 H2O has been inserted as a COMPONENT
  6   2
2003002    -6.8730   103.0519
    813     0.0000     0.0000
  2  16
8113302 =FeOH2+          0.0000    7.2900   0.000   0.000 1.00 0.00 0.00   0.0000
0.00 3   1.000 811   1.000 330   1.000 813   0.000   0   0.000   0   0.000   0
 0.000   0   0.000   0   0.000   0   0.000   0   0.000   0   0.000   0   0.000   0
0  0.000   0   0.000   0   0.000   0
0  0.000   0   0.000   0   0.000   0   0.000   0
0  0.000   0   0.000   0   0.000   0   0.000   0
8113301 =FeO-            0.0000   -8.9300   0.000   0.000-1.00 0.00 0.00   0.000
0.00 3   1.000 811  -1.000 330  -1.000 813   0.000   0   0.000   0   0.000   0
 0.000   0   0.000   0   0.000   0   0.000   0   0.000   0   0.000   0   0.000   0
0  0.000   0   0.000   0   0.000   0
0  0.000   0   0.000   0   0.000   0   0.000   0
0  0.000   0   0.000   0   0.000   0   0.000   0
8111500 =FeOHCa+2        0.0000    4.9700   0.000   0.000 2.00 0.00 0.00   0.000
0.00 3   1.000 811   1.000 150   2.000 813   0.000   0   0.000   0   0.000   0
 0.000   0   0.000   0   0.000   0   0.000   0   0.000   0   0.000   0   0.000   0
0  0.000   0   0.000   0   0.000   0
0  0.000   0   0.000   0   0.000   0   0.000   0
0  0.000   0   0.000   0   0.000   0   0.000   0
8117320 =FeSO4-          0.0000    7.7800   0.000   0.000-1.00 0.00 0.00   0.000
0.00 5   1.000 811   1.000 732   1.000 330  -1.000   2  -1.000 813   0.000   0
 0.000   0   0.000   0   0.000   0   0.000   0   0.000   0   0.000   0   0.000   0
0  0.000   0   0.000   0   0.000   0
0  0.000   0   0.000   0   0.000   0   0.000   0
0  0.000   0   0.000   0   0.000   0   0.000   0
8117321 =FeOHSO4-2       0.0000    0.7900   0.000   0.000-2.00 0.00 0.00   0.000
0.00 3   1.000 811   1.000 732  -2.000 813   0.000   0   0.000   0   0.000   0
 0.000   0   0.000   0   0.000   0   0.000   0   0.000   0   0.000   0   0.000   0
0  0.000   0   0.000   0   0.000   0
0  0.000   0   0.000   0   0.000   0   0.000   0
0  0.000   0   0.000   0   0.000   0   0.000   0
8112120 =FeCrO4-         0.0000   10.8500   0.000   0.000-1.00 0.00 0.00   0.000
0.00 5   1.000 811   1.000 212   1.000 330  -1.000   2  -1.000 813   0.000   0
 0.000   0   0.000   0   0.000   0   0.000   0   0.000   0   0.000   0   0.000   0
0  0.000   0   0.000   0   0.000   0
0  0.000   0   0.000   0   0.000   0   0.000   0
0  0.000   0   0.000   0   0.000   0   0.000   0
8112121 =FeOHCrO4-2      0.0000    3.9000   0.000   0.000-2.00 0.00 0.00   0.000
0.00 3   1.000 811   1.000 212  -2.000 813   0.000   0   0.000   0   0.000   0
 0.000   0   0.000   0   0.000   0   0.000   0   0.000   0   0.000   0   0.000   0
0  0.000   0   0.000   0   0.000   0
0  0.000   0   0.000   0   0.000   0   0.000   0
0  0.000   0   0.000   0   0.000   0   0.000   0
8123302 =FeOH2+          0.0000    7.2900   0.000   0.000 1.00 0.00 0.00   0.000
0.00 3   1.000 812   1.000 330   1.000 813   0.000   0   0.000   0   0.000   0
 0.000   0   0.000   0   0.000   0   0.000   0   0.000   0   0.000   0   0.000   0
0  0.000   0   0.000   0   0.000   0
0  0.000   0   0.000   0   0.000   0   0.000   0
0  0.000   0   0.000   0   0.000   0   0.000   0
8123301 =FeO-            0.0000   -8.9300   0.000   0.000-1.00 0.00 0.00   0.000
0.00 3   1.000 812  -1.000 330  -1.000 813   0.000   0   0.000   0   0.000   0
 0.000   0   0.000   0   0.000   0   0.000   0   0.000   0   0.000   0   0.000   0
0  0.000   0   0.000   0   0.000   0
0  0.000   0   0.000   0   0.000   0   0.000   0
0  0.000   0   0.000   0   0.000   0   0.000   0
8121500 =FeOCa+          0.0000   -5.8500   0.000   0.000 1.00 0.00 0.00   0.000
0.00 4   1.000 812   1.000 150  -1.000 330   1.000 813   0.000   0   0.000   0
 0.000   0   0.000   0   0.000   0   0.000   0   0.000   0   0.000   0   0.000   0
0  0.000   0   0.000   0   0.000   0
0  0.000   0   0.000   0   0.000   0   0.000   0
0  0.000   0   0.000   0   0.000   0   0.000   0
```

```
8126000 =FeOPb+          0.0000    0.3000   0.000   0.000 1.00 0.00 0.00    0.0000
0.00 4   1.000 812   1.000 600  -1.000 330   1.000 813   0.000   0   0.000   0
 0.000   0   0.000   0   0.000   0   0.000   0   0.000   0   0.000   0
0  0.000   0   0.000   0   0.000   0
0  0.000   0   0.000   0   0.000   0   0.000   0
0  0.000   0   0.000   0   0.000   0   0.000   0
8127320 =FeSO4-          0.0000    7.7800   0.000   0.000-1.00 0.00 0.00    0.0000
0.00 5   1.000 812   1.000 732   1.000 330  -1.000   2  -1.000 813   0.000   0
 0.000   0   0.000   0   0.000   0   0.000   0   0.000   0   0.000   0
0  0.000   0   0.000   0   0.000   0

0  0.000   0   0.000   0   0.000   0   0.000   0
0  0.000   0   0.000   0   0.000   0   0.000   0
8127321 =FeOHSO4-2       0.0000    0.7900   0.000   0.000-2.00 0.00 0.00    0.0000
0.00 3   1.000 812   1.000 732  -2.000 813   0.000   0   0.000   0   0.000   0
 0.000   0   0.000   0   0.000   0   0.000   0   0.000   0   0.000   0
0  0.000   0   0.000   0   0.000   0
0  0.000   0   0.000   0   0.000   0   0.000   0
0  0.000   0   0.000   0   0.000   0   0.000   0
8122120 =FeCrO4-         0.0000   10.8500   0.000   0.000-1.00 0.00 0.00    0.0000
0.00 5   1.000 812   1.000 212   1.000 330  -1.000   2  -1.000 813   0.000   0
 0.000   0   0.000   0   0.000   0   0.000   0   0.000   0   0.000   0
0  0.000   0   0.000   0   0.000   0
0  0.000   0   0.000   0   0.000   0   0.000   0
0  0.000   0   0.000   0   0.000   0   0.000   0
8122121 =FeOHCrO4-2      0.0000    3.9000   0.000   0.000-2.00 0.00 0.00    0.0000
0.00 3   1.000 812   1.000 212  -2.000 813   0.000   0   0.000   0   0.000   0
 0.000   0   0.000   0   0.000   0   0.000   0   0.000   0   0.000   0
0  0.000   0   0.000   0   0.000   0
0  0.000   0   0.000   0   0.000   0   0.000   0
0  0.000   0   0.000   0   0.000   0   0.000   0
8116000 =FeOPb+          0.0000    4.6500   0.000   0.000 1.00 0.00 0.00    0.0000
0.00 4   1.000 811   1.000 600  -1.000 330   1.000 813   0.000   0   0.000   0
 0.000   0   0.000   0   0.000   0   0.000   0   0.000   0   0.000   0
0  0.000   0   0.000   0   0.000   0
0  0.000   0   0.000   0   0.000   0   0.000   0
0  0.000   0   0.000   0   0.000   0   0.000   0
```

INPUT DATA BEFORE TYPE MODIFICATIONS

ID	Name	ACTIVITY GUESS	log GUESS	ANAL TOTAL
330	H+1	1.000E-04	-4.000	-1.008E-01
770	H4SiO4	8.710E-02	-1.060	8.738E-02
30	Al+3	4.786E-02	-1.320	4.767E-02
281	Fe+3	1.000E-12	-12.000	1.478E-02
150	Ca+2	2.884E-03	-2.540	2.853E-03
460	Mg+2	3.715E-03	-2.430	3.721E-03
500	Na+1	9.772E-04	-3.010	9.681E-04
410	K+1	2.344E-03	-2.630	2.335E-03
732	SO4-2	1.622E-03	-2.790	1.624E-03
992	Acetate	1.000E-01	-1.000	1.000E-01
61	H3AsO4	3.890E-06	-5.410	3.853E-06
100	Ba+2	7.943E-05	-4.100	7.932E-05
110	Be+2	5.888E-06	-5.230	5.841E-06
160	Cd+2	6.310E-08	-7.200	6.379E-08
212	CrO4-2	1.413E-05	-4.850	1.399E-05
361	Hg(OH)2	2.512E-08	-7.600	2.493E-08
600	Pb+2	1.202E-06	-5.920	1.204E-06
762	SeO4-2	1.122E-06	-5.950	1.133E-06
903	VO2+1	2.692E-05	-4.570	2.679E-05
950	Zn+2	6.166E-05	-4.210	6.190E-05
811	ADS1TYP1	1.230E-06	-5.910	1.236E-06
812	ADS1TYP2	4.898E-05	-4.310	4.944E-05
813	ADS1PSIo	1.000E+00	0.000	0.000E+00
2	H2O	1.000E+00	0.000	0.000E+00

Charge Balance: UNSPECIATED

Sum of CATIONS= 1.033E-01 Sum of ANIONS = 1.033E-01

PERCENT DIFFERENCE = 2.241E-02 (ANIONS - CATIONS)/(ANIONS + CATIONS)

IMPROVED ACTIVITY GUESSES PRIOR TO FIRST ITERATION:		
H4SiO4	Log activity guess:	-1.06
Al+3	Log activity guess:	-1.37
Fe+3	Log activity guess:	-5.25
SO4-2	Log activity guess:	-2.79
H3AsO4	Log activity guess:	-7.18
CrO4-2	Log activity guess:	-11.41
Hg(OH)2	Log activity guess:	-7.64
SeO4-2	Log activity guess:	-5.95

PART 2 of OUTPUT FILE

MINTEQA2 for Windows v1.50 DATE OF CALCULATIONS:

CONSTRAINTS ON COMPONENT ACTIVITIES

As specified, this chemical system is OPEN with respect to the following components:

H2O

Activities of the following components are constrained by the species shown:

COMPONENT	SPECIES	TYPE
H2O	H2O	3

PART 3 of OUTPUT FILE

MINTEQA2 for Windows v1.50 DATE OF CALCULATIONS:

PARAMETERS OF THE COMPONENT MOST OUT OF BALANCE:

ITER	NAME	TOTAL mol/L	DIFF FXN	LOG ACTVTY	RESIDUAL
0	ADS1PSIo	0.000E+00	9.873E-02	0.00000	9.873E-02
***	Temporarily holding ionic strength constant				
1	ADS1PSIo	1.051E-06	1.357E-02	-0.17851	1.357E-02
2	ADS1PSIo	-4.801E-05	1.331E+02	2.55576	1.331E+02
3	ADS1PSIo	-4.865E-05	1.832E+01	2.56723	1.832E+01
4	ADS1PSIo	-1.501E-05	2.483E+07	1.56723	2.483E+07
5	ADS1PSIo	-1.515E-05	1.435E+05	1.57467	1.435E+05
6	ADS1PSIo	-1.569E-05	5.920E+03	1.60352	5.920E+03
7	ADS1PSIo	-1.986E-05	1.700E+02	1.80039	1.700E+02
8	ADS1PSIo	-5.371E-06	-2.054E+01	0.80039	2.054E+01
9	ADS1PSIo	-4.110E-06	5.121E-01	0.64273	5.121E-01
10	ADS1PSIo	-5.452E-06	5.590E-02	0.80994	5.590E-02
11	ADS1PSIo	1.120E-06	7.453E+00	-0.19006	7.453E+00
12	ADS1PSIo	1.027E-06	7.628E-01	-0.17443	7.628E-01
13	ADS1PSIo	9.717E-07	8.282E-02	-0.16520	8.282E-02
14	ADS1PSIo	1.692E-06	5.479E-03	-0.28422	5.479E-03
15	ADS1PSIo	1.700E-06	7.069E-04	-0.28552	7.069E-04
16	ADS1PSIo	1.058E-05	-1.250E-04	-1.28552	1.250E-04
17	ADS1PSIo	1.071E-05	-4.935E-05	-1.29533	4.935E-05
18	ADS1PSIo	1.205E-05	-3.128E-05	-1.38881	3.128E-05
19	ADS1PSIo	7.452E-06	-6.509E-06	-1.02194	6.509E-06
20	ADS1PSIo	6.892E-06	-2.427E-06	-0.96655	2.427E-06
21	ADS1PSIo	6.290E-06	-1.418E-06	-0.90377	1.418E-06
22	ADS1PSIo	5.334E-06	1.488E-06	-0.79607	1.488E-06
23	ADS1PSIo	5.131E-06	1.390E-07	-0.77194	1.390E-07
24	ADS1PSIo	5.093E-06	2.806E-07	-0.76729	2.806E-07
25	ADS1PSIo	5.090E-06	-1.173E-08	-0.76695	1.171E-08
26	ADS1PSIo	5.101E-06	-4.986E-08	-0.76826	4.983E-08
27	ADS1PSIo	5.094E-06	1.253E-08	-0.76746	1.251E-08
28	ADS1PSIo	5.095E-06	-4.487E-09	-0.76762	4.465E-09
29	ADS1PSIo	5.094E-06	-3.922E-10	-0.76749	3.700E-10
30	ADS1PSIo	5.094E-06	5.133E-10	-0.76746	4.910E-10
31	ADS1PSIo	5.094E-06	-5.576E-11	-0.76746	3.353E-11
32	ADS1PSIo	5.094E-06	-3.843E-11	-0.76746	1.620E-11
33	ADS1PSIo	5.094E-06	-4.658E-11	-0.76746	2.435E-11
34	VO2+1	2.679E-05	3.994E+12	-7.08000	3.994E+12
35	VO2+1	2.679E-05	1.393E+12	-7.12575	1.393E+12
36	VO2+1	2.679E-05	4.856E+11	-7.17151	4.856E+11
37	VO2+1	2.679E-05	1.693E+11	-7.21727	1.693E+11
38	VO2+1	2.679E-05	5.903E+10	-7.26303	5.903E+10
39	VO2+1	2.679E-05	2.058E+10	-7.30878	2.058E+10
40	VO2+1	2.679E-05	7.177E+09	-7.35454	7.177E+09
41	VO2+1	2.679E-05	2.503E+09	-7.40029	2.503E+09
42	VO2+1	2.679E-05	8.726E+08	-7.44604	8.726E+08
43	VO2+1	2.679E-05	3.043E+08	-7.49179	3.043E+08
44	VO2+1	2.679E-05	1.061E+08	-7.53752	1.061E+08
45	VO2+1	2.679E-05	3.700E+07	-7.58323	3.700E+07
46	VO2+1	2.679E-05	1.290E+07	-7.62890	1.290E+07
47	VO2+1	2.679E-05	4.501E+06	-7.67449	4.501E+06
48	VO2+1	2.679E-05	1.570E+06	-7.71992	1.570E+06
49	VO2+1	2.679E-05	5.484E+05	-7.76507	5.484E+05
50	ADS1PSIo	5.099E-06	-3.250E-11	-0.76811	1.025E-11
51	ADS1PSIo	5.104E-06	-1.156E-10	-0.76868	9.332E-11
52	ADS1PSIo	5.113E-06	-4.069E-10	-0.76975	3.846E-10
53	ADS1PSIo	5.130E-06	-1.403E-09	-0.77176	1.381E-09
54	ADS1PSIo	5.160E-06	-4.653E-09	-0.77542	4.631E-09
55	ADS1PSIo	5.215E-06	-1.442E-08	-0.78191	1.440E-08
56	ADS1PSIo	5.307E-06	-4.019E-08	-0.79289	4.017E-08
57	ADS1PSIo	5.455E-06	-9.709E-08	-0.81027	9.707E-08
58	ADS1PSIo	5.678E-06	-1.996E-07	-0.83599	1.996E-07
59	ADS1PSIo	5.997E-06	-3.515E-07	-0.87182	3.514E-07
60	ADS1PSIo	6.436E-06	-5.346E-07	-0.91933	5.346E-07
61	ADS1PSIo	7.003E-06	-6.814E-07	-0.97774	6.814E-07
62	ADS1PSIo	7.604E-06	-6.405E-07	-1.03649	6.405E-07
63	ADS1PSIo	7.991E-06	-2.970E-07	-1.07257	2.969E-07
64	ADS1PSIo	8.069E-06	-1.869E-08	-1.07970	1.866E-08
65	ADS1PSIo	8.000E-06	-6.918E-09	-1.07340	6.891E-09
66	ADS1PSIo	7.894E-06	-1.730E-08	-1.06369	1.728E-08
67	ADS1PSIo	7.806E-06	-1.156E-08	-1.05552	1.154E-08
68	ADS1PSIo	7.811E-06	-7.200E-11	-1.05597	4.584E-11
69	ADS1PSIo	7.819E-06	-1.057E-10	-1.05673	7.952E-11
70	VO2+1	2.679E-05	2.476E-04	-8.84033	2.476E-04
71	VO2+1	2.679E-05	5.564E-05	-9.12879	5.564E-05
72	VO2+1	2.679E-05	9.216E-06	-9.33960	9.216E-06
73	VO2+1	2.679E-05	5.644E-07	-9.41260	5.643E-07
74	VO2+1	2.679E-05	2.747E-09	-9.41819	2.721E-09
***	Releasing hold on I.S. due to convergence				
76	ADS1PSIo	8.670E-06	-8.507E-07	-1.05669	8.507E-07
77	ADS1PSIo	8.581E-06	-9.055E-08	-1.04394	9.053E-08
78	ADS1PSIo	8.572E-06	-7.246E-09	-1.04261	7.220E-09
79	ADS1PSIo	8.571E-06	-5.083E-10	-1.04250	4.819E-10
80	ADS1PSIo	8.571E-06	-3.623E-11	-1.04249	9.796E-12

ITERATIONS= 81: SOLID QUARTZ PRECIPITATES

ITERATIONS= 81: SOLID HEMATITE PRECIPITATES

PART 2 of OUTPUT FILE

MINTEQA2 for Windows v1.50 DATE OF CALCULATIONS:

CONSTRAINTS ON COMPONENT ACTIVITIES

As specified, this chemical system is OPEN with respect to the following components:

H2O

Activities of the following components are constrained by the species shown:

COMPONENT	SPECIES	TYPE
Fe+3	HEMATITE	4
H4SiO4	QUARTZ	4
H2O	H2O	3

PART 3 of OUTPUT FILE

MINTEQA2 for Windows v1.50 DATE OF CALCULATIONS:

PARAMETERS OF THE COMPONENT MOST OUT OF BALANCE:

ITER	NAME	TOTAL mol/L	DIFF FXN	LOG ACTVTY	RESIDUAL
81	Zn+2	6.190E-05	-1.943E-05	-5.12364	1.943E-05
***	Temporarily holding ionic strength constant				
82	ADS1TYP1	1.236E-06	-2.232E-07	-6.88017	2.232E-07
83	ADS1TYP1	1.236E-06	6.474E-07	-6.70830	6.474E-07
84	ADS1TYP1	1.236E-06	-4.605E-07	-7.17801	4.605E-07
85	ADS1TYP1	1.236E-06	7.216E-08	-7.02361	7.215E-08
86	ADS1TYP1	1.236E-06	3.544E-11	-7.04658	3.421E-11
***	Releasing hold on I.S. due to convergence				
88	Zn+2	6.190E-05	7.297E-07	-5.12808	7.296E-07
89	ADS1TYP1	1.236E-06	-2.426E-10	-7.05306	2.413E-10
90	ADS1TYP1	1.236E-06	-1.347E-12	-7.05345	1.114E-13
91	Zn+2	6.190E-05	2.136E-10	-5.13173	1.517E-10

ITERATIONS= 92: SOLID GIBBSITE PRECIPITATES

PART 2 of OUTPUT FILE

MINTEQA2 for Windows v1.50 DATE OF CALCULATIONS:

CONSTRAINTS ON COMPONENT ACTIVITIES

As specified, this chemical system is OPEN with respect to the following components:

H2O

Activities of the following components are constrained by the species shown:

COMPONENT	SPECIES	TYPE
Al+3	GIBBSITE	4
Fe+3	HEMATITE	4
H4SiO4	QUARTZ	4
H2O	H2O	3

PART 3 of OUTPUT FILE

MINTEQA2 for Windows v1.50 DATE OF CALCULATIONS:

PARAMETERS OF THE COMPONENT MOST OUT OF BALANCE:

ITER	NAME	TOTAL mol/L	DIFF FXN	LOG ACTVTY	RESIDUAL
92	Zn+2	6.190E-05	-1.988E-05	-5.13173	1.988E-05
***	Temporarily holding ionic strength constant				
93	Zn+2	6.190E-05	6.088E-06	-4.74620	6.088E-06
94	Zn+2	6.190E-05	1.811E-07	-4.77596	1.810E-07
95	Zn+2	6.190E-05	-2.626E-08	-4.78846	2.619E-08
96	Zn+2	6.190E-05	-1.019E-08	-4.79674	1.013E-08
97	VO2+1	2.679E-05	1.120E-06	-6.65923	1.120E-06
98	VO2+1	2.679E-05	1.205E-08	-6.66820	1.203E-08
99	Pb+2	1.204E-06	-1.200E-08	-7.12222	1.200E-08
100	Pb+2	1.204E-06	-6.124E-09	-7.11617	6.123E-09
101	Pb+2	1.204E-06	-7.948E-10	-7.11375	7.936E-10
102	Pb+2	1.204E-06	-1.785E-11	-7.11359	1.665E-11
103	CrO4-2	1.399E-05	1.666E-11	-7.51702	2.668E-12
***	Releasing hold on I.S. due to convergence				
105	Zn+2	6.190E-05	-1.640E-05	-4.79731	1.640E-05
106	Zn+2	6.190E-05	-2.588E-06	-4.66029	2.588E-06
107	Zn+2	6.190E-05	-2.762E-07	-4.64179	2.762E-07
108	Zn+2	6.190E-05	-3.017E-08	-4.63984	3.011E-08
109	Zn+2	6.190E-05	-3.277E-09	-4.63963	3.215E-09
110	Zn+2	6.190E-05	-3.556E-10	-4.63961	2.937E-10

ITERATIONS= 111: SOLID BARITE PRECIPITATES

PART 2 of OUTPUT FILE

MINTEQA2 for Windows v1.50 DATE OF CALCULATIONS:

CONSTRAINTS ON COMPONENT ACTIVITIES

As specified, this chemical system is OPEN with respect to the following components:

H2O

Activities of the following components are constrained by the species shown:

COMPONENT	SPECIES	TYPE
Ba+2	BARITE	4
Al+3	GIBBSITE	4
Fe+3	HEMATITE	4
H4SiO4	QUARTZ	4
H2O	H2O	3

PART 3 of OUTPUT FILE

MINTEQA2 for Windows v1.50 DATE OF CALCULATIONS:

PARAMETERS OF THE COMPONENT MOST OUT OF BALANCE:

ITER	NAME	TOTAL mol/L	DIFF FXN	LOG ACTVTY	RESIDUAL
111	VO2+1	2.679E-05	-3.707E-06	-6.60653	3.707E-06
***	Temporarily holding ionic strength constant				
112	VO2+1	2.679E-05	4.497E-06	-6.57136	4.497E-06
113	VO2+1	2.679E-05	1.775E-07	-6.60374	1.774E-07
114	VO2+1	2.679E-05	6.881E-10	-6.60415	6.613E-10
***	Releasing hold on I.S. due to convergence				
116	VO2+1	2.679E-05	-1.141E-08	-6.60416	1.139E-08
117	VO2+1	2.679E-05	-1.244E-09	-6.60398	1.217E-09
118	VO2+1	2.679E-05	-1.352E-10	-6.60396	1.084E-10
119	SeO4-2	1.133E-06	-2.610E-12	-6.21997	1.477E-12

ITERATIONS= 120: SOLID GIBBSITE DISSOLVES BY DISSOLUTION RULE 2.

ITERATIONS= 120: SOLID KAOLINITE PRECIPITATES

PART 2 of OUTPUT FILE

MINTEQA2 for Windows v1.50 DATE OF CALCULATIONS:

CONSTRAINTS ON COMPONENT ACTIVITIES

As specified, this chemical system is OPEN with respect to the following components:

H2O

Activities of the following components are constrained by the species shown:

COMPONENT	SPECIES	TYPE
Al+3	KAOLINITE	4
Ba+2	BARITE	4
Fe+3	HEMATITE	4
H4SiO4	QUARTZ	4
H2O	H2O	3

PART 3 of OUTPUT FILE

MINTEQA2 for Windows v1.50 DATE OF CALCULATIONS:

PARAMETERS OF THE COMPONENT MOST OUT OF BALANCE:

ITER	NAME	TOTAL mol/L	DIFF FXN	LOG ACTVTY	RESIDUAL
120	VO2+1	2.679E-05	-3.696E-06	-6.60396	3.696E-06
***	Temporarily holding ionic strength constant				
121	VO2+1	2.679E-05	3.652E-06	-6.51044	3.652E-06
122	VO2+1	2.679E-05	3.195E-07	-6.50290	3.194E-07
123	VO2+1	2.679E-05	3.272E-09	-6.50138	3.245E-09
***	Releasing hold on I.S. due to convergence				
125	VO2+1	2.679E-05	-1.695E-07	-6.50139	1.695E-07
126	VO2+1	2.679E-05	-1.195E-08	-6.50086	1.192E-08
127	VO2+1	2.679E-05	-9.298E-10	-6.50083	9.030E-10
128	VO2+1	2.679E-05	-6.810E-11	-6.50082	4.131E-11

ID No	Name	Total Conc(M)	Conc (M)	log Activity	Diff fxn
330	H+1	-1.008E-01	1.349E-04	-3.93481	-3.960E-10
813	ADS1PSIo	5.593E-06	4.512E-02	-1.34567	9.170E-12
811	ADS1TYP1	1.236E-06	6.653E-09	-8.17698	-5.434E-18
812	ADS1TYP2	4.944E-05	2.692E-07	-6.56995	-2.150E-16
150	Ca+2	2.853E-03	2.412E-03	-2.87707	-1.949E-09
460	Mg+2	3.721E-03	3.103E-03	-2.76763	-2.526E-09
500	Na+1	9.681E-04	9.587E-04	-3.08316	-1.885E-10
410	K+1	2.335E-03	2.311E-03	-2.70102	-4.547E-10
732	SO4-2	1.624E-03	8.606E-04	-3.32465	-7.428E-10
992	Acetate	1.000E-01	1.483E-02	-1.89368	-1.535E-09
61	H3AsO4	3.853E-06	6.541E-08	-7.18195	-7.453E-13
950	Zn+2	6.190E-05	4.400E-05	-4.61595	-3.716E-11
110	Be+2	5.841E-06	2.828E-06	-5.80799	-2.732E-12
160	Cd+2	6.379E-08	3.503E-08	-7.71495	-3.221E-14
212	CrO4-2	1.399E-05	5.184E-08	-7.54478	-2.496E-12
361	Hg(OH)2	2.493E-08	1.586E-10	-9.79733	2.294E-16
600	Pb+2	1.204E-06	1.951E-07	-6.96916	-2.986E-13
762	SeO4-2	1.133E-06	1.126E-06	-6.20770	-8.850E-13

903	VO2+1	2.679E-05	3.665E-07	-6.50082	-4.968E-12
2	H2O	-6.939E-18	3.489E-02	-0.00119	0.000E+00
770	H4SiO4	8.738E-02	9.891E-05	-4.00238	0.000E+00
281	Fe+3	1.478E-02	1.180E-12	-12.51165	0.000E+00
100	Ba+2	7.932E-05	4.019E-07	-6.65535	0.000E+00
30	Al+3	4.767E-02	3.160E-04	-4.08396	0.000E+00

Type I - COMPONENTS AS SPECIES IN SOLUTION

ID No	Name	Conc (M)	log Act	Charge	Act Coef	New logK
330	H+1	1.349E-04	-3.93481	1.00	0.86128	0.065
770	H4SiO4	9.891E-05	-4.00238	0.00	1.00554	-0.002
30	Al+3	3.160E-04	-4.08396	3.00	0.26079	0.584
281	Fe+3	1.180E-12	-12.51165	3.00	0.26079	0.584
150	Ca+2	2.412E-03	-2.87707	2.00	0.55026	0.259
460	Mg+2	3.103E-03	-2.76763	2.00	0.55026	0.259
500	Na+1	9.587E-04	-3.08316	1.00	0.86128	0.065
410	K+1	2.311E-03	-2.70102	1.00	0.86128	0.065
732	SO4-2	8.606E-04	-3.32465	-2.00	0.55026	0.259
992	Acetate	1.483E-02	-1.89368	-1.00	0.86128	0.065
61	H3AsO4	6.541E-08	-7.18195	0.00	1.00554	-0.002
100	Ba+2	4.019E-07	-6.65535	2.00	0.55026	0.259
110	Be+2	2.828E-06	-5.80799	2.00	0.55026	0.259
160	Cd+2	3.503E-08	-7.71495	2.00	0.55026	0.259
212	CrO4-2	5.184E-08	-7.54478	-2.00	0.55026	0.259
361	Hg(OH)2	1.586E-10	-9.79733	0.00	1.00554	-0.002
600	Pb+2	1.951E-07	-6.96916	2.00	0.55026	0.259
762	SeO4-2	1.126E-06	-6.20770	-2.00	0.55026	0.259
903	VO2+1	3.665E-07	-6.50082	1.00	0.86128	0.065
950	Zn+2	4.400E-05	-4.61595	2.00	0.55026	0.259
811	ADS1TYP1	6.653E-09	-8.17698	0.00	1.00000	0.000
812	ADS1TYP2	2.692E-07	-6.56995	0.00	1.00000	0.000

Type II - OTHER SPECIES IN SOLUTION OR ADSORBED

ID No	Name	Conc (M)	log Act	Charge	Act Coef	New logK
8116000	=FeOPb+	1.239E-08	-7.90700	1.00	1.00000	4.650
4109921	K[Acetate]	1.612E-05	-4.79020	0.00	1.00554	-0.198
3613300	Hg+2	6.150E-12	-11.47058	2.00	0.55026	6.453
3300020	OH-	1.003E-10	-10.06338	-1.00	0.86128	-13.932
6003300	PbOH+	2.706E-11	-10.63254	1.00	0.86128	-7.532
6003301	Pb(OH)2 (aq)	6.334E-17	-16.19591	0.00	1.00554	-17.096
6003302	Pb(OH)3-	6.391E-24	-23.25929	-1.00	0.86128	-28.026
6003303	Pb2OH+3	1.521E-16	-16.40170	3.00	0.26079	-5.813
6003304	Pb3(OH)4+2	1.579E-29	-29.06098	2.00	0.55026	-23.629
6003305	Pb(OH)4-2	2.117E-31	-30.93367	-2.00	0.55026	-39.440
6003306	Pb4(OH)4+4	8.083E-32	-32.13014	4.00	0.09168	-18.950
303300	AlOH+2	1.294E-05	-5.14734	2.00	0.55026	-4.738
303301	Al(OH)2+	5.677E-07	-6.31072	1.00	0.86128	-10.029
303303	Al(OH)3 (aq)	8.385E-10	-9.07409	0.00	1.00554	-16.793
303302	Al(OH)4-	1.065E-11	-11.03747	-1.00	0.86128	-22.623
9503300	ZnOH+	2.430E-10	-9.67933	1.00	0.86128	-8.932
9503301	Zn(OH)2 (aq)	2.850E-15	-14.54271	0.00	1.00554	-17.796
9503302	Zn(OH)3-	1.441E-21	-20.90608	-1.00	0.86128	-28.026
9503303	Zn(OH)4-2	7.762E-30	-29.36946	-2.00	0.55026	-40.229
1603300	CdOH+	1.537E-14	-13.87832	1.00	0.86128	-10.032
1603301	Cd(OH)2 (aq)	7.176E-21	-20.14170	0.00	1.00554	-20.296
1603302	Cd(OH)3-	4.424E-29	-28.41908	-1.00	0.86128	-32.440
1603303	Cd(OH)4-2	9.794E-40	-39.26845	-2.00	0.55026	-47.029
1603304	Cd2OH+3	4.903E-21	-20.89327	3.00	0.26079	-8.813
3613302	HgOH+	1.352E-11	-10.93396	1.00	0.86128	2.862
3613303	Hg(OH)3-1	2.014E-21	-20.76071	-1.00	0.86128	-14.832
2813300	FeOH+2	3.122E-11	-10.76503	2.00	0.55026	-1.928
2813301	Fe(OH)2+	6.706E-10	-9.23841	1.00	0.86128	-4.529
2813302	Fe(OH)3 (aq)	5.331E-14	-13.27078	0.00	1.00554	-12.562
2813303	Fe(OH)4-	5.008E-19	-18.36516	-1.00	0.86128	-21.523
2813304	Fe2(OH)2+4	1.066E-19	-20.01006	4.00	0.09168	-1.816
2813305	Fe3(OH)4+5	3.412E-27	-28.08846	5.00	0.02391	-4.667
1103301	BeOH+	6.216E-08	-7.27137	1.00	0.86128	-5.332
1103302	Be(OH)2 (aq)	2.903E-12	-11.53475	0.00	1.00554	-13.596
1103303	Be(OH)3-	7.358E-18	-17.19812	-1.00	0.86128	-23.126
1103304	Be(OH)4-2	6.280E-28	-27.46150	-2.00	0.55026	-37.129
1103305	Be2OH+3	5.301E-11	-10.85936	3.00	0.26079	-2.593
1103306	Be3(OH)3+3	1.422E-14	-14.43070	3.00	0.26079	-8.224
4603300	MgOH+	2.795E-11	-10.61850	1.00	0.86128	-11.720
1503300	CaOH+	2.657E-12	-11.64045	1.00	0.86128	-12.632
1003300	BaOH+	9.686E-17	-16.07873	1.00	0.86128	-13.292
3307320	HSO4-	6.199E-06	-5.27252	-1.00	0.86128	2.052
6007320	PbSO4 (aq)	2.476E-08	-7.60381	0.00	1.00554	2.688
6007321	Pb(SO4)2-2	1.291E-10	-10.14846	-2.00	0.55026	3.729
307320	AlSO4+	3.518E-04	-3.51861	1.00	0.86128	3.955
307321	Al(SO4)2-	1.785E-06	-5.81326	-1.00	0.86128	4.985
9507320	ZnSO4 (aq)	2.495E-06	-5.60060	0.00	1.00554	2.338
9507321	Zn(SO4)2-2	1.880E-08	-7.98525	-2.00	0.55026	3.539
1607320	CdSO4 (aq)	2.128E-09	-8.66959	0.00	1.00554	2.368
1607321	Cd(SO4)2-2	2.484E-11	-10.86424	-2.00	0.55026	3.759
3617320	HgSO4 (aq)	4.172E-13	-12.37723	0.00	1.00554	8.610
2817320	FeSO4+	1.899E-12	-11.78630	1.00	0.86128	4.115
2817321	Fe(SO4)2-	1.923E-14	-13.78095	-1.00	0.86128	5.445
9037320	VO2SO4-	4.144E-09	-8.44747	-1.00	0.86128	1.443
1107321	BeSO4 (aq)	1.135E-07	-6.94264	0.00	1.00554	2.188
1107322	Be(SO4)2-2	2.501E-10	-9.86129	-2.00	0.55026	2.855
4607320	MgSO4 (aq)	1.463E-04	-3.83228	0.00	1.00554	2.258
1507320	CaSO4 (aq)	1.432E-04	-3.84172	0.00	1.00554	2.358
5007320	NaSO4-	2.438E-06	-5.67781	-1.00	0.86128	0.795
4107320	KSO4-	7.690E-06	-5.17894	-1.00	0.86128	0.912
3307620	HSeO4-1	4.191E-09	-8.44251	-1.00	0.86128	1.765
9507620	ZnSeO4	2.312E-09	-8.63365	0.00	1.00554	2.188
9507621	Zn(SeO4)2-2	2.655E-15	-14.83535	-2.00	0.55026	2.455
1607620	CdSeO4 (aq)	2.213E-12	-11.65265	0.00	1.00554	2.268
3300613	AsO4-3	3.208E-16	-16.07751	-3.00	0.26079	-20.116
3300612	HAsO4-2	5.586E-09	-8.51232	-2.00	0.55026	-8.941
3300611	H2AsO4-	3.782E-06	-5.48714	-1.00	0.86128	-2.175
3307701	H2SiO4-2	3.231E-18	-17.75010	-2.00	0.55026	-21.358
3307700	H3SiO4-	1.170E-10	-9.99657	-1.00	0.86128	-9.864
2123300	HCrO4-	1.245E-05	-4.96959	-1.00	0.86128	6.575
2123301	H2CrO4 (aq)	1.005E-09	-8.99561	0.00	1.00554	6.416
2123302	Cr2O7-2	7.268E-09	-8.39800	-2.00	0.55026	14.819
2127320	CrO3SO4-2	3.275E-10	-9.74417	-2.00	0.55026	9.253
5002120	NaCrO4-	1.359E-10	-9.93164	-1.00	0.86128	0.761
4102120	KCrO4-	2.449E-10	-9.67581	-1.00	0.86128	0.635

9033303	VO4-3	4.166E-21	-20.96395	-3.00	0.26079	-29.616
9033302	HVO4-2	4.578E-11	-10.59876	-2.00	0.55026	-15.641
9033301	H2VO4-	1.353E-06	-5.93358	-1.00	0.86128	-7.235
9033300	H3VO4 (aq)	1.347E-06	-5.86839	0.00	1.00554	-3.302
9030020	V2O7-4	2.520E-20	-20.63634	-4.00	0.09168	-30.202
9030021	HV2O7-3	3.824E-14	-14.00115	-3.00	0.26079	-20.086
9030022	H3V2O7-	1.186E-05	-4.99078	-1.00	0.86128	-3.725
9030023	V3O9-3	6.406E-12	-11.77716	-3.00	0.26079	-15.296
9030024	V4O12-4	8.875E-15	-15.08955	-4.00	0.09168	-19.522
9030025	V10O28 -6	1.513E-24	-26.15505	-6.00	0.00463	-21.759
9030026	HV10O28 -5	5.227E-21	-21.90316	-5.00	0.02391	-14.286
9030027	H2V10O28-4	2.555E-20	-20.63037	-4.00	0.09168	-9.662
3309921	H[Acetate]	8.435E-02	-1.07149	0.00	1.00554	4.755
6009921	Pb[Acetate]	7.621E-07	-6.18284	1.00	0.86128	2.745
6009922	Pb[Acetate]2	2.095E-07	-6.67652	0.00	1.00554	4.078
9509921	Zn[Acetate]	1.365E-05	-4.92963	1.00	0.86128	1.645
9509922	Zn[Acetate]2	1.729E-06	-5.75991	0.00	1.00554	2.641
1609921	Cd[Acetate]	2.434E-08	-7.67863	1.00	0.86128	1.995
1609922	Cd[Acetate]2	2.266E-09	-8.64230	0.00	1.00554	2.858
3619920	Hg[Acetate]	1.001E-09	-9.06426	1.00	0.86128	10.559
3619921	Hg[Acetate]2	2.375E-08	-7.62194	0.00	1.00554	13.828
2819920	Fe[Acetate]	7.542E-11	-10.38193	2.00	0.55026	4.283
2819921	Fe[Acetate]2	2.178E-09	-8.72671	1.00	0.86128	7.637
2819922	Fe[Acetate]3	2.464E-09	-8.60599	0.00	1.00554	9.584
1109921	Be[Acetate]	2.583E-06	-5.65277	1.00	0.86128	2.114
1109922	Be[Acetate]2	2.545E-07	-6.59195	0.00	1.00554	3.001
4609920	Mg[Acetate]	4.716E-04	-3.39131	1.00	0.86128	1.335
1509920	Ca[Acetate]	2.979E-04	-3.59075	1.00	0.86128	1.245
1009921	Ba[Acetate]	3.853E-08	-7.47903	1.00	0.86128	1.135
5009920	Na[Acetate]	6.930E-06	-5.15684	0.00	1.00554	-0.182
8113302	=FeOH2+	6.800E-07	-6.16746	1.00	1.00000	7.290
8113301	=FeO-	1.491E-12	-11.82650	-1.00	1.00000	-8.930
8111500	=FeOHCa+2	1.677E-09	-8.77540	2.00	1.00000	4.970
8117320	=FeSO4-	4.903E-07	-6.30958	-1.00	1.00000	7.780
8117321	=FeOHSO4-2	9.544E-09	-8.02028	-2.00	1.00000	0.790
8112120	=FeCrO4-	3.470E-08	-7.45971	-1.00	1.00000	10.850
8112121	=FeOHCrO4-2	7.406E-10	-9.13042	-2.00	1.00000	3.900
8123302	=FeOH2+	2.751E-05	-4.56043	1.00	1.00000	7.290
8123301	=FeO-	6.033E-11	-10.21947	-1.00	1.00000	-8.930
8121500	=FeOCa+	1.959E-13	-12.70788	1.00	1.00000	-5.850
8126000	=FeOPb+	2.239E-11	-10.64997	1.00	1.00000	0.300
8127320	=FeSO4-	1.984E-05	-4.70255	-1.00	1.00000	7.780
8127321	=FeOHSO4-2	3.861E-07	-6.41325	-2.00	1.00000	0.790
8122120	=FeCrO4-	1.404E-06	-5.85268	-1.00	1.00000	10.850
8122121	=FeOHCrO4-2	2.996E-08	-7.52339	-2.00	1.00000	3.900

Type III - SPECIES WITH FIXED ACTIVITY

ID No	Name	Conc (M)	New logK	Enthalpy
2	H2O	3.489E-02	0.001	0.000

Type IV - FINITE SOLIDS (present at equilibrium)

ID No	Name	Conc (M)	New logK	Enthalpy
2077002	QUARTZ	4.029E-02	4.000	-22.360
3028100	HEMATITE	7.390E-03	1.418	128.987
6010000	BARITE	7.888E-05	9.980	-23.000
8603001	KAOLINITE	2.349E-02	-7.435	148.000

Type V - UNDERSATURATED SOLIDS (not present at equilibrium)

ID No	Name	Conc (M)	New logK	Enthalpy
2095004	Zn(OH)2 (epsilon)	5.215E-09	-11.534	81.800
2095005	ZnO (active)	1.159E-08	-11.188	88.760
2095006	ZINCITE	8.289E-09	-11.334	89.620
2016000	Cd(OH)2 (am)	2.644E-14	-13.730	86.902
2016001	Cd(OH)2	3.223E-14	-13.644	94.620
2016002	MONTEPONITE	1.122E-15	-15.103	103.400
2036100	MONTROYDITE	6.980E-07	3.640	38.900
2036101	Hg(OH)2	5.000E-07	3.496	0.000
2028100	FERRIHYDRITE	1.254E-04	-3.191	73.374
2028102	GOETHITE	6.301E-02	-0.491	60.584
2021200	CrO3	6.270E-13	3.211	5.209
2011001	Be(OH)2 (am)	7.333E-06	-7.194	0.000
2011002	Be(OH)2 (alpha)	1.463E-05	-6.894	0.000
2011003	Be(OH)2 (beta)	3.675E-05	-6.494	0.000
2046000	BRUCITE	1.801E-12	-16.844	113.996
2046001	PERICLASE	3.286E-17	-21.584	151.230
2046002	Mg(OH)2 (active)	2.021E-14	-18.794	0.000
2015000	LIME	1.959E-28	-32.699	193.910
2015001	PORTLANDITE	1.535E-18	-22.804	128.620
2010001	Ba(OH)2:8H2O	6.433E-24	-24.394	54.320
3006100	As2O5	8.582E-22	-6.706	22.640
3003000	Al2O3	6.095E-05	-19.652	258.590
2095001	Zn(OH)2	1.125E-09	-12.200	0.000
3028101	MAGHEMITE	1.570E-08	-6.386	0.000
3028102	LEPIDOCROCITE	8.306E-03	-1.371	0.000
3090300	V2O5	1.686E-04	1.360	-34.000
3046000	SPINEL	4.904E-17	-36.848	388.012
3046001	MAGNESIOFERRITE	6.654E-14	-16.860	278.920
6060000	LARNAKITE	1.096E-09	0.434	21.830
6060001	Pb3O2SO4	6.582E-20	-10.686	79.140
6060002	Pb4O3SO4	3.364E-30	-21.877	136.450
6060003	ANGLESITE	3.135E-03	7.790	-12.000
6060004	Pb4(OH)6SO4	1.997E-29	-21.100	0.000
6003000	AlOHSO4	5.689E-01	3.230	0.000
6003001	Al4(OH)10SO4	9.456E-04	-22.700	0.000
6095000	Zn2(OH)2SO4	6.467E-13	-7.500	0.000
6095001	Zn4(OH)6SO4	2.590E-27	-28.400	0.000
6095002	Zn3O(SO4)2	2.869E-32	-18.914	258.080
6095003	ZINCOSITE	1.348E-12	-3.930	82.586
6095004	ZnSO4:1H2O	4.968E-08	0.638	44.070
6095005	BIANCHITE	6.566E-07	1.765	0.669
6095006	GOSLARITE	1.154E-06	2.011	-14.210
6016000	Cd3(OH)4SO4	5.070E-34	-22.560	0.000
6016001	Cd3OH2(SO4)2	2.307E-29	-6.710	0.000
6016002	Cd4(OH)6SO4	1.041E-39	-28.400	0.000
6016003	CdSO4	1.357E-11	0.172	51.980
6016004	CdSO4:1H2O	4.845E-10	1.726	31.540
6016005	CdSO4:2.67H2O	6.764E-10	1.873	17.991

6036100	HgSO4	2.690E-12	9.419	-14.686
6028100	Fe2(SO4)3	5.458E-32	3.734	242.028
6028101	H-JAROSITE	3.815E-13	12.100	230.748
6050000	Na-JAROSITE	3.422E-13	11.200	151.377
6041002	K-JAROSITE	3.284E-09	14.800	130.875
6046000	EPSOMITE	1.061E-04	2.127	-11.560
6015000	ANHYDRITE	1.440E-02	4.360	7.200
6015001	GYPSUM	2.546E-02	4.610	-1.000
2095003	Zn(OH)2 (gamma)	3.291E-09	-11.734	0.000
6050001	MIRABILITE	4.085E-09	1.114	-79.442
6050002	THENARDITE	1.539E-10	-0.322	9.121
6041000	K-ALUM	5.266E-09	5.170	-30.209
6041001	ALUNITE	6.175E-21	1.400	210.000
3021212	PbCrO4	1.219E-02	12.600	-44.180
3021208	MgCrO4	2.030E-16	-5.380	88.952
3015000	CaCrO4	6.980E-09	2.266	26.945
3021201	BaCrO4	2.950E-05	9.670	-33.000
3021210	Na2CrO4	2.284E-17	-2.930	19.630
3021211	Na2Cr2O7	5.902E-20	9.895	-22.196
3021205	K2CrO4	3.686E-13	0.513	-18.270
3021206	K2Cr2O7	7.627E-12	17.242	-80.750
6160000	PbSeO4	4.604E-07	6.840	-15.000
6195001	ZnSeO4:6H2O	4.889E-10	1.520	0.000
6116001	CdSeO4:2H2O	8.413E-13	1.850	0.000
6146001	MgSeO4:6H2O	1.650E-08	1.200	0.000
6115001	CaSeO4:2H2O	8.567E-07	3.020	8.300
6110001	BaSeO4	3.953E-06	7.460	-22.000
6111001	BeSeO4:4H2O	8.309E-10	2.940	0.000
6150002	Na2SeO4	2.218E-14	-1.280	0.000
6141001	K2SeO4	1.319E-11	0.730	0.000
7260000	Pb3(AsO4)2	3.447E-18	-5.800	0.000
7203000	AlAsO4:2H2O	5.447E-05	-4.800	0.000
7295000	Zn3AsO42:2.5H2O	5.548E-19	-13.650	0.000
7228100	FeAsO4:2H2O	5.110E-09	-0.400	0.000
7215000	Ca3(AsO4)2:4H2O	2.037E-22	-22.300	0.000
7210000	Ba3(AsO4)2	1.545E-02	8.910	-11.046
7349000	NH4VO3	1.166E-09	-3.800	-30.000
7360000	Pb3(VO4)2	2.658E-09	-6.140	72.634
7360001	Pb2V2O7	3.676E-02	1.900	26.945
7346000	Mg(VO3)2	4.871E-12	-11.280	136.649
7346001	Mg2V2O7	5.110E-22	-26.360	255.224
7315001	Ca(VO3)2	1.578E-06	-5.660	84.768
7315002	Ca3(VO4)2	7.601E-30	-38.960	293.466
7315003	Ca2V2O7	2.236E-13	-17.500	159.494
7315004	Ca3(VO4)2:4H2O	9.465E-31	-39.860	0.000
7315005	Ca2V2O7:2H2O	1.973E-17	-21.552	0.000
7310001	Ba3(VO4)2:4H2O	3.642E-35	-32.940	0.000
7310002	Ba2V2O7:2H2O	2.622E-19	-15.872	0.000
7350000	NaVO3	2.668E-06	-3.858	30.180
7350001	Na3VO4	2.020E-37	-36.681	184.610
7350002	Na4V2O7	7.430E-40	-37.400	201.083
8603000	HALLOYSITE	7.246E-03	-9.575	181.430
2003003	GIBBSITE	2.666E-01	-8.291	95.395
8646000	CHRYSOTILE	1.259E-25	-32.200	196.000
8646003	SEPIOLITE	2.738E-18	-15.760	114.089
2076200	SeO3	7.583E-36	-21.044	146.377
2077000	CHALCEDONY	3.548E-01	3.550	-19.700
2077001	CRISTOBALITE	2.239E-01	3.350	-20.006
2095000	Zn(OH)2 (am)	5.988E-10	-12.474	80.620
2077003	SiO2 (am,gel)	5.129E-02	2.710	-14.000
2077004	SiO2 (am,ppt)	5.495E-02	2.740	-15.150
2060000	MASSICOT	1.012E-12	-12.894	66.848
2060001	LITHARGE	1.604E-12	-12.694	65.501
2060002	PbO:0.3H2O	8.296E-13	-12.980	0.000
2060004	Pb(OH)2	5.599E-08	-8.150	58.534
2060005	Pb2O(OH)2	4.068E-25	-26.188	0.000
2003000	Al(OH)3 (am)	8.259E-04	-10.800	111.000
2003001	BOEHMITE	1.381E-01	-8.578	117.696
8646004	SEPIOLITE (A)	2.615E-21	-18.780	0.000
2095002	Zn(OH)2 (beta)	3.143E-09	-11.754	83.140

Type VI - EXCLUDED SPECIES (not included in mole balance)

ID No	Name	Conc (M)	New logK	Enthalpy
813	ADS1PSIo	4.512E-02	0.000	0.000
2003002	DIASPORE	7.000E+00	-6.873	103.052

PART 4 of OUTPUT FILE

MINTEQA2 for Windows v1.50 DATE OF CALCULATIONS:

PERCENTAGE DISTRIBUTION OF COMPONENTS AMONG
TYPE I and TYPE II (dissolved and adsorbed) species

H+1			
	99.8	Percent bound in species #3309921	H[Acetate]
ADS1PSIo			
	12.2	Percent bound in species #8113302	=FeOH2+
	491.9	Percent bound in species #8123302	=FeOH2+
ADS1TYP1			
	1.0	Percent bound in species #8116000	=FeOPb+
	55.0	Percent bound in species #8113302	=FeOH2+
	39.7	Percent bound in species #8117320	=FeSO4-
	2.8	Percent bound in species #8112120	=FeCrO4-
ADS1TYP2			
	55.7	Percent bound in species #8123302	=FeOH2+
	40.1	Percent bound in species #8127320	=FeSO4-

	2.8	Percent bound in species #8122120	=FeCrO4-
Ca+2			
	84.5	Percent bound in species # 150	Ca+2
	5.0	Percent bound in species #1507320	CaSO4 (aq)
	10.4	Percent bound in species #1509920	Ca[Acetate]
Mg+2			
	83.4	Percent bound in species # 460	Mg+2
	3.9	Percent bound in species #4607320	MgSO4 (aq)
	12.7	Percent bound in species #4609920	Mg[Acetate]
Na+1			
	99.0	Percent bound in species # 500	Na+1
K+1			
	99.0	Percent bound in species # 410	K+1
SO4-2			
	55.7	Percent bound in species # 732	SO4-2
	22.8	Percent bound in species # 307320	AlSO4+
	9.5	Percent bound in species #4607320	MgSO4 (aq)
	9.3	Percent bound in species #1507320	CaSO4 (aq)
	1.3	Percent bound in species #8127320	=FeSO4-
Acetate			
	14.8	Percent bound in species # 992	Acetate
	84.4	Percent bound in species #3309921	H[Acetate]
H3AsO4			
	1.7	Percent bound in species # 61	H3AsO4
	98.2	Percent bound in species #3300611	H2AsO4-
Zn+2			
	71.1	Percent bound in species # 950	Zn+2
	4.0	Percent bound in species #9507320	ZnSO4 (aq)
	22.1	Percent bound in species #9509921	Zn[Acetate]
	2.8	Percent bound in species #9509922	Zn[Acetate]2
Be+2			
	48.4	Percent bound in species # 110	Be+2
	1.1	Percent bound in species #1103301	BeOH+
	1.9	Percent bound in species #1107321	BeSO4 (aq)
	44.2	Percent bound in species #1109921	Be[Acetate]
	4.4	Percent bound in species #1109922	Be[Acetate]2
Cd+2			
	54.9	Percent bound in species # 160	Cd+2
	3.3	Percent bound in species #1607320	CdSO4 (aq)
	38.1	Percent bound in species #1609921	Cd[Acetate]
	3.6	Percent bound in species #1609922	Cd[Acetate]2
CrO4-2			
	89.0	Percent bound in species #2123300	HCrO4-
	10.0	Percent bound in species #8122120	=FeCrO4-
Hg(OH)2			
	4.0	Percent bound in species #3619920	Hg[Acetate]
	95.3	Percent bound in species #3619921	Hg[Acetate]2
Pb+2			
	16.2	Percent bound in species # 600	Pb+2
	1.0	Percent bound in species #8116000	=FeOPb+
	2.1	Percent bound in species #6007320	PbSO4 (aq)
	63.3	Percent bound in species #6009921	Pb[Acetate]
	17.4	Percent bound in species #6009922	Pb[Acetate]2
SeO4-2			
	99.4	Percent bound in species # 762	SeO4-2
VO2+1			
	1.4	Percent bound in species # 903	VO2+1
	5.1	Percent bound in species #9033301	H2VO4-

	5.0	Percent bound in species #9033300	H3VO4 (aq)
	88.5	Percent bound in species #9030022	H3V2O7-
H2O			
	38.9	Percent bound in species # 303300	AlOH+2
	3.4	Percent bound in species # 303301	Al(OH)2+
	8.1	Percent bound in species #9033301	H2VO4-
	8.1	Percent bound in species #9033300	H3VO4 (aq)
	106.8	Percent bound in species #9030022	H3V2O7-
H4SiO4			
	100.0	Percent bound in species # 770	H4SiO4
Fe+3			
	12.4	Percent bound in species #2813301	Fe(OH)2+
	1.4	Percent bound in species #2819920	Fe[Acetate]
	40.2	Percent bound in species #2819921	Fe[Acetate]2
	45.4	Percent bound in species #2819922	Fe[Acetate]3
Ba+2			
	91.3	Percent bound in species # 100	Ba+2
	8.7	Percent bound in species #1009921	Ba[Acetate]
Al+3			
	46.3	Percent bound in species # 30	Al+3
	1.9	Percent bound in species # 303300	AlOH+2
	51.5	Percent bound in species # 307320	AlSO4+

PART 5 of OUTPUT FILE

MINTEQA2 for Windows v1.50 DATE OF CALCULATIONS:

---------- EQUILIBRATED MASS DISTRIBUTION ----------

IDX	Name	DISSOLVED mol/L	DISSOLVED percent	SORBED mol/L	SORBED percent	PRECIPITATED mol/L	PRECIPITATED percent
330	H+1	8.445E-02	99.9	4.995E-05	0.1	0.000E+00	0.0
150	Ca+2	2.853E-03	100.0	1.677E-09	0.0	0.000E+00	0.0
460	Mg+2	3.721E-03	100.0	0.000E+00	0.0	0.000E+00	0.0
500	Na+1	9.681E-04	100.0	0.000E+00	0.0	0.000E+00	0.0
410	K+1	2.335E-03	100.0	0.000E+00	0.0	0.000E+00	0.0
732	SO4-2	1.524E-03	93.9	2.072E-05	1.3	7.888E-05	4.9
992	Acetate	1.000E-01	100.0	0.000E+00	0.0	0.000E+00	0.0
61	H3AsO4	3.853E-06	100.0	0.000E+00	0.0	0.000E+00	0.0
950	Zn+2	6.190E-05	100.0	0.000E+00	0.0	0.000E+00	0.0
110	Be+2	5.841E-06	100.0	0.000E+00	0.0	0.000E+00	0.0
160	Cd+2	6.379E-08	100.0	0.000E+00	0.0	0.000E+00	0.0
212	CrO4-2	1.252E-05	89.5	1.469E-06	10.5	0.000E+00	0.0
361	Hg(OH)2	2.493E-08	100.0	0.000E+00	0.0	0.000E+00	0.0
600	Pb+2	1.192E-06	99.0	1.241E-08	1.0	0.000E+00	0.0
762	SeO4-2	1.133E-06	100.0	0.000E+00	0.0	0.000E+00	0.0
903	VO2+1	2.679E-05	100.0	0.000E+00	0.0	0.000E+00	0.0
770	H4SiO4	9.891E-05	0.1	0.000E+00	0.0	8.728E-02	99.9
281	Fe+3	5.423E-09	0.0	0.000E+00	0.0	1.478E-02	100.0
100	Ba+2	4.404E-07	0.6	0.000E+00	0.0	7.888E-05	99.4
30	Al+3	6.831E-04	1.4	0.000E+00	0.0	4.699E-02	98.6

Charge Balance: SPECIATED

Sum of CATIONS = 1.667E-02 Sum of ANIONS 1.663E-02

PERCENT DIFFERENCE = 1.390E-01 (ANIONS - CATIONS)/(ANIONS + CATIONS)

EQUILIBRIUM IONIC STRENGTH (m) = 2.401E-02

EQUILIBRIUM pH = 3.935

******* DIFFUSE LAYER ADSORPTION MODEL ********

**** Parameters For Adsorbent Number 1 ****
Electrostatic Variables: psi0 = 0.079603 sig0 = 0.040884
psib = 0.000000 sigb = 0.000000
psid = 0.000000 sigd = 0.000000
Adsorbent Concentration (g/l): 0.022
Specific Surface Area (sq. meters/g): 600.00

DATE ID NUMBER: 20040515
TIME ID NUMBER: 19341158

PART 6 of OUTPUT FILE

MINTEQA2 for Windows v1.50 DATE OF CALCULATIONS:

Saturation indices and stoichiometry of all minerals

ID No	Name	SI	Composition by stoich. of components
2076200	SeO3	-35.120	[1.000]762 [2.000]330 [-1.000] 2
2077000	CHALCEDONY	-0.450	[1.000]770 [-2.000] 2
2077001	CRISTOBALITE	-0.650	[1.000]770 [-2.000] 2
2077002	QUARTZ	0.000	[1.000]770 [-2.000] 2
2077003	SiO2 (am,gel)	-1.290	[1.000]770 [-2.000] 2
2077004	SiO2 (am,ppt)	-1.260	[1.000]770 [-2.000] 2
2060000	MASSICOT	-11.995	[1.000]600 [1.000] 2 [-2.000]330
2060001	LITHARGE	-11.795	[1.000]600 [1.000] 2 [-2.000]330
2060002	PbO:0.3H2O	-12.081	[-2.000]330 [1.000]600 [1.330] 2
2060004	Pb(OH)2	-7.252	[-2.000]330 [1.000]600 [2.000] 2
2060005	Pb2O(OH)2	-24.391	[2.000]600 [3.000] 2 [-4.000]330
2003000	Al(OH)3 (am)	-3.083	[1.000] 30 [3.000] 2 [-3.000]330
2003001	BOEHMITE	-0.860	[-3.000]330 [1.000] 30 [2.000] 2
2003002	DIASPORE	0.845	[-3.000]330 [1.000] 30 [2.000] 2
2003003	GIBBSITE	-0.574	[1.000] 30 [3.000] 2 [-3.000]330
2095000	Zn(OH)2 (am)	-9.223	[1.000]950 [2.000] 2 [-2.000]330
2095001	Zn(OH)2	-8.949	[-2.000]330 [1.000]950 [2.000] 2
2095002	Zn(OH)2 (beta)	-8.503	[1.000]950 [2.000] 2 [-2.000]330
2095003	Zn(OH)2 (gamma)	-8.483	[1.000]950 [2.000] 2 [-2.000]330
2095004	Zn(OH)2 (epsilon)	-8.283	[1.000]950 [2.000] 2 [-2.000]330
2095005	ZnO (active)	-7.936	[-2.000]330 [1.000]950 [1.000] 2
2095006	ZINCITE	-8.082	[1.000]950 [1.000] 2 [-2.000]330
2016000	Cd(OH)2 (am)	-13.578	[-2.000]330 [1.000]160 [2.000] 2
2016001	Cd(OH)2	-13.492	[1.000]160 [2.000] 2 [-2.000]330
2016002	MONTEPONITE	-14.950	[-2.000]330 [1.000]160 [1.000] 2
2036100	MONTROYDITE	-6.156	[1.000]361 [-1.000] 2
2036101	Hg(OH)2	-6.301	[1.000]361
2028100	FERRIHYDRITE	-3.902	[1.000]281 [3.000] 2 [-3.000]330
2028102	GOETHITE	-1.201	[1.000]281 [2.000] 2 [-3.000]330
2021200	CrO3	-12.203	[1.000]212 [2.000]330 [-1.000] 2
2011001	Be(OH)2 (am)	-5.135	[1.000]110 [2.000] 2 [-2.000]330
2011002	Be(OH)2 (alpha)	-4.835	[1.000]110 [2.000] 2 [-2.000]330
2011003	Be(OH)2 (beta)	-4.435	[1.000]110 [2.000] 2 [-2.000]330
2046000	BRUCITE	-11.744	[1.000]460 [2.000] 2 [-2.000]330
2046001	PERICLASE	-16.483	[-2.000]330 [1.000]460 [1.000] 2
2046002	Mg(OH)2 (active)	-13.694	[1.000]460 [2.000] 2 [-2.000]330
2015000	LIME	-27.708	[-2.000]330 [1.000]150 [1.000] 2
2015001	PORTLANDITE	-17.814	[1.000]150 [2.000] 2 [-2.000]330
2010001	Ba(OH)2:8H2O	-23.192	[1.000]100 [10.000] 2 [-2.000]330
3006100	As2O5	-21.066	[2.000] 61 [-3.000] 2
3003000	Al2O3	-4.215	[2.000] 30 [3.000] 2 [-6.000]330
3028100	HEMATITE	0.000	[2.000]281 [3.000] 2 [-6.000]330
3028101	MAGHEMITE	-7.804	[-6.000]330 [2.000]281 [3.000] 2

ID No	Name	SI	Composition by stoich. of components
			[1.000] 2
6060001	Pb3O2SO4	-19.182	[-4.000]330 [3.000]600 [1.000]732
			[2.000] 2
6060002	Pb4O3SO4	-29.473	[-6.000]330 [4.000]600 [1.000]732
			[3.000] 2
6060003	ANGLESITE	-2.504	[1.000]600 [1.000]732
6060004	Pb4(OH)6SO4	-28.700	[-6.000]330 [4.000]600 [1.000]732
			[6.000] 2
6003000	AlOHSO4	-0.245	[-1.000]330 [1.000] 30 [1.000]732
			[1.000] 2
6003001	Al4(OH)10SO4	-3.024	[-10.000]330 [4.000] 30 [1.000]732
			[10.000] 2
6095000	Zn2(OH)2SO4	-12.189	[-2.000]330 [2.000]950 [2.000] 2
			[1.000]732
6095001	Zn4(OH)6SO4	-26.587	[-6.000]330 [4.000]950 [6.000] 2
			[1.000]732
6095002	Zn3O(SO4)2	-31.542	[-2.000]330 [3.000]950 [2.000]732
			[1.000] 2
6095003	ZINCOSITE	-11.870	[1.000]950 [1.000]732
6095004	ZnSO4:1H2O	-7.304	[1.000]950 [1.000]732 [1.000] 2
6095005	BIANCHITE	-6.183	[1.000]950 [1.000]732 [6.000] 2
6095006	GOSLARITE	-5.938	[1.000]950 [1.000]732 [7.000] 2
6016000	Cd3(OH)4SO4	-33.295	[-4.000]330 [3.000]160 [4.000] 2
			[1.000]732
6016001	Cd3OH2(SO4)2	-28.637	[-2.000]330 [3.000]160 [2.000] 2
			[2.000]732
6016002	Cd4(OH)6SO4	-38.983	[-6.000]330 [4.000]160 [6.000] 2
			[1.000]732
6016003	CdSO4	-10.867	[1.000]160 [1.000]732
6016004	CdSO4:1H2O	-9.315	[1.000]160 [1.000]732 [1.000] 2
6016005	CdSO4:2.67H2O	-9.170	[1.000]160 [1.000]732 [2.670] 2
6036100	HgSO4	-11.570	[1.000]361 [1.000]732 [2.000]330
			[-2.000] 2
6028100	Fe2(SO4)3	-31.263	[2.000]281 [3.000]732
6028101	H-JAROSITE	-12.419	[-5.000]330 [3.000]281 [2.000]732
			[7.000] 2
6050000	Na-JAROSITE	-12.466	[-6.000]330 [1.000]500 [3.000]281
			[2.000]732 [6.000] 2
6041002	K-JAROSITE	-8.484	[-6.000]330 [1.000]410 [3.000]281
			[2.000]732 [6.000] 2
6046000	EPSOMITE	-3.974	[1.000]460 [1.000]732 [7.000] 2
6015000	ANHYDRITE	-1.842	[1.000]150 [1.000]732
6015001	GYPSUM	-1.594	[1.000]150 [1.000]732 [2.000] 2
6010000	BARITE	0.000	[1.000]100 [1.000]732

ID No	Name	SI	Composition by stoich. of components
3028102	LEPIDOCROCITE	-2.081	[-3.000]330 [1.000]281 [2.000] 2
3090300	V2O5	-3.773	[2.000]903 [1.000] 2 [-2.000]330
3046000	SPINEL	-16.309	[-8.000]330 [1.000]460 [2.000] 30
			[4.000] 2
3046001	MAGNESIOFERRITE	-13.177	[-8.000]330 [1.000]460 [2.000]281
			[4.000] 2
6060000	LARNAKITE	-8.960	[-2.000]330 [2.000]600 [1.000]732

ID No	Name	SI	Composition by stoich. of components
6050001	MIRABILITE	-8.389	[2.000]500 [1.000]732 [10.000] 2
6050002	THENARDITE	-9.813	[2.000]500 [1.000]732
6041000	K-ALUM	-8.279	[1.000]410 [1.000] 30 [2.000]732
			[12.000] 2
6041001	ALUNITE	-20.209	[1.000]410 [3.000] 30 [2.000]732
			[6.000] 2
3021212	PbCrO4	-1.914	[1.000]600 [1.000]212
3021208	MgCrO4	-15.693	[1.000]212 [1.000]460

3015000	CaCrO4	-8.156	[1.000]	150	[1.000]	212					
3021201	BaCrO4	-4.530	[1.000]	100	[1.000]	212					
3021210	Na2CrO4	-16.641	[1.000]	212	[2.000]	500					
3021211	Na2Cr2O7	-19.229	[2.000]	212	[2.000]	500	[2.000]	330	[-1.000]	2	
3021205	K2CrO4	-12.433	[1.000]	212	[2.000]	410					
3021206	K2Cr2O7	-11.118	[2.000]	212	[2.000]	410	[2.000]	330	[-1.000]	2	
6160000	PbSeO4	-6.337	[1.000]	600	[1.000]	762					
6195001	ZnSeO4:6H2O	-9.311	[1.000]	950	[1.000]	762	[6.000]	2			
6116001	CdSeO4:2H2O	-12.075	[1.000]	160	[1.000]	762	[2.000]	2			
6146001	MgSeO4:6H2O	-7.782	[1.000]	460	[1.000]	762	[6.000]	2			
6115001	CaSeO4:2H2O	-6.067	[1.000]	150	[1.000]	762	[2.000]	2			
6110001	BaSeO4	-5.403	[1.000]	100	[1.000]	762					
6111001	BeSeO4:4H2O	-9.080	[1.000]	110	[1.000]	762	[4.000]	2			
6150002	Na2SeO4	-13.654	[2.000]	500	[1.000]	762					
6141001	K2SeO4	-10.880	[2.000]	410	[1.000]	762					
7260000	Pb3(AsO4)2	-17.463	[3.000]	600	[2.000]	61	[-6.000]	330			
7203000	AlAsO4:2H2O	-4.264	[1.000]	30	[1.000]	61	[2.000]	2	[-3.000]	330	
7295000	Zn3AsO42:2.5H2O	-18.256	[3.000]	950	[2.000]	61	[2.500]	2	[-6.000]	330	
7228100	FeAsO4:2H2O	-8.292	[1.000]	281	[1.000]	61	[2.000]	2	[-3.000]	330	
7215000	Ca3(AsO4)2:4H2O	-21.691	[3.000]	150	[2.000]	61	[4.000]	2	[-6.000]	330	
7210000	Ba3(AsO4)2	-1.811	[3.000]	100	[2.000]	61	[-6.000]	330			
7349000	NH4VO3	-8.933	[2.000]	903	[1.000]	2	[-2.000]	330			
7360000	Pb3(VO4)2	-8.575	[-8.000]	330	[3.000]	600	[2.000]	903	[4.000]	2	
7360001	Pb2V2O7	-1.435	[-6.000]	330	[2.000]	600	[2.000]	903	[3.000]	2	
7346000	Mg(VO3)2	-11.312	[-4.000]	330	[1.000]	460	[2.000]	903	[2.000]	2	
7346001	Mg2V2O7	-21.292	[-6.000]	330	[2.000]	460	[2.000]	903	[3.000]	2	
7315001	Ca(VO3)2	-5.802	[-4.000]	330	[1.000]	150	[2.000]	903	[2.000]	2	
7315002	Ca3(VO4)2	-29.119	[-8.000]	330	[3.000]	150	[2.000]	903	[4.000]	2	
7315003	Ca2V2O7	-12.650	[-6.000]	330	[2.000]	150	[2.000]	903	[3.000]	2	
7315004	Ca3(VO4)2:4H2O	-30.024	[3.000]	150	[2.000]	903	[8.000]	2	[-8.000]	330	

ID No	Name	SI	Composition by stoich. of components								
7315005	Ca2V2O7:2H2O	-16.705	[2.000]	150	[2.000]	903	[5.000]	2	[-6.000]	330	
7310001	Ba3(VO4)2:4H2O	-34.439	[3.000]	100	[2.000]	903	[8.000]	2	[-8.000]	330	
7310002	Ba2V2O7:2H2O	-18.581	[2.000]	100	[2.000]	903	[5.000]	2	[-6.000]	330	
7350000	NaVO3	-5.574	[-2.000]	330	[1.000]	500	[1.000]	903	[1.000]	2	
7350001	Na3VO4	-36.695	[-4.000]	330	[3.000]	500	[1.000]	903	[2.000]	2	
7350002	Na4V2O7	-39.129	[-6.000]	330	[4.000]	500	[2.000]	903	[3.000]	2	
8603000	HALLOYSITE	-2.140	[2.000]	30	[2.000]	770	[1.000]	2	[-6.000]	330	
8603001	KAOLINITE	0.000	[2.000]	30	[2.000]	770	[1.000]	2	[-6.000]	330	
8646000	CHRYSOTILE	-24.900	[3.000]	460	[2.000]	770	[1.000]	2	[-6.000]	330	
8646003	SEPIOLITE	-17.563	[2.000]	460	[3.000]	770	[-4.000]	330	[-0.500]	2	
8646004	SEPIOLITE (A)	-20.583	[-0.500]	2	[2.000]	460	[3.000]	770	[-4.000]	330	